Complexity

Modelling Economic and Financial Networks: Heterogeneous, Dynamic, and Interactive

Lead Guest Editor: Huajiao Li
Guest Editors: Xueyong Liu and Matteo Zignani

Modelling Economic and Financial Networks: Heterogeneous, Dynamic, and Interactive

Complexity

Modelling Economic and Financial Networks: Heterogeneous, Dynamic, and Interactive

Lead Guest Editor: Huajiao Li
Guest Editors: Xueyong Liu and Matteo Zignani

Contents

Hindawi
Complexity
Volume 2022, Article ID 8856009, 12 pages
https://doi.org/10.1155/2022/8856009

Research Article

Complexity Analysis of a 2D-Piecewise Smooth Duopoly Model: New Products versus Remanufactured Products

S. S. Askar and A. Al-khedhairi

Department of Statistics and Operations Research, College of Science, King Saud University, P.O. Box 2455, Riyadh 11451, Saudi Arabia

Correspondence should be addressed to S. S. Askar; s.e.a.askar@hotmail.co.uk

Received 21 September 2020; Revised 16 February 2022; Accepted 9 April 2022; Published 30 April 2022

Academic Editor: Xueyong Liu

Recent studies on remanufacturing duopoly games have handled them as smooth maps and have observed that the bifurcation types that occurred in such maps belong to generic classes like period-doubling or Neimark-Sacker bifurcations. Since those games yield piecewise smooth maps, their bifurcations belong to the so-called border-collision bifurcations, which occur when the map's fixed points cross the borderline between the smooth regions in the phase space. In the current paper, we present a proper systematic analysis of the local stability of the map's fixed points both analytically and numerically. This includes studying the border-collision bifurcation depending on the map's parameters. We present different multistability scenarios of the dynamics of the game's map and show different types of periodic cycles and chaotic attractors that jump from one region to another or just cross the borderline in the phase space.

1. Introduction

Recently, many countries have adopted the remanufacturing process in order to promote their economy. This process requires remanufacturing of used or default products as remanufacturing is considered a friendly environmental process. There are many popular firms that have commenced this process, such as Ford, Xerox, and Caterpillar [1, 2]. Indeed, the remanufacturing process may be beneficial for some companies to increase their profits, but it may be worse for other companies. It may not be useful for companies which produce new products because it may deprive sales of new products and therefore hurt their expected profits. For these reasons, companies that produce new or original products prefer not to follow remanufacturing and designate this strategy to third-party companies. Based on environmental conditions, those third-party companies accumulate used or default products so that they remanufacture them again and then send them to the market for selling [3–6]. According to USA economy magazines, the industry of remanufacturing in the USA is worth $53 billion [7, 8]. It reveals the fact that original products manufacturers face a competitive threat from remanufacturer companies. Such competition between those companies and its complex dynamic characteristics can be described and investigated by duopoly games.

Competition in duopoly games includes only two competed firms whose strategies may be quantities (as in Cournot) or prices (as in Bertrand). Duopoly games and their complex dynamic characteristics have been analyzed by several authors in the literature. For instance, the duality of quantities and prices in a differentiated duopoly game proposed by Dixit has been analyzed in [9]. In [10], the dynamics of a Cournot duopoly game whose players are boundedly rational and adopt a gradient adjustment mechanism have been investigated. A duopoly game with firms that adopted two different adjustment mechanisms, local monopolistic approximation and gradient-based, has been studied in [11]. Price competition of a nonlinear duopoly game has been illustrated when price demand elasticity varies in [12]. For more information on the adjustment mechanisms, readers are advised to see [13]. In [14], a

Bertrand duopoly game whose players want to maximize their relative profits has been introduced and discussed. Different duopoly models based on Cobb-Douglas utility have been analyzed in [15]. A duopoly model of technological innovation based on constant conjectural variation and boundedly rational players has been studied in [16]. In [17], the dynamic properties of a Bertrand duopoly game with two-stage delay have been investigated. For more detailed studies and information on the complex dynamic characteristics of duopoly games, we refer to the literature [18–22].

There are few studies on the remanufacturing of duopoly games in literature. Those studies have introduced such games based on smooth models and hence they have investigated the stability conditions of the fixed points of that models. For example, the dynamic characteristics of the fixed points of this game have been introduced and discussed in [3, 23]. In spite of the stability investigations given in those previous references, they have improperly handled their games. They have studied their games as a game described by a smooth discrete dynamical system. The current paper is motivated by the game given in [3]. Our motivation gives rise to a proper investigation of the game and in addition, introduces a rich analysis of the stability of the game's fixed point by analyzing the border-collision bifurcation by which the fixed point becomes unstable. Indeed, such games should be described by a piecewise smooth map as given in the current manuscript. Piecewise-smooth map means that the map is defined by many parts and the phase plane is divided into regions separated by a border curve. Consequently, the dynamic of map in these regions should not be studied separately as given in [3, 23], simply because the dynamic of destabilization of the map's fixed point is usually never related to only one region. The dynamics of the map should be studied based on parameter values belonging to these regions where the map is defined.

The current paper gives a proper description of the map used to define this game in [3]. Before that, we recall some important aspects of piecewise smooth maps. There are several applications of different disciplines in the literature that were modeled using piecewise-smooth maps. Such applications include physiological and economic systems, mechanical systems, and switching circuits. They have reported many interesting observations regarding the kinds of bifurcations that destabilize such maps. They have observed that the bifurcation that occurred in these piecewise smooth maps does not belong to a generic class of bifurcation such as period doubling or Neimark-Sacker. Instead, new types of bifurcations have emerged from these maps when the fixed point crosses the border curve separating the smooth regions on where the maps are defined. Now, we report some important studies on the complex dynamic characteristics of piecewise smooth maps. For example, in [24], a general three-dimensional piecewise smooth map and its multiple attractors have been investigated. A global analysis of a piecewise-smooth Cournot duopoly model derived from an isoelastic demand function has been performed in [25]. In [26], multistability investigations and border bifurcations have been discussed for a 2D piecewise-smooth map. In [27], a 2D map that is continuous, noninvertible, and piecewise smooth has been used to characterize the innovation activities in the model of trade and product innovation of two countries. The global dynamics of the piecewise-smooth map that describes the spatial distribution of long-run industrial activity for the economic geography model have been analyzed in [28]. Interesting readers of piecewise smooth maps and their dynamic characteristics may be directed to see literature [29–34].

Further, we have to highlight other investigations in literature that uphold this research direction and raise new directions in future work. In [35], a review report on new research directions on evolutionary games and their rules which are adopted to exploit the benefits of cooperation that might be occurred among players. The characteristics of cooperation under the synergies between evolutionary game and networks have been reviewed in [36]. Discussing the factors that might affect the overall performance of a firm has been determined and analyzed in [37]. Recently, in [38], the authors have identified the most influential invaders in cooperative communities based decomposition of the weighted-degree mechanism.

After the above introduction, the current paper is briefly organized as follows. In Section 2, we give a proper version of the map used to describe the remanufacturing game presented in [3]. In Section 3, local analysis of the map's fixed point on the smooth regions where the map is defined is analytically investigated. Section 3 presents rich numerical simulation experiments which uphold obtained results in Section 2. In Section 5, we give a brief conclusion.

2. The Model

Let us consider an economic market populated by two competed firms. The first firm is called a manufacturer and supports the market with new products, while the second firm is called a third-party remanufacturer and supports the market with differentiated remanufactured products. The customers are willing to pay for productions by those two firms. The demand productions sent to the market by firms are denoted by x_1 and x_2. The competition between these firms is carried out in discrete time periods, $t = 0, 1, 2, \ldots$. The first firm sends the new quantity x_1 for selling in the market at time t, while the second firm can receive returned quantity x_2 for remanufacturing and sells it again in the market at time $t + 1$. According to the literature [3, 23], this discussion can be described by the following inverse demand functions (The inverse demand functions areas in [1]). But the authors have defined their game's map as a smooth one which is incorrect. They have studied each part of the map separately; however, it had to be studied as a piecewise-smooth map. In a addition, they had to investigate the fixed points as a function of the map's parameters when they belong to two different regions separated by border line on where the piecewise map was defined. This is for simple reason that is the dynamics of destabilization of the fixed points are usually never related to only one region. Thus the map's dynamics had to be really analyzed as a piecewise one with points jumping from one region to the other:

$$p_1 = 1 - x_1 - \delta x_2,$$
$$p_2 = \delta(1 - x_1 - x_2). \tag{1}$$

The parameter δ has an important meaning in this game. If $\delta = 1$, it means that the customers are prepared to pay the same price for new and remanufactured products. From an economic perspective, this may not be approved. If $\delta = 0$, the customers will not pay any price for remanufactured products. Because of the variety of customers, we restrict this parameter to $\delta \in (0, 1)$. Assuming that $C_i(x_i)$ refers to the cost of the quantity x_i and is given by the following linear form:

$$C_i(x_i) = c_i x_i, \quad i = 1, 2, \tag{2}$$

where c_1 and c_2 refer to the marginal costs for both firms, respectively. Therefore, the profits of both firms are given as follows:

$$\pi_1 = (1 - x_1 - \delta x_2 - c_1)x_1,$$
$$\pi_2 = (\delta(1 - x_1 - x_2) - c_2)x_2. \tag{3}$$

And their marginal functions become as follows:

$$\frac{\partial \pi_1}{\partial x_1} = 1 - 2x_1 - \delta x_2 - c_1,$$
$$\frac{\partial \pi_2}{\partial x_2} = \delta(1 - x_1 - 2x_2) - c_2. \tag{4}$$

Due to incomplete information both firms can get from the market, they update their productions based on partial information. So we assume that the two firms are heterogeneous and adopt different adjustment mechanisms in order to update their productions. We presume that the first firm will behave as a bounded rational firm and consequently will maximize its profit. It is easy to see that for $\delta \in (0, 1)$ and $c_1 > c_2$, the marginal profit $(\partial \pi_1 / \partial x_1)$ is always positive and lies within the first quadrant. Therefore, the first firm will increase its output to get the maximum of its profit. This mechanism is called bounded rationality and has been intensively adopted in the literature ([10–15]) to describe such firm's behavior. Based on this reasoning the first firm will update its output at period $t + 1$ according to the following form:

$$x_{1,t+1} = x_{1,t} + k x_{1,t} \frac{\partial \pi_{1,t}}{\partial x_{1,t}}, \tag{5}$$

where k is a positive parameter. On the other hand, we assume that the second firm seeks to share the market with a certain profit. The weighted sum method [39] is used to handle this behavior. It starts with assuming that it seeks a complete market share maximization. This makes $\pi_2 = 0$ and then its optimum output becomes as follows:

$$\overline{x}_2 = 1 - x_1 - \frac{c_2}{\delta}. \tag{6}$$

But when it completely seeks profit maximization, its marginal profit will vanish and then we have the following:

$$\widehat{x}_2 = \frac{1}{2}\left(1 - x_1 - \frac{c_2}{\delta}\right). \tag{7}$$

According to some weights, the second firm will be traded off between market share and profit as follows:

$$\widetilde{x}_2 = \omega \overline{x}_2 + (1 - \omega)\widehat{x}_2 = \frac{1 + \omega}{2}\left(1 - x_1 - \frac{c_2}{\delta}\right), \tag{8}$$

where $\omega \in (0, 1)$. When $\omega = 0$, it means the second firm seeks profit maximization only while $\omega = 1$ means it seeks market share maximization. But as it trades off between both, we have restricted the parameter ω to the interval $(0, 1)$. Now we assume this firm updates its output according to the following adaptive mechanism:

$$x_{2,t+1} = (1 - \beta)x_{2,t} + \beta \widetilde{x}_2, \tag{9}$$

where β is a positive parameter and is restricted to the interval $\beta \in (0, 1)$. Since the output of the second firm at time $t + 1$ should be less than or equal to those of the first firm at time t, $x_{1,t+1} \le x_{1,t}$, therefore, (9) will be modified as follows:

$$x_{2,t+1} = \min\left\{(1 - \beta)x_{2,t} + \beta \widetilde{x}_2, x_{1,t}\right\}. \tag{10}$$

Using (5) and (10), one gets the map that describes this game as follows:

$$x_{1,t+1} = x_{1,t} + k x_{1,t}\left(1 - 2x_{1,t} - \delta x_{2,t} - c_1\right),$$
$$x_{2,t+1} = \min\left\{(1 - \beta)x_{2,t} + \beta \widetilde{x}_2, x_{1,t}\right\}, \tag{11}$$

The map (11) is a two-dimensional piecewise smooth map and is constructed to describe the proposed duopoly game in this paper. In order to study the stability of its fixed points we should study it as a piecewise-smooth map not as in [3]. It is worthwhile to mention that the authors in [3] have improperly studied their map as a smooth map. Here, in this paper we introduce a proper investigation for the map (11). The stability of this map depends on the second equation where the function $\mathsf{F} = (1 - \beta)x_{2,t} + \beta \widetilde{x}_2$ exists. It means that any order pair (x_1, x_2) belongs to $\mathsf{F} < x_1$ gives only one part of the map to be dynamically studied, while if $\mathsf{F} > x_1$ the other part of the map should be studied. Hence, we get the fact that there is a borderline $\mathsf{F} = x_1$ where the map is continuous. Furthermore, the map's phase plane will be divided by the border line into two regions (Left region, R_ℓ and right region R_r). This borderline takes the following form:

$$x_1 = \frac{1}{2 + \beta(1 + \omega)}\left[2(1 - \beta)x_2 + \frac{\beta}{\delta}(1 + \omega)(\delta - c_2)\right] =: g(x_2). \tag{12}$$

So the map (11) is modified to the following:

$$x_{1,t+1} = x_{1,t} + kx_{1,t}\left(1 - 2x_{1,t} - \delta x_{2,t} - c_1\right),$$

$$x_{2,t+1} = \begin{cases} x_{2,t+1} = (1-\beta)x_2 + \frac{1}{2}\beta(1+\omega)\left(1 - x_1 - \frac{c_2}{\delta}\right), & \text{if } x_{1,t} \geq g(x_2), \\ x_{1,t}, & \text{if } x_{1,t} \leq g(x_2). \end{cases} \tag{13}$$

or, equivalently, it becomes as follows:

$$\left(x_{1,t+1}, x_{2,t+1}\right) = \begin{cases} x_{1,t} + kx_{1,t}\left(1 - 2x_{1,t} - \delta x_{2,t} - c_1\right), \\ x_{2,t+1} = (1-\beta)x_2 + \frac{1}{2}\beta(1+\omega)\left(1 - x_1 - \frac{c_2}{\delta}\right), \end{cases} \quad \text{if } x_{1,t} \geq g(q_2) \text{ (region } R_r), \tag{14}$$

$$\left(x_{1,t+1}, x_{2,t+1}\right) = \begin{cases} x_{1,t} + kx_{1,t}\left(1 - 2x_{1,t} - \delta x_{2,t} - c_1\right), \\ x_{1,t} \end{cases} \quad \text{if } x_{1,t} \leq g(q_2) \text{ (region } R_\ell).$$

Now, we come to the fact that the stability of the map (14) depends on points located in region R_r from the borderline or on points located in the region R_ℓ. Furthermore, other attracting sets may appear at the same parameter values. But when the map's fixed points are destabilized, this means that their dynamics are usually never related to only one region in the phase space. As a result, the dynamic of the map (14) must be studied as a piecewise smooth map with points jumping from region R_r to region R_ℓ and vice versa.

3. Local Analysis

It is clear that the map (14) is defined in two different regions separated by a borderline. This gives rise to two fixed points in the two regions. We denote these two points E_r (for the one in region R_r) and E_ℓ (for the point in region R_ℓ), where

$$E_r = \left(\frac{2(1-c_1) - (1+\omega)(\delta - c_2)}{4 - (1+\omega)\delta}, \frac{(1+\omega)\left((1+c_1)\delta - 2c_2\right)}{(4-(1+\omega)\delta)\delta}\right),$$

$$E_\ell = \left(\frac{1-c_1}{2+\delta}, \frac{1-c_1}{2+\delta}\right). \tag{15}$$

These fixed points are positive under the conditions, $(\delta/2)(1-c_1)(1+\omega) < (1+\omega)(\delta - c_2) < 2(1-c_1)$ and $c_1 < 1$. The Jacobian matrices at (15) become as follows:

$$J_r = \begin{bmatrix} 1 - \frac{4(1-c_1) - 2(1+\omega)(\delta - c_2)}{4 - (1+\omega)\delta}k & -\frac{2(1-c_1) - (1+\omega)(\delta - c_2)}{4 - (1+\omega)\delta}\delta k \\ -\frac{(1+\omega)\beta}{2} & 1 - \beta \end{bmatrix},$$

$$J_\ell = \begin{bmatrix} 1 - \frac{2(1-c_1)}{\delta + 2}k & -\frac{\delta(1-c_1)}{\delta+2}k \\ 1 & 0 \end{bmatrix}. \tag{16}$$

The eigenvalues for the above Jacobian matrices take the form, $\lambda_{1,2} = (1/2)(\tau \pm \sqrt{\tau^2 - 4\Delta})$, where τ and Δ refer to the trace and determinant respectively. It should be noted that τ and Δ may be taken as τ_r and Δ_r (or τ_ℓ and Δ_ℓ) depending on whether the fixed point lies within region R_r (or region R_ℓ). Those traces and determinants in both regions take the following form:

$$\begin{aligned}
\tau_r &= 2-\beta-\frac{2\left[2\left(1-c_1\right)-(1+\omega)\left(\delta-c_2\right)\right]}{4-(1+\omega)\delta}k,\\
\tau_\ell &= 1-\frac{2\left(1-c_1\right)}{\delta+2}k,\\
\Delta_r &= 1-\beta+\frac{\left[\beta(1+\omega)^2\delta^2+\delta(1+\omega)\left(4-c_2\beta(1+\omega)-2\beta\left(3-c_1\right)\right)-4(1-\beta)\left(2\left(1-c_1\right)+c_2(1+\omega)\right)\right]}{2[4-(1+\omega)\delta]}k,\\
\Delta_\ell &= \frac{\delta\left(1-c_1\right)}{\delta+2}k.
\end{aligned} \tag{17}$$

and the eigenvalues are as follows:

$$\begin{aligned}
\lambda_{1r,2r} &= 1-\frac{\beta}{2}-A_1k\pm\sqrt{\frac{\beta^2}{4}-\frac{\beta}{2}A_2k-A_1^2k^2},\\
\lambda_{1\ell,2\ell} &= \frac{1}{2}-\left(\frac{1-c_1}{2+\delta}\right)k\pm\sqrt{\frac{1}{4}-\frac{\left(1-c_1\right)(1+\delta)}{2+\delta}k+\left(\frac{1-c_1}{2+\delta}\right)^2k^2},
\end{aligned} \tag{18}$$

where $A_1=(2(1-c_1)-(1+\omega)(\delta-c_2)/4-(1+\omega)\delta)$ and $B=([2-(1+\omega)\delta]$ $[2(1-c_1)-(1+\omega)(\delta-c_2)]/4-(1+\omega)\delta)$. Or equivalently,

$$\begin{aligned}
\lambda_{1r,2r} &= \frac{1}{2}\left(\tau_r\pm\sqrt{\tau_r^2-4\Delta_r}\right),\\
\lambda_{1\ell,2\ell} &= \frac{1}{2}\left(\tau_\ell\pm\sqrt{\tau_\ell^2-4\Delta_\ell}\right).
\end{aligned} \tag{19}$$

We should highlight that the map (14) is continuous, and it also has continuous derivatives in each region. Its derivative is discontinuous at the borderline $\mathsf{F}=x_1$. Moreover, the map may have no fixed point in half of the phase space. It means that the location E_ℓ (or E_ℓ) may turn out to be in region R_r (or region R_ℓ) and consequently, the character of a virtual fixed point uprises. Furthermore, the triangle of stability for each fixed point is given by the following:

$$\begin{aligned}
S_r &= \left\{(\tau_r,\Delta_r):\ 1+\tau_r+\Delta_r>0, 1-\tau_r+\Delta_r>0, 1-\Delta_r>0\right\},\\
S_\ell &= \left\{(\tau_\ell,\Delta_\ell):\ 1+\tau_\ell+\Delta_\ell>0, 1-\tau_\ell+\Delta_\ell>0, 1-\Delta_\ell>0\right\},
\end{aligned} \tag{20}$$

where

$$\begin{aligned}
1+\tau_r+\Delta_r &= 8-4\beta-\frac{\left[2\left(1-c_1\right)-(1+\omega)\left(\delta-c_2\right)\right]\left[(1+\omega)\delta\beta+4(2-\beta)\right]}{4-(1+\omega)\delta}k,\\
1-\tau_r+\Delta_r &= \frac{\beta}{2}\left[2\left(1-c_1\right)-(1+\omega)\left(\delta-c_2\right)\right]k,\\
1-\Delta_r &= \beta-\frac{\left[2\left(1-c_1\right)-(1+\omega)\left(\delta-c_2\right)\right]\left[(1+\omega)\delta\beta+4(1-\beta)\right]}{2[4-(1+\omega)\delta]}k,\\
1+\tau_\ell+\Delta_\ell &= 2-\frac{\left(1-c_1\right)(2-\delta)}{2+\delta}k,\\
1-\tau_\ell+\Delta_\ell &= \left(1-c_1\right)k,\\
1-\Delta_\ell &= 1-\frac{\delta\left(1-c_1\right)}{2+\delta}k.
\end{aligned} \tag{21}$$

4. Simulation

We carry out in this section several simulation experiments to get more insights into the local and global analysis of the map (14). This simulation will deeply investigate different qualitative behaviors of that map. We analyze the influences of map's parameters on the stability of the fixed points using some tools of numerical simulations such as 1D and 2D bifurcation diagrams, largest Lyapunov exponent, time series plot, phase diagram, and

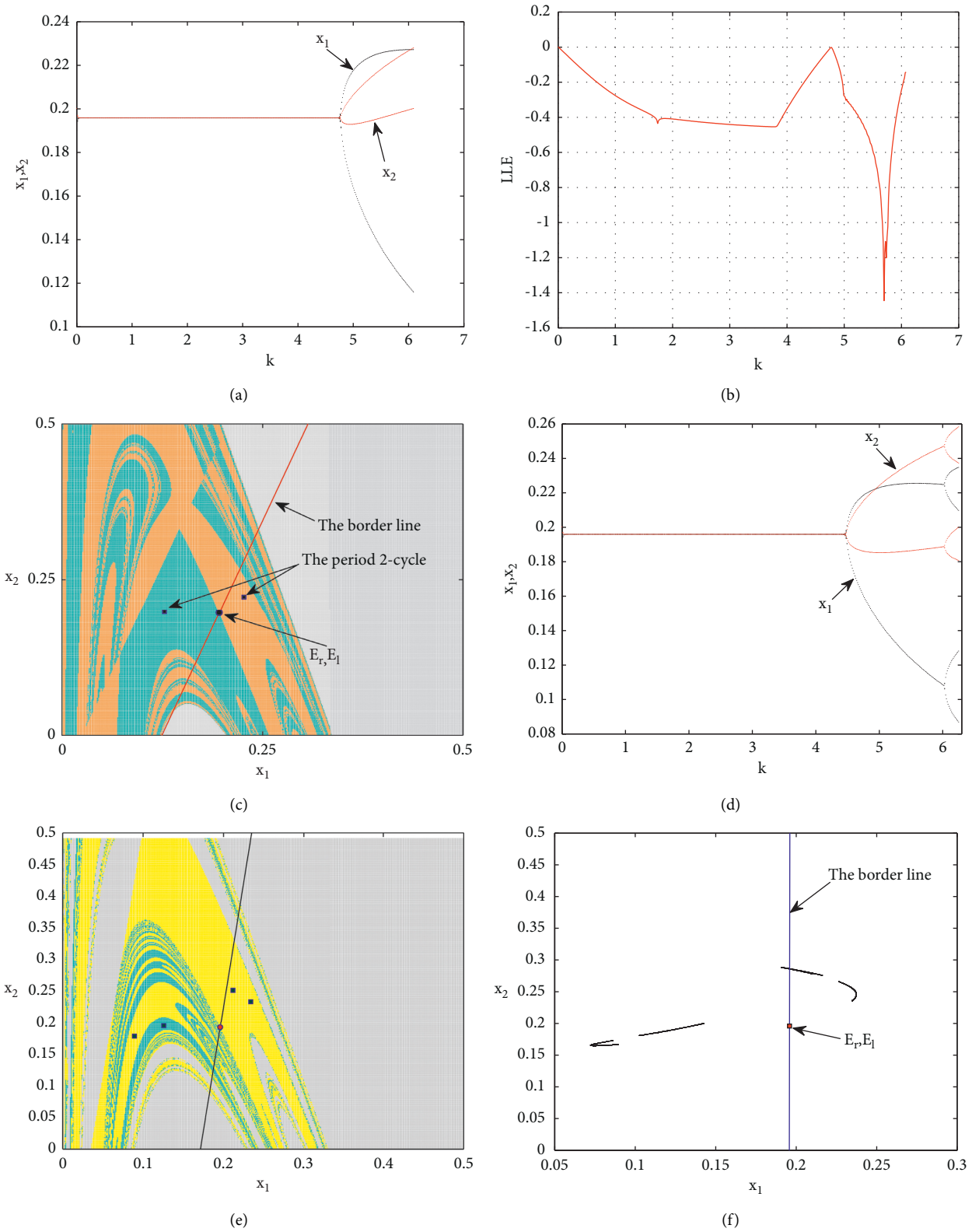

Figure 1: (a) The stable period 2-cycle when varying the parameter k at the parameter values: $\omega = 0.5, c_1 = 0.5, c_2 = 0.3, \delta = 0.5525470489$, and $\beta = 0.5$. (b) Largest Lyapunov exponent corresponds to the bifurcation diagram in Figure 1(a). (c) Basin of attraction of the stable period 2-cycle at $\omega = 0.5, c_1 = 0.5, c_2 = 0.3, \delta = 0.5525470489, \beta = 0.5$ and $k = 5.72$. (d) The stable period 2-cycle when varying the parameter k at the parameter values: $\omega = 0.5, c_1 = 0.5, c_2 = 0.3, \delta = 0.5525470489$ and $\beta = 0.8$. (e) Basin of attraction of the stable period 4-cycle at $\omega = 0.5, c_1 = 0.5, c_2 = 0.3, \delta = 0.5525470489, \beta = 0.8$ and $k = 6.2$. (f) Phase plane for the chaotic attractor at: $\omega = 0.5, c_1 = 0.5, c_2 = 0.3, \delta = 0.5525470489, \beta = 0.999$ and $k = 6.2$.

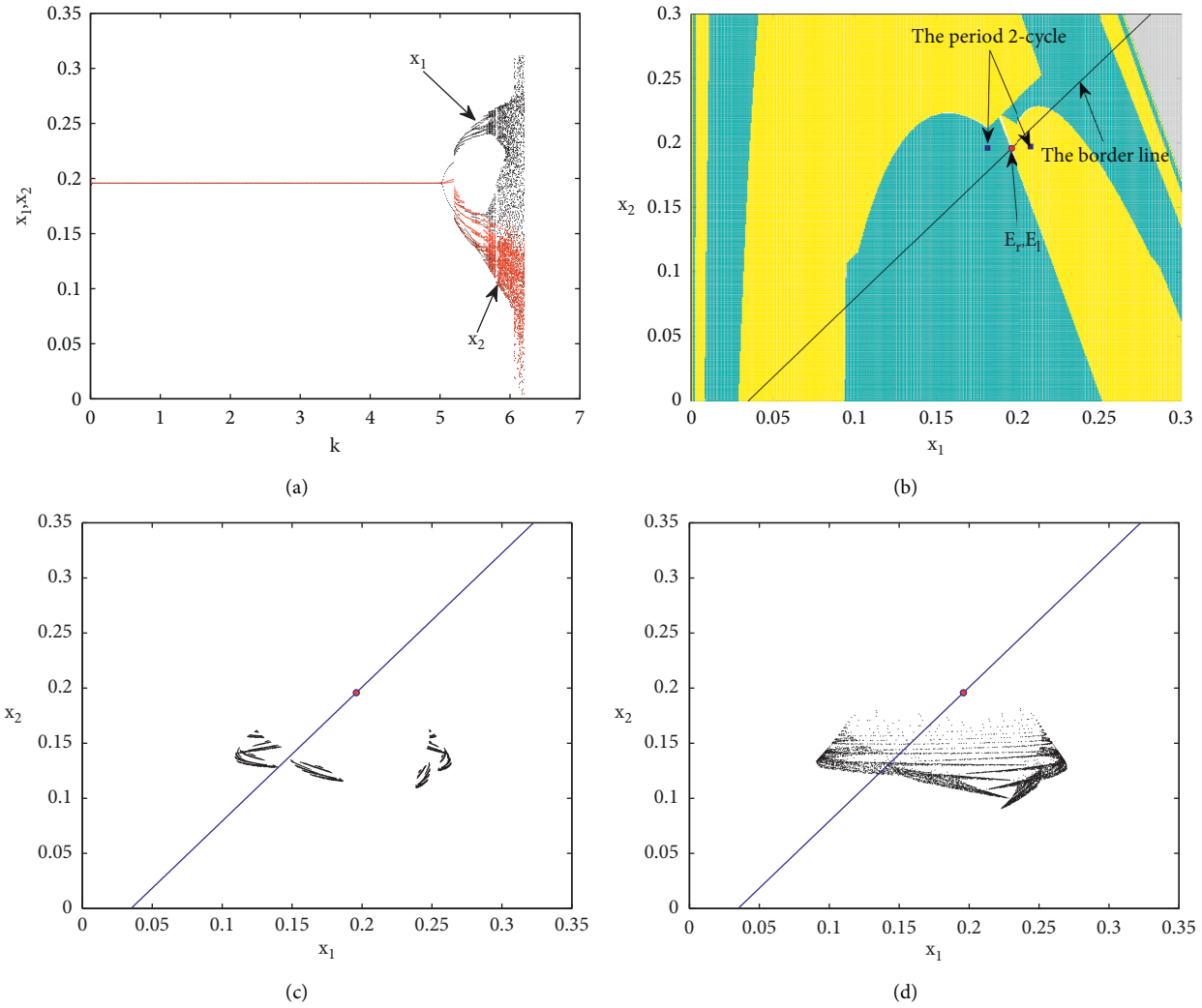

FIGURE 2: (a) Bifurcation diagram at varying the parameter k. (b) Basin of attraction of the period 5-cycle at $k_2 = 5.1$. (c) Phase plane for the chaotic attractor at $\omega = 0.5, c_1 = 0.5, c_2 = 0.3, \delta = 0.5525470489, \beta = 0.11$ and $k = 5.78$. (d) Phase plane for the chaotic attractor at $\omega = 0.5, c_1 = 0.5, c_2 = 0.3, \delta = 0.5525470489, \beta = 0.11$ and $k = 5.95$.

basin of attraction. We start our numerical experiments with the initial datum $(x_{1,0}, x_{2,0}) = (0.19, 0.15)$ with the parameter values, $\omega = 0.5$, $c_1 = 0.5$, $c_2 = 0.3$, and $\delta = 0.5525470489$. At these parameter values we get $E_r = E_\ell = (0.19588, 0.0.19588)$. This means that we have two coincided fixed points born in the border line $\mathsf{F} = x_1$. At the same time, the other two parameters k and β are considered the bifurcation parameters. Both the Jacobians defined in (16) depend on those parameters and to calculate them we assume $\beta = 0.5$ and $k = 5.72$. This gives the following:

$$J_\ell = \begin{bmatrix} -1.2409 & -0.61910 \\ 1 & 0 \end{bmatrix}, \quad J_r = \begin{bmatrix} -1.2409 & -0.61910 \\ -0.375 & 0.5 \end{bmatrix}, \tag{22}$$

where $\Delta_r = -0.85261$, $\tau_r = -0.7409$, $\Delta_\ell = 0.61910$, and $\tau_\ell = -1.2409$ with $\lambda_{1\ell,2\ell} = -0.62045 \pm 0.48388i$ and $(\lambda_{1r}, \lambda_{2r}) = (0.62446, -1.3654)$. It is clear that $|\Delta_r| < 1$ and $|\Delta_\ell| < 1$ that means the map's dynamics in both regions are dissipative. Furthermore, we have $-1 < \Delta_r < 0, 0 < \lambda_{1r} < 1$ and $\lambda_{2r} < -1$ and hence a transverse homoclinic intersection may not exist and the obtained attractor may not be chaotic. But since $1 + \tau_r\tau_\ell - \Delta_r - \Delta_\ell + \Delta_r\Delta_\ell > 0$, then the attractor will be a cycle of 2-period only. Figure 1(a) shows the bifurcation diagram at those parameter values when varying k. The figure gives rise to a bifurcation diagram that stops at the cycle of 2-period only for any increase of that parameter. That is confirmed in the corresponding Largest Lyapunov exponent (or LLE) given in Figure 1(b). In Figure 1(c), one can see that there are three different sections and the border line crosses them. Those sections are colored by cyan, yellow, and grey. The cyan and yellow colors show the basin of attraction of the locally stable period 2-cycle while the grey one depicts the basin of attraction of diverging trajectories. Moreover, the border line contains the two coincided fixed points born on it. Fixing the previous parameter values and increasing β above gives rise to higher periodic cycles with respect to k. For example, at $\beta = 0.8$ a stable period 4-cycle

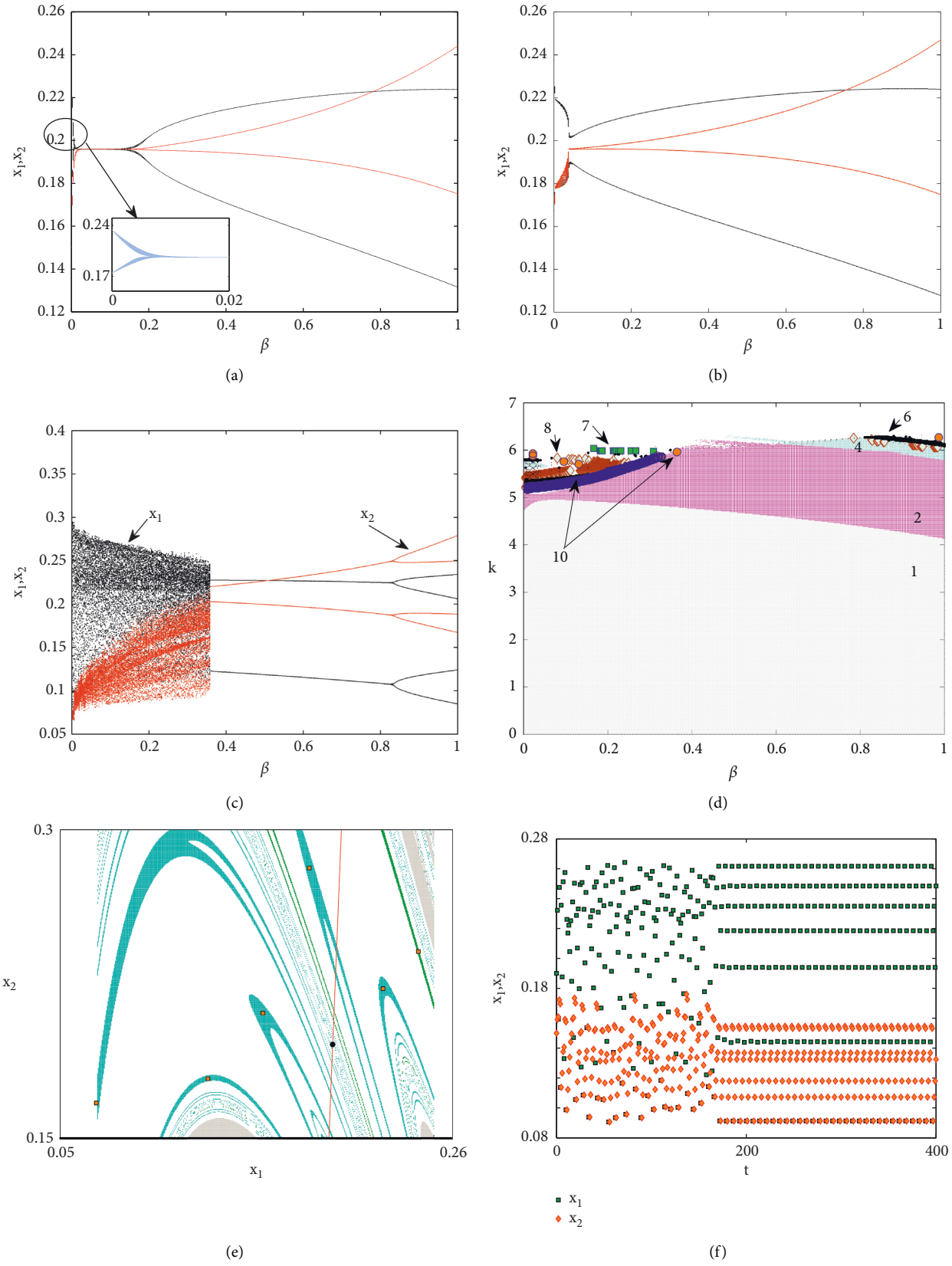

Figure 3: (a) Bifurcation diagram at varying the parameter β. (b) Bifurcation diagram at varying the parameter β and $k = 5.09$. (c) Bifurcation diagram at varying the parameter β and $k = 6$. (d) 2D Bifurcation diagram at $\omega = 0.5, c_1 = 0.5, c_2 = 0.3, \delta = 0.5525470489$. (e) The basin of attraction of stable period 6-cycle. (f) The time series for the periodic 7-cycle.

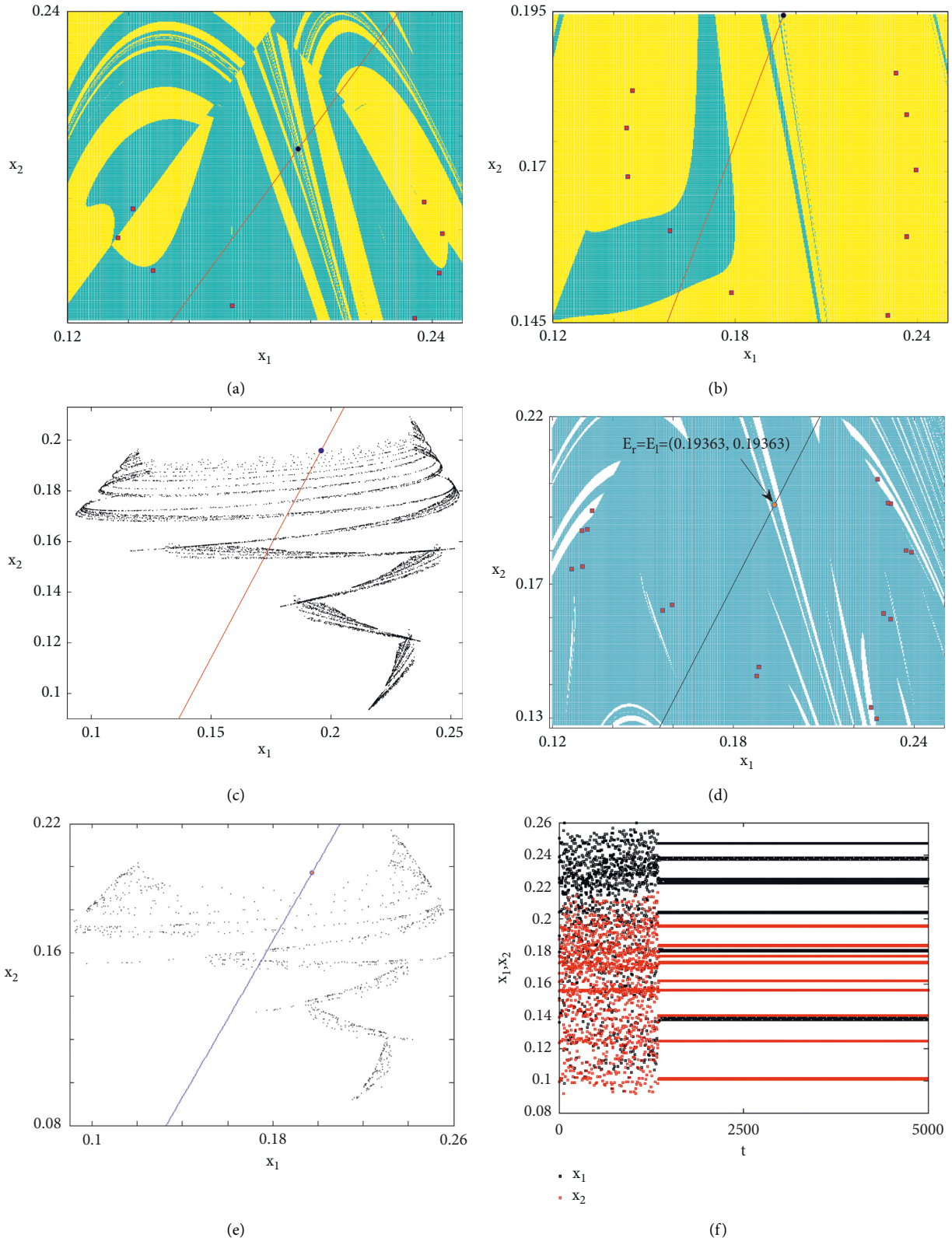

Figure 4: (a) Basin of attraction of the period 8-cycle. (b) Basin of attraction of the period 10-cycle. (c) Phase space of chaotic attractor. (d) Basin of attraction of the period 18-cycle. (e) Chaotic attractor that is changed into stable period 18-cycle. (f) Times series for the chaotic attractor given in Figure 4(e).

exists when varying the parameter k. Figure 2(c) presents a stable period 4-cycle that is born due to period-doubling bifurcation. The basin of attraction of this cycle is given in Figure 1(e). Increasing β further makes periodic cycles such as period-8, period-16, and higher period cycles appear till β approaches close to 1 on, where the dynamics of the map evolve in a chaotic attractor. Figure 1(e) shows four unconnected chaotic areas in both regions. Now, we investigate the influence of the parameter k when β takes values close to 0. At the parametr values, $\omega = 0.5$, $c_1 = 0.5$, $c_2 = 0.3$, $\delta = 0.5525470489$, $\beta = 0.11$ and $k = 5$ we get the following:

$$J_\ell = \begin{bmatrix} -0.95883 & -0.54117 \\ 1 & 0 \end{bmatrix}, \quad J_r = \begin{bmatrix} -0.95883 & -0.54117 \\ -0.0825 & 0.89 \end{bmatrix}, \tag{23}$$

where $\Delta_r = -0.8980$, $\tau_r = -0.06883$, $\Delta_\ell = 0.54117$, and $\tau_\ell = -0.95882$ with $\lambda_{1\ell,2\ell} = -0.47941 \pm 0.55797i$ and $(\lambda_{1r}, \lambda_{2r}) = (0.91384, -0.98267)$. It is clear that $|\Delta_r| < 1$ and $|\Delta_\ell| < 1$ that means the map's dynamics in both regions are also dissipative. Simulation shows that at small values of the parameter β, the influence of the parameter k becomes very bad. Figure 2(a) shows the bifurcation diagram when varying the parameter k at the same parameter values. At $k = 5.1$ the dynamic of the map gives a stable period 2-cycle. Its basin of attraction is given in Figure 2(b) where there are two periodic points separated by the border line. Increasing the parameter k more gives unstable periodic cycle and routes to chaotic attractors are obtained as shown in Figures 2(c) and 2(d). Both figures present chaotic attractors that are separated by the border line or cross it.

Now, we analyze the impact of the parameter β on the map's dynamic while keeping the other parameter values fixed. Let us assume $\omega = 0.5$, $c_1 = 0.5$, $c_2 = 0.3$, $\delta = 0.5525470489$, and $k = 5$. Figure 3(a) presents the bifurcation diagram when varying β. It is clear that the two fixed points born on the border line are locally stable and above $\beta = 0.1473$ a period 2-cycle arises. Numerical experiments show that the influence of the parameter β changes as k increases further. For example, at $k = 5.09$ and keeping the other parameter values fixed, a bifurcation diagram is given in Figure 3(b). Another bad impact of the parameter β on the map's dynamics is given in the bifurcation diagram in Figure 3(c) at $k = 6$. This makes us investigate more the dynamic behavior of the map when assuming different values of those two parameters. This can be done by plotting the 2D bifurcation diagram for them. It is depicted in Figure 3(d) on where different periodic cycles can be obtained. The numbers from 1 to 10 show different types of periodic cycles. For the parameter values $\omega = 0.5, c_1 = 0.5, c_2 = 0.3, \delta = 0.5525470489, \beta = 0.9244$, and $k = 6.1133$, the basin of attraction of stable period 6-cycle is depicted in Figure 3(e). At the same set of parameter values used in Figure 3(e) but for $\beta = 0.182$ and $k = 5.989$, we get a chaotic behavior of the map's dynamic which after that is turned into a stable period 7-cycle. We simulate this behavior of the map by the time series given in Figure 3(f).

At the same set of parameters and for $\beta = 0.158$ and $k = 5.491$ a stable period 8-cycle arises and is distributed in both regions from the border line. Another stable period 10-cycle is given in Figure 4(b) at the same set of parameter values but for $\beta = 0.158$ and $k = 5.413$. Carrying out more numerical experiments about the dynamic of the map (14) gives rise to more complicated behavior of it. For example, at the same set of parameter values used in Figures 4(a) and 4(b) and for $\beta = 0.3088$ and $k = 5.9733$, a one-piece chaotic attractor that crosses the border line is given in Figure 4(c). From the above discussions that are obtained when the second firm uses symmetric weights ($\omega = 0.5$), we conclude that the smooth-piecewise map (14) describing the heterogeneous duopoly is characterized by higher degree of unpredictability. In order to end our discussion in this paper, we give two examples for the asymmetric case (when $\omega \neq 0.5$). Assuming the following parameter values, $\omega = 0.33$, $c_1 = 0.5$, $c_2 = 0.3$, $\delta = 0.5822914793$, $\beta = 0.3088$ and $k = 5.7$ a stable period of 18-cycle arises. This cycle is plotted with the coincided fixed points born on the border line in Figure 4(d). Assuming the following parameter values, $\omega = 0.65$, $c_1 = 0.5, c_2 = 0.3$, $\delta = 0.5326030850$, $\beta = 0.3088$ and $k = 6$, Figure 4(e) presents a chaotic behavior of the map that is changed into a stable period 18-cycle. The time series given in Figure 4(f) simulates the behavior given in Figure 4(e).

5. Conclusion

We have analyzed in this paper the dynamic behavior of a remanufactured duopoly game. Previous works in literature have studied and discussed such a game as a smooth map. In the present paper, we have given a proper investigation of the competition carried out between firms in this game. Our investigation and analysis are entirely different than those given in [3, 23] for the same game. Analytically, we have analyzed the piecewise-smooth map describing such a game and illustrated the local stability conditions of its fixed points in both regions where the map was defined. Numerically, we have enriched this paper with intensive numerical simulation experiments about the global analysis of the map's fixed points that have shown how the map's dynamics may become quite complex. To the extent of our knowledge, the obtained results in this paper have provided new analytical results and proper investigations of the model investigated by the authors in [3]. This includes studying the game's model as a piecewise smooth map. Our interesting results have detected different scenarios of multistability situations and period cycles points jumping from one region to another or passing through the borderline. Our future studies will be directed to the importance of networks in dealing with such remanufacturing games.

Data Availability

All data are included in the paper.

Conflicts of Interest

The authors declare that they have no conflicts of interest.

Acknowledgments

This paper was supported by Research Supporting Project number (RSP-2022/167), King Saud University, Riyadh, Saudi Arabia. This project was funded by King Saud University, Riyadh, Saudi Arabia.

References

[1] A. Atasu, M. Sarvary, and L. N. Van Wassenhove, "Remanufacturing as a marketing strategy," *Management Science*, vol. 54, no. 10, pp. 1731–1746, 2008.

[2] R. Subramanian, M. E. Ferguson, and L. Beril Toktay, "Remanufacturing and the component commonality decision," *Production and Operations Management*, vol. 22, no. 1, pp. 36–53, 2013.

[3] L. Shi, Z. Sheng, and F. Xu, "Complexity analysis of remanufacturing duopoly game with different competition strategies and heterogeneous players," *Nonlinear Dynamics*, vol. 82, no. 3, pp. 1081–1092, 2015.

[4] G. Ferrer and J. M. Swaminathan, "Managing new and remanufactured products," *Management Science*, vol. 52, no. 1, pp. 15–26, 2006.

[5] M. E. Ferguson and L. B. Toktay, "The effect of competition on recovery strategies," *Production and Operations Management*, vol. 15, no. 3, pp. 351–368, 2006.

[6] P. Majumder and H. Groenevelt, "Competition in remanufacturing," *Production and Operations Management*, vol. 10, no. 2, pp. 125–141, 2001.

[7] S. Mitra and S. Webster, "Competition in remanufacturing and the effects of government subsidies," *International Journal of Production Economics*, vol. 111, no. 2, pp. 287–298, 2008.

[8] G. Ferrer and J. M. Swaminathan, "Managing new and differentiated remanufactured products," *European Journal of Operational Research*, vol. 203, no. 2, pp. 370–379, 2010.

[9] N. Singh and X. Vives, "Price and quantity competition in a differentiated duopoly," *The RAND Journal of Economics*, vol. 15, no. 4, pp. 546–554, 1984.

[10] A. Agliari, A. K. Naimzada, and N. Pecora, "Nonlinear dynamics of a Cournot duopoly game with differentiated products," *Applied Mathematics and Computation*, vol. 281, pp. 1–15, 2016.

[11] F. Cavalli, A. Naimzada, and F. Tramontana, "Nonlinear dynamics and global analysis of a heterogeneous Cournot duopoly with a local monopolistic approach versus a gradient rule with endogenous reactivity," *Communications in Nonlinear Science and Numerical Simulation*, vol. 23, no. 1-3, pp. 245–262, 2015.

[12] L. Gori and M. Sodini, "Price competition in a nonlinear differentiated duopoly," *Chaos, Solitons & Fractals*, vol. 104, pp. 557–567, 2017.

[13] C. Hommes, *Behavioral Rationality and Heterogeneous Expectations in Complex Economic Systems*, Cambridge University Press, Cambridge, UK, 2013.

[14] S. S. Askar and A. Al-khedhairi, "Dynamic investigations in a duopoly game with price competition based on relative profit and profit maximization," *Journal of Computational and Applied Mathematics*, vol. 367, Article ID 112464, 2020.

[15] S. S. Askar and A. Al-khedhairi, "Cournot duopoly games: models and investigations," *Mathematics*, vol. 7, no. 11, p. 1079, 2019.

[16] Y. Li and L. Wang, "Chaos in a duopoly model of technological innovation with bounded rationality based on constant conjectural variation," *Chaos, Solitons & Fractals*, vol. 120, pp. 116–126, 2019.

[17] J. Ma and F. Si, "Complex dynamics of a continuous Bertrand duopoly game model with two-stage delay," *Entropy*, vol. 18, no. 7, p. 266, 2016.

[18] A. A. Elsadany, "Dynamics of a Cournot duopoly game with bounded rationality based on relative profit maximization," *Applied Mathematics and Computation*, vol. 294, pp. 253–263, 2017.

[19] S. Askar, "The rise of complex phenomena in Cournot duopoly games due to demand functions without inflection points," *Communications in Nonlinear Science and Numerical Simulation*, vol. 19, no. 6, pp. 1918–1925, 2014.

[20] S. S. Askar, "Duopolistic Stackelberg game: investigation of complex dynamics and chaos control," *Operational Research*, 2018.

[21] A. K. Naimzada and R. Raimondo, "Chaotic congestion games," *Applied Mathematics and Computation*, vol. 321, pp. 333–348, 2018.

[22] J. Ma, L. Sun, S. Hou, and X. Zhan, "Complexity study on the Cournot-Bertrand mixed duopoly game model with market share preference," *Chaos: An Interdisciplinary Journal of Nonlinear Science*, vol. 28, no. 2, Article ID 023101, 2018.

[23] Y. Peng, Q. Lu, Y. Xiao, and X. Wu, "Complex dynamics analysis for a remanufacturing duopoly model with nonlinear cost," *Physica A: Statistical Mechanics and Its Applications*, vol. 514, no. C, pp. 658–670, 2019.

[24] M. Patra, "Multiple attractor bifurcation in three-dimensional piecewise linear maps," *International journal of Bifurcation and chaos*, vol. 28, no. 10, Article ID 1830032, 2018.

[25] F. Tramontana, L. Gardini, and T. Puu, "Global bifurcations in a piecewise-smooth Cournot duopoly game," *Chaos, Solitons & Fractals*, vol. 43, no. 1-2, pp. 15–24, 2010.

[26] P. Commendatore, I. Kubin, and I. Sushko, "Dynamics of a developing economy with a remote region: agglomeration, trade integration and trade patterns," *Communications in Nonlinear Science and Numerical Simulation*, vol. 58, pp. 303–327, 2018.

[27] I. Sushko, L. Gardini, and K. Matsuyama, "Coupled chaotic fluctuations in a model of international trade and innovation: some preliminary results," *Communications in Nonlinear Science and Numerical Simulation*, vol. 58, pp. 287–302, 2018.

[28] P. Commendatore, I. Kubin, and I. Sushko, "Typical bifurcation scenario in a three region identical New Economic Geography model," *Mathematics and Computers in Simulation*, vol. 108, pp. 63–80, 2015.

[29] L. Gardini, I. Sushko, and K. Matsuyama, "2D discontinuous piecewise linear map: emergence of fashion cycles," *Chaos: An Interdisciplinary Journal of Nonlinear Science*, vol. 28, no. 5, Article ID 055917, 2018.

[30] P. Commendatore, I. Kubin, C. Petraglia, and I. Sushko, "Regional integration, international liberalisation and the dynamics of industrial agglomeration," *Journal of Economic Dynamics and Control*, vol. 48, pp. 265–287, 2014.

[31] P. Commendatore, I. Kubin, P. Mossay, and I. Sushko, "The role of centrality and market size in a four-region asymmetric new economic geography model," *Journal of Evolutionary Economics*, vol. 27, no. 5, pp. 1095–1131, 2017.

[32] D. Radi, L. Gardini, L. Gardini, and V. Avrutin, The role of constraints in a segregation model: the symmetric case," *Chaos, Solitons & Fractals*, vol. 66, pp. 103–119, 2014.

[33] D. Radi, L. Gardini and V. Avrutin, The role of constraints in a segregation model: the asymmetric case," *Discrete Dynamics in Nature and Society*, vol. 2014, Article ID 569296, 17 pages, 2014.

[34] A. Agliari, L. Gardini, and T. Puu, "Global bifurcations in duopoly when the Cournot point is destabilized via a subcritical Neimark bifurcation," *International Game Theory Review*, vol. 8, no. 1, pp. 1–20, 2006.

[35] M. Perc and A. Szolnoki, "Coevolutionary games-A mini review," *Biosystems*, vol. 99, no. 2, pp. 109–125, 2010.

[36] Z. Wang, L. Wang, A. Szolnoki, and M. Perc, "Evolutionary games on multilayer networks: a colloquium," *The European Physical Journal B*, vol. 88, no. 5, p. 124, 2015.

[37] S. M. Kamal, Y. Al-Hadeethi, F. A. Abolaban, F. M. Al-Marzouki, and M. Perc, "An evolutionary inspection game with labour unions on small-world networks," *Scientific Reports*, vol. 5, 2015.

[38] G. Yang, T. P. Benko, M. Cavaliere, J. Huang, and M. Perc, "Identification of influential invaders in evolutionary populations," *Scientific Reports*, vol. 9, p. 7305, 2019.

[39] Y. Collette and P. Siarry, *Multiobjective Optimization: Principles and Case Studies*, Springer-Verlag, Berlin Heidelberg, 2004.

Hindawi
Complexity
Volume 2021, Article ID 8875794, 13 pages
https://doi.org/10.1155/2021/8875794

Research Article

Evolutionary Game Analysis of Capital-Constrained Supplier's and Manufacturer's Financing Schemes

Suyong Zhang[1,2] **Panos. M. Pardalos,**[2] **and Xiaodan Jiang**[1]

[1]*College of Transport and Communication, Shanghai Maritime University, Shanghai, China*
[2]*Center for Applied Optimization, Department of Industrial and Systems Engineering, University of Florida, Gainesville, FL 32611, USA*

Correspondence should be addressed to Suyong Zhang; soonchueng@foxmail.com

Received 23 September 2020; Revised 8 February 2021; Accepted 23 October 2021; Published 18 December 2021

Academic Editor: M. De Aguiar

Purchase order financing (POF) and buyer direct financing (BDF) are both innovative financing schemes aiming to help financial constrained suppliers secure financing for production. In this paper, we investigate the interaction mechanism between suppliers' financing strategy selection and manufacturers' loans offering strategy adoption under two innovative financing schemes. We developed an evolutionary game model to effectively investigate the interaction mechanism between suppliers and manufacturers and analyzed the evolutionary stable strategies of the game model. Then we used system dynamics to present the performance of the evolutionary game model and took a sensitivity analysis to verify the theoretical results. The main conclusions are as follows: in the supply chain, to deal with the noncooperation among suppliers and manufacturers on innovative financing schemes, the revenue of manufacturers, the rate of manufacturer loan, and the proper financial risk factor should be relatively high.

1. Introduction

To reduce operating costs, many manufacturers in developed regions purchase source from small suppliers. But the limited working capital of small suppliers affects production decisions, and enterprises desire to obtain finance from the bank to execute their production. However, small and startup suppliers have obstruction accessing from the bank, because of their lack of credit history. According to the British Commercial Bank survey, nearly 100,000 SMEs are rejected by banks each year when financing from the bank [1]. These suppliers often rely on two ways for loans. One of the ways is the loans offered by banks and secured by suppliers' assets, such as factories [2]. The other way is turning down the orders from reputable manufacturers because these manufacturers can offer direct financing or guarantee for suppliers to obtain the bank loans [3]. Inevitably, suppliers without financing directly affect the operation of supply chain, such as fail to deliver, higher retail price, and even worse end products to consumers.

To satisfy the financing needs of the small suppliers, two innovative nonasset-based financing schemes have recently come out. The first is purchase order financing (POF) which indicates that the bank lends to suppliers based on purchase order issued by reputable manufacturers [4, 5]. Since POF loans are only granted based on purchase orders issued by reputable buyers, the main risk associated with POF is not the buyer's credit risk, but the supplier's performance risk; that is, the supplier may not be able to deliver the order quality as specified by the buyer [6]. The second scheme is buyer direct financing (BDF) which indicates that the manufacturer acts as both the buyer and the lender, and finances suppliers for production [3]. BDF has been adopted by manufacturers and suppliers in both developed and developing markets. Rolls-Royce has provided loans of more than 500 million pounds to small suppliers who cannot obtain sufficient financing through other channels.

Similarly, GSK has lent billions of pounds to its small suppliers [7]. As both purchase order financing (POF) and buyer direct financing (BDF) are still taking shape, researchers are investigating whether banks or manufacturers are in a better position to finance suppliers.

In the complex and ever-changing economic environment, it brings various risks to the supply chain. However, financial risk has become increasingly prominent and critical in today's economic world. According to the survey result shown by "McKinsey & Company" [8]; the financial uncertainty is a top factor that could influence supply chain decisions. Thus, it is meaningful for us to investigate the supply chain members financing strategies under the consideration of financial risk.

To investigate the abovementioned topic, we investigate the interaction mechanism between suppliers' financing strategy selection and manufacturers' loans offering strategy adoption under two innovative financing schemes, by using evolutionary game theory (EGT). In the proposed game theory method, the population of suppliers and manufacturers are named as players. To adopt the optimal strategy at each time, manufacturers and suppliers choose the strategy that they have the utmost expected utility. We all know EGT is used in many fields, such as strategy interaction [9], mobile health [10], players cooperation [11], and social rumor control [11]. Due to the emergence of two innovative financial schemes for manufacturers, small size and setup suppliers have subsequently gained two ways to solve their financial problems to ensure the continued stability of the capital chain. By using EGT to develop a novel model under two innovative financing schemes, manufacturers have two types of choices—BDF (buyer direct financing) and POF (purchase order financing)—and suppliers also have two strategies—BF (bank financing) and MF (manufacturer financing). In reality, rational manufacturers seek to maximize their profits. When suppliers choose BF (bank financing) strategy, they will obtain loan from the bank which offers a variety of financing options for suppliers' business to purchase inventory and materials. When suppliers choose MF (manufacturer financing) strategy, they will obtain loan from the manufacturer which offers two innovative financing schemes (BDF and POF).

Firstly, under the two innovative financing schemes, the model of evolutionary game between manufacturers and suppliers is developed. Secondly, the payoff matrix of suppliers and manufacturers under two innovative financing schemes was analyzed and the evolutionary stable strategies were obtained. By using the evolutionary game, this study is for analysis of the long-term behaviors of the two innovative financing schemes of populations of manufacturers and suppliers considering the financial risk.

The remainder of this paper is organized as follows. Section 2 introduces a review of the literature. In Section 3, an evolutionary game model under two innovative financing schemes (BDF and POF) is developed, and the evolutionary stable strategies are obtained. In Section 4, a numerical example is examined with system dynamics simulation, presenting the performance of the evolutionary game model. Section 5 summarizes the main results and describes the future research.

2. Literature Review

Our research is related to three research streams: supply chain finance scheme, the financial risk management, and the application of evolutionary game theory.

2.1. The Influence of Financing Scheme on Supply Chain Management. The supply chain finance is an important research topic in supply chain operations. Modigliani and Miller [12] pointed out that operational and financial decisions can be made separately in a perfect capital market. Pakhira et al. [13] consider the financial scheme under the retailer's budget constraint in a supplier-retailer supply chain. Johari et al. [14] coordinated the supply chain by considering the financial scheme. Kaur [15] investigates the financial scheme for a two-echelon SC considering default risk. Babich and Sobel [16] investigated how to coordinate the operational and financial decisions with the increase likelihood of a successful initial public offering (IPO). Lin and He [17] considered three financing strategies, bank financing (BF), a guaranteed contract with a buy-back clause (GBB), a guaranteed contract with a wholesale price discount clause (GWD), and investigated the influence of supplier's asset structure in financing strategies on the supply chain consist of one retailer, one capital-constraint supplier, and one bank. Buzacott and Zhang [2] incorporate financing into supply chain operation decisions and indicate financing scheme is profitable for the supply chain partners. Babich and Tang [18] studied the financing mechanism for dealing with product adulteration problems. Rui and Lai [19] studied the deferred payment and inspection mechanisms for mitigating supplier product adulteration. Tang et al. [3] examined the relative efficiency of POF and BDF under both endogenous supplier performance risk and information asymmetry. These researches are not based on different financial schemes (i.e., POF and BDF). Although Tang et al. considered both POF and BDF as we do, they did not investigate the difference between POF and BDF by using the evolutionary game theory. Our paper studies the interaction mechanism between suppliers' financing strategy selection and manufacturers' loans offering strategy adoption under two innovative financing schemes (POF and BDF).

2.2. The Financial Risk Measurement Methods. Many papers focused on the risk measurement methods. Liu and Cruz [20] studied the impact of financial risk on optimal supply chain decisions by using the net present value method (NPV). Applequist et al. [21] proposed a new method to evaluate the risk and uncertainty of chemical manufacturing supply chains. Soni and Kodali [22] developed PROMETHEE-II model to assess the global supply chain risk.

Krystofik et al. [23] developed a framework for the risk assessment of delaying the delivery of shipments to customers in the presence of incomplete information. Bandaly et al. [24] developed an integrated risk management model to test the level of supply chain risk management. Munir et al. [25] explored the association between supply chain

integration (SCI) and supply chain risk management (SCRM) based on the information processing view of risk management to improve operational performance.

Zeng and Yen [26] applied topology theory and Markov chain to measure the resilience of supply chain financial risk from the perspective of partnership. Cardoso et al. [27] proposed a mixed integer linear programming model to measure the financial risk in the design of closed-loop supply chains. The above literature shows that multicriteria risk measurement methods, such as NPV and MILP, all belong to static analysis methods. However, we all know that the supply chain's response strategy to financial risk is dynamically changing with time, which is a continuous learning process. After realizing this issue, we develop evolutionary game models to analyze the impact of financial risks on supply chain financing strategy adoption.

2.3. The Evolutionarily Game Theory to Examine the Long-Term Behaviors of Populations. Wang et al. [28] explore the long-term evolutionary behavior of sustainability. Hosseini-Motlagh et al. [29] investigate sustainable financing for a financially constrained manufacturer using a one-population evolutionary game. Wu et al. [30] established an evolutionary game model between government and enterprises in the context of low carbon and studied the impact of government incentive policies on enterprises' emission reduction strategies. Fan et al. [31] developed the evolutionary game model of government and enterprises under the conditions of government supervision and no-government supervision, respectively. Zhang et al. [32] used evolutionary game to study the interaction mechanism between manufacturer's green technology strategy selection and government regulation. To obtain more insight on dynamic supply chain financing strategy, our research investigates the interaction mechanism between suppliers' financing strategy selection and manufacturers' loans offering strategy adoption under two innovative financing schemes by using evolutionary game theory (EGT).

The contributions of this paper are reflected in the following, many scholars have employed general game theory to discuss financial decisions in supply chain management, such as signaling game and Stackelberg game. They usually focus on static problems. To obtain more insight on dynamic supply chain financing strategy, our research is based on the evolutionary game to investigate the interaction mechanism between suppliers' financing strategy selection and manufacturers' loans offering strategy adoption under two innovative financing schemes. By theoretical analysis and numerical study, this paper can offer references for the construction of financing market.

3. Evolutionary Game Model

3.1. Model Description. We assume both players of the game are bounded rationality. Two strategies for each of the players are considered in this evolutionary game model. Suppliers strategy space is defined as $S =$ (BF, MF), BF (bank financing) represents the supplier's loan from the bank which offers a variety of financing options for suppliers' business to purchase inventory and materials. MF (manufacturer financing) represents the supplier's loan from the manufacturer which offers two innovative financing schemes. Manufacturers' strategy space is defined as $M =$ (BDF, POF). BDF (buyer direct financing) indicates that the manufacturer acts as both the buyer and the lender and finances suppliers for production [3]. POF (purchase order financing) indicates that the bank lends suppliers based on purchase order issued by reputable manufacturers [4, 5]. In the long-term environment, we model four different scenarios of two populations under four strategy profiles: (1) (BDF, MF): when the manufacturer directly issued a loan to the supplier and the supplier happened to accept this financial scheme; (2) (POF, MF): when the manufacturer bank lends suppliers based on purchase order issued by reputable manufacturers and the supplier is willing to accept this financial scheme; (3) (BDF, BF): when the manufacturer directly issued a loan to the supplier, the supplier happened to refuse this financial scheme, and the supplier switches to bank loans directly. (4) (POF, BF): when the manufacturer bank lends suppliers based on purchase order issued by reputable manufacturers, the supplier happened to refuse this financial scheme, and the supplier switches to bank loans directly. The difference between this scenario and scenario (BDF, BF) is that the manufacturer's willingness to provide financial guarantees for the supplier often depends on the supplier's reliability.

x is the probability that suppliers adopt MF strategy, and then $1 - x$ represents the probability that suppliers adopt BF strategy. y is the probability that manufacturers adopt BDF strategy, and then $1 - y$ represents the probability that manufacturers adopt POF strategy. Hence, the evolutionary game model is defined as $f = \{(x, 1-x), (y, 1-y)\}$. In the long term, the financing issues of the two populations are modeled under four strategies which are played between manufacturers and suppliers. The major notations related to our research are listed in Table 1. Table 2 indicates payoffs of manufacturers and suppliers under different strategies.We have

$$\pi_{\mathrm{SM1}} = V_s - C_s - L_S(1+\gamma_m), \tag{1}$$

$$\pi_{\mathrm{SM2}} = V_s - C_s - L_S(1+\gamma_b)e^{-\alpha}, \tag{2}$$

$$\pi_{\mathrm{SB3}} = V_s - C_s - L_S(1+\gamma_b), \tag{3}$$

$$\pi_{\mathrm{SB4}} = V_s - C_s - L_S(1+\gamma_b), \tag{4}$$

$$\pi_{\mathrm{MB1}} = L_S(1+\gamma_m) - C_m, \tag{5}$$

$$\pi_{\mathrm{MP2}} = R_m - C_m - L_S(1+\gamma_b)(1-e^{-\alpha}), \tag{6}$$

$$\pi_{\mathrm{MB3}} = L_S - C_m, \tag{7}$$

$$\pi_{\mathrm{MP4}} = R_m - C_m. \tag{8}$$

Table 1: Major notations.

Notations	Explanation
π_{SMi}	The profits of the supplier who takes MF strategy
π_{SBi}	The profits of the supplier who takes BF strategy
π_{MBi}	The profits of the manufacturer with BDF strategy
π_{MPi}	The profits of the manufacturer with POF strategy
V_s	The revenue of supplier
γ_m	Interest rate of manufacturer loans. $\gamma_m \in [0,1]$
γ_b	Interest rate of bank loans $\gamma_b \in [0,1]$
L_S	The suppliers' loans
C_m	The production costs of the manufacturer
C_s	The production costs of the supplier
R_m	The revenue of the manufacturer
α	Financial risk factor. $\alpha > 0$

Table 2: Payoff matrix.

		Manufacturers	
		BDF	POF
Suppliers	MF	π_{SM1} π_{MB1}	π_{SM2} π_{MP2}
	BF	π_{SB3} π_{MB3}	π_{SB4} π_{MP4}

The proportion of suppliers who choose strategy MF over time is noted by y, which is $0 \le y \le 1$; moreover, the proportion of manufacturers who select strategy BDF is indicated by x, which is $0 \le x \le 1$. Let U_{MF} be the expected utility of the supplier who takes MF strategy, U_{BF} the expected utility of the supplier who takes BF strategy, and E_{BDF} and E_{POF} the expected utility of the manufacturer who takes divergent strategies (BDF or POF, respectively). According to Table 2 and equations (1)–(8), we can obtain the mixed strategy utilities of suppliers and manufacturers as follows:

$$U_{MF} = y\left(V_s - C_s - L_S\left(1+\gamma_m\right)\right) + (1-y)\left(V_s - C_s - L_S\left(1+\gamma_b\right)e^{-\alpha}\right), \tag{9}$$

$$U_{BF} = y\left(V_s - C_s - L_S\left(1+\gamma_b\right)\right) + (1-y)\left(V_s - C_s - L_S\left(1+\gamma_b\right)\right), \tag{10}$$

$$E_{BDF} = x\left(L_S\left(1+\gamma_m\right) - C_m\right) + (1-x)\left(L_S - C_m\right), \tag{11}$$

$$E_{POF} = x\left(R_m - C_m - L_S\left(1+\gamma_b\right)\left(1-e^{-\alpha}\right)\right) + (1-x)\left(R_m - C_m\right). \tag{12}$$

Therefore, the mean utility of suppliers and manufacturers is obtained. Let $\overline{U}$ and $\overline{E}$ represent suppliers' mean utility and manufacturers' mean utility, respectively, and $\overline{U}$ and $\overline{E}$ are, respectively, presented as the following:

$$\overline{U} = xU_{MF} + (1-x)U_{BF}, \tag{13}$$

$$\overline{E} = yE_{BDF} + (1-y)E_{POF}. \tag{14}$$

According to Zhang et al. [32], the replicator dynamic equations of financing strategy MF adopted by suppliers $F(x)$ and strategy BDF selected by manufacturers $F(y)$ are determined as

$$F(x) = \frac{dx}{dt} = x\left(U_{MF} - \overline{U}\right), \tag{15}$$

$$F(y) = \frac{dy}{dt} = y\left(E_{GT} - \overline{E}\right). \tag{16}$$

By substituting (9), (11), (13), and (14) into (15) and (16), the replicator dynamic equations can be obtained as

$$F(x) = e^{-\alpha}(-1+x)xL_s\left(\left(-1+e^{\alpha}\right)(-1+y) - \left(-1+e^{\alpha}+y\right)\gamma_b + e^{\alpha}y\gamma_m\right). \tag{17}$$

$$F(y) = -e^{-\alpha}(-1+y)y\left(-e^{\alpha}R_m + L_s\left(e^{\alpha} - x + e^{\alpha}x + \left(-1+e^{\alpha}\right)x\gamma_b + e^{\alpha}x\gamma_m\right)\right). \tag{18}$$

Let $F(x) = 0$ and $F(y) = 0$; a solution that does not change over time will be equilibrium.

Proposition 1. *For the above model,*

(a) $(0,0)$, $(0,1)$, $(1,0)$, $(1,1)$ *are the fixed equilibrium points.*

(b) If $0 < (e^{\alpha}(R_m - L_s))/(L_s(-1+e^{\alpha} - \gamma_b + e^{\alpha}\gamma_b + e^{\alpha}\gamma_m)) < 1$, $0 < ((-1+e^{\alpha})(1+\gamma_b))/(-1+e^{\alpha} - \gamma_b + e^{\alpha}\gamma_m) < 1$, (x^*, y^*) *is the equilibrium point and* (x^*, y^*)*are shown as follows:*

$$(x^*, y^*) = \left(\frac{e^{\alpha}(R_m - L_s)}{L_s\left(-1+e^{\alpha} - \gamma_b + e^{\alpha}\gamma_b + e^{\alpha}\gamma_m\right)}, \frac{\left(-1+e^{\alpha}\right)(1+\gamma_b)}{-1+e^{\alpha} - \gamma_b + e^{\alpha}\gamma_m}\right). \tag{19}$$

Proof. Proposition 1 (a) can easily be obtained. Referring to, the equilibrium points must satisfy $F(x) = 0$, $F(y) = 0$. As $0 < x < 1$, $0 < y < 1$, (x^*, y^*) can be obtained.

Proposition 1 shows the equilibrium points from the evolutionary game model, whether these points are the ESS that should be discussed next.

Proposition 2. *For the above equilibrium points, the stability analysis of evolutionary game is as follows:*

(i) The fixed equilibrium points are all unstable, except the point $(0,1)$*; the evolutionary game cannot achieve stability at these four fixed points*

(ii) The center point (x^*, y^*) *is the saddle point*

Proof. According to Lyapunov stability analysis, the Jacobian matrix J (Hofbauer and Sigmund, 1998) is

$$J = \begin{bmatrix} \dfrac{\partial F(x)}{\partial x} & \dfrac{\partial F(x)}{\partial y} \\ \dfrac{\partial F(y)}{\partial x} & \dfrac{\partial F(y)}{\partial y} \end{bmatrix} = \begin{bmatrix} \alpha_{11} & \alpha_{12} \\ \alpha_{21} & \alpha_{22} \end{bmatrix}, \tag{20}$$

where

$$\begin{aligned} \alpha_{11} &= e^{-\alpha}(-1+2x)L_s\left(\left(-1+e^{\alpha}\right)(-1+y) - \left(-1+e^{\alpha}+y\right)\gamma_b + e^{\alpha}y\gamma_m\right), \\ \alpha_{12} &= e^{-\alpha}(-1+x)xL_s\left(-1+e^{\alpha} - \gamma_b + e^{\alpha}\gamma_m\right), \\ \alpha_{21} &= -e^{-\alpha}(-1+y)yL_s\left(-1+e^{\alpha} + \left(-1+e^{\alpha}\right)\gamma_b + e^{\alpha}\gamma_m\right), \\ \alpha_{22} &= -e^{-\alpha}(-1+2y)\left(-e^{\alpha}R_m + L_s\left(e^{\alpha} - x + e^{\alpha}x + \left(-1+e^{\alpha}\right)x\gamma_b + e^{\alpha}x\gamma_m\right)\right). \end{aligned} \tag{21}$$

The det J and tr J of five strategies are shown in Table 3, where $\det J = \alpha_{11}\alpha_{22} - \alpha_{12}\alpha_{21}$ and $\mathrm{tr}J = \alpha_{11} + \alpha_{22}$.

As shown in Table 3, it is uncertain whether det J and tr J of $(0,1)$, $(1,0)$, $(1,1)$ strategies are bigger or smaller than zero. The asymptotical stable strategy pair must satisfy $\det J \geq 0$ and $\mathrm{tr}\, J < 0$ and should be disturbance rejection, which meets the condition $\partial F(x)/\partial x < 0$, $\partial F(y)/\partial y < 0$. By calculating, $(0,1)$ is the ESS for this game model. Proposition 2 (i) is proven.

The central point (x^*, y^*) adapts to the basic conditions of evolutionary stable strategy. (x^*, y^*) is the Lyapunov stability. Then we should investigate the stability nature of point (x^*, y^*). If it is the asymptotically stability, (x^*, y^*) is the evolutionary stable strategy.

Considering the center point, the Jacobian Matrix J' is

$$J' = \begin{bmatrix} b_{11} & b_{12} \\ b_{21} & b_{22} \end{bmatrix}, \tag{22}$$

where

$$\begin{aligned} b_{11} &= \frac{\left(L_s - R_m\right)\left(-1+e^{\alpha} - \gamma_b + e^{\alpha}\gamma_m\right)\left(-e^{\alpha}R_m + L_s\left(-1+2e^{\alpha} + \left(-1+e^{\alpha}\right)\gamma_b + e^{\alpha}\gamma_m\right)\right)}{L_s\left(-1+e^{\alpha} + \left(-1+e^{\alpha}\right)\gamma_b + e^{\alpha}\gamma_m\right)^2}, \\ b_{12} &= b_{21} = 0, \\ b_{22} &= -\frac{\left(-1+e^{\alpha}\right)L_s(1+\gamma_b)\left(\gamma_b - \gamma_m\right)\left(-1+e^{\alpha} + \left(-1+e^{\alpha}\right)\gamma_b + e^{\alpha}\gamma_m\right)}{\left(-1+e^{\alpha} - \gamma_b + e^{\alpha}\gamma_m\right)^2}. \end{aligned} \tag{23}$$

Table 3: The det J and tr J of five strategies.

Strategy	det J	tr J
$(0, 0)$	$e^{-\alpha}L_s((1-e^{\alpha})(1+\gamma_b))(R_m - L_s)$	$-e^{-\alpha}L_s((1-e^{\alpha})(1+\gamma_b)) + (L_s - R_m)$
$(0, 1)$	0	$L_s(\gamma_b - \gamma_m) + (L_s - R_m)$
$(1, 0)$	$e^{-\alpha}L_s((1-e^{\alpha})(1+\gamma_b))(-R_m + L_s(2 - e^{-\alpha} + (-e^{-\alpha}+1)\gamma_b + \gamma_m))$	$e^{-\alpha}L_s((1-e^{\alpha})(1+\gamma_b)) + (-R_m + L_s(2 - e^{-\alpha} + (-e^{-\alpha}+1)\gamma_b + \gamma_m))$
$(1, 1)$	$L_s(\gamma_m - \gamma_b)(R_m + L_s(2 - e^{-\alpha} + (-e^{-\alpha}+1)\gamma_b + \gamma_m))$	$L_s(\gamma_m - \gamma_b) + (R_m + L_s(2 - e^{-\alpha} + (-e^{-\alpha}+1)\gamma_b + \gamma_m))$
(x^*, y^*)	+	0

The characteristic equation of Jacobian Matrix J' is $\dot{J}' = \lambda E - J'$, let$|J'| = 0$, the characteristic roots $\lambda_{1,2}$ can be deduced as

$$\lambda_{1,2} = \pm \frac{i\sqrt{A * B}}{\sqrt{L_s}(-1 + e^{\alpha} + (-1 + e^{\alpha})\gamma_b + e^{\alpha}\gamma_m)(-1 + e^{\alpha} - \gamma_b + e^{\alpha}\gamma_m)}, \tag{24}$$

where

$$\begin{aligned} A &= (L_s - R_m)(-1 + e^{\alpha} - \gamma_b + e^{\alpha}\gamma_m)(-e^{\alpha}R_m \\ &\quad + L_s(-1 + 2e^{\alpha} + (-1 + e^{\alpha})\gamma_b + e^{\alpha}\gamma_m)) \\ B &= (-1 + e^{\alpha})L_s(1 + \gamma_b)(\gamma_b - \gamma_m)(-1 + e^{\alpha} \\ &\quad + (-1 + e^{\alpha})\gamma_b + e^{\alpha}\gamma_m) \end{aligned} \tag{25}$$

Matrix J' causes virtual characteristic roots, so the point (x^*, y^*) is not asymptotically stable. And it is not the evolutionary stable strategy. Proposition 2 (ii) is proven.

As Proposition 2 shown, $(0, 1)$ is the only ESS in this dynamic system, so every subtle change may not have an impact on the behaviors of suppliers and manufacturers.

The phase diagram of the evolution path is shown in Figure 1. Point $O(0, 1)$ stands for the stable strategy among manufacturers and suppliers. And it proves suppliers are willing to adopt the BF strategy while manufacturers would like to take BDF strategy. So the dynamic system will evolve to the equilibrium point $O(0, 1)$.

We define the area of $OA_4A_2A_3$ as $S_{OA_4A_2A_3}$, and $S_{OA_4A_2A_3}$ depicts the evolutionary proportion of (BF, BDF) strategy. From the coordinates of A_4, we can easily obtain

$$S_{OA_4A_2A_3} = \frac{1}{2}\left(\frac{e^{\alpha}(R_m - L_s)}{L_s(-1 + e^{\alpha} - \gamma_b + e^{\alpha}\gamma_b + e^{\alpha}\gamma_m)} + 1 - \frac{(-1 + e^{\alpha})(1 + \gamma_b)}{-1 + e^{\alpha} - \gamma_b + e^{\alpha}\gamma_m}\right). \tag{26}$$

Corollary 1. *The number of manufacturers and suppliers who adopt strategy pair (BF, BDF) increases with increasing of α.*

Proof. The first-order partial derivation of $S_{OA_4A_2A_3}$ with respect to financial risk factor α is determined by the following:

$$\frac{\partial S_{OA_4A_2A_3}}{\partial \alpha} = \frac{e^{\alpha} Log[e](L_s - R_m)(1 + \gamma_b)}{L_s(1 + \gamma_b - e^{\alpha}(1 + \gamma_b + \gamma_m))^2} < 0. \tag{27}$$

Thus, $S_{OA_4A_2A_3}$ is decreasing with the increase of financial risk factor. That means the point A_4 evolves into point A_3 and the probability that the replicator dynamic system will converge to strategy pair (BF, BDF).

Corollary 2. *It implies the impacts of financial risk factor on the probability that game players adopt strategy pair (BF, BDF). As the financial risks grow, suppliers tend to choose BF strategy and manufacturers are willing to adopt BDF strategy. The game players choose this strategy pair to maintain stability in the financial risks. When the financial risk is relatively high, the small supplier access to manufacturer financing will be hazardous. Manufacturers choose the buyer direct financing scheme to suppliers who were unable to give suppliers a guarantee. Apparently, strategy pair (BF, BDF) can ensure the profits of manufacturers and suppliers to a large extent.*

Corollary 3. *The number of manufacturers and suppliers who adopt strategy pair (BF, BDF) increases with increasing of γ_b.*

Proof. The first-order partial derivation of $S_{OA_4A_2A_3}$ with respect to interest rate of bank loans γ_b is determined by the following:

$$\frac{\partial S_{OA_4A_2A_3}}{\partial \gamma_b} = \frac{e^{\alpha}(-1 + e^{\alpha})(L_s - R_m)}{L_s(1 + \gamma_b - e^{\alpha}(1 + \gamma_b + \gamma_m))^2} < 0. \tag{28}$$

Therefore, $S_{OA_4A_2A_3}$ is decreasing with the increase of bank loans rate. That means the point A_4 evolves into point A_3; the probability that the replicator dynamic system will evolve to strategy pair (BF, BDF) increases with the increase of γ_b.

Corollary 2 shows the impacts of interest rate of the bank loans on the probability that game players adopt strategy pair (BF, BDF). However, the game players adopt strategy pair (BF, BDF) to maintain stability in the high-level interest rate of the bank loans. As we all know that strategy pair (BF, BDF) can ensure the profits of game players to a large extent. Thus it is beneficial to the profit of manufacturers and suppliers when the interest rate of the bank loans is relatively high.

Corollary 4. *The number of manufacturers and suppliers who adopt strategy pair (BF, BDF) increases with increasing of γ_m.*

Proof. The first-order partial derivation of $S_{OA_4A_2A_3}$ with respect to interest rate of the manufacturer loans γ_m is determined by the following:

$$\frac{\partial S_{OA_4A_2A_3}}{\partial \gamma_m} = \frac{e^{2\alpha}(L_s - R_m)}{L_s(1 + \gamma_b - e^{\alpha}(1 + \gamma_b + \gamma_m))^2} < 0. \tag{29}$$

Therefore, $S_{OA_4A_2A_3}$ is decreasing with the increase of interest rate of the manufacturer loans. That means the point A_4 evolves into point A_3; the probability that the replicator dynamic system will evolve to strategy pair (BF, BDF) increases with the increase of γ_m.

Corollary 3 indicates the impacts of interest rate of the manufacturer loans on the probability that game players adopt strategy pair (BF, BDF). As the interest rate of the manufacturer loans increases, the probability that the

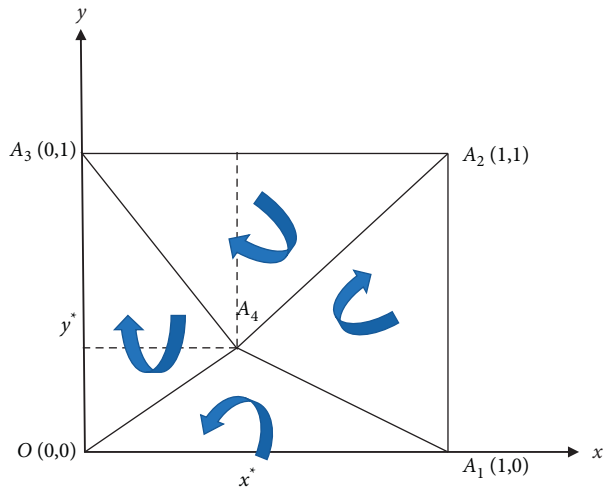

FIGURE 1: Manufacturers' evolutionary stable strategy and suppliers' evolutionary stable strategy evolve to (0, 1).

replicator dynamic system will evolve to strategy pair (BF, BDF) increases. The game players adopt this strategy pair to maintain stability in the high-level interest rate of the bank loans. Clearly, strategy pair (BF, BDF) always can ensure the profits of game players to a large extent. Therefore, $S_{OA_4A_2A_3}$ is decreasing with the increase of interest rate of the manufacturer loans, which means $S_{OA_4A_2A_1}$ increases with the increase of interest rate of the manufacturer loans and point A_4 gets far away from point A_3. Thus, it is not beneficial for the system evolving to (MF, POF) when the interest rate of the manufacturer loans is relatively high.

Corollary 5. *The number of manufacturers and suppliers who adopt strategy pair (BF, BDF) increases with increasing of L_s.*

Proof. The first-order partial derivation of $S_{OA_4A_2A_3}$ with respect to the suppliers' loans L_s is determined by the following:

$$\frac{\partial S_{OA_4A_2A_3}}{\partial L_s} = -\frac{e^{\alpha} R_m}{L_s^2\left(-1-\gamma_b+e^{\alpha}\left(1+\gamma_b+\gamma_m\right)\right)} < 0. \quad (30)$$

Therefore, $S_{OA_4A_2A_3}$ is decreasing with the increase of the supplier loans. That means the point A_4 evolves into point A_3; the probability that the replicator dynamic system will evolve to strategy pair (BF, BDF) increases with the suppliers' loans L_s.

Corollary 4 shows the impacts of the suppliers' loans on the probability that game players adopt strategy pair (BF, BDF). As the supplier loans increase, suppliers tend to choose BF strategy and manufacturers are not willing to adopt POF strategy. The game players adopt (BF, BDF) strategy pair to maintain stability when the suppliers' loans are relatively high. $S_{OA_4A_2A_3}$ decrease as the L_s increases; it means manufacturers and suppliers are not willing to adopt strategy pair (MF, POF). Clearly, strategy pair (BF, BDF) can ensure the profits of game players to a large extent; thus it is harmful for the system evolve to (MF, POF) when the suppliers' loans are relatively high.

Corollary 6. *The number of manufacturers and suppliers who adopt strategy pair (MF, POF) increases with increasing of R_m.*

Proof. The first-order partial derivation of $S_{OA_4A_2A_3}$ with respect to the revenue of the manufacturer R_m is determined by the following:

$$\frac{\partial S_{OA_4A_2A_3}}{\partial L_s} = \frac{1}{L_s\left(1+\gamma_b-e^{-\alpha}\left(1+\gamma_b\right)+\gamma_m\right)} > 0. \quad (31)$$

Therefore, $S_{OA_4A_2A_3}$ is increasing with the increase of the revenue of the manufacturer. That means the point A_4 evolves into point A_1; the probability that the replicator dynamic system will evolve to strategy pair (MF, POF) increases with the revenue of the manufacturer R_m.

Corollary 5 shows the impacts of R_m on the probability that game players adopt strategy pair (MF, POF). As the manufacturers' revenue increases, suppliers tend to choose MF strategy and manufacturers are not willing to adopt BDF strategy. The game players adopt (MF, POF) strategy pair to maintain stability when R_m is relatively high. Thus, it is harmful for the system to evolve to (MF, POF) when the revenue of the manufacturer is relatively low.

4. Numerical Study

We use Vensim PLE to test the performance of evolutionary game model. The system dynamics model (SD model) is developed before we use Vensim PLE to show the dynamics behavior among suppliers and manufacturers. A series of numerical studies are implemented by a financial chain with groups of suppliers and manufacturers. The two sections are considered: Section 1 discussed how game players respond to different initial values; Section 2 assessed the influencing factors of strategy pair (MF, POF).

4.1. SD Model. The system dynamics model of the evolutionary game among suppliers and manufacturers is shown in Figure 2.

The system dynamics model consists of two flow rates, eight intermediate variables, four flows, and eight external variables. Two flow rates try to depict the change in the probability of suppliers (manufacturers) adopting MF (BDF) strategy. The four flows are used to indicate the probability of suppliers (manufacturers) choosing MF (BDF) strategy or BF (POF) strategy. Eight external variables correspond to eight variables in the game payoff matrix.

4.2. The Evolution Tendency of Game Players. To simulate the evolutionary game model, three sets of numerical experiments are carried out. Numerical studies are obtained by solving the replicator dynamics equation by using SD method. This section is for observation of evolution tendency among the different initial values. To make this purpose, we set up a

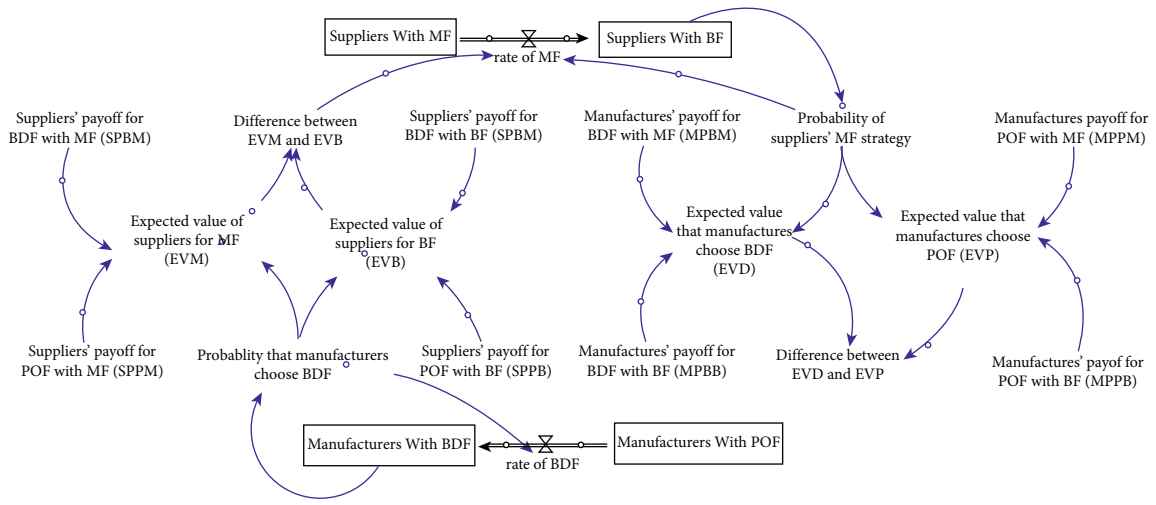

Figure 2: System dynamics model of suppliers and manufacturers behavior.

SD model with three scenarios; the initial values are determined in Table 4. If we change the initial value, we can get two ESS (0, 1) and (1, 0), but the dynamic system will never evolve to the points (0, 0) and (1, 1).

Figure 3 shows the probability of game players adopting (BF, BDF) strategy, where the blue lines represent the probability of suppliers adopting MF strategy and the red lines show the manufacturers' strategy tendency. The numerical experiments are depicted in the scenario (i)–(iii). After 100 simulations, the evolutionary game can catch the ESS in scenarios (i) and (iii). In scenario (i), the dynamic system converges to the strategy pair (BF, BDF) when the revenue of the manufacturer $R_m = 2.1$. In scenario (ii), the dynamic system cannot converge to the strategy pair (MF, BDF) and (BF, POF) when the revenue of the manufacturer $R_m = 1.4$. In scenario (iii), the dynamic system converges to the strategy pair (MF, POF) when the revenue of the manufacturer $R_m = 3$, and the cost of manufacturer $C_m = 0.15$ is relatively high. The manufacturers want to choose POF strategy and the suppliers are willing to adopt MF strategy when the manufacturers' revenue and cost are relatively high.

Figure 3 indicates that the evolution results are related to the manufacturers' revenue. As shown in Figure 3(a), if the manufacturer sells low premium items, the dynamic system cannot reach stability in the evolution of financial strategies. This is because the manufacturer who without competitiveness cannot provide a convincing guarantee for the supplier is even more unable to fund suppliers directly. Therefore, suppliers should establish supply chain relationships with manufacturers with high brand influence, to obtain a more stable capital chain and gradually strengthen the cooperative relationship among supply chain members. When the two parties establish a mutually beneficial cooperative relationship, the company can help suppliers find ways to reduce costs, thereby reducing prices. Furthermore, when the two parties have established a good cooperative relationship, many tasks can be simplified, such as ordering, statistics, and quality inspection, thereby reducing cost.

Table 4: The external variable values in simulation.

Group	i	ii	iii
V_s	2	2	2
γ_m	0.05	0.05	0.05
γ_b	0.04	0.04	0.04
L_S	1.5	1.5	1.5
C_m	0.1	0.05	0.15
C_s	0.2	0.2	0.2
R_m	2.1	1.4	3
α	1	1	1

As shown in Figure 3(b), if the manufacturer produces proper premium items, the dynamic system converges to the strategy pair (BF, BDF). The manufacturer has insufficient cash flows and is unwilling to provide financing guarantees for suppliers funding from the bank, suppliers are more willing to choose bank financing strategy to ensure that their capital chain does not break. Manufacturers with proper premium products are more willing to provide partners with BDF financial strategies, directly provide sources of funds to suppliers, further cooperate with suppliers, increase product innovation and transformation, and gradually expand market share.

As shown in Figure 3(c), if the manufacturer sells high-premium products, the dynamic system converges to the strategy pair (MF, POF). The manufacturer has sufficient cash flows and is willing to provide financing guarantees for suppliers funding from the bank, and suppliers are more willing to choose manufacturer financing strategy to ensure that their capital chain does not break. Small size and startup suppliers often have difficulty accessing financing from the bank because of their lack of credit history. Thus, when high-premium product manufacturers cooperate with suppliers, suppliers prefer to choose manufacturer financing strategy, and it is more profitable for manufacturers to provide financial guarantees for suppliers instead of directly lending suppliers.

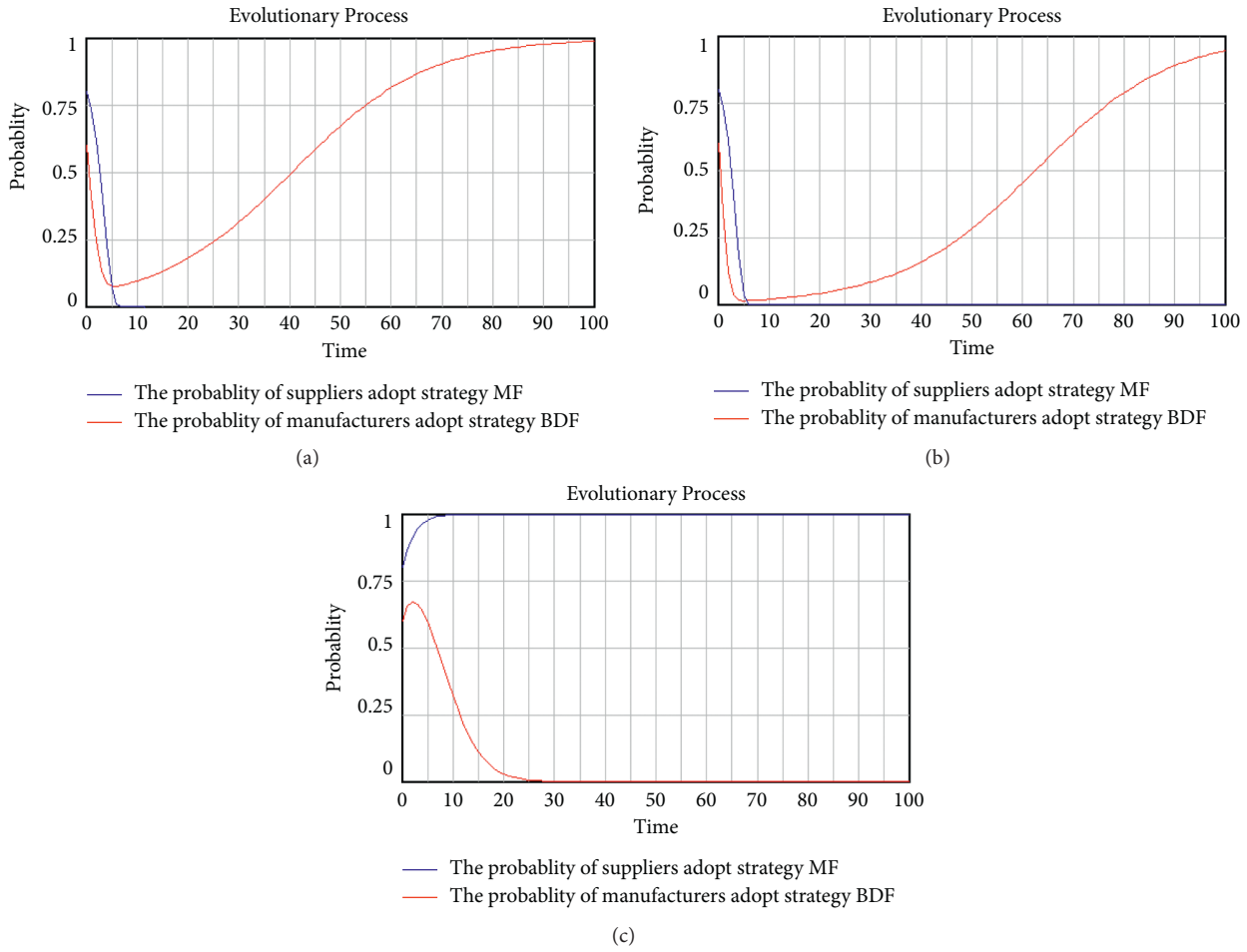

Figure 3: The evolutionary process.

4.3. The Influencing Factors of Strategy Pair (BF, BDF). In this section, a sensitivity analysis is performed to better understand the above theoretical results. The sensitivity analysis based on $S_{OA_4A_2A_3}$ is decided by various parameters.

Figure 4 shows the number of manufacturers and suppliers who adopt strategy pair (BF, BDF) increases with increasing of financial risk factor α. Given a fixed value of financial risk factor, the high value of manufacturers' revenue brings about the high proportion of selecting strategy pair (MF, POF). However, with increasing of financial risk factor, the changes in the proportion of selecting strategy pair (BF, BDF) tend to be flat. Thus, when $\alpha < 3$, reducing the financial risk factor can promote the dynamic system evolving to the strategy pair (MF, POF).

Figure 5 illustrates the impacts of the bank loan rate γ_b and financial risk factor α on the evolutionary proportion of selecting strategy pair (BF, BDF). The sensitivity analysis results certificate Corollary 2. It reveals the probability that the replicator dynamic system will evolve to strategy pair (BF, BDF) increases with the increase of γ_b. Given a fixed value of the bank loan rate, the high value of financial risk factor brings about the high proportion of selecting strategy pair (BF, BDF).

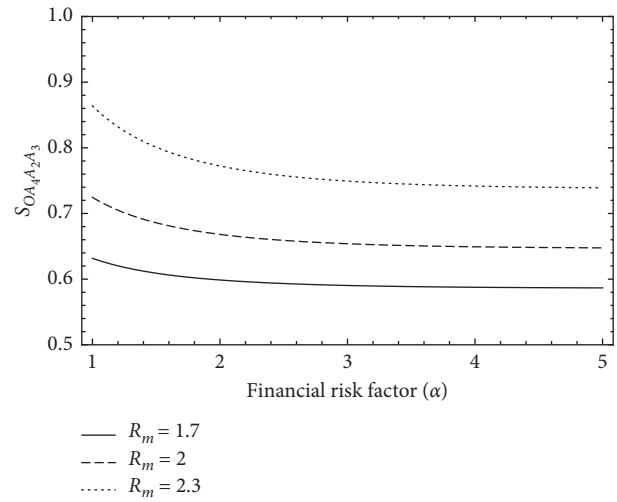

Figure 4: The impacts of financial risk factor on $S_{OA_4A_2A_3}$ with various manufacturers' revenue.

Figure 6 depicts the impacts of the manufacturer loan rate γ_m and financial risk factor α on the evolutionary proportion of selecting strategy pair (BF, BDF). It reveals

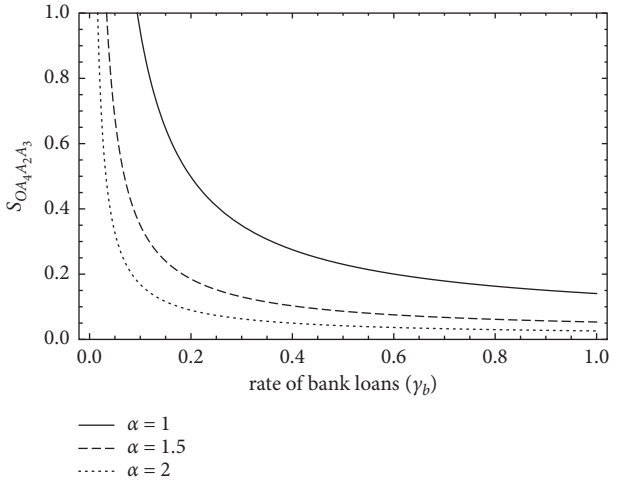

Figure 5: The impacts of the bank loan rate on $S_{OA_4A_2A_3}$ with various financial risk factors.

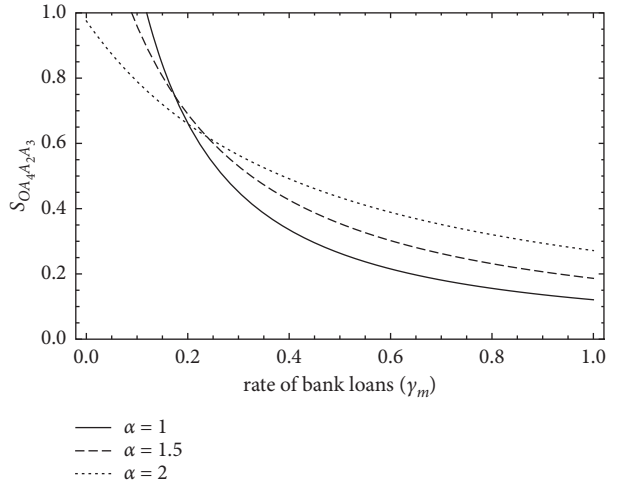

Figure 6: The impacts of the manufacturer loan rate on $S_{OA_4A_2A_3}$ with various financial risk factors.

the probability that the replicator dynamic system will evolve to strategy pair (BF, BDF) increases with the increase of γ_m. When $\gamma_m > 0.2$, given a fixed value of the manufacturer loan rate, the high value of financial risk factor brings about the high proportion of selecting strategy pair (BF, BDF). When $\gamma_m > 0.2$, given a fixed value of the manufacturer loan rate, the high value of financial risk factor brings about the high proportion of selecting strategy pair (MF, POF).

Figure 7 reveals the impacts of the suppliers' loans L_s and manufacturers' revenue R_m on the evolutionary proportion of selecting strategy pair (BF, BDF). The sensitivity analysis results certificate Corollary 4. The $S_{OA_4A_2A_3}$ decrease as the L_s increases, it means manufacturers and suppliers are not willing to adopt strategy pair (MF, POF) when L_s is relatively high. In addition, the suppliers' loan L_s increases as manufacturers' revenue R_m.

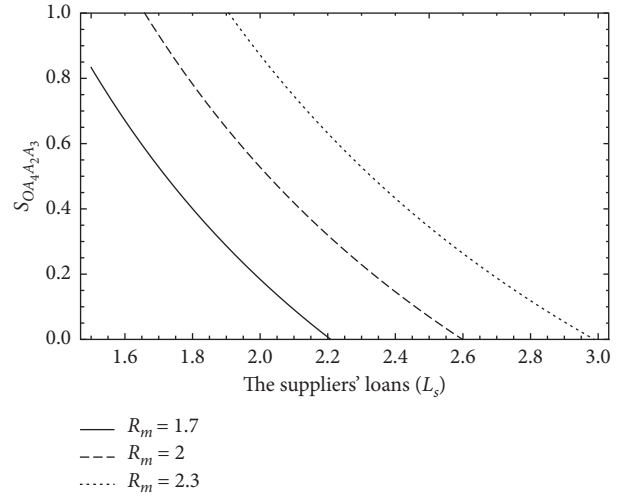

Figure 7: The impacts of the suppliers' loans on $S_{OA_4A_2A_3}$ with various manufacturers' revenue.

5. Conclusions

POF and BDF are both innovative financing schemes aiming to help financial constrained suppliers secure financing for production. In this paper, we investigate the interaction mechanism between suppliers' financing strategy selection and manufacturers' loans offering strategy adoption under two innovative financing schemes. Firstly, we proposed an evolutionary game model to effectively investigate the interaction mechanism between suppliers and manufacturers. Secondly, the payoff matrix of suppliers and manufacturers under two innovative financing schemes was analyzed and the evolutionary stable strategies were obtained. Finally, we use system dynamics to present the performance of the evolutionary game model and took a sensitivity analysis to verify the theoretical results.

We can draw the following conclusions: Firstly, the evolutionary model can reach the stability strategy pair (BF, BDF); if we change the initial value, we can get another stability strategy pair (MF, POF) when manufacturers' revenue and cost are relatively high. Secondly, when high-premium product manufacturers cooperate with suppliers, suppliers prefer to choose manufacturer financing strategy, and it is more profitable for manufacturers to provide financial guarantees for suppliers instead of directly lending suppliers. Thirdly, for manufacturers to participate in the game, the initial conditions need to be changed to make sure the evolutionary game evolves to the strategy pair (MF, POF). When the rate of manufacturer loan is relatively high, the high value of financial risk factor brings about the high proportion of selecting strategy pair (MF, POF). And the financial risk factor becomes larger in a moderate range, which can accelerate the evolution of the system to (MF, POF) much faster.

As the first attempt at understanding the interaction mechanism between suppliers' financing strategy selection and manufacturers' loans offering strategy adoption under BDF and POF financing schemes, our research is not

without limitations though; we take the evolutionary game model to encourage manufacturers and suppliers to reach financial cooperation and obtain the approaches to promote the dynamic system evolving to the strategy pair (MF, POF). Nevertheless, we assume that the information between players is symmetry. We should consider information between players is asymmetry in the future research. We only focus on the static rate of loans in our model; it is interesting to explore how the dynamic rate of loans affects the evolutionary system. Furthermore, how to implement the dynamic rate of loans should be further discussed.

Data Availability

The data used to support the findings of this study are included within the article.

Conflicts of Interest

The authors declare that they have no conflicts of interest.

Acknowledgments

This research was supported by MOE (Ministry of Education in China) Project of Humanities and Social Sciences (project no. 21YJCZH223) and also sponsored by Shanghai Sailing Program (no. 21YF1416500).

References

[1] G. Liu, W. Zhao, and X. Zhao, "A new firm entry under capital constraint," 2018, https://ssrn.com/abstract=3324336.

[2] J. A. Buzacott and R. Q. Zhang, "Inventory management with asset-based financing," *Management Science*, vol. 50, no. 9, pp. 1274–1292, 2004.

[3] C. S. Tang, S. A. Yang, and J. Wu, "Sourcing from suppliers with financial constraints and performance risk," *Manufacturing & Service Operations Management*, vol. 20, no. 1, pp. 70–84, 2018.

[4] A. Martin, *The Places They Go when Banks Say No*, New York Times, New York, NY, USA, 2010, http://www.nytimes.com/2010/01/31/business/smallbusiness/31order.html?dbk.

[5] C. Tice, *Can a Purchase Order Loan Keep Your Business Growing? Entrepreneur*, http://www.entrepreneur.com/article/207058, 2010.

[6] Gustin D. (2014) Purchase Order Finance, the Tough Nut to Crack. Trade Financing Matters (April 28), http://spendmatters.com/tfmatters/purchase%20order-finance-the-tough-nut-to-crack/.

[7] S. Watkins, *Top UK Firms Lend Billions to Struggling Suppliers as They Are Forced to Act as Banks*, Daily Mail, London, UK, 2012, http://www.dailymail.co.uk/money/news/article-2220517/Top-UK-firms-lend%20billions-suppliers-forced-act-banks.html.

[8] McKinsey & Company, *Managing Global Supply Chains: McKinsey Global Survey Results*, McKinsey Quarterly, Shanghai, China, 2008.

[9] L. Liu, J. J. Lv, J. Y. Li, and Y. Z. Wang, "Evolutionary game model of information interaction in social network," *Journal of Information and Computational Science*, vol. 12, no. 6, pp. 2375–2388, 2015.

[10] Y. Chen, S. Ding, H. Zheng, Y. Zhang, and S. Yang, "Exploring diffusion strategies for mHealth promotion using evolutionary game model," *Applied Mathematics and Computation*, vol. 336, pp. 148–161, 2018.

[11] M. Perc, J. J. Jordan, D. G. Rand, Z. Wang, S. Boccaletti, and A. Szolnoki, "Statistical physics of human cooperation," *Physics Reports*, vol. 687, pp. 1–51, 2017.

[12] F. Modigliani and M. H. Miller, "The cost of capital, corporation finance and the theory of investment," *The American Economic Review*, vol. 48, no. 3, pp. 261–297, 1958.

[13] N. Pakhira, M. K. Maiti, and M. Maiti, "Uncertain multi-item supply chain with two level trade credit under promotional cost sharing," *Computers & Industrial Engineering*, vol. 118, pp. 451–463, 2018.

[14] M. Johari, S.-M. Hosseini-Motlagh, M. Nematollahi, M. Goh, and J. Ignatius, "Bi-level credit period coordination for periodic review inventory system with price-credit dependent demand under time value of money," *Transportation Research Part E: Logistics and Transportation Review*, vol. 114, pp. 270–291, 2018.

[15] A. Kaur, "Two-level trade credit with default risk in the supply chain under stochastic demand," *Omega*, vol. 88, pp. 4–23, 2019.

[16] V. Babich and M. J. Sobel, "Pre-IPO operational and financial decisions," *Management Science*, vol. 50, no. 7, pp. 935–948, 2004.

[17] Q. Lin and J. He, "Supply chain contract design considering the supplier's asset structure and capital constraints," *Computers & Industrial Engineering*, vol. 137, Article ID 106044, 2019.

[18] V. Babich and C. S. Tang, "Managing opportunistic supplier product adulteration: deferred payments, inspection, and combined mechanisms," *Manufacturing & Service Operations Management*, vol. 14, no. 2, pp. 301–314, 2012.

[19] H. Rui and G. Lai, "Sourcing with deferred payment and inspection under supplier product adulteration risk," *Production and Operations Management*, vol. 24, no. 6, pp. 934–946, 2015.

[20] Z. Liu and J. M. Cruz, "Supply chain networks with corporate financial risks and trade credits under economic uncertainty," *International Journal of Production Economics*, vol. 137, no. 1, pp. 55–67, 2012.

[21] G. E. Applequist, J. F. Pekny, and G. V. Reklaitis, "Risk and uncertainty in managing chemical manufacturing supply chains," *Computers & Chemical Engineering*, vol. 24, no. 9-10, pp. 2211–2222, 2000.

[22] G. Soni and R. Kodali, "A decision framework for assessment of risk associated with global supply chain," *Journal of Modelling in Management*, vol. 8, no. 1, pp. 25–53, 2013.

[23] M. Krystofik, C. J. Valant, J. Archbold, P. Bruessow, and N. G. Nenadic, "Risk assessment framework for outbound supply-chain management," *Information*, vol. 11, no. 9, p. 417, 2020.

[24] D. Bandaly, A. Satir, and L. Shanker, "Integrated supply chain risk management via operational methods and financial instruments," *International Journal of Production Research*, vol. 52, no. 7, pp. 2007–2025, 2014.

[25] M. Munir, M. S. Sadiq Jajja, K. A. Chatha, and S. Farooq, "Supply chain risk management and operational performance: the enabling role of supply chain integration," *International Journal of Production Economics*, vol. 227, Article ID 107667, 2020.

[26] B. Zeng and B. P.-C. Yen, "Rethinking the role of partnerships in global supply chains: a risk-based perspective,"

International Journal of Production Economics, vol. 185, pp. 52–62, 2017.

[27] S. R. Cardoso, A. P. Barbosa-Póvoa, and S. Relvas, "Integrating financial risk measures into the design and planning of closed-loop supply chains," *Computers & Chemical Engineering*, vol. 85, pp. 105–123, 2016.

[28] Z. Wang, Q. Wang, B. Chen, and Y. Wang, "Evolutionary game analysis on behavioral strategies of multiple stakeholders in E-waste recycling industry," *Resources, Conservation and Recycling*, vol. 155, Article ID 104618, 2020.

[29] S.-M. Hosseini-Motlagh, M. Nematollahi, M. Johari, and B. R. Sarker, "A collaborative model for coordination of monopolistic manufacturer's promotional efforts and competing duopolistic retailers' trade credits," *International Journal of Production Economics*, vol. 204, pp. 108–122, 2018.

[30] B. Wu, P. Liu, and X. Xu, "An evolutionary analysis of low-carbon strategies based on the government-enterprise game in the complex network context," *Journal of Cleaner Production*, vol. 141, pp. 168–179, 2017.

[31] R. Fan, L. Dong, W. Yang, and J. Sun, "Study on the optimal supervision strategy of government low-carbon subsidy and the corresponding efficiency and stability in the small-world network context," *Journal of Cleaner Production*, vol. 168, pp. 536–550, 2017.

[32] S. Zhang, C. Wang, and C. Yu, "The evolutionary game analysis and simulation with system dynamics of manufacturer's emissions abatement behavior under cap-and-trade regulation," *Applied Mathematics and Computation*, vol. 355, pp. 343–355, 2019.

Hindawi
Complexity
Volume 2021, Article ID 6673158, 13 pages
https://doi.org/10.1155/2021/6673158

Research Article

Research on the Complex Mechanism of Placeness, Sense of Place, and Satisfaction of Historical and Cultural Blocks in Beijing's Old City Based on Structural Equation Model

Jing Zhang[1,2] **and Qiang Li**[1]

[1]*Faculty of Architecture, Civil and Transportation Engineering, Beijing University of Technology, Beijing 1001241, China*
[2]*Department of Tourism Management, School of Landscape Architecture, Beijing University of Agriculture, Beijing 102206, China*

Correspondence should be addressed to Qiang Li; liqiang@bjut.edu.cn

Received 24 December 2020; Accepted 27 May 2021; Published 5 July 2021

Academic Editor: Xueyong Liu

Using a structural equation model, this study explores the complex influence mechanism between the place experience and satisfaction of the historical and cultural blocks in the old city of Beijing and the mechanism differences between different types. Based on the data obtained in the questionnaire survey, this study uses the structural equation model method to propose a theoretical model of the relationship between place experience and satisfaction, and through path analysis, the theoretical model of the path relationship between the dimensions of placeness, sense of place, and satisfaction is estimated and tested. Through the mathematical verification of the structural model, on the basis of establishing the final theoretical model, the hypothesis to be proved is further verified. This study also uses the bootstrap method to test the significance of the mediating effect of place experience and uses multiple-group analysis to try to explore the moderating role of residents' and tourists' identity types in the model. The study found that there are multiple correlations among placeness, sense of place, and place satisfaction in the historical and cultural blocks in the old city of Beijing. The placeness is the foundation and the sense of place is the intermediary variable, which both affect satisfaction; furthermore, tourists and residents have differences in the mechanism of placeness and sense of place on satisfaction. On the one hand, the perception of placeness directly affects satisfaction, and on the other hand, the sense of place has an indirect effect on satisfaction. The positive effects of tourists' placeness on sense of place and sense of place on satisfaction are greater than that of residents. However, the positive effect of residents' placeness on satisfaction is greater than that of tourists.

1. Introduction

Place experience is the process of interaction and construction between people as a subject and the place as an object. Existing domestic and foreign related studies have proved that place experience has been studied from multiple angles, but it mainly contains two aspects. One is the research of people's cognition of place environmental elements, or the study of placeness; the second is the study of the emotional relationship between people and place, or the study of the sense of place. At the same time, studies have shown that environmental satisfaction is indeed closely related to relevant place experience [1]. However, the existing problems in related studies at home and abroad are as follows. First of all, the study on place experience, in terms of study content, either focuses on the attribute of placeness or the sense of place, and the study on place experience lacks completeness. Moreover, existing study perspectives generally start from place users (such as residents, immigrants, real estate owners, tourists, recreationists, and tourism operators, resp.), focusing on one of them. It is rare to conduct simultaneous surveys on residents and tourists, which brings about one-sidedness in the study content and study results. Secondly, the relationship between environmental satisfaction and place experience has no consistent results. In addition, as the most unique areas in the city, the

historical and cultural blocks are not only the material carrier of the history and culture of the place, but also a lively stage of social life. This is a collection of place complex subjects and rich connotations. The contradiction between its protection and development has always been a hot topic for many scholars. However, at present, there are still few comprehensive researches from the multiple subjects of residents and tourists, as well as the multiple dimensions of placeness, sense of place, and satisfaction.

Beijing is an ancient capital with a history of more than 3,000 years. Since the early years of the Western Zhou Dynasty (c.11th century–711 BC), there have been many relics left around the city, especially the 33 historical and cultural blocks distributed in the old city as the most representative. However, in recent years, the placeness of historical and cultural blocks in the old city of Beijing has suffered a greater impact driven by globalization and modernity, and these blocks are facing place restructuring in the process of protection and development. Therefore, this article intends to conduct a multidimensional and multisubject survey and analysis of the place experience in these blocks in the old city of Beijing, tries to portray place experience from both placeness and sense of place, and explores its complex relationship with the survey subject's 20 satisfaction. At the same time, through group analysis, the mechanism differences of the model in different subjects are further revealed, to provide guidance and reference for the targeted protection and renewal of the historical and cultural blocks in the old city of Beijing.

2. Definition of Related Concepts

At present, there is no clear definition of place experience in the academic circle. It involves two dimensions: placeness and sense of place. Tuan [2] earlier proposed that place experience is closely related to the place. The related concepts have gradually deepened from place [2–4] to placeness [3, 5, 6] and sense of place [7–11]. The sense of place has derived place dependence, place attachment, and place identity [12–21]. These three concepts are often mixed whether in empirical or theoretical research. Each concept may involve other concepts [22]. Lalli [23] thinks that place identity is the main concept and place attachment is a subset of it. Place attachment is widely considered as a synonym for sense of place, and place identity and place dependence are its two subconcepts [14, 15] in the research of environmental psychology.

Placeness refers to the physical environmental elements of a place and people's cognition of them [24]. It is the quality of coming from a place, or placeness [25]. Sense of place refers to people's emotional response to place and the emotional relationship between them [6–8], and it is people's overall perception of local environment. From the perspective of the man–land relationship, placeness is more from the perspective of "place" of the object, and the sense of place is more from the perspective of "man" of the subject.

This paper divides the place experience of historical and cultural blocks into two dimensions: placeness and sense of place. The placeness of these blocks is defined as local elements and people's cognition of local elements. The local elements of these blocks refer to relevant studies [26–33], mainly including elements of natural environment, elements of historical and cultural value, elements of architecture and space, and local service elements. The sense of place of these blocks is defined as people's overall perception of these blocks and the emotional connection with these blocks. Based on the classical theoretical framework of place attachment proposed by Williams [14, 15] and the dimensional research on sense of place by some scholars [11, 34–38], this paper divides the sense of place into three dimensions: place dependence, place attachment, and place identity. Place dependence emphasizes people's functional attachment to place; place attachment emphasizes the emotional connection between people and place; and place identity emphasizes the relationship between people and place, which is the dimension of people and place's related identities (Figure 1).

3. Literature Review

Place experience research since the 1990s has focused on the relationship among placeness, sense of place, and satisfaction. Its research methods have gradually expanded from qualitative analysis to principal component analysis, regression analysis, structural equation modeling, and other quantitative research. The research mainly focuses on the following three aspects:

First, the correlation between sense of place and satisfaction: Some researches in the field of tourism have confirmed that the sense of place positively affects satisfaction. If tourists have a stronger sense of identity with the destination, they are more likely to evaluate the destination positively, or the emotion between people and places plays an important role in the formation of tourist satisfaction [39–43]. In the field of residential satisfaction research, some scholars believe that identifying with a place will lead to positive evaluation and attitude towards the place [20, 23, 44, 45], or the sense of place has a positive impact on residential satisfaction [46–49]. However, some scholars believe that satisfaction is an influencing factor of place identity, and satisfaction tends to identify [50–52].

Second, the correlation between placeness (objective attribute of place or environment) and satisfaction: In the study on residents, some scholars think that residential satisfaction is a complex phenomenon, which depends on a series of factors. Residents' cognition of community is based on physical [53, 54], social [54–56], and personal factors [47, 57], which are intertwined and affect residents' satisfaction [58]. Amerigo and Aragones [59] constructed a theoretical model of residential satisfaction based on the interaction between the objective attributes of the environment and people through qualitative analysis. The model reveals three paths of the objective attribute of environment affecting residential satisfaction: directly acting on residential satisfaction; turning into subjective after the valuator's evaluation and resulting in a certain degree of satisfaction; and filtering the objective attributes through individual personality characteristics, thus affecting

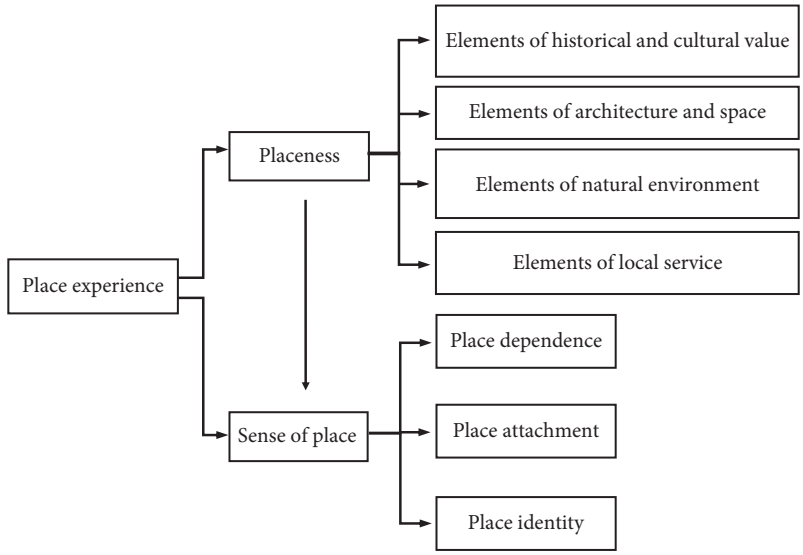

Figure 1: Conceptual map of place experience in historic and cultural blocks.

residents' satisfaction. However, some scholars believe that the objective characteristics of the place do not determine the satisfaction, but also refer to the subjective interpretation of these objective characteristics [45, 60–64]. In the research on tourists, some scholars [25, 65] have also proved that some local factors of tourist destinations have a significant positive impact on tourists' satisfaction through quantitative analysis methods.

Third, the relationship between placeness and sense of place: Some scholars have established conceptual models of the relationship between placeness and sense of place. They think that sense of place is the reaction of people stimulated by environmental factors such as material environment, social environment [3, 8, 9], natural environment, and management environment [10], or placeness is the key factor to form sense of place. Other scholars have studied the relationship between placeness and sense of place through empirical analysis. Wardhani and Kusumowidagdo [32] used qualitative interviews to reveal the influence of physical factors on the formation of place sense. Özkan and Yilmaz [33] used regression analysis to verify that there is a significant positive correlation between environmental attributes of open space and place dependence. Zhang and Duan [29], Kyle et al. [66], and Tang [67] used structural equation models to verify the causal relationship between tourists' or residents' placeness and sense of place.

According to the review, relevant studies have proved that there are correlations between sense of place and satisfaction, placeness and satisfaction, and placeness and sense of place, but there is no consistent conclusion on the causal relationship among them. What is more, there are few studies on the mechanism of action among placeness, sense of place, and satisfaction. Besides, the existing researches only start from residents or tourists unilaterally, which are also one-sided. Taking the historical and cultural blocks in Beijing's old city as the research object, this paper attempts to explore the causal relationship and influencing mechanism among placeness, sense of place, and satisfaction from the perspective of residents and tourists.

4. Theoretical Model and Data Collection

4.1. Construction of the Proposed Model. Based on the review of relevant research at home and abroad, this study finally determined three variables of placeness, sense of place, and satisfaction (Figure 2), and the following hypotheses were proposed: H1: placeness has a significant positive impact on the sense of place; H2: placeness has a significant positive impact on satisfaction; H3: sense of place has a significant positive impact on satisfaction; H4: sense of place has a significant mediating effect on the relationship between placeness and satisfaction; and H5: when identity type is used as a moderating variable, the correlation strength between variables will change significantly.

4.2. Research Design and Data Collection. The study uses a combination of structured questionnaire surveys and observation interviews to obtain basic sample data. The content of the questionnaire consists of four parts: a measurement table of placeness and sense of place (Table 1), satisfaction, and demographic characteristics. Moreover, this study is formed on the basis of soliciting the opinions of relevant experts, using the five-point Likert scale method, with "strongly disagree-strongly agree" or "Very dissatisfied-very satisfied" corresponding to an evaluation scale of 1 to 5 points. Among them, the scale of placeness and sense of place is based on relevant research and has been modified as necessary to adapt to the current survey. Therefore, exploratory factor analysis (EFA) was conducted on the placeness scale and the sense of place scale by principal component analysis, and the observed variables X_{18}, X_{22}, X_{12}, X_{13}, and Y_8 were deleted on this basis. The investigation time was from September 25, 2017, to October 6, 2017, and from March 26, 2018, to April 6, 2018, the survey was

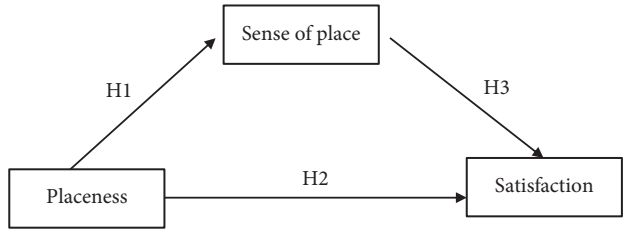

Figure 2: Hypothesis structure relationship model.

Table 1: Measurement index system.

Basic dimensions		Observation variables	Reference Sources
Placeness	Elements of historical and cultural value	X_1, characteristics of traditional culture; X_2, folk custom and intangible cultural heritage; X_3, cultural value; X_4, era characteristics; X_5, historical remains; X_6, historical character events or historical background	[28, 29]
	Elements of architecture and space	X_7, street system; X_8, courtyard space; X_9, building features; X_{10}, space layout; X_{11}, overall landscape; X_{12}, landscape sketch; X_{13}, overall style	
	Elements of local service	X_{14}, public service management; X_{15}, environmental sanitation facilities; X_{16}, infrastructure; X_{17}, identification and interpretation system; X_{18}, external transportation; X_{19}, public service facilities	
	Elements of natural environment	X_{20}, overall natural environment; X_{21}, plant landscape; X_{22}, animal landscape; X_{23}, courtyard natural environment	
Sense of place	Place dependence	Y_1, this is the best place for me to do my hobby Y_2, there is nowhere comparable to this Y_3, I will come here often/live here whenever possible Y_4, this is a good place for work, travel, and life Y_5, this place can meet my needs better than other places (get relaxed, gain knowledge, get friends, etc.)	[14, 15]
	Place attachment	Y_6, this place makes me happy Y_7, this place makes me feel relaxed Y_8, this is my favorite place Y_9, I will miss this place when I cannot come for a long time Y_{10}, the scenery and life atmosphere here make me feel that I belong to this place	
	Place identity	Y_{11}, this place means a lot to me Y_{12}, my personality and characteristics can be fully displayed here Y_{13}, I feel like this is a part of my life Y_{14}, I can be my true self Y_{15}, this place is very special to me Y_{16}, I quite agree with this place	

conducted in Dashilan, Nanluoguxiang, Fuchengmen Inner Street, and Dongsi North Santiao to Batiao in the historical and cultural districts of Beijing's old city. And the random sampling surveys of tourists on the streets and random household surveys are conducted on residents. The survey actually distributed 1,300 questionnaires, of which 1,224 were recovered, with a recovery rate of 94.15%. Excluding 87 invalid questionnaires, 1137 valid questionnaires were finally obtained, with an effective rate of 92.89%. Among them, a total of 563 questionnaires were returned by tourists and 574 questionnaires were returned by residents. SPSS 22.0 statistical software was used to process the sample data for the recovered data and combined with the use of AMOS 22.0 for structural equation model verification analysis.

4.3. Construction of Structural Model. The causal relationship model between placeness, sense of place, and satisfaction constructed in this study includes two latent variables of placeness, sense of place, and one observed variable of satisfaction. According to the results of exploratory factor analysis, the observed variables of placeness and sense of place are represented by the arithmetic mean of the scores of the items contained in each factor by the internal consistency approach of item packaging. Therefore, the observed variables of latent variable of placeness include elements of historical and cultural value, elements of architecture and space, elements of natural environment, and local service elements; the observed variables of latent variable of sense of place include place dependence, place attachment, and place identity.

5. Validation Analysis of Empirical Results

5.1. Structural Characteristics of the Sample. The proportion of female tourists (58.1%) is slightly higher than that of males (41.9%). The age distribution is dominated by young and middle-aged under 44, with a cumulative percentage of 80.5%; among them, young people under 34 account for 62.2%. Their occupations are widely distributed, with a relatively large proportion of students, accounting for 30.4%, followed by business/service personnel and enterprise and institution management personnel, accounting for 15.2% and 14%, respectively. The average monthly income is not high, and those with a monthly income of less than 10,000 yuan or a low-income group (including current students) account for 91.6%. Highly educated people, with a college degree or above, account for 83.9%. The source of tourists is mainly domestic, with tourists from other provinces accounting for 55.7% and local tourists from Beijing accounting for 41.2%. The degree of involvement of tourists was not high before they came, and the percentage of tourists who did not understand and only knew a little reached 69.9%. The proportion of first-time visitors and revisiting tourists is the same, and the proportion of tourists who visit twice or more is 55.2%. Sightseeing and leisure and entertainment are the main motives for traveling, accounting for 79.5% of the total. Tourists stay mainly within half a day, with a cumulative percentage of 89.6%.

The proportion of female residents (55.7%) is slightly higher than that of men (44.3%). The age distribution is dominated by middle-aged and elderly people over 45 years old. The cumulative proportion of people over 45 years old accounts for 82.1%; among them, the proportion of people over 55 years old reaches 63.2%. The occupation distribution is dominated by retirees, with a proportion of 68.9%, followed by business/service personnel with a proportion of 14.2%. The average monthly income is low, and those with a monthly income of less than 5,000 yuan (excluding current students) account for 89.2%. The education level is not high, and the accumulative proportion of college degrees (excluding colleges) is 77.8%. The main types of residents are aboriginals, with a total of 77.8% of people living for more than 20 years, followed by new immigrants, with 14.2% of people living for less than 5 years. The type of property ownership is mainly public rental housing, which accounts for 67.9% of the total, while people with private property rights and those who rent property rights to others each account for 16%.

5.2. Reliability and Validity Testing of the Scale. Use SPSS 22.0 statistical software to calculate the Cronbach α of latent variables such as elements of historical and cultural value, elements of architecture and space, local service elements, natural environment elements, place dependence, place attachment, and place identity. The results show (Table 2) that the Cronbach α of the above latent variables is between 0.737 and 0.934, which has good internal consistency and stability.

The comprehensive reliability (CR) of each scale is greater than 0.7, and the average variance extracted (AVE) is greater than 0.5, indicating that the scale has good internal reliability and discriminant validity.

5.3. Inspection and Evaluation of the Measurement Model

5.3.1. Testing of the Measurement Model. Using AMOS22.0 to test the degree of fit of the measurement model, the study obtains the index value of the degree of fit, shown in Table 3. It can be seen from Table 3 that the RMSEA (0.082) in the absolute fitting index is slightly greater than 0.08 and the PGFI (0.452) in the simple fitting index is slightly less than 0.5, which does not meet the fitting requirements; the other indicators meet the fitting requirements. It can be seen that the degree of fitting between the measurement model and the data are at a better level, the external quality of the model is good, and no further correction is needed.

5.3.2. Evaluation of the Measurement Model. Using the confirmatory factors to analyze and evaluate the measurement model, Table 4 lists the path coefficients of the measurement model; among them, the standardized coefficients are all above 0.6 and the standard deviations are all less than 0.1, all of which have passed the significance test. The load value of the standardized factor of each measurement index in the latent variable is between 0.626 and 0.877, which meets the standard of factor load greater than 0.5; each research variable has no negative measurement error, and the standard deviation is relatively small, lower than 0.05; the critical ratios are all greater than 3.29, and the parameter estimates all reach the significant level of 0.001 ($P < 0.001$, represented by the ***symbol), indicating that each factor index has a strong explanatory power for the measurement model, and the basic fitness of the model is good.

5.4. Correlation Analysis and Discriminant Validity. It can be seen from Table 5 that the correlation coefficients between the variables are all lower than 0.7, and there is no multicollinearity. The bold numbers are the square root of the AVE of the corresponding variables. The nonbold numbers are the correlation coefficients of the corresponding variables. The bold numbers are all greater than the absolute value of the nonbold numbers, indicating that the discriminant validity is better; that is, there is a certain degree of discrimination between variables.

5.5. Inspection and Evaluation of Structural Model

5.5.1. Testing of the Structural Model. Using AMOS22.0 to test the degree of fit of the conceptual model, the study obtains the index value of the degree of fit shown in Table 6. It can be seen from Table 6 that the RMSEA (0.084) in the absolute fitting index is slightly greater than 0.08 and the PGFI (0.483) in the simple fitting index is slightly less than 0.5, which does not meet the fitting requirements; the other indicators meet the fitting requirements. It can be seen that

Table 2: Reliability test results of the observed variables and latent variables*.

The name of the factor	Reliability (*coefficient)	Composite reliability (CR)	Average variance extracted (AVE) values
Elements of historical and cultural value	0.855	0.893	0.584
Elements of architecture and space	0.878	0.911	0.673
Elements of local service	0.737	0.881	0.598
Elements of natural environment	0.800	0.884	0.717
Place dependence	0.907	0.931	0.729
Place attachment	0.840	0.907	0.764
Place identity	0.934	0.947	0.719

*represents the measured value after eliminating the observed variables X_{18}, X_{22}, X_{12}, X_{13}, and Y_8.

Table 3: Overall measurement model indices.

Index	Absolute fitting index				Value-added fitting index			Simple fitting index	
Specific classification	$\chi 2$/df	GFI	RMR	RMSEA	NFI	TLI	CFI	PGFI	PNFI
Judgment criteria	<3	>0.9	<0.08	<0.08	>0.9	>0.9	>0.9	>0.5	>0.5
Fitting results	8.689*	0.966	0.029	0.082	0.958	0.941	0.962	0.452	0.616
Fitting evaluation		Good				Very good		Good	

*The sample size in this paper is $n = 1137$, so the $\chi 2$/df index is not referenced. Note: when the sample size is greater than 1,000, the index has no reference significance [68].

Table 4: Estimation of path coefficients for measurement models.

Relationship between potential variables and observed variables			Unstandardized estimation	S.E.	C.R.	P	Standardized estimation	SMC	1-SMC	CR	AVE
Elements of historical and cultural value	<---	Placeness	1				0.791	0.626	0.374		
Elements of architecture and space	<---	Placeness	1.002	0.043	23.378	***	0.780	0.608	0.392	0.809	0.517
Elements of natural environment	<---	Placeness	0.860	0.044	19.503	***	0.626	0.392	0.608		
Elements of local service	<---	Placeness	0.772	0.037	20.723	***	0.666	0.444	0.556		
Place identity	<---	Sense of place	1			***	0.877	0.770	0.230		
Place attachment	<---	Sense of place	0.777	0.026	30.180	***	0.778	0.605	0.395	0.881	0.712
Place dependence	<---	Sense of place	0.935	0.028	33.612	***	0.872	0.760	0.240		

***At the 0.001 level (2-tailed), the correlation is significant.

Table 5: Discriminant validity matrix.

	Placeness	Sense of place	Satisfaction
Placeness	**0.719**		
Sense of place	.207**	**0.844**	
Satisfaction	.413**	.446**	1

**At the 0.01 level (2-tailed), the correlation is significant.

the degree of fitting between the measurement model and the data is at a better level, the external quality of the model is good, and no further correction is needed.

5.5.2. Evaluation of the Structural Model. The software AMOS22.0 is used to evaluate the structural relationship between the latent variables of the initial conceptual model, and the specific results are shown in Table 7. From Table 7, the absolute value of the critical value (CR) of each coefficient is greater than 3.29, and the parameter estimates are all up to 0.001 (P value is ***, representing significant at the 0.001 level) significance level, that is, all passing the significance test. Among them, the standardized path coefficient of placeness and sense of place is 0.212, indicating that the respondents' perception of placeness has a significant positive impact on the formation of sense of place; the standardized path coefficient of placeness and satisfaction is 0.366, indicating that the respondents' perception of placeness has a significant positive impact on their

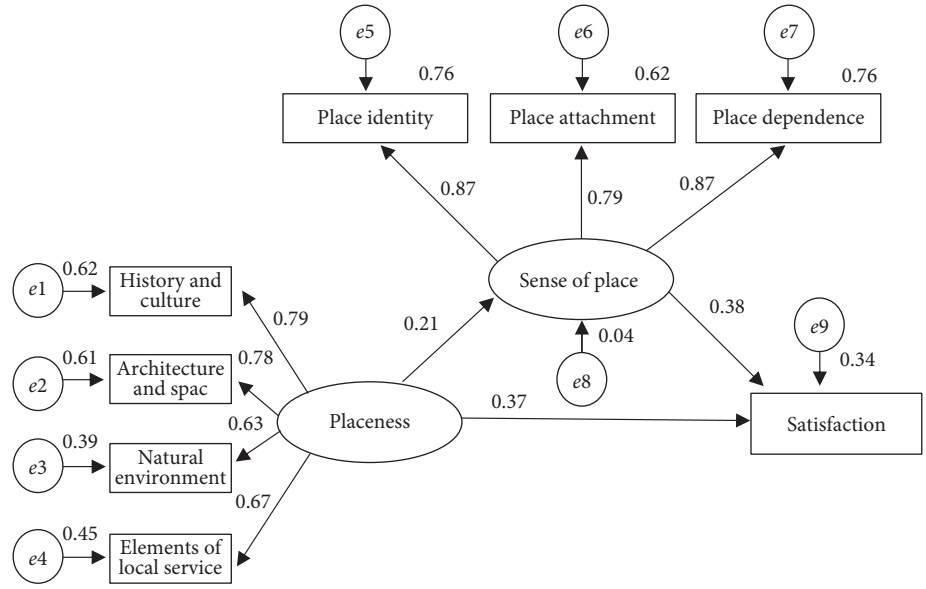

Figure 3: Ultimate structural equation modeling.

satisfaction; the standardized path coefficient between place and satisfaction is 0.382, indicating that the sense of place formed by the survey has a significant positive impact on satisfaction. Through the comparison of the size of the path coefficient, it can be seen that the degree of influence of the respondents' sense of place on satisfaction is greater than the influence of their perception of placeness on satisfaction (Figure 3).

5.6. Analysis of Mediating Effect. This study uses the bias-corrected percentile bootstrap method to test the significance of the mediating effect. First, the study uses the method of repeated random sampling to extract 2,000 bootstrap samples from the original data ($N = 1137$), and then fit the model based on these samples, generate and save the estimated value of 1,000 mediation effects, from an approximate sampling distribution, and calculate the average path value of the mediation effect, and these effect values are sorted by numerical value. Finally, the study uses the 2.5th percentile and the 97.5th percentile to estimate the 95% confidence interval of the mediation effect. If the 95% confidence interval of these path coefficients does not include 0, it indicates that the mediating effect is significant. Then, look at whether the confidence interval (or significance) of the standardized direct effect contains 0, if it contains 0 (that is, it is not significant), it is full mediation; otherwise, it is partial mediation.

It can be seen from Table 8 that the 95% confidence interval of the indirect effect of placeness on satisfaction is [0.049, 0.115], which does not contain 0, so the mediating effect is significant. The 95% confidence interval of the direct effect of placeness on satisfaction is [0.308, 0.427], which does not include 0, so partial mediating effects are significant. The indirect effect value was 0.081, while the direct effect value was 0.366, and the total effect value was 0.447. All passed the test of significance level (0.001). The ratio of indirect effect to total effect was $0.081/0.447 = 0.181$. That is to say, 18.1% of the variation was caused by the sense of place when placeness affected overall satisfaction.

It can be proved that the respondents' perception of placeness can not only directly affect satisfaction, but also form an indirect effect on satisfaction through the sense of place. The sense of place can be used as an intermediary variable for the influence of placeness on satisfaction.

5.7. Analysis of Moderating Effect. To test whether the constructed model has cross-group stability, this study uses the model to perform multiple-group path analysis with different identity type (resident or tourist) variables. If there is no significant difference, it means that the identity type variable has no effect on the model; if there is a significant difference, it means that the identity type variable has a moderating effect.

When the multiple-group structural equation model is running, Amos 22.0 sets five parameter restriction models, so the multiple-group model includes six models: unrestricted model, measurement weighted model, structure weighted model, structure covariance model, structure residual error model, and measurement residual model. Two judgments are required for multigroup analysis: whether each model is recognized and whether the recognized model meets the standard. If the sample data of each group is large, the chi-square value that limits the overall fitness statistics of the model should be used as one of the reference standards, and the overall judgment needs to be made from the fitness situation of each fitness statistics [69]. If there are more than two identified models that meet the standard, the optimal model needs to be judged based on AIC and ECVI. The model with the smallest value of AIC and ECVI is the best model. The overall fitness test results of the multiple-group model are

Table 6: Structural equation model indices.

Index	Absolute fitting index				Value-added fitting index			Simple fitting index	
Specific classification	$\chi 2$/df	GFI	RMR	RMSEA	NFI	TLI	CFI	PGFI	PNFI
Judgment criteria	<3	>0.9	<0.08	<0.08	>0.9	>0.9	>0.9	>0.5	>0.5
Fitting results	9.069*	0.966	0.029	0.084	0.958	0.941	0.962	0.483	0.616
Fitting evaluation		Good				Very good			Good

*The sample size in this paper is $n = 1137$, so the $\chi 2$/df index is not referenced. When the sample size is greater than 1,000, this index has no reference significance [68].

Table 7: Path coefficient estimation of the structural equation model.

Path relationship among potential variables			Unstandardized estimation	Standardized estimation	Standard error	Critical value	P value
Sense of place	<---	Placeness	0.286	0.212	0.047	6.102	***
Satisfaction	<---	Placeness	0.573	0.366	0.047	12.263	***
Satisfaction	<---	Sense of place	0.443	0.382	0.033	13.61	***

***At the 0.001 level (2-tailed), the correlation is significant.

Table 8: Bootstrap analysis for the significance test of mediation effect.

	Effect value	95% confidence interval		P	Intermediary judgment
		Lower limit	Upper limit		
Indirect effect	0.081	0.049	0.115	0.001	Intermediary existed
Direct effect	0.366	0.308	0.427	0.001	Part of the intermediary
Total effect	0.447	0.388	0.506	0.001	

Table 9: Multigroup modeling indicators comparison of the overall adaptation.

Test statistic	Reference standard	Unrestricted model	Measurement weighting model	Structure weighted model	Structural covariance model	Structural residual model	Measurement residual model
CMIN/DF	<3	4.282	4.429	5.617	5.526	5.524	7.506
P	>0.05	≤0.001	≤0.001	≤0.001	≤0.001	≤0.001	≤0.001
RMR	<0.05	0.023	0.030	0.061	0.059	0.068	0.073
RMSEA	<0.05	0.054	0.055	0.064	0.063	0.063	0.076
GFI	>0.9	0.968	0.960	0.951	0.951	0.950	0.923
NFI	>0.9	0.959	0.949	0.934	0.934	0.932	0.892
CFI	>0.95	0.968	0.960	0.945	0.945	0.944	0.905
PNFI	>0.5	0.617	0.729	0.734	0.750	0.766	0.860
PGFI	>0.5	0.484	0.574	0.581	0.594	0.607	0.692
AIC	The smaller the better	226.148	248.449	303.159	302.676	306.109	441.309
ECVI	The smaller the better	0.199	0.219	0.267	0.267	0.270	0.389

shown in Table 9. Through the comparison and analysis of the fitness of the six hypothetical models, the multigroup model with identity type as moderator variables after comparison, the measurement weighted model is determined as the best model.

According to the model comparison in Table 10, there are significant differences between the unrestricted model and the restricted model. The p value was less than 0.05, which passed the significance test. Therefore, there are significant differences in the models of different identity types, that is, identity types play a moderating role.

By sorting out the data calculation results, the estimation results of the multiple-group structural equation model of two different identity types are obtained, as shown in Table 11, and the specific path diagrams are shown in Figures 4 and 5.

The analysis results of the multiple-group structural equation model show that in the path H1 of the positive influence of placeness on the sense of place, the influence of tourists and local residents is very significant ($P < 0.001$), and the influence effects of the two types of identity are quite different. Among them, the impact effect of tourists (0.601) is greater than that of local residents (0.257). In the path H2 of the positive influence of placeness on satisfaction, the influence of tourists and local residents is very significant ($P < 0.001$), and the

Table 10: Comparison between unrestricted model and restricted model (measurement weighted model).

Model	DF	CMIN	P	NFI Delta-1	IFI Delta-2	RFI rho-1	TLI rho2
Measurement weights	7	36.301	0.000	0.010	0.010	0.002	0.002

Table 11: Estimated results of multigroup structural equation modeling based on tourists and residents.

Route	Respondents	
	Tourist	Resident
H1: sense of place<---placeness	0.601***	0.257***
H2: satisfaction <--- placeness	0.289***	0.306***
H3: satisfaction <--- sense of place	0.454***	0.334***

*denotes $P < 0.05$, **denotes $P < 0.01$, *** indicates $P < 0.001$; paths H1, H2, and H3 are consistent with the previous hypothesis.

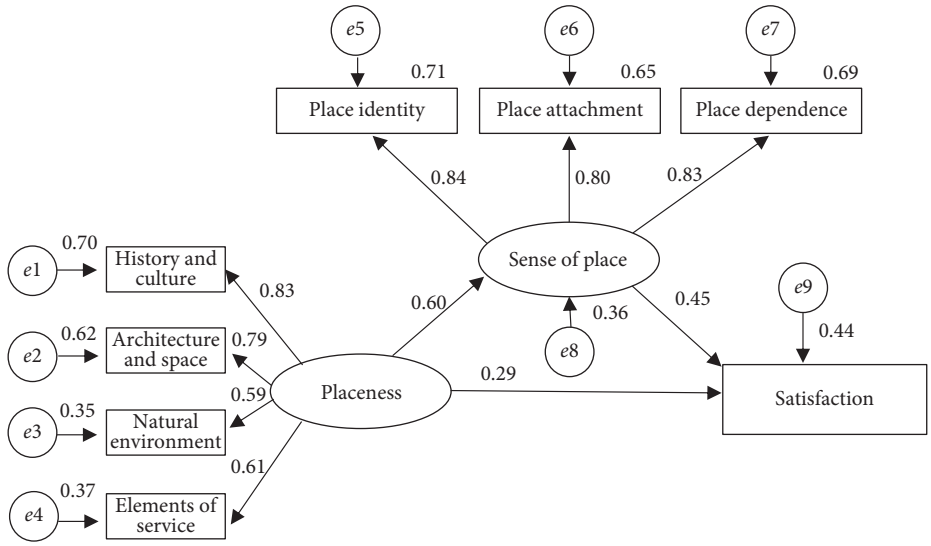

Figure 4: Standardized path coefficient of multi-group structural equation modeling for tourists.

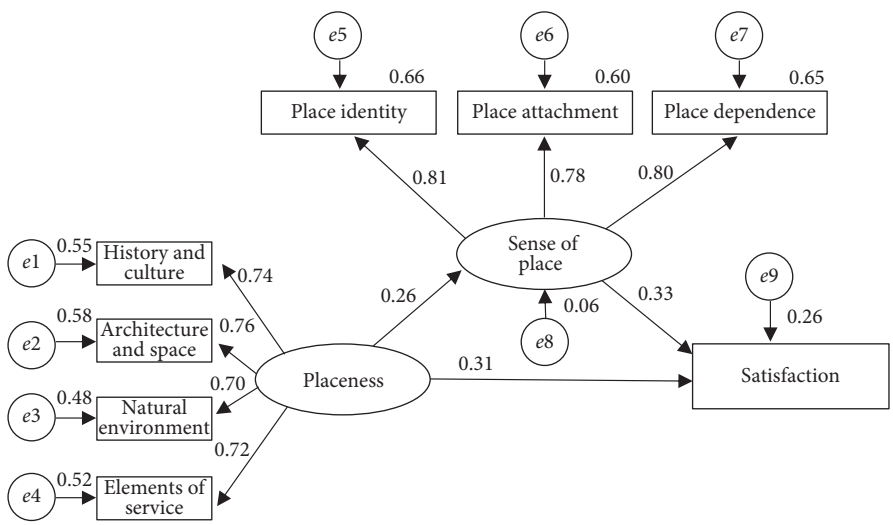

Figure 5: Standardized path coefficient of multi-group structural equation modeling for residents.

difference is large. Among them, the influence of tourists (0.289) is smaller than that of local residents (0.306). In path H3, where the sense of place has a positive impact on satisfaction, the impact of tourists and local residents is very significant ($P < 0.001$), and there are large differences. Among them, the impact effect of tourists (0.454) is greater than that of local residents (0.334).

6. Conclusion and Discussion

6.1. Conclusion. In summary, based on relevant studies at home and abroad and previous studies, this paper constructs a causal model of placeness, sense of place, and satisfaction in the historical and cultural blocks in the old city of Beijing, and then, the model and research hypothesis proposed in this study were tested through the analysis of the covariance structure provided by AMOS. The test results show that all five hypotheses proposed in this study are valid.

First, direct effect: The two dimensions of place experience (placeness and sense of place) of residents and tourists in historical and cultural blocks of Beijing's old city have a remarkable positive impact on their satisfaction. Placeness has a significant positive impact on sense of place, hypothesis 1 is tenable; placeness has a significant positive impact on satisfaction, hypothesis 2 is tenable; sense of place has a significant positive impact on satisfaction, hypothesis is tenable. Moreover, the sense of place formed by the respondents has a slightly greater impact on satisfaction than placeness.

Second, indirect effect: Sense of place has a prominent mediating effect on the relationship between placeness and satisfaction. From the research results, we can see that placeness not only has a significant direct effect on satisfaction, but also has a significant indirect effect on satisfaction through sense of place.

Thirdly, when identity type is used as a moderating variable, the correlation strength among placeness, sense of place, and satisfaction will change significantly. The results show that the causalities of the three for residents and tourists are consistent, but the influence intensities are significantly different.

6.2. Discussion. This study aims to take Beijing's historical and cultural district as the object, organize the three variables of placeness, sense of place, and satisfaction into a model by the structural equation, build the causal model of placeness, sense of place, and satisfaction, and compare the differences of causal mechanism for residents and tourists. The following results are obtained:

Firstly, it eliminates the differences of causality between placeness and satisfaction and between sense of place and satisfaction based on regression analysis and other research methods and obtains the definite causality among placeness, sense of place, and satisfaction.

Secondly, it reveals that the influence mechanisms of residents' and tourists' sense of place and satisfaction in historical and cultural blocks originate from placeness. Placeness is the foundation, and sense of place is the intermediary variable, and they affect satisfaction jointly. However, in the age of globalization and modernization, the landscape of these blocks in various places gradually tends to be similar, and the historical authenticity and placeness are gradually lost. The results of this study show that improving the local characteristics of these blocks in the old city of Beijing and accelerating sense of place for residents and tourists are the core of improving the satisfaction.

Thirdly, it reveals the direct and indirect effects of placeness on satisfaction, and the effect intensity varies on residents and tourists. The results show that the residents' satisfaction with Beijing's historical and cultural blocks is more directly influenced by placeness and less by local emotional links. Tourists' satisfaction is rooted in the indirect influence of placeness, or the emotional connection between tourists and places. The authors think that this may be because the local characteristics of Beijing's historical and cultural blocks have not been effectively protected. Tourists conduct local experience activities in a particular way and time constraints. In the process of tourism, tourists form sense of place through mutual confirmation and stimulus of the on-the-spot feelings based on the objective elements and the memory and imagination before tourism, and then their satisfaction evaluations are affected. However, residents' living environment has changed from the original pure living environment into tourist destinations under tourism development. This change often disrupts residents' place dependence and place attachment, thus affecting the promotion effect of sense of place on satisfaction.

7. Research Deficiency and Prospect

Firstly, the research subject is not extensive enough. The development of a historical and cultural district involves a wide range of participants, including residents, tourists, business operators, developers, and local governments. Different subjects have different experiences and interests, as well as different perceptions of the place experience of historical and cultural blocks, resulting in different appeals and satisfaction. This study only focuses on residents and tourists, which has certain limitations. In the future, we can further expand research subjects and make a comparative study among multiple subjects, so as to more comprehensively reflect the local characteristics of historical and cultural districts and the place significance given by different subjects.

Secondly, the research variables can be further expanded. This study provides a basic research framework for the formation of place experience and its impact on the satisfaction of residents and tourists in historical and cultural blocks. Through the model analysis, it can be concluded that for different subjects, residents and tourists, the effects of placeness and sense of place on satisfaction are different. This shows that the formation of sense of place and satisfaction not only comes from placeness, but may also be affected by other variables. For example, Tang [67] thinks that the formation of sense of place is an evaluation process based on environmental perception combined with personal behavior goals, and the level of personal knowledge and

experience is a vital factor in this evaluation process. Therefore, demographic factors affect the formation of sense of place in many cases. In addition, some studies have shown that there is a relationship between satisfaction and future behavior intention [70–73]. Therefore, variables such as demographic characteristics and place revisit intention can be added to expand the model variables in the future, so as to further reveal the complex mechanism between place experience and satisfaction.

Data Availability

All data used to support the findings of this study are available from the corresponding author upon request.

Conflicts of Interest

The authors declare that they have no conflicts of interest regarding the publication of this paper.

Acknowledgments

This study was supported by the Key Program of Beijing Social Science Foundation (19GLA001), the Major Program of the National Social Science Foundation of China (20ZDA086), and the General Program of the National Natural Science Foundation of China (52078006).

References

[1] G. Fleury-Bahi, M.-L. Félonneau, and D. Marchand, "Processes of place identification and residential satisfaction," *Environment and Behavior*, vol. 40, no. 5, pp. 669–682, 2008.

[2] Y. Tuan, "Place: an experiential perspective," *Geographical Review*, vol. 65, no. 2, pp. 151–165, 1975.

[3] E. Relph, *Place and Placelessness*, Pion, London, UK, 1976.

[4] J. D. Sime, "Creating places or designing spaces?" *Journal of Environmental Psychology*, vol. 6, no. 1, pp. 49–63, 1986.

[5] S. A. Shumaker and R. B. Taylor, *Toward a Clarification of People-Place Relationships: A Model of Attachment to Place*, Environmental Psychology: Directions and Perspectives, Praeger, New York, NY, USA, 1983.

[6] D. Hummon, *Community Attachment: Local Sentiment and Sense of place*, Place Attachment, New York press, New York, NY, USA, 1992.

[7] Y. Tuan, "Rootedness versus sense of place," *Landscape*, vol. 24, pp. 3–8, 1980.

[8] F. Steele, *The Sense of Place*, CBI Publishing Company Inc., Boston, MA, USA, 1981.

[9] E. H. Zube, J. L. Sell, and J. G. Taylor, "Landscape perception: research, application and theory," *Landscape Planning*, vol. 9, no. 1, pp. 1–33, 1982.

[10] T. C. Greene, *Cognition and the Management of Place in the Nature and the Human Spirit*, Venture Publishing, State College, PA, USA, 1996.

[11] B. S. Jorgensen and R. C. Stedman, "Sense of place as an attitude: lakeshore owners attitudes toward their properties," *Journal of Environmental Psychology*, vol. 21, no. 1, pp. 233–248, 2001.

[12] H. M. Prohansky, A. K. Fabian, and R. Kaminoff, "Place-identity: physical world socialization of the self," *Journal of Environmental Psychology*, vol. 3, no. 1, pp. 57–83, 1983.

[13] G. M. Breakwell, *Coping with Threatened Identity*, Methuen, London, UK, 1986.

[14] D. R. Williams and J. W. Roggenbuck, "Measuring place attachment: some preliminary results. Proceeding of NRPA symposium on leisure research," in *Proceedings of the NRPA Symposium on Leisure Research*, vol. 9, San Antonio, TX, USA, October 1989.

[15] D. R. Williams, M. E. Patterson, J. W. Roggenbuck, and A. E. Watson, "Beyond the commodity metaphor: examining emotional and symbolic attachment to place," *Leisure Sciences*, vol. 14, no. 1, pp. 29–46, 1992.

[16] M. V. Giuliani and R. Feldman, "Place attachment in a developmental and cultural context," *Journal of Environmental Psychology*, vol. 13, no. 3, pp. 267–274, 1993.

[17] K. S. Bricker and D. L. Kerstetter, "Level of specialization and place attachment: an Exploratory study of Whitewater Recreationists," *Leisure Sciences*, vol. 22, no. 4, pp. 233–257, 2000.

[18] K. De Bres and J. Davis, "Celebrating group and place identity: a case study of a new regional festival," *Tourism Geographies*, vol. 3, no. 3, pp. 326–337, 2001.

[19] K. S. Bricker and D. L. Kerstetter, "An interpretation of special place meanings whitewater recreationists attach to the south Fork of the American River," *Tourism Geographies*, vol. 4, no. 4, pp. 396–425, 2002.

[20] G. Kyle, A. Graefe, R. Manning, and J. Bacon, "An examination of the relationship between leisure activity involvement and place attachment among hikers along the appalachian trail," *Journal of Leisure Research*, vol. 35, no. 3, pp. 249–273, 2003.

[21] G. Kyle, A. Graefe, R. Manning, and J. Bacon, "Effects of place attachment on users' perceptions of social and environmental conditions in a natural setting," *Journal of Environmental Psychology*, vol. 24, no. 2, pp. 213–225, 2004.

[22] M. A. Abou-Shouk, N. Zoair, M. N. El-Barbary, and M. M. Hewedi, "Sense of place relationship with tourist satisfaction and intentional revisit: evidence from Egypt," *International Journal of Tourism Research*, vol. 20, no. 2, pp. 172–181, 2018.

[23] M. Lalli, "Urban-related identity: theory, measurement, and empirical findings," *Journal of Environmental Psychology*, vol. 12, no. 4, pp. 285–303, 1992.

[24] E. Relph, "Placeness, place, placelessness," 2019, http://www.placeness.com.

[25] Y. Xiao, *Research on Regional Gene of Historical and Cultural Blocks Based on Tourist Satisfaction*, Zhejiang University of technology and industry, Hangzhou, China, 2018.

[26] F. Wang, X. Huang, and X. Yu, "Tourist cognition of sense of place in tourism attractions," *Acta Geographica Sinica*, vol. 64, no. 10, pp. 1267–1277, 2009.

[27] F. Wang, L. Yan, X. Xiong, and B. Wu, "A study on tourist cognition of urban memory in historic sites: a case study of alley nanluogu historic site in beijing," *Acta Geographica Sinica*, vol. 67, no. 4, pp. 545–556, 2012.

[28] M. Zhang and F. Wang, "Research on the sense of place in the historical area of Beijing residents," *Urban*, vol. 218, no. 9, pp. 43–51, 2013.

[29] Z. Zhang and H. Duan, "Analysis on the relation mechanism between environmental locality and Tourists'Sense of place based on Amos7. 0 platform: a case study of xi'an daming palace national archaeological park," *Tourism Science*, vol. 28, no. 4, pp. 81–94, 2014.

[30] G. Gabriela, V. Aziliz, and V. B. Koenraad, "Place attachment and challenges of historic cities: a qualitative empirical study on heritage values in cuenca, Ecuador," *Journal of Cultural*

Heritage Management and Sustainable Development, vol. 8, no. 3, pp. 387–399, 2018.

[31] A. Kusumowidagdo and D. K. Wardhani, "Investigating a sense of place at a historic commercial street corridor: visitor perception of social aspects," in *Proceedings of the Cities' Identity through Architecture and Arts: Proceedings of the International Conference on Cities' Identity through Architecture and Arts (CITAA 2017)*, Routledge, Cairo, Egypt, May 2017.

[32] D. K. Wardhani and A. Kusumowidagdo, *Authenticity of the Physical Environment that Influences a Sense of Place: A Qualitative Study at Ampel Street Corridor, Surabaya, Indonesia*, Cities' Identity Through Architecture and Arts, Routledge, London, UK, 2018.

[33] D. G. Özkan and S. Yilmaz, "The effects of physical and social attributes of place on place attachment," *Archnet-IJAR: International Journal of Architectural Research*, vol. 13, no. 1, pp. 133–150, 2019.

[34] B. Nanzer, "Measuring sense of place: a scale for Michigan," *Administrative Theory & Praxis*, vol. 26, no. 3, pp. 362–382, 2004.

[35] L. K. Harmon, H. C. Zinn, and M. Gleason, "Place identity, place dependence, and place- based affect: examining their relationship to participation in educational and interpretive programs at isle royale national park," in *Proceedings of the People, Places, and Parks: Proceedings of the 2005 George Wright Society Conference on Parks, Protected Areas, and Cultural Sites*, The George Wright Society, Hancock, MI, USA, August 2006.

[36] G. T. Kyle, A. J. Mowen, J. D. Absher, and M. E. Havitz, "Commitment to public leisure service providers: a conceptual and psychometric analysis," *Journal of Leisure Research*, vol. 38, no. 1, pp. 78–103, 2006.

[37] K. Deutsch and K. Goulias, *Investigating the Impact of Sense of Place on Travel Behavior Using an Intercept Survey Methodology*, University of California Transportation Center, UC Berkeley, Berkeley, CA, USA, 2009.

[38] S. Tapsuwan, Z. Leviston, and D. Tucker, "Community values and attitudes towards land use on the gnangara groundwater System: a sense of place study in perth, western Australia," *Landscape and Urban Planning*, vol. 100, no. 1-2, pp. 24–34, 2011.

[39] A. Yuksel, F. Yuksel, and Y. Bilim, "Destination attachment: effects on customer satisfaction and cognitive, affective and conative loyalty," *Tourism Management*, vol. 31, no. 2, pp. 274–284, 2010.

[40] Y. Yu, J. Tian, and J. Su, "A study of the relativity between place attachment and post-tour behavioral tendencies of visitors: taking value perception and satisfaction experience as intermediary variables," *Tourism Science*, vol. 24, no. 2, pp. 54–62,74, 2010.

[41] G. Prayag and C. Ryan, "Antecedents of tourists' loyalty to Mauritius," *Journal of Travel Research*, vol. 51, no. 3, pp. 342–356, 2012.

[42] H. Ramkissoon, L. D. G. Smith, and B. Weiler, "Relationships between place attachment, place satisfaction and pro-environmental behaviour in an Australian national park," *Journal of Sustainable Tourism*, vol. 21, no. 3, pp. 434–457, 2013a.

[43] H. Ramkissoon, L. D. Graham Smith, and B. Weiler, "Testing the dimensionality of place attachment and its relationships with place satisfaction and pro-environmental behaviours: a structural equation modelling approach," *Tourism Management*, vol. 36, pp. 552–566, 2013b.

[44] B. P. Kaltenborn, "Effects of sense of place on responses to environmental impacts," *Applied Geography*, vol. 18, no. 2, pp. 169–189, 1998.

[45] C. C. M. Adriaanse, "Measuring residential satisfaction: a residential environmental satisfaction scale (RESS)," *Journal of Housing and the Built Environment*, vol. 22, no. 3, pp. 287–304, 2007.

[46] F. Rojo Perez, G. Fernandez-Mayoralas Fernandez, E. Pozo Rivera, and J. Manuel Rojo Abuin, "Ageing in place: predictors of the residential satisfaction of elderly," *Social Indicators Research*, vol. 54, no. 2, pp. 173–208, 2001.

[47] D. W. Chapman and J. R. Lombard, "Determinants of neighborhood satisfaction in fee-based gated and nongated communities," *Urban Affairs Review*, vol. 41, no. 6, pp. 769–799, 2006.

[48] K. M. Smith, *The Relationship between Residential Satisfaction, Sense of Community, Sense of Belonging and Sense of Place in a Western Australian Urban Planned Community*, Edith Cowan University, Perth, Australia, 2011.

[49] X. Li, *Research on Relantionship between Sense of Place of Inhabitants and Satisfaction of Inhabitants-A Case Study of LiJingmen Historical and Cultural Blocks of LuoYang*, Jiangxi Normal University, Nanchang, China, 2018.

[50] D. Uzzell, E. Pol, and D. Badenas, "Place identification, social cohesion, and enviornmental sustainability," *Environment and Behavior*, vol. 34, no. 1, pp. 26–53, 2002.

[51] E. D. Brocato, *Place Attachment: An Investigation of Environments and Outcomes in Service Context*, University of Texas at Arlington, Arlington, TX, USA, 2006.

[52] K. Y. Lee and M. G. Jeong, "Residential environmental satisfaction, social capital, and place attachment: the case of Seoul, Korea," *Journal of Housing and the Built Environment*, vol. 36, no. 2, pp. 559–575, 2020.

[53] M. Bonnes, M. Bonaiuto, and A. P. Ercolani, "Crowding and residential satisfaction in the urban environment," *Environment and Behavior*, vol. 23, no. 5, pp. 531–552, 1991.

[54] M. Braubach, "Residential conditions and their impact on residential environment satisfaction and health: results of the who large analysis and review of european housing and health status (lares) study," *International Journal of Environment and Pollution*, vol. 30, no. 3/4, pp. 384–403, 2007.

[55] M. Aragonés and J. Aragones, "A theoretical and methodological approach to the study of residential satisfaction," *Journal of Environmental Psychology*, vol. 17, no. 1, pp. 47–57, 1997.

[56] J. Potter and R. Cantarero, "How does increasing population and diversity affect resident satisfaction? A small community case study," *Environment and Behavior*, vol. 38, no. 5, pp. 605–625, 2006.

[57] M. Bonaiuto, A. Aiello, M. Perugini, M. Bonnes, and A. P. Ercolani, "Multidimensional perception of residential environment quality and neighbourhood attachment in the urban environment," *Journal of Environmental Psychology*, vol. 19, no. 4, pp. 331–352, 1999.

[58] J. Bardo, "Dimensions of community satisfaction in a British new town," *Multivariate Experimental Clinical Research*, vol. 2, no. 3, pp. 129–134, 1976.

[59] M. Aragonés and J. Aragones, "Residential satisfaction in council housing," *Journal of Environmental Psychology*, vol. 10, no. 4, pp. 313–325, 1990.

[60] G. C. Galster and G. W. Hesser, "Residential satisfaction," *Environment and Behavior*, vol. 13, no. 6, pp. 735–758, 1981.

[61] J. B. Hughey and J. W. Bardo, "The structure of community satisfaction in a southeastern American city," *The Journal of Social Psychology*, vol. 123, no. 1, pp. 91–99, 1984.
[62] M. Lu, "Analyzing migration decisionmaking: relationships between residential satisfaction, mobility intentions, and moving behavior," *Environment and Planning A*, vol. 30, no. 8, pp. 1473–1495, 1998.
[63] M. Lu, "Determinants of residential satisfaction: ordered logit vs. Regression models," *Growth and Change*, vol. 30, no. 2, pp. 264–287, 1999.
[64] D. Carro, S. Valera, and T. Vidal, "Perceived insecurity in the public space: personal, social and environmental variables," *Quality & Quantity*, vol. 44, no. 2, pp. 303–314, 2010.
[65] D. Krešić, J. Mikulić, and K. Miličević, "The factor structure of tourist satisfaction at pilgrimage destinations: the case of Medjugorje," *International Journal of tourism Research*, vol. 15, no. 5, pp. 484–494, 2013.
[66] G. T. Kyle, A. Mowen, and M. Tarrant, "Linking place preferences with place meaning: an examination of the relationship between place motivation and place attachment," *Journal of Environmental Psychology*, vol. 24, no. 4, pp. 439–454, 2004.
[67] W. Tang, *The Sense of Place in Tourism Destination*, Social Science academic press, Beijing, China, 2013.
[68] Z. Wen, J. Hou, and M. Herbert, "Structural equation model test: fitting index and chi-square criterion," *Acta Psychologica Sinica*, vol. 36, no. 2, pp. 186–194, 2004.
[69] M. Wu, *Questionnaire Statistical Analysis Practice-SPSS Operation and Application*, Chongqing University Press, Chongqing, China, 2010.
[70] P. Kotler, D. Haider, and I. Rein, "There's no place like our place! the marketing of cities, regions, and nations," *Public Management*, vol. 76, pp. 15–18, 1994.
[71] M. Kozak and M. Rimmington, "Tourist satisfaction with Mallorca, Spain, as an off-season holiday destination," *Journal of Travel Research*, vol. 38, pp. 260–269, 2000.
[72] J. E. Bigné, M. I. Sánchez, and J. Sánchez, "Tourism image, evaluation variables and after-purchase behavior: inter-relationship," *Tourism Management*, vol. 22, no. 6, pp. 607–616, 2001.
[73] C. Chi and H. Qu, "Examining the structural relationships of destination image, tourist satisfaction and destination loyalty: an integrated approach," *Tourism Management*, vol. 29, pp. 624–636, 2008.

Hindawi
Complexity
Volume 2021, Article ID 6649894, 13 pages
https://doi.org/10.1155/2021/6649894

Research Article

Spatial Association and Explanation of China's Digital Financial Inclusion Development Based on the Network Analysis Method

Xiaojie Liu,[1,2] Jiannan Zhu,[1,2] Jianfeng Guo ,[1,2] and Changnan Cui[3]

[1]*Institutes of Science and Development, Chinese Academy of Sciences, Beijing 100190, China*
[2]*School of Public Policy and Management, University of Chinese Academy of Sciences, Beijing 100049, China*
[3]*National Technology Transfer Center of Chinese Academy of Sciences, Beijing 100086, China*

Correspondence should be addressed to Jianfeng Guo; guojf@casipm.ac.cn

Received 22 December 2020; Accepted 9 May 2021; Published 24 May 2021

Academic Editor: Huajiao Li

As an essential direction for developing inclusive finance, digital financial inclusion breaks through the time and space constraints of inclusive finance development and has extensive connections between different regions. However, no research has modelled the network connections and the role and position of different digital financial inclusion development regions. This study constructed the spatial association network of China's digital financial inclusion development and used the network analysis method and the quadratic assignment procedure (QAP) method to study the structural and locational properties and the influencing factors of the network. We found that (1) although the network had a relatively low density, its connectivity and stability were excellent, and the network structure is not hierarchical; (2) the centrality of some rapidly developing central and western provinces was greater than that of some developed eastern provinces; (3) developed eastern provinces played a net spillover role, driving the development of digital financial inclusion in central and western provinces; and (4) the spatial association was affected by the development level of the PC Internet and economy, the industrial structure, and the spatial adjacency. This study enriches the research on digital financial inclusion and provides a scientific basis for the formulation and implementation of policies to promote the further development of digital financial inclusion.

1. Introduction

With the recent rapid development of information technologies, the integration of digital technology and inclusive finance has continued to deepen [1, 2], further improving the accessibility and affordability of inclusive financial services and expanding its coverage [3]. Accordingly, digital financial inclusion is gradually becoming an essential direction for financial inclusion [4]. Depending on digital technology, digital financial inclusion gradually eliminates the time and space constraints for developing inclusive finance, making it possible to provide round-the-clock and full coverage financial services to any corner of the world. This trend requires a holistic approach to explore the development of digital financial inclusion. Unlike the methods used in the existing literature, we adopt a comprehensive approach to construct and analyze the network of digital financial inclusion development in this study.

Similar to financial inclusion [5], existing research on digital financial inclusion mainly focuses on its effect on economic development [6–10], poverty reduction [11–13], and financial stability [14, 15]. These studies only focus on the impact of digital financial inclusion and do not consider the possibility of connections of digital financial inclusion development between regions. This is very important because the development of inclusive finance has apparent spatial spillover effects [16], which are even more pronounced in the development of digital financial inclusion that incorporates digital technology. Guo et al. [17] studied the development of digital financial inclusion among cities in China. They found that the development of digital financial inclusion among cities has a significant positive spatial autocorrelation, that is, a significant positive spatial spillover effect. Furthermore, this effect shows an increasing trend year by year. Similarly, Shen et al. [18] took 101 countries as the research objects and found that countries

with a higher level of digital financial inclusion will influence the development of digital financial inclusion in neighboring countries through spillover effects.

Existing evidence shows that the development of digital financial inclusion is widely connected in different regions. Therefore, it should be regarded as a digital service network that provides around-the-clock and full coverage financial services when studying it. However, to the best of our knowledge, no research explicitly models the network connections and the role and position of different digital financial inclusion development regions. Therefore, this study takes China, the world's largest digital financial inclusion market [19], as the research object and attempts to fill this gap by constructing a spatial association network of digital financial inclusion development. Meanwhile, we use the network analysis method and the quadratic assignment procedure (QAP) method to study the structural and locational properties and the influencing factors of the network in order to identify the spatial characteristics and the critical influencing factors of the development of digital financial inclusion. All findings provide an essential scientific basis for the formulation and implementation of policies for further developing digital financial inclusion, which is vital to realize the sustainable development of inclusive finance.

2. Methods and Data

2.1. Construction of the Spatial Association Network. China's spatial association network for the development of digital financial inclusion comprises relationships of digital financial inclusion development between provinces. In the network, the nodes are provinces, and the edges are relationships. The key to constructing a spatial association network is to depict the spatial associations between provinces. According to the research of Mantegna [20], we define a spatial metric through the function of the correlation coefficient and then use this spatial metric (Euclidean distance in this study) as a distance to construct these relationships. The appropriate function is

$$D_{ij} = \sqrt{2\left(1 - C_{ij}\right)}, \tag{1}$$

where $i, j = 1, 2, \ldots, N$ represents any two different provinces in the 31 provinces (municipalities and autonomous regions collectively referred to as "provinces," excluding Hong Kong, Macao, and Taiwan); D_{ij} is the Euclidean distance between province i and j; C_{ij} is the correlation coefficient between two vectors, concretely given by the following formula:

$$C_{ij} = \frac{\sum_{t=1}^{T}\left(x_{it} - \overline{x_i}\right)\left(x_{jt} - \overline{x_j}\right)}{\sqrt{\sum_{t=1}^{T}\left(x_{it} - \overline{x_i}\right)^2 \sum_{t=1}^{T}\left(x_{jt} - \overline{x_j}\right)^2}}, \tag{2}$$

where $x_{it} = (x_{i1}, x_{i2}, \ldots, x_{it}, \ldots, x_{iT})$ and $x_{jt} = (x_{j1}, x_{j2}, \ldots, x_{jt}, \ldots, x_{jT})$, respectively, denote China's digital financial inclusion index of provinces i and j from $t = 1$ to $t = T$.

Motivated by the research of Yang and Liu [21], we can acquire the spatial association matrix between provinces according to equation (3) after obtaining the Euclidean distance matrix.

$$Q(i, j) = \begin{cases} 1, & Q_{ij} \geq \dfrac{1}{N}\sum_{j=1}^{N} Q_{ij}, \\ 0, & Q_{ij} < \dfrac{1}{N}\sum_{j=1}^{N} Q_{ij}, \end{cases} \tag{3}$$

where $Q(i, j)$ represents the spatial association between provinces i and j; Q_{ij} represents the reciprocal of D_{ij}; and the spatial association matrix $Q(i, j)$ equals to $(Q_{ij})_{N\times N}$. Considering that the calculated spatial association matrix is asymmetric, the spatial association network of the digital financial inclusion development we constructed is directional. In addition, compared with traditional network construction methods, our approach eliminates the disadvantage in which the gravity model and the VAR Granger causality model are susceptible to multiple factors [21].

2.2. Characterization of the Spatial Association Network

2.2.1. Whole Network. In this study, we take four indicators, that is, network density, network connectedness, network hierarchy, and network efficiency, to measure the structural characteristics of the whole network of digital financial inclusion development [22].

Network density is an indicator that reflects the interconnectedness of the provinces in the network [23]. It can be defined as the ratio of actual relationships to the total possible relationships, and its calculation formula is as follows:

$$\text{density} = \frac{L}{N \times (N - 1)}, \tag{4}$$

where L denotes the actual number of relationships; N represents the network's size.

Network connectedness is used to measure the reachability between provinces in the network. If some provinces are not accessible to each other, then the network's connectedness must be small, whereas if the provinces can be directly and indirectly accessible to each other, the network's connectedness must be large. Therefore, network connectedness can be calculated as follows:

$$\text{connectedness} = 1 - \frac{2V}{N \times (N - 1)}, \tag{5}$$

where V represents the number of unreachable node pairs in the network; N represents the network's size.

Network hierarchy can measure the extent to which each province in the network is asymmetrically connected to the other, thereby reflecting the hierarchical status of each province. Specifically, its calculation formula is as follows:

$$\text{hierarchy} = 1 - \frac{P}{\max(P)}, \tag{6}$$

where P denotes the number of symmetrically reachable node pairs in the network; $\max(P)$ denotes the maximum possible number of symmetrically reachable node pairs.

Network efficiency refers to the extent to which redundant connections exist in the network. In our spatial association network, the lower the network efficiency, the more the relationships between provinces and the more the spatial spillover channels for the development of digital financial inclusion. The calculation formula of network efficiency is as follows:

$$\text{efficiency} = 1 - \frac{Q}{\max(Q)}, \tag{7}$$

where Q represents the number of excess connections in the network; $\max(Q)$ represents the maximum possible number of redundant connections.

2.2.2. Centrality. As for the locational characteristics of each province in the spatial association network of digital financial inclusion development, we focus on three aspects, namely, degree centrality, betweenness centrality, and closeness centrality [24], which can be used to measure the connectivity, intermediation, and accessibility [25] of different provinces in the network.

Degree centrality measures the extent to which a province is in direct contact or is adjacent to many other provinces in the network. It can be defined as the ratio of the number of provinces directly connected to a province to the number of provinces most likely to be directly connected to the province. Degree centrality can be calculated as follows:

$$C_{\text{deg}}(i) = \frac{n(i)}{N-1}, \tag{8}$$

where $C_{\text{deg}}(i)$ denotes the degree centrality of province i; $n(i)$ denotes the number of provinces directly connected to the province i in the network; N represents the size of the network.

Betweenness centrality measures the extent to which a province is in the middle of other provinces in the network and reflects the degree of control of a province on the interconnection between other provinces. Its calculation formula is as follows:

$$C_{\text{btw}}(i) = \frac{2\sum_{J}^{N}\sum_{k}^{N} b_{jk}(i)}{N^2 - (3N+2)}, \tag{9}$$

where

$$b_{jk}(i) = \frac{d_{jk}(i)}{d_{jk}}, \tag{10}$$

where $C_{\text{btw}}(i)$ represents the betweenness centrality of province i; d_{jk} represents the number of shortest paths between provinces j and k; $d_{jk}(i)$ represents the number of shortest paths that pass through province i and connect provinces j and k; N represents the size of the network.

Closeness centrality measures the closeness between provinces in the network and represents a measure not controlled by other provinces. If a province in the network is close to all other provinces, that province has a high closeness centrality. The calculation formula of closeness centrality is as follows:

$$C_{\text{close}}(i) = \frac{\sum_{j=1}^{N} d_{ij}}{N-1}, \tag{11}$$

where $C_{\text{close}}(i)$ denotes the closeness centrality of province i; d_{ij} denotes the shortest path between provinces i and j; N represents the size of the network.

2.2.3. Block Model. Block model analysis was first proposed by White, Boorman, and Breiger to better analyze the role and position of each province in the spatial association network [26]. On the basis of this method, 31 provinces can be divided into four blocks: the first one is the "primary beneficial" block. Its members have more relations within the block and fewer relations outside the block. The second one is the "net spillover" block. Its members mainly send out relations to other blocks. However, few relations are received from other blocks. The third one is the "bidirectional spillover" block, in which members send relations outside and inside the block. The fourth one is the "broker" block. Its members receive relationships from the members of the outside block and send them to the other block members; however, the internal members have relatively few connections.

Accordingly, we use UCINET software and the CONCOR method to divide the 31 provinces in the spatial association network of digital financial inclusion development into the four blocks mentioned above in this study.

2.3. Quadratic Assignment Procedure

2.3.1. Theoretical Model. On the one hand, digital finance can theoretically break through the limitations of traditional geographic space to provide people with financial services in remote areas cheaply and conveniently; on the other hand, the promotion of many businesses of digital finance still depends on geographical factors and its development also shows a robust spatial clustering [17]. Therefore, we speculate that the geographical adjacency may increase the probability of establishing the spatial association of digital financial inclusion development between provinces. Besides, as a new form of financial development, digital finance still follows the fundamental laws of financial development; that is, its development still relies on the real economy and traditional finance [27]. Meanwhile, the development of digital finance also depends to no small extent on the development of information technology [28] and mobile technology [1, 6, 11]. Moreover, tertiary industries have more digital finance demand than primary and secondary industries when considering the industrial structure. Hence, we speculate that the differences between provinces in terms of the development level of the economy, traditional finance and the Internet (PC Internet and mobile Internet), and the industrial structure may also affect the establishment of the spatial association of digital financial inclusion development between provinces.

In summary, we consider five kinds of factors to study the influencing factors of the spatial association of digital financial inclusion development. The specific information on these factors and their representative indicators is shown in Table 1.

Accordingly, we set up the following model:

$$R = f(S, E, F, N, M, I). \tag{12}$$

Equation (12) expresses the relationship between relational data, and these relational data consist of a series of matrices. The dependent variable R is the spatial association network of digital financial inclusion development; the corresponding spatial association matrix directly represents it. The independent variable S is the spatial adjacency matrix determined by the geographical location. If two provinces are adjacent in the spatial adjacency matrix, then the value is 1; otherwise, the value is 0. For the remaining variables, we take the average value of the corresponding indicator of each province during the sample period and then use the absolute difference of those average values to construct the difference matrix.

2.3.2. QAP Analysis Method. Given that our empirical data are relational, it contains attribute information and relational structure [29] and does not satisfy the assumption of "variable independence" in the sense of conventional statistics. Hence, most multivariate statistical methods cannot be used. In this study, we adopt a nonparametric QAP method, which can be used for hypothesis testing at the relationship-relationship level, to study the influencing factors of the spatial association network. QAP analysis includes QAP correlation analysis and QAP regression analysis.

QAP correlation analysis, which is based on the replacement of matrix data, is a method of comparing the similarity of the grid values in two square matrices and, at the same time, performing a nonparametric test [30]. The specific practice has the following three steps: first, the correlation coefficient between the long vectors formed by the known matrices is calculated. Next, the rows and corresponding columns of one matrix are randomly replaced simultaneously, and then the correlation coefficient between the replaced matrix and the other matrix is calculated. Repeating this process hundreds or even thousands of times obtains a distribution of correlation coefficients. Lastly, by comparing the actual correlation coefficient calculated in the first step with the distribution of the correlation coefficient calculated under random rearrangement, we can see whether the actual correlation coefficient falls into the rejection domain or the acceptance domain and then make a judgment.

The principle of QAP regression analysis is the same as that of QAP correlation analysis. The purpose of the QAP regression analysis is to study the regression relationship between multiple matrices and one matrix and evaluate the significance of the determination coefficient R^2. The specific calculation has two steps. First, regular multiple regression analysis is performed on the long vector corresponding to the independent and dependent variable matrix. Secondly, the rows and corresponding columns of the dependent variable matrix are randomly permutated simultaneously, and then the regression is recalculated. This step is repeated hundreds or even thousands of times to estimate the standard error of the statistics.

2.4. Data Sources. The core data used in this study are the "Peking University Digital Financial Inclusion Index of China," which is compiled on the basis of hundreds of millions of microdata from a representative digital financial institution in China; this dataset reflects the cross-section and cross-time changes in the acquisition and use of digital financial services in China [31]. The index covers 31 provinces, 337 prefecture-level cities (regions, autonomous prefectures, and leagues collectively referred to as "cities"), and nearly 2,800 counties (county-level cities, banners, and municipal districts collectively referred to as "counties"). The province-level and prefecture-level index span from 2011 to 2018, and the county-level index spans from 2014 to 2018. In addition to the overall index, the "Peking University Digital Financial Inclusion Index of China" also includes the coverage breadth subindex, the use depth subindex, and the digitization degree subindex [32]. Hence, the "Peking University Digital Financial Inclusion Index of China" can comprehensively portray the development trend of digital financial inclusion in different regions of China. However, to reflect the spatial association of China's digital financial inclusion development from a general view, we only consider the provincial overall index in our study. The other QAP analysis data come from the "China Statistical Yearbook" and "China Financial Statistical Yearbook." Besides, to remove the temporal trend, we also process the data logarithmically.

3. Analysis of Results

3.1. Empirical Results and Analysis of the Spatial Association Network. To study the structural and locational properties of spatial association network of digital financial inclusion development intuitively and clearly, we use NetDraw software to draw a diagram, as shown in Figure 1. From the figure, we can see that the associations between the 31 provinces are dense. Meanwhile, the developed eastern provinces are mainly located on the network's right, whereas the central and western provinces are interwoven in the middle and left sides of the network.

3.1.1. Whole Network Analysis. The emphasis of the whole network analysis is on the structural characteristics of the spatial association network of digital financial inclusion development and its impact on the development of the provinces within the network.

Network density describes the number of spatial associations in the network. In the spatial association network of digital financial inclusion development, the maximum possible association between 31 provinces is 930, and the actual existing association is 359; hence, according to

Table 1: Variables and indicators.

Variable		Indicator	Variable description
Dependent variable	Network relations	Spatial association network of digital financial inclusion development (R)	Spatial association matrix of digital financial inclusion development
Independent variable	Spatial adjacency relations	Spatial adjacency relation (S)	Spatial adjacency matrix
	Economic development level	Difference in per capita GDP (E)	Per capita GDP difference matrix
	Traditional finance development level	Difference in the total credit balance of financial institutions per unit of GDP (F)	Total credit balance of financial institutions per unit of GDP difference matrix
	PC Internet development level	Difference in the Internet penetration rate (N)	Internet penetration rate difference matrix
	Mobile Internet development level	Difference in the mobile phone penetration rate (M)	Mobile phone penetration rate difference matrix
	Industrial structure	Difference in the tertiary industry output value per unit of GDP (I)	Tertiary industry output value per unit of GDP difference matrix

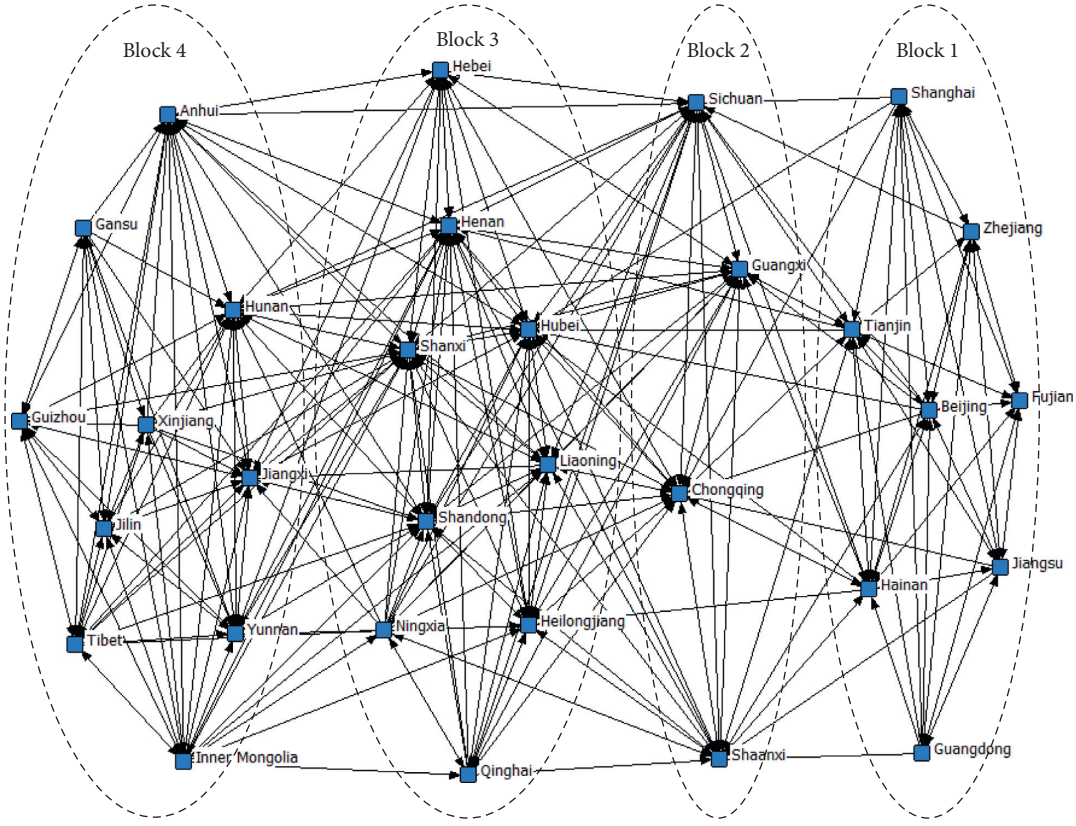

Figure 1: Spatial association network of China's digital financial inclusion development from 2011 to 2018.

formula (4), the network density is 0.386. This result reflects that the degree of interconnectedness between provinces regarding digital financial inclusion development is relatively low. It can be seen that the situation of direct and comprehensive communication and the mutually beneficial cooperation in terms of digital financial inclusion between provinces within the network are not optimistic.

Network connectedness, network hierarchy, and network efficiency describe the pattern of spatial associations in the network. On the basis of formulas (5)–(7), the network connectedness, network hierarchy, and network efficiency of the spatial association network for the digital financial inclusion development can be calculated. The network connectedness is 1, indicating that the network has a high relational degree and

good connectivity. In other words, this result implies that the provinces in the network can be directly and indirectly accessible to each other to a large extent. The network hierarchy is 0, indicating no hierarchical structure of spatial associations and spatial spillover effects between provinces in the network; that is, spatial associations and spatial spillover effects could also exist between provinces with the different development level of digital financial inclusion. The network efficiency is 0.577, indicating the existence of multiple overlapping overflow channels of digital financial inclusion development between provinces in the network; hence, the network structure is relatively stable. On the whole, the current spatial association pattern of high connectivity, nonhierarchy, and strong stability is very conducive to the exchange of information and the sharing of resources between provinces regarding the development of digital financial inclusion.

3.1.2. Centrality Analysis. Centrality analysis is to describe and measure the locational characteristics of each province in the spatial association network of the development of digital financial inclusion. Provinces that are more important or prominent in terms of connectivity, intermediation, and accessibility occupy the more central and vital location in the network.

Based on formula (8), the calculation results of degree centrality show that provinces with the degree centrality greater than 50 have the most considerable effect on other provinces in the development of digital financial inclusion. Besides, in terms of connectivity, these provinces are at the core of China's spatial association network of digital financial inclusion development. Among these provinces, the rapidly developing central and western provinces (Shanxi, Henan, Hubei, Sichuan, Hunan, Chongqing, Inner Mongolia, Anhui, Jiangxi, Guangxi, Shaanxi, and Ningxia) account for more than 85%. These provinces are in direct contact or are adjacent to many other provinces and could be recognized by other provinces as major channels to transmit digital financial inclusion development information. However, the degree centrality of eastern coastal provinces, such as Shanghai, Jiangsu, Zhejiang, Guangdong, and Fujian, is relatively low, which indicates that these economically developed provinces have limited direct or indirect spatial connections with other provinces in terms of digital financial inclusion development; hence, these provinces are in a relatively marginal location with respect to connectivity in the network. Part of the reason for this phenomenon lies with the fact that the aforementioned central and western provinces are located in the middle of China's geographic space. Therefore, relying on the geographical advantage of connecting east-west and north-south, these provinces can strengthen connections with more provinces in the development of digital financial inclusion, thereby establishing more spatial associations. In contrast, restricted by geographical conditions, the aforesaid eastern provinces have more connections with the central provinces and fewer connections with the western provinces. As a result, these provinces only establish the spatial associations of digital financial inclusion with fewer provinces.

According to the results of betweenness centrality calculated on the basis of formulas (9) and (10), the average betweenness centrality of 31 provinces is 29.548; the betweenness centrality of 15 provinces is higher than the average. Among them, the Shaanxi, Sichuan, and Shanxi provinces are the most critical nodes because they have the highest betweenness centrality. These three relatively fast-developing central and western provinces play an essential role in neighboring provinces and have a strong ability to control interprovincial digital financial inclusion development. In other words, these provinces are in the central location with respect to intermediation and play the critical "intermediary" and "bridge" role in the spatial association network, connecting the development of digital financial inclusion in eastern and western provinces. This phenomenon may be inseparable from the geographical advantage of these provinces. These provinces are located not only in the middle of China's geographic space but also along the Heihe-Tengchong Line which represents China's demographic, geographic, and economic boundaries. Therefore, relying on the advantage of "intermediary" and "bridge" in geographical location, these provinces occupy the central location in terms of intermediation and control the cooperation in digital financial inclusion between other provinces in the network. The betweenness centrality of Guizhou, Gansu, Jiangsu, Zhejiang, Qinghai, Fujian, Guangdong, and Xinjiang are all less than 5. Among them, half of the provinces are in the developed eastern region, whereas the other half is in the underdeveloped western region. However, these provinces all have relatively limited influence on neighboring provinces in the development of digital financial inclusion. This phenomenon may be caused by these provinces being located at the edge of China's geographic space; hence, they are not dominant geographically. This is also reflected in their location in the spatial association network; that is, these provinces are at the edge of the network, so they have weak abilities to control the digital financial inclusion cooperation between other provinces.

According to the calculation results of closeness centrality based on formula (11), the mean value of 31 provinces is 60.055; 15 provinces have a higher value than the average. Among them, rapidly developing central and western provinces (Shanxi, Hunan, Hubei, Sichuan, Guangxi, Chongqing, Hunan, Shaanxi, Ningxia, Heilongjiang, Anhui, Jiangxi, and Qinghai) account for more than 86%. These provinces are relatively close to other provinces in the spatial association network; that is, they can quickly interact with other provinces regarding digital financial inclusion development. Hence, these provinces occupy the central location with respect to accessibility of the spatial association network of digital financial inclusion development and are the central actors. It is worth noting that these provinces are almost the same as the central and western provinces with a degree centrality greater than 50. Therefore, these provinces that occupy the central location of the spatial association network can also be attributed to their superior location which connects east-west and north-south. Due to this locational advantage, these provinces can establish closer

spatial associations with other provinces in terms of digital financial inclusion development. The last ten provinces are Beijing, Shanghai, Xinjiang, Jilin, Guizhou, Zhejiang, Jiangsu, Guangdong, Gansu, and Fujian. Among these provinces, the eastern provinces account for 60%, and the central and western provinces account for 40%. However, they are all marginal actors in the spatial association network and may need to rely on other provinces to relay digital financial inclusion development information. This may also be because these provinces are located at the edge of China's geographic space (i.e., eastern and western regions). Therefore, they need to rely on the central provinces to establish spatial associations with other provinces.

It can be seen from the above analysis that some rapidly developing central and western provinces occupy the central location in terms of connectivity, intermediation, and accessibility in the spatial association network of China's digital financial inclusion development. In addition to being affected by geographical factors, we believe that this kind of locational characteristics of the spatial association network is also affected by policy factors to a certain extent. At the end of 2015, the Chinese government issued the "Plan for Promoting Inclusive Finance Development (2016–2020)," making more specific arrangements for inclusive finance development. Correspondingly, the Ministry of Finance of China began to implement the plan in 2016 by allocating special funds for the development of inclusive finance to all provinces. As shown in Figure 2, from 2016 to 2018, the Ministry of Finance of China mainly allocated special funds to provinces such as Yunnan, Henan, Shaanxi, Hubei, Jiangxi, Hunan, Guizhou, Gansu, Sichuan, and Anhui. These provinces are all located in the central and western regions of China, reflecting the Chinese government's strong support for developing inclusive finance in central and western provinces. Since digital financial inclusion is an essential direction of inclusive finance, the development of digital financial inclusion in central and western provinces accelerates accordingly, which helps these provinces establish more spatial associations with other provinces. Overall, the central and western provinces have occupied the central location in the spatial association network of China's digital financial inclusion development mainly due to their superior geographical location and strong government support.

3.1.3. Block Model Analysis. The focus of block model analysis is to identify and determine the role and position of each province in the spatial association network of the development of digital financial inclusion so as to find the "subgroups" in the network. Using UCINET software and setting the maximum segmentation depth and convergence criterion to 2 and 0.2, respectively, four digital financial inclusion development blocks can be obtained (as shown in Figure 1). Block 1 has eight members, all located in the economically developed eastern region, including Beijing, Tianjin, Jiangsu, Guangdong, Zhejiang, Hainan, Fujian, and Shanghai. Block 2 has four members, all of which are relatively fast-developing western provinces, namely, Guangxi, Chongqing, Sichuan, and Shaanxi. Block 3 has nine members, including provinces with strong economic growth (Hebei, Shandong, Henan, Hubei, and Liaoning) and provinces with relatively slow economic growth (Qinghai, Shanxi, Heilongjiang, and Ningxia). Block 4 has ten members, mainly the relatively backward provinces in the central and western regions, namely, Jilin, Inner Mongolia, Hunan, Yunnan, Tibet, Guizhou, Gansu, Jiangxi, Anhui, and Xinjiang.

In the actual 359 associations in the spatial association network, the number of associations within the four blocks is 198, and the number of associations between the four blocks is 161, demonstrating the existence of spatial associations and spillover effects between the blocks. Specifically, according to Table 2, we can observe that Block 1 sends 24 relationships to other blocks but only receives 9 relationships from Block 2. The number of relationships that Block 1 sends out to the other blocks is approximately three times the number of relationships that is received from the other blocks. Therefore, Block 1 can be considered as a "net spillover" block. Block 2 receives 55 relationships from other blocks and simultaneously sends 40 relationships to other blocks; however, there are only a few relationships between the internal members of Block 2. Therefore, Block 2 is a typical "broker" block. Block 3 sends 60 relationships to other blocks and receives 69 relationships from other blocks; the expected internal relation ratio is 26.67%, and the actual internal relation ratio is 48.72%. Hence, Block 3 fits the condition of a "primary beneficiary" block. Block 4 sends 75 relationships within the block and 37 relationships to other blocks. The expected internal relation ratio is 30.00%, and the actual internal relation ratio is 66.96%. Thus, Block 4 meets the condition of a "bidirectional spillover" block.

According to the distribution of the associations between blocks, the density matrix (as shown in Table 3) can be calculated to reflect the distribution of spillover effects among blocks. With the entire network density being 0.386, there will be a tendency to concentrate in the block when the density of one block is greater than 0.386. Hence, by assigning a value greater than 0.386 in the density matrix as 1, otherwise, assigning as 0, the image matrix as shown in Table 4 can be obtained. The image matrix can clearly show the spillover effects between blocks. According to Tables 3 and 4, we can observe that the spillover effect of Block 1 is mainly reflected in itself and Block 2, that of Block 2 is mainly reflected in itself and Block 3, and that of Block 3 is mainly reflected in itself and Block 2. By contrast, the spillover effect of Block 4 is only reflected in itself.

The image matrix also clearly shows the transmission mechanism of the development of digital financial inclusion in China. Figure 3 shows that, first of all, the development of China's digital financial inclusion has a noticeable "club" effect. This indicates that abundant associations exist within each block; that is, the members within the block are closely related to each other. Second, Block 1 is the engine for the development of China's digital financial inclusion and transmits the development's momentum to Block 2. Third, as an important "bridge" and "link," Block 2 transmits the development's momentum to Block 3. And next, part of the development's momentum is returned to Block 2 by Block 3. Hence, it can be seen that this transmission mechanism has the characteristics of gradient spillover and bidirectional spillover. Overall, the members of Block 1 (Beijing, Tianjin, Jiangsu, Guangdong, Zhejiang, Hainan, Fujian, and

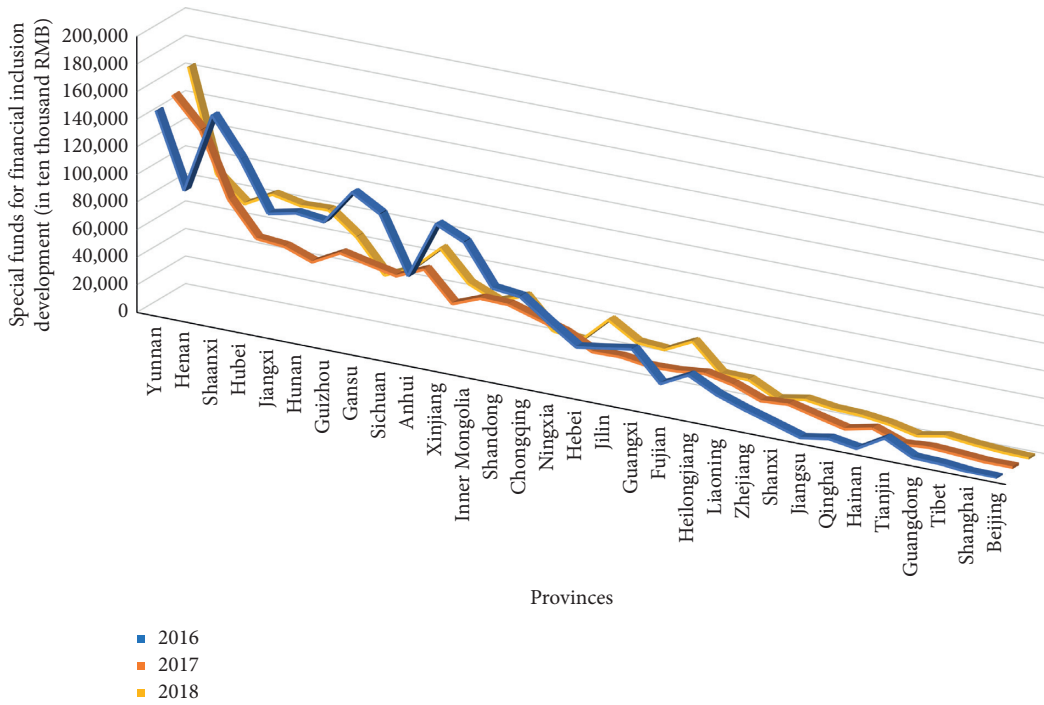

Figure 2: The allocation of special funds for financial inclusion development in various provinces in China from 2016 to 2018.

Table 2: Analysis of spillover effects between various blocks.

Block	Block 1	Block 2	Block 3	Block 4	Block membership	Expected internal relation ratio (%)	Actual internal relation ratio (%)	Total relations received from other blocks	Total relations sent to other blocks	Block role
Block 1	54	18	6	0	8	23.33	69.23	9	24	Net spillover
Block 2	9	12	29	2	4	10.00	23.08	55	40	Broker
Block 3	0	34	57	26	9	26.67	48.72	69	60	Primary beneficial
Block 4	0	3	34	75	10	30.00	66.96	28	37	Bidirectional spillover

Table 3: Density matrix of the blocks.

	Block 1	Block 2	Block 3	Block 4
Block 1	0.964	0.563	0.083	0.000
Block 2	0.281	1.000	0.806	0.050
Block 3	0.000	0.944	0.792	0.289
Block 4	0.000	0.075	0.378	0.833

Table 4: Image matrix of the blocks.

	Block 1	Block 2	Block 3	Block 4
Block 1	1	1	0	0
Block 2	0	1	1	0
Block 3	0	1	1	0
Block 4	0	0	0	1

Shanghai) serving as the engine are all located in the developed eastern region with rapid economic growth and financial development. Therefore, these provinces can lead other provinces in the development of digital financial inclusion based on their economic and financial development advantages. However, the driving effect of Block 1 on Block 3 (economically developed areas and economically backward areas) is not directly realized but indirectly realized through Block 2 (relatively fast-developing western provinces).

3.1.4. Method Effectiveness Analysis. In graph theory, Minimum Spanning Tree (MST) is a standard approach used to describe network structure. A network constructed based on the MST approach can intuitively reflect the most critical connections and information between nodes in the network with the simplest structure [20, 33, 34]. Therefore, we refer to

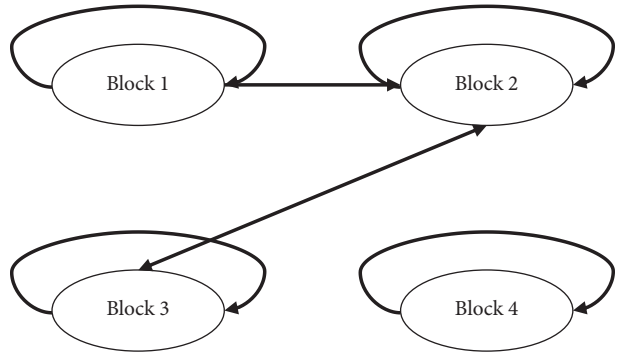

Figure 3: Relationship between China's four digital financial inclusion development blocks.

the work of Yang and Liu [21] and verify the effectiveness of our method of constructing the network mentioned above by establishing a network based on the MST method. The basis of the network, which is constructed on the basis of the MST method, is also the correlation coefficient. After calculating the correlation coefficient in accordance with equation (2), we can convert it into Euclidean distance in accordance with equation (1). Then, we can use Prim's algorithm to construct MST [35].

The concise network of digital financial inclusion development in China built based on the MST method is shown in Figure 4. Figure 4 provides some convincing information. Except for Chongqing, the role and position of other provinces in the network constructed based on the MST method are basically the same as before. In this tree structure, the eight developed eastern provinces (i.e., Guangdong, Jiangsu, Fujian, Beijing, Zhejiang, Shanghai, Tianjin, and Hainan) are clustered in Block 1 on the upper right. Block 2 connected to Block 1 includes three relatively fast-developing western provinces, that is, Shaanxi, Guangxi, and Sichuan. Their structure of association is relatively simple. As a critical node, Hebei is connected to Blocks 3 and 4. Compared with the previous network, besides five provinces with strong economic growth (Hebei, Shandong, Henan, Hubei, and Liaoning) and four provinces with relatively slow economic growth (Qinghai, Shanxi, Heilongjiang, and Ningxia), Block 3 also includes Chongqing which used to belong to Block 2. Block 4 is the same as before and mainly includes Jilin, Inner Mongolia, Hunan, Yunnan, Tibet, Guizhou, Gansu, Jiangxi, Anhui, and Xinjiang, which are relatively underdeveloped central and western provinces. Moreover, Block 1 and Block 3 are not directly connected but indirectly connected through Block 2.

In conclusion, by comparing the network constructed based on our method with the network constructed based on the MST approach, we find that the role and position of the provinces in the network are basically the same as before. Therefore, the effectiveness of our network construction method is well confirmed.

3.2. Influencing Factors of the Spatial Association Network

3.2.1. QAP Correlation Analysis. We use UCINET software and select 5000 random permutations to test the correlation between the spatial association matrix and the matrices of the influencing factors, and the results obtained are shown in Table 5. In Table 5, "Value" represents the actual correlation coefficients between the spatial association matrix and the influencing factor matrices; "Significance" represents the significance level; "Average" and "Std. dev" represent the average value and the standard deviation of the correlation coefficients calculated from 5000 random permutations; "Min" and "Max" denote the minimum and maximum values in the randomly calculated correlation coefficients; "Prop $\geqq 0$" and "Prop $\leqq 0$" indicate the probability that the correlation coefficients of these random calculations are no less than and no more than the actual correlation coefficients, respectively.

The QAP correlation analysis results show a significantly positive correlation between the spatial association matrix R and the spatial adjacency matrix S, with a correlation coefficient of 0.123. This result indicates that the geographical adjacency between provinces has a significantly positive effect on the spatial association and spatial overflow between provinces. The correlation coefficients between the spatial association matrix R and the other difference matrices reflecting the development level of the economy, traditional finance and the Internet (PC Internet and mobile Internet), and the industrial structure are all significantly negative. This result means that these four kinds of critical factors also affect the spatial association and spatial spillover between provinces.

Furthermore, we perform a QAP correlation analysis on the matrices of the influencing factor. The results in Table 6 show that the matrices of influencing factors are highly correlated and statistically significant. Therefore, the effect of these influencing factors on spatial association matrix R may overlap, which is a characteristic of relational data. Hence, we must use the QAP method to deal with the "multicollinearity" problem between these relational data.

3.2.2. QAP Regression Analysis. We use UCINET software and select 5000 random permutations to test the effect of the matrices of various influencing factors on the spatial association matrix R, and the results obtained are shown in Tables 7 and 8. The model-fitting results in Table 7 show that the determination coefficient is 0.142, and its adjusted value is 0.137. This result indicates that when a linear relationship

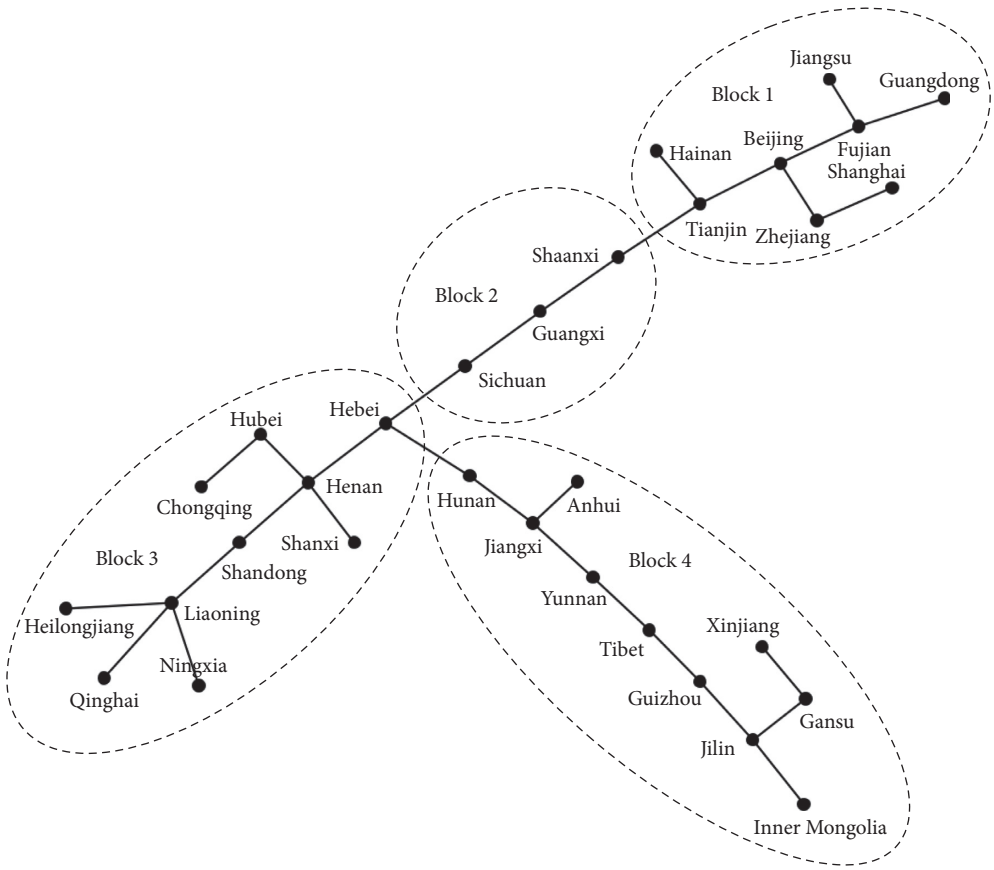

Figure 4: Network structure of digital financial inclusion development in China from 2011 to 2018 based on the MST approach.

Table 5: QAP correlation analysis of spatial association matrix R and its influencing factor matrices.

Variable	Value	Significance	Average	Std. dev	Min	Max	Prop ≥ 0	Prop ≤ 0
S	0.123^{***}	0.007	0.000	0.043	−0.151	0.166	0.007	0.995
E	-0.315^{***}	0.000	−0.001	0.050	−0.207	0.138	1.000	0.000
F	-0.098^{**}	0.038	−0.000	0.051	−0.257	0.136	0.963	0.038
N	-0.335^{***}	0.000	−0.000	0.051	−0.270	0.137	1.000	0.000
M	-0.246^{***}	0.000	−0.001	0.054	−0.205	0.157	1.000	0.000
I	-0.109^{**}	0.021	0.000	0.056	−0.172	0.154	0.980	0.021

Note. *** and ** denote significance at 1% and 5% levels, respectively.

exists between the spatial association matrix R and the influencing factor matrices that we considered in this study, the matrices of the influencing factors with a significant influence can explain 13.7% of the variation of the spatial association matrix R.

The regression coefficients and the test indicators of each variable are shown in Table 8. In Table 8, "Unstandardized coefficient" and "Standardized coefficient" represent the unstandardized and standardized regression coefficients of the variable matrices; "Significance" represents the significance level; "Prop ≧ 0" and "Prop ≦ 0" indicate the probability that these randomly calculated regression coefficients are no less than and no more than the actual regression coefficients, respectively. The results show that the regression coefficients of difference matrices N and E, −0.236 and −0.171, are both significantly negative at the 1% significance level, indicating that when the difference of the development level of the PC Internet and economy decreases by 1%, the probability of establishing the spatial association between two provinces can be increased by 0.236% and 0.171%, respectively. The regression coefficient of difference matrix I is 0.195 and significant at the 1% significance level, indicating that when the industrial structure's difference increases by 1%, the probability of building two provinces' spatial association can be increased by 0.195%. The regression coefficient of spatial adjacency matrix S is 0.062 and significant at the 10% significance level, indicating that if two provinces are adjacent, the probability of establishing the spatial association between these two provinces can be increased by 0.062%, whereas the regression coefficients of difference matrices M and F are insignificant, indicating that the difference in the development level of the mobile Internet

Table 6: QAP correlation analysis between influencing factors matrices.

Variable	S	E	F	N	M	I
S	1.000***	−0.148***	−0.115***	−0.151***	−0.108***	−0.079**
E	−0.148***	1.000***	0.270***	0.710***	0.550***	0.453***
F	−0.115***	0.270***	1.000***	0.324***	0.476***	0.667***
N	−0.151***	0.710***	0.324***	1.000***	0.790***	0.546***
M	−0.108***	0.550***	0.476***	0.790***	1.000***	0.723***
I	−0.079**	0.453***	0.667***	0.546***	0.723***	1.000***

Note. *** and ** denote significance at 1% and 5% levels, respectively.

Table 7: Results of model fitting.

R^2	Adjusted R^2	Observations	Permutations
0.142	0.137	930	5000

Table 8: QAP regression results of spatial association matrix R and its influencing factor matrices.

Variable	Unstandardized coefficient	Standardized coefficient	Significance	Prop ≧ 0	Prop ≦ 0
Interception	0.386	0.000	—	—	—
S	0.085	0.062*	0.061	0.061	0.940
E	−0.247	−0.171***	0.006	0.994	0.006
F	−0.095	−0.066	0.117	0.883	0.117
N	−1.136	−0.236***	0.005	0.995	0.005
M	−0.002	−0.068	0.210	0.791	0.210
I	1.087	0.195***	0.007	0.007	0.994

Note. *** and * denote significance at 1% and 10% levels, respectively.

and traditional finance has almost no effect on the spatial association between provinces.

4. Conclusions and Implications

This study constructs a spatial association network of digital financial inclusion development and uses the network analysis method and the QAP method to analyze the network's structural and locational properties and the influencing factors. Concretely, we first set up a spatial association network based on the Euclidean distance; then, we study the structural and locational properties of the network and the role and position of the provinces within the network through the analysis of the whole network, centrality, and block model; lastly, we explore the influencing factors of the spatial association by using the QAP method. According to the research results, we draw the following conclusions:

(1) The spatial association network of China's digital financial inclusion development has high connectivity, nonhierarchy, and strong stability; however, its density is relatively low. Hence, further communication and cooperation between provinces to develop digital financial inclusion can still be promoted. The centrality of some rapidly developing central and western provinces located in the middle of China's geographic space is relatively high. By contrast, the centrality of some developed eastern provinces is relatively low. We believe that this result is mainly affected by geographical factors and policy factors. On the one hand, based on the geographical advantage of connecting east-west and north-south, these rapidly developing central and western provinces are able to establish spatial associations with more provinces for the development of digital financial inclusion. On the other hand, relying on the strong support of the Chinese government, digital financial inclusion in the central and western provinces has made considerable progress, which has also promoted the establishment of spatial associations with more provinces.

(2) Provinces in the spatial association network of China's digital financial inclusion development can be roughly divided into four blocks. As a net spillover block, Block 1 includes eight developed eastern provinces: Beijing, Tianjin, Jiangsu, Guangdong, Zhejiang, Hainan, Fujian, and Shanghai. Block 2 plays the role of the broker and is composed of four relatively fast-developing western provinces, which are located in the middle of China's geographic space (i.e., Guangxi, Chongqing, Sichuan, and Shaanxi). Block 3 is the primary beneficiary block, including provinces with strong economic growth (i.e., Hebei, Shandong, Henan, Hubei, and Liaoning) and provinces with relatively slow economic growth (i.e., Qinghai, Shanxi, Heilongjiang, and Ningxia). Block 4 consists of relatively backward provinces in the central and western regions (i.e., Jilin, Inner

Mongolia, Hunan, Yunnan, Tibet, Guizhou, Gansu, Jiangxi, Anhui, and Xinjiang) and plays the role of bidirectional spillover in the network. Among the four blocks, Block 1 is the engine that promotes the digital financial inclusion development in China, and its driving effect on Block 3 is not directly realized but indirectly realized through Block 2.

(3) The similarity in the development level of the PC Internet and economy, the difference in the industrial structure, and the spatial adjacency are the main influencing factors of the interprovincial spatial association of China's digital financial inclusion development. On the contrary, the interprovincial spatial association of China's digital financial inclusion development is hardly affected by the development level of the mobile Internet and traditional finance. Among these influencing factors, it is worth noting that, first of all, spatial adjacency is still an important factor affecting the spatial association. This reflects that although digital financial inclusion can break through the limitations of time and space, its development is still influenced by the geographical factor to some extent. Second, the development level of traditional finance hardly affects the spatial association, indicating that although digital financial inclusion still follows the essence of financial development, its development does not mainly depend on the development level of traditional finance.

The policy implications of the conclusion are as follows: First of all, based on the characteristics of low density, high connectivity, nonhierarchy, and strong stability of spatial association network of China's digital financial inclusion development, policymakers can further strengthen the communication and docking among provinces and actively establish consultation and cooperation mechanism so as to effectively promote the information exchange and resources sharing of digital financial inclusion development among provinces. Second, policymakers can highlight the central position of the rapidly developing central and western provinces represented by Shanxi, Sichuan, Hunan, and Hubei in terms of connectivity, intermediation, and accessibility in the spatial association network of China's digital financial inclusion development. On the one hand, policymakers can fully tap the potential of these provinces in transmitting the information of digital financial inclusion development. On the other hand, policymakers can give full play to the role of these provinces as the "bridge" and "link" in promoting the coordinated development of digital financial inclusion among provinces. Third, policymakers can bring the radiating and leading role of the eastern developed provinces in the spatial association network of China's digital financial inclusion development into full play. By disseminating the valuable experience and feasible path of developing digital financial inclusion in the developed eastern provinces to the central and western provinces, it will drive and help the central and western provinces develop digital financial inclusion. Lastly, in order to increase the probability of establishing the spatial association between provinces and amplify the interprovincial spatial spillover effect, policymakers can make efforts in several ways, including comprehensively increasing the national PC Internet penetration rate, promoting the coordinated development of regional economies, and forming an interprovincially differentiated industrial structure.

Although we have conducted a relatively comprehensive analysis, our research still has limitations in some aspects. First, limited by the data, we have not investigated the evolutionary characteristics of the spatial association network from a dynamic perspective and have only merely described the static characteristics. Hence, we will conduct dynamic evolution research on the spatial association network in the future. In addition to Euclidean distance, we can consider using other spatial metrics as the distance to construct network connections. We can then compare and analyze networks with different spatial metrics to further understand digital financial inclusion development's spatial association.

Data Availability

The core data used to support the findings of the study are the "Peking University Digital Financial Inclusion Index of China," which is compiled by the Institute of Digital Finance, Peking University. The data can be accessed from https://idf.pku.edu.cn/yjcg/zsbg/485016.htm.

Conflicts of Interest

The authors declare that there are no conflicts of interest regarding the publication of this paper.

Acknowledgments

This study was supported by the National Natural Science Foundation of China, "Financial Market Web Feature Theory Integrating Spatial Semantic Analysis under the Big Data Environment" (no. 71671180).

References

[1] A. Demirguc-Kunt, L. Klapper, D. Singer, S. Ansar, and J. Hess, *The Global Findex Database 2017: Measuring Financial Inclusion and the Fintech Revolution*, World Bank, Washington, DC, USA, 2018.

[2] D. Gabor and S. Brooks, "The digital revolution in financial inclusion: international development in the fintech era," *New Political Economy*, vol. 22, no. 4, pp. 423–436, 2016.

[3] K. Lauer and T. Lyman, *Digital Financial Inclusion: Implications for Customers, Regulators, Supervisors, and Standard-Setting Bodies*, Consultative Group to Assist the Poor, Washington, DC, USA, 2015.

[4] T. Sun, "Balancing innovation and risks in digital financial inclusion-experiences of ant financial services group," in *Handbook of Blockchain, Digital Finance, and Inclusion Volume*, Academic Press, Cambridge, MA, USA, 2018.

[5] World Bank, *Global Financial Development Report 2014: Financial Inclusion*, World Bank Publications, Washington, DC, USA, 2013.

[6] J. Manyika, S. Lund, M. Singer, O. White, and C. Berry, *Digital Finance for All: Powering Inclusive Growth in Emerging Economies*, McKinsey Global Institute, San Francisco, CA, USA, 2016.

[7] L. Yang and Y. Zhang, "Digital financial inclusion and sustainable growth of small and micro enterprises-evidence based on China's new third board market listed companies," *Sustainability*, vol. 12, no. 9, p. 3733, 2020.

[8] J. Li, Y. Wu, and J. J. Xiao, "The impact of digital finance on household consumption: evidence from China," *Economic Modelling*, vol. 86, pp. 317–326, 2020.

[9] Q. Song, J. Li, Y. Wu, and Z. Yin, "Accessibility of financial services and household consumption in China: evidence from micro data," *The North American Journal of Economics and Finance*, vol. 53, Article ID 101213, 2020.

[10] Z. Yin, X. Gong, P. Guo, and T. Wu, "What drives entrepreneurship in digital economy? Evidence from China," *Economic Modelling*, vol. 82, pp. 66–73, 2019.

[11] S. Gammage, A. Kes, L. Winograd et al., *Gender and Digital Financial Inclusion: What Do We Know and What Do We Need to Know*, International Center for Research on Women, Washington, DC, USA, 2017.

[12] X. Wang and G. He, "Digital financial inclusion and farmers' vulnerability to poverty: evidence from rural China," *Sustainability*, vol. 12, no. 4, p. 1668, 2020.

[13] D. Radcliffe and R. Voorhies, "A digital pathway to financial inclusion," *SSRN Electronic Journal*, Article ID 2186926, 2012.

[14] P. K. Ozili, "Impact of digital finance on financial inclusion and stability," *Borsa Istanbul Review*, vol. 18, no. 4, pp. 329–340, 2018.

[15] M. N. A. Siddik and S. Kabiraj, "Digital finance for financial inclusion and inclusive growth," in *Digital Transformation in Business and Society*, Springer, Berlin, Germany, 2020.

[16] X. Wang and J. Guan, "Financial inclusion: measurement, spatial effects and influencing factors," *Applied Economics*, vol. 49, no. 18, pp. 1751–1762, 2017.

[17] F. Guo, J. Wang, F. Wang et al., "Measuring China's digital financial inclusion: index compilation and spatial characteristics," *Jingjixue Jikan (China Economic Quarterly)*, vol. 19, no. 4, pp. 1401–1418, 2019.

[18] Y. Shen, C. J. Hueng, and W. Hu, "Measurement and spillover effect of digital financial inclusion: a cross-country analysis," *Applied Economics Letters*, pp. 1–6, 2020.

[19] L. Li, "China will become the world's largest digital financial market," 2020, https://k.sina.com.cn/article_6465571420_18160ca5c01900n1y5.html?from=movie.

[20] R. N. Mantegna, "Hierarchical structure in financial markets," *The European Physical Journal B*, vol. 11, no. 1, pp. 193–197, 1999.

[21] C. Yang and S. Liu, "Spatial correlation analysis of low-carbon innovation: a case study of manufacturing patents in China," *Journal of Cleaner Production*, vol. 273, Article ID 122893, 2020.

[22] D. Krackhardt, "Graph theoretical dimensions of informal organizations," *Computational Organization Theory*, vol. 89, no. 112, pp. 123–140, 1994.

[23] M. Dozier, M. Harris, and H. Bergman, "Social network density and rehospitalization among young adult patients," *Psychiatric Services*, vol. 38, no. 1, pp. 61–65, 1987.

[24] L. C. Freeman, "Centrality in social networks conceptual clarification," *Social Networks*, vol. 1, no. 3, pp. 215–239, 1978.

[25] S. Chen, J. Xi, M. Liu, and T. Li, "Analysis of complex transportation network and its tourism utilization potential: a case study of Guizhou expressways," *Complexity*, vol. 2020, Article ID 1042506, 22 pages, 2020.

[26] H. C. White, S. A. Boorman, and R. L. Breiger, "Social structure from multiple networks. I. Blockmodels of roles and positions," *American Journal of Sociology*, vol. 81, no. 4, pp. 730–780, 1976.

[27] F. Guo, S. T. Kong, and J. Wang, "General patterns and regional disparity of internet finance development in China: evidence from the Peking University Internet finance development index," *China Economic Journal*, vol. 9, no. 3, pp. 253–271, 2016.

[28] J. Xu, "China's internet finance: a critical review," *China & World Economy*, vol. 25, no. 4, pp. 78–92, 2017.

[29] J. Neville, M. Adler, and D. Jensen, "Clustering relational data using attribute and link information," in *Proceedings of the Text Mining and Link Analysis Workshop, 18th International Joint Conference on Artificial Intelligence*, Acapulco, Mexico, August 2003.

[30] M. Everett, *Social Network Analysis, Textbook at Essex Summer School in SSDA*, LinkedIn, Mountain View, CA, USA, 2002.

[31] J. T. Lai, I. K. M. Yan, X. Yi, and H. Zhang, "Digital financial inclusion and consumption smoothing in China," *China & World Economy*, vol. 28, no. 1, pp. 64–93, 2020.

[32] F. Guo, T. Kong, J. Wang et al., *The Peking University Digital Financial Inclusion Index of China (2011–2018)*, Institute of Digital Finance, Peking University, Beijing, China, 2019.

[33] Q. Ji and Y. Fan, "Evolution of the world crude oil market integration: a graph theory analysis," *Energy Economics*, vol. 53, pp. 90–100, 2016.

[34] J.-P. Onnela, A. Chakraborti, K. Kaski, J. Kertesz, and A. Kanto, "Dynamics of market correlations: taxonomy and portfolio analysis," *Physical Review E*, vol. 68, no. 5, Article ID 056110, 2003.

[35] H. Marfatia, W.-L. Zhao, and Q. Ji, "Uncovering the global network of economic policy uncertainty," *Research in International Business and Finance*, vol. 53, Article ID 101223, 2020.

Hindawi
Complexity
Volume 2021, Article ID 6679580, 11 pages
https://doi.org/10.1155/2021/6679580

WILEY | Hindawi

Research Article

Evolution Characteristics and Regional Roles' Influencing Factors of Interprovincial Population Mobility Network in China

Wei Fang,[1,2] **Pengli An**,[1,2] **and Siyao Liu**[1,2]

[1]*School of Economics and Management, China University of Geosciences, Beijing 100083, China*
[2]*Key Laboratory of Carrying Capacity Assessment for Resource and Environment, Ministry of Natural Resources, Beijing 100083, China*

Correspondence should be addressed to Wei Fang; davifang@163.com

Received 25 December 2020; Accepted 26 April 2021; Published 13 May 2021

Academic Editor: Xueyong Liu

This paper analyses the evolutionary characteristics of the interprovincial population mobility network structure in China and explores the roles of provinces from 2010 to 2015. By constructing the interprovincial population mobility network, we examine the provinces' functions during periods of population mobility through population mobility diversity, population mobility, and population mobility intermediation. The results show that the coverage and tightness of the interprovincial population mobility network were influenced by national economic development, increasing steadily from 2010 to 2014 and then suddenly falling in 2015. The regions that played essential roles in the province's mobility diversity and intermediation showed a dispersion trend. In contrast, areas that played a vital role in the inflows or outflows were relatively concentrated and stable. Additionally, this work further explores how economic factors, e.g., GDP, residents' consumption levels, total population, unemployment rate, and consumer price index, are used as independent variables to analyse the provinces' roles in the interprovincial population mobility network. The analysis shows that the inflow or outflow volumes are easily affected by the five indices. These five indices are significantly related to network role indicators to different extents.

1. Introduction

Population flow and regional development are interactive processes [1]. During migration, material, information, capital, and technology also flow among regions [2]. In the case of unbalanced regional development and a heterogenous population distribution in China, a vast number of people move among different areas every year. As mentioned in the Report on the Development of China's Floating Population [3], there was a floating population of 230 million in China in 2010 that reached 244 million by 2017. This accounted for nearly 18 percent of the total population in China. Most were migrant workers, and similar cases are common in emerging economies such as India and Brazil. In these countries, the regional development paces are asynchronous, leading to a mismatch of population and wage levels in different areas. In detail, there are always surplus labourers and lower wages in underdeveloped regions. In contrast, in developed areas, labour is scarce, and salaries are high. Thus, such a significant imbalance prompts migration. Naturally, with population mobility, resources, information, capital, and technology will also spill over and reallocate among regions. In the long run, with gradual changes in regional socioeconomic factors, the interregional population mobility features and the roles of migration areas will correspondingly transform. As the largest emerging country, China has an extraordinary household registration regime, which greatly supports population movement statistics. Therefore, analysing China's interprovincial population movement features and evolution trends, exploring the roles the provinces play in migration, and excavating the underlying impact factors could provide references for emerging economies when making population mobility policies.

Previous research on population flow mainly focuses on how people move among different countries, such as

immigration [4–7], travel abroad [8], or refugee migration [9, 10]. Additionally, they also focus on how residents float around the country. Inside a country, travel is a short-term pattern of population mobility; thus, some research studies primarily explore tourism impacts on local economies and the environment [11, 12]. Additionally, some unique festivals will temporally motivate people to move, such as New Year's Festivals in Asia and Christmas in Western countries. Given the large scale and seasonal effects, scholars mainly explore how this type of population mobility affects transportation and consumption in the short run [13]. Finally, many labourers migrate to other areas permanently for jobs [14].

In recent years, based on the fifth and sixth censuses in China, some scholars have explored the features of interprovincial population floating [15, 16]. They analysed the relationship between population mobility and related socioeconomic indicators, such as the urban-rural income gap [17, 18], regional economic growth [19–21], epidemic diffusion [22, 23], and market potential and anticipated revenue [18]. However, due to the lack of continuity in data, it is hard to demonstrate how population mobility evolves and how evolution gradually influences economic development [24]. Therefore, some research has introduced network theory, building population mobility models among different provinces and exploring the rules and evolutionary features of interprovincial population floating in a precise and systematic way. In addition, some scholars describe the features of population mobility through network theory. Jiang explored daily population hovering features among 334 cities in China using Baidu Migration Big Data [2]. Ye et al. [25] found that a significant rich-club phenomenon occurred in Chinese population movements during the 2015 Spring Festival. Zhang et al. [26] used Tencent location big data to explore population movement characteristics among 234 cities in China. However, previous research has mainly focused on temporal changes in migration, especially patterns on holidays, and has not explored gradual trends and influencing factors.

In terms of residential movement among the different provinces, economic development, marketization, spatial distance, and information can influence its pattern. Therefore, this paper explored the role played by each province in the population flow from a global perspective, inferring how their roles are influenced by the factors mentioned above. We built five interprovincial population mobility networks and explored each province's functions during migration from the diversity of population flow, the amount of flow, and the intermediary of migration. In addition, by introducing the panel regression model, we examined how the gross regional production, total population, household purchase level, unemployment rate, and consumer price index impact the different roles that the provinces played in migration. Moreover, due to quantification uncertainty and protracted nature of the household registration system's reform, this paper mainly considers the total population without deeply analysing the impacts of the reform on urban and rural populations.

2. Data and Methodology

2.1. Data. We downloaded the dataset describing the interprovincial population movement from the National Earth System Science Data Center at the National Science & Technology Infrastructure of China (http://www.geodata.cn). This dataset contains the population inflow and outflow of 31 provinces, municipalities, and autonomous regions. It also includes the outflow of population from Hong Kong, Taipei, and Macau to the other provinces in mainland China.

Additionally, we downloaded the gross provincial production, household consumption level, total population, unemployment rate, and consumer price index for each province from the National Bureau of Statistics (http://data.stats.gov.cn/).

The entirety of the data spans from 2010 to 2015.

2.2. Methodology

2.2.1. Networks of Population Moving Interprovincially. We applied a node to represent each province for the network construction, with the directed edges depicting the migrant and the edges' weights measuring mobility. We exhibit the migrant structures from 2010 to 2015 in Figure 1.

In this figure, the size of the node reflects the population inflow and outflow. A larger node corresponds to a greater number of migrants. The direction of the edge describes the citizens' movement direction, and the thickness of the edges reflects the amount of the population flow between these areas. Additionally, we used the same colour to mark provinces with close population mobility relationships. Since there are only outflow data from Hong Kong, Taipei, and Macau, we did not explore the factors influencing these three areas' roles in the network.

Furthermore, we calculated the network density, the average shortest path for exploring the interprovincial population structure, and its evolutionary features. Specifically, network density measures the level of coverage of interprovincial population movements, and the average shortest path length reflects the closeness among the provinces:

$$D = \frac{1}{u} \sum_{i,j \in N, i \neq j} e_{ij}\left(p_{ij}\right), \tag{1}$$

where D is the network density, u is the largest possible number of edges in the population flow network, and e_{ij} is the weight of the edge between node i and node j. If p_{ij} (the population flow between province i and j) is larger than zero, it equals 1; otherwise, it equals 0:

$$L_t = < L_{ij} > = \text{Average}\left(\sum_{ij \in N, i \neq j} \text{Min}\left(\text{Path}\left(i \longrightarrow j\right)\right)\right), \tag{2}$$

where $\langle L_{ij} \rangle$ is the average shortest length path between node i and node j [27].

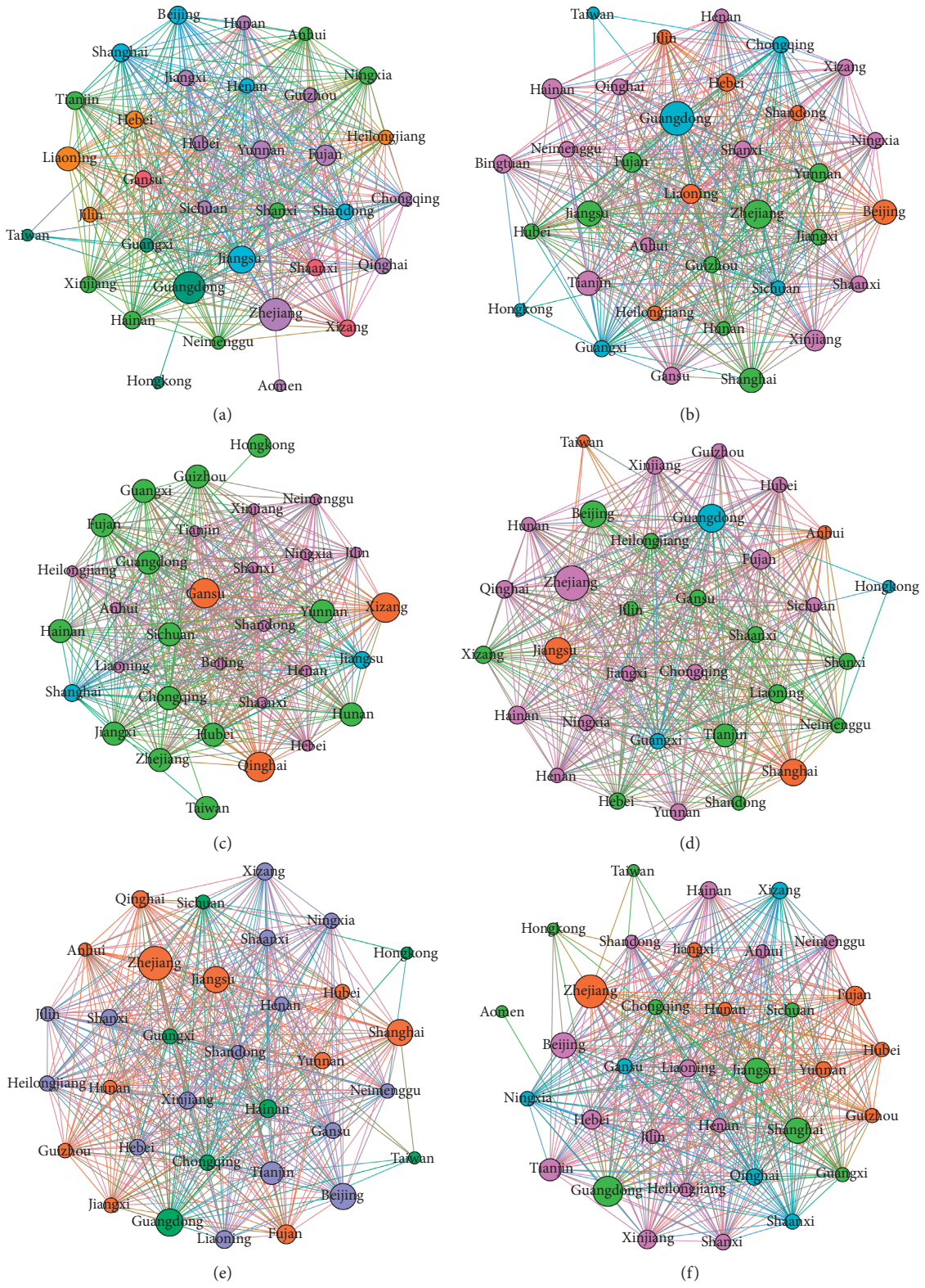

Figure 1: China's interprovincial population flow network from 2010 to 2015. (a) 2010. (b) 2011. (c) 2012. (d) 2013. (e) 2014. (f) 2015.

Population mobility reflects the mutual influence of economic development among the provinces. The average shortest length in the network measures the least number of provinces that need to be crossed to get from one province to another. Therefore, the value of L_t could exhibit closeness among the provinces.

2.2.2. The Roles of the Provinces in the Network. In network theory, there are several indices used to measure the roles of the nodes. This paper selected in-degree, out-degree, in-strength, out-strength, and betweenness centrality to explore the diversity of population movement, gross population mobility, and population flow medium.

In this paper, in-degree (as shown in function (3)) was applied to represent the inflow population diversity, which measures how many provinces have population migrating to a particular province. The out-degree (as shown in function (4)) was used to explain the outflow population diversity, which measures the number of provinces to which the people migrate from a specific province. In function 5, the in-strength calculates the total number of people who move to a particular province. Correspondingly, in function (6), the out-strength estimates the population that moves from a specific province. In addition, to depict the medium of population flow (i.e., some areas play the role of bridges during migration), we introduced betweenness centrality, as shown in function (7) [28]:

$$d_i^{\text{in}} = \sum_{k=1}^{m} e(p_{ki}), \tag{3}$$

where d_i^{in} is the in-degree of the node, i.e., the diversity of the inflow population.

When $p_{ki} > 0$, $e(p_{ki})$ equals 1; otherwise, $e(p_{ki})$ equals 0:

$$d_i^{\text{out}} = \sum_{k=1}^{m} e(p_{ki}), \tag{4}$$

where d_i^{out} is the out-degree of the node, i.e., the diversity of the outflow population. As shown above, when $p_{ki} > 0$, $e(p_{ki})$ equals 1; otherwise, $e(p_{ki})$ equals 0:

$$wd_i^{\text{in}} = \sum_{k=1}^{m} p_{ki}, \tag{5}$$

where wd_i^{in} is the in-strength of the node, i.e., the total number of inflow populations:

$$wd_i^{\text{out}} = \sum_{k=1}^{m} p_{ki}, \tag{6}$$

where wd_i^{out} is the out-strength of the node, i.e., the total number of outflow populations:

$$C(i) = \frac{\sum_{s \neq i \neq t} \sigma_{st}(i)/\sigma_{st}}{(N-1)(N-2)}, \tag{7}$$

where $C(i)$ is the betweenness centrality of the node, i.e., the medium of population mobility. The variable σ_{st} is the number of shortest paths between node$_s$ and node$_t$, $\sigma_{st}(i)$ is the number of shortest paths across node$_i$ between node$_s$ and node$_t$, and N is the number of nodes in the population migration network.

2.2.3. Factors Influencing the Roles of Provinces in the Population Migration Network. Since interprovincial population migration will be impacted by several factors, such as regional economic development, demographics, and employment, we further explore which factors influence interprovincial population migration and the magnitude of their impacts.

(1) Regional Economic Development. Uneven economic development among provinces is the core driving factor that accounts for population movement. Rapid economic growth could provide more employment and raise the income level (hence, coastal areas such as Guangdong, Zhejiang, and Shanghai have always been significant regions for attracting people). Therefore, we selected gross regional production to represent regional economic development, the household consumption level to exhibit the average living cost of the local citizen, and the consumer price index (CPI) to measure the gaps between labour wage levels and real purchasing power.

(2) Demographics. When economic development is comparable and employment opportunities are limited, competitiveness in heavily populated areas is higher than that in other areas, and the labour wage per capita is relatively lower. Therefore, in some provinces with a large population, people will be inclined to leave for other provinces with better economic performances. Consequently, we select the total number of people to reflect the demographic factor.

(3) Employment. To some extent, demographics could reflect the total number of working forces provided by a region. However, the employment rate could reflect the relationship between the province's available employment positions and the number of working-age people willing to work.

This paper selected gross regional production, household purchase level, total population, unemployment rate, and customer price index as explanatory variables above all. To explore how these variables influence the interprovincial population flow, we selected inflow population diversity, outflow population diversity, the total number of inflow populations, the total number of outflow populations, and the medium of population mobility as the explained variables. We then establish a panel regression model of these variables to explore how these factors influence population mobility across provinces.

During the analysis, we algorithmize the model as in the following function:

$$\ln \overset{i}{Y}t = \beta 0 + \beta 1 \ln X1t + \beta_2 \ln X2t + \beta_3 \ln X3 + \beta_4 \ln X4t + \beta_5 \ln X5t + \beta_6 \ln et, \quad (8)$$

where $\overset{i}{Y}_t$ represents the value of the i^{th} role of a province in year t and $X1_t \sim X5_t$, respectively, represent the gross regional production, household consumption level, total population, unemployment rate, and consumer price index of each area.

3. Results

3.1. Evolutionary Features of Interprovincial Population Mobility. As shown in Figure 2, from 2010 to 2015, except for Hong Kong, Taipei, and Macau, the other 31 provinces or autonomous regions all have inflow and outflow migrants. Additionally, from 2010 to 2014, the coverage of the bilateral population flowing among these areas increased year by year and then dropped in 2015, which exactly corresponded to China's economic development. China's economy grew rapidly from 2011–2014. However, influenced by the weak behaviour of the global economy in 2015, China's economy entered a new normal, caused by a significant drop in exports and excess domestic production capacity. We additionally noticed that the bilateral population flow tightness among the provinces exhibited a similar trend. Although there was a slight upswing in 2015, the tightness during the six years was below 1.2, which means that the population could migrate from one province to another through 1.2 provinces on average. This shows that, except for Hong Kong, Taipei, and Macau, there are frequent population flows among the 31 provinces in mainland China. Another profile indicates that mainland China's economic development is quite active, and the provincial economy performs unevenly and has significant structural differences. Influenced by the slowdown of the economy in 2015, the population flow's activeness correspondingly declined.

3.2. Roles of Provinces in the Interprovincial Population Mobility Network. Based on the five indices in Section 1.2.2, we analysed the provincial role in interprovincial population mobility from 2010 to 2015 and ranked the values. We present the top 5 provinces for each year in Tables 1–5.

According to the in-degree and out-degree of each node in the network, we can obtain the source and flow direction of population mobility, reflecting the diversity of population mobility. The outflow of population from each province is widely scattered throughout the country, while the provinces with the most inflow are mainly concentrated in the more developed coastal provinces. Regarding the diversity of population mobility, we can notice from Tables 1 and 2 that compared to the inflow population, the outflows are more dispersive. During 2010–2015, Guangdong and Shanghai exhibited significant diversity in inflow population, and they persistently ranked in the top 5. This means that these two provinces received migrants from all the other areas in mainland China. In addition, Jiangsu, Sichuan, Hebei, Zhejiang, Henan, Shaanxi, Gansu, Fujian, Jiangxi, Shandong, Hunan, Hubei, and Anhui have prominent advantages in the diversity of the outflow population.

By further analysing the out-strength and in-strength of each node in the network, we can obtain the number of inflow and outflow populations for each province. Tables 3 and 4 show that the top 5 provinces with the highest annual amounts of inflow and outflow populations counted. Regarding the population mobility amount, all the provinces behave more stably than the diversity of mobility. Notably, the five eastern developed regions, including Zhejiang, Guangdong, Jiangsu, Shanghai, and Tianjin, attracted the most migrants in 2011–2015. Therefore, regional economic development is the core factor influencing the population to move in. Furthermore, the five major central provinces, i.e., Sichuan, Anhui, Henan, Hunan, and Hubei, sent the most people to other areas. Correspondingly, these five provinces are the ones with larger populations and weaker economic performances. This shows that the main factors affecting population mobility remain to be the level of regional economic development, employment opportunities, and personal income.

Furthermore, Table 5 shows that all the provinces' values change significantly for the medium population flow. Notably, Guangdong has consistently performed as the most potent in medium population flow for the five years. Combined with Guangdong's results in Tables 1–4, we find that Guangdong has received a mass of labourers from the other provinces but sent less to the others during the economic development period. There is a consensus that Guangdong performed as a substantial economic growth engine. While attracting migrants, Guangdong also channelled labour to the other areas through investment. After 2013, Jiangsu and Zhejiang exhibited increasingly prominent medium roles, playing a similar function to Guangdong. Hainan and Chongqing—famous places to live and travel in China—have also played a more vital medium role.

3.3. Factors Influencing the Roles of the Province in the Population Mobility Network. As mentioned above, each province plays a different and distinct position in the population mobility network. Regions that have significant diversity and intermediation roles are scattered, distributed and change over time. Population flow amounts are mainly concentrated in certain crucial provinces, and the distribution is stable over time. We further analysed how regional economic and social factors influence these provinces' roles based on these significant population mobility features.

Therefore, we selected the network indices we obtained in Section 3.2 as explanatory variables, i.e., population inflow and outflow diversity, the number of population inflows and outflows, and mobility intermediation. We determined the gross regional production, household consumption level, total population, unemployment rate, and consumer price index as explained variables to build five panel regression models.

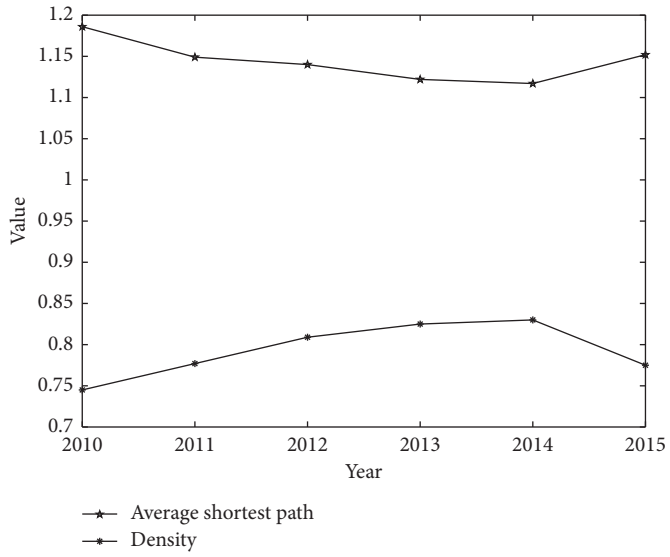

Figure 2: Coverage and tightness of the interprovincial population mobility network.

Table 1: The top 5 provinces for population inflow diversity in 2010–2015.

	2010	2011	2012	2013	2014	2015
Guangdong	32	32	30	31	31	32
Jiangsu	30			31	30	30
Liaoning	29				30	30
Shanghai	29	29	31	29	31	30
Sichuan	29	29			30	
Hainan	29			29	30	
Tibet Autonomous Region	29				30	
Beijing		30	30	29		
Tianjin		30		29	30	30
Guangxi Zhuang Autonomous Region		29		29	30	
Chongqing			30		30	30
Qinghai			30			
Shanxi				30		
Zhejiang				30	31	31
Hebei				29		
Shaanxi				29		
Gansu				29		
Fujian						30

Thus, to ascertain the model's robustness and validity, we tested the variables before regression. First, we explored the correlations between these variables. As shown in Table 6, the correlation coefficients between the five explanatory variables are relatively small. Second, we applied the variance inflation factor to check the multicollinearity of the five explanatory variables. The results show that the largest variance inflation factor was VIF = 7.80, indicating that they all passed the test. Third, we introduced the ADF test (augmented Dickey–Fuller test) to examine the variables' stationarity, with the results showing that they are second-order stationary. Fourth, we conducted a cointegration test of these variables and found that they have long-term cointegration relationships.

The panel regression results (shown in Table 7) found that the household purchase level has a significant positive correlation with inflow population diversity. The standardized correlation coefficient is 0.531, which indicates that the household purchase level is the primary factor influencing the population's inflow diversity. Consistent with common sense, high local purchasing implies that the income level overwhelms the purchasing power, and people who live in other areas will be keen to migrate here. In contrast, the unemployment rate was negatively correlated with the inflow population diversity. In most cases, a high unemployment rate means an unstable external living environment, and the people outside this area will be reluctant to move here.

The population's outflow diversity is positively correlated with the total population, household purchasing level, and unemployment rate. This shows that the combined effects of these factors will induce people to migrate to other

Table 2: The top 5 provinces for population outflow diversity in 2010–2015.

	2010	2011	2012	2013	2014	2015
Guangdong	30			30	30	
Jiangsu	30	31	30	30	30	30
Sichuan	30	31	30	30	30	30
Hebei	30	31	30	30	30	30
Zhejiang	30	31	30	30	30	30
Henan	30	31	30	30	30	30
Shaanxi	30	31	30	30	30	30
Gansu	30	31	30	30	30	30
Shanxi	30	31	30	30	30	
Fujian	30	31	30	30	30	30
Jiangxi	30	31	30	30	30	30
Shandong	30	31	30	30	30	30
Hunan	30	31	30	30	30	30
Heilongjiang	30		30	30	30	30
Hubei	30	31	30	30	30	30
Anhui	30	31	30	30	30	30
Guizhou	30		30		30	
Chongqing		31	30	30	30	30
Yunnan		31		30	30	30
Qinghai			30	30		
Jilin			30	30	30	30
Guangxi				30		
Liaoning				30	30	30
Inner Mongolia				30		

Table 3: The top 5 provinces for inflow populations in 2010–2015.

	2010	2011	2012	2013	2014	2015
Zhejiang	6517	5291	8883	12493	12473	12461
Guangdong	6363	7086	8445	8547	8706	10693
Jiangsu	4859	4271	5383	8122	8050	7851
Liaoning	3826					
Fujian	2795					
Tianjin	2000	4000				
Shanghai	2000	4000	14993	7974	7999	7995
Beijing	2000	4000	5994	8000	7997	7999

Table 4: The top 5 provinces for outflow populations in 2010–2015.

	2010	2011	2012	2013	2014	2015
Sichuan	6718	7798	9695	11207	10876	11667
Anhui	6559	6660	11113	12029	11923	11656
Henan	5699	7256	8667	10809	10353	10879
Hunan	3725	4404	5350	6227	6273	6380
Jiangxi	3284					
Hubei		4146	4989	5861		5820
Shandong					5774	

provinces (even to underdeveloped regions) to find working opportunities and lower their living costs. Among these factors, the total population is the major one, of which the standardized coefficient is 1.165.

In addition, the amount of population mobility has significant positive correlations with gross regional production, household purchase level, and consumer price index. Despite the costly living standard exhibited by the consumption level and price index, the results show that the advanced economy still attracted people to migrate. For example, Guangdong, Shanghai, and Beijing have always been places where young people dream to live. Additionally, the negative correlations between unemployment and population outflow show that the unemployment rate plays a vital role in population inflow. Moreover, the total population is positively correlated with the outflow population

Table 5: The top 5 provinces for population mobility intermediation in 2010–2015.

	2010	2011	2012	2013	2014	2015
Guangdong	45.50	26.17	32.94	33.59	16.31	43.05
Yunnan	32.62					
Sichuan	14.30	6.24		3.19	14.59	
Jiangsu	9.95			33.59	6.48	9.53
Jiangxi	8.47	13.48				
Guangxi		19.48				
Chongqing		16.00	23.55			
Shanghai			13.51			
Qinghai			5.17			
Shanxi			4.69	3.59		
Zhejiang				3.59	9.71	13.82
Inner Mongolia					9.31	
Henan						8.24
Guizhou						7.44

and is the most significant influencing factor (with the standardized coefficient reaching 0.914).

For the population mobility intermediation, the results show that gross regional production is a significant negative factor. This shows that developed areas are more likely to act as population mobility destinations than intermediation destinations. In contrast, the household purchase level, total population, and consumer price index are positively correlated with mobility intermediation. This shows that the more people there are and the higher the province's living cost, the more likely this area will become an intermediary in population mobility. Notably, the total population mostly influenced the intermediary function of the province regarding population flow.

From the above analysis, we can see that the total population, unemployment rate, and consumption level are the most important factors affecting interprovincial population flow. They not only affect the diversity of population mobility but also affect the amount of population mobility. However, they are different in the direction of influence; the regional GDP, consumption level, total population, and consumer price index determine the regional economic growth to a large extent. The higher the GDP and the consumption level of a province, the more likely it is to be a destination for migrants.

4. Discussion and Conclusion

According to China's population statistics, this paper introduced network theory to explore interprovincial population mobility during 2010–2015 from different perspectives. Specifically, this paper analysed the evolutionary features of the topological structure of interprovincial population mobility and provincial roles during the flow of population, extracting the factors that influence their functions. This paper systematically reveals the regular pattern and evolution characteristics of interprovincial population mobility from the network perspective and analyses the influence intensity of each influencing factor by constructing a panel regression model between the main influencing factors and network indicators.

First, based on the coverage of the population mobility relationship (graph density) and the closeness of the population mobility relationship (average shortest path), we explored the evolutionary features of China's interprovincial population mobility network structure from 2010 to 2015. From 2010 to 2014, we found that the population flow across the province gradually increased but then dropped in 2015. This indicates that active and imbalanced regional economic development facilitated frequent population mobility across provinces. Especially in 2015, with structure regulation, China proposed a new normal for developing the economy. Thus, the overall topological feature of population mobility exhibits a different pattern. This conclusion reflects that the characteristics of employment-based population mobility are different from those of tourism or holiday populations. From the existing literature, China's tourism and holiday population flow has been increasing annually in recent years [20, 29].

Second, we explored each province's roles in population mobility from three perspectives, i.e., diversity (in-degree and out-degree), amount (in-strength and out-strength), and the intermediary of population mobility. We obtain some different population flow characteristics from other studies that only consider holiday population mobility [13] and tourism [2]. The results showed that the provinces that have advantages in the diversity of population mobility change over time. The population's outflow diversity especially exhibits a more distinct scattered distribution of the provinces than the inflow. Regarding the population flow, people who lived in the midwestern regions were more inclined to migrate out to the other areas, and eastern provinces were more likely to act as hosts. Similarly, the provinces that play significant intermediary roles in population flows also change over time. However, Guangdong, Zhejiang, and Jiangsu performed extraordinarily compared to the others. In particular, Guangdong has always played an essential intermediate role in migration. Some provinces famous for travel or living environments (such as Hainan, Chongqing, and Guangxi) also act as vital intermediaries during population flows.

Third, to explore the factors that impact the different provincial functions related to population flows, we built five

Table 6: Correlation coefficient between variables.

	Inflow diversity	Outflow diversity	Inflow population	Outflow population	Intermediary of flow	Gross regional production	Household purchasing level	Total population	Unemployment rate	CPI
Gross regional production	0.2955	0.3707	0.4625	0.3045	0.4603	1.0000	—	—	—	—
Household purchasing level	0.4491	−0.1089	0.7339	−0.1973	0.1836	0.4556	1.0000	—	—	—
Total population	0.0715	0.5628	0.0719	0.6128	0.4032	0.6222	0.0251	1.0000	—	—
Unemployment rate	−0.4119	0.2624	−0.4016	0.1889	−0.1590	−0.1465	−0.2626	0.0559	1.0000	—
CPI	−0.1239	−0.0645	−0.1421	−0.2305	0.0133	−0.2249	−0.2821	−0.1209	0.0774	1.000

Table 7: Estimation of panel regression models by the least squares method (standardized coefficients and t).

	Inflow diversity	Outflow diversity	Inflow population	Outflow population	Intermediary of flow
Gross regional production	0.4552182 (1.043562)	−0.5892163 (−1.744970)	0.200232* (2.150312)	−0.1485215 (−0.583230)	−1.318329*** (−3.13820575)
Household purchasing level	0.53137612** (2.587326)	0.3262172** (2.043505)	0.719328*** (6.704840)	−0.2124816** (−1.762216)	0.826172*** (4.161051)
Total population	0.3486712 (0.963121)	1.1652187*** (4.701748)	−0.035481 (−0.121224)	0.91399212*** (4.328284)	1.4913473*** (4.282643)
Unemployment rate	−0.2813984*** (−4.074657)	0.1724173*** (3.201550)	0.093291* (1.662168)	0.15321229*** (3.787326)	−0.047103 (−0.700281)
CPI	0.0243217 (0.346621)	0.1721269 (1.300935)	0.200232* (2.150312)	−0.18733215*** (−4.546379)	0.252485*** (3.714374)

Note: the value in the bracket is the t-value, * means $p < 0.1$; ** means $p < 0.05$; *** means $p < 0.01$.

panel regression models by separately setting the gross regional production, household purchase level, total population, unemployment rate, and consumer price index as explanatory variables and the five network indices as the explained variables. Although some studies have analysed the influencing factors of population mobility in China, most of them use cross-sectional data on population mobility [22, 25]; thus, it is difficult to analyse the influence, direction, and intensity of different factors on population mobility by time-series data. The results show that the total population, unemployment rate, and household purchase level are significant factors influencing the diversity of people inflows. People who live in regions with more people, higher unemployment rates, and higher purchase levels are more inclined to migrate to underdeveloped areas. Thus, the outflows of the people take an air of diversity. Additionally, the five factors all exert significant impacts on the total amount of population flow. Therefore, to ascertain the population's stable and orderly flow, local governments should regulate the policy based on each factor's strength of influence. Specifically, the gross regional production, household purchase level, and consumer price index significantly influenced provinces' population inflows. The total population is the most significant factor in inducing people to move out to other regions. In addition, some provinces are more likely to act as population flow destinations with advantages in their gross regional product, household purchase level, total population, and consumer price proportional to the province's intermediary values.

This work analysed how the population migrated across China's provinces and explored the external factors that influence provincial functions during periods of population flow. In this research, we mainly selected indicators extensively applied in socioeconomic research as external factors. In future works, we will broadly focus on many more factors that might influence provincial migration roles and that will help propose more worthwhile policies.

Data Availability

In this paper, we downloaded the dataset describing the interprovincial population movement from the National Earth System Science Data Center, National Science & Technology Infrastructure of China (http://www.geodata.cn).

Conflicts of Interest

The authors declare that they have no conflicts of interest.

Acknowledgments

This work was supported by Beijing Social Science Foundation of China (Grant no. 20GLB016) and National Natural Science Foundation of China (Grant nos. 71991483 and 71991480).

References

[1] H. Zhao, W. Zhang, and T. Ha, "Network characteristics of urban population migration," *Journal of Northeastern University (Natural Science)*, vol. 27, no. 2, pp. 169–172, 2006, in Chinese.

[2] X. Jiang and S. Wang, "Research on China's urban population mobility network: based on Baidu migration big data," *Chinese Journal of Population Science*, vol. 2, pp. 35–46, 2017, in Chinese.

[3] National Health Commission of the PRC, *Report on the Development of China's Floating Population*, China Population Publishing House, Beijing, China, 2018.

[4] L. Putterman and D. N. Weil, "Post-1500 population flows and the long-run determinants of economic growth and inequality," *The Quarterly Journal of Economics*, vol. 125, no. 4, pp. 1627–1682, 2010.

[5] E. Tranos, M. Gheasi, and P. Nijkamp, "International migration: a global complex network," *Environment and Planning B Planning and Design*, vol. 42, no. 1, pp. 4–22, 2014.

[6] V. Danchev and M. A. Porter, "Neither global nor local: heterogeneous connectivity in spatial network structures of world migration," *Social Networks*, vol. 53, pp. 4–19, 2017.

[7] P. Müller and M. Franz, "Transnational labour migration and the offshoring of knowledge-intensive business services within global production networks: the case of a German automotive company in Turkey," *Environment and Planning A: Economy and Space*, vol. 51, no. 6, pp. 1350–1369, 2019.

[8] L. Jun, Y. Zhang, Y. Yan, and Q. Qin, "Investigating the impact of human activity on land use/cover change in China's Lijiang river basin from the perspective of flow and type of population," *Sustainability*, vol. 9, 2017.

[9] A. Nagurney, P. Daniele, and G. Cappello, "Human migration networks and policy interventions: bringing population distributions in line with system optimization," *International Transactions in Operational Research*, vol. 28, no. 1, pp. 5–26, 2020.

[10] N. Kortendiek, "How to govern mixed migration in Europe: transnational expert networks and knowledge creation in international organizations," *Global Networks*, vol. 21, no. 2, pp. 320–338, 2020.

[11] Y. Li, B. Zhou, L. E. Wang et al., "Effect of tourist flow on province-scale food resource spatial allocation in China," *Journal of Cleaner Production*, vol. 239, no. Dec.1, pp. 117931.1–117931.12, 2019.

[12] N. Mou, Y. Zheng, T. Makkonen et al., "Tourists' digital footprint: the spatial patterns of tourist flows in Qingdao, China," *Tourism Management*, vol. 81, Article ID 104151, 2020.

[13] J. Lai and J. Pan, "China's city network structural characteristics based on population flow during spring festival travel rush: empirical analysis of "tencent migration" big data," *Journal of Urban Planning and Development*, vol. 2, no. 146, Article ID 04020018, 2020.

[14] R. C. D. Carvalho and E. Charles-Edwards, "The evolution of spatial networks of migration in Brazil between 1980 and 2010," *Population Space and Place*, vol. 26, no. 3, p. e2332, 2020.

[15] H. Wang, "Research on spatial pattern of demographic changes since 1982——based on four census data," *Industrial Economy Review*, vol. 3, no. 6, pp. 670–677, 2016, in Chinese.

[16] H. Ma and X. Wang, "An empirical analysis of the causes of inter-provincial urban-rural migration in China: evidence from the 6th population census," *Population and Development*, vol. 2303, pp. 25–36, 2017, in Chinese.

[17] D. Luo and C. Xing, "Population adjustments in response to local demand shifts in China," *Journal of Housing Economics*, vol. 33, no. sep, pp. 101–114, 2016.

[18] X. Hou and R. Yang, "Biased policies, mobility and urban-rural income gap: a study based on spatial heterogeneity interaction effect," *Nankai Economic Studies*, vol. 6, pp. 59–74, 2017, in Chinese.

[19] J. Li and C. Miao, "Impact of population flow on regional economic disparities in the Yangtze River economic belt," *Acta Geographica Sinica*, vol. 72, no. 2, pp. 197–212, 2017, In Chinese.

[20] X. Han, J. Zhang, L. Chen, and J. Guo, "Research on population mobility and regional economic development in poor areas," *Review of Economic Research*, vol. 34, pp. 22–27, 2018, in Chinese.

[21] G. Shi and Z. Li, "Research on the mechanism of population mobility promoting regional economic growth: based on panel data of the Yangtze River delta urban agglomeration," *East China Economic Management*, vol. 34, no. 6, pp. 10–18, 2020, in Chinese.

[22] T. Liu and Y. Jin, "Human mobility and spatio-temporal dynamics of COVID-19 in China: comparing survey data and big data," *Population Research*, vol. 44, no. 5, pp. 44–59, 2020, in Chinese.

[23] Y. Liu, D. Yang, G. Dong, H. Zhang, and C. Miao, "The spatio-temporal spread characteristics of 2019 novel coronavirus pneumonia and risk assessment based on population movement in henan province: analysis of 1 243 individual case reports," *Economic Geography*, vol. 40, no. 3, pp. 24–32, 2020, in Chinese.

[24] T. Liu, Y. Qi, and G. Cao, "China's floating population in the 21st century: uneven landscape, influencing factors, and effects on urbanization," *Acta Geographica Sinica*, vol. 70, no. 4, pp. 567–581, 2015, in Chinese.

[25] W. Ye, W. Song, C. Xiu et al., "The rich-club phenomenon of China's population flow network during the country's spring festival," *Applied Geography*, vol. 96, pp. 77–85, 2018.

[26] W. Zhang, Z. Chong, X. Li, and G. Nie, "Spatial patterns and determinant factors of population flow networks in China: analysis on tencent location big data," *Cities*, vol. 99, p. 102640, 2020.

[27] H. Li, H. An, W. Fang, Y. Wang, W. Zhong, and L. Yan, "Global energy investment structure from the energy stock market perspective based on a heterogeneous complex network model," *Applied Energy*, vol. 194, pp. 648–657, 2017.

[28] U. Brandes, "A faster algorithm for betweenness centrality*," *The Journal of Mathematical Sociology*, vol. 25, no. 2, pp. 163–177, 2001.

[29] J. Pan and J. Lai, "Research on spatial pattern of population mobility among cities: a case study of "tencent migration" big data in "national day–mid-autumn festival" vacation," *Geographical Research*, vol. 38, no. 7, pp. 1678–1693, 2019, in Chinese.

Hindawi
Complexity
Volume 2021, Article ID 6645406, 23 pages
https://doi.org/10.1155/2021/6645406

Research Article

The Study of the Spatial Heterogeneity and Structural Evolution of the Producer Services Trade Network

Yan Li, Xuehan Liang, and Qingbo Huang

School of Maritime Economics and Management, Dalian Maritime University, Dalian 116026, China

Correspondence should be addressed to Qingbo Huang; huangqingbo@dlmu.edu.cn

Received 21 December 2020; Revised 7 April 2021; Accepted 12 April 2021; Published 26 April 2021

Academic Editor: Huajiao Li

Constructing an all-directional, multilevel, and composite interconnection network, accelerating the free flow of producer services elements across regions, and further improving the efficiency of resource integration demand to conduct a comprehensive and systematic analysis of producer services trade. Thus, using bilateral trade data, this paper builds producer services trade network composed of 61 major countries and innovatively combines the methods of social network and economic geography to explore its spatiotemporal evolution and system properties. The results show that, firstly, the producer services trade network has spatial heterogeneity, which is characterized by high-value agglomerations in Western Europe and East Asia, and low-value agglomerations in Southern Europe and Southeast Asia. Secondly, most countries tend to choose trading partners with close geographical locations or common cultures to establish a cohesive subgroup. Thirdly, the producer services trade network has a significant core-periphery structure, the "spaghetti bowl" effect, which leads to a downward trend in the number of core and semi-peripheral countries. Finally, the trade agreement relations, language relations, and differences in economy, geography, institution, and technology all have a significant impact on the evolution of producer services trade network, but this change has little relationship with the population size divergences of different countries.

1. Introduction

As the world economy has presented a trend of transformation from industrial type to being service-oriented, the service industry has become the focus of international trade, among which producer services industry is the most critical branch because it gathers a lot of knowledge and capital [1, 2]. Affected by the application of information technology [3, 4], the elements of producer services are redistributed in the global market; more countries carry out trade activities as exporters or importers, thus forming a gigantic relationship network of producer services trade. Whether it can become a key node with control power in producer services trade network determines the construction of a "service-driven country," and reflects the position of international division of labor and the distribution of interests in the economic globalization. Therefore, it is of great significance to study the spatiotemporal evolution and the complex features of producer services trade network for complementing the study of competitiveness evaluation based on trade volume accounting and formulating adaptive and feasible trade strategies. It is also the practice of network analysis method in a specific industry level.

Along with global economic integration, more mainstream standpoints can recognize the conclusion that the producer services can be a major component of trade flow for a long time [5]. In 1995, the General Agreement on International Trade in service (GATS), which was led by WTO, came into force. As a result of the unbalanced development of service industry in various countries and the differences in negotiations, the liberalization of services trade under the framework of GATS has made slow progress, and regional services trade agreements have gradually sprung up, such as the "Trans-Pacific Partnership Agreement (TPP)" and "International Trade in Services Agreement (TISA)." These changes in regional economic and trade cooperation also increase the uncertainty of the future development of the producer services trade network.

Moreover, the enhancement of the extroversion characteristics of producer services has changed the view of the traditional urban basic economic model [6], that is, "services can only be sold within a limited distance, and cannot be exported to other regions to generate income for the local area." Since then, the spatial flow of producer services gradually infiltrates into regional or urban research areas. Majority of those studies focus on the location selection and driving factors of producer services enterprises, or the spatial agglomeration and influence mechanism of industry at the micro level [7–9]. However, there are few studies that combine the spatial heterogeneity of producer services with macro trade data and use the network method to analyze.

The purpose of this article was to capture the dynamic and heterogeneous features of producer services trade network, and focus on the following issues: What are the spatial characteristics and influencing factors of the structural evolution of producer services trade network? Has the development of producer services in emerging economies changed their position in the trade network and the pattern of global interests? Are the core countries and the marginal countries regularly carrying out trade interaction to promote them to integrate into producer services trade network? The solution of these problems will help to optimize the trade network structure, and build an all-directional, multilevel, composite interconnection network.

The main contributions are as follows: firstly, previous studies, reviewed in Sections 1 and 2, are mostly based on the micro perspective of industry and enterprise, or the analysis of commodity trade network. This paper makes up for the gap of service trade network from the global and national macro level. Secondly, the social network analysis method is introduced into the field of producer services trade to identify the functions of different countries in trade network and the factors affecting the evolution of network structure, and to supplement the methods of competitiveness evaluation and previous empirical studies limited to the dual relationship between the two sides of trade. Finally, applying GIS technology to trade data for spatial exploratory analysis, this paper expands the research content related to economic geography, reveals the general characteristics and evolution law of producer services trade network, and provides scientific support for the establishment of an open and inclusive services trade system.

The rest of the research mainly consists of four parts. Section 2 is literature review. Section 3 includes an overview of the research area, data sources, and methods of this article. Section 4 describes the spatiotemporal characteristics and impact factors of producer services trade network, and the final part puts forward conclusions, policy recommendations, and the future research directions.

2. Literature Review

Taking trade network as an example, the complexity of the socioeconomic system is an interdisciplinary issue that combines economics, geography, and network science [10–13]. Only by establishing a multiple analysis framework can we holistically explore its structure and evolution trend. However, most of the existing researches on the producer services trade system are based on a single dimension, mainly including two categories. The first category is about the perspective of economics. These studies focus on the driving mechanism of the development of producer services trade and its basic role in the transformation and upgrading of economic structure. Research and development investment, infrastructure construction, and foreign investment are considered as the essential elements to enhance the competitiveness of producer services trade [14, 15]. In terms of the utility in macroeconomic operation, producer services trade can provide key missing factors for final products and improve domestic total factor productivity through technology transfer and spillover [16]. The second category focuses on the geographical perspective. These studies point out that the producer services trade flow structure is composed of export cities, circulation systems, and market cities, and find that the role of producer service trade in regional and urban system is such that its unbalanced distribution will bring about the adjustment of regional economic structure, thus leading to the outward development of service trade [17].

Related research methods have become more abundant over time. Traditional analytical approaches mainly include simple international comparison based on revealed comparative advantage index or trade competitiveness index, and applying classical gravity model or other econometric methods to investigate the binary relationship between trade subjects [18, 19]. Social network is an emerging systematic method [20]. Since the scale-free network was proposed, using this method to analyze international trade issues has become the focal point of most researches [21–25]. In particular, Quadratic Assignment Procedure (QAP) belongs to the hypothesis test of "relationship-relationship" level in the social network method, which is considered to be one of the most effective tools for empirical analysis of network science [26, 27]. However, the objects of existing studies are mainly the goods trade network [28–30]. Limited by the difficulty of bilateral data acquisition, only a few literatures focus on the services trade network. Xu uses QAP weighted network to find that there is a significant correlation between various sectors of services trade. When exploring the impact of common human relations on the services trade network, he believes that common trade agreements play the most critical role, and the same language and religion are also major determinants [31, 32]. Besides, QAP regression analysis also shows that the differences of economic scale, technological innovation, and geographical distance affect the changes of services trade network structure in the region [33].

Summing up previous studies, we can find that there are still some deficiencies in the comprehensive application of economic geography and network theory to analyze the producer services trade relationship. Considering its strategic significance in the global industrial network and value chain, as well as the gaps in related fields, we explore the spatial-temporal variation and influencing factors of the producer services trade network, lay an empirical foundation for its balanced development, and put forward policy

suggestions for effectively improving the status of countries in the trade network.

3. Research Methods and Data Sources

3.1. Data Sources and Trade Network. The primary trade data source of this study is the OECD database. Based on the latest available annual data of producer services trade in 2000, 2004, 2008, and 2012, 61 countries[1] with total services trade accounting for more than 90% of the world's total services trade are involved, covering major economies in the world. The classification standard of producer services refers to the definitions of Browning and Singlemann [34], which mainly include six subindustries, namely: (1) transportation industry; (2) communication industry; (3) finance industry; (4) insurance industry; (5) computer and information services industry; and (6) concession rights and patent royalties, integrating the data of various industries to establish the producer services trade network. The logical framework of this paper is as follows (Figure 1):

The complex system G of trade network can be represented by a tuple: $G = (V, E)$. Among them, $V = \{v_1, v_2, \ldots, v_n\}$ is the node set, $E = \{e_{ij}\}$ is the edge set, and each edge e_{ij} in E has a pair of nodes (v_i, v_j) in Vcorresponding to it.

In this paper, we use 61 sample countries and the trade flows between countries as nodes and edges, respectively, to construct trade network. The adjacency matrix $A = [a_{ij}]$ denotes the unweighted network. If there is a trade relationship between the two countries, $a_{ij} = 1$, otherwise $a_{ij} = 0$, in the undirected network, $a_{ij} = a_{ji}$. The adjacency matrix $W = [w_{ij}]$ represents the weighted trade network. In the directed network, the edge weight is expressed by the export volume (million US dollars) from v_i tov_j. In the undirected network, the total trade volume (million US dollars) between v_i and $v_j$is used to represent the edge weight, that is, $w_{ij} = w_{ji}$. Where $w_{ij} = w_{ij}^e + w_{ij}^m$, $(i, j = 1, 2, \ldots, n)$, $w_{ij}^e\,(w_{ij}^m)$ represents the trade amount that the v_i exports (imports) to v_j. Referring to Cerina's method [35], set 100 million US dollars as the threshold of trade flows, the trade volume of each network after taking the threshold value over the years accounts for more than 90% of the total trade volume of the corresponding fully connected trade network, which indicates that the network after extracting the threshold value is relatively representative. After determining the threshold value, the edge whose trade flows is greater than it is assigned to 1, otherwise it is assigned to 0, so as to halve the weighted network to obtain the unweighted trade network.

3.2. Research Methods

3.2.1. Network Analysis. Social network analysis is a comprehensive method to analyze the structure and attribute of "social actors as nodes and their relationship set"; this method is widely used in investment relations, population migration, and knowledge spillover relations because it can reveal the network structural features from multiple angles [36]. The selection and analysis of specific research indicators in this paper are carried out according to the following ideas: the first is the overall analysis of the network, which aims to explore the whole evolutionary trend, including network density, average degree, average path length, and average clustering coefficient. The second is the node analysis of the network, which studies the status and function of trade entities in the network, including degree centrality, closeness centrality, and betweenness centrality, and the node strength. Finally, the cohesive subgroup structure and core-periphery structure are synthetically determined based on the index features to divide the subgroups and levels in the network. Relevant indicators are shown in Table 1.

3.2.2. Empirical Model. The existing literatures usually consider the influence of economic scale, geographical distance, and institutional differences on trade relations and flows [37, 38]. In addition, participating in common regional trade agreements may reduce the cost of trade, but it is necessary to pay attention to the negative effects due to their asymmetric impact on countries [39]. The function of informal institutions such as culture in trade cannot be ignored, Selmier et al. pointed out that the positive communication of language culture will reduce the blind area of bilateral trade cognition and the cost of information acquisition [40]. Because the producer services are technology-intensive industries, technological innovation also plays a major role in the development of producer services trade [33]. Besides, affected by trade demands and transaction markets, population size may change the global trade pattern [41].

Based on this, we build the following model to analyze the factors influencing the evolution of producer services trade network:

$$Y = F(\text{Dis\_}gdp, \text{Comfta}, \text{Dis\_cap}, \text{Dis\_ins}, \text{Comlan}, \text{Dis\_tec}, \text{Dis\_pop}), \quad (1)$$

where Y is the producer services trade relation matrix; Dis_gdp, Dis_cap, Dis_ins, Dis_tec, Dis_pop represent the differences in economic scale, geographical distance, institution, technology, and population size, respectively, while Comfta and Comlan represent the trade agreement and language relationship between the two countries; the specific variable representation and data sources are shown in Table 2.

The variables belong to relational data and have structural autocorrelation; traditional multiple regression analysis based on ordinary least squares cannot reflect the correlation between them. QAP regression is a

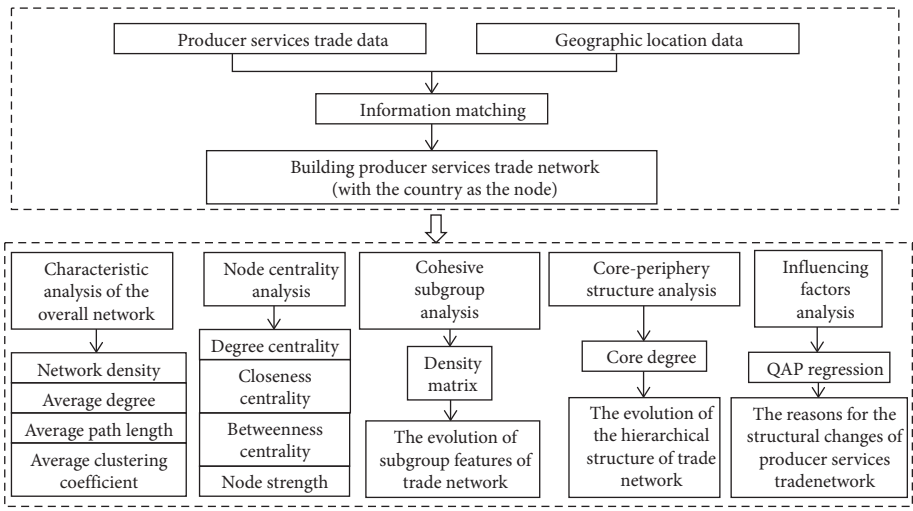

Figure 1: Logical framework.

Table 1: Network analysis indicators.

Indicators	Formulation	Index explanation	Actual meaning
Network density	$D = (2m/(n(n-1)))$	D refers to the proportion of the actual number of node connections in the network to the maximum number of possible node connections.	The activity of producer services trade links among countries.
Average degree	$\overline{k} = (1/n)\sum_i^n k(v_i)$	$\overline{k}$ refers to the average of the degrees of all nodes, $k(v_i)$ represents the degree of node. v_i.	The connectivity of the whole trade network.
Average path length	$L = (1/(n(n-1)))\sum_{i,j} d_{ij}$	L refers to the average number of the shortest path between each pair of nodes, d_{ij} represents the shortest path between nodes v_i and v_j.	The transmission efficiency of trade network.
Average clustering coefficient	$\overline{C} = (1/n)\sum_{i=1}^n C(v_i)$ $= (1/n)\sum_{i=1}^n (\sum_{j,k\in G} a_{ij}a_{jk}a_{ki}/k(v_i)(k(v_i)-1))$	$\overline{C}$ is the mean value of the clustering coefficients of all nodes. $C(v_i)$ represents the clustering coefficient of node v_i.	The degree of aggregation and adjacency of trade network.
Degree centrality	$C_D(v_i) = ((\sum_{j=1}^n a_{ij}(i \neq j))/(n-1))$	$C_D(v_i)$ describes the ability of direct contact of node v_i with others.	The possibility of direct trade links between a country and other countries.
Closeness centrality	$C_C(v_i) = ((n-1)/\sum_{v_j \in V, i \neq j} d_{ij})$	$C_C(v_i)$ refers to the sum of the shortest path between an individual node and all other nodes.	The relative spatial accessibility of countries in trade network.
Betweenness centrality	$C_B(v_i) = (\sum_{j<k}(g_{jk}(v_i)/g_{jk})/((1/2)(n-1)(n-2)))$	$C_B(v_i)$ refers to the probability that a node is in the shortcut between node pairs. g_{jk} is the number of shortcuts between node v_j and v_k. $g_{jk}(v_i)$ is the number of shortcuts between node v_j and v_k that passes through the node v_i.	The transfer function of countries in trade network.
Node strength	$S(v_i) = \sum_{j=1}^n a_{ij}w_{ij}$	$S(v_i)$ is the sum of weights of all edges connected to the node v_i. In the directed network, it can be divided into out-strength and in-strength.	Trade volume between countries in a weighted trade network.
Core degree	$\rho = \sum_{i,j} a_{ij}\delta_{ij}$ $\delta_{ij} = c_i \times c_j$	By iterating different pattern matrices δ to obtain the maximum value ρ. At this time, δ is the actual corresponding core-periphery structure matrix. c represents the core degree of node, a_{ij} is the element in adjacency matrix$A$, δ_{ij} is the element in pattern matrix δ of the core-periphery structure, and ρ represents the correlation between matrix $A$and matrix δ.	The status and importance of a country in trade network.

Table 2: Variable description and data sources.

Driving factors	Variable description	Data sources
Economic scale difference	The absolute difference of GDP growth rate between v_i and v_j countries.	The WDI database
Trade agreement relation	If countries v_i and v_j have a common trade agreement, it is 1, otherwise it is 0.	The CEPII database
Geographical distance difference	The actual distance between the capitals of v_i and v_j countries.	The CEPII database
Institutional difference	The calculation formula is: Dis_ins = $(1/6)\sum_h^6 \lvert((I_{ih} - I_{jh})/(\max I_h - \min I_h))\rvert$, h represents six dimensions to measure the national institution, namely, control of corruption, government effectiveness, political stability and absence of violence, regulatory quality, rule of law, voice and accountability, I_h represents the score on the h dimension [42].	The WGI database
Language relationship	If countries v_i and v_j have common official language, it is 1, otherwise it is 0.	The CEPII database
Technical difference	The absolute difference in the number of patent applications between v_i and v_j countries.	The WDI database
Population size difference	The absolute difference in population scale between v_i and v_j countries.	The CEPII database

nonparametric test method, which is used to analyze the regression relationship between multiple matrices and one matrix, avoiding the error problem caused by data "multicollinearity" in traditional measurement methods. Therefore, we use the method of QAP regression to explore the factors that affect the structural changes of producer services trade network.

4. Spatial Analysis of the Topological Feature of the Producer Services Trade Network

4.1. Spatial Pattern Evolution of the Producer Services Trade Network. This paper uses ArcGIS 10.4 to take countries as network nodes, the bilateral import and export volume of producer services trade as weight, and selects the data of four time periods of 2000, 2004, 2008, and 2012 to construct the structure chart of undirected producer services trade network to study its spatial and temporal evolution.

The evolution of producer services trade pattern can be described simply by the node strength of each country and trade flows between countries. The following conclusions can be drawn from Figure 2: the node strength of each country and the edge weight of neighboring node countries were increasing, and the trade links among countries were closer, forming an integrated and interdependent trade network. The reason is that the deepening of economic globalization and the adjustment strategy of industrial structure incline to service industry, the status of producer services industry in the domestic economy is rising, and the trade development continues to be active. Except for the most significant trade volume between the United States and Japan in 2000, the scale of producer services trade between the United Kingdom and the United States was the largest in the remaining years. Because spatial proximity was an important driving factor for the occurrence of regional trade phenomena, other closely related trading partners were generally countries with closer geographical location, such as Germany-the United Kingdom, the United Kingdom-France, the United States-Canada, the United States-Mexico. The establishment of the North American Free Trade Area and the foundation of the European Union also promoted intra-regional trade links. Since the United States was the absolute core of the trade network, and the trade mode has evolved from intra-regional clusters to trans-continental trade (such as the United States-China, the United States-India), the spatial pattern of producer services trade network has gradually transformed from a dual-core pattern of "the United States-Western Europe" to a cross-regional radial pattern with the United States as the explosive point.

The change of international demand structure and the difference of industrial chain status in different countries lead to more and more regional and national imbalances in the development of producer services trade, which is reflected in the spatial heterogeneity in the network. The whole network presented two high-value trade concentration regions, namely, East Asia and Western Europe. Southern European countries, such as Croatia, Bulgaria and Slovenia, as well as Southeast Asian countries, such as Cambodia, Vietnam, and Brunei, have formed low-scale trade agglomeration areas in space. In terms of node significance, the most critical trade nodes in North America were the United States and Canada, and the United States had the highest node strength each year. Other developed countries such as Germany, the United Kingdom and France, as secondary links, occupied the central position and supported the development of trade network. Before 2008, China, South Korea, Singapore, and Japan were essential nodes in the Asian region. After 2008, policy reform, technological progress, deepening division of labor, investment inclination, and other factors have jointly promoted the growth of producer services in India, so it became another vital node in Asia. This shows that in recent years, the status of a subset of emerging economies in the producer services trade network has risen, but it has not gradually changed the leading position of developed countries.

Over time, geographical factors were no longer a factor restricting trade exchanges, and the degree of trade globalization was strengthening, so the trade links between various countries were characterized by diversification. For example,

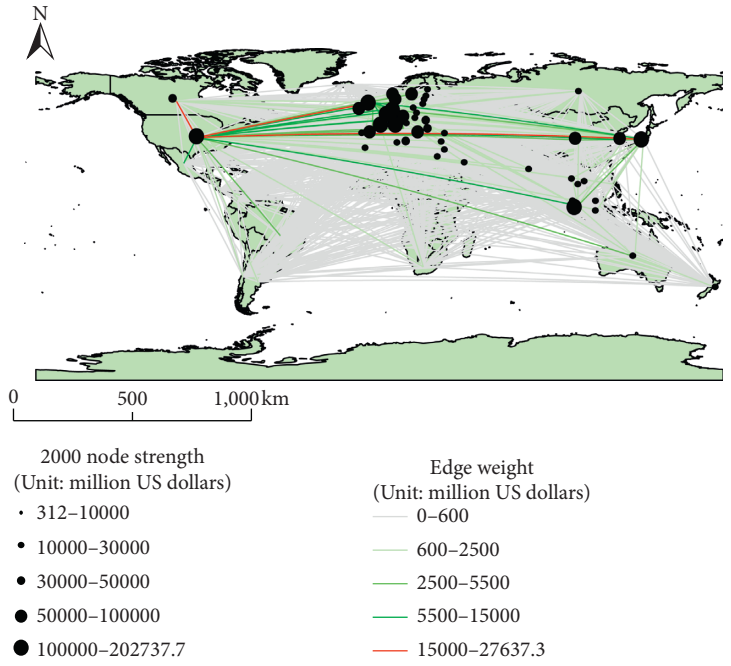

(a)

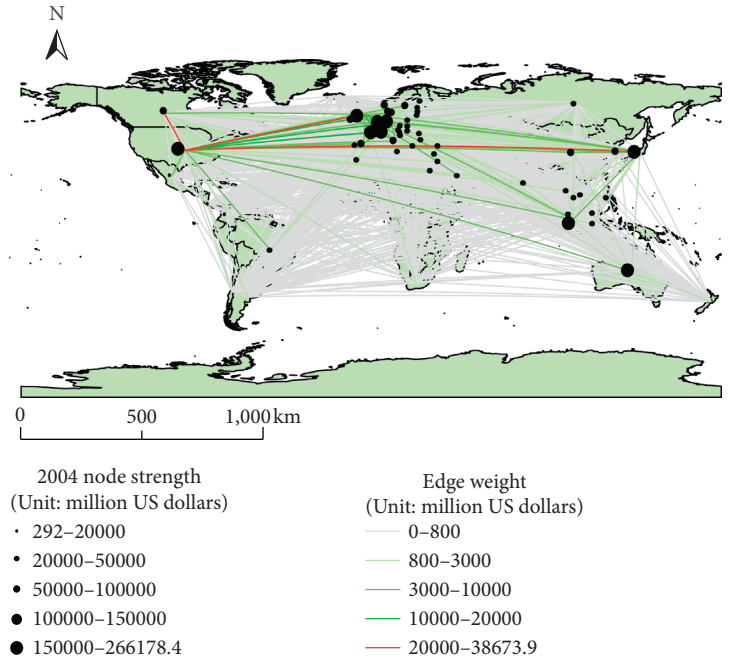

(b)

Figure 2: Continued.

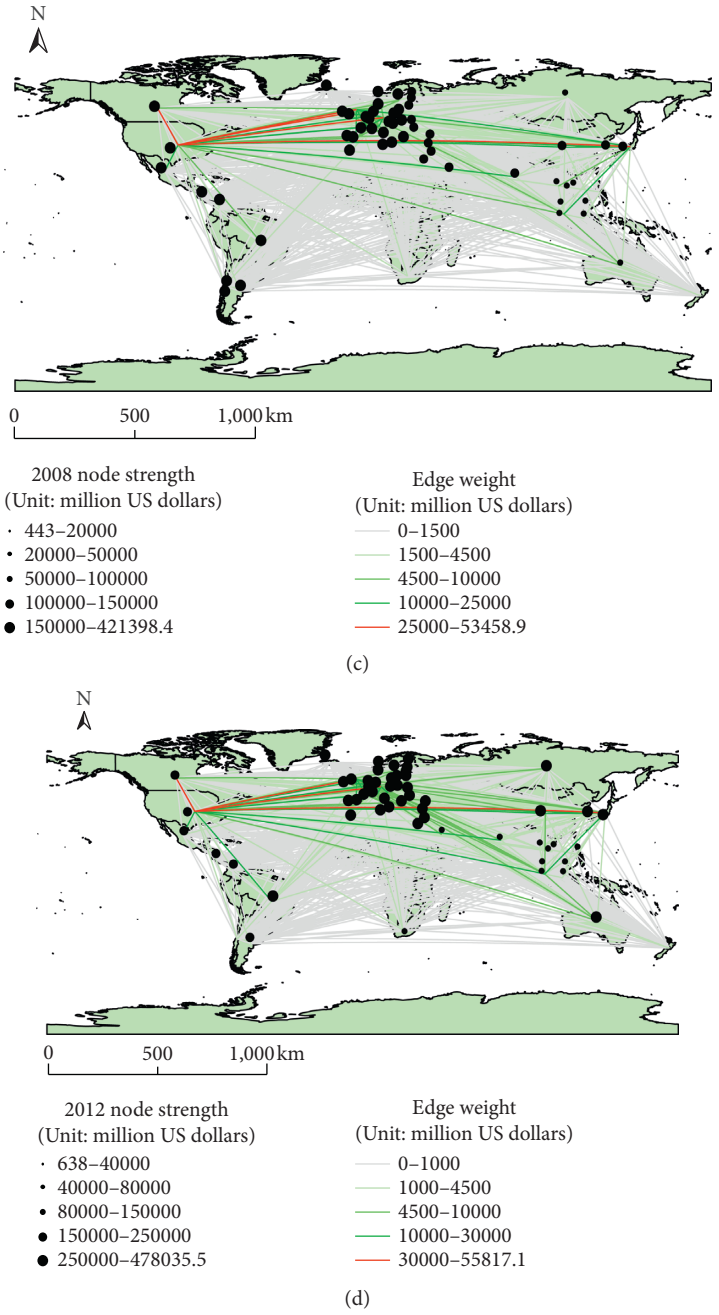

Figure 2: Spatial structure diagram of the producer services trade network.

China only had strong trade ties with a limited number of countries such as the United States, Japan, and South Korea in 2000. By 2012, these countries were still the closest partners in cooperation with China, while the "triangular trade" of producer services between China, Japan, and South Korea in Asia showed a weakening trend, and Singapore, France, and Germany have become significant trade options.

4.2. Analysis of the Overall Network Topology Characteristics. Then, this paper calculates topology indexes to reflect the overall characteristics of producer services trade network.

In comparison to the changes in network indicators from 2000 to 2012, the following conclusions can be drawn as shown in Table 3: the increase in the number of edges connecting node countries and density shows that the producer services trade network has a tendency of intensification, which is mainly due to the enhanced tradability of service industry in the era of knowledge economy. Network density grew fastest between 2004 and 2008; after 2008, it was relatively stable. The possible reason is that the financial crisis in 2008 has a more significant impact on services trade, and countries have to maintain conservative trade relations to deal with its occurrence.

Table 3: Characteristic statistics of the overall network of producer services trade.

Year	Number of edges	Network density	Average degree	Average path length	Average clustering coefficient
2000	509	0.28	16.68	1.74	0.55
2004	658	0.36	21.57	1.64	0.61
2008	857	0.47	28.09	1.53	0.70
2012	892	0.49	29.25	1.51	0.71

The upward momentum of the average degree suggests that the connectivity of the network is enhanced. In 2000, the average path length was close to 2, and each pair of countries with trade needs to establish an indirect relationship through another country. After 2000, the average path length shortened; more and more producer services products can arrive without passing through transit nodes, saving time and transportation costs, and improving the efficiency of trade transactions.

The average clustering coefficient has been rising from 2000 to 2012, which indicates that the producer services trade network had a more obvious phenomenon of trade clusters. Generally speaking, compared with random network with the same number of nodes and edges, a small world network has a smaller average path length and a larger average clustering coefficient [43]. Because the average path length of producer services trade network is in the range of 1.51 – 1.74, which is slightly lower than the theoretical value of the random network of the same scale (1.78 –2.14), and the average clustering coefficient is in the range of 0.55 –0.71, which is much higher than the average clustering coefficient of the random network (0.13 – 0.24), it can be considered that this network is a small world network, that is to say, the producer services trade network exhibits the aggregation features of a few nodes as the core; these nodes have a high number of connections, while most other nodes only have fewer connections [44].

4.3. Network Centrality Analysis

4.3.1. Centrality of the Unweighted Network. This paper calculates the centrality indicators of all sample countries to explore the individual characteristics of nodes, and then uses Arcgis10.4 for data visualization. Due to space constraints, the top 15 countries and values in 2000 and 2012 are shown in Table 4. In addition, we study the status of countries in the network according to their rankings.

The evolution of centrality index of producer services trade network is shown in Table 4 and Figure 3. The degree centrality of a node represents the number of trade relations and it is the simplest indicator to evaluate its position in the trade network; the results indicate that the top three key nodes are stable in the United States (USA), the United Kingdom (GBR), and Germany (DEU). Due to the lack of location advantages and breakthrough technology, some countries had limited ability to participate in the specialized division, resulting in weaker producer services trade attractiveness, such as Cambodia (CAM) and Costa Rica (CRC), which had the lowest degree centrality. Regarding spatial layout, among the top 15 countries, in 2000, there were 2 in North America, 9 in Europe, and 4 in Asia. In 2012, Asian countries increased to 5, North American countries decreased to 1, and the number of European countries remained unchanged. With the development of service outsourcing as a new mode of service trade, developing countries have increased investment in communication, computer and information services, and actively undertaken the outsourcing business of developed countries. China (CHN), India (IND), and other countries have gradually become regional or global service outsourcing centers. In particular, benefited from the high concentration of services trade, India showed a trend of long-term rapid growth, making its degree centrality increase significantly. Constrained by the economic slowdown brought by the financial crisis, the activity of producer services trade in developed regions has decreased, resulting in the decline of the average annual growth rate of degree centrality of countries in Europe and American, which are located at the core of the network. But on the whole, the degree centrality of developed countries is still higher than that of the developing countries; developed economies generally have stronger international competitiveness in producer services trade.

The closeness centrality is used to characterize the ability to be "not controlled by other countries." Due to the high degree of trade facilitation and the less dependence on other countries to establish trade relations, countries in the central position, such as the United States and the United Kingdom, usually had higher closeness centrality. The existence of these countries played a vital role in the spatial flow of industrial resources and they acted as the resource "connectors" in the trade network. Conversely, countries that needed more steps or intermediaries to establish trade relations had lower closeness centrality, such as Cambodia and Brunei (BRU). These countries had low efficiency in connecting with other countries and found it difficult to gain spatial advantages.

The betweenness centrality measures the node's ability to control other nodes. The higher the degree, the more the node can serve as a "bridge" in the network. The United States, the United Kingdom, and Germany were still at the forefront; they played an important "intermediary" role and transit capacity in producer services trade network and controlled the links between other countries. The node with the fastest growth in betweenness centrality was Luxembourg, with an average annual growth rate of 48.2%, which may be related to its highly developed finance, insurance services and securities market. As a financial center, a number of service enterprises have formed an outstanding service network. However, emerging economies such as

Table 4: Centrality analysis of the producer services trade network (Top 15).

Rank	2000						2012					
	Degree centrality		Closeness centrality		Betweenness centrality		Degree centrality		Closeness centrality		Betweenness centrality	
	Country	Value	Country	Value	Country	Value	Country	Value	Country	Value	Country	Value
1	USA	98.33	USA	98.36	USA	26.62	USA	100.00	USA	100.00	USA	10.75
2	DEU	85.00	DEU	86.96	GBR	10.39	GBR	95.00	GBR	95.24	GBR	4.78
3	GBR	80.00	GBR	83.33	JPN	7.21	DEU	93.33	DEU	93.75	DEU	4.05
4	JPN	75.00	JPN	80.00	ITA	6.26	FRA	88.33	FRA	89.55	FRA	3.10
5	FRA	68.33	FRA	75.95	AUT	4.20	NLD	86.67	NLD	88.24	JPN	2.93
6	ITA	65.00	ITA	74.07	CAN	3.97	SUI	85.00	SUI	86.96	NLD	2.76
7	NLD	61.67	NLD	72.29	FRA	3.57	JPN	81.67	JPN	84.51	SIN	2.60
8	SUI	61.67	SUI	72.29	CHN	2.72	ITA	81.67	ITA	84.51	SUI	2.50
9	SIN	55.00	SIN	68.18	SIN	2.07	DNK	80.00	DNK	83.33	ITA	2.35
10	DNK	51.67	DNK	67.42	SUI	1.69	SIN	78.33	SIN	82.19	DNK	2.04
11	ESP	50.00	ESP	65.93	IND	1.60	BEL	78.33	BEL	82.19	KOR	1.97
12	CHN	45.00	CHN	64.52	BEL	1.27	KOR	78.33	KOR	82.19	BEL	1.81
13	KOR	45.00	KOR	64.52	KOR	0.98	CHN	76.67	CHN	81.08	CHN	1.27
14	CAN	43.33	CAN	63.83	BRA	0.98	SWE	71.67	SWE	77.92	AUT	1.01
15	BEL	40.00	BEL	61.86	DEU	0.62	IND	70.00	IND	76.92	SWE	0.98

India, China had relatively small betweenness centrality, indicating that they do not yet have the same industrial advantages and control power as European and American countries. In 2000, there were 25 countries whose betweenness centrality value was 0, and it was reduced to 12 countries in 2012; the intermediary capacity of each country in producer services trade network still has excellent disparity, which is an alternative expression of the dependence between trade supply and demand countries.

4.3.2. Centrality of the Weighted Network. In order to show more clearly the changes in trade flow and volume over the long term, a $61 * 61$ relationship matrix was constructed for the weighted and directed network of producer services trade in 2000 and 2012. The rows of the matrix represent the importing country, the columns show the exporting country, and the cells suggest the trade flow from column nodes to row nodes.

Figure 4 shows the export heat map of producer services trade. The shades of color represent the export volume of producer services trade products of various countries. The larger the export volume, the darker the color. Comparing the export heat maps of 2000 and 2012, we can find that orange cells are more densely distributed, which suggests that the interaction between trade entities and the breadth of trade flow are gradually enhanced. However, both heat maps are dominated by light blue cells; it can be found that although the trade volume in this stage has increased significantly, countries with weak trade exchanges of producer services products still have a considerably large proportion, shaping "center-remoteness" block matrix feature. The United States, Germany, the United Kingdom, Japan, Singapore, and other countries with frequent trade contacts form the internal network of the central countries. From the color change of cells, the trade interaction between the central group countries was significantly raised in 2012, while the density of trade flow between central countries and external countries, as well as within external countries, was relatively small. This may be because the radiation and driving force of the countries located in the central plate is relatively limited, and the industrial foundation of the marginal countries is weak So, it is difficult to form deep integration in a short time.

Furthermore, we use the node strength to discuss the centrality features in weighted network. Among them, the out-strength and in-strength are expressed by the weighted out-degree and weighted in-degree of the node, respectively.

Figure 5 describes the changes in the out-strength of various countries. From 2000 to 2012, the export value of producer services trade showed a rapid growth trend; the United States, the United Kingdom, and Germany were in the first echelon of out-strength ranking. The advanced production system and economic strength determined the competitiveness and attractiveness of these countries. From the perspective of spatial distribution, the countries with higher out-strength were mainly concentrated in the European region. Countries such as France, the Netherlands, and Switzerland had strong supply capacity of producer services products. Tunisia in Africa, Brunei and Cambodia in Southeast Asia were the main low out-strength countries. Japan and Singapore were in the leading position of Asia in the network. In 2000, the range of out-strength was 114,366 million U.S. dollars, and in 2012 it rose to 275,008 million U.S. dollars. This indicates that there is spatial polarization in the network, and the Matthew effect of the export of producer services is prominent.

Emerging economies such as China and India have gradually increased their ability to participate in producer services trade. India is the country with the fastest growth in out-strength, with an annual growth rate of 18.82%. From 2000 to 2012, China's out-strength increased from 22nd to 14th; the reason is that China has considerable advantages in many emerging markets such as foreign labor export

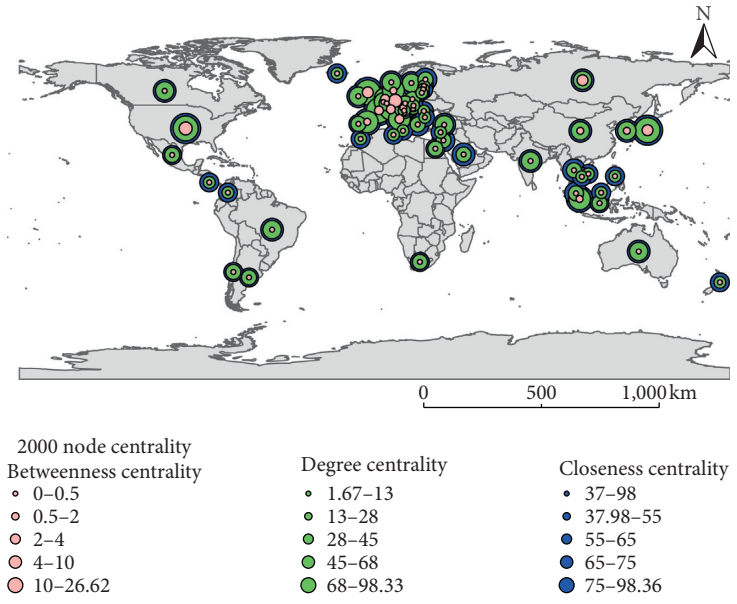

(a)

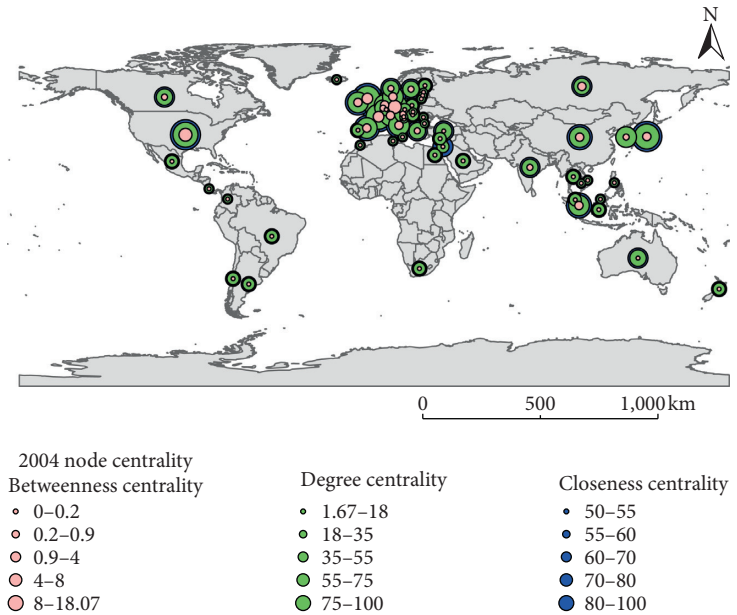

(b)

Figure 3: Continued.

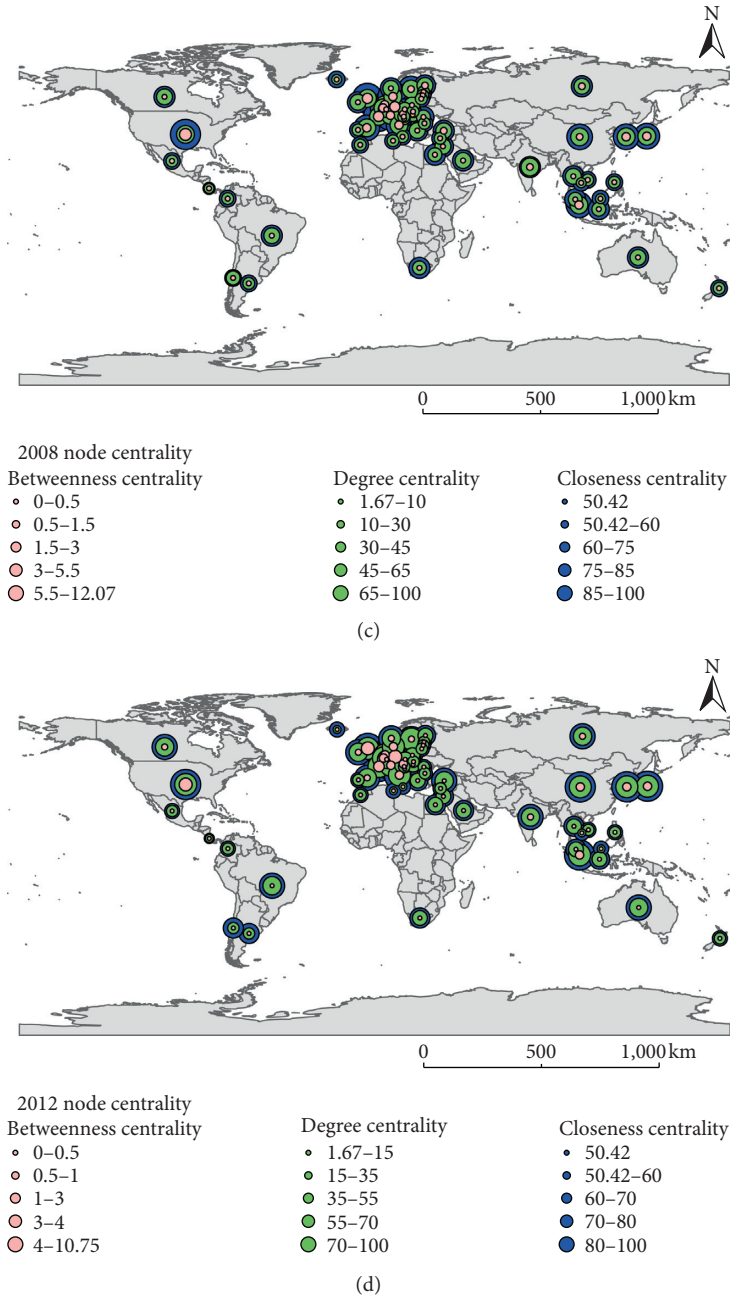

Figure 3: The evolution of centrality of the producer services trade network.

(including engineering), international tourism, transportation and logistics, which is the main direction of service trade export. As a result of the negative effect of the global financial crisis, the average annual growth rate of the out-strength of primary countries declined from 2008 to 2012, and even the out-strength index of the United Kingdom, Italy, Sweden, and other countries that were greatly affected did not increase but decreased in 2012.

Figure 6 shows the modification of the in-strength of producer services trade network. Since the influence of weight on node strength is considered, the importance of some countries has gradually improved with the increase of trade flows, such as India and China, but the performance is relatively different. India is driven by a large number of exports, while China is mainly pulled by the growth of imports. It can be said that India's out-strength effect is more potent than its in-strength effect, while China's is on the contrary, which may depend on the fact that China is a typical producer services consumption country and has a high degree of external dependence. China's weight in-degree increased from the 16th in 2000 to the 4th in 2012. It was the fastest-growing country in the sample, with an average annual growth rate of 19.38%. Among them, the United States, Japan, South Korea were the primary sources of imports.

Due to the lack of information technology and human capital, as well as the obstacles of opening-up level and

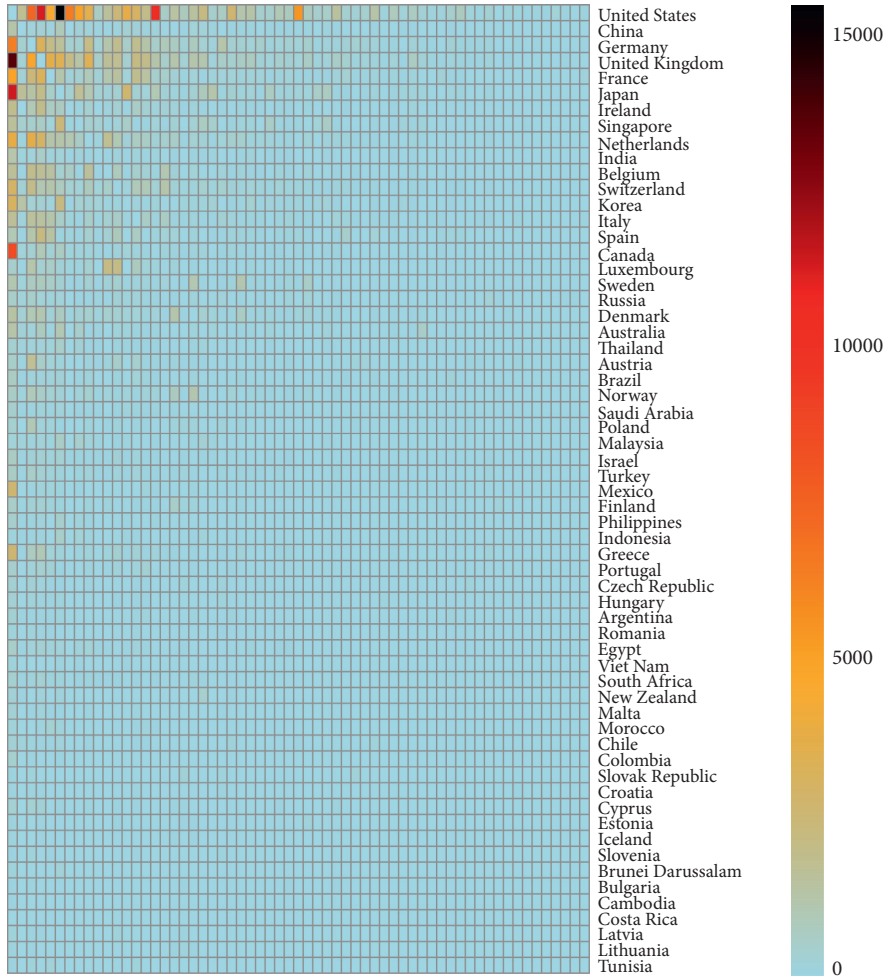

(a)

Figure 4: Continued.

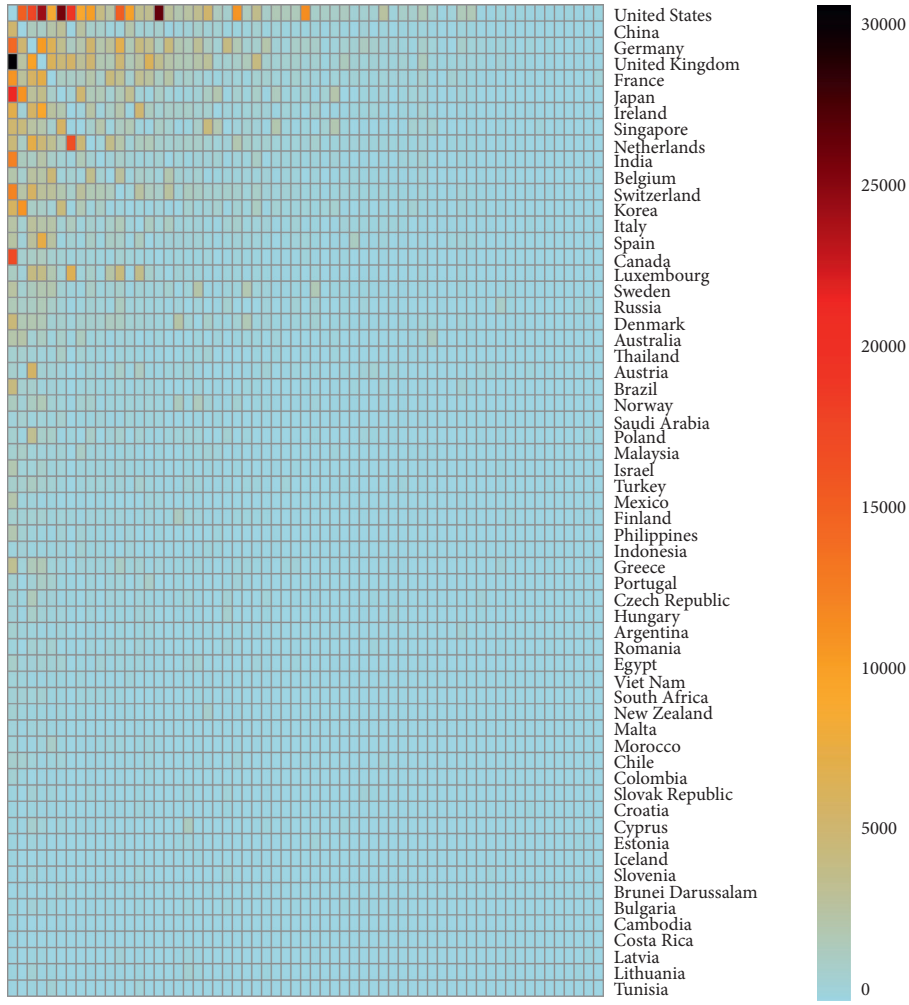

(b)

Figure 4: Export heat map of producer services trade. (a) 2000; (b) 2012.

management organization, the out-strength and in-strength of Eastern European countries such as Estonia, Lithuania, and Latvia, as well as the southern European countries such as Bulgaria and Croatia remained weak. So, they had only low comprehensive influence. Further, the in-strength shows the Matthew effect of increasing range, which is the same as that of out-strength.

Compared with the centrality analysis in the unweighted network to explore which countries have a wider trade scope and greater control over resources and information, the centrality index in the weighted network, node strength, considers more deeply the impact of trade volume on the status of countries in the network. Typically, several emerging developing economies have not shown remarkable core power in the unweighted network, but their position in the weighted network has risen significantly due to the consideration of trade scale. Integrating the centrality research results of the two kinds of networks, we found that there is a strong positive correlation between them; countries with more trading partners tend to have higher trade strength. For instance, countries such as the United States, the United Kingdom, and Germany with higher node centrality indicators in the unweighted network are consistent with countries with upper node strength in the weighted network; these countries have both extensive trade links and substantial foreign trade. The reason lies in that the developed countries have a solid base of producer services and provide comprehensive policy support for producer services trade. Under their competitive advantages in knowledge-intensive and technology-intensive services industries, they can choose more trade target countries and generate massive trade flows, thus becoming a powerful producer services trade country.

5. Cohesive Subgroup Analysis and Core-periphery Structure Analysis

5.1. Cohesive Subgroup Analysis. In the formation process of producer services trade network, the trade entities will conform subgroups due to the affinity of trade relations. Therefore, referring to Wang's research method [45], considering that the subgroup division is more robust after long-

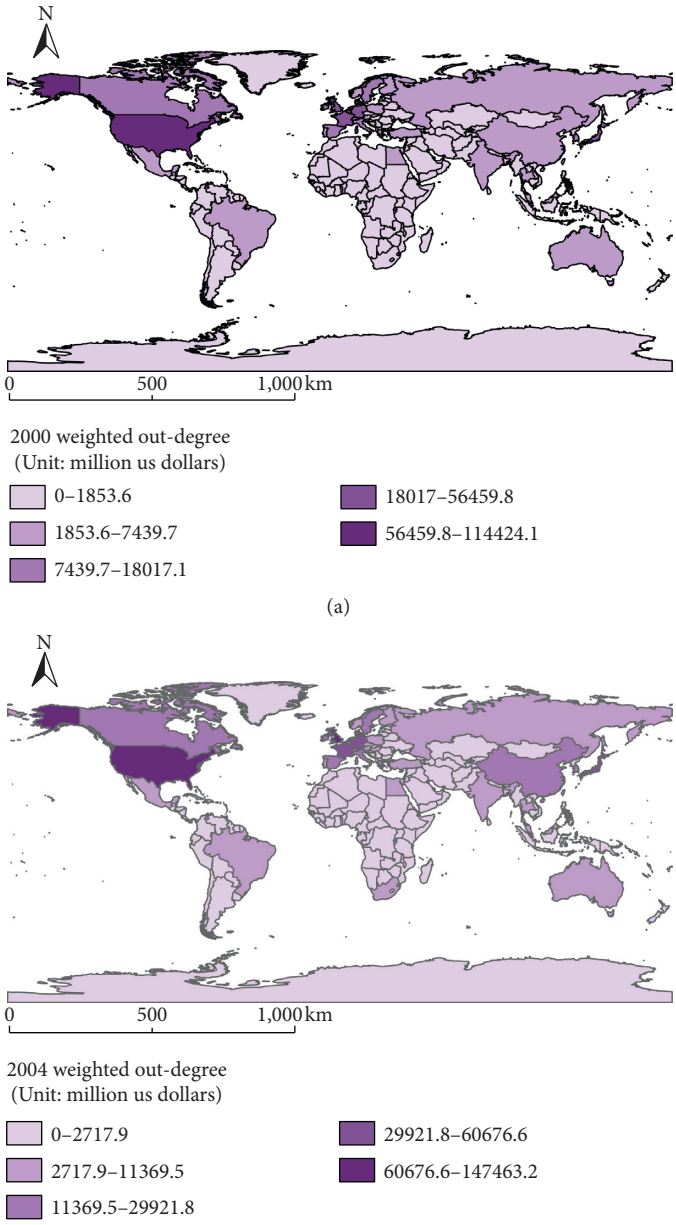

Figure 5: Continued.

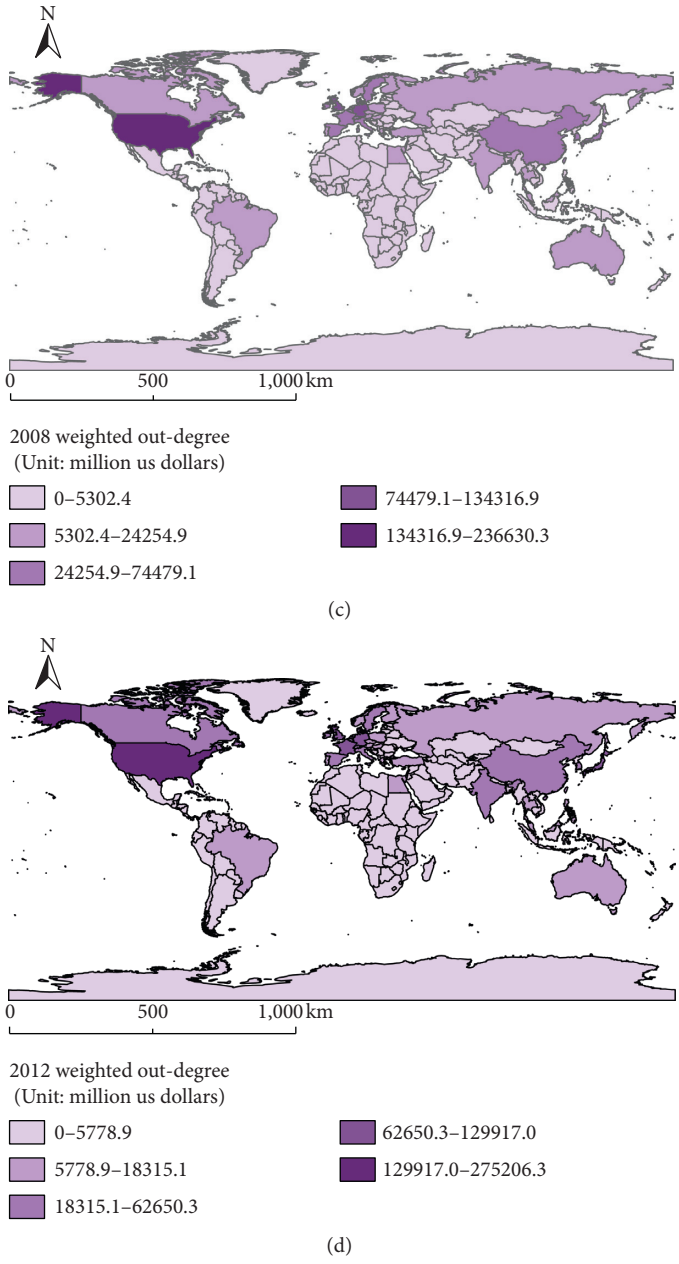

Figure 5: Out-strength spatial distribution of the weighted and directed network.

term development, this paper selects 2000 and 2012 as the representative years, and uses the CONCOR algorithm to carry out cohesive subgroup analysis, so as to determine the number of subgroups and the members included in them, and explore the spatial spillover relationship, with the purpose of studying the evolution of producer services trade network from the perspective of subgroup structure.

The calculation results show that the producer services trade network has cohesive subgroup structure, and the classification of cohesive subgroups is not strictly based on the economic level. According to Figure 7(a), the producer services trade network in 2000 was divided into four subgroups, of which subgroup I was represented by the United States, Netherlands, and the United Kingdom. This subgroup was agglomerated by the attraction of economic strength to form an American and European community composed of 13 countries. Subgroup II had the most enormous scale. Due to geopolitical and cultural factors, it had formed an Asia-Europe association represented by China, India, including 29 Asian, European, and African countries such as South Korea and Singapore. Subgroup III was represented by Hungary, including 15 European and South American countries such as Czech and Chile. Subgroup IV was an independent community consisting of Croatia, Cambodia, Bulgaria, and Lithuania. Shown by Figure 7(b), the number of subgroups did not change in 2012, but the community differentiation within the subgroups was modified. China, South Korea, and other rapidly

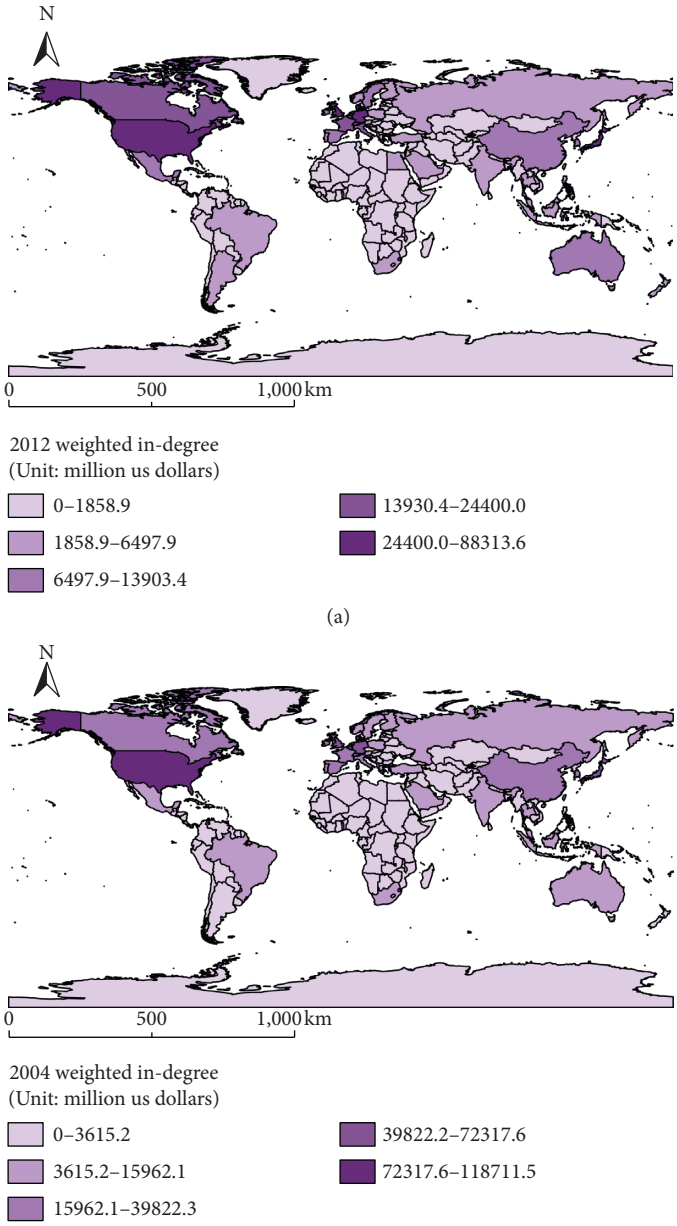

Figure 6: Continued.

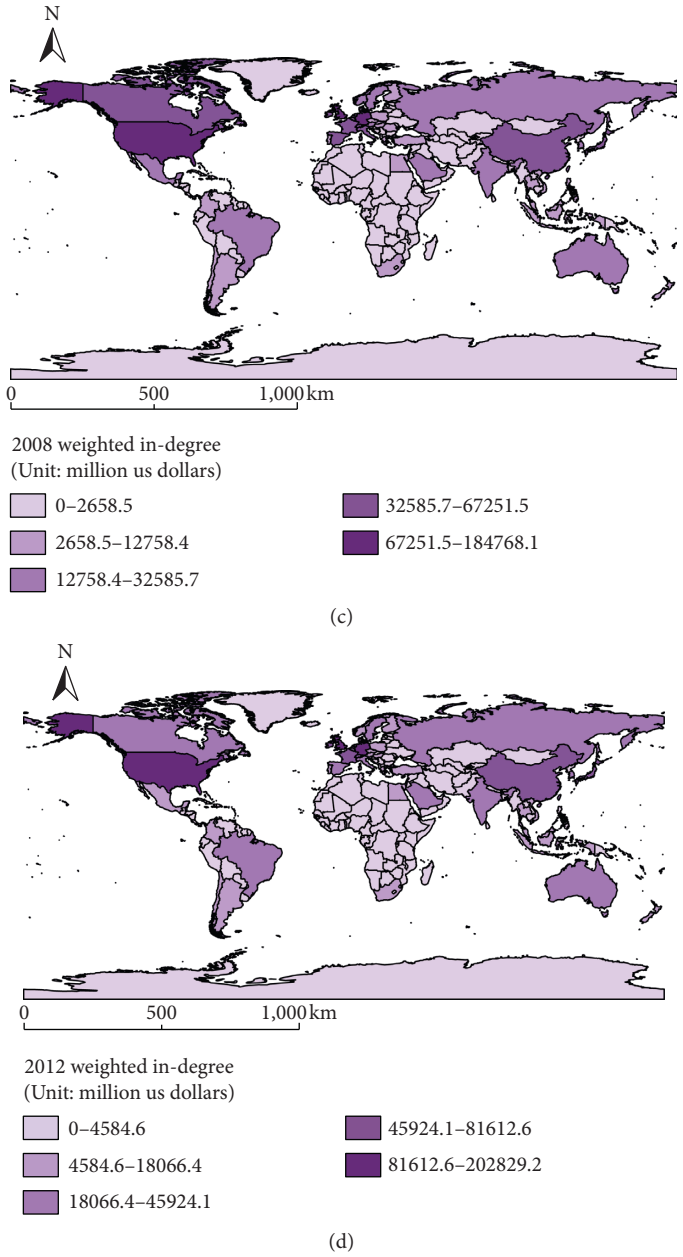

Figure 6: In-strength spatial distribution of the weighted and directed network.

developing Asian countries entered subgroup I from subgroup II, and integrated with developed countries into a community. Subgroup II was still the community with the largest number of members. The close geographical distance made Croatia and Bulgaria enter subgroup III from subgroup IV; thus, subgroup III became an association with southern European countries as its main members, while the subgroup belonging to other major countries in the world, such as Russia and Canada, had little change. Countries such as the United States, Germany, the United Kingdom, France, and Japan were all in the same subgroup in 2000 and 2012; these countries tend to choose each other based on the principle of reciprocity and have stronger condensation effect compared with trade linkages among other countries.

Table 5 shows the spatial spillover relationship between cohesive subgroups, and the value of the diagonal of the density matrix reflects the density of the internal association of the subgroups. In 2000, the density value within subgroup I was the largest, the trade ties among the member states in the plate were relatively sufficient, and subgroup I had a distinctive feature of reflexivity. The reason is that subgroup I, including the United States, Germany, the United Kingdom, and other traditional powers of producer services trade, can exert significant influence on trade by making use of location attraction and industry advantages. In addition, subgroup I had a strong spillover effect on subgroup II, and the import of producer services trade of subgroup II mainly came from

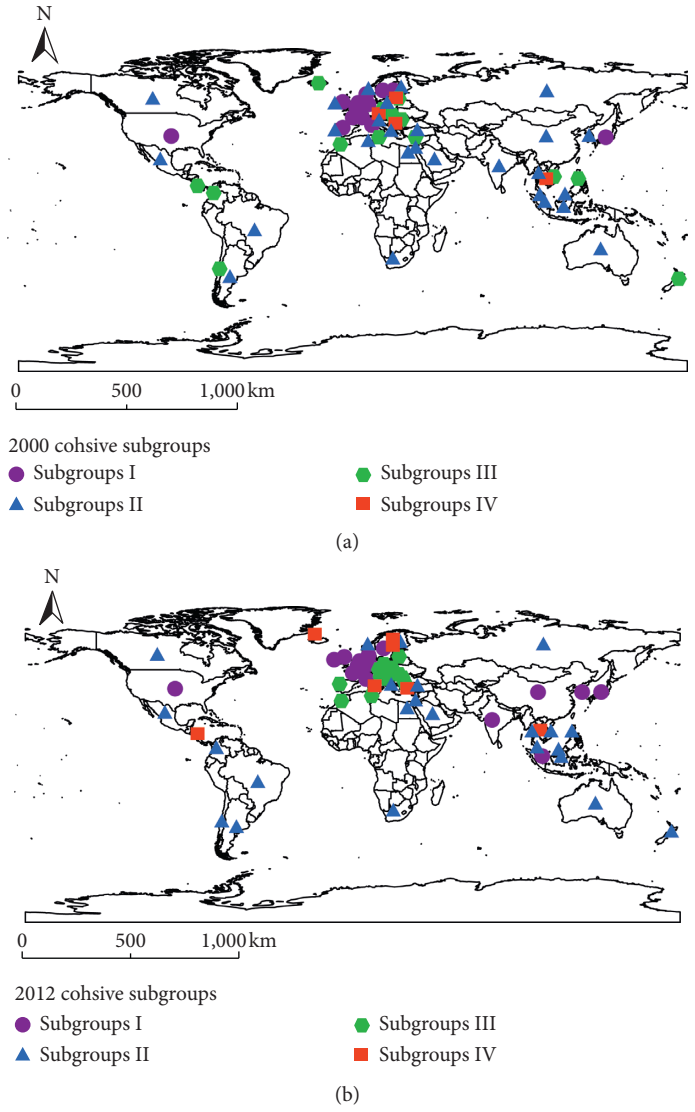

Figure 7: Cohesive subgroups of the producer services trade network in 2000 and 2012.

Table 5: Density matrix of cohesive subgroups of the producer services trade network.

	2000					2012			
	I	II	III	IV		I	II	III	IV
I	0.833	0.515	0.144	0.000	I	0.980	0.797	0.427	0.103
II	0.509	0.081	0.028	0.000	II	0.652	0.190	0.033	0.043
III	0.149	0.021	0.010	0.000	III	0.491	0.054	0.244	0.011
IV	0.000	0.009	0.000	0.000	IV	0.183	0.037	0.022	0.048

subgroup I. Subgroup II also had spillover effect on subgroup I, while the internal relationship was weak. Subgroup III only had fairly sparse trade relationship with subgroup I, and subgroup IV even did not have any acceptance or sending links with other subgroups. In 2000, both subgroup III and subgroup IV were in an extremely isolated position in the network. It can also be seen that the radiation effect of subgroup I on subgroup III and subgroup IV was still less, and the whole network was in a very unbalanced development stage.

In 2012, the density coefficient did not appear to a value of 0, and the values in the density matrix were all greater than those in 2000, indicating that the correlation between and within each subgroup was closer than that in 2000. Subgroup I was still in the plate with the closest internal trade connection, and it not only had significant spillover effect on subgroup II and subgroup III but also had a stimulating effect on the trade development of subgroup IV. From the point of view of the relationship between subgroups, subgroup II and subgroup I had the closest trade

relations, and the economies within these subgroups enhanced each other's influence through stable trade cooperation. Subgroup III also had spillover effect on subgroup I, and the internal trade linkage strength had been dramatically improved. This may be benefited by the evolution of subgroup III into a Southern European community in 2012, and the spatial proximity made the trade cooperation within the subgroup more intimate. However, the trade relationship between subgroup IV and other subgroups was still fairly sparse, making it difficult for each subgroup in the trade network to form a closed transmission mechanism in space. The subgroup agglomerated by countries with powerful economic forces (the United States, the United Kingdom, etc.) had radiative impact on both the inner and outer subgroups, which can be considered as an obvious two-way spillover effect, while the members who were in the position of the orphan depend on the supply from that subgroup.

5.2. Core-Periphery Structure Analysis. The core-periphery structure analyzes the spatial pattern evolution from the perspective of the network secondary structure. Chen Yinfei pointed out that the world economic structure can be divided into three levels, namely, the core layer, the semi-periphery layer, and the periphery layer. It is believed that the countries with the core degree greater than 0.1 are located in the core layer, countries with core degree greater than 0.01 but less than 0.1 are in the semi-periphery layer, and countries with core degree less than 0.01 are in the periphery layer [46]. Compared with other indexes, the core degree can directly reflect the national status and spatial hierarchy structure of the network. Most notably, the centrality and core degree are not necessarily the same; the centrality index reflects the growth of trade link and volume between countries, while the core country refers to the part of the subjects with strong interaction in the countries with high centrality. In the case of the lack of linkages between actors with high centrality, their core degree may be low.

As can be seen from Table 6, there is a "core-semi-periphery-periphery" structure in producer services trade network, but the number and members of each layer change, resulting in the reorganization of the hierarchical structure. The number of core layer countries only increased significantly in 2004, showing an inverted U-shaped trend of first rising and then falling. Most of the countries were in the semi-periphery areas, while the number of periphery countries has significantly increased from 2000 to 2012. The possible reason for this phenomenon is that the core countries are mainly developed countries, which have the right to speak and formulate rules of producer services trade. In order to maximize their own interests, many trade agreements have been signed. However, the existing rules have not adequately solved the problem of trade liberalization. Instead, the different preferential treatment and origin rules of each agreement are intertwined to form the "spaghetti bowl" effect, leading to the marginalization of some underdeveloped countries. As the trade network is supported by fewer core countries and semi-periphery countries, the control power has slightly decreased, which makes the network vulnerable, necessitating its structure to be optimized and improved

The results in Table 7 show that the core degree of each country fluctuated from 2000 to 2012. The top ten countries in the core degree were mainly powerful nations in Western Europe, such as the United Kingdom (GBR), France (FRA), and Netherlands (NLD). Regarding specific changes, the core degree of the United States declined significantly in 2004 and 2012. The reason may be that China's accession to the WTO and the official circulation of Euro increased the core degree of China, Germany, and France, resulting in the core degree of the United States declining for the first time. After the subprime crisis of 2008, the core degree of the United States declined for the second time. The core degrees of European Union (EU) member states, Germany and France, maintained the same change trend from 2000 to 2012. The Euro currency promoted the trade status of member nations, so the core degree of both countries improved greatly in 2004. Due to the impact of the financial crisis, the core degree in 2008 was lower than that in 2004, but after that, their core degree resumed the upward trend with the gradual recovery of the economy. Furthermore, countries with a high degree of centrality such as France and Denmark do not have a high core degree, which verifies the conclusion that the centrality index and core degree are not entirely the same. In terms of emerging economies, the core degree of BRICs member countries, namely, Brazil (0.062 to 0.085), China (0.02 to 0.099), Russia (0.038 to 0.05), and India (0.044 to 0.094), have significantly improved from 2000 to 2012, reflecting the increasing competitiveness and importance of these trading entities and the apparent tendency of diversification of the network.

6. Analysis of the Influencing Factors of the Producer Service Trade Network

After exploring the spatial heterogeneity and dynamicity of the producer services trade network, we further use the method of QAP regression to study the determinants of the evolution of network structure. In order to evade the great impact of the financial crisis on the structural changes of producer services trade network, this paper selects 2012, when the market gradually recovers stability and economic growth, and 2000, the first year of the statistical year, for QAP regression analysis. The corresponding matrix of the variables was brought into the regression model; after 2000 random permutations, the QAP regression results of the unweighted network and weighted network (shown in Table 8) are obtained. The models all pass the significance test of 1%.

By comparing the results in Table 8, it can be found that the estimated coefficient of economic distance was significantly negative in each regression model, indicating that the smaller the difference in economic development level between countries, the more conducive to the generation of trade relations and the increase of trade flows. The reason is that countries with small difference in economic levels have similar consumption structures, which increases the possibility of producer services trade. Trade agreement relations

Table 6: Number of core, semi-periphery, and periphery countries, 2000–2012.

Year	2000	2004	2008	2012
Core layer	12	15	11	12
Semi-periphery layer	46	38	42	38
Periphery layer	3	8	8	11

Table 7: Core degree of the producer services trade network (Top 10).

Year	2000		2004		2008		2012	
Rank	Country	Core	Country	Core	Country	Core	Country	Core
1	USA	0.626	USA	0.577	USA	0.679	USA	0.620
2	GBR	0.473	GBR	0.410	GBR	0.367	GBR	0.396
3	DEU	0.251	DEU	0.307	DEU	0.256	DEU	0.273
4	JPN	0.248	JPN	0.268	JPN	0.238	JPN	0.249
5	NLD	0.198	CAN	0.217	IRL	0.192	SUI	0.211
6	SUI	0.166	FRA	0.212	SUI	0.185	IRL	0.189
7	FRA	0.160	NLD	0.196	KOR	0.185	CAN	0.187
8	ITA	0.148	SUI	0.174	FRA	0.171	NLD	0.184
9	BEL	0.144	IRL	0.164	NLD	0.169	FRA	0.176
10	ESP	0.129	ESP	0.135	IND	0.152	SIN	0.124

Table 8: QAP regression result of the producer services trade network.

Variable	Unweighted network		Weighted network	
	2000	2012	2000	2012
Dis_gdp	−0.041*	−0.062*	−0.034*	−0.060**
Comfta	0.131***	0.026	0.045*	−0.058*
Dis_cap	−0.057	−0.144***	−0.037	−0.110***
Dis_ins	0.016	0.044*	−0.063***	−0.062***
Comlan	0.108***	0.083***	0.108***	0.130***
Dis_tec	0.261***	0.201***	0.178**	0.172**
Dis_pop	0.086*	−0.001	0.028	−0.028

Notes: ***represents $p < 0.01$, **represents $p < 0.05$, *represents $p < 0.1$.

had an important positive impact on the trade network in 2000, with common trade agreements facilitating trade exchanges. However, in the 2012 unweighted network, the regression coefficient did not pass the significance test of 1%. In the weighted network, it was significantly negative. The reason may be that the signing of a variety of bilateral and regional services trade agreements has formed the phenomenon of a "spaghetti bowl," and the producer services trade faces greater disputes, which on the contrary inhibits the trade cooperation among countries. The estimated coefficient of geographic distance was not significant in the two networks in 2000. In 2012, it was negative in both the unweighted and weighted network, and has passed the significance test of 1%, which shows that the producer services trade is also affected by geographic distance. This may be related to the fact that some producer services trade relies on goods trade and people's spatial transformation, such as the transportation industry, which is vulnerable to the influence of geographical distance, resulting in spatial proximity changing the structure of trade network. The regression coefficient of institutional distance was not significant in the unweighted network in 2000, but it is positive in 2012, and has passed the significance test of 10%; the institutional difference between the two countries had a certain impact on the establishment of trade ties. However, in the weighted network of 2000 and 2012, the regression coefficient of institutional distance had an extremely remarkable negative effect on trade network, indicating that countries had greater trade volume with partners adjacent to their own systems. This depends on the smaller institutional difference to reduce the distortion of resource allocation and the occurrence of corruption, and the lack of effective institutional guarantee will make international trade prone to friction and disputes. Language relationship had a notable positive impact on the formation of producer services trade network. The reason is that the linguistic homogeneity may mean that they are in the same cultural circle, communication barriers and risks in trade are less, thus it is easier to create trade links, and trade scale is larger than in countries with greater cultural difference. The regression coefficient of technical distance was significantly positive, which was consistent with the research conclusion of Yang Chen, who analyzed the factors influencing the services trade network structure from the perspective of industry heterogeneity. The difference in

technological level is in favor of the occurrence of new services trade relations such as finance and communication industry [33]. The regression coefficient of population size difference was only positive in the 2000 unweighted network, but not in other networks. It shows that in 2000, countries with large populations tended to establish trade links with small population countries, but they did not significantly increase trade scale. Because the difference of population size cannot directly affect the opening of the service market, this variable has little effect on the changes of producer services trade network.

7. Discussion and Conclusion

This paper constructs producer services trade network and explores its spatial heterogeneity and structural evolution. The main contribution lies in the innovative analysis framework of integrating social network and economic geography, deepening the comprehending of network topological function and interaction in producer services trade system, and providing reference for policy-makers to adopt appropriate trade strategies. The leading conclusions are as follows.

Geographically, the producer services trade network has evolved from a dual-core structure of "USA-Western Europe" to the radial mode with the United States as the explosive point. The spatial heterogeneity reflects the imbalance of trade pattern; frequent trade activities are primarily concentrated in developed countries in East Asia, North America, and Western Europe, and the low-value trade agglomeration areas in southern Europe and Southeast Asia are the "depressions" that hinder the process of economic integration. Topologically, the density and average degree of the network have an upward trend, and the phenomenon of small world network is increasingly apparent. The entire network exhibits the structural feature of "core-semi-peripheral-periphery"; Western Europe is a gathering area of core countries, and Japan and the United States have the most principal forces in Asia and North America, respectively. Due to the negative impact of various asymmetric trade agreements, the number of marginal countries continues to increase, which is detrimental to the stable and complete development of the trade network. Thus, we need to consider relative convergence when formulating new and amending trade rules, set comparatively uniform origin rules, eliminate rule overlaps and conflicts, and establish efficient rule implementation and dispute settlement institutions.

The QAP regression analysis shows that this structure evolution of the producer services trade network is often conditioned by trade agreement relations, language relations, and differences in economy, geography, institution, and technology between the two countries. In particular, the language difference and technological distance have greater impact in each model. Therefore, each country still needs to strengthen trade ties with partners in the same cultural circle, unite with similar stakeholders to implement diversified trade market strategies, and cultivate the core technological advantages of domestic producer services to enhance the status of international division of labor.

In terms of competitiveness evaluation, countries with superior centrality and core degree, such as the United States, the United Kingdom, and Germany, have undoubted leading power and sufficient producer services supply capacity, and assume the role of bridges and supporters in the network. China, India, and other emerging economies have benefited from increased node strength and improved their position in the network, but it did not change the trade configuration dominated by developed countries. Due to the high technical threshold, it is difficult for most developing countries to occupy the export market. Therefore, they need to enhance the industrial attraction and competitive advantage through innovation-driven endeavors. For example, relevant enterprises are encouraged to increase the investment of capital, technology, and talents, and establish research and development centers, so as to improve the export quality of producer services trade.

With regard to the system interaction, cohesive subgroup analysis reveals that the producer services trade network has spatial spillover relations; major traditional service trade powers in Europe are condensed in the same subgroup based on the principle of reciprocity, but its radiation and driving power for isolated subgroups is still very small, which is not conducive for the integration of member states into the trade network. Thus, isolated subgroups need to strengthen cooperation with countries with strong spillover effects, import appropriate production factors, and form optimal allocation with domestic resources to stimulate development potential and trade participation, and ultimately establish a mutually beneficial and win-win trading system.

However, this article still has some limitations, which can be further improved and supplemented in future work:

(1) Due to the problem of data availability, the research interval is relatively lagging at this stage. When the data are easy to obtain, we will further analyze the complexity and systematic characteristics of producer services trade network in recent years, especially the impact of trade war and COVID-19 epidemic on the network.

(2) This article is a holistic analysis that integrates the trade data of producer services industries. The next step is to conduct a more detailed study of each subindustry and explore the changes in the trade pattern from multiple industrial dimensions.

(3) At present, this paper still stays at the basic level of the analysis of the characteristics of producer services trade network, without an in-depth theoretical research. In the future, we need to use more complex system theory to explore the dynamic features and evolution mechanism of the trade network.

Data Availability

The relevant data of this paper can be obtained from the corresponding author.

Conflicts of Interest

The authors declare no conflicts of interest.

Acknowledgments

This research was supported by grant from the National Social Science Foundation of China (Grant No. 17BJY071).

References

[1] Y. Bi, W. R. J. Alexander, and Z. Pei, "Factors affecting trade in services: evidence from panel data," *Applied Economics*, vol. 51, no. 34, pp. 3730–3739, 2019.

[2] M. Afzal, S. Shoaib Ahmed, and M. Waseem Shahzad, "Impact of merchandize and services trade on economic growth of Pakistan," *Journal of Contemporary Research in Business, Economics and Finance*, vol. 1, no. 2, pp. 30–36, 2019.

[3] P. Guerrieri and V. Meliciani, "Technology and international competitiveness: the interdependence between manufacturing and producer services," *Structural Change and Economic Dynamics*, vol. 16, no. 4, pp. 489–502, 2005.

[4] H. Breinlich, "Producer services and trade liberalization," *International Encyclopedia of Geography: People, the Earth, Environment and Technology*, pp. 1–9, 2017.

[5] W. J. Coffey, "Producer services research in Canada," *The Professional Geographer*, vol. 47, no. 1, pp. 74–81, 1995.

[6] S. Illeris, "The role of services in regional and urban development: a reappraisal of our understanding," *The Service Industries Journal*, vol. 25, no. 4, pp. 447–460, 2005.

[7] Y. Zhao, J. Liu, F. Zhang, and M. Liu, "Research on the spatial distribution pattern of producer service firms in urban Harbin," *Proceedings of the ICA*, vol. 2, pp. 1–6, 2019.

[8] R. O. Pereira and B. Derudder, "The cities/services-nexus: determinants of the location dynamics of advanced producer services firms in global cities," *The Service Industries Journal*, vol. 30, no. 12, pp. 2063–2080, 2010.

[9] Y. Wu, P. Fan, and H. You, "Spatial evolution of producer service sectors and its influencing factors in cities: a case study of hangzhou, China," *Sustainability-Basel*, vol. 10, 2018.

[10] D. Haberly and D. Wójcik, "Regional blocks and imperial legacies: mapping the global offshore fdi network," *Economic Geography*, vol. 91, no. 3, pp. 251–280, 2015.

[11] Z. Liao, Z. Wang, and K. Guo, "The dynamic evolution of the characteristics of exchange rate risks in countries along "the belt and road" based on network analysis," *Plos One*, vol. 14, 2019.

[12] H. Li, H. An, W. Fang, Y. Wang, W. Zhong, and L. Yan, "Global energy investment structure from the energy stock market perspective based on a heterogeneous complex network model," *Applied Energy*, vol. 194, pp. 648–657, 2017.

[13] D. Zhou, H. Li, Z. Li, J. Zhou, and D. Lin, "Structure characteristics analysis of diesel sales in complex network method," *Cluster Computing*, vol. 22, no. 3, pp. 5635–5635, 2019.

[14] S. Robinson, Z. Wang, and W. Martin, "Capturing the implications of services trade liberalization," *Economic Systems Research*, vol. 14, no. 1, pp. 3–33, 2002.

[15] B. Hoekman and A. Mattoo, "Services trade and growth," *International Journal of Services Technology and Management*, vol. 17, p. 1, 2008.

[16] J. Markusen, T. F. Rutherford, and D. Tarr, "Trade and direct investment in producer services and the domestic market for expertise," *Canadian Journal of Economics/Revue Canadienne D'conomique*, vol. 38, no. 3, pp. 758–777, 2005.

[17] P. W. Daniels, "Producer services research in the United Kingdom," *The Professional Geographer*, vol. 47, no. 1, pp. 82–87, 1995.

[18] B. Balassa, "Trade liberalisation and "revealed" comparative advantage," *The Manchester School*, vol. 33, no. 2, pp. 99–123, 1965.

[19] X. Liu and J. Shi, "A new method for interindustry linkage analysis based on demand-driven and multisector input-output model and its application in China's manufacturing and producer services," *Complexity*, vol. 2020, pp. 1–16, 2020.

[20] H. An, W. Zhong, Y. Chen, H. Li, and X. Gao, "Features and evolution of international crude oil trade relationships: a trading-based network analysis," *Energy*, vol. 74, pp. 254–259, 2014.

[21] M. A. Serrano and M. Boguna, "Topology of the world trade web," *Physical Review E*, vol. 68, Article ID 015101, 2003.

[22] D. Garlaschelli and M. I. Loffredo, "Structure and evolution of the world trade network," *Physica A: Statistical Mechanics and Its Applications*, vol. 355, no. 1, pp. 138–144, 2005.

[23] M. C. Mahutga, "The persistence of structural inequality? A network analysis of international trade, 1965–2000," *Social Forces*, vol. 84, pp. 1863–1889, 2006.

[24] L. De Benedictis and L. Tajoli, "The world trade network," *The World Economy*, vol. 34, no. 8, pp. 1417–1454, 2011.

[25] G. Fagiolo, J. Reyes, and S. Schiavo, "On the topological properties of the world trade web: a weighted network analysis," *Physica A: Statistical Mechanics and Its Applications*, vol. 387, no. 15, pp. 3868–3873, 2008.

[26] L. W. Jin, L. W. Kyung, S. S. Young, and Z. K. Gao, "Patent network analysis and quadratic assignment procedures to identify the convergence of robot technologies," *PLoS One*, vol. 11, Article ID e0165091, 2016.

[27] J. Huang, W. Zhang, and W. Ruan, "Spatial spillover and impact factors of the internet finance development in China," *Physica a Statistical Mechanics and Its Applications*, p. 527, 2019.

[28] T. Long, H. Pan, C. Dong, T. Qin, and P. Ma, "Exploring the competitive evolution of global wood forest product trade based on complex network analysis," *Physica A: Statistical Mechanics and Its Applications*, vol. 525, pp. 1224–1232, 2019.

[29] T. Kitamura and S. Managi, "Driving force and resistance: network feature in oil trade," *Applied Energy*, vol. 208, pp. 361–375, 2017.

[30] G. Fagiolo, J. Reyes, and S. Schiavo, "The evolution of the world trade web: a weighted-network analysis," *Journal of Evolutionary Economics*, vol. 20, no. 4, pp. 479–514, 2010.

[31] H. Xu and L. Cheng, "The qap weighted network analysis method and its application in international services trade," *Physica A: Statistical Mechanics and Its Applications*, vol. 448, pp. 91–101, 2016.

[32] H. Xu and L. Cheng, "The study of the influence of common humanistic relations on international services trade-from the perspective of multi-networks," *Physica A: Statistical Mechanics and Its Applications*, vol. 523, pp. 642–651, 2019.

[33] C. Yang, H. Wang, and Q. Han, "Identification of the structural characteristics and influencing factors of the international service trade network based on the sna method: empirical evidence from the Asia-Pacific region," *International Business*, pp. 65–75, 2017, in Chinese.

[34] H. L. Browning, J. Singelmann, and A. P. R. C. Texas Univ, *The Emergence of a Service Society: Demographic and Sociological*

*Aspects of the Sectoral Transformation of the Labor Force in the U.S.A.*ERIC Clearinghouse, Washington, DC, USA, 1975.

[35] F. Cerina, Z. Zhu, A. Chessa, and M. Riccaboni, "World input-output network," *PLoS One*, vol. 10, 2015.

[36] Y. Yokura, H. Matsubara, and R. Sternberg, "R&d networks and regional innovation: a social network analysis of joint research projects in Japan," *Area*, vol. 45, 2013.

[37] Z. Chong, C. Qin, and S. Pan, "The evolution of the belt and road trade network and its determinant factors," *Emerging Markets Finance and Trade*, vol. 55, no. 14, pp. 3166–3177, 2019.

[38] Bedassa, Tadesse, Roger, and White, "Cultural distance as a determinant of bilateral trade flows: do immigrants counter the effect of cultural differences?" *Applied Economics Letters*, 2009.

[39] Marjan, "Southeastern european trade analysis: a role for endogenous cefta-2006?" *Emerging Markets Finance and Trade*, vol. 49, pp. 26–44, 2013.

[40] W. T. Selmier and C. H. Oh, *The Power of Major Trade Languages in Trade and Foreign Direct Investment*, Social Science Electronic Publishing, Rochester, NY, USA.

[41] F. Kimura and H. H. Lee, "The gravity equation in international trade in services," *Review of World Economics (Weltwirtschaftliches Archiv)*, p. 142, 2006.

[42] B. Kogut and H. Singh, "The effect of national culture on the choice of entry mode," *Journal of International Business Studies*, vol. 19, no. 3, pp. 411–432, 1988.

[43] W. Wang and Z. Li, "The evolution of China's interregional coal trade network, 1997–2016," *Physica A: Statistical Mechanics and Its Applications*, vol. 536, p. 120974, 2019.

[44] D. J. Watts and S. H. Strogatz, "Collective dynamics of 'small-world' networks," *Nature*, vol. 393, no. 6684, pp. 440–442, 1998.

[45] Q. Wang, D. Du, Y. Zhang, and Q. Gui, "Research on the evolutionary characteristics of global mobile trade network," *World Regional Studies*, vol. 28, pp. 170–178, 2019, in Chinese.

[46] Y. Chen, "Social network analysis of the world trade pattern from 2000 to 2009," *International Trade Issues*, pp. 31–42, 2011, in Chinese.

Hindawi
Complexity
Volume 2021, Article ID 6657191, 13 pages
https://doi.org/10.1155/2021/6657191

Research Article

Understanding the Impact of Startups' Features on Investor Recommendation Task via Weighted Heterogeneous Information Network

Sen Wu, Ruojia Chen, Guiying Wei, Xiaonan Gao, and Lifang Huo

School of Economics and Management, University of Science and Technology Beijing, Beijing 100083, China

Correspondence should be addressed to Xiaonan Gao; gaoxiaonan0001@163.com

Received 24 December 2020; Revised 23 March 2021; Accepted 12 April 2021; Published 22 April 2021

Academic Editor: Huajiao Li

Investor recommendation is a critical and challenging task for startups, which can assist startups in locating suitable investors and enhancing the possibility of obtaining investment. While some efforts have been made for investor recommendation, few of them explore the impact of startups' features, including partners, rounds, and fields, to investor recommendation performance. Along this line, in this paper, with the help of the heterogeneous information network, we propose a FEatures' COntribution Measurement approach of startups on investor recommendation, named FECOM. Specifically, we construct the venture capital heterogeneous information network at first. Then, we define six venture capital metapaths to represent the features of startups that we focus on. In this way, we can measure the contribution of startups' features on the investor recommendation task by validating the recommendation performance based on different metapaths. Finally, we extract four practical rules to assist in further investment tasks by using our proposed FECOM approach.

1. Introduction

Venture capital (VC) is an important source of funding for startups [1]. It plays a key role in startups' sustainable growth and performance [2] and the innovation in the economy [3]. Investment companies provide financial support for startups. Besides that, they provide startups with necessary experience and knowledge for their development. However, there is information asymmetry between startups and investment companies, and it is challenging for startups to find suitable investors, especially for the startups that have no previous investors before [4]. Finance is an integral part of the startups' process, yet obtaining it is challenging [5]. For this reason, an investor-filtering system for startups can be extremely beneficial [4]. Therefore, achieving information filtering and then recommending suitable investors for startups who can meet their personalized financial needs by using recommendation techniques have become a key problem to be solved in the domain of VC.

In the domain of VC, the extensive recommendation studies mainly focus on helping VC companies to find suitable startups [1, 6–8], while effective methods that support startups in finding investors are relatively rare. Xu et al. [4] achieved the investor recommendation by constructing a tripartite network representation containing virtual links. Antonio et al. [9] pointed out that finding a suitable investor who is interested in the startups' fields usually requires long-term research, which is especially difficult for new startups. Furthermore, recommending suitable investors who are interested in the startups' features is also challenging due to their inexperience. However, as for the new startups which have not been invested before, the resources they can utilize is limited. They have no previous investors to be mined, and the features of startups are the limited resources available for finding suitable investors for them. Along this line, we try to employ the startups' features to study the investor recommendation problem, by measuring the contribution of startups' features on the investor recommendation performance. The features we care about in this paper include partners, rounds, and field. An example of startups is shown in Table 1, the startup Ziroom and Bitmain have the same round, the startup Vxiaoke is in

Table 1: An example of startups.

Investor	Startup	Partner	Round	Field
Sequoia Capital (China)	Ziroom	Lin Xiong and Guowei Li	A	Real Estate
Sequoia Capital (China)	Bitmain	Jihan Wu and Yuesheng Ge	A	Finance
IDG Capital	Vxiaoke	Yunchang Wu and Xiaoguang Li	Angel Investment	Electronic Commerce

Angel Investment, and the former two startups have the same investor, while the investor of the third startup is different from them. Therefore, we consider that the feature of round may affect the decision of investors. And, there may be various impacts on investors by different startups' features. To this end, how to measure the contribution of startups' features on the investor recommendation performance is a vital task for startups. In this paper, we aim to address startups' features contribution measurement problem.

For exploring the impact of startups' features on the investor recommendation task, there are two challenges that need to be solved. (1) How to represent the features related to the investor recommendation task? (2) How to recommend a investor to a startup based on the focused features? Notably, the VC network is a typical heterogeneous information network (HIN), which contains multiple types of nodes and multiple edges between nodes. There is rich structural information and semantic information in the VC network, which provides us the opportunity to address the two challenges based on HIN.

HIN has been successfully applied in recommender systems [10]. Therefore, in this paper, we propose a features' contribution measurement approach of startups on investor recommendation named FECOM, based on HIN. The purpose of this paper is to explore the impact of startups' features on the investor recommendation task and extract the rules to assist in further investment tasks. Specifically, we integrate various types of VC data into the form of HIN at first, by which the venture capital heterogeneous information network (VC-HIN) can be constructed. Then, the venture capital metapaths (VC-metapaths) are defined to represent the features of startups that we focus on. Based on this, we propose the FECOM approach, which can conduct the investor recommendation task by utilizing different VC-metapaths. In this way, we can measure the contribution of startups' features on the investor recommendation task according to different VC-metapaths, and extract beneficial rules to assist in further investment tasks, by analysing the recommendation performance.

The main contributions of this paper can be summarized as follows:

(1) We define the venture capital heterogeneous information network (VC-HIN), by which the structural information contained in the VC network can be expressed.

(2) We formulate the venture capital metapaths (VC-metapaths) to represent the features related to the investor recommendation task, and the semantic information contained in the VC network can be indicated.

(3) We propose a features' contribution measurement approach of startups on investor recommendation named FECOM. On the basis of it, we can analyse the impact of startups' features on investor recommendation by validating the recommendation performance based on different metapaths.

(4) We extract four practical rules by exploiting the proposed FECOM approach, which are beneficial for further investment tasks.

The paper is structured as follows. In Section 2, we introduce the related works. In Section 3, we propose two definitions about the proposed FECOM, which are the basis of FECOM. In Section 4, we provide the framework and the details of the proposed FECOM. In Section 5, we explore the impact of startups' features on investor recommendation and extract four practical rules to assist in further investment tasks through experiments. In Section 6, we conclude the paper.

2. Related Work

In this section, we briefly review related works on the VC, VC recommendations, and HIN.

In recent years, related research studies in the domain of VC have continued to grow. Chircop et al. [11] studied the influence of religious belief on VC decision-making. Andrieu and Groh [12] established a startups' investor selection model and found that startups would select investors based on the factors such as the quality of the investor support. Tian et al. [13] confirmed the nonlinear relationship between the geographic distance between the investors and the startups and the startups' performance through the research. Cheng and Tang [14] conducted the research on the impact of investment partner selection strategy, the industry of the startup, and geographic uncertainty on VC. Wu et al. [15] studied the influence of the network structure on VC alliance's successful exit from emerging markets. Zhang et al. [16] used multilayer network analysis to simulate the spread of risks in the VC market when external shocks affect investment companies or startups. Luo [17] put forward the countermeasures for the company's financial risk investment by predicting the stock premium. Salamzadeh and Kesim [5] tried to conceptualize the phenomenon "startup" and recognize the challenges they might face. Antonio et al. [9] examined the association between the presence of venture capital and the growth of startups.

However, as for the VC recommendation, there are few research studies focusing on that. Stone et al. [1] demonstrated the effectiveness of the collaborative filtering recommendation technique in the new application domain of finance and improved the recommendation quality of

investment opportunities. Zhao et al. [6] proposed a portfolio optimization framework to solve the problem of information filtering in VC, which can predict the new investment of investment companies. Wu et al. [7] applied a personalized recommendation technique to the domain of VC recommendation to complete the recommendation of VC projects. Xu et al. [4] combine with probs diffusion algorithm, develop the investor recommendation by constructing a tripartite network representation containing virtual links. The existing recommendation research studies in the domain of VC mainly concentrate on the recommendation of VC startups and seldom study the recommendation of investors based on the needs of startups. However, due to the information asymmetry between investors and startups, the financing process is usually challenging, especially for the startups that have not yet been invested before [4]. As the features of startups without investment are the limited resources available for them to find suitable investors, we try to exploit the features and measure the contribution of startups' features on the investor recommendation performance and then extract beneficial rules to assist in the further investment recommendation problem by analysing the recommendation performance.

As an emerging direction, HIN has attracted the attention of many scholars. HIN contains rich structural and semantic information [18]. The recommendation based on HIN can naturally simulate the rich information contained in the network and then realize personalized recommendation. Node similarity measurement, as a key part of information extraction from HIN-based recommendation, has been widely studied. Haveliwala [19] proposed the personalized PageRank algorithm (PRANK recommendation), which measures the similarity between nodes by randomly walking between nodes; Jeh and Widom [20] proposed the SimRank algorithm, which calculates the similarity between nodes through the similarity of their neighbors. However, both PRANK and SimRank ignored the semantic information contained in the HIN. In addition to those algorithms, there are many HIN-based recommendation techniques considering the metapath-based similarity [21]. Sun et al. [18] proposed the PathSim algorithm based on symmetric metapaths to achieve similarity measurement between nodes of the same type in the network; Lao and Cohen [22] proposed the PCRW algorithm to measure the similarity between different types of nodes in the network through a random walk model with path constraints; Shi et al. [23] proposed the HeteSim algorithm based on the arbitrary metapath, which can measure the similarity between any type of node in the network. The above three algorithms all use metapath-based similarity to measure the node similarity of network semantic information, but they do not consider the network structure information. All the above similarity measurement techniques have some limitations because they fail to consider the structure or semantic information of HIN at the same time. Lee et al. [24] proposed the PathRank algorithm to calculate the similarity between nodes by using the one-way random walk model. It realizes the measurement of nodes' similarity on the basis of fully extracting the structure and semantic information of HIN. Compared with the above node similarity measurement methods, the PathRank algorithm can utilize the rich information contained in the VC network. Furthermore, we will calculate the scores of investors to be recommended on the basis of the PathRank algorithm in the following sections by considering the rich structural information and semantic information in the VC network.

Among the above existing literature studies, there is less attention from scholars that has been devoted to the evaluation of the impact of startups' features on the investor recommendation task. Motivated by these observations, we propose a features' contribution measurement approach of startups on investor recommendation named FECOM. According to the proposed FECOM, the practical rules could be obtained to support the investment task by evaluating the recommendation performance based on different metapaths.

3. Preliminaries

In this section, we propose two definitions about the proposed FECOM approach, namely, venture capital heterogeneous information network (VC-HIN) and venture capital metapaths (VC-metapaths) in the VC network, which are the basis of the model. Specifically, VC-metapaths can provide various semantic information for the investor recommendation task.

Definition 1. Venture capital heterogeneous information network (VC-HIN).

Venture capital heterogeneous information network (VC-HIN) is defined as a weighted heterogeneous information network constructed based on venture capital data, including different types of nodes and weighted edges. Specifically, VC-HIN is indicated by $G = (V, E)$, where $V = \{C, P, R, F, I\}$ is the node set containing five kinds of node, namely, C-company, P-company partner, R-investment round, F-field, and I-investor, and E refers to the edge set including 14 kinds of edge types between different nodes, which are directed and reveal the relations between corresponding nodes. As for the weights of edges in VC-HIN, we define different weight calculation methods for different kinds of edges. In terms of the edge between I and C, its weight is the total number of times of the investor who used to invest in the startup. For the edge between I and P, the weight is the number of times of the investor invested in the companies built by P. Similarly, as to the edge between I and R, its weight is the number of times of the investor invested in companies in round R. And, the weight of the edge between I and F is the number of times of the investor invested in companies in field F. Particularly, the weights of edges between C and P, R, and F are defined as 1.

An example of VC-HIN is shown in Figure 1. There are two company nodes $C1$ and $C2$, two investor nodes $I1$ and $I2$, two company partner nodes $P1$ and $P2$, two round nodes $R1$ and $R2$, and one field node $F1$. The lines represent the edges between nodes, and thicker lines indicate the edges with larger weights. For example, the line between $I2$ and $F1$ is thicker than that between $I1$ and $F1$, which indicates that the

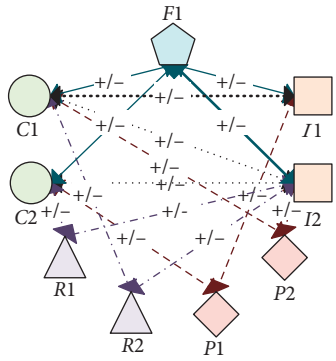

Figure 1: An example of Venture Capital Heterogeneous Information Network.

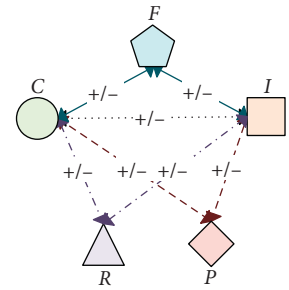

Figure 2: Venture capital heterogeneous information network schema.

weight of the edge linking $I2$ and $F1$ is larger than the edge linking $I1$ and $F1$. It proves that the investor $I2$ invests more in companies in the field F than $I1$. Similarly, the weight of the edge linking $I1$ and $C1$ is larger than the edge linking $I2$ and $C1$, revealing that the company $C1$ is invested by the investor $I1$ more than $I2$. Furthermore, the edges between different nodes are directed and reveal the relations between corresponding nodes, and the edges have two kinds of directions "+" and "−." For example, the edge $C1 \longrightarrow^{\text{invest in}^-} I1$ indicates that the company $C1$ is invested by the investor $I1$. And, the edge $I1 \longrightarrow^{\text{invest in}^+} C1$ implies that the investor $I1$ invests in the company $C1$.

Definition 2. Venture capital metapaths (VC-metapaths).

The venture capital metapaths (VC-metapaths) in VC-HIN are defined specifically to the investor recommendation task studied in this paper. We first formulate the venture capital heterogeneous information network schema $TG = (A, R)$ shown in Figure 2 with the node type mapping function $\phi_V: V \longrightarrow A$ and the edge type mapping function $\phi_E: E \longrightarrow R$, where A represents the node type set and R represents the edge type set. Based on TG, we define VC-metapaths, which can represent the compound relation between different nodes in VC-HIN. A VC-metapath can be represented as $g_k = v_1 \longrightarrow^{e_1} v_2 \ldots v_i \longrightarrow^{e_i} v_i + 1$, where each element in set $\langle v_1, v_2, \ldots, v_i \rangle$ represents a node in the network, and the element in set $\langle e1, e2, \ldots, ei \rangle$ represents an edge in VC-HIN. We are supposed to recommend suitable investors for startups; therefore, the first node in the VC-metapath is fixed as a company node, and the last node must be an investor node. As shown in Figure 2, there are five kinds of node types in the set A and 14 kinds of edge types including directions in the set R.

As we focus on the contribution of the target startups' features on the investor recommendation task, the commonly used features include startups' partners, rounds, and fields. As shown in Table 2, we formulate six VC-metapaths based on these three kinds of startups' features. The longer the metapath, the fuzzier the corresponding semantic information and the lower the reliability of the similarity measure [18]. Therefore, we define that there will be no more than four nodes in VC-metapaths. The six VC-metapaths cannot only exploit the semantic information behind the different types of nodes and edges in VC-HIN but also simulate several classical recommendation methods, such as collaborative filtering recommendation and content-based filtering. Table 2 lists the six VC-metapaths, their semantic analysis conclusions, and similar methods. For example, the VC-metapath CPI can mine the semantic information behind startups' partners and the edge linking P and I contained in the metapath. This metapath recommends investors who have invested in the partners of target companies, which is similar to the paradigm of content-based recommendation.

Figure 3 shows the six VC-metapaths, where the edges contained in the metapath are represented by solid lines. CPI and CPCI are shown in Figure 3(a), where CPI consists of the edge linking C and P and the edge linking P and I, while CPCI is composed of the edge linking C and P and the edge linking C and I. For the metapath CRI and CRCI in Figure 3(b), the edge linking C and R and the edge linking R and I make up CRI, and CRCI is comprised of the edge linking C and R and the edge linking C and I. Similarly, CFI and CFCI are shown in Figure 3(c), where CFI consists of the edge linking C and F and the edge linking F and I, while CFCI is composed of the edge linking C and F and the edge linking C and I.

Based on the basic concepts mentioned above, the proposed FECOM can consider the structure information contained in VC-HIN and the semantic information contained in multiple VC-metapaths at the same time, which will fully mine the rich information contained in the VC network and is able to explore the impact of startups' features to the investor recommendation task. The details about FECOM will be introduced in the next section.

4. FECOM Approach

In this section, we first provide the overall framework of the proposed FECOM approach and then illustrate its details.

4.1. Overview of FECOM. In this section, we introduce the framework of FECOM.

The framework of the proposed FECOM is shown in Figure 4, consisting of two main components:

(1) *Constructing Layer.* We construct the VC-HIN and specify the VC-metapaths of VC-HIN in this layer

Table 2: VC-metapaths of VC-HIN

VC-metapaths	Semantic analysis	Similar method
CPCI	Recommend investors who have invested in the companies with the same partners as target startups	Collaborative filtering recommendation
CPI	Recommend investors who have invested in the partners of target startups	Content-based recommendation
CRCI	Recommend investors who have invested in the companies with the same rounds as target startups	Collaborative filtering recommendation
CRI	Recommend investors who have invested in the rounds of target startups	Content-based recommendation
CFCI	Recommend investors who have invested in the companies with the same fields as target startups	Collaborative filtering recommendation
CFI	Recommend investors who have invested in the fields of target startups	Content-based recommendation

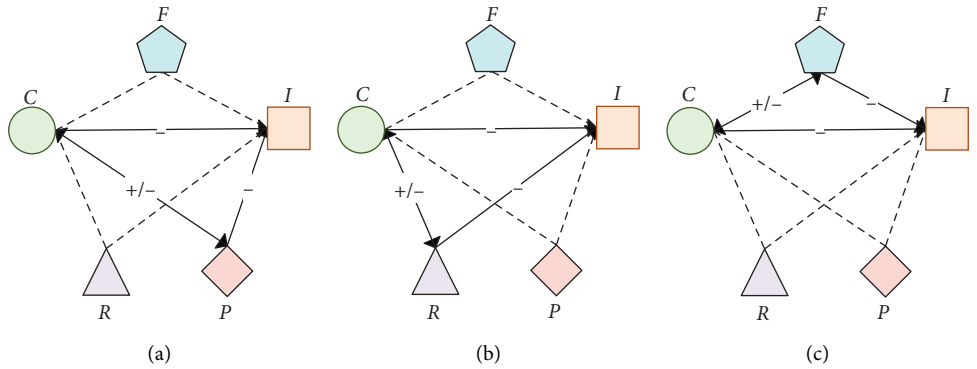

Figure 3: Examples of VC-metapaths. (a) The metapath CPI and CPCI. (b) The metapath CRI and CRCI. (c) The metapath CFI and CFCI.

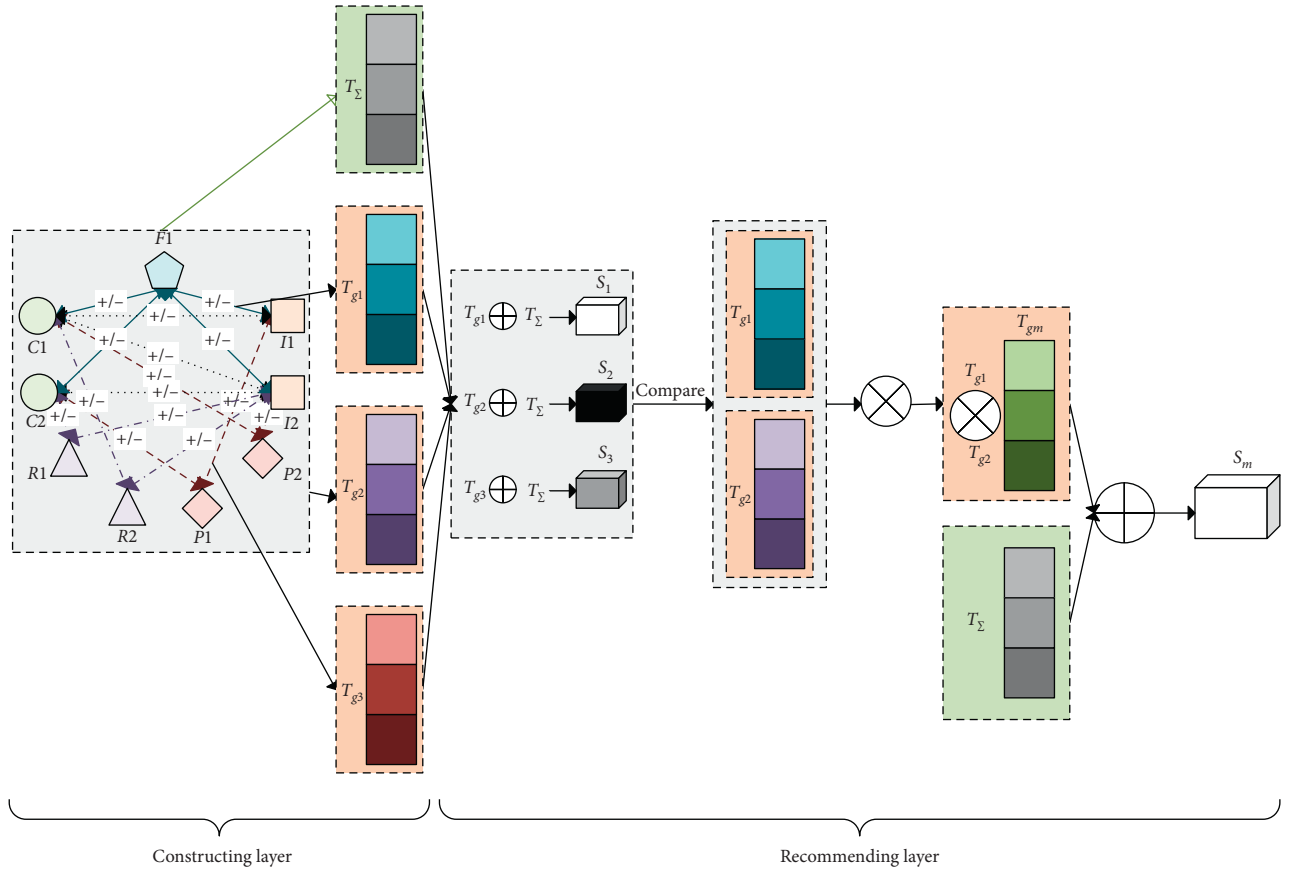

Figure 4: Framework of the proposed FECOM where the left part shows the constructing layer and the right part presents the recommending layer.

firstly. The VC-HIN is built according to the VC data collected in advance, which is similar to Figure 1; however, it is bigger and more complex than Figure 1. The VC-metapaths are designed according to the information to be mined; since the target startups in this paper have no investors before, the partners, rounds, and fields of them can be exploited to realize the investor recommendation. As shown in Table 2 and Figure 3, the VC-metapaths in this paper have been designed. Herein, we give two kinds of transition matrices, the VC-HIN transition matrix $T_{\sum}$ and the VC-metapath transition matrix T_{gk}, $k \in \{1, 2, \ldots, 6\}$, for each VC-metapath g_k, $k \in \{1, 2, \ldots, 6\}$. Since there are six metapaths in Table 2, k is an integer less than or equal to 6. The VC-HIN transition matrix $T_{\sum}$ is extracted from VC-HIN, which can express the structural information of VC-HIN. Similarly, the VC-metapath transition matrix T_{gk} is calculated based on the VC-metapath, indicating the semantic information contained in the metapath.

(2) *Recommending Layer.* This layer requires the VC-HIN transition matrix $T_{\sum}$ and the VC-metapath transition matrix T_{gk} as input and conducts the investor recommendation. The recommending layer contains two personalized investor recommendation strategies, which are based on the single metapath and the mixed metapath. The investor recommendation of the mixed metapath is derived from recommendation results of different single metapaths. As shown in the recommending layer, the VC-HIN transition matrix $T_{\sum}$ and the VC-metapaths' transition matrices T_{g1}, T_{g2}, and T_{g3} are obtained in the constructing layer. Next, we utilize the VC-HIN transition matrix $T_{\sum}$ and the VC-metapaths' transition matrices containing T_{g1}, T_{g2}, and T_{g3} in Figure 4, respectively, to obtain the optimal investor recommendation sets S_1, S_2, and S_3 based on the single metapaths g_1, g_2, and g_3. The VC-metapaths' transition matrices T_{g1} and T_{g2} with better recommendation effectiveness will be selected to generate the mixed metapath transition matrix T_{gm} of the mixed metapath g_m after comparing the recommendation performance on each single metapath. In the end, the optimal investor recommendation set S_m can be obtained based on the VC-HIN transition matrix $T_{\sum}$ and the mixed metapath transition matrix T_{gm}. By evaluating the performance of the recommendation set, we can analyse the impact of the corresponding VC-metapath on the investor recommendation task.

Next, based on the framework of FECOM mentioned above, the technical details about the constructing layer and recommending layer are interpreted, respectively.

4.2. Constructing Layer. In the constructing layer, we are supposed to construct the VC-HIN and design the VC-metapaths based on the VC data collected before firstly. Next, we compute the VC-HIN transition matrix $T_{\sum}$ and the VC-metapath transition matrix T_{gk} based on the adjacency matrix P and the edge adjacency matrix P_{Rn}, $n \in \{1, 2, \ldots, 14\}$, respectively. Since there are 14 edge types in TG = (A, R), n is an integer less than or equal to 14.

For the adjacency matrix P, it is represented as a $|V| \times |V|$ matrix, where $|V|$ is the total numbers of all the nodes in VC-HIN. And, the element $P(i, j)$ of P represents the weight of the edge between the node v_i and v_j.

Based on the adjacency matrix P, the VC-HIN transition matrix $T_{\sum}$ can be computed according to equation (1), which is a $|V| \times |V|$ matrix:

$$T_{\sum}(i, j) = \begin{cases} \dfrac{w_{ij}}{\sum_j P(i, j)}, & \text{if } e_i \text{ linking } v_i \text{ and } v_j \in E \wedge i \le |V| \wedge j \le |V|, \\ 0, & \text{otherwise,} \end{cases} \tag{1}$$

where $T_{\sum}(i, j)$ is the element of the ith row and the jth column in $T_{\sum}$, representing the probability of the transition between the node v_i and the node v_j.

As for the edge adjacency matrix P_{Rn}, it is also a $|V| \times |V|$ matrix, where R_n is one of the edge types in the edge type set R and $|V|$ is the total numbers of all the nodes in VC-HIN. The element $P_{Rn}(i, j)$ of P_{Rn} reveals the weight of the edge linking the node v_i and v_j whose edge type belongs to the edge type R_n.

For the metapath $g_k = v_1 \longrightarrow^{e_1} v_2 \ldots v_i \longrightarrow^{e_i} v_i + 1$ mentioned in Section 3, its transition matrix T_{gk} can be calculated after normalizing the edge adjacency matrix P_{Rn}. The normalized P_{Rn} will be represented as N_{Rn}, which is defined as follows:

$$N_{Rn}(i, j) = \begin{cases} \dfrac{w_{ij}}{\sum_j P_{Rn}(i, j)}, & \text{if the edge type of } e_i \text{ linking } v_i \text{ and } v_j \in R_n \wedge i \le |V| \wedge j \le |V| \wedge n \le |R|, \\ 0, & \text{otherwise,} \end{cases} \tag{2}$$

where $N_{Rn}(i, j)$ is the element of the ith row and the jth column in N_{Rn}, demonstrating the probability of the random walk between the node v_i and the node v_j.

The VC-metapath transition matrix T_{gk} can also be denoted as a $|V| \times |V|$ matrix, which can be represented as follows:

$$T_{gk} = N_{R1} \times N_{R2} \ldots \times N_{Rn}. \quad (3)$$

The basic idea is that the transition matrix of the metapath g_k can be obtained by multiplying the normalized edge adjacency matrices of all the edges contained in the metapath g_k.

In this section, on the basis of the adjacency matrix P and the edge adjacency matrix P_{Rn} mentioned above, we introduce the calculation process of the VC-HIN transition matrix $T_{\sum}$ and the VC-metapath transition matrix T_{gk}. Hereafter, we interpret the recommending layer in detail.

4.3. Recommending Layer. For exploring the contribution of different startups' features on investor recommendation task T_{gk}, we utilize different types of metapaths to carry out the investor recommendation, respectively, in this layer. We will explain how to obtain the investor recommendation set for target startups under the single metapath and the mixed metapath in this section.

4.3.1. Investor Recommendation Based on the Single Metapath. The single metapaths are the VC-metapaths defined based on the venture capital heterogeneous information network schema, which can represent the compound relation between different nodes in VC-HIN. In this paper, the single metapath refers to the six VC-metapaths shown in Table 2 and Figure 3. The investor recommendation based on the single metapath mainly relies on the VC-metapaths mentioned before. We can obtain the investor recommendation sets according to the partners, rounds, and fields of startups. The investor recommendation based on the single metapath such as CPCI, CRCI, and CFCI can simulate the procedure of collaborative filtering recommendation. It will address the investor recommendation task for startups by exploring the performance of its features including partners, rounds, and fields. In addition, the investor recommendation based on the single metapath such as CPI, CRI, and CFI simulates the content-based recommendation.

FECOM exploits the VC-HIN transition matrix $T_{\sum}$ and the VC-metapath transition matrix T_{gk} to calculate the scores of investors based on PathRank [24]. As shown in equation (4), we first input the VC-HIN transition matrix $T_{\sum}$ and the VC-metapath transition matrix T_{gk} of each single metapath, respectively, to obtain the score set of all the investors to be recommended. Then, the investor recommendation set is generated after sorting the scores of all the investors in the descending order:

$$\vec{r} = w_{\mathrm{trans}} \times \vec{r} \times T_{\sum} + w_{\mathrm{path}} \times \vec{r} \times T_{gk} + w_{re} \times \vec{t}. \quad (4)$$

As shown in equation (4), $\vec{r}$ represents the score set of all the investors to be recommended, which is a $1 \times |V|$ vector. We first initialize and then continuously optimize $\vec{r}$ by equation (4). When $\vec{r}$ no longer changes, it will be the optimal score set.w_{trans}, w_{path}, and w_{re} are all the probability weight parameters, t is represented as a $1 \times |V|$ restart vector, and the element $\vec{t}\,(i)$ of $\vec{t}$ is 1 when its corresponding node v_i is the target startup.

Next, as there are several probability weight parameters in equation (4), we will obtain different investor recommendation sets by setting different values for the parameters. After comparing the performance of each single metapath under different parameter configurations, we can acquire the optimal performance of each single metapath. Meanwhile, the optimal investor recommendation sets can be produced. Finally, several single metapaths with better recommendation effectiveness will be selected to generate the mixed metapath g_m.

We realize the investor recommendation based on the single metapaths in this section. Along this line, the investor recommendation based on the mixed metapath will be provided.

4.3.2. Investor Recommendation Based on the Mixed Metapath. The mixed metapath is generated by the single metapaths mentioned above. In this paper, the mixed metapath is built by combining several single metapaths with good recommendation performance, where the number of metapaths to generate the mixed metapath is not fixed. We choose single metapaths based on their performance. The investor recommendation based on the mixed metapath can simulate the hybrid recommendation. It can realize the investor recommendation by mixing startups' various features including the partner, round, and field information. For example, the mixed metapath based on CPCI and CRI can consider the partners and rounds of the startups at the same time.

The generation process of the mixed metapath is shown in Figure 5. Firstly, we can obtain the VC-HIN transition matrix $T_{\sum}$ and the VC-metapaths' transition matrices T_{g1}, T_{g2}, and T_{g3} for the metapath g_1, g_2, and g_3 from the constructing layer. Then, the investor recommendation sets based on different single metapaths under different parameter configurations can be acquired. After comparing their performance, we can know the optimal performance of each single metapath. As shown in Figure 5, the investor recommendation sets S_1, S_2, and S_3 are the optimal investor recommendation sets based on the metapath g_1, g_2, and g_3. As the mixed metapath is built by combining several single metapaths with good recommendation performance, we compare the recommendation effectiveness of different investor recommendation sets S_1, S_2, and S_3 by using evaluation metrics. And, the VC-metapaths' transition matrices T_{g1} and T_{g2} will be input into equation (5) to generate the mixed metapath transition matrix T_{gm}, which derived from PathRank [24], because S_1 and S_2 perform better than S_3:

$$T_{\mathrm{gm}} = w_1 T_{g1} + w_2 T_{g2} + \cdots + w_k T_{\mathrm{gk}}. \quad (5)$$

As shown in equation (5), T_{gm} represents the mixed metapath transition matrix of the mixed metapath gm, which is a $|V| \times |V|$ matrix just like the VC-metapath transition matrix T_{gk}. T_{gk} represents the VC-metapath

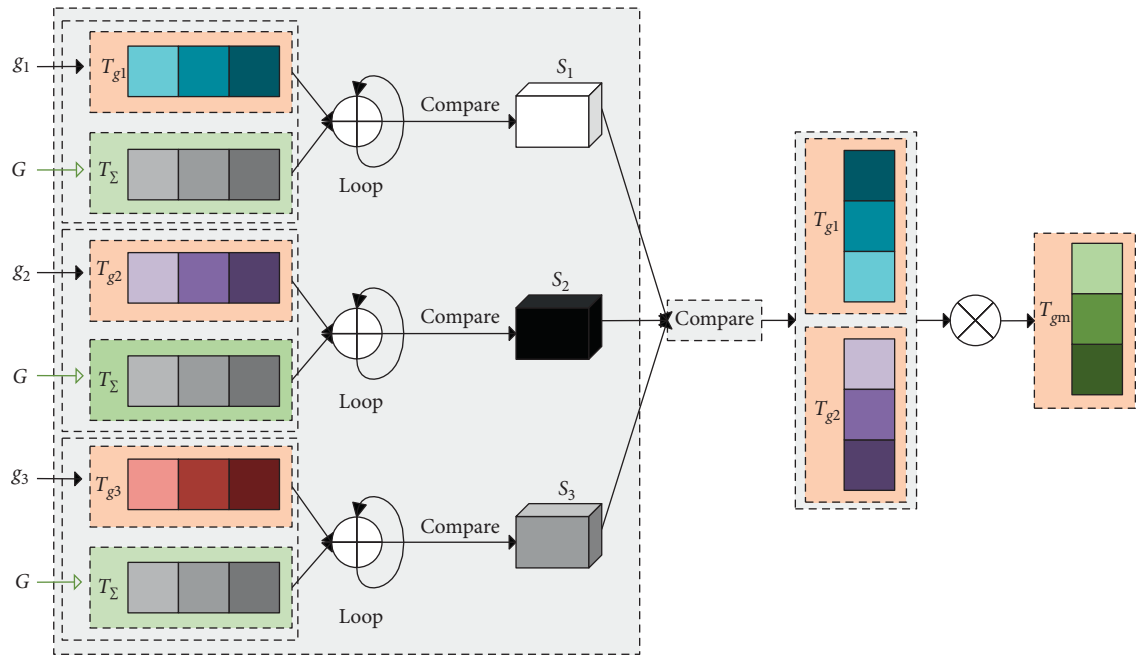

Figure 5: The mixed metapath of FECOM.

transition matrix of the metapath gk, and wk is the metapath weight of the metapath g_k.

After getting the mixed metapath transition matrix T_{gm}, we will introduce the investor recommendation based on the mixed metapath. Firstly, we can obtain the score set of the investors by inputting the VC-HIN transition matrix $T_\sum$ and the mixed metapath transition matrix T_{gm} into equation (4). Then, the optimal investor recommendation set of the mixed metapath can be collected after comparing the performance of the mixed metapath under different parameters.

In brief, after comparing the optimal investor recommendation sets based on different single metapaths and the mixed metapath by using evaluation metrics, the optimal investor recommendation set can be obtained. Along this line, we can know the contribution of each VC-metapath on the investor recommendation task; based on this, the impact of startups' features will be explored.

5. Experiments

In this section, we first evaluate the recommendation performance of FECOM on different single metapaths and the mixed metapath through real VC data. Along this line, we can analyse the effectiveness of different metapaths to the investor recommendation task.

5.1. Dataset. The experimental dataset is collected from http://www.itjuzi.com. We delete the investment events with missing fields, rounds, and partners and remove the investors who have invested less than three times and their corresponding investment events, so as to avoid the cold-start problem for investors, which leaves us with 13573 investment events. As shown in Table 3, there are 6816 companies, 1328 investors, 4862 partners, 15 rounds, and 19 fields in the experimental dataset.

Table 3: Dataset description.

Data field	Data description
Investment event	Total 13573 investment events
Company	Total 6816 companies
Investor	Total 1328 Investors
Partner	Total 4862 partners
Round	Total 15 rounds
Field	Total 19 fields

We divide the dataset into the training set and the testing set in the chronological order. The training set takes the first 80% of the original data, and the testing set takes the rest part. Besides, we aim to recommend investors to new startups that have no previous investors before; to this end, there are only 1602 investment events in the testing set. Since some startups appear in multiple investment events, there are actually 995 startups involved in the testing set.

5.2. Evaluation Metrics. We choose two evaluation metrics, the ranking score (RS) [25] and the AUC (area under receiver operator curve) [26], to evaluate the effectiveness of our proposed FECOM in the investor recommendation task.

5.2.1. Ranking Score (RS). The ranking score (RS) is an important indicator to measure the relative ranking of the investors in the recommendation set. For the target startup, the relevant investor refers to the investor whose investment record exists in the testing set, and the irrelevant investor refers to the investor who has not invested in the target startup in the training set. RS can measure the relative

ranking of relevant investors and measure the degree of uniformity between the recommendation set and the actual investor set. The smaller the RS, the more accurate the relative ranking of the investors in the recommendation set. On the contrary, the higher the RS, the less accurate the ranking. Since there are few actual investors for the target startup, the RS is a better evaluation metric than Precision and Recall [4].

As shown in equation (6), L_u represents the number of investors to be ranked for the target startup and l_{ua} represents the ranking of the investors to be ranked in the recommended list. The mean ranking score can be obtained by averaging the ranking scores of all the startups:

$$\mathrm{RS}_{ua} = \frac{l_{ua}}{L_u}. \tag{6}$$

5.2.2. AUC (Area under Receiver Operator Curve). The AUC can be approximated as the probability that the utility of the relevant investor is higher than the utility of the irrelevant investor. It can measure the ability of the recommendation technique to distinguish relevant investors from irrelevant investors. For the target startup, the higher the AUC, the stronger the ability of the recommended technique to distinguish relevant investors from irrelevant investors, the better the recommendation effectiveness, and the easier for the startup to find suitable investors. On the contrary, the lower the AUC, the more difficult for the startup to find suitable investors.

As shown in equation (7), for the target startup, a relevant investor and an irrelevant investor are randomly selected, n' means the number of times that the score of the relevant investor is greater than the score of the irrelevant investor, n'' represents the number of times the two scores are equal, and n represents the number of startups. The mean AUC can be obtained by averaging the AUC of all the startups:

$$\mathrm{AUC} = \frac{n' + 0.5n''}{n}. \tag{7}$$

5.3. Recommendation Performance on VC-Metapaths. We evaluate the investor recommendation based on the single metapath and the mixed metapath according to the evaluation metrics mentioned above in this section.

5.3.1. Recommendation Performance on Single Metapaths. For locating the optimal recommendation result on each metapath, we set multiple probability parameters w_{trans}, w_{path}, and w_{re}, where w_{trans} ranges from 0 to 0.4, w_{path} ranges from 0.6 to 1, and w_{re} ranges from 0 to 0.2, and the step size of them are all 0.05. Specifically, when w_{trans} and w_{re} are 0, the recommendation effectiveness is poor, which is not reported in this paper. The values of RS and AUC based on each single metapath are shown in Tables 4 and 5. The values that need to be paid attention are in bold.

As shown in Table 4, among all the metapaths, when w_{trans} is 0.2, w_{path} is 0.6, and w_{re} is 0.2, the recommendation based on the metapaths CPCI and CPI performs better. The best RS of CPCI is 0.211807, while the best RS of CPI is 0.213887. Furthermore, the investor recommendation based on the metapath CPCI performs better than the metapath CPI. Besides, when w_{trans} is 0.35, w_{path} is 0.6, and w_{re} is 0.05, and the recommendation based on the metapaths CRCI, CRI, CFCI, and CFI performs best. Except for this, the recommendation based on the metapaths CFCI and CFI performs better than the metapaths CRCI and CRI.

As for AUC results shown in Table 5, when w_{trans} is 0.15, w_{path} is 0.7, and *wre* is 0.15, the investor recommendation based on the metapath CPCI performs best. Furthermore, when w_{trans} is 0.15, w_{path} is 0.7, and w_{re} is 0.15, the investor recommendation based on the metapath CPI performs best. Among all the metapaths, the investor recommendation based on the two metapaths performs better than the other metapaths. At the same time, when w_{trans} is 0.2, w_{path} is 0.6, and w_{re} is 0.2, the performance of the investor recommendation based on the two metapaths is still better. Additionally, the investor recommendation based on the metapath CPI performs better than the metapath CPCI. And, the investor recommendation based on the metapaths CFCI and CFI performs better than the metapaths CRCI and CRI.

In summary, the obtained results demonstrate that when w_{trans} is 0.2, w_{path} is 0.6, and w_{re} is 0.2, the investor recommendation based on the metapaths CPCI and CPI performs better than other metapaths.

5.3.2. Recommendation Performance on the Mixed Metapath. After optimizing the investor recommendation based on different single metapaths mentioned above, we plot their performance in Figures 6 and 7. The investor recommendation based on the metapath CPCI and CPI performs better than those based on other four metapaths apparently. Therefore, we choose the two better single metapaths CPCI and CPI. Next, we will select the optimal parameter configuration and VC-metapaths' CPCI and CPI to generate the mixed metapath and conduct the investor recommendation. The metapath weight parameter of the single metapath CPCI is set to w_1, the metapath weight parameter of CPI is set to w_2, and $w_1 + w_2 = 1$. Furthermore, in the experiment, the step size of the two parameters is 0.1.

The experiment results of the investor recommendation on the mixed metapath are shown in Figures 8 and 9. It shows that the RS and AUC of the investor recommendation based on the mixed metapath vary with the metapath weight parameters. The RS gradually decreases as w_1 increases. Meanwhile, the performance of the investor recommendation based on the mixed metapath is getting better and better. The AUC is relatively volatile; however, it is generally on the rise. Besides, the investor recommendation based on the mixed metapath performs better in general. When the metapath weight parameter w_1 is 1 and w_2 is 0, the RS and AUC both perform best. It indicates that the performance of investor recommendation based on the single metapath

Table 4: Recommendation performance of six single metapaths on RS.

w_{trans}	w_{path}	w_{re}	CPCI	CPI	CRCI	CRI	CFCI	CFI
0.05	0.75	0.2	0.219222	0.22135	0.277106	0.270169	0.250546	0.243982
	0.8	0.15	0.221655	0.223362	0.277828	0.270873	0.250666	0.244244
	0.85	0.1	0.225599	0.220296	0.278481	0.27176	0.251109	0.244576
	0.9	0.05	0.234695	0.222552	0.279313	0.273044	0.251627	0.245053
0.1	0.7	0.2	0.213694	0.216187	0.262471	0.25895	0.242316	0.238706
	0.75	0.15	0.214787	0.217409	0.263718	0.260653	0.243208	0.239471
	0.8	0.1	0.216373	0.219011	0.264582	0.261073	0.244014	0.239913
	0.85	0.05	0.219776	0.222534	0.265447	0.262304	0.24427	0.240644
0.15	0.65	0.2	0.21261	0.2147	0.251039	0.247022	0.233613	0.230515
	0.7	0.15	0.213292	0.215465	0.252235	0.248369	0.234637	0.23212
	0.75	0.1	0.213675	0.216258	0.253453	0.249991	0.235588	0.232905
	0.8	0.05	0.215354	0.218043	0.254979	0.252041	0.236634	0.23409
0.2	0.6	0.2	**0.211807**	**0.213887**	0.244265	0.240331	0.227102	0.224867
	0.65	0.15	0.21266	0.214897	0.245381	0.241693	0.228164	0.225873
	0.7	0.1	0.213779	0.216197	0.246371	0.242599	0.229241	0.22663
	0.75	0.05	0.216248	0.218739	0.247331	0.244195	0.230016	0.22762
0.25	0.6	0.15	0.212023	0.213949	0.240456	0.237147	0.223524	0.221577
	0.65	0.1	0.212548	0.214742	0.241443	0.238426	0.224411	0.222593
	0.7	0.05	0.214052	0.216359	0.242718	0.239425	0.225425	0.223164
0.3	0.6	0.1	0.212974	0.214543	0.23785	0.235392	0.221116	0.219334
	0.65	0.05	0.213756	0.215409	0.238975	0.236847	0.221975	0.220426
0.35	0.6	0.05	0.214028	0.21612	**0.236006**	**0.234157**	**0.219589**	**0.218322**

Table 5: Recommendation performance of six single metapaths on AUC.

w_{trans}	w_{path}	w_{re}	CPCI	CPI	CRCI	CRI	CFCI	CFI
0.05	0.75	0.2	0.781749	0.780472	0.713146	0.727824	0.748564	0.752393
	0.8	0.15	0.783025	0.775367	0.717294	0.718571	0.757498	0.753669
	0.85	0.1	0.770262	0.783025	0.734205	0.717613	0.749202	0.758775
	0.9	0.05	0.767709	0.776005	0.725271	0.734844	0.752393	0.762285
0.1	0.7	0.2	0.794512	0.776643	0.737396	0.737396	0.760689	0.758137
	0.75	0.15	0.774729	0.784939	0.748245	0.740587	0.754308	0.761966
	0.8	0.1	0.790045	0.788449	0.741863	0.736439	0.761327	0.758137
	0.85	0.05	0.789726	0.768666	0.746011	0.738354	0.76037	0.758456
0.15	0.65	0.2	0.784301	**0.79866**	0.758137	0.761008	0.760051	0.773452
	0.7	0.15	**0.798022**	0.78813	0.739949	0.751117	0.766114	0.767071
	0.75	0.1	0.786216	0.789726	0.751755	0.746331	0.765795	0.77792
	0.8	0.05	0.788449	0.784939	0.753989	0.740587	0.761646	0.762604
0.2	0.6	0.2	**0.783344**	**0.79164**	0.748883	0.75335	0.762285	0.7709
	0.65	0.15	0.788449	0.770262	0.765795	0.762285	0.775048	0.782387
	0.7	0.1	0.781429	0.789407	0.756222	0.763242	0.783663	0.773133
	0.75	0.05	0.765795	0.773133	0.751436	0.770581	0.754308	0.779515
0.25	0.6	0.15	0.791002	0.789087	0.765475	0.762285	0.77441	0.77792
	0.65	0.1	0.787492	0.776643	0.759094	0.766752	0.772176	**0.782706**
	0.7	0.05	0.777281	0.776643	**0.76739**	0.753031	0.778558	0.775367
0.3	0.6	0.1	0.792916	0.796426	0.762923	**0.772176**	0.776962	0.781749
	0.65	0.05	0.793235	0.787811	0.76037	0.765475	0.777281	0.773772
0.35	0.6	0.05	0.785897	0.78111	0.754627	0.769943	**0.789087**	0.766433

CPCI is better, compared with the results based on the mixed metapath.

5.4. Analysis of VC-Metapaths. After assessing the performance of the investor recommendation based on the single metapath and the mixed metapath, we can now analyse the impact of each defined single metapath on the investor recommendation task and summarize four rules to assist in further investment tasks.

(1) The partners of startups contain much more precise semantic information for investor recommendation than the fields and rounds of startups.

As shown in Tables 4 and 5, among all the VC-metapaths, the investor recommendation based on

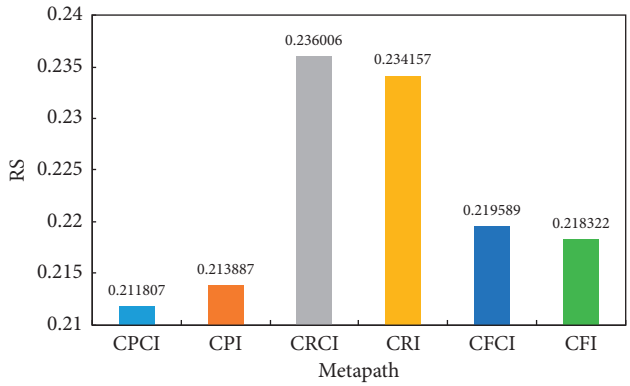

Figure 6: Recommendation performance of different metapaths on RS.

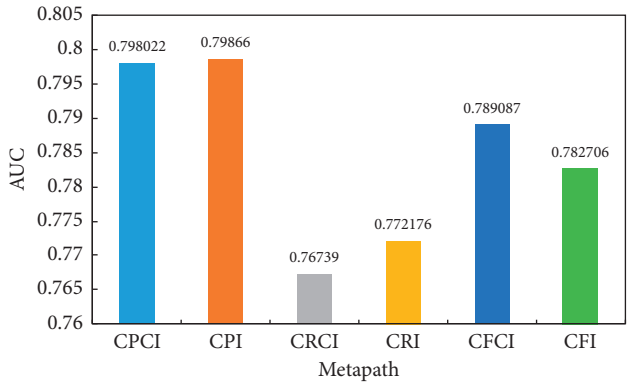

Figure 7: Recommendation performance of different metapaths on AUC.

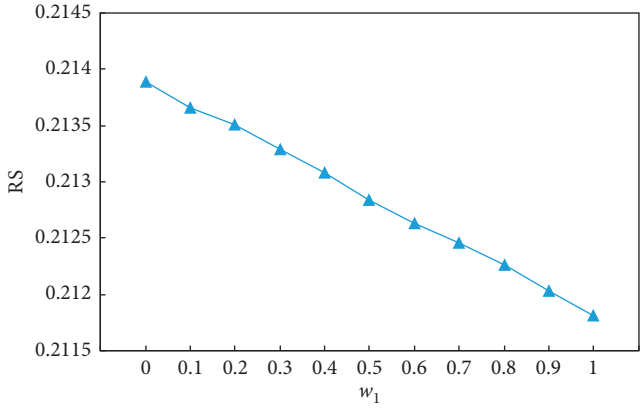

Figure 8: Recommendation performance of the mixed metapath on RS.

the metapaths CPCI and CPI performs better than the other metapaths. It indicates that the metapaths CPCI and CPI can imply rich semantic information. Correspondingly, the partners involved in the two metapaths contain more precise semantic information than the fields and rounds of startups. Therefore, the partners of startups could be followed when recommending investors for startups. For example,

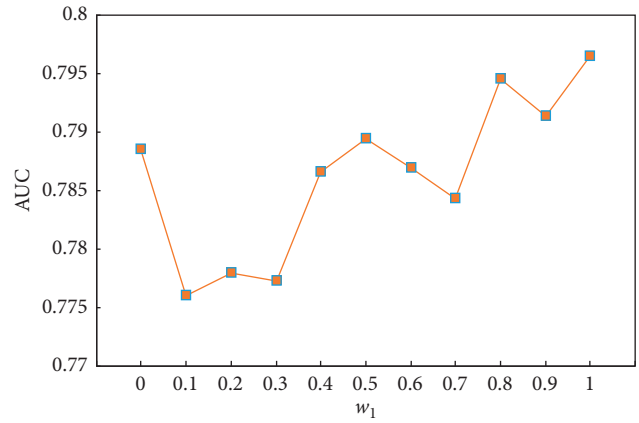

Figure 9: Recommendation performance of the mixed metapath on AUC.

as for the startup Ziroom shown in Table 1, if we recommend investors for it based on its partners, rounds, or fields, its partners Lin Xiong and Guowei Li could contain more useful semantic information than its field Real Estate and its round A, and we could obtain good recommendation performance by mining its partners.

(2) The fields of startups include richer related information about investor recommendation than the rounds.

Tables 4 and 5 show that the recommendation based on the metapaths CFCI and CFI performs better than the metapaths CRCI and CRI, which illustrates that the metapaths CFCI and CFI include more plentiful information than the metapaths CRCI and CRI. Along this line, the fields of startups contain richer information than the rounds. Thereby, we could focus on their fields in the investor recommendation task. Also, for the startup Ziroom shown in Table 1, if we recommend investors on the basis of its rounds or fields, its field Real Estate could contribute more to the recommendation task than its round A, and we could get good recommendation effectiveness by utilizing its field.

(3) The companies with the same partners as the target startup could contribute much more information to the investor recommendation task, than its partners.

As shown in Table 4, the investor recommendation based on the VC-metapath CPCI is more effective than the investor recommendation based on the metapath CPI. The results indicate that it will make the relative ranking of relevant investors in the corresponding investor recommendation set more accurate when we mine the companies with the same partners as the target startup and recommend investors for the target startup. However, when we focus on the partners of startups and recommend investors for the target startup who have invested in the partners of the target startup, the accuracy of the relative ranking of relevant investors will be reduced.

Therefore, the companies with the same partners as the target startup could contribute much more information to the investor recommendation task, than its partners. For example, if we recommend investors for the startup Ziroom shown in Table 1 based on its partners, Lin Xiong and Guowei Li, we could first focus on the companies with partners Lin Xiong and Guowei Li and then recommend the investors who have invested in those companies for Ziroom.

(4) It will lead to worse performance, when the investor recommendation task is conducted by simultaneously utilizing the companies with the same partners as the target startup and the partners of the target startup.

The experimental results shown in Tables 4 and 5 illustrate that the partners of startups are more important than the other features, such as fields and rounds of startups. As shown in Figures 8 and 9, when the metapath weight parameter w_1 is 1 and w_2 is 0, the RS and AUC of the investor recommendation based on the mixed metapath both perform best. As the metapath weight parameter w_1 is 1 and w_2 is 0, it indicates that the performance of investor recommendation based on the single metapath CPCI is better, compared with the result based on the mixed metapath. It shows that the mixed metapath generated by the metapaths CPCI and CPI will make the semantic information contained in the metapath fuzzier, which will lead to worse recommendation performance. For example, if we recommend investors for the startup Ziroom shown in Table 1 based on its partners Lin Xiong and Guowei Li, we define the investors who have invested in the companies with the same partners as the first kind of investor and the investors who are interested in the partners as the second kind of investor, and we could only recommend investors for Ziroom based on the first kind of investor. Furthermore, it will make the recommendation performance worse if we recommend investors for Ziroom on the basis of the two kinds of investors.

6. Conclusions

In this paper, we investigate how to mine practical rules to assist in further investment tasks, by measuring the impact of startups' features on the investor recommendation task. Along this line, we propose a features' contribution measurement approach of startups on investor recommendation, named FECOM. Specifically, we first construct the VC-HIN and design six VC-metapaths based on three startups' features, including partners, rounds, and fields. Then, the two recommendation strategies contained in FECOM could be accomplished by exploiting different types of VC-metapaths. To this end, we could analyse the impact of startups' features on investor recommendation by validating the recommendation performance and summarize the practical rules beneficial for further investment tasks. Finally, four practical rules about the startups' features for the investment task are extracted based on a real-world dataset, which can be employed to guide in further investor recommendation.

However, if there is a large amount of VC data to be processed, the proposed FECOM will be time consuming. In the future, we will put efforts into reducing the time cost of FECOM. Besides, we will study the optimal number of single metapaths to generate the mixed metapath.

Data Availability

The data used to support the findings of this study are available from the corresponding author via gaoxiaonan0001@163.com upon request.

Conflicts of Interest

The authors declare that there are no conflicts of interest regarding the publication of this paper.

Acknowledgments

This work was supported in part by the National Natural Science Foundation of China (no. 71971025).

References

[1] T. Stone, W. Zhang, and X. Zhao, "An empirical study of top-n recommendation for venture finance," in *Proceedings of the 22nd ACM International Conference on Information & Knowledge Management*, pp. 1865–1868, ACM, San Francisco, CA, USA, December 2013.

[2] J. Jeong, J. Kim, H. Son, and D. Nam, "The role of venture capital investment in startups' sustainable growth and performance: focusing on absorptive capacity and venture capitalists' reputation," *Sustainability*, vol. 12, no. 8, Article ID 3447, 2020.

[3] J. Lerner and R. Nanda, "Venture capital's role in financing innovation: what we know and how much we still need to learn," *Journal of Economic Perspectives*, vol. 34, no. 3, pp. 237–261, 2020.

[4] S. Xu, Q. Zhang, M. S. Lü, and M. Mariani, "Recommending investors for new startups by integrating network diffusion and investors' domain preference," *Information Sciences*, vol. 515, pp. 103–115, 2020.

[5] A. Salamzadeh and H. K. Kesim, "Startup companies: life cycle and challenges," in *Proceedings of the 4th International Conference on Employment, Education and Entrepreneurship (EEE)*, Belgrade, Serbia, October 2015.

[6] X. Zhao, W. Zhang, and J. Wang, "Risk-hedged venture capital investment recommendation," in *Proceedings of the 9th ACM Conference on Recommender Systems*, pp. 75–82, Vienna, Austria, September 2015.

[7] S. Wu, H. Li, and L. Liu, "A venture capital recommendation algorithm based on heterogeneous information network," *International Journal of Computers Communications & Control*, vol. 15, no. 1, Article ID 1009, 2020.

[8] H. Li, S. Wu, and L. Liu, "Venture capital recommendation based on meta path ranking in heterogeneous information network," in *Proceedings of the 7th IEEE International*

Conference on Logistics, Informatics and Service Sciences (LISS'2017), pp. 1063–1067, Kyoto, Japan, July 2017.

[9] D. Antonio, G. Foster, and M. Gupta, "Venture capital financing and the growth of startup firms," *Journal of Business Venturing*, vol. 18, no. 6, pp. 689–708, 2003.

[10] C. Shi, Y. Li, J. Zhang, Y. Sun, and S. Y. Philip, "A survey of heterogeneous information network analysis," *IEEE Transactions on Knowledge and Data Engineering*, vol. 29, no. 1, pp. 17–37, 2016.

[11] J. Chircop, S. Johan, and M. Tarsalewska, "Does religiosity influence venture capital investment decisions?" *Journal of Corporate Finance*, vol. 62, Article ID 101589, 2020.

[12] G. Andrieu and A. P. Groh, "Specialist versus generalist investors: trading off support quality, investment horizon and control rights," *European Economic Review*, vol. 101, pp. 459–478, 2018.

[13] X. Tian, G. Kou, and W. Zhang, "Geographic distance, venture capital and technological performance: evidence from Chinese enterprises," *Technological Forecasting and Social Change*, vol. 158, Article ID 120155, 2020.

[14] C.-Y. Cheng and M.-J. Tang, "Partner-selection effects on venture capital investment performance with uncertaintiesffects on venture capital investment performance with uncertainties," *Journal of Business Research*, vol. 95, pp. 242–252, 2019.

[15] J. Wu, C. Luo, and L. Liu, "A social network analysis on venture capital alliance's exit from an emerging market," *Complexity*, vol. 2020, Article ID 4650160, 10 pages, 2020.

[16] X. Zhang, L. Valdez, H. Stanley, and L. Braunstein, "Modelling risk contagion in the venture capital market: a multilayer network approach," *Complexity*, vol. 2019, Article ID 9209345, 11 pages, 2019.

[17] T. Luo, "Research on decision-making of complex venture capital based on financial big data platform," *Complexity*, vol. 2018, Article ID 5170281, 12 pages, 2018.

[18] Y. Sun, J. Han, X. Yan, P. S. Yu, and T. Wu, "PathSim," *Proceedings of the VLDB Endowment*, vol. 4, no. 11, pp. 992–1003, 2011.

[19] T. H. Haveliwala, "Topic-sensitive PageRank: a context-sensitive ranking algorithm for Web search," *IEEE Transactions on Knowledge and Data Engineering*, vol. 15, no. 4, pp. 784–796, 2003.

[20] G. Jeh and J. Widom, "SimRank: a measure of structural-context similarity," in *Proceedings of the Eighth ACM SIGKDD International Conference on Knowledge Discovery and Data Mining*, pp. 538–543, Edmonton, Alberta, Canada, July 2002.

[21] Y. Wen, J. Hou, Z. Yuan, and D. Zhou, "Heterogeneous information network-based scientific workflow recommendation for complex applications," *Complexity*, vol. 2020, Article ID 4129063, 16 pages, 2020.

[22] N. Lao and W. W. Cohen, "Relational retrieval using a combination of path-constrained random walks," *Machine Learning*, vol. 81, no. 1, pp. 53–67, 2010.

[23] C. Shi, X. Kong, Y. Huang, P. S. Yu, and B. Wu, "HeteSim: a general framework for relevance measure in heterogeneous networks," *IEEE Transactions on Knowledge and Data Engineering*, vol. 26, no. 10, pp. 2479–2492, 2014.

[24] S. Lee, S. Park, M. Kahng, and S. Lee, "PathRank: a novel node ranking measure on a heterogeneous graph for recommender systems," in *Proceedings of the 21st ACM International Conference on Information and Knowledge Management*, pp. 1637–1641, Maui, HI, USA, November 2012.

[25] T. Zhou, J. Ren, M. Medo, and Y. Zhang, "Bipartite network projection and personal recommendation," *Physical Review*, vol. 76, no. 4, Article ID 046115, 2007.

[26] J. A. Hanley and B. J. McNeil, "The meaning and use of the area under a receiver operating characteristic (ROC) curve," *Radiology*, vol. 143, no. 1, pp. 29–36, 1982.

Hindawi
Complexity
Volume 2021, Article ID 6687544, 14 pages
https://doi.org/10.1155/2021/6687544

Research Article

Dynamics of a Heterogeneous Constraint Profit Maximization Duopoly Model Based on an Isoelastic Demand

S. S. Askar,[1,2] **A. Ibrahim**,[3] **and A. A. Elsadany**[4]

[1]*Department of Statistics and Operations Research, College of Science, King Saud University, Riyadh, Saudi Arabia*
[2]*Department of Mathematics, Faculty of Science, Mansoura University, Mansoura, Egypt*
[3]*Department of Mathematics and Statistics, School of Quantitative Science, UUM College of Arts and Sciences, Universiti Utara Malaysia, 06010 Sintok, Kedah, Malaysia*
[4]*Department of Basic Science, Faculty of Computers and Informatics, Suez Canal University, Ismailia 41522, Egypt*

Correspondence should be addressed to A. A. Elsadany; aelsadany1@yahoo.com

Received 20 December 2020; Revised 17 February 2021; Accepted 18 March 2021; Published 28 March 2021

Academic Editor: Xueyong Liu

A Cournot duopoly game is a two-firm market where the aim is to maximize profits. It is rational for every company to maximize its profits with minimal sales constraints. As a consequence, a model of constrained profit maximization (CPM) occurs when a business needs to be increased with profit minimal sales constraints. The CPM model, in which companies maximize profits under the minimum sales constraints, is an alternative to the profit maximization model. The current study constructs a duopoly game based on an isoelastic demand and homogeneous goods with heterogeneous strategies. In the event of sales constraint and no sales constraint, the local stability conditions of the Cournot equilibrium are derived. The initial results show that the duopoly model would be easier to stabilize if firms were to impose certain minimum sales constraints. Two routes to chaos are analyzed by numerical simulation using 2D bifurcation diagram, one of which is period doubling bifurcation and the other is Neimark–Sacker bifurcation. Four forms of coexistence of attractors are demonstrated by the basin of attraction, which is the coexistence of periodic attractors and chaotic attractors, the coexistence of periodic attractors and quasiperiodic attractors, and the coexistence of several chaotic attractors. Our findings show that the effect of game parameters on stability depends on the rules of expectations and restriction of sales by firms.

1. Introduction

In 1838, Antoine Augustin Cournot introduced the concept of duopoly in his book titled Researches on the Mathematical Principles of the Theory of Wealth. He considered the situation of two firms competing in a market by producing a homogeneous product that would maximize their profits. A number of studies on Cournot games has been conducted for two (duopoly) or more players, phrased as dynamic games on discrete time domains [1–6]. Most discrete time oligopoly dynamics that have been considered in the past two decades were based on the single objective of maximizing profit of firms [7–10]. More recently, the stable, periodic, and chaotic dynamic behaviors of these markets can be analyzed on the basis of these models [11–15].

From an economic point of view, multiobjective games have the advantage of being more realistic in many cases. Typically, one maximizes profits in oligopoly models as a single objective. This is not realistic since many cases have more than one objective. Baumol [16] proposed an alternative model called constraint sales maximization where a business maximizes its sales on the basis of a minimum constraint of profit. The idea for Baumol's model was based on his experience as a business consultant, which he found that businesses maximize sales rather than profits. Fisher [17, 18] concluded that maximizing profits which subject to minimum sales constraints are more rational for a business, thus leading to a new model called constraint profit maximization. Since then, there have been a few studies on the dynamics of oligopoly models with constraints. The earliest was by Kamerschen and Smith [19], who showed that the stability of their duopoly model depends on the production cost and the coefficients in the linear demand function. In their work, by including risk minimization into their profit

maximization oligopoly model, Ahmed et al. [20] showed that giving more weight to risk minimization decreases profit. In another work, Ahmed et al. [21] showed that a multiobjective oligopoly model is more stable than a single objective one. Mert [22] showed that, in a duopoly model under a hybrid of sales and profit maximization goal, Nash equilibrium occurs at sales maximization conditions rather than profit maximization conditions. More recently, Ibrahim [23] derived the local stability conditions for a Nash equilibrium of duopoly model subject to minimum sales constraint.

Decision mechanism plays an important role in the output adjustment process of a firm. Some common mechanisms are naive expectation, adaptive expectation, bounded rationality, and local approximation. All the abovementioned studies consider the case of homogeneous players, where the duopolists or oligopolists adopt the same decision mechanism. However, in practical, a more realistic assumption is the players adopting heterogeneous decision mechanisms, which characterized the works by Léonard and Nishimura [24], Den Haan [25], Agiza and Elsadany [26, 27], and Tramontana and Elsadany [28]. Dubiel-Teleszynski [29] studied a heterogeneous Cournot game with nonlinear cost function and explored the nonlinear dynamics of this game. Tramontana [30] and Ding et al. [31] analyzed a heterogeneous duopoly game with isoelastic and linear demand function, respectively. Both works showed the existent of two different routes to complicated dynamics. Cavalli et al. [32] investigated a dynamic Cournot duopoly with heterogeneous players based on a local monopolistic approach versus a gradient rule with endogenous reactivity local monopolistic approach. Pecora and Sodini [33] analyzed the stability switching curves in the heterogeneous Cournot duopoly with delay.

The literature review reported above has shown that the issue of profit maximization for firms has been discussed without constraints in dynamic situation. Recently, certain games models have been investigated and have given rise to complex dynamics with some constraints, such as global analysis and multistability of Cournot duopoly market game based on consumer surpluses [34, 35]. The effect of model parameters on game dynamics, coexisting attractors, and global dynamics of constrained competition games by both corporate social responsibility (CSR) and social welfare (SW) has been studied in [36, 37].

The goal of this work is to reconsider the CPM Cournot duopoly game by providing an isoelastic demand function with heterogeneous players and to develop the Tramontana model [30] on the basis of a minimum sales constraint. In this paper, we analyze a similar duopoly game to Tramontana [30], but the profit maximization is subject to minimum sales constraint. The dynamic equilibrium-point structure reflects corresponding economic explanations. Jury stability criterion [38] and numerical simulation provide local stability of boundary equilibrium and Nash equilibrium for obtaining the game's internal complexity. The theoretical stability of the equilibrium point and the derivation of critical curves of noninvertiable map are studied, and the game's dynamic behavior is simulated numerically. We demonstrate that the sequential change in game parameters not only causes the stability of the game to collapse but also increases the complexity of consequent game behaviors such as the number of coexisting attractors, the critical bifurcation of attractors, and the global bifurcation of the attraction basin.

The paper is organized as follows. In Section 2, a duopoly model and the nonlinear system describing the dynamics of the productions of the firms are described. In Section 3, the local stability conditions for the Nash equilibrium are determined. In Section 4, we present the numerical simulations as well as an analysis of the local bifurcations, basin of attractions, critical curves, and route to complex dynamics. Finally, some remarks are presented in Section 5.

2. Model

We consider a market dominated by two firms producing perfect substitute goods. Let q_i be the output of firm $i = 1, 2$ and Q denote the total output of the two firms. We recall an isoelastic demand function, which is based on the Cobb–Douglas utility function governing the market [39]:

$$p = \frac{1}{Q} = \frac{1}{q_1 + q_2}, \tag{1}$$

where p is the goods price. Let the cost function for each company be

$$C_i(q_i) = c_i q_i. \tag{2}$$

Now, each company's profit is

$$\pi_i(q_1, q_2) = \frac{q_i}{Q} - c_i q_i. \tag{3}$$

i considers S_i to be a constant constraint of sales. The firm i is maximizing its profit subject to its sales constraint:

$$\begin{aligned} &\text{maximizes} \quad \frac{q_i}{Q} - c_i q_i \\ &\text{subject to} \quad \frac{q_i}{Q} \geq S_i, \end{aligned} \tag{4}$$

which is equivalent to maximizing the payoff function as the objective function of firm i:

$$L_i = \frac{q_i}{Q} - c_i q_i - \mu_i \left(\frac{q_i}{Q} - S_i \right), \tag{5}$$

where μ_i is positive parameter and associated with the sales constraint. By differentiating the payoff function L_i with respect to q_i, we obtain

$$\frac{\partial L_i}{\partial q_i} = \frac{q_{-i}(1 - \mu_i)}{Q^2} - c_i = 0, \tag{6}$$

where q_{-i} represents the output of the other duopolist. The solution of (6) gives the firm's i reaction function as follows:

$$q_i = \sqrt{\frac{q_{-i}(1 - \mu_i)}{c_i}} - q_{-i}. \tag{7}$$

The response of the firm i to the output of the other firm is the response function.

We consider the situation where each firm adopts different mechanisms in adjusting its output in each time period. Following Tramontana and Elsadany [28] and Tramontana [30], we assume firm 1 to have bounded rationality, where an increase or decrease of its output is dependent on the marginal payoff function of the last period. This adjustment process is given by

$$q_1(t+1) = q_1(t) + \alpha q_1(t)\frac{\partial L_1}{\partial q_1}, \tag{8}$$

where $\alpha > 0$ represents the speed of adjustment.

For firm 2, we assume that it naively expects that the output of its rival is the same as the last period, i.e., $q_1^e(t+1) = q_1(t)$. Given this assumption, using the best reaction function in (7), firm 2 will determine its output in period $t+1$ using the following the adjustment process:

$$q_2(t+1) = \sqrt{\frac{q_1(t)(1-\mu)}{c_2}} - q_1(t). \tag{9}$$

The dynamics of the outputs of the two firms are expressed by the discrete dynamical system as follows:

$$T(q_1, q_2): \begin{cases} q_1(t+1) = q_1(t) + \alpha q_1(t)\left(\dfrac{q_2(t)(1-\mu_1)}{(q_1(t)+q_2(t))^2} - c_1\right), \\ \\ q_2(t+1) = \sqrt{\dfrac{q_1(t)(1-\mu_2)}{c_2}} - q_1(t), \end{cases} \tag{10}$$

where $0 < \mu_2 < 1$. When $\mu_1 = \mu_2 = 0$, system (10) is reduced to the game considered by Tramontana [30].

System (10) is a noninvertible two-dimensional map whose iteration determines competing firms' trajectories. We investigate the effect of parameters on this system's dynamics. To discuss the local qualitative behaviors of the solutions of system (10), first, we need to investigate the local stability and bifurcation of equilibrium points of the game (10) between these two firms.

3. Nash Equilibrium and Local Stability

The equilibrium points of system (10) are obtained through the fixed point conditions $q_1(t+1) = q_1(t) = q_1^*$ and $q_2(t+1) = q_2(t) = q_2^*$ in the discrete system (10), and we obtain

$$\alpha q_1^*\left(\frac{q_2^*(1-\mu_1)}{(q_1^*+q_2^*)^2} - c_1\right) = 0, \tag{11}$$

$$\sqrt{\frac{q_1^*(1-\mu_2)}{c_2}} - q_1^* - q_2^* = 0. \tag{12}$$

Solving equations (11) and (12) simultaneously yields the following Nash equilibrium point:

$$E = (q_1^*, q_2^*) = \left(\frac{c_2(1-\mu_2)(1-\mu_1)^2}{[c_1(1-\mu_2)+c_2(1-\mu_1)]^2}, \frac{c_1(1-\mu_1)(1-\mu_2)^2}{[c_1(1-\mu_2)+c_2(1-\mu_1)]^2}\right), \tag{13}$$

where E is a positive equilibrium provided that $\mu_i < 1, i = 1, 2$. The Nash equilibrium E of game (10) is a unique fixed point and is the same equilibrium in Tramontana [30] when $\mu_1 = \mu_2 = 0$. The Jacobian matrix of system (10) is

$$J = \begin{bmatrix} 1 - \alpha c_1 + \dfrac{\alpha(1-\mu_1)\left(q_2^2 - q_1 q_2\right)}{(q_1+q_2)^3} & \dfrac{\alpha(1-\mu_1)\left(q_1^2 - q_1 q_2\right)}{(q_1+q_2)^3} \\ \\ \dfrac{1}{2}\sqrt{\dfrac{1-\mu_2}{c_2 q_1}} - 1 & 0 \end{bmatrix}, \tag{14}$$

with characteristic polynomial

$$f(\lambda) = \lambda^2 - \mathrm{tr}(J(E))\lambda + \det(J(E)), \tag{15}$$

where $\mathrm{tr}(J)$ and $\det(J)$ are the trace and determinant of the Jacobian matrix in (14), respectively.

The required condition of the local asymptotic stability of Nash equilibrium point is that the eigenvalues of the corresponding Jacobian matrix are inside the unit circle. According to the Jury criterion [34], the local stability conditions of the Nash equilibrium point are as follows:

$$\begin{aligned} &f(-1) = 1 + \mathrm{tr}(J(E)) + \det(J(E)) > 0,\\ &f(1) = 1 - \mathrm{tr}(J(E)) + \det(J(E)) > 0,\\ &\det(J) < 1. \end{aligned} \tag{16}$$

If only two of the three inequalities in (16) hold, one of the following three behaviors occurs [38]:

(i) A period doubling bifurcation is obtained when $f(-1) = 0$

(ii) A transcritical or fold bifurcation is obtained when $f(1) = 0$

(iii) A Neimark–Sacker bifurcation is obtained when $\det(J) < 1$

Proposition 1. *The Nash equilibrium point (13) is stable provided that* $\alpha < \min\{\alpha_f, \alpha_{ns}\}$, *where*

$$\begin{aligned} \alpha_f &= \frac{4(1-\mu_2)[c_1(1-\mu_2) + c_2(1-\mu_1)]}{(1-\mu_2)^2 c_1^2 + 6(1-\mu_1)(1-\mu_2)c_1c_2 - 3(1-\mu_1)^2 c_2^2},\\ \alpha_{ns} &= \frac{2(1-\mu_2)[c_1(1-\mu_2) + c_2(1-\mu_2)]}{3(1-\mu_1)^2 c_2^2 - 2(1-\mu_1)(1-\mu_2)c_1c_2 - (1-\mu_2)^2 c_1^2}. \end{aligned} \tag{17}$$

Proof. The proof depends on the Jacobian matrix of map (10) given in (14), which when evaluated at the Nash equilibrium point (13) becomes

$$J_M = \begin{bmatrix} 1 - \alpha\left(\dfrac{2c_1c_2(1-\mu_1)}{c_1(1-\mu_2) + c_2(1-\mu_1)}\right) & \alpha\left(\dfrac{c_2(1-\mu_1)[c_2(1-\mu_1) - c_1(1-\mu_2)]}{(1-\mu_2)[c_1(1-\mu_2) + c_2(1-\mu_1)]}\right) \\ -\dfrac{1}{2}\dfrac{c_1(1-\mu_2) + 3c_2(1-\mu_1)}{c_2(1-\mu_1)} & 0 \end{bmatrix}, \tag{18}$$

and the trace and determinant of matrix (18) are

$$\begin{aligned} \mathrm{tr}(J(E)) &= 1 - \alpha\left(\frac{2c_1c_2(1-\mu_1)}{c_1(1-\mu_2) + c_2(1-\mu_1)}\right),\\ \det(J(E)) &= \frac{[c_2(1-\mu_1) - c_1(1-\mu_2)][c_1(1-\mu_2) + 3c_2(1-\mu_1)]}{2(1-\mu_2)[c_1(1-\mu_2) + c_2(1-\mu_1)]}. \end{aligned} \tag{19}$$

Substituting (19) in (16) and after some algebraic calculations, the first condition of (16) is satisfied if $3c_2(1-\mu_1) > c_1(1-\mu_2)$, while the other two conditions are reduced to $\alpha < \alpha_f$ and $\alpha < \alpha_{ns}$. This completes the proof. □

Proposition 2. *The Nash equilibrium point (13) can be unstable by either period-doubling or Neimark–Sacker bifurcation if*

$$\begin{aligned} &\alpha_{ns} \le \alpha_f \Longleftrightarrow \frac{1}{\sqrt{3}}\left(\frac{1-\mu_1}{1-\mu_2}\right)c_2 \le c_1 \le 3\left(\frac{1-\mu_1}{1-\mu_2}\right)c_2,\\ &\alpha_{ns} \ge \alpha_f \Longleftrightarrow c_1 \le \frac{1}{\sqrt{3}}\left(\frac{1-\mu_1}{1-\mu_2}\right)c_2 \cup c_1 \ge 3\left(\frac{1-\mu_1}{1-\mu_2}\right)c_2. \end{aligned} \tag{20}$$

Proof. The proof is straightforward and is obtained by reducing the expression $\alpha_{ns} - \alpha_f$.

In Section 4, the features of bifurcation and chaos are demonstrated in depth through local analysis numerical simulation such as chaotic attractors, initial sensitivity, intermittent chaos, and multistationary properties. The hidden complexity of the game is studied using chaos and bifurcation theories to reveal the complexity of competition between two heterogeneous firms. □

4. Numerical Simulation of Dynamic Game Behaviors

The numerical simulations in this section show some insights about the local stability of the Nash equilibrium point (13) and confirm our results in Section 2. In fact, we will see that the dynamics of map (10) becomes more complex due to the map's trajectories behaving differently when there is a slight change in the initial datum. For example, by fixing the

parameters $c_1 = 0.35, c_2 = 0.2, \mu_1 = 0.1$, and $\mu_2 = 0.5$, we get $\alpha_f \approx 5.8$ and $\alpha_{ns} \approx 99.3$, which means that $\alpha_f < \alpha_{ns}$, and hence, the Nash equilibrium becomes unstable due to period doubling bifurcation. Interestingly, at the initial data $(x_{0,1}, x_{0,2}) = (0.20, 0.40)$ and $(x_{0,1}x_{0,2}) = (0.40, 0.11)$, we report two different bifurcation diagrams corresponding to $c_1 = 0.35, c_2 = 0.2, \mu_1 = 0.1$, and $\mu_2 = 0.5$ on varying the parameter α. Figure 1(a) shows these bifurcation diagrams, where the blue one is for $(x_{0,1}, x_{0,2}) = (0.20, 0.40)$ while the red one is for $(x_{0,1}, x_{0,2}) = (0.40, 0.11)$. As we can see, a period 2-cycle arises even before $\alpha_f \approx 5.8$, particularly at $\alpha \approx 5.69$. This indicates that different attractors may coexisted on varying the parameter α. Such attractors are important and we give detailed investigations about them later. Now, we focus and report some attractors of map (10) at the initial datum $(x_{0,1}, x_{0,2}) = (0.40, 0.11)$ by keeping the other parameter values fixed. At the bifurcation threshold $\alpha_f \approx 5.8$, we obtain

$$J_M = \begin{bmatrix} -1.0586 & 0.029408 \\ -1.9861 & 0 \end{bmatrix}, \tag{21}$$

whose eigenvalues are $\lambda_1 = -1.0002$ and $\lambda_2 = -0.058395$, both of which are real with one having an absolute value greater than 1. This means that the Nash equilibrium becomes unstable due to period doubling bifurcation.

Figure 1(b) shows that the map's dynamic begins with the period 2-cycle, which is represented by squares while the Nash equilibrium point is represented by a circle. In order to investigate the evolution of the map's dynamic, we have carried out further numerical simulations, as shown in Figures 1(c)–1(f). In Figure 1(c), we present a stable period 4-cycle at $\alpha = 6.58$. This dynamic is followed by a stable period 8-cycle and a stable period 16-cycle which occurred at $\alpha = 6.738$ and $\alpha = 6.77$, respectively (Figure 1(d)). After that and particularly at $\alpha = 6.773$, a stable period 32-cycle arises. We should highlight that the basin of attraction of those stable period cycles becomes more complicated as we approach period 32-cycle. Further increase in the parameter α to 6.78 gives rise to a dynamic of four unconnected areas that turns into four connected areas as α goes to 6.782 (Figure 1(e)). Moreover, the dynamic of the map then goes to an unstable period 20-cycle ($\alpha = 6.787$) followed by four pieces of chaotic areas ($\alpha = 6.788$) which turn into an unstable period 12-cycle ($\alpha = 6.795$). Eventually, the map's behavior changes into a two-piece chaotic at $\alpha = 6.85$ which then finally evolved into a one-piece chaotic attractor (Figure 1(f)).

All numerical simulations performed so far was at parameter values that satisfied the second condition of (16). Conversely, we assume now parameter values that satisfy the first condition. Let us assume the following parameter values, $c_1 = 0.1, c_2 = 0.22, \alpha = 2, \mu_1 = 0.3$, and $\mu_2 = 0.7$ with the same initial datum $(x_{0,1}x_{0,2}) = (0.40, 0.11)$. Substituting in (18), one obtains

$$J_M = \begin{bmatrix} 0.66522 & 0.69188 \\ -1.5974 & 0 \end{bmatrix}, \tag{22}$$

whose eigenvalues are $\lambda_{1,2} = 0.33261 \pm 0.99729i$ which are complex and have an absolute value greater than 1. This means the stable Nash equilibrium point will become unstable due to Neimark–Sacker bifurcation on varying the parameter α above the critical value α_{ns}. In Figure 2(b), at $\alpha = 7.10$, the attractor becomes a stable spiral point (red color), and as the parameter α increases, the stable spiral enlarges in size (yellow color). The Nash equilibrium point is represented by circle in the previous figure. As α continues to increase, the spiral becomes larger before changing into an attracting invariant closed curve with rough selvedge due to Neimark–Sacker bifurcation. These spiral and selvedge are plotted in Figure 2(c) at $\alpha = 7.17$ (red color) and $\alpha = 7.18$ (blue color), respectively. At $\alpha = 7.19$ and $\alpha = 7.195$, the attracting invariant closed curves becomes larger with some rough edges as shown in Figure 2(d). It is clear from the close values of the parameter α how quasi-periodic motions are produced around Nash point due to this type of bifurcation. Increasing α furthermore gives rise to continued invariant closed curves around the Nash point, but their selvedges begin to vanish as plotted in Figure 2(e) (blue color). After that and particularly when α approaches 7.847, the closed invariant curve is turned into a stable period 7-cycle, as illustrated by the squares in Figure 2(f). This figure analyzes the basin of attraction of this cycle where the cyan color refers to the basin of Nash point, while the yellow color represents the basin of the cycle. When we increase the parameter α until it is equal to 7.894, the previous cycle becomes a closed invariant curve.

Other invariant closed curves that are different from the previous ones are constructed for the map at $\alpha = 8.10$ and $\alpha = 8.12$, as shown in Figure 3(a). Following this dynamic situation, in Figure 3(b), we obtain an interesting behavior of the map after increasing $\alpha$to 8.143, that is, the coexistence of multiple stable period 10-cycle. Increasing the parameter α again changes the period 10-cycle into a chaotic attractor which then becomes a stable period 23-cycle at $\alpha = 8.149$. In Figure 3(c), we plot this period 23-cycle with its complicated basin of attraction. The gray color in this figure indicates divergent trajectories. Moving above $\alpha = 8.149$ and, particularly, in the interval $[8.150, 8.154]$, the dynamic evolution of map (10) will be mutual between period 23-cycle and chaotic attractors. Consequently, a stable period 26-cycle is formed around the Nash point in Figure 3(d) at $\alpha = 8.1565$, and above this value, the dynamic evolution of map (10) becomes a chaotic attractor, as evidenced in Figures 3(e) and 3(f).

So far, we have discussed the complex dynamics of map (10) by varying the parameter α and keeping the other parameter values fixed. Now, we are going to analyze the behavior of the map when either μ_1 or μ_2 varies and the other parameters become fixed including α. Let us start our investigation by assuming the following parameter values, $c_1 = 0.35, c_2 = 0.2, \mu_1 = 0.1$, and $\alpha = 5$, while μ_2 is considered as the bifurcation parameter.

In Figure 4(a), a period doubling bifurcation diagram is reported on varying μ_2. Increasing μ_2 further gives rise to a cascade of period doubling bifurcations ensued by periods of higher periodicity appeared and routes to chaos are formed. A confirmation of existence of chaos is the largest Lyapunov exponent corresponding to the bifurcation parameter μ_2. As

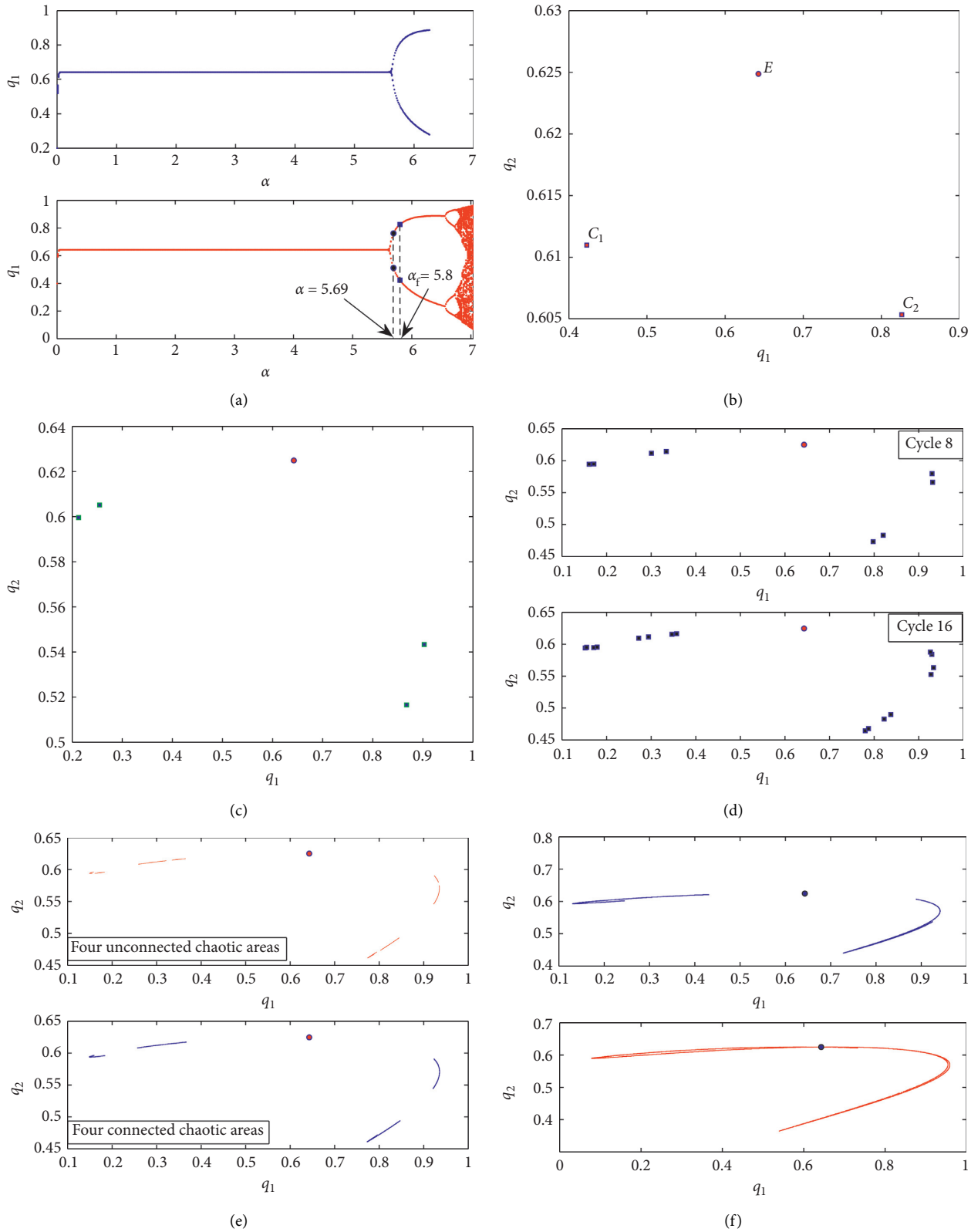

Figure 1: The fixed parameters are $c_1 = 0.35, c_2 = 0.2, \mu_1 = 0.1$, and $\mu_2 = 0.5$. (a) Bifurcation diagram of q_1 with respect to α at the initial data $(x_{0,1}, x_{0,2}) = (0.40, 0.11)$ (red color) and $(x_{0,1}, x_{0,2}) = (0.20, 0.40)$ (blue color). (b) Phase plane for period 2-cycle at $\alpha = 5.8$. (c) Phase plane for period 4-cycle at $\alpha = 6.58$. (d) Phase plane for period 8-cycle and 16-cycle at $\alpha = 6.738$ and $\alpha = 6.77$, respectively. (e) Phase plane of the four pieces chaotic areas at $\alpha = 6.78$ and $\alpha = 6.82$, respectively. (f) Phase plane of the one-piece and two-piece chaotic areas.

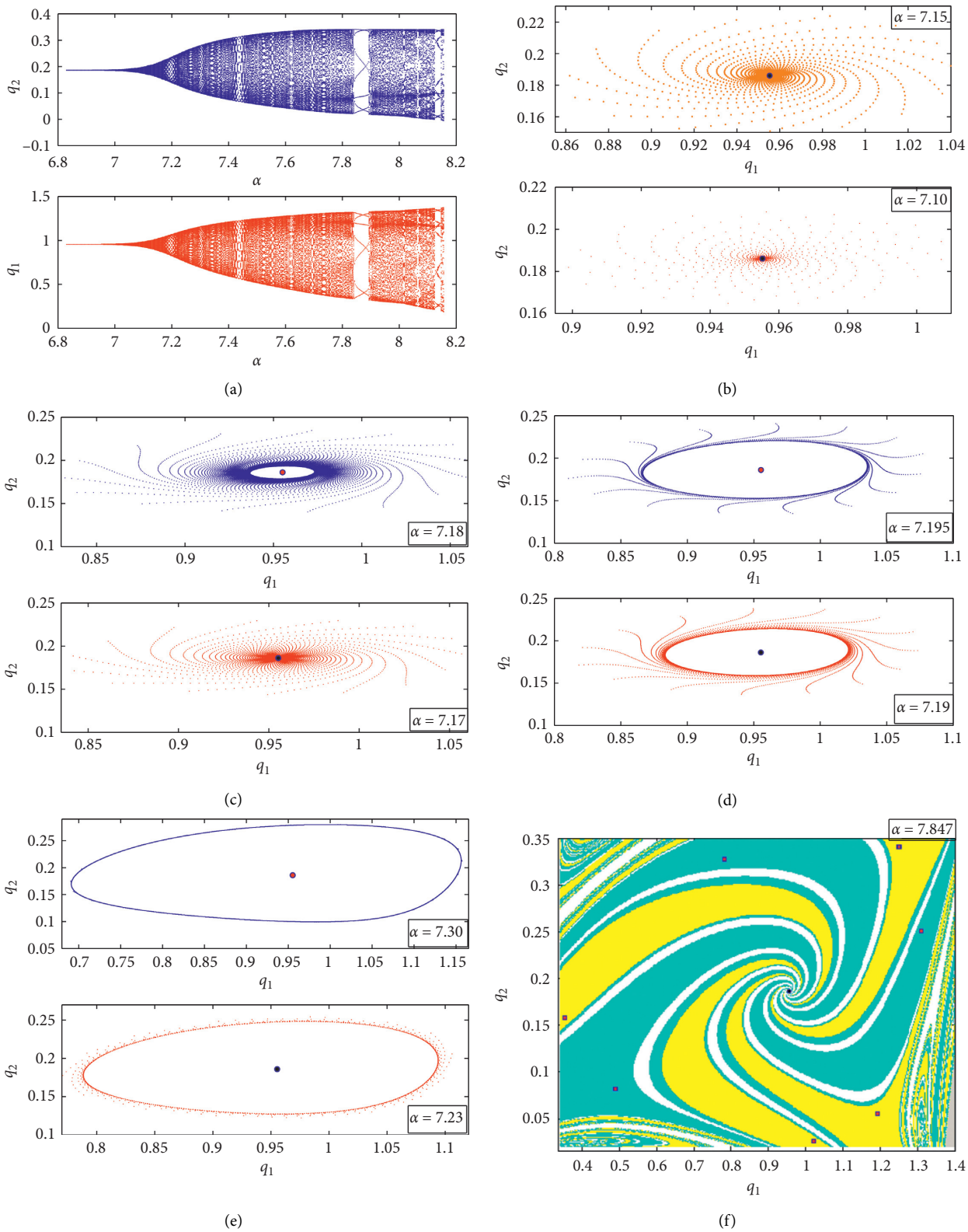

Figure 2: The fixed parameter values are $c_1 = 0.1, c_2 = 0.22, \alpha = 2, \mu_1 = 0.3$, and $\mu_2 = 0.7$. (a) Bifurcation diagrams of q_1 and q_2 on varying the parameter α at the initial datum (the red color) $(x_{0,1}, x_{0,2}) = (0.40, 0.11)$. (b) Phase plane of a stable spiral point. (c) Phase plane of a stable spiral point at $\alpha = 7.17$ and $\alpha = 7.18$. (d) Phase plane of an invariant closed curve at $\alpha = 7.19$ and $\alpha = 7.195$. (e) Phase plane of an invariant closed curve at $\alpha = 7.23$ and $\alpha = 7.30$. (f) Stable period 7-cycle and its basin of attraction at $\alpha = 7.847$.

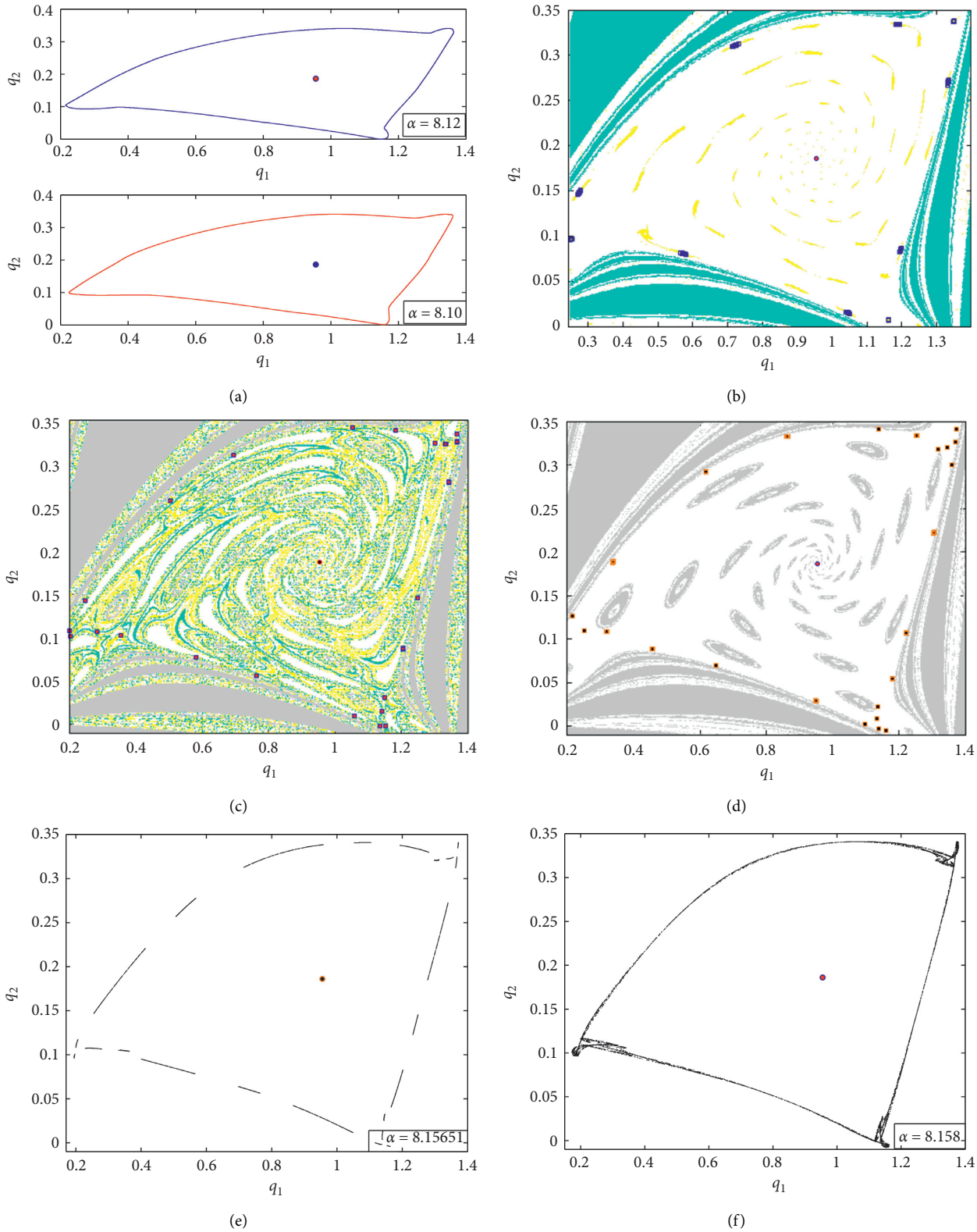

FIGURE 3: The fixed parameter values are $c_1 = 0.1, c_2 = 0.22, \alpha = 2, \mu_1 = 0.3$, and $\mu_2 = 0.7$. (a) Phase plane of an invariant closed curve at $\alpha = 8.10$ and $\alpha = 8.12$. (b) Basin of attraction of multiple stable period 10-cycle at $\alpha = 8.143$. (c) Stable period 23-cycle and its basin of attraction at $\alpha = 8.149$. (d) Stable period 23-cycle and its basin of attraction at $\alpha = 8.1565$. (e) Phase plane of chaotic attractor at $\alpha = 8.15651$. (f) Phase plane of chaotic attractor at $\alpha = 8.158$.

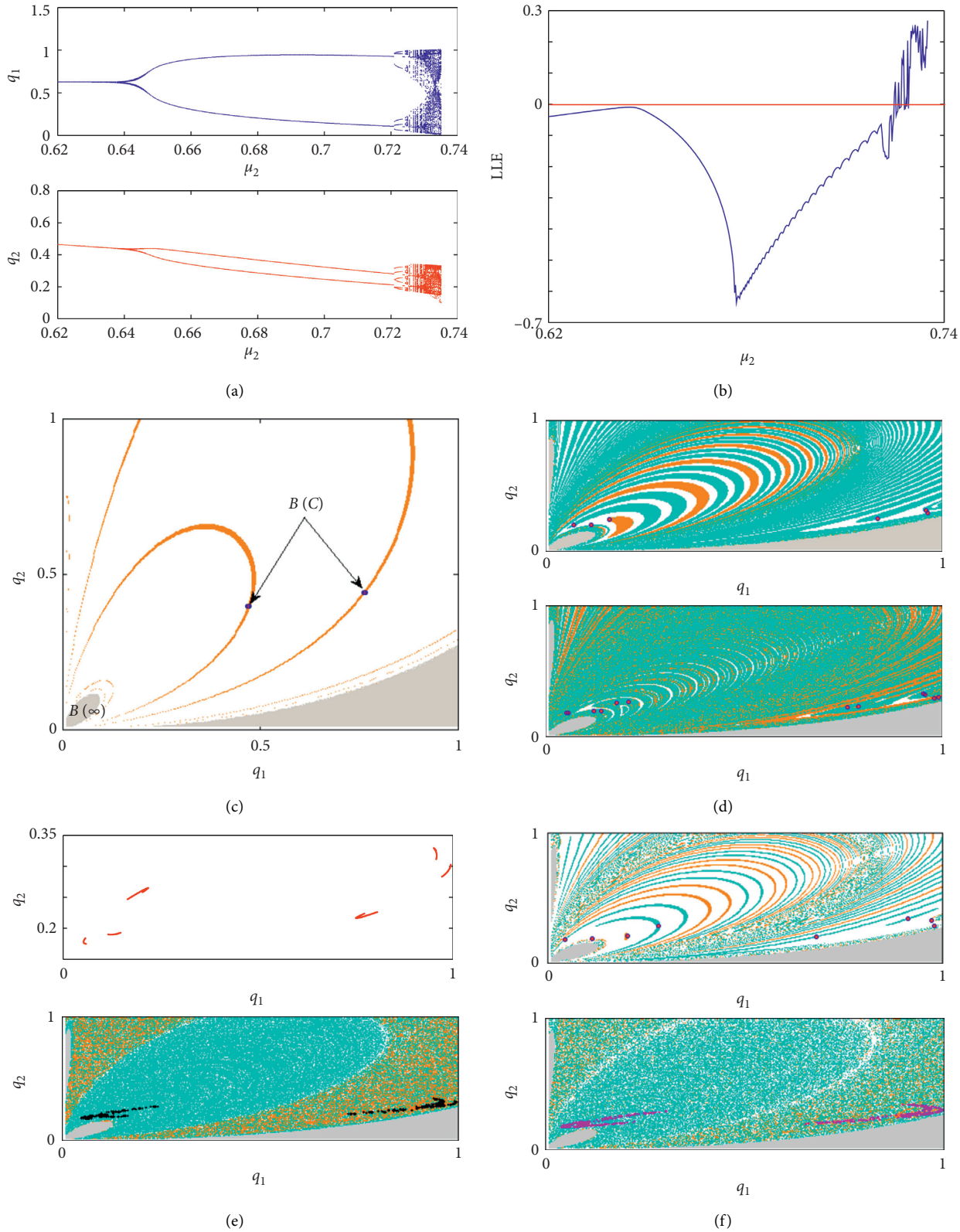

FIGURE 4: The fixed parameter values are $c_1 = 0.35, c_2 = 0.2, \mu_1 = 0.1$, and $\alpha = 5$. (a) Bifurcation diagrams of q_1 and q_2 on varying the parameter μ_2. (b) Largest Lyapunov exponent with respect to μ_2. (c) Basin of attraction of the period 2-cycle at $\mu = 0.648$. (d) Basin of attraction of the periods 6-cycle and 12-cycle at $\mu_2 = 0.721$ and $\mu_2 = 0.7245$, respectively. (e) The phase plane of the six pieces chaotic attractors at $\mu_2 = 0.725$ and the basin of attraction of the chaotic behavior converted to a period 2-cycle at $\mu_2 = 0.7257$. (f) The basin of attraction of period 8-cycle at $\mu_2 = 0.7259$ and the chaotic behavior converted to two spirals at $\mu_2 = 0.7269$.

can be seen in Figure 4(b), the largest Lyapunov exponent is negative for $\mu_2 < 0.7247$. Actually, the first period doubling occurs at $\mu_2 = 0.648$. It is plotted in Figure 4(c) with its basin of attraction at the same parameter values and $\mu_2 = 0.648$. The gray color denotes the divergent and unfeasible trajectories ($B(\infty)$), while the white color indicates nonconvergent points. As μ_2 increases, the period 2-cycle continues to appear till μ_2 approaches 0.721 at which a period 6-cycle arises. Increasing the parameter μ_2 further to 0.7245 gives rise to a period 12-cycle. The basin of attraction of those two cycles is given in Figure 4(d). Shifting this parameter to 0.725 causes six-piece chaotic attractors to emerge. The phase plane of these attractors is given in Figure 4(e) with an interesting behavior, that is, the dynamic of map (10) changes from a chaotic attractor to a stable period 2-cycle whose basin is given in the same figure.

We end this part of numerical investigation by the following dynamic behaviors of the map given by Figures 4(f) and 5(a). They give information about a stable period 8-cycle, a chaotic attractor that changes to two spiral points, and two closed invariant curves with chaotic attractor due to Neimark–Sacker bifurcation. Conversely, when $c_1 < c_2$, a Neimark–Sacker bifurcation with respect to the parameter μ_2 takes place. We give in Figure 5 some numerical simulations showing different behaviors of the map for different values of the bifurcation parameter.

5. Noninvertible Map and Critical Curves

Due to the complex structure of the basin of attraction, we discuss here some important characteristics of map (10). By setting $q_{1,t+1} = q_1$ and $q_{2,t+1} = q_2$ in the two-dimensional map (10), the time evolution of the two competing firms is obtained by the iteration of the map T: $(q_1, q_2) \longrightarrow (q_1, q_2)$ given by

$$T: \begin{cases} \acute{q}_1 = q_1 + \alpha q_1 \left(\dfrac{(1-\mu_1)q_2}{(q_1+q_2)^2} - c_1 \right), \\ \acute{q}_2 = \sqrt{\dfrac{(1-\mu_2)q_1}{c_2}} - q_1. \end{cases} \tag{23}$$

To understand the structure of basin and its qualitative changes, the inverse of the above map becomes important. Map (23) is a noninvertible map. This can be obtained from the fact that given a point $(q_1, q_2) \in \mathbb{R}$, its rank-1 preimages may be up to four; those four points are computed by solving the algebraic system given in (23) with respect to q_1 and q_2. The phase space can be divided into several regions denoted by Z_i, where i refers to the number of rank-1 preimages corresponding to each region in the phase plane. Any two contiguous regions are different from each other by two real preimages. The critical curve (LC) which generalizes the critical value (local maximum or minimum) of one dimension to the two-dimensional framework is the locus which has two or more coincide preimages. Similarly, LC_{-1} denotes the set of critical points (local extreme points). LC_{-1} contains all the points at which the following Jacobian determinant of (23) vanishes:

$$\frac{\alpha(1-\mu_1)q_1(q_1-q_2)\left(2c_2\sqrt{c_2(1-\mu_2)q_1} + \mu_2 - 1\right)}{(q_1+q_2)^3\sqrt{c_2(1-\mu_2)q_1}} = 0. \tag{24}$$

We should highlight that map (23) is not defined at $(q_1, q_2) = (0, 0)$. This means that LC_{-1} becomes $\mathrm{LC}_{-1} \subseteq \{(q_1, q_2) \in \mathbb{R}^2_+ : q_1 = q_2, q_1 \neq 0 \neq q_2\}$. The critical curve can be obtained easily from $\mathrm{LC} = T(\mathrm{LC}_{-1})$. One can see from Figure 6(b) that LC separates the phase plane into two regions: Z_0 and Z_2. The region Z_0 has no preimages of rank-1, while the region Z_2 has two preimages or rank-1. Even if we are unable to get analytical expressions for these preimages, we can still use numerical calculation to obtain those points. At the parameter values $c_1 = 0.35, c_2 = 0.2, \mu_1 = 0.1$, $\mu_2 = 0.5$, and $\alpha = 5.8$, we get only two rank-1 preimages' points located in region Z_2. One of which is located below LC_{-1} and the other point located above it, as shown in Figure 6(b). Therefore, map (23) is a $Z_0 - Z_1$ noninvertible map. Figure 6(a) represents the phase plane corresponding to the same parameter values. The gray color refers to the divergent and unfeasible trajectories denoted by $B(\infty)$. The other two colors indicate the basin of attraction of the Nash point and the basin of attraction of the period 2-cycle coexisting with the Nash point, denoted by $B(E)$ and $B(C)$, respectively. In general, divergent trajectories along the q_2-axis can be obtained starting from an initial condition out of this axis. This means that the preimages on this axis can be calculated as follows. Let the point $(q_1, 0) \in \mathbb{R}^2_+$. Then, its preimages are the real solutions of the following algebraic system obtained by substituting this point in (23):

$$\begin{cases} \acute{q}_1 = q_1 + \alpha q_1 \left(\dfrac{(1-\mu_1)q_2}{(q_1+q_2)^2} - c_1 \right), \\ 0 = \sqrt{\dfrac{(1-\mu_2)q_1}{c_2}} - q_1. \end{cases} \tag{25}$$

From the second equation of (25), one can see that the preimages of that point are either located on the same invariant axis $q_1 = 0$ or on the straight line $q_1 = 1 - \mu_2/c_2$.

Proposition 3. *The real preimages of the point* $(0, \acute{q}_2) \in \mathbb{R}^2_+$ *belong to the same invariant axis* $q_1 = 0$ *or lie on the curve:*

$$q_2 = \frac{\alpha(1-\mu_1)}{2(\alpha c_1 - 1)} - q_1 + \sqrt{\frac{\alpha(1-\mu_1)}{(\alpha c_1 - 1)}\left[\frac{\alpha(1-\mu_1)}{4(\alpha c_1 - 1)} - q_1\right]}, \quad q_1 \leq \frac{\alpha(1-\mu_1)}{4(\alpha c_1 - 1)}. \tag{26}$$

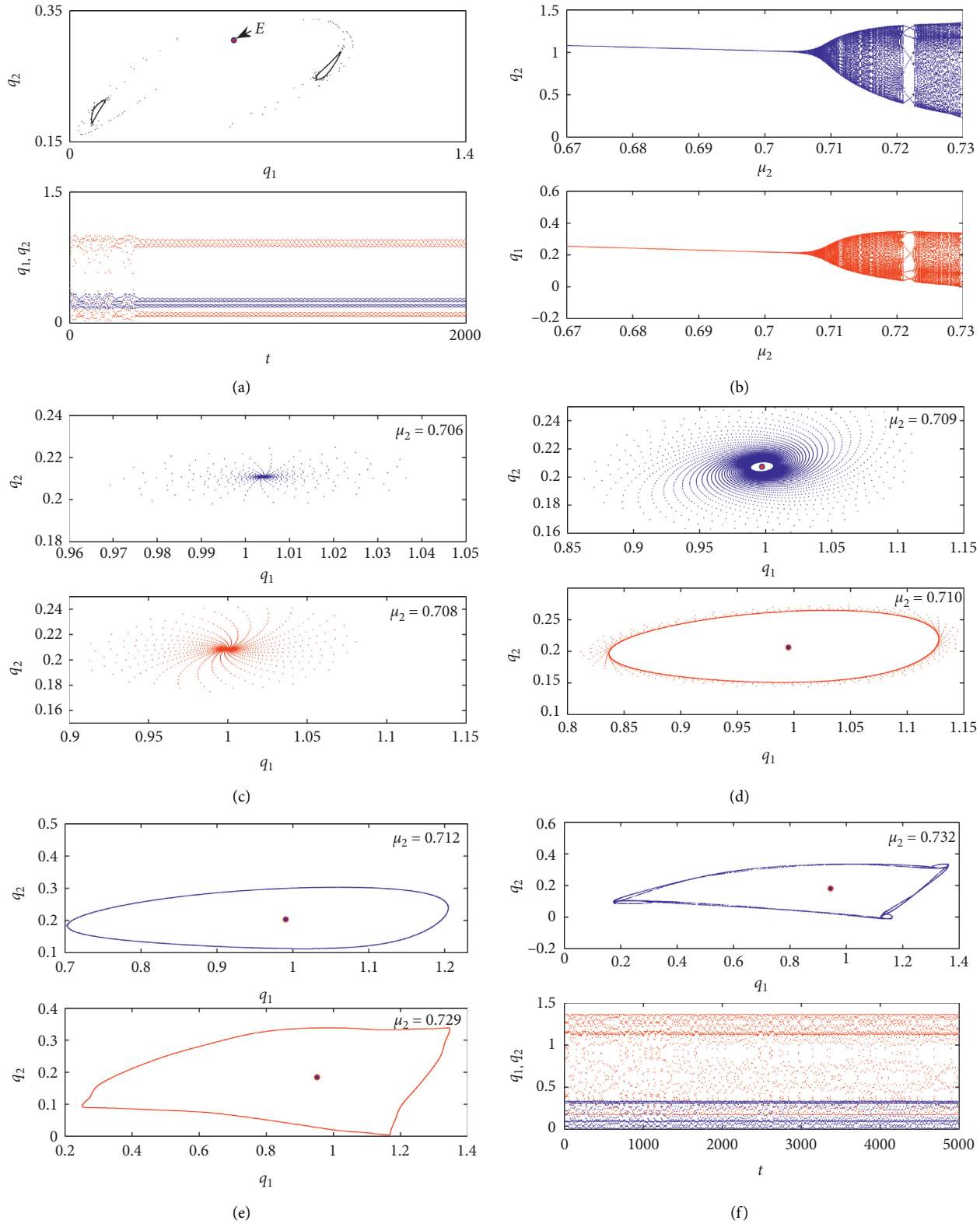

FIGURE 5: The fixed parameter values are $(q_{0,1}, q_{0,2}) = (0.40, 0.11), c_1 = 0.1, c_2 = 0.2, \mu_1 = 0.3$, and $\alpha = 8$. (a) Two closed invariant curves at $\mu_2 = 0.73$. The time series of q_1 and q_2 corresponding to these two invariant curves are also shown. (b) Bifurcation diagrams of q_1 and q_2 on varying the parameter μ_2. (c–f) Different behaviors of the map at different values of the bifurcation parameter μ_2. Time series of q_1 and q_2 corresponding to the chaotic attractor are also shown.

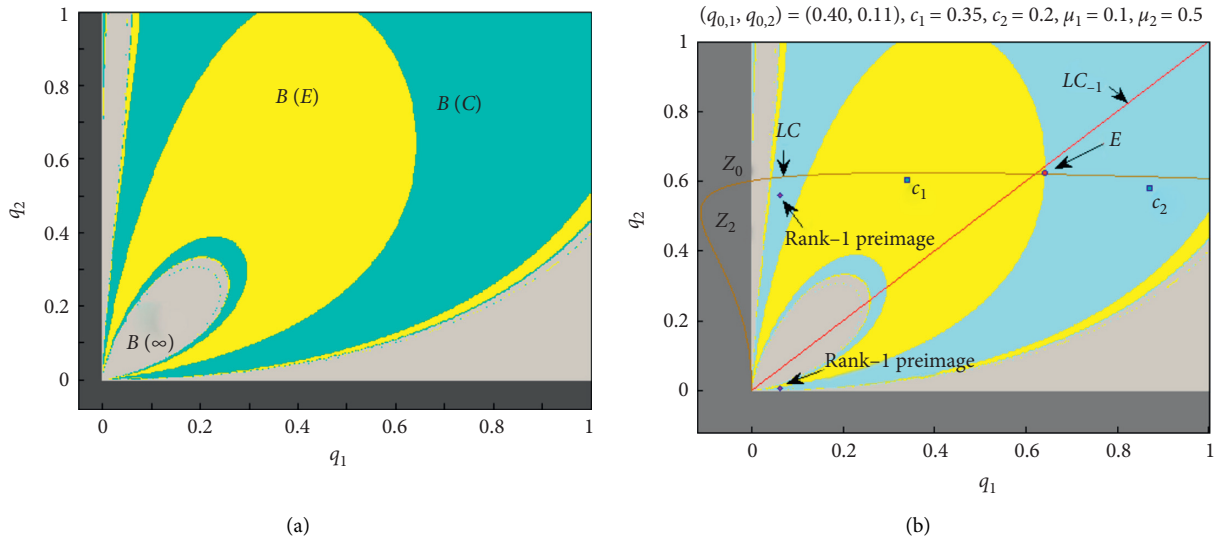

FIGURE 6: (a and b) Phase plane corresponding to the parameter values $c_1 = 0.35, c_2 = 0.2, \mu_1 = 0.1, \mu_2 = 0.5$, and $\alpha = 5.8$. The gray color refers to the divergent and infeasible trajectories, while the other two colors are for the basin of attraction of Nash point and the period 2-cycle coexisting with it.

Proof. Substituting $(0, \acute{q}_2)$ in (23), we obtain

$$\begin{cases} 0 = q_1 + \alpha q_1 \left(\dfrac{(1-\mu_1)q_2}{(q_1+q_2)^2} - c_1 \right), \\ \acute{q}_2 = \sqrt{\dfrac{(1-\mu_2)q_1}{c_2}} - q_1. \end{cases} \tag{27}$$

From the first equation of (27), the preimages of that point belong to the same invariant axis $q_1 = 0$ or lie on the curve defined by the following equation:

$$0 = 1 - \alpha c_1 + \frac{\alpha(1-\mu_1)}{(q_1+q_2)^2} q_2. \tag{28}$$

From (28), the term $(q_1 + q_2)^2 = (\alpha(1-\mu_1)/\alpha c_1 - 1)q_2$ must be positive under the condition $\alpha c_1 \geq 1$. Solving (28) with respect to q_2 completes the proof. □

Proposition 4. *Map (23) has two real preimages $O_{-1}^{(1)}$ and $O_{-1}^{(2)}$, where*

$$\begin{aligned} O_{-1}^{(1)} &= \left(0, \frac{\alpha(1-\mu_1)}{\alpha c_1 - 1}\right), \\ O_{-1}^{(2)} &= \left(\frac{1-\mu_2}{c_2}, \frac{\alpha(1-\mu_1)}{2(\alpha c_1 - 1)} - q_1 + \sqrt{\frac{\alpha(1-\mu_1)}{(\alpha c_1 - 1)}\left[\frac{\alpha(1-\mu_1)}{4(\alpha c_1 - 1)} - q_1\right]}\right), \\ q_1 &\leq \frac{\alpha(1-\mu_1)}{4(\alpha c_1 - 1)}. \end{aligned} \tag{29}$$

Proof. The proof is straightforward and is obtained by substituting $q_1 = 0$ or $q_1 = 1 - \mu_2/c_2$ in (27).

Therefore, the two preimages $O_{-1}^{(1)}$ and $O_{-1}^{(2)}$ are corner points on the hyperplane that describes the basin of attraction. All the points outside this hyperplane cannot generate any feasible trajectories. □

6. Conclusion and Future Work

This paper features complex behaviors of heterogeneous Cournot duopoly game in which players optimize their profits under minimal sales constraints. In cases of sales constraints and no sales constraints, the steady states points and the local stability conditions of the Nash equilibrium have been obtained. We have proven that the proposed game inherently produces two routes to chaos: the flip and Neimark–Sacker bifurcation, even though different values of the parameters of the minimum sales constraints are present in the firms. The plots of 1D bifurcation diagrams are used to further illustrate those two routes to chaos. We also use numerical simulations to describe the dynamic phenomenon of the game through 2D bifurcation diagram, 1D bifurcation diagram, Lyapunov

maximum exponent, time series map, phase diagram, basins of attractions, and so forth.

Our numerical results show the Nash equilibrium point is very sensitive to any change in the adjustment speed and minimal sales constraints parameters, the latter parameter being the main difference between this study and Tramontana [30]. Furthermore, the two routes to chaos give rise to complex dynamic behaviors when the changes in the parameters are large. Numerical simulations also show that the basin of attractions of the feasible and unfeasible trajectories of map (10) depend on the cost, adjustment speed, and minimum sales constraint parameters.

Based on the result in this study, economical firms have better chance of reaching the Nash equilibrium by setting their minimum sales constraints to a certain value while varying their adjustment speed from time to time according to the stability condition. However, if this is not possible, another approach that can control their output towards a stable Nash is by employing a controlling parameter method such as delayed feedback control, which can be explored in future study.

Data Availability

The data used to support the findings of this study are included within the article.

Conflicts of Interest

The authors declare that there are no conflicts of interest regarding the publication of this paper.

Acknowledgments

This work was supported by the Research Supporting Project Number (RSP-2021/167), King Saud University, Riyadh, Saudi Arabia.

References

[1] A. Cournot, *Recherches sur les Principes Mathematics de la Theorie de la Richesse*, Hachette, Paris, France, 1838.

[2] H. Hotelling, "Stability in competition," *The Economic Journal*, vol. 39, no. 153, pp. 41–57, 1929.

[3] K. Okuguchi, "Adaptive expectations in an oligopoly model," *The Review of Economic Studies*, vol. 37, no. 2, pp. 233–237, 1970.

[4] A. Dixit, "Comparative statics for oligopoly," *International Economic Review*, vol. 27, no. 1, pp. 107–122, 1986.

[5] N. Singh and X. Vives, "Price and quantity competition in a differentiated duopoly," *The RAND Journal of Economics*, vol. 15, no. 4, pp. 546–554, 1984.

[6] T. Puu, "Complex dynamics with three oligopolists," *Chaos, Solitons & Fractals*, vol. 7, no. 12, pp. 2075–2081, 1996.

[7] G. I. Bischi and A. Naimzada, "Global analysis of a dynamic duopoly game with bounded rationality," *Advances in Dynamic Games and Applications*, vol. 5, pp. 361–385, 2000.

[8] G. I. Bischi and M. Kopel, "Equilibrium selection in a nonlinear duopoly game with adaptive expectations," *Journal of Economic Behavior & Organization*, vol. 46, no. 1, pp. 73–100, 2001.

[9] A. Agliari, L. Gardini, and T. Puu, "Global bifurcations of basins in a triopoly game," *International Journal of Bifurcation and Chaos*, vol. 12, no. 10, pp. 2175–2207, 2002.

[10] E. Ahmed, M. F. Elettreby, and A. S. Hegazi, "On Puu's incomplete information formulation for the standard and multi-team Bertrand game," *Chaos, Solitons & Fractals*, vol. 30, no. 5, pp. 1180–1184, 2006.

[11] W. Wu, Z. Chen, and W. H. Ip, "Complex nonlinear dynamics and controlling chaos in a Cournot duopoly economic model," *Nonlinear Analysis: Real World Applications*, vol. 11, no. 5, pp. 4363–4377, 2010.

[12] S. Askar, "The rise of complex phenomena in Cournot duopoly games due to demand functions without inflection points," *Communications in Nonlinear Science and Numerical Simulation*, vol. 19, no. 6, pp. 1918–1925, 2014.

[13] L. C. Baiardi and A. K. Naimzada, "An oligopoly model with rational and imitation rules," *Mathematics and Computers in Simulation*, vol. 156, pp. 254–278, 2019.

[14] J. Andaluz, A. A. Elsadany, and G. Jarne, "Dynamic Cournot oligopoly game based on general isoelastic demand," *Nonlinear Dynamics*, vol. 99, no. 2, pp. 1053–1063, 2020.

[15] S. S. Askar and A. Al-khedhairi, "Dynamic investigations in a duopoly game with price competition based on relative profit and profit maximization," *Journal of Computational and Applied Mathematics*, vol. 367, Article ID 112464, 2020.

[16] W. J. Baumol, *Business Behavior, Value and Growth*, Macmillan, New York, NY, USA, 1959.

[17] F. M. Fisher, "Business behavior, value and growth. William J. Baumol," *Journal of Political Economy*, vol. 68, no. 3, pp. 314-315, 1960.

[18] F. M. Fisher, "On the goals of the firm: comment," *The Quarterly Journal of Economics*, vol. 79, no. 3, pp. 500–503, 1965.

[19] D. R. Kamerschen and P. Smith, "Stability in duopoly models," *Economic Studies Quarterly*, vol. 22, pp. 39–49, 1971.

[20] E. Ahmed, A. S. Hegazi, and A. T. A. El-Hafez, "On multiobjective oligopoly," *Nonlinear Dynamics, Psychology, and Life Sciences*, vol. 7, no. 2, pp. 205–219, 2003.

[21] E. Ahmed, G. A. Ashry, and S. S. Askar, "On multi-objective optimization and game theory in production management," *International Journal of Nonlinear Science*, vol. 24, no. 1, pp. 29–33, 2017.

[22] M. Mert, "What does a firm maximize? A simple explanation with regard to economic growth," *International Journal of Engineering Business Management*, vol. 10, pp. 1–13, 2018.

[23] A. Ibrahim, "Local stability condition of the equilibrium of a constraint pro t maximization duopoly model," *AIP Conference Proceedings*, vol. 2138, no. 1, Article ID 030020, 2019.

[24] D. Léonard and K. Nishimura, "Nonlinear dynamics in the Cournot model without information," *Annals of Operations Research*, vol. 89, pp. 165–173, 1999.

[25] W. J. Den Haan, "The importance of the number of different agents in a heterogeneous asset-pricing model," *Journal of Economic Dynamics and Control*, vol. 25, no. 5, pp. 721–746, 2001.

[26] H. N. Agiza and A. A. Elsadany, "Nonlinear dynamics in the cournot duopoly game with heterogeneous players," *Physica A: Statistical Mechanics and its Applications*, vol. 320, pp. 512–524, 2003.

[27] H. N. Agiza and A. A. Elsadany, "Chaotic dynamics in nonlinear duopoly game with heterogeneous players," *Applied Mathematics and Computation*, vol. 149, no. 3, pp. 843–860, 2004.

[28] F. Tramontana and A. E. A. Elsadany, "Heterogeneous triopoly game with isoelastic demand function," *Nonlinear Dynamics*, vol. 68, no. 1-2, pp. 187–193, 2012.
[29] T. Dubiel-Teleszynski, "Nonlinear dynamics in a heterogeneous duopoly game with adjusting players and diseconomies of scale," *Communications in Nonlinear Science and Numerical Simulation*, vol. 16, no. 1, pp. 296–308, 2011.
[30] F. Tramontana, "Heterogeneous duopoly with isoelastic demand function," *Economic Modelling*, vol. 27, no. 1, pp. 350–357, 2010.
[31] Z. Ding, Q. Li, S. Jiang, and X. Wang, "Dynamics in a Cournot investment game with heterogeneous players," *Applied Mathematics and Computation*, vol. 256, pp. 939–950, 2015.
[32] F. Cavalli, A. Naimzada, and F. Tramontana, "Nonlinear dynamics and global analysis of a heterogeneous Cournot duopoly with a local monopolistic approach versus a gradient rule with endogenous reactivity," *Communications in Nonlinear Science and Numerical Simulation*, vol. 23, no. 1–3, pp. 245–262, 2015.
[33] N. Pecora and M. Sodini, "A heterogenous Cournot duopoly with delay dynamics: hopf bifurcations and stability switching curves," *Communications in Nonlinear Science and Numerical Simulation*, vol. 58, pp. 36–46, 2018.
[34] Y. Cao, W. Zhou, T. Chu, and Y. Chang, "Global dynamics and synchronization in a duopoly game with bounded rationality and consumer surplus," *International Journal of Bifurcation and Chaos*, vol. 29, no. 11, Article ID 1930031, 2019.
[35] W. Zhou, N. Zhao, T. Chu, and Y. X. Chang, "Stability and multistability of a bounded rational mixed duopoly model with homogeneous product," *Complexity*, vol. 2020, Article ID 4580415, 12 pages, 2020.
[36] W. Zhou, T. Chu, and X. X. Wang, "Stability, global dynamics, and social welfare of a two-stage game under R&D spillovers," *Mathematical Problems in Engineering*, vol. 18, p. 2021, 2021.
[37] W.-n. Li, A. A. Elsadany, W. Zhou, and Y.-l. Zhu, "Global analysis, multi-stability and synchronization in a competition model of public enterprises with consumer surplus," *Chaos, Solitons & Fractals*, vol. 143, Article ID 110604, 2021.
[38] G. I. Bischi, C. Chiarella, M. Kopel, and F. Szidarovszky, *Nonlinear Oligopolies: Stability and Bifurcations*, Springer-Verlag Berlin Heidelberg, Berlin, Germany, 2010.
[39] T. Puu, "Chaos in duopoly pricing," *Chaos, Solitons & Fractals*, vol. 1, no. 6, pp. 573–581, 1991.

Hindawi
Complexity
Volume 2021, Article ID 8839218, 20 pages
https://doi.org/10.1155/2021/8839218

WILEY | Hindawi

Research Article

Rebate Strategy Selection and Channel Coordination of Competing Two-Echelon Supply Chains

Ziling Wang,[1] Rong Zhang,[2] and Bin Liu[1]

[1]*School of Economics and Management, Shanghai Maritime University, Pudong 201306, Shanghai, China*
[2]*Research Center of Logistics, Shanghai Maritime University, Pudong 201306, Shanghai, China*

Correspondence should be addressed to Bin Liu; liubin@shmtu.edu.cn

Received 16 September 2020; Revised 24 January 2021; Accepted 6 March 2021; Published 22 March 2021

Academic Editor: Xueyong Liu

Rebate has long been a crucial tool that has attracted researchers from a diverse range of fields including marketing and supply chain management. When a manufacturer uses a retailer for reaching end customers, the rebate strategy undertakes an additional dimension. Here we show whether the two rebate strategies, manufacturer rebate and channel rebate, can be the optimal choice for the manufacturer and the retailer. And we aim at full coordination with rebate. Game theory is exploited to identify the equilibrium rebate decisions, which are fully characterized with two rebate strategies considering rebate sensitivity. Furthermore, we demonstrate how the decisions depend on parameters, such as market size, rebate redemption rate, and competition intensity in monopoly and duopoly supply chain systems. Our work also coordinates the supply chain with two coordination policies and examines if they can achieve full coordination. Counterintuitive findings suggest that the channel rebate with sensitivity and discrimination is not effective and the manufacturer rebate is the unique optimal option. Besides, the coordination can be realized with a centralized rebate in monopoly setting when the manufacturer forgoes her own interest. Then full coordination can be achieved in duopoly setting with a new coordination policy, rebate combination, given the redemption rate for the channel rebate is lower compared with the manufacturer rebate. Managerial insights are suggested that offering rebates with discrimination can have significant inventory and coordination policy implications and can lead to a double win under a well-controlled redemption rate.

1. Introduction

Rebate, admittedly, is a modern and salient type of sale promotion in the marketing mix toward consumers' daily lives. According to an industrial survey, about 50% of supply chain members utilize rebates as part of their customer loyalty and promotional mix [1]. A study of UK shopper behavior reveals that one in three customers prefer rebates on consumer packaged goods and three in four customers are inclined to instant rebates on appliances and electronics [2]. Firms regard rebate as a useful tool or strategy [3–7]. Rebates will not lower the customers' future price expectations, especially in consumer electronics, automotive, and food product industries for a few purposes. In some cases, rebates are commonly applied to increase sales, expand demands, decrease inventories, and coordinate supply chains [8, 9].

Different implementations exist for all kinds of rebates in monopoly and duopoly supply chain systems. As an illustration, a manufacturer provides a rebate of US$100 to end customers for every Nikon Digital camera sold for US$600. Channel rebates are epidemic in the network hardware switching industry [10] and pervasive in the software industry, for instance, Lotus and Symantec [11, 12]. Unilever and P&G, two major manufacturers of the fast-moving consumer goods industry, generally tender manufacturer rebates to consumers. Furthermore, Canon and Epson, two oligarch competitors of the electronics industry, distribute substitutable products through retailers, such as Staples. Both also offer manufacturer rebates for a valid purchase. Retailers can benefit from a high demand due to manufacturers' rebate programs. Thus, retailers are in an incentive to subsidize manufacturers. Many retailers, such as Walmart

and Staples, invest resources to promote these programs in their stores and on their websites. Some retailers support manufacturer rebate programs in the form of sharing the fixed cost [13]. A properly designed channel rebate can achieve channel coordination [14]. Channel rebates can also coordinate supply chains under special arrangements, for example, long-term relationship contract, where the wholesale price and retail price, respectively, can be modified by the manufacturer and the retailer [15].

However, these existing theories only investigate redemption with customers' sensitivity to the manufacturer rebate and do not involve channel rebates. In effect, channel rebate's realizing coordination is based upon the condition that customers are homogeneous and retailers cannot engage in discrimination. Although few customers redeem rebates for a particularly low redemption rate [16–23], redemption with regard to rebate sensitivity is noteworthy either [24]. Therefore, we fill this gap by expressly addressing the following research questions:

(1) What is the incentive for manufacturers to furnish the manufacturer rebate when they sell to a common retailer?

(2) How does customers' sensitivity to the channel rebate with or without discrimination affect supply chain members' profits?

(3) Does centralized profit or coordination exist under such an assigned rebate strategy? If not, is there any other rebate strategy that can bring about coordination or full coordination?

We present two supply chain systems: a monopoly supply chain system of one manufacturer selling to one retailer and a duopoly one with two competing manufacturers selling substitutable products through a common retailer to customers. Note that these customers are heterogeneous in their rebate sensitivity. We also focus on the two most popular rebate strategies, manufacturer rebate and channel rebate. The former is the payment from the manufacturer to the end customers upon the purchase of the manufacturer's product. The manufacturer can take full advantage of the "slippage effect" to implement rebate discrimination with less than 100% redemption rate. The latter is a rebate the manufacturer passes to the retailer on the basis of the quantity ordered. In turn, the retailer may pass a fraction of the rebate to the end customers. Moreover, we implement customers' sensitivity to realistic channel rebates and outline whether the strategy is effective with or without discrimination.

In this paper, we shall first identify customers' redemption rates related to sensitivity for both two rebate strategies and competition intensity as the key performance drivers. We then characterize how they affect firm decisions and profits. Our analysis demonstrates collusion may occur among supply chain members with the manufacturer rebate in the two systems, and it is the unique optimal choice without coordination. The manufacturer rebate can also create a win-win situation where the retailer can obtain a free ride to gain the most profit, whereas in the channel rebate with customers' sensitivity and discrimination, the profit of the overall supply chain is no better than that of the no-rebate strategy. Next, a centralized rebate policy is implemented to examine whether the two supply chain systems can achieve coordination. Our results indicate that coordination can be realized in the monopoly system when the manufacturer is willing to forgo her own interest. Otherwise, the overall supply chain can be better off with a comparatively small market size. On the contrary, the coordination may fail in the duopoly setting. Thus, we put forward a new coordination policy of mixing the manufacturer rebate and the channel rebate with discrimination. The overall supply chain here can be fully coordinated with a rebate combination if the redemption rate for the channel rebate is lower than the manufacturer rebate.

Our work is related to the large volume of literature on rebates in the past several decades. Most studies in the field focus on the effectiveness and impact of rebates. Gerstner and Hess [8] examined the use of retailer and manufacturer rebates and revealed that offering rebates is profitable for manufacturers without price discrimination. Taylor [14] introduced a new form of channel rebates-target rebate, in which the rebate is paid for each unit sold beyond a specified target level, on the basis of the linear rebate paid just for each unit sold. Arcelus et al. [25] explored the joint influences of integrated pricing, rebate, and ordering decisions on the channel rebate and the manufacturer rebate within a stochastic price-dependent demand framework. Khouja [3] revealed that proposing rebates can have good pricing and inventory policy implications and lead to an increase in profit. Aydin and Porteus [26] indicated that manufacturer rebate can boost a retailer's margin but not the whole system, whereas channel rebate may simultaneously perform better. Demirag et al. [27] developed a game-theoretical model to investigate the impact of retailer incentives and customer rebate promotions on pricing and ordering policies. They implied that customer rebates can be more profitable than retailer incentives in some cases. Arcelus et al. [28] outlined the two rebate strategies of manufacturer rebate and retailer rebate may be equally advantageous.

In this stream, a considerable amount of studies have been conducted on a one-manufacturer-one-retailer relationship. Gerstner and Hess [29] examined four types of price promotions including trade deals only, manufacturer rebates only, their combination, and channel rebates with two consumer segments. They observed conditions under which a retailer motivates to effectively serve both segments. Chen et al. [16] used a case study comparing rebates with coupons and indicated that the rebate can play an efficient role in price discrimination among consumers. Lu and Moorthy [30] analyzed the difference between a rebate and coupon when uncertain redemption costs are resolved and identified. They revealed that rebates perform better in price discrimination. Cho et al. [31] studied the equilibrium of a vertical competition game between a manufacturer and a retailer and investigated the effect of competition on rebate decisions. Baysar et al. [32] conducted a Stackelberg game in a monopoly supply chain system. They argued that uncertain market conditions are more beneficial to manufacturer

rebates. However, retailer incentive is always out a good figure with deterministic demand. Given structure power in the supply chain, Khouja and Jing [33] analyzed a Stackelberg game with a manufacturer offering rebates as a leader and a retailer acting as a follower.

Supply chain coordination, on which we exhaustively review the latest research here, is relevant to our work. Consulting cost-sharing, Liu et al. [34] discussed the efficacy of cost-sharing in advertising with a model of two competing manufacturer-retailer supply chains' selling partially substitutable products that may differ in market size. They suggested that firms performing advertising can rather bear the costs entirely. Pu et al. [35] suggested a cost-sharing contract to achieve more profitable outcomes. Chen et al. [36] revealed that profit-sharing can coordinate the dual-channel supply chain. Xu et al. [37] indicate a two-way revenue-sharing contract can coordinate the supply chain and achieves a double win. Heydari and Ghasemia [38] proposed a customized revenue-sharing strategy, which can also coordinate the two-echelon reverse supply chain. Li et al. [39] develop the impact of revenue-sharing and cost-sharing contracts presented by a retailer on emission reduction efforts and firms' profitability. Other coordination contrasts and their effectiveness comparison were also implied, like buyback, risk-sharing, and return policy [40–43]. Modak et al. [44] explored channel coordination and profit division issues of a manufacturer-distributor-duopolistic retailers supply chain. They found the manufacturer prefers collusion, Stackelberg, and Cournot, while the retailer prefers the reverse and both prefer backward sequential bargaining.

Rebate contracts, the focus of this study, however, have gained relatively little attention. Taylor [14] first demonstrated that a designed target rebate can achieve coordination and a win-win outcome when demand is not influenced by sales effort. Taylor and Xiao [45] characterized the optimal rebate and return contracts. They claimed that a retailer and manufacturer, including the total system, may benefit from rebate contracts instead of return contrasts. Chiu et al. [46] developed two target sales rebates (TSR): (1) an innovative menu of TSR contracts with fixed order quantity and (2) a sophisticated case. The differences between them are analytically examined, thereby generating meaningful managerial insights.

Our research is closely related to research by Ha et al. [13], Wang et al. [47], and Muzaffar et al. [15]. Ha et al. [13] pioneered a multistage game, including two manufacturers selling substitutable products through a common retailer with less than 100% redemption rate called the slippage effect. Wang et al. [47] further investigated the impacts of leadership strategy on profits and study rebate decisions under different strategies. However, they both only considered the manufacturer rebate. The new contribution of this paper to the literature is that it considers the slippage effect of customers' sensitivity involved in both systems of the manufacture rebate and channel rebate with and without discrimination. Muzaffar et al. [15] included manufacturer and channel rebates and showed that the latter can coordinate supply chains under special arrangements. On the contrary, a wholesale price discount does not confer the supply chain coordination mechanism, and the retailer must pass a portion of the discount to the end customers. Accordingly, such coordination becomes collusion. However, their work only considered a one-to-one supply chain, where customers are homogeneous in sensitivity for the channel rebate, and the manufacturer and retailer cannot engage in discrimination on them, to wit, 100% redemption rate. Our contribution to the literature is that we develop a duopoly supply chain with two competing manufacturers, on the basis of the one-to-one system, selling substitutable products through a common retailer to customers, where these customers are heterogeneous in their rebate sensitivity. We show that the channel rebate cannot realize coordination with respect to rebate discrimination on heterogeneous customers. Additionally, we propose a new coordination policy of mixing the manufacturer rebate and the channel rebate, where the retailer exerts discrimination on consumers in the channel rebate, and full coordination can be achieved.

2. Materials and Methods

2.1. Model Setting. We first set out to determine a monopoly supply chain system involving one manufacturer (she) selling a single product through a common retailer (he) to consumers who are heterogeneous in their rebate sensitivity. The manufacturer is viewed as the Stackelberg leader, whereas the retailer is the follower. We investigate the manufacturer and channel rebates in the two-echelon supply chains, where the manufacturer can select either type of the rebate strategy denoted as $T = \{M, C\}$, that is to say, two rebate settings, a manufacturer rebate only (denoted as the superscript M) and a channel rebate only (denoted as the superscript C). We assume that the manufacturer should decide whether to provide a rebate before other decisions because launching a rebate is time-consuming.

The supply chain system can be described as a multistage game with the following sequence of events:

(1) The manufacturer must decide either to offer the rebate, denoted by R, or not to do it, denoted by N, with a related fixed cost. Consequently, we denote the manufacturer's rebate decisions as $Z^s = \{R, N\}$.

(2) After observing the rebate decision, the manufacturer selects the type of rebate strategy T. The manufacturer has three combinations, $Z^sT = \{RM, RC, NN\}$, where $Z^sT = NN$ is designated as the benchmark.

(3) Then, the manufacturer determines her wholesale price ω^{Z^sT} and rebate value r^{RM} if she selects the manufacturer rebate.

(4) Given the manufacturer's rebate strategies and price decisions, the retailer determines his retail price p^{Z^sT} and rebate value r^{RC} if the manufacturer chooses the channel rebate.

(5) The manufacturer produces to meet her demands, and the firms acquire their payoffs.

We next develop the monopoly supply chain system to a duopoly system, including two manufacturers (indexed by X or Y) selling substitutable products through a common retailer to consumers who are heterogeneous in their rebate sensitivity. The system also conforms to the manufacturer Stackelberg process. The multistage game in the duopoly system is the same as the monopoly one. Each manufacturer i(i = X, Y) determines her wholesale price $\omega_{\mathrm{i}}^{\mathrm{Z^dT}}$ and rebate value $r_{\mathrm{i}}^{\mathrm{Z^dM}}$, if any. By contrast, the retailer determines his retail prices $p_{\mathrm{i}}^{\mathrm{Z^dT}}$ and rebate value $r_{\mathrm{i}}^{\mathrm{Z^dC}}$, if any. In addition, we assume that the two manufacturers move simultaneously to make price decisions in the duopoly system, where we only consider the symmetric setting. That is, both manufacturers either offer rebates or not. Therefore, the manufacturer's rebate decisions are denoted as $\mathrm{Z^d} = \mathrm{Z}_X^d$ $\mathrm{Z}_Y^d = \{\mathrm{RR, NN}\}$. The first and second letters denote manufacturer X and manufacturer Y's rebate decisions, respectively, where $Z_X^d = \{\mathrm{R, N}\}$ and $\mathrm{Z}_Y^d = \{\mathrm{R, N}\}$. Consequently, the manufacturer has three combinations, $\mathrm{Z^dT} = \{\mathrm{RRM, RRC, NNN}\}$. The multistage game in the duopoly setting is similar to the monopoly setting.

2.2. Demand Function. Research by Cai [48] suggested that rebates help discriminate consumers who are heterogeneous in their price sensitivity as not every consumer redeems rebates. We divide consumers into two segments, where they are heterogeneously rebate-sensitive and rebate-insensitive, respectively. Research by Lu and Moorthy [30] argued that consumers with different incomes may have different opportunity costs of time, so they can incur different redemption costs. As a result, we assume rebate-sensitive consumers incur a low redemption cost C_{L}. On the contrary, rebate-insensitive consumers incur a high redemption cost C_{H} for the complexity of the redemption steps or their high cost of time, where $0 \le C_{\mathrm{L}} < C_{\mathrm{H}}$. We derive the demand functions in the duopoly supply chain system by following a similar approach from research by Ha et al. [13] and Wang et al. [47]. The approach was also developed from research by Zhang et al. [49] and Chung [50]. The utility function of a representative consumer is given by

$$\begin{aligned}&\left(q_X^{Z^dT} + q_Y^{Z^dT}\right)a - (1/2)\left[\left(q_X^{Z^dT}\right)^2 + \left(q_Y^{Z^dT}\right)^2 + 2\gamma q_X^{Z^dT} q_Y^{Z^dT}\right]\\ &\quad - \left\{p_X^{Z^dT} - \max\left[\theta r_X^{Z^dC}, \left(r_X^{Z^dC} - C_C\right)\right] - \max\left[m r_X^{Z^dM}, \left(r_X^{Z^dM} - C_M\right)\right]\right\} q_X^{Z^dT}\\ &\quad - \left\{p_Y^{Z^dT} - \max\left[\theta r_Y^{Z^dC}, \left(r_Y^{Z^dC} - C_C\right)\right] - \max\left[m r_Y^{Z^dM}, \left(r_Y^{Z^dM} - C_M\right)\right]\right\} q_Y^{Z^dT},\end{aligned} \tag{1}$$

where a is the market size; $q_{\mathrm{i}}^{\mathrm{Z^dT}}$, $p_{\mathrm{i}}^{\mathrm{Z^dT}}$, and $r_{\mathrm{i}}^{\mathrm{Z^dT}}$ are the consumption quantity, retail price, and rebate value of product i produced by manufacturer i, respectively; and C_{C} and C_{M} are consumers' estimated redemption costs of manufacturer and channel rebates. Here, $\gamma \in [0, 1)$, which is generally interpreted as the competition intensity among manufacturers, capturing the substitutability of the two products. We suppose that the customers are homogeneous in their redemption costs of rebates proposed by two competing manufacturers.

Moreover, research by Chen et al. [51] pointed out through some studies that consumers insidiously display overconfidence in the personal forecast. Such an optimism bias is called "slippage effect," which can let customers overestimate their likelihood of redeeming a rebate offer and commit a blunder in estimating the effort involved in the redemption. Research by Tasoff and Letzler [52] indicated that the expected redemption rates exceed the actual redemption rates by 49% because of stamp and envelope costs, cost of time, and loss of form, all of which explain a high redemption cost. Therefore, to contemplate the "slippage effect" in differentiating heterogeneous consumers in terms of their rebate sensitivity, we follow the methods of research by Wang et al. [47] and view $m \in (0, 1]$ as the redemption rate for the manufacturer rebate and $\theta \in (0, 1]$ as the one for the channel rebate in the utility function. Namely, if $C_{\mathrm{M}} = C_{\mathrm{C}} = C_{\mathrm{L}} = 0$, then consumers are rebate-sensitive and can incur a 100% redemption rate ($m = \theta = 1$). If $C_{\mathrm{M}} = C_{\mathrm{C}} = C_{\mathrm{H}}$, then the redemption costs are high such that the consumers are rebate-insensitive and can incur redemption rates less than 100% ($m \in (0, 1), \theta \in (0, 1)$), instead of being prohibited from redeeming rebates. For tractability, the proportion of rebate-sensitive consumers is made identical to rebate-insensitive consumers in the market (otherwise, too many parameters can be stacked in the formulas).

Hence, the utility function of a representative rebate-sensitive consumer is given by

$$\begin{aligned}&\left(q_{\mathrm{X}}^{\mathrm{Z^dT}} + q_{\mathrm{Y}}^{\mathrm{Z^dT}}\right)a - (1/2)\left[\left(q_{\mathrm{X}}^{\mathrm{Z^dT}}\right)^2 + \left(q_{\mathrm{Y}}^{\mathrm{Z^dT}}\right)^2 + 2\gamma q_{\mathrm{X}}^{\mathrm{Z^dT}} q_{\mathrm{Y}}^{\mathrm{Z^dT}}\right]\\ &\quad - \left(p_{\mathrm{X}}^{\mathrm{Z^dT}} - r_{\mathrm{X}}^{\mathrm{Z^dC}} - r_{\mathrm{X}}^{\mathrm{Z^dM}}\right) q_{\mathrm{X}}^{\mathrm{Z^dT}} - \left(p_{\mathrm{Y}}^{\mathrm{Z^dT}} - r_{\mathrm{Y}}^{\mathrm{Z^dC}} - r_{\mathrm{Y}}^{\mathrm{Z^dM}}\right) q_{\mathrm{Y}}^{\mathrm{Z^dT}}.\end{aligned} \tag{2}$$

Given $p_{\mathrm{i}}^{\mathrm{Z^dT}}$ and $r_{\mathrm{i}}^{\mathrm{Z^dT}}$, the optimal consumption quantities $t_{\mathrm{i}}^{\mathrm{Z^dT}}$ for rebate-sensitive consumers are stated by the following demand functions:

$$t_{\mathrm{X}}^{\mathrm{Z^dT}} = \frac{(1-\gamma)a - \left(p_{\mathrm{X}}^{\mathrm{Z^dT}} - r_{\mathrm{X}}^{\mathrm{Z^dC}} - r_{\mathrm{X}}^{\mathrm{Z^dM}}\right) + \gamma\left(p_{\mathrm{Y}}^{\mathrm{Z^dT}} - r_{\mathrm{Y}}^{\mathrm{Z^dC}} - r_{\mathrm{Y}}^{\mathrm{Z^dM}}\right)}{1-\gamma^2},$$
$$t_{\mathrm{Y}}^{\mathrm{Z^dT}} = \frac{(1-\gamma)a - \left(p_{\mathrm{Y}}^{\mathrm{Z^dT}} - r_{\mathrm{Y}}^{\mathrm{Z^dC}} - r_{\mathrm{Y}}^{\mathrm{Z^dM}}\right) + \gamma\left(p_{\mathrm{X}}^{\mathrm{Z^dT}} - r_{\mathrm{X}}^{\mathrm{Z^dC}} - r_{\mathrm{X}}^{\mathrm{Z^dM}}\right)}{1-\gamma^2}. \tag{3}$$

The utility function of a representative rebate-insensitive consumer is as follows:

$$\left(q_{\mathrm{X}}^{\mathrm{Z^dT}} + q_{\mathrm{Y}}^{\mathrm{Z^dT}}\right)a - (1/2)\left[\left(q_{\mathrm{X}}^{\mathrm{Z^dT}}\right)^2 + \left(q_{\mathrm{Y}}^{\mathrm{Z^dT}}\right)^2 + 2\gamma q_{\mathrm{X}}^{\mathrm{Z^dT}} q_{\mathrm{Y}}^{\mathrm{Z^dT}}\right] - \left(p_{\mathrm{X}}^{\mathrm{Z^dT}} - \theta r_{\mathrm{X}}^{\mathrm{Z^dC}} - m r_{\mathrm{X}}^{\mathrm{Z^dM}}\right)q_{\mathrm{X}}^{\mathrm{Z^dT}} - \left(p_{\mathrm{Y}}^{\mathrm{Z^dT}} - \theta r_{\mathrm{Y}}^{\mathrm{Z^dC}} - m r_{\mathrm{Y}}^{\mathrm{Z^dM}}\right)q_{\mathrm{Y}}^{\mathrm{Z^dT}}. \tag{4}$$

Given $p_{\mathrm{i}}^{\mathrm{Z^dT}}$, the optimal consumption quantities $k_{\mathrm{i}}^{\mathrm{Z^dT}}$ for rebate-insensitive consumers are stated by the following demand functions:

$$k_{\mathrm{X}}^{\mathrm{Z^dT}} = \frac{(1-\gamma)a - \left(p_{\mathrm{X}}^{\mathrm{Z^dT}} - \theta r_{\mathrm{X}}^{\mathrm{Z^dC}} - m r_{\mathrm{X}}^{\mathrm{Z^dM}}\right) + \gamma\left(p_{\mathrm{Y}}^{\mathrm{Z^dT}} - \theta r_{\mathrm{Y}}^{\mathrm{Z^dC}} - m r_{\mathrm{Y}}^{\mathrm{Z^dM}}\right)}{1-\gamma^2},$$
$$k_{\mathrm{Y}}^{\mathrm{Z^dT}} = \frac{(1-\gamma)a - \left(p_{\mathrm{Y}}^{\mathrm{Z^dT}} - \theta r_{\mathrm{Y}}^{\mathrm{Z^dC}} - m r_{\mathrm{Y}}^{\mathrm{Z^dM}}\right) + \gamma\left(p_{\mathrm{X}}^{\mathrm{Z^dT}} - r\theta_{\mathrm{X}}^{\mathrm{Z^dC}} - m r_{\mathrm{X}}^{\mathrm{Z^dM}}\right)}{1-\gamma^2}. \tag{5}$$

Let $D_i^{\mathrm{Z^dT}} = (1/2)\left(t_i^{\mathrm{Z^dT}} + k_i^{\mathrm{Z^dT}}\right)$ as the total demand of the product i. The relevant demand functions displayed in Appendix A in the monopoly supply chain system can be inferred from the duopoly system. No data are used to support this study.

3. Results and Discussion

3.1. Monopoly Supply Chain System. In light of the rebate decision $\mathrm{Z^s}$ and rebate strategy T from the manufacturer, we solve for the equilibrium retail price, wholesale price, and rebate value, if any, by optimizing the profit functions of the retailer and manufacturer. We also obtain firm profits. The fixed cost of the rebate is not involved in the manufacturer's profit functions because it is a sunk cost and does not have any impact on the manufacturer's decisions, and rebate discrimination is wielded in the manufacturer rebate. All the equilibrium results are summarized in Table 1, and all proofs are provided in Appendix B.

3.1.1. Benchmark. If the manufacturer does not launch any rebate program, given $\overset{\mathrm{NN}}{\omega}$, the retailer maximizes his profit $\pi_{\mathrm{R}}^{\mathrm{NN}} = (p^{\mathrm{NN}} - \omega^{\mathrm{NN}})D^{\mathrm{NN}}$. Then the manufacturer maximizes her profit $\pi_{\mathrm{M}}^{\mathrm{NN}} = \omega^{\mathrm{NN}} D^{\mathrm{NN}}$, and the optimal wholesale price, retail price, and profits can be obtained.

3.1.2. Manufacturer Rebate. If the manufacturer presents the manufacturer rebate, given ω^{RM} and r^{RM}, the retailer maximizes his profit $\pi_{\mathrm{R}}^{\mathrm{RM}} = (p^{\mathrm{RM}} - \omega^{\mathrm{RM}})D^{\mathrm{RM}}$. Then, the manufacturer maximizes her profit $\pi_{\mathrm{M}}^{\mathrm{RM}} = (1/2)(\omega^{\mathrm{RM}} - m r^{\mathrm{RM}})t^{\mathrm{RM}} + (1/2)\omega^{\mathrm{RM}} k^{\mathrm{RM}}$, and the other optimal prices and profits involved can be derived.

Lemma 1. *For the manufacturer rebate in the monopoly supply chain, we have the following:*

(i) ω^{RM^*}, r^{RM^*}, p^{RM^*}, $\pi_{\mathrm{R}}^{\mathrm{RM}^*}$, *and* $\pi_{\mathrm{M}}^{\mathrm{RM}^*}$ *initially decrease and then increase in* m

Table 1: Equilibrium results in the monopoly supply chain system.

	Benchmark	Manufacturer rebate
ω^*	$(a/2)$	$(am(5-4m)/8m-8m^2-1)$
r^*	—	$(2a/8m-8m^2-1)$
p^*	$(3a/4)$	$(am(7-6m)/8m-8m^2-1)$
π_R^*	$(a^2/16)$	$(4a^2(1-m)^2m^2/(8m-8m^2-1)^2)$
π_M^*	$(a^2/8)$	$(a^2(1-m)m/8m-8m^2-1)$

(ii) A threshold exists in m for the manufacturer and retailer

Lemma 1 elucidates that, at a relatively low redemption level, the higher the redemption level, the lower the wholesale price and profits for the manufacturer. Videlicet, the manufacturer can only lower the wholesale price to stimulate rebate sensitivity for improving the redemption level at a low redemption rate. However, as the wholesale price is lowered to a certain point, the redemption rate can reach a relevant threshold. In addition, the higher the redemption rate, the higher the wholesale price and profits for the manufacturer. At a comparatively high redemption level, the market demand is close to saturation, and the low wholesale price set cannot boost the demand anymore. Therefore, as the redemption rate becomes comparatively high, the manufacturer can fix a high wholesale price to earn additional profits. The impacts of the redemption rate on retailers are similar.

Rebate value may always be expected to decrease in the redemption rate due to the assumption that a manufacturer raises the rebate value to enhance the redemption level. Thus, when redemption becomes high, the manufacturer can reduce the rebate value. Nevertheless, the retail price is related to the wholesale price and rebate value. If the negative influence of the redemption rate is greater than its positive influence, the retailer may be worse off. Here, we acknowledge that retailers must set a high retail price to gain profit when the redemption rate reaches a relatively high level.

3.1.3. Channel Rebate. If the manufacturer furnishes the channel rebate, given ω^{RC} and r^{RC}, the retailer maximizes his profit $\pi_R^{RC} = (1/2)(p^{RC} - \omega^{RC})t^{RC} + (1/2)[p^{RC} - \omega^{RC} + (1-\theta)r^{RC}]k^{RC}$ by not exerting rebate discrimination on customers. Then the manufacturer must maximize her profit $\pi_M^{RC} = (\omega^{RC} - r^{RC})D^{RC}$, and we can only obtain an optimal relationship between the wholesale price and rebate value, $\omega^{RC^*} = r^{RC^*} + (a/2)$. The same equilibrium results as the benchmark are then derived.

If employing rebate discrimination on customers, the retailer maximizes his profit $\pi_R^{RC} = (1/2)[p^{RC} - \omega^{RC} + (1-\theta)r^{RC}]t^{RC} + (1/2)(p^{RC} - \omega^{RC} + r^{RC})\ k^{RC}$. Then the optimal wholesale price and rebate value for the manufacturer become negative.

Lemma 2. *The channel rebate is ineffective whether the retailer implements rebate discrimination on customers or not.*

The effects of the channel rebate on the manufacturer and retailer are counterintuitive. For the retailer not to exert rebate discrimination on customers, the manufacturer only decides her price margin. That is, no matter how many rebate values the retailer sets; she can make an increment of $(a/2)$. The retail margin aggrandized by the rebate might not offset the increase in the wholesale price. Consequently, the retailer selects the no-rebate strategy, resulting in the manufacturer's profit identical to the benchmark. Conversely, if the retailer exerts rebate discrimination, the manufacturer may be reluctant in offering a channel rebate. Therefore, whether the retailer implements rebate discrimination, a conflict exists between the manufacturer and retailer under the channel rebate. The following proposition presents the optimal choice of rebate strategy in the monopoly supply chain system.

Proposition 1. *For* $Z^sT = \{RM, RC, NN\}$*: (a)* $\pi_M^{RC^*} = \pi_M^{NN^*} < \pi_M^{RM^*}$*. (b)* $\pi_R^{RC^*} = \pi_R^{NN^*} < \pi_R^{RM^*}$.

Proposition 1 confirms collusion among supply chain members with the manufacturer rebate in the monopoly system. Collusion can create a win-win situation. The increasing rebate value can reduce the double marginalization caused by the high wholesale price, and the retailer can obtain a free ride to gain the most profit, as depicted in Figure 1. In the long run, the channel rebate has the same impact as the no-rebate policy. Customers' sensitivity to the channel rebate affects supply members more than the manufacturer rebate, regardless of the discrimination. Accordingly, in the monopoly supply chain system without coordination, the manufacturer rebate is the unique optimal choice.

3.2. Duopoly Supply Chain System. Considering the rebate decision Z^d and rebate strategy T from competing manufacturers, we figure out the equilibrium retail prices, wholesale prices, and rebate values, if any, by optimizing the profit functions of the manufacturers and retailer, and we also obtain firm profits. Similarly, the fixed costs do not have any impact on manufacturers' decisions, and rebate discrimination is involved in the manufacturer rebate. All the equilibrium results are summarized in Table 2.

3.2.1. Benchmark. If the two competing manufacturers do not undertake any rebate program, given ω_i^{NNN}, the retailer maximizes his profit $\pi_R^{NNN} = (p_X^{NNN} - \omega_X^{NNN})D_X^{NNN} + (p_Y^{NNN} - \omega_Y^{NNN})D_Y^{NNN}$. Then the manufacturers should maximize their profits $\pi_i^{NNN} = \omega_i^{NNN}D_i^{NNN}$, and the optimal wholesale prices, retail prices, and profits can be obtained.

3.2.2. Manufacturer Rebate. If the manufacturers provide the manufacturer rebate, given ω_i^{RRM} and r_i^{RRM}, the retailer

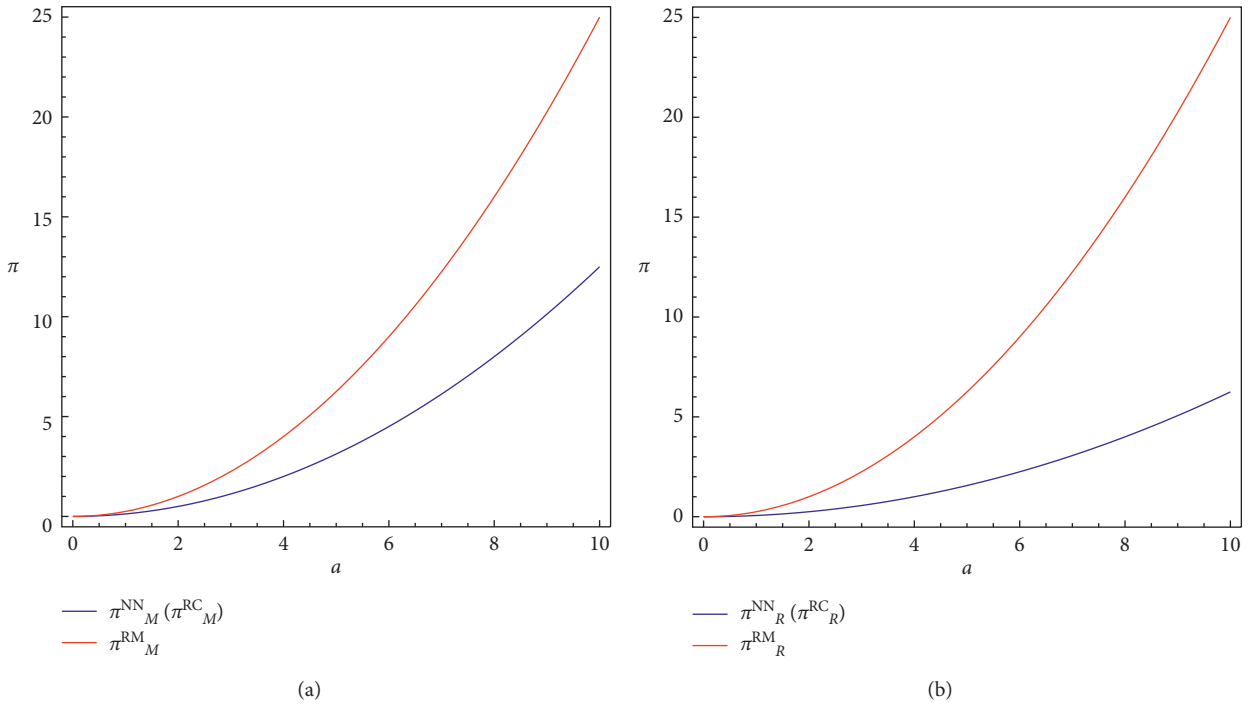

Figure 1: Manufacturer's and retailer's profits in the monopoly supply chain system versus a ($m = 1/2$). (a) Manufacturer's profits. (b) Retailer's profits.

Table 2: Equilibrium results in the duopoly supply chain system.

	Benchmark	Manufacturer rebate
ω_i^*	$(a(1-\gamma)/2-\gamma)$	$(am(5+2m(-2+\gamma)-2\gamma)(-1+\gamma)/1-2m(-2+\gamma)^2+2m^2(-2+\gamma)^2-\gamma)$
r_i^*	—	$(2a(-1+\gamma)/1-2m(-2+\gamma)^2+2m^2(-2+\gamma)^2-\gamma)$
p_i^*	$(a(3-2\gamma)/2(2-\gamma))$	$(am[-7+8\gamma-2\gamma^2+m(6-7\gamma+2\gamma^2)]/1-2m(-2+\gamma)^2+2m^2(-2+\gamma)^2-\gamma)$
π_R^*	$(a^2/2(2-\gamma)^2(1+\gamma))$	$(2a^2(1-m)^2m^2(2-\gamma)^2/(1+\gamma)[-1+2m(-2+\gamma)^2-2m^2(-2+\gamma)^2+\gamma]^2)$
π_i^*	$(a^2(1-\gamma)/2(2-\gamma)^2(1+\gamma))$	$(a^2(1-m)m(-1+\gamma)/[1-2m(-2+\gamma)^2+2m^2(-2+\gamma)^2-\gamma](1+\gamma))$

maximizes his profit $\pi_R^{RRM} = (p_X^{RRM} - \omega_X^{RRM})D_X^{RRM} + (p_Y^{RRM} - \omega_Y^{RRM})D_Y^{RRM}$. Then, the manufacturers maximize their profits $\pi_i^{RRM} = (1/2)(\omega_i^{RRM} - mr_i^{RRM})t_i^{RRM} + (1/2)\omega_i^{RRM}k_i^{RRM}$, and the other associated optimal decisions are derived.

Lemma 3. *For the manufacturer rebate in the duopoly supply chain, we have the following:*

(i) $\omega_i^{RRM^*}$ *initially decreases and then increases in* m *if* $\gamma < \gamma_1$

(ii) $\omega_i^{RRM^*}$ *constantly increases in* m *for* $\gamma \geq \gamma_1$

(iii) $p_i^{RRM^*}$ *initially decreases and then increases in* m *if* $\gamma < \gamma_2$

(iv) $p_i^{RRM^*}$ *perpetually increases in* m *for* $\gamma \geq \gamma_2$, *where* $\gamma_1 \leq \gamma_2$

Lemma 3 shows that, compared with the monopoly supply chain system, the redemption rate has different influences on the wholesale price with comparable substitutability in the duopoly system. When the competition between two manufacturers is less intense (i.e.,$\gamma < \gamma_1$), the impact of the redemption level on the wholesale price is similar to the monopoly setting. When the competition is intense (i.e.,$\gamma \geq \gamma_1$), the wholesale price always increases in the redemption rate. That is to say, when both manufacturers offer rebates in a competitive market, they are confronted with a low wholesale price. Therefore, they can no longer reduce the price to raise the redemption level. A threshold also exists in product substitutability, allowing the redemption rate to make a difference to the retailer price.

Lemma 4. *For the manufacturer rebate in the duopoly supply chain system,* $r_i^{RRM^*}$, $\pi_i^{RRM^*}$, *and* $\pi_R^{RRM^*}$ *decrease and then increase in* m *with any* γ.

Lemma 4 indicates that the impact of customers' redemption rate on rebate values and supply chain members' profits is not subject to competition level between the two manufacturers. The effect is concordant with the result of the manufacturer rebate in the monopoly supply chain system. In addition, a threshold exists in the redemption rate for the members' profits.

The interaction between the redemption rate and substitutability reflects that the instinct in manufacturer

competition is price competition and the coaction between manufacturers is greater than that between retailers. Based on our analysis, both manufacturers can only lessen rebate values, not wholesale prices with exceedingly competitive substitutability. Doing so raises the redemption rate at a low redemption level for capturing a potential demand.

3.2.3. Channel Rebate. If the manufacturers tender the channel rebate, the retailer maximizes his profit $\pi_R^{RRC} = (1/2)\sum_{i=X,Y}\{(p_i^{RRC} - \omega_i^{RRC})t_i^{RRC} + [p_i^{RRC} - \omega_i^{RRC} + (1 - \theta)r_i^{RRC}]k_i^{RRC}\}$ by not exerting rebate discrimination on customers. Then, the manufacturers maximize their profits $\pi_i^{RRC} = (\omega_i^{RRC} - r_i^{RRC})D_i^{RRC}$. Similarly, we can only obtain the optimal relationship between wholesale prices and rebate values for the manufacturers, $\omega_i^{RRC^*} = r_i^{RRC^*} + (a(1-\gamma)/(2-\gamma))$. And the equilibrium results are also identical to the benchmark. If wielding rebate discrimination on customers, the retailer maximizes his profit $\pi_R^{RRC} = (1/2)\sum_{i=X,Y}\{[p_i^{RRC} - \omega_i^{RRC} + (1-\theta)r_i^{RRC}]t_i^{RRC} + (p_i^{RRC} - \omega_i^{RRC} + r_i^{RRC})k_i^{RRC}\}$. Then, the manufacturers can maximize their profits. The optimal wholesale prices and rebate values are also negative.

The effectiveness of the channel rebate in the duopoly supply chain system is similar to the monopoly setting. With the increment of the wholesale prices fixed by the manufacturers, the retailer not exerting rebate discrimination on customers can decide the nonzero rebate values. However, the retailer is inflicted with a negative profit. Consequently, the retailer can also select the no-rebate strategy, compelling the manufacturers' profits no better than the benchmark. The following proposition illuminates the optimal choice of the rebate strategy in the duopoly supply chain system.

Proposition 2. *For $Z^dT = \{\text{RRM}, \text{RRC}, \text{NNN}\}$, we have the following:*

(i) $\pi_i^{RRC^*} = \pi_i^{NNN^*} < \pi_i^{RRM^*}$

(ii) $\pi_R^{RRC^*} = \pi_R^{NNN^*} < \pi_R^{RRM^*}$

Proposition 2 implies that, similar to the monopoly supply chain system, the manufacturer rebate can result in a double win, as depicted in Figure 2, and tacit collusion is developed between the two manufacturers although they are in a competitive relationship. Furthermore, the retailer can likewise take a free ride with the manufacturer rebate instead of the channel rebate. Moreover, sensitivity to the channel rebate has a greater effect on the supply chain in contrast to the manufacturer rebate. Accordingly, in the duopoly supply chain system without coordination, indubitably, the manufacturer rebate is still the exclusive optimal choice.

3.3. Coordination in the Rebate Strategy

3.3.1. Centralized Rebate. This work has examined the rebate strategy in a decentralized supply chain. However, the supply chain coordination is a pursuit of the largest interest normally achievable through a centralized system. A centralized rebate represents a supply chain where only one decision is made. Moreover, all the members maximize the overall supply chain profits by offering the maximum rebate instead of their own profits. As the manufacturer rebate strategy is the exclusive optimal selection for both the monopoly and duopoly supply chain systems, we just coordinate the supply chain with the manufacturer rebate in this section. If the profit of the overall supply chain is improved with the centralized rebate, then we manifest this supply chain coordinated.

In the monopoly supply chain system, the total supply chain profit is $\pi^{sTSC} = (1/2)(p^{RM} - mr^{sTSC})(a - p^{RM} + r^{sTSC}) + (1/2)p^{RM}(a - p^{RM} + mr^{sTSC})$. We can obtain the optimal rebate value $r^{sTSC*} = (2a(-2+m^2)/1 - 8m + 8m^2)$ and derive the corresponding profits with coordination.

The retailer must sometimes forgo his own profits to make up to the optimal rebate value because the manufacturer cannot readily take on all the rebates under optimality. Correspondingly, how much is the manufacturer willing to sacrifice? We then investigate the maximum bound for the manufacturer. By substituting ω^{RM^*} into the manufacturer's profit π_M^{RM}, we can give the manufacturer's upper bound $r_M^{sTSC^*} \le (a(-3+m^2)/1 - 8m + 8m^2)$ for the rebate.

Proposition 3. *For creating a centralized rebate in the monopoly supply chain, we have the following:*

(i) The manufacturer and the retailer or the manufacturer alone must raise rebate up to r^{sTSC*}

(ii) If the manufacturer offers the rebate of r^{sTSC*}, then she is no better than the no-coordination policy

(iii) If the manufacturer offers the maximum rebate $r_M^{sTSC*} = (a(-3+m^2)/1 - 8m + 8m^2)$, then the retailer cannot pocket all his profits

In Part (ii), a Pareto improvement exists, indicating that the overall supply chain profit is enhanced. The manufacturer is no better than the no-rebate policy. By contrast, the retailer has a free ride to gain additional profits. This condition is illustrated as $\pi_R^{sTSC^*}$ in Figure 3. In Part (iii), if the manufacturer does not present all the rebates for a centralized rebate, then the retailer must promote the rebate value to r^{sTSC^*} by forgoing his own profit margin as a consumer discount. Therefore, the overall supply chain is in a good position (Pareto optimal) when the market size is comparatively small (i.e., $a < (3 + 7m + 4m^2/2 + 8m + 2m^2)$), as depicted in Figure 4. The increase in a manufacturer's profit can countervail the decrease in a retailer's profit. The end of the curve up warp suggests that when customers' redemption rate becomes relatively high, the Pareto optimal zone enlarges by boosting the potential demand.

In the duopoly supply chain system likewise, we can obtain the optimal rebate $r_i^{dTSC^*} = (a(-8 + 9\gamma + m\gamma - 2\gamma^2 + 2m^2(2 - 3\gamma + \gamma^2))/2(1 - 2m(-2+\gamma)^2 + 2m^2(-2+\gamma)^2 - \gamma))$ by substituting $p_i^{RRM^*}$ into the related total supply chain profit function. Then we can derive the corresponding profits with coordination. Besides, the manufacturers' upper bound for the rebate is $r_M^{dTSC^*} \le (a(-3+m^2)(1-\gamma)/1 - 2m(-2+\gamma)^2 + 2m^2(-2+\gamma)^2 - \gamma)$.

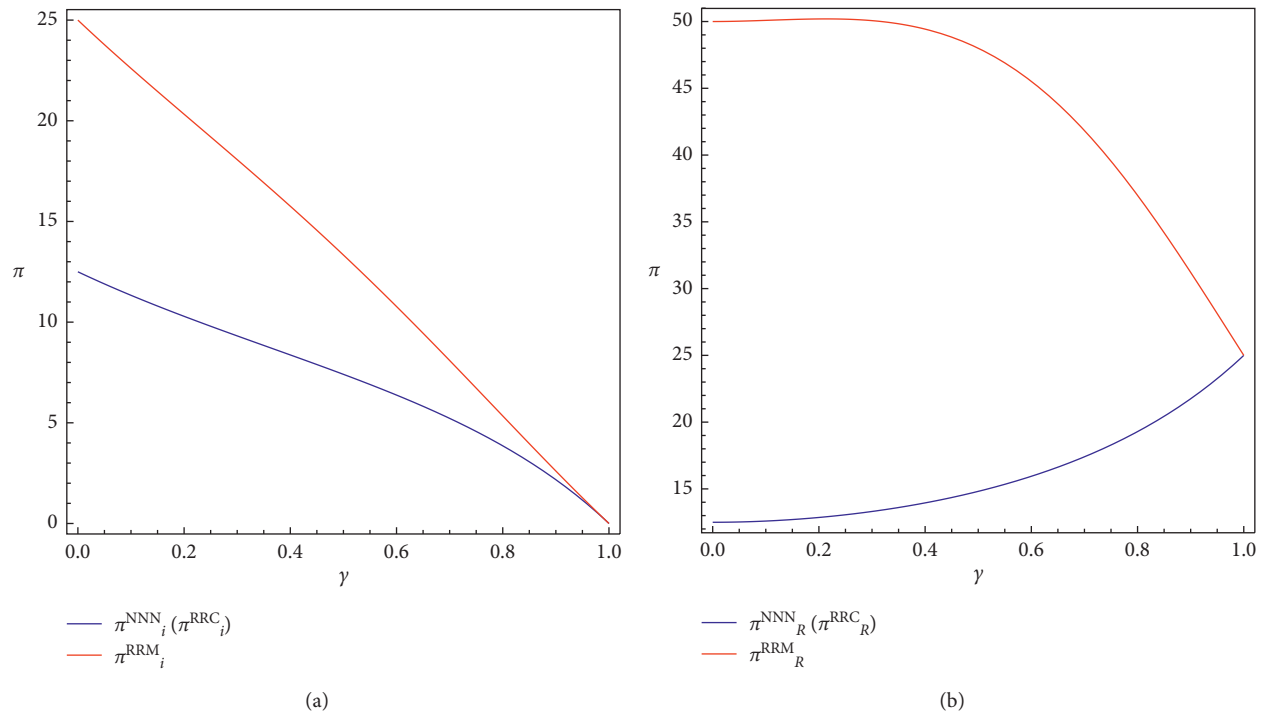

Figure 2: Manufacturers' and retailer's profits in the duopoly supply chain system versus $\gamma\,(a = 10, m = (1/2))$. (a) Manufacturers' profits. (b) Retailer's profits.

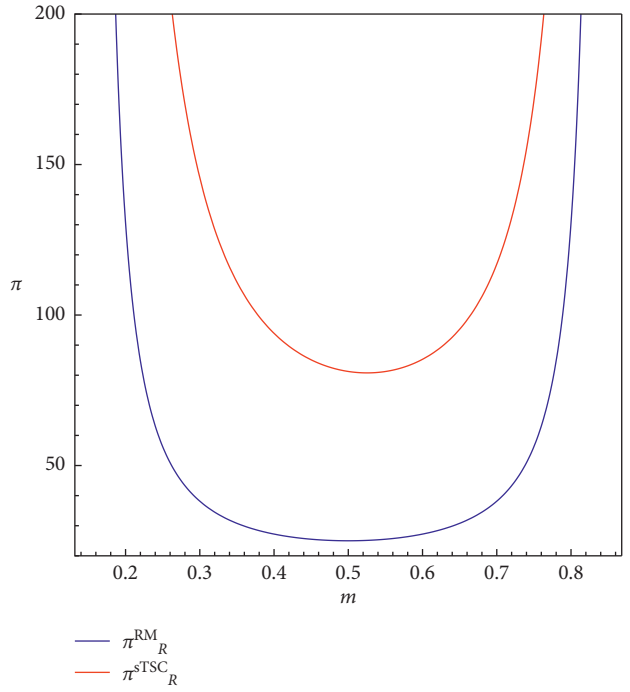

Figure 3: Comparison of the retailer's profit for the manufacturer and centralized rebates with manufacturer's offering r^{sTSC*}.

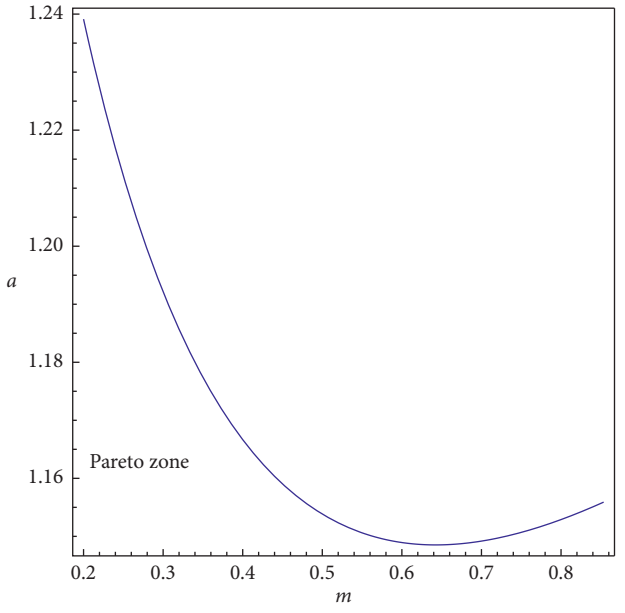

Figure 4: Pareto zone for full coordination under the centralized rebate with manufacturer's offering r_M^{sTSC*}.

Proposition 4. *For creating a centralized rebate in the duopoly supply chain system,*

(i) The manufacturers and the retailer or the manufacturers alone must raise the rebate up to $r_i^{dTSC^*}$

(ii) If the manufacturers offer the rebate of $r_i^{dTSC^*}$*, then they are worse off than the no-coordination policy*

(iii) The manufacturers and the retailer fail to coordinate in the supply chain if the manufacturers merely offer the maximum rebate $r_M^{dTSC^*} = (a(-3+m^2)(1-\gamma)/1-2m(-2+\gamma)^2+2m^2(-2+\gamma)^2-\gamma)$

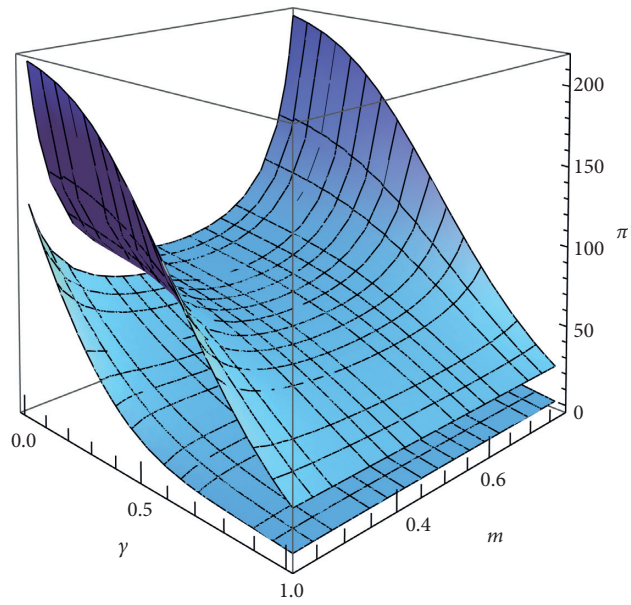

Figure 5: Changes in the overall supply chain profit under the centralized rebate with manufacturers' offering $r_i^{dTSC^*}$.

In Part (ii), the manufacturers might go downhill in the duopoly setting. Nevertheless, compared with the decentralized system, the overall supply chain is potentially ideal, as illustrated in Figure 5. The above and below curve surfaces represent the changes in the overall supply chain profit with redemption rate and substitutability. Such changes are attributed to the retailer's profit increment making up the manufacturers' wastage. To actualize the full coordination, the two competing manufacturers prefer to sacrifice themselves to expand the overall supply chain profit. In Part (iii), the overall supply chain profit could become aggravated compared with the monopoly system, even if the retailer would like to forgo his own interest to raise the rebate up to r_i^{dTSC*}. Note that the manufacturers' offering is only a part of the rebate values to customers. In other words, the centralized rebate policy in this condition may fail.

3.3.2. Rebate Combination. Based on our interpretation, the supply chain is unnecessarily better off in the centralized rebate if the manufacturer does not undertake all manufacturer rebates. Thus, we recommend rebate combination as a new coordination policy, where the manufacturers and retailer take rebate as a means to encourage demand. And the retailer implements discrimination on customers similar to manufacturers. On the one hand, the channel rebate is a practical and attractive price-controlling strategy. Specifically, it allows the manufacturers to control the retail price setting in the supply chain system, and the manufacturers might act as such to motivate the retailer to take further inventory. On the other hand, realizing the centralized rebate in real life is indeed tricky.

If the overall supply chain profit ameliorates compared with the no-rebate program, we treat the rebate combination as an effective coordination scheme. In addition, we assume that the customers may be simultaneously sensitive or insensitive to the rebates. All the equilibrium results are summarized in Table 3.

For the monopoly supply chain system, given ω^{BR}, r^{BRM}, and r^{BRC}, the retailer maximizes his profit $\pi_R^{BR} = (1/2)[p^{BR} - \omega^{BR} + (1-\theta)r^{BRM}]t^{BR} + (1/2)\ (p^{BR} - \omega^{BR} + r^{BRM})k^{BR}$, where r^{BRM} and $\underset{r}{}^{BRC}$ represent the rebate provided by the manufacturer and retailer, respectively. Then the manufacturer maximizes her profit $\pi_M^{BR} = (1/2)(\omega^{BR} - mr^{BRM} - r^{BRC})t^{BR} + (1/2)(\omega^{BR} - r^{BRC})k^{BR}$, and we can obtain the other optimal decisions.

For the duopoly supply chain system, given ω_i^{BRR}, r_i^{BRRM}, and r_i^{BRRC}, the retailer maximizes his profit $\pi_R^{BRR} = (1/2)\sum_{i=X,Y}\{[p_i^{BRR} - \omega_i^{BRR} + (1-\theta)r_i^{BRR}]t_i^{BRR} + (p_i^{BRR} - \omega_i^{BRR} + r_i^{BRR})k_i^{BRR}\}$, where r_i^{BRRM} and r_i^{BRRC} represent the rebate offered by the manufacturers and retailer, respectively. Then the manufacturers maximize their profits $\pi_i^{BRR} = (1/2)(\omega_i^{BRR} - mr_i^{BRRM} - r_i^{BRRC})t_i^{BRR} + (1/2)(\omega_i^{BRR} - r_i^{BRRC})\ k_i^{BRR}$, and we can obtain other related optimal results.

Proposition 5. *For the rebate combination in the monopoly and duopoly supply chain systems, the Pareto optimal zone for the overall supply chain exists to achieve full coordination with* $\theta < m$.

Proposition 5 indicates that, in both supply chain systems, the manufacturers and the retailer are better off with any $0 \le \gamma < 1$, if the redemption rate for the channel rebate is lower than the manufacturer rebate. To wit, the redemption rate for the channel rebate has a greater impact than the manufacturer rebate on the overall supply chain with the rebate combination. When $\theta \le 0.5$ and $\theta < m < 1$, the Pareto optimal zone maximization comes into reality for the overall supply chain to achieve full coordination. When $\theta > 0.5$ and $\theta < m < \underset{m}{}^{\theta>0.5}$, redemption rate goes relatively high. Otherwise, the Pareto optimal zone could become narrow when the redemption rate for the manufacturer rebate increases, as outlined in Figure 6.

Table 3: Equilibrium results in the rebate combination.

	Monopoly	Duopoly
$\omega^*_{(i)}$	$(a(-2+7m-2\theta-5m\theta+2m\theta^2)/2(m+\theta-4m\theta+2m\theta^2))$	$(a\{2-2\gamma+2\theta+m[-7+5\theta-2\theta^2+\gamma(5-5\theta+2\theta^2)]\}/(-2+\gamma)(m+\theta-4m\theta+2m\theta^2))$
$r^{M*}_{(i)}$	$(a(1-\theta)/m+\theta-4m\theta+2m\theta^2)$	$(2a(1-\gamma)(1-\theta)/(2-\gamma)(m+\theta-4m\theta+2m\theta^2))$
$r^{C*}_{(i)}$	$(a(-1+2m-\theta)/m+\theta-4m\theta+2m\theta^2)$	$(2a[1+m(-2+\gamma)-\gamma+\theta]/(-2+\gamma)(m+\theta-4m\theta+2m\theta^2))$
$p^*_{(i)}$	$(a(-\theta(1+\theta)+m(4-5\theta+3\theta^2))/2(m+\theta-4m\theta+2m\theta^2))$	$(a\{\theta(1-\gamma+\theta)+m[-4+5\theta-3\theta^2+\gamma(3-4\theta+2\theta^2)]\}/(-2+\gamma)(m+\theta-4m\theta+2m\theta^2))$
π^*_R	$(a^2(-1+\theta)(\theta^2(1+\theta)-m\theta(1+3\theta)+m^2(-1+5\theta-3\theta^2+\theta^3))/4(m+\theta-4m\theta+2m\theta^2)^2)$	$(2a^2(-1+\theta)\Delta(m,\theta,\gamma)/(-2+\gamma)^2(1+\gamma)(m+\theta-4m\theta+2m\theta^2)^2)$
$\pi^*_{(i)}$	$(a^2m(-1+\theta)^2/4(m+\theta-4m\theta+2m\theta^2))$	$(a^2m(1-\gamma)(1-\theta)^2/(2-\gamma)^2(1+\gamma)(m+\theta-4m\theta+2m\theta^2))$

Note: $\Delta(m,\theta,\gamma)=\theta^2(1-\gamma+\theta)+m\theta(-1+\gamma-3\theta+\gamma\theta)+m^2[-1-(-5+\gamma)\theta-3\theta^2+\theta^3]$.

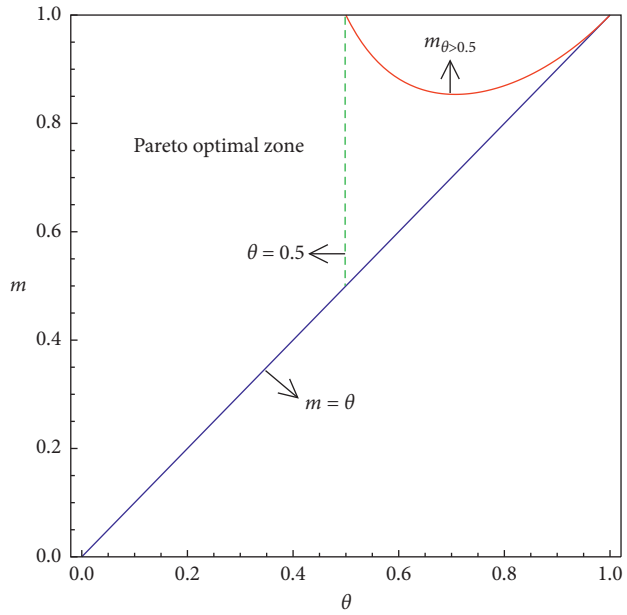

Figure 6: Pareto optimal zone under the rebate combination in both supply chain systems.

3.3.3. Managerial Insights. Our work offers crucial managerial insights for practitioners to further understand various rebate strategies in practice. For the monopoly and duopoly supply chain systems, if the manufacturers must deal with outdated stocks or style products to increase profits and embody the win-win situation, they should inspire the retailer to present channel rebates with noninstant redemption and redeeming efforts required so that the retailer can implement rebate discrimination on consumers. Moreover, for the sake of achieving the goal for double interests with rebate combination, the supply chain members should well control the redemption rate, and especially, the retailer has to dominate it for the channel rebate. Also, a retailer can purchase products from more than one manufacturer for additional profits, if appropriate competition exists under the rebate combination.

4. Conclusion

In this study, we examine the two most popular rebate strategies: (1) monopoly supply chain system with one manufacturer selling to one retailer and (2) duopoly supply chain system with two competing manufacturers selling to a common retailer. We also identify customers' redemption rates related to sensitivity for the manufacturer and channel rebates and competition intensity as the key performance drivers. What is more, we characterize how they affect firm decisions and profits. Then, we propose two coordination policies in the rebate strategy to meliorate the overall supply chain. Our analysis reveals novel and counterintuitive results. First, in the monopoly and duopoly supply chain systems, collusion may occur among supply chain members with the manufacturer rebate. This rebate is the unique optimal choice without coordination and can create a win-win situation where the retailer obtains a free ride to gain the most profit. In contrast, the overall supply chain is no better than the no-rebate policy under the channel rebate with customers' sensitivity, and competition intensity makes no difference to the manufacturers and the retailer. Second, with a centralized rebate on the manufacturer rebate strategy, coordination can be realized when the manufacturer is willing to forgo her own interest. Otherwise, the overall supply chain can be better off with a comparatively small market size in the monopoly system. By contrast, the coordination may fail in the duopoly setting. Accordingly, we develop a rebate combination as a new coordination policy with manufacturers and retailer offering rebates. Our analysis demonstrates that the overall supply chain can be fully coordinated with rebate combination if the redemption rate for the channel rebate is lower compared with the manufacturer rebate. Moreover, the Pareto optimal zone could be narrowed down with the increasing redemption level.

In addition, we have some implications for rebate programs in practice. If the manufacturer has many products in stock, then she must stimulate the retailer to participate in the channel rebate where the retailer can implement rebate discrimination on consumers. In addition, if the supply chain members prefer full coordination with proper competition intensity, the supply chain members should keep the redemption rate from increasing too much. Otherwise, the manufacturers and the retailer may be disadvantaged, thus ceasing rebate offers.

Our work has several limitations for application in real-life problems. For instance, we suppose that the redemption rate of the two rebate strategies is constant. However, it does not necessarily correspond with reality. It would be meaningful to extend our model to a more general situation, i.e., by considering that the redemption rate follows the uniform distribution. Besides, this study only views the manufacturer as the Stackelberg leader and does not consider the impact of power structure. With the development of retailing, retailers have a big say in the market. Thus, Nash bargaining may be an interesting topic to study in rebate decision. Finally, our work also does not account for the cost of rebating efforts, such as advertising, which is widely used in market expansion. Given that uncertainty still remains as to all the issues, we anticipate future research for resolution how the cost of rebate promotion affects the rebate strategy and who should bear the cost.

Appendix

Demand functions of the monopoly system

In the monopoly supply chain system, the utility function of a representative consumer is given by $q^{Z^sT}a - (1/2)q^{Z^sT} - (p^{Z^sT} - \max[\theta r^{Z^sC}, (r^{Z^sC} - C_C)] - \max[mr^{Z^sM}, (r^{Z^sM} - C_M)])q^{Z^sT}$, where a is the market size and q^{Z^sT},p^{Z^sT}, and r^{Z^sT} are the consumption quantity, retail price, and rebate value of product produced by the manufacturer, respectively.

The utility function of a representative rebate-sensitive consumer is given by $q^{Z^sT}a - (1/2)q^{Z^sT} - (p^{Z^sT} - r^{Z^sC} - r^{Z^sM})q^{Z^sT}$. Given p^{Z^sT} and r^{Z^sT}, the optimal consumption

quantities t^{Z^sT*} for the rebate-sensitive consumers are given by the following demand functions: $t^{Z^sT} = a - p^{Z^sT} + r^{Z^sC} + r^{Z^sM}$.

The utility function of a representative rebate-insensitive consumer is given by $q^{Z^sT}a - (1/2)q^{Z^sT} - (p^{Z^sT} - \theta r^{Z^sC} - mr^{Z^sM})q^{Z^sT}$. Given p^{Z^sT}, the optimal consumption quantities k^{Z^sT*} for the rebate-insensitive consumers are given by the following demand functions: $k^{Z^sT} = a - p^{Z^sT} + \theta r^{Z^sC} + mr^{Z^sM}$. Let $D^{Z^sT} = (1/2)(t^{Z^sT} + k^{Z^sT})$ as the total demand of the product.

Proofs

In the monopoly supply chain system, we have the following:

(1) For $Z^sT = NN$, the retailer and manufacturer maximize their profits with the negative Hessian matrices due to $(\partial^2\pi_R^{NN}/\partial p^{NN^2}) = -2 < 0$ and $(\partial^2\pi_M^{NN}/\partial\omega^{NN^2}) = -1 < 0$. Thus, the profits of the retailer and manufacturer satisfy the second-order condition for the maximum.

(2) For $Z^sT = RM$, the retailer and manufacturer maximize their profits with the negative Hessian matrices due to $(\partial^2\pi_R^{RM}/\partial p^{RM^2}) = -2 < 0$, $(\partial^2\pi_M^{RM}/\partial\omega^{RM^2}) = -1 < 0$, $(\partial^2\pi_M^{RM}/\partial r^{RM^2}) = 1/4(-3 + m)m < 0$, and $(\partial^2\pi_M^{RM}/\partial\omega^{RM^2})(\partial^2\pi_M^{RM}/\partial r^{RM^2}) - (\partial^2\pi_M^{RM}/\partial\omega^{RM}\partial r^{RM})(\partial^2\pi_M^{RM}/\partial r^{RM}\partial\omega^{RM}) = (-8m^2 + 8m - 1/16) > 0$ for any $m \in ((2 - \sqrt{2}/4), (2 + \sqrt{2}/4))$. Therefore, the profits of the retailer and manufacturer satisfy the second-order condition for the maximum.

(3) For $Z^sT = RC$, the retailer and manufacturer maximize their profits with the negative Hessian matrices due to $(\partial^2\pi_R^{RC}/\partial p^{RC^2}) = -2 < 0$, $(\partial^2\pi_M^{RC}/\partial\omega^{RC^2}) = -1 < 0$, $(\partial^2\pi_M^{RC}/\partial r^{RC^2}) < 0$, and $(\partial^2\pi_M^{RC}/\partial\omega^{RC^2})(\partial^2\pi_M^{RC}/\partial r^{RC^2}) - (\partial^2\pi_M^{RC}/\partial\omega^{RC}\partial r^{RC})(\partial^2\pi_M^{RC}/\partial r^{RC}\partial\omega^{RC}) \geq 0$ for any $\theta \in (0, 1]$. Thus, the profits of the retailer and manufacturer satisfy the second-order condition for the maximum.

In the duopoly supply chain system, we have the following:

(1) For $Z^dT = NNN$, the retailer and manufacturers maximize their profits with the negative Hessian matrices due to

$$\frac{\partial^2\pi_R^{NNN}}{\partial p_i^{NNN^2}} = -\frac{2}{1-\gamma^2} < 0,$$

$$\frac{\partial^2\pi_R^{NNN}}{\partial p_X^{NNN^2}}\frac{\partial^2\pi_R^{NNN}}{\partial p_Y^{NNN^2}} - \frac{\partial^2\pi_R^{NNN}}{\partial p_X^{NNN}\partial_Y^{NNN}}\frac{\partial^2\pi_R^{NNN}}{\partial p_Y^{NNN}\partial p_X^{NNN}} = \frac{4}{1-\gamma^2} > 0, \tag{B.1}$$

$$\frac{\partial^2\pi_i^{NNN}}{\partial\omega_i^{NNN^2}} = -\frac{1}{1-\gamma^2} < 0,$$

for any $\gamma \in [0, 1)$. Therefore, the profits of the retailer and manufacturers satisfy the second-order condition for the maximum.

(2) For $Z^dT = RRM$, the retailer and manufacturers maximize their profits with the negative Hessian matrices due to

$$\frac{\partial^2 \pi_{\mathrm{R}}^{\mathrm{RRM}}}{\partial p_{\mathrm{i}}^{\mathrm{RRM}^2}} = -\frac{2}{1-\gamma^2} < 0,$$

$$\frac{\partial^2 \pi_{\mathrm{R}}^{\mathrm{RRM}}}{\partial p_{\mathrm{X}}^{\mathrm{RRM}^2}} \frac{\partial^2 \pi_{\mathrm{R}}^{\mathrm{RRM}}}{\partial p_{\mathrm{Y}}^{\mathrm{RRM}^2}} - \frac{\partial^2 \pi_{\mathrm{R}}^{\mathrm{RRM}}}{\partial p_{\mathrm{X}}^{\mathrm{RRM}} \partial_{\mathrm{Y}}^{\mathrm{RRM}}} \frac{\partial^2 \pi_{\mathrm{R}}^{\mathrm{RRM}}}{\partial p_{\mathrm{Y}}^{\mathrm{RRM}} \partial p_{\mathrm{X}}^{\mathrm{RRM}}} = \frac{4}{1-\gamma^2} > 0,$$

$$\frac{\partial^2 \pi_{\mathrm{i}}^{\mathrm{RRM}}}{\partial \omega_{\mathrm{i}}^{\mathrm{RRM}^2}} = -\frac{1}{1-\gamma^2} < 0, \tag{B.2}$$

$$\frac{\partial^2 \pi_{\mathrm{i}}^{\mathrm{RRM}}}{\partial r_{\mathrm{i}}^{\mathrm{RRM}^2}} = -\frac{3}{2\left(1-\gamma^2\right)} < 0,$$

$$\frac{\partial^2 \pi_{\mathrm{i}}^{\mathrm{RRM}}}{\partial \omega_{\mathrm{i}}^{\mathrm{RRM}^2}} \frac{\partial^2 \pi_{\mathrm{i}}^{\mathrm{RRM}}}{\partial r_{\mathrm{i}}^{\mathrm{RRM}^2}} - \frac{\partial^2 \pi_{\mathrm{i}}^{\mathrm{RRM}}}{\partial \omega_{\mathrm{i}}^{\mathrm{RRM}} \partial r_{\mathrm{i}}^{\mathrm{RRM}}} \frac{\partial^2 \pi_{\mathrm{i}}^{\mathrm{RRM}}}{\partial r_{\mathrm{i}}^{\mathrm{RRM}} \partial \omega_{\mathrm{i}}^{\mathrm{RRM}}} = \frac{-8m^2 + 8m - 1}{16\left(1-\gamma^2\right)} > 0,$$

for any $m \in ((2-\sqrt{2}/4), (2+\sqrt{2}/4))$ and $\gamma \in [0, 1)$. Therefore, the profits of the retailer and manufacturer satisfy the second-order condition for the maximum.

(3) For $\mathrm{Z^dT} = \mathrm{RRC}$, the retailer and manufacturers maximize their profits with the negative Hessian matrices due to

$$\frac{\partial^2 \pi_{\mathrm{R}}^{\mathrm{RRC}}}{\partial p_{\mathrm{i}}^{\mathrm{RRC}^2}} = -\frac{2}{1-\gamma^2} < 0,$$

$$\frac{\partial^2 \pi_{\mathrm{R}}^{\mathrm{RRC}}}{\partial p_{\mathrm{X}}^{\mathrm{RRC}^2}} \frac{\partial^2 \pi_{\mathrm{R}}^{\mathrm{RRC}}}{\partial p_{\mathrm{Y}}^{\mathrm{RRM}^2}} - \frac{\partial^2 \pi_{\mathrm{R}}^{\mathrm{RRC}}}{\partial p_{\mathrm{X}}^{\mathrm{RRC}} \partial_{\mathrm{Y}}^{\mathrm{RRC}}} \frac{\partial^2 \pi_{\mathrm{R}}^{\mathrm{RRC}}}{\partial p_{\mathrm{Y}}^{\mathrm{RRC}} \partial p_{\mathrm{X}}^{\mathrm{RRC}}} = \frac{4}{1-\gamma^2} > 0,$$

$$\frac{\partial^2 \pi_{\mathrm{i}}^{\mathrm{RRC}}}{\partial \omega_{\mathrm{i}}^{\mathrm{RRC}^2}} = -\frac{1}{1-\gamma^2} < 0, \tag{B.3}$$

$$\frac{\partial^2 \pi_{\mathrm{i}}^{\mathrm{RRC}}}{\partial r_{\mathrm{i}}^{\mathrm{RRC}^2}} < 0,$$

$$\frac{\partial^2 \pi_{\mathrm{i}}^{\mathrm{RRC}}}{\partial \omega_{\mathrm{i}}^{\mathrm{RRC}^2}} \frac{\partial^2 \pi_{\mathrm{i}}^{\mathrm{RRC}}}{\partial r_{\mathrm{i}}^{\mathrm{RRC}^2}} - \frac{\partial^2 \pi_{\mathrm{i}}^{\mathrm{RRC}}}{\partial \omega_{\mathrm{i}}^{\mathrm{RRC}} \partial r_{\mathrm{i}}^{\mathrm{RRC}}} \frac{\partial^2 \pi_{\mathrm{i}}^{\mathrm{RRC}}}{\partial r_{\mathrm{i}}^{\mathrm{RRC}} \partial \omega_{\mathrm{i}}^{\mathrm{RRC}}} \geq 0,$$

for any $\theta \in (0, 1]$ and$\gamma \in [0, 1)$. Thus, the profits of the retailer and manufacturer satisfy the second-order condition for the maximum.

Proof of Lemma 1

For Part (i), ω^{RM}, r^{RM}, p^{RM}, $\pi_{\mathrm{R}}^{\mathrm{RM}}$, and $\pi_{\mathrm{M}}^{\mathrm{RM}}$ initially decrease and then increase in m because

$$\frac{\partial \omega^{\mathrm{RM}}}{\partial m} = \frac{a\left(-5 + 8m + 8m^2\right)}{\left(1 - 8m + 8m^2\right)^2} < 0, \quad \text{for } m \in \left(\frac{2-\sqrt{2}}{4}, \frac{\sqrt{14}-2}{4}\right),$$

$$\frac{\partial \omega^{\mathrm{RM}}}{\partial m} = \frac{a\left(-5 + 8m + 8m^2\right)}{\left(1 - 8m + 8m^2\right)^2} > 0, \quad \text{for } m \in \left[\frac{\sqrt{14}-2}{4}, \frac{2+\sqrt{2}}{4}\right),$$

$$\frac{\partial r^{\mathrm{RM}}}{\partial m} = \frac{2a\left(-8 + 16m\right)}{\left(1 - 8m + 8m^2\right)^2} < 0, \quad \text{for } m \in \left(\frac{2-\sqrt{2}}{4}, \frac{1}{2}\right),$$

$$\frac{\partial r^{\mathrm{RM}}}{\partial m} = \frac{2a\left(-8 + 16m\right)}{\left(1 - 8m + 8m^2\right)^2} > 0, \quad \text{for } m \in \left[\frac{1}{2}, \frac{2+\sqrt{2}}{4}\right),$$

$$\frac{\partial p^{\mathrm{RM}}}{\partial m} = \frac{a\left(-7 + 12m + 8m^2\right)}{\left(1 - 8m + 8m^2\right)^2} < 0, \quad \text{for } m \in \left[\frac{1}{2}, \frac{2+\sqrt{2}}{4}\right),$$

$$\frac{\partial p^{\mathrm{RM}}}{\partial m} = \frac{a\left(-7 + 12m + 8m^2\right)}{\left(1 - 8m + 8m^2\right)^2} < 0, \quad \text{for } m \in \left(\frac{2-\sqrt{2}}{4}, \frac{\sqrt{23}-3}{4}\right), \tag{B.4}$$

$$\frac{\partial p^{\mathrm{RM}}}{\partial m} = \frac{a\left(-7 + 12m + 8m^2\right)}{\left(1 - 8m + 8m^2\right)^2} > 0, \quad \text{for } m \in \left[\frac{\sqrt{23}-3}{4}, \frac{2+\sqrt{2}}{4}\right),$$

$$\frac{\partial \pi_{\mathrm{R}}^{\mathrm{RM}}}{\partial m} = \frac{8a^2 m\left(1 - 3m + 2m^2\right)}{\left(1 - 8m + 8m^2\right)^3} < 0, \quad \text{for } m \in \left(\frac{2-\sqrt{2}}{4}, \frac{1}{2}\right),$$

$$\frac{\partial \pi_{\mathrm{R}}^{\mathrm{RM}}}{\partial m} = \frac{8a^2 m\left(1 - 3m + 2m^2\right)}{\left(1 - 8m + 8m^2\right)^3} > 0, \quad \text{for } m \in \left[\frac{1}{2}, \frac{2+\sqrt{2}}{4}\right),$$

$$\frac{\partial \pi_{\mathrm{M}}^{\mathrm{RM}}}{\partial m} = \frac{a^2\left(-1 + 2m\right)}{\left(1 - 8m + 8m^2\right)^2} < 0, \quad \text{for } m \in \left(\frac{2-\sqrt{2}}{4}, \frac{1}{2}\right),$$

$$\frac{\partial \pi_{\mathrm{M}}^{\mathrm{RM}}}{\partial m} = \frac{a^2\left(-1 + 2m\right)}{\left(1 - 8m + 8m^2\right)^2} > 0, \quad \text{for } m \in \left[\frac{1}{2}, \frac{2+\sqrt{2}}{4}\right).$$

For Part (ii), we can derive the conclusion from these details. □

Proof of Lemma 2

In the monopoly supply chain system, if the retailer does not exert rebate discrimination on customers with rebate sensitivity under the channel rebate, then we can obtain $\frac{\mathrm{RC}}{r} = 0$. If the retailer exerts rebate discrimination on customers with rebate sensitivity under the channel rebate, then we can derive $\omega^{\mathrm{RC}} = r^{\mathrm{RC}} - 2a < 0$. □

Proof of Proposition 1

With the profits of the manufacturer and retailer indicated in the monopoly system, for $a > 0$ and

$$m \in \left(\frac{2-\sqrt{2}}{4}, \frac{2+\sqrt{2}}{4}\right),$$

$$\pi_{\mathrm{M}}^{\mathrm{RM}} - \pi_{\mathrm{M}}^{\mathrm{NN}}\left(\pi_{\mathrm{M}}^{\mathrm{RC}}\right) = -\frac{a^2}{8\left(1 - 8m + 8m^2\right)} > 0, \tag{B.5}$$

$$\pi_{\mathrm{R}}^{\mathrm{RM}} - \pi_{\mathrm{R}}^{\mathrm{NN}}\left(\pi_{\mathrm{R}}^{\mathrm{RC}}\right) = \frac{a^2\left[16\left(1-m\right)m - 1\right]}{16\left[1 + 8\left(-1 + m\right)m\right]^2} > 0.$$

□

Proof of Lemma 3

For Parts (i) and (ii), $\omega_{\mathrm{i}}^{\mathrm{RRM}}$ initially decreases and then increases in m if $\gamma < \gamma_1$, where $\gamma_1 = 0.477592$. Given that $0 < \gamma < 0.477592$,

$$\frac{\partial \omega_{\mathrm{i}}^{\mathrm{RRM}}}{\partial m} = \frac{a(1-\gamma)\left[-5+2m^2(-2+\gamma)^2+7\gamma-2\gamma^2+4m\left(2-3\gamma+\gamma^2\right)\right]}{\left[-1+2m(-2+\gamma)^2-2m^2(-2+\gamma)^2+\gamma\right]^2} < 0, \quad \text{with } m \in \left(\frac{2-\sqrt{2}}{4}, \frac{\sqrt{14}-2}{4}\right),$$
$$\frac{\partial \omega_{\mathrm{i}}^{\mathrm{RRM}}}{\partial m} = \frac{a(1-\gamma)\left[-5+2m^2(-2+\gamma)^2+7\gamma-2\gamma^2+4m\left(2-3\gamma+\gamma^2\right)\right]}{\left[-1+2m(-2+\gamma)^2-2m^2(-2+\gamma)^2+\gamma\right]^2} > 0, \quad \text{with } m \in \left[\frac{\sqrt{14}-2}{4}, \frac{2+\sqrt{2}}{4}\right). \tag{B.6}$$

However, for $0.477592 \le \gamma < 1$,

$$\frac{\partial \omega_{\mathrm{i}}^{\mathrm{RRM}}}{\partial m} = \frac{a(1-\gamma)\left[-5+2m^2(-2+\gamma)^2+7\gamma-2\gamma^2+4m\left(2-3\gamma+\gamma^2\right)\right]}{\left[-1+2m(-2+\gamma)^2-2m^2(-2+\gamma)^2+\gamma\right]^2} > 0, \quad m \in \left(\frac{2-\sqrt{2}}{4}, \frac{2+\sqrt{2}}{4}\right). \tag{B.7}$$

For Parts (iii) and (iv), the conclusion with respect to $p_{\mathrm{i}}^{\mathrm{RRM}}$ is true because for $0 < \gamma < 0.792893$,

$$\frac{\partial p_{\mathrm{i}}^{\mathrm{RRM}}}{\partial m} = \frac{a(1-\gamma)\left[-7+2m^2(-2+\gamma)^2+8\gamma-2\gamma^2+2m\left(6-7\gamma+2\gamma^2\right)\right]}{\left[-1+2m(-2+\gamma)^2-2m^2(-2+\gamma)^2+\gamma\right]^2} < 0, \quad \text{with } m \in \left(\frac{2-\sqrt{2}}{4}, \frac{\sqrt{23}-3}{4}\right),$$
$$\frac{\partial p_{\mathrm{i}}^{\mathrm{RRM}}}{\partial m} = \frac{a(1-\gamma)\left[-7+2m^2(-2+\gamma)^2+8\gamma-2\gamma^2+2m\left(6-7\gamma+2\gamma^2\right)\right]}{\left[-1+2m(-2+\gamma)^2-2m^2(-2+\gamma)^2+\gamma\right]^2} > 0, \quad \text{with } m \in \left[\frac{\sqrt{23}-3}{4}, \frac{2+\sqrt{2}}{4}\right). \tag{B.8}$$

However, for $0.792893 \le \gamma < 1$,

$$\frac{\partial p_{\mathrm{i}}^{\mathrm{RRM}}}{\partial m} = \frac{a(1-\gamma)\left[-7+2m^2(-2+\gamma)^2+8\gamma-2\gamma^2+2m\left(6-7\gamma+2\gamma^2\right)\right]}{\left[-1+2m(-2+\gamma)^2-2m^2(-2+\gamma)^2+\gamma\right]^2} > 0, \quad \text{with } m \in \left(\frac{2-\sqrt{2}}{4}, \frac{2+\sqrt{2}}{4}\right), \tag{B.9}$$

where $\gamma_2 = 0.792893$. □

Proof of Lemma 4

$r_{\mathrm{i}}^{\mathrm{RRM}}$, $\pi_{\mathrm{i}}^{\mathrm{RRM}}$, and $\pi_{\mathrm{R}}^{\mathrm{RRM}}$ initially decrease and then increase in m with any γ because

$$\frac{\partial r_{\mathrm{i}}^{\mathrm{RRM}}}{\partial m} = \frac{4a(-1+2m)(-2+\gamma)^2(1-\gamma)}{\left[-1+2m(-2+\gamma)^2-2m^2(-2+\gamma)^2+\gamma\right]^2} < 0,$$
$$\frac{\partial \pi_{\mathrm{R}}^{\mathrm{RRM}}}{\partial m} = \frac{4a^2 m\left(1-3m+2m^2\right)(-2+\gamma)^2(1-\gamma)}{\left[1-2m(-2+\gamma)^2+2m^2(-2+\gamma)^2-\gamma\right]^3(1+\gamma)} < 0, \tag{B.10}$$
$$\frac{\partial \pi_{\mathrm{M}}^{\mathrm{RM}}}{\partial m} = \frac{a^2(-1+2m)(-1+\gamma)^2}{(1+\gamma)\left[-1+2m(-2+\gamma)^2-2m^2(-2+\gamma)^2+\gamma\right]^2} < 0, \quad \text{for } m \in \left(\frac{2-\sqrt{2}}{4}, \frac{1}{2}\right).$$

In addition,

$$\frac{\partial r_i^{RRM}}{\partial m} = \frac{4a(-1+2m)(-2+\gamma)^2(1-\gamma)}{\left[-1+2m(-2+\gamma)^2-2m^2(-2+\gamma)^2+\gamma\right]^2} > 0,$$
$$\frac{\partial \pi_R^{RRM}}{\partial m} = \frac{4a^2 m\left(1-3m+2m^2\right)(-2+\gamma)^2(1-\gamma)}{\left[1-2m(-2+\gamma)^2+2m^2(-2+\gamma)^2-\gamma\right]^3(1+\gamma)} > 0, \tag{B.11}$$
$$\frac{\partial \pi_M^{RM}}{\partial m} = \frac{a^2(-1+2m)(-1+\gamma)^2}{(1+\gamma)\left[-1+2m(-2+\gamma)^2-2m^2(-2+\gamma)^2+\gamma\right]^2} > 0, \quad \text{for } m \in \left[\frac{1}{2}, \frac{2+\sqrt{2}}{4}\right).$$

□

Proof of Proposition 2

With the profits of the manufacturers and retailer provided in the duopoly system, for $0 \le \gamma < 1$ and $m \in (2-\sqrt{2}/4, (2+\sqrt{2}/4))$,

$$\pi_M^{RRM} - \pi_M^{NNN}\left(\pi_M^{RRC}\right) = -\frac{a^2(-1+\gamma)^2}{2\left[1-2m(-2+\gamma)^2+2m^2(-2+\gamma)^2-\gamma\right](-2+\gamma)^2(1+\gamma)} > 0,$$
$$\pi_R^{RRM} - \pi_R^{NNN}\left(\pi_R^{RRC}\right) = \frac{a^2\left(1+4(-1+m)m(-2+\gamma)^2-\gamma\right)(-1+\gamma)}{2(-2+\gamma)^2(1+\gamma)\left[-1-2(-1+m)m(-2+\gamma)^2+\gamma\right]^2} > 0. \tag{B.12}$$

□

Proof of Proposition 3

For Part (ii), if the manufacturer offers $r^{sTSC} = (2a(-2+m^2)/1-8m+8m^2)$, then we can derive $\pi_M^{sTSC} = (a^2(-1+m)m/1-8m+8m^2)$, which is equal to the no-coordination policy. For Part (iii), if the manufacturer offers $r_M^{sTSC} = (a(-3+m^2)/1-8m+8m^2)$, then we can obtain

$$\pi_R^{sTSC} = -\frac{a^2(-1+m)^2 m\left[-4m+a\left(1+4m+m^2\right)\right]}{\left(1-8m+8m^2\right)^2} < \pi_R^{RM} = \frac{4a^2(-1+m)^2m^2}{[1+8(-1+m)m]^2}, \quad m \in \left(\frac{2-\sqrt{2}}{4}, \frac{2+\sqrt{2}}{4}\right). \tag{B.13}$$

□

Proof of Proposition 4

For Part (ii), if the manufacturer offers $r^{dTSC} = (a[-8+9\gamma+m\gamma-2\gamma^2+2m^2(2-3\gamma+\gamma^2)]/2[1-2m(-2+\gamma)^2+2m^2(-2+\gamma)^2-\gamma])$, then we can derive

$$\pi_M^{dTSC} - \pi_M^{RRM} = \frac{a^2(-1+m)^2 m\gamma\left[-12+4m^2(-2+\gamma)^2(-1+\gamma)+23\gamma-16\gamma^2+4\gamma^3+m\left(-28+54\gamma-36\gamma^2+8\gamma^3\right)\right]}{8(1+\gamma)\left[-1+2m(-2+\gamma)^2-2m^2(-2+\gamma)^2+\gamma\right]^2} < 0,$$
$$\text{for } m \in \left(\frac{2-\sqrt{2}}{4}, \frac{2+\sqrt{2}}{4}\right), \tag{B.14}$$

and $0 \le \gamma < 1$. For Part (iii), if the manufacturer offers $r_M^{dTSC} = (a(-3+m^2)(1-\gamma)/1-2m(-2+\gamma)^2+2m^2(-2+\gamma)^2-\gamma)$, then we can obtain

$$\pi_R^{dTSC} - \pi_R^{RRM} = \frac{a^2(-1+m)^2\left[8+4m^3(-2+\gamma)(-1+\gamma)^3-22\gamma+27\gamma^2-16\gamma^3+4\gamma^4+2m^2\left(4-43\gamma+61\gamma^2-32\gamma^3+6\gamma^4\right)+m\left(40-104\gamma+117\gamma^2-60\gamma^3+12\gamma^4\right)\right]}{4(1+\gamma)\left[-1+2m(-2+\gamma)^2-2m^2(-2+\gamma)^2+\gamma\right]^2} < 0,$$

$$\pi_M^{dTSC} - \pi_M^{RRM} = \frac{a^2(-1+m)^2 m(-1+\gamma)\left[2(-1+\gamma)^2(-3+2\gamma)+2m^2(-2+\gamma)^2(-1+2\gamma)+m\left(-14+39\gamma-32\gamma^2+8\gamma^3\right)\right]}{4(1+\gamma)\left[-1+2m(-2+\gamma)^2-2m^2(-2+\gamma)^2+\gamma\right]^2} < 0, \quad \text{for } m \in \left(\frac{2-\sqrt{2}}{4}, \frac{2+\sqrt{2}}{4}\right), \tag{B.15}$$

and $0 \le \gamma < 1$. □

Proof of Proposition 5

Given π_M^{NN}, π_M^{BR}, π_R^{NN}, and π_R^{BR} in the monopoly setting, we can derive that

$$\pi_M^{BR} - \pi_M^{NN} = \left(a^2(m-\theta)/8\{\theta + m[1+2(-2+\theta)\theta]\}\right) > 0, \tag{B.16}$$

for $0 < \theta \le 0.5$, $\theta < m < 1$, and $0.5 < \theta < 1$; $\theta < m < -(\theta/1-4\theta+2\theta^2)$, and

$$\pi_R^{BR} - \pi_R^{NN} = \frac{a^2\left[2m\theta\left(1+8\theta-8\theta^2\right)+\theta^2\left(-5+4\theta^2\right)+m^2\left(3-16\theta+12\theta^2\right)\right]}{16\left(m+\theta-4m\theta+2m\theta^2\right)^2} > 0, \tag{B.17}$$

for $0 < \theta \le 0.5\theta < m < 1$, and $0.5 < \theta < 1$; $\theta < m < (-5\theta + 4\theta^3/3 - 16\theta + 12\theta^2)$. Given π_M^{NNN}, π_M^{BRR}, π_R^{NNN}, and π_R^{BRR} in the duopoly setting, we can derive that

$$\pi_M^{BRR} - \pi_M^{NNN} = \frac{a^2(1-\gamma)(m-\theta)}{2(-2+\gamma)^2(1+\gamma)\left(m+\theta-4m\theta+2m\theta^2\right)} > 0, \tag{B.18}$$

for $0 < \theta \le 0.5$, $\theta < m < 1$, $0 \le \gamma < 1$, and $0.5 < \theta < 1$, $\theta < m < -(\theta/1-4\theta+2\theta^2)$, $0 \le \gamma < 1$, and

$$\pi_R^{BRR} - \pi_R^{NNN} = \frac{-a^2(m-\theta)\left\{\theta\left[-5-4\gamma(-1+\theta)+4\theta^2\right]+m\left[-3-4(-4+\gamma)\theta+4(-3+\gamma)\theta^2\right]\right\}}{2(-2+\gamma)^2(1+\gamma)\left(m+\theta-4m\theta+2m\theta^2\right)^2} > 0, \tag{B.19}$$

for $0 < \theta \le 0.5$, $\theta < m < 1$, $0 \le \gamma < 1$, and $0.5 < \theta < 1$, $\theta < m < -(\theta/1-4\theta+2\theta^2)$, $0 \le \gamma < 1$ or $-(\theta/1-4\theta+2\theta^2) < m \le (-\theta-4\theta^2+4\theta^3/3-12\theta+8\theta^2)$, $0 \le \gamma < 1$, or $(-\theta-4\theta^2+4\theta^3/3-12\theta+8\theta^2) < m < (-5\theta+4\theta^3/3-16\theta+12\theta^2)$, $0 \le \gamma < (3m+5\theta-16m\theta+12m\theta^2-4\theta^3/4\theta-4m\theta-4\theta^2+4m\theta^2)$. Moreover, $m_{\theta>0.5} = -(\theta/1-4\theta+2\theta^2)$ because $-(\theta/1-4\theta+2\theta^2) < (-\theta-4\theta^2+4\theta^3/3-12\theta+8\theta^2) < (-5\theta+4\theta^3/3-16\theta+12\theta^2)$. □

Data Availability

No data were used to support this study.

Conflicts of Interest

The authors declare that there are no conflicts of interest regarding the publication of this paper.

Acknowledgments

The authors would like to disclose this research was supported by National Natural and Science Foundation of China (Grant number 71971134) and Cruise Program from the Ministry of Industrial Information and Technology of China (Grant number MC-201917-C09).

References

[1] P. R. Newswire, "One in every two retailers using rebates to drive customer responsiveness," 2011, http://www.prnewswire.com/news-releases/one-in-every-two-retailers-usingrebates-to-drive-customer -responsiveness-121651153.html.

[2] R. Parago, "2014 UK shopper behavior study," 2014, http://www.slideshare.net/Parago/uk-shopperweb.

[3] M. Khouja, "A joint optimal pricing, rebate value, and lot sizing model," *European Journal of Operational Research*, vol. 174, no. 2, pp. 706–723, 2006.

[4] License, "Shopping trips," *License*, vol. 8, no. 5, pp. 44-45, 2005.
[5] R. Lieber, "Finding extra discounts online," *Wall Street Journal–Eastern Edition*, vol. 246, no. 114, 2015.
[6] S. Mitra, "Analysis of a two-echelon inventory system with returns☆," *Omega*, vol. 37, no. 1, pp. 106–115, 2009.
[7] J. Pocock, "Complete systems," *Apply*, vol. 5, no. 7, pp. 4–7, 2005.
[8] E. Gerstner and J. D. Hess, "Pull promotions and channel coordination," *Marketing Science*, vol. 14, no. 1, pp. 43–60, 1995.
[9] D. Xing and T. Liu, "Sales effort free riding and coordination with price match and channel rebate," *European Journal of Operational Research*, vol. 219, no. 2, pp. 264–271, 2012.
[10] F. Preston, *Consolidated Industry Seeks Out Top VARs*, p. 41, Computer Reseller News, Westborough, MA, USA, 1999.
[11] E. F. Moltzen, *Lotus Targets VARs to Beef up Support*, p. 721, Computer Reseller News, 1997.
[12] L. Pender, *Symantec Woos VAR Channel*, pp. 159-160, Computer Reseller News, 1998.
[13] A. Y. Ha, W. Shang, and Y. Wang, "Manufacturer rebate competition in a supply chain with a common retailer," *Production and Operations Management*, vol. 26, no. 11, pp. 1–15, 2017.
[14] T. A. Taylor, "Supply chain coordination under channel rebates with sales effort effects," *Management Science*, vol. 48, no. 8, pp. 992–1007, 2002.
[15] A. Muzaffar, M. N. Malik, and A. Rashid, "Rebate mechanism for the manufacturer in two-level supply chains," *Asia Pacific Management Review*, vol. 23, no. 4, pp. 301–309, 2018.
[16] Y. Chen, S. Moorthy, and Z. J. Zhang, "Research note-price discrimination after the purchase: rebates as state-dependent discounts," *Management Science*, vol. 51, no. 7, pp. 1131–1140, 2005.
[17] S. M. Gilpatric, "Slippage in rebate programs and present-biased preferences," *Marketing Science*, vol. 28, no. 2, pp. 229–238, 2009.
[18] M. Khouja and F. E. Vergara, "Single-period inventory model with a delayed incentive option for selling excess inventory," *International Transactions in Operational Research*, vol. 15, no. 3, pp. 359–379, 2008.
[19] M. Kinsman, "The hard sell," *PROMO Source Book*, vol. 16, p. 19, 2004.
[20] V. Kumar, V. Madan, and S. S. Srinivasan, "Price discounts or coupon promotions: does it matter?" *Journal of Business Research*, vol. 57, no. 9, pp. 933–941, 2004.
[21] J. Wechsler, "Drug spending slows," *Pharmaceutical Executive*, vol. 27, no. 2, p. 28, 2007.
[22] A. Wolf, "FTC issues rebate warning to retailers," *TWICE: This Week in Consumer Electronics*, vol. 20, no. 7, p. 6, 2005.
[23] S. Yang, C. L. Munson, and B. Chen, "Using MSRP to enhance the ability of rebates to control distribution channels," *European Journal of Operational Research*, vol. 205, no. 1, pp. 127–135, 2010.
[24] M. Khouja, S. S. Robbins, and H. K. Rajagopalan, "Optimal pricing and delayed incentives in heterogeneous consumer market," *Journal of Revenue and Pricing Management*, vol. 7, no. 1, pp. 85–105, 2006.
[25] F. J. Arcelus, S. Kumar, and G. Srinivasan, "Retailer's response to alternate manufacturer's incentives under a single-period, price-dependent, stochastic-demand framework," *Decision Sciences*, vol. 36, no. 4, pp. 599–626, 2005.
[26] G. Aydin and E. L. Porteus, "Manufacturer-to-retailer versus manufacturer-to-consumer rebates in a supply chain," in *Retail Supply Chain Management," International Series in Operations Research & Management Science*, N. Agrawal and S. A. Smith, Eds., vol. vol. 122, pp. 237–270, Springer, Boston, MA, USA, 2009.
[27] O. C. Demirag, O. Baysar, P. Keskinocak, and J. L. Swann, "The effects of customer rebates and retailer incentives on a manufacturer's profits and sales," *Naval Research Logistics (NRL)*, vol. 57, no. 1, pp. 88–108, 2010.
[28] F. J. Arcelus, R. Gor, and G. Srinivasan, "Price, rebate and order quantity decisions in a newsvendor framework with rebate-dependent recapture of lost sales," *International Journal of Production Economics*, vol. 140, no. 1, pp. 473–482, 2012.
[29] E. Gerstner and J. D. Hess, "A theory of channel price promotions," *American Economic Review*, vol. 81, no. 4, pp. 872–886, 1991.
[30] Q. Lu and S. Moorthy, "Coupons versus rebates," *Marketing Science*, vol. 26, no. 1, pp. 67–82, 2007.
[31] S. Cho, K. F. McCardle, and C. S. Tang, "Optimal Pricing and rebate strategies in a two-level supply chain," *Production and Operations Management*, vol. 18, no. 4, pp. 424–446, 2009.
[32] O. Baysar, O. Demirag, P. Keskinocak, and J. Swann, "The effects of customer rebates and retailer incentives on a manufacturer's profits and sales," *Naval Research Logistics*, vol. 57, no. 1, pp. 88–108, 2009.
[33] M. Khouja and J. Zhou, "The effect of delayed incentives on supply chain profits and consumer surplus," *Production and Operations Management*, vol. 19, no. 2, pp. 172–197, 2010.
[34] B. Liu, G. G. Cai, and A. A. Tsay, "Advertising in asymmetric competing supply chains," *Production and Operations Management*, vol. 23, no. 11, pp. 1845–1858, 2014.
[35] X. Pu, L. Gong, and X. Han, "Consumer free riding: coordinating sales effort in a dual-channel supply chain," *Electronic Commerce Research and Applications*, vol. 22, pp. 1–12, 2017.
[36] J. Chen, H. Zhang, and Y. Sun, "Implementing coordination contracts in a manufacturer Stackelberg dual-channel supply chain," *Omega*, vol. 40, no. 5, pp. 571–583, 2012.
[37] G. Xu, B. Dan, X. Zhang, and C. Liu, "Coordinating a dual-channel supply chain with risk-averse under a two-way revenue sharing contract," *International Journal of Production Economics*, vol. 147, pp. 171–179, 2014.
[38] J. Heydari and M. Ghasemi, "A revenue sharing contract for reverse supply chain coordination under stochastic quality of returned products and uncertain remanufacturing capacity," *Journal of Cleaner Production*, vol. 197, pp. 607–615, 2018.
[39] T. Li, R. Zhang, S. Zhao, and B. Liu, "Low carbon strategy analysis under revenue-sharing and cost-sharing contracts," *Journal of Cleaner Production*, vol. 212, no. 1, pp. 1462–1477, 2019.
[40] H. Krishnan, R. Kapuscinski, and D. A. Butz, "Coordinating contracts for decentralized supply chains with retailer promotional effort," *Management Science*, vol. 50, no. 1, pp. 48–63, 2014.
[41] B. Liu, R. Zhang, and M. Xiao, "Joint decision on production and pricing for online dual channel supply chain system," *Applied Mathematical Modelling*, vol. 34, no. 12, pp. 4208–4218, 2010.
[42] B. Li, P.-W. Hou, P. Chen, and Q.-H. Li, "Pricing strategy and coordination in a dual channel supply chain with a risk-averse retailer," *International Journal of Production Economics*, vol. 178, pp. 154–168, 2016.
[43] S. Zhang and J. Zhang, "Contract preference with stochastic cost learning in a two-period supply chain under asymmetric

information," *International Journal of Production Economics*, vol. 196, pp. 226–247, 2018.

[44] N. M. Modak, S. Panda, and S. S. Sana, "Three-echelon supply chain coordination considering duopolistic retailers with perfect quality products," *International Journal of Production Economics*, vol. 182, pp. 564–578, 2016.

[45] T. A. Taylor and W. Xiao, "Incentives for retailer forecasting: rebates vs. Returns," *Management Science*, vol. 55, no. 10, pp. 1654–1669, 2009.

[46] C.-H. Chiu, T.-M. Choi, G. Hao, and X. Li, "Innovative menu of contracts for coordinating a supply chain with multiple mean-variance retailers," *European Journal of Operational Research*, vol. 246, no. 3, pp. 815–826, 2015.

[47] Z. Wang, J. J. Mi, and B. Liu, "Rebate decisions and leadership strategy in competing supply chain with heterogeneous consumers," *Mathematical Problems in Engineering*, vol. 2018, Article ID 2598415, 20 pages, 2018.

[48] G. Cai, Y. Dai, and W. Zhang, "Modeling multichannel supply chain management with marketing mixes: a survey," *Social Science Electronic Publishing*, vol. 15, 2015.

[49] R. Zhang, B. Liu, and W. Wang, "Pricing decisions in a dual channels system with different power structures," *Economic Modelling*, vol. 29, no. 2, pp. 523–533, 2012.

[50] H. Chung and E. Lee, "Asymmetric relationships with symmetric suppliers: strategic choice of supply chain price leadership in a competitive market," *European Journal of Operational Research*, vol. 259, no. 2, pp. 564–575, 2017.

[51] X. Chen, C.-L. Li, B.-D. Rhee, and D. Simchi-Levi, "The impact of manufacturer rebates on supply chain profits," *Naval Research Logistics*, vol. 54, no. 6, pp. 667–680, 2007.

[52] J. Tasoff and R. Letzler, "Everyone believes in redemption: nudges and overoptimism in costly task completion," *Journal of Economic Behavior & Organization*, vol. 107, pp. 107–122, 2014.

Hindawi
Complexity
Volume 2021, Article ID 6641852, 15 pages
https://doi.org/10.1155/2021/6641852

Research Article

On Comparing between Two Nonlinear Cournot Duopoly Models

S. S. Askar [1,2]

[1]*Department of Statistics and Operations Research, College of Science, King Saud University, Riyadh, Saudi Arabia*
[2]*Department of Mathematics, Faculty of Science, Mansoura University, Mansoura, Egypt*

Correspondence should be addressed to S. S. Askar; s.e.a.askar@hotmail.co.uk

Received 11 October 2020; Revised 28 January 2021; Accepted 5 February 2021; Published 16 February 2021

Academic Editor: Matteo Zignani

The comparison between two nonlinear duopoly models constructed based on symmetric utility function that is derived from Cobb–Douglas is investigated in this paper. The first model consists of two firms which update their outputs using gradient-based mechanism called bounded rationality. The second model contains a bounded rational firm that is competing with a firm whose outputs depend on a trade-off between market share maximization and profit maximization. For the two models, the fixed points are calculated and their conditions of stability are analyzed. The obtained results show that the second model is more stabilizing provided that the second firm adopts low weights of trade-offs. We show that the two models can be destabilized via flip bifurcation only. Furthermore, the noninvertibility of the two models that can give rise to several stable attractors is discussed.

1. Introduction

Literature has reported several works that have studied the complex dynamic characteristics of Cournot duopoly games. Such games have given rise to interesting results about the models describing them. These results have included investigations of the types of bifurcation responsible for instability of games' equilibrium points and chaos routes. Some of those games have been formed based on popular utility function such as Cobb–Douglas [1], constant elasticity of substitution (CES) [2], and Singh and Vives utility function [3]. There are other utility production functions that have been adopted to model Cournot games like, for example, the isoelastic utility derived from Cobb–Douglas (see [4]). The current paper adopts a symmetric utility function that is derived from the well-known Cobb–Douglas one. Although the adopted symmetric utility in the current paper is simple, the two models formed based on it are complicated and provide interesting results about their dynamics as will be shown later.

In order to make the current paper self-contained, we report in the introduction some important works that have been cited in this direction of research. For instance, we cite from literature the reported works ([5–10]) which have discussed and investigated the routes of chaos in Cournot games whose models have been constructed based on naive expectations. Such works have analyzed the chaotic behaviors on those models via detecting the types of bifurcations appeared on them. In [11], a gradient-based mechanism called bounded rationality has been adopted to globally study the competition of Cournot game. In this study, a rich analysis has shown that the game's equilibrium points can be destabilized due to coexistence of periodic cycles and chaotic behaviors. The adoption of bounded rationality approach has opened the gate to several studies on its influences on duopoly games and it has been applied to other games whose players may be homogeneous or heterogeneous. In [12–15], the authors have applied the bounded rationality and other approaches such as Puu's approach in order to analyze Cournot games and the cooperation that might be occurred between their players. These studies have confirmed what has been reported in literature on the destabilization routes of chaos that affected the stability of the equilibrium points in those games. Other useful works have been reported in [16, 17], in which Agiza et al. have investigated oligopoly games with both linear and nonlinear inverse demand function that have been used to study those games under limited rationality. In [18], chaos has been controlled in a duopoly game of master and slave players after the game's dynamics have been analyzed and

routes to chaos have been identified. The complex dynamic characteristics of both triopoly Cournot and Bertrand games whose players produce differentiated commodities have been investigated in [19]. Here, we cannot ignore to cite two important works of Bischi et al. ([20, 21]) which introduced an intensive analysis of bifurcation and chaos occurred in the dynamics of oligopoly games. In [22], a Cournot duopoly game whose players are homogeneous and their inverse demand functions are isoelastic has been introduced and its dynamic characteristics have been discussed. For more works in this direction of research, interesting readers are advised to see the literature [23–30].

The current paper belongs to both homogeneous and heterogeneous duopoly games in which games' players adopt similar and different decisional mechanisms. The main results of this paper concern with the comparison between two nonlinear duopoly games which are formed based on a symmetric utility function derived from Cobb–Douglas well-known production utility. The comparison includes investigation of routes where the equilibrium points can be destabilized, analyzing the global behaviors of the two models describing the games that include investigation of the structure of attractive basins. Our obtained results show that the equilibrium points of both models cannot preserve their stabilities due to flip bifurcation only. Moreover, they show that the model with heterogeneous players seems to be more stable if the second firm uses low trade-off weights between market share and profit maximization. The structure of basins for both models may be quite complicated as we deal with noninvertible maps.

After this introduction, we can summarize the parts of the paper as follows. Section 2 introduces the two maps describing the duopoly games in this paper. In Section 3, we analyze the properties of the first map and this includes discussing the stability conditions of its equilibrium points and proves it is a noninvertible map. As in Section 3, Section 4 discusses the second map and analyzes its complex characteristics. Some comparisons between the two maps are given in Section 5. In Section 6 ,we end the paper with some conclusions and future works.

2. The Game of Competition

We consider a game of two firms (or players) whose decision variables in the market are quantities. We take q_1 and q_2 as the quantities produced by each firm. We recall the Cobb–Douglas function of two variables appearing in many economic models as follows:

$$U = q_1^a q_2^b, \quad 0 < a, b < 1. \tag{1}$$

This function is popular as Cobb–Douglas (this function is a production function used to organize production possibilities for firms from different and various branches [31]. In the application to production, as a firm's output is something measurable, the sum $a + b >$ or <1 makes sense as watershed between increasing and decreasing returns to scale. In our assumption in this paper, maximizing utility $U = \sqrt{q_1 q_2}$ returns $(p_1/p_2) = (q_2/q_1)$ or $p_1 q_1 = p_2 q_2$ that means the total revenue for both firms is equal and this is due to the assumed symmetry as we take $a = b$.) function which should properly be called Wicksell function since the Swedish economist Knut Wicksell was the first to introduce this production function [32]. It represents the agent's preferences. Both a and b are constants. It has the following properties:

(i) It is a monotonic function under the transformation $u = \ln U$. This means that $(\partial u/\partial q_1) = (a/q_1)$ and $(\partial u/\partial q_2) = (b/q_2)$ and hence the marginal utility of each quantity is positive.

(ii) It is a concave utility function. This means that $(\partial^2 u/\partial q_1^2) = (-a/q_1^2) < 0$ and $(\partial^2 u/\partial q_2^2) = (-b/q_2^2) < 0$ and hence the marginal utility of each quantity is decreasing.

(iii) It is strongly additive. This means that $(\partial^2 u/\partial q_1 \partial q_2) = 0$ and hence the marginal of the quantity q_1 is independent of the quantity q_2. So, the quantities cannot represent substitutes or complements.

(iv) It is a homothetic function. This means that if $x = (q_1, q_2)$, $y = (\breve{q}_1, \breve{q}_2)$, $u(x) = u(y)$, and $\theta > 0$, then $u(\theta x) = u(\theta y)$.

We assume the symmetric case, $a = b = (1/2)$, with the budget constraint $p_1 q_1 + p_2 q_2 = 1$ where p_i is the price of $q_i, i = 1, 2$. Now, we have the following maximization problem:

$$\begin{aligned} &\max U = \sqrt{q_1 q_2}, \\ &\text{s.t. } p_1 q_1 + p_2 q_2 = 1. \end{aligned} \tag{2}$$

Solving (2) gives the following prices:

$$\begin{aligned} p_1 &= \frac{1}{2}\sqrt{\frac{q_2}{q_1}}, \\ p_2 &= \frac{1}{2}\sqrt{\frac{q_1}{q_2}}. \end{aligned} \tag{3}$$

At the economic market, each competitor wants to maximize its profit given by

$$\begin{aligned} \pi_1 &= \frac{1}{2}\sqrt{q_1 q_2} - c_1 q_1^2, \\ \pi_2 &= \frac{1}{2}\sqrt{q_1 q_2} - c_2 q_2^2, \end{aligned} \tag{4}$$

where $C(q_i) = c_i q_i^2$ is the cost function of each quantity. It is a quadratic function and is often met in applications. For example, in the modeling of renewable resources exploitation, such as fisheries [33], in [34], it has been considered in order to investigate the role of convexity. So, the marginal cost is not constant, $(\partial C(q_i)/\partial q_i) = 2c_i q_i$, and $c_i, i = 1, 2$ is a constant parameter. The marginal profits take the following form:

$$\begin{aligned} \frac{\partial \pi_1}{\partial q_1} &= \frac{1}{4}\sqrt{\frac{q_2}{q_1}} - 2c_1 q_1, \\ \frac{\partial \pi_2}{\partial q_2} &= \frac{1}{4}\sqrt{\frac{q_1}{q_2}} - 2c_2 q_2. \end{aligned} \tag{5}$$

Here, we discuss two situations. The first situation assumes that both firms use a gradient-based mechanism such as the bounded rationality defined in the literature [4, 35–37]. Using this mechanism, we get the following discrete dynamical system:

$$T(q_1,q_2):\begin{cases} q_1(t+1)=q_1(t)+k_1q_1(t)\left(\frac{1}{4}\sqrt{\frac{q_2(t)}{q_1(t)}}-2c_1q_1(t)\right),\\ q_2(t+1)=q_2(t)+k_2q_2(t)\left(\frac{1}{4}\sqrt{\frac{q_1(t)}{q_2(t)}}-2c_2q_2(t)\right), \end{cases} \tag{6}$$

where $k_i, i=1,2$ is a speed of adjustment parameter. The second situation is a heterogeneous situation. We assume that the second firm shares the market with certain profit. It trades off between market share maximization and profit maximization. The market share means it seeks the optimum output by putting $\pi_2=0$ and then we get the optimum, $\breve{q}_2=\sqrt[3]{(q_1/4c_2^2)}$, while the profit maximization gives $\widehat{q}_2=(1/4)\sqrt[3]{(q_1/c_2^2)}$. Since it is traded off between those, we get the following:

$$\widetilde{q}_2=\omega\breve{q}_2+(1-\omega)\widehat{q}_2, \tag{7}$$

where $\omega\in(0,1)$. When the second firm shares market maximization only, we take $\omega=1$, while $\omega=0$ means it seeks profit maximization only. Now, the second firm updates its output according to the following:

$$q_2(t+1)=(1-s)q_2(t)+s\left(\frac{\omega}{\sqrt[3]{4}}+\frac{1-\omega}{4}\right)\sqrt[3]{\frac{q_1(t)}{c_2^2}}, \tag{8}$$

where $s\in(0,1)$ is a constant weight. So, we have another model with heterogeneous players given by

$$T_1(q_1,q_2):\begin{cases} q_1(t+1)=q_1(t)+kq_1(t)\left(\frac{1}{4}\sqrt{\frac{q_2(t)}{q_1(t)}}-2c_1q_1(t)\right),\\ q_2(t+1)=(1-s)q_2(t)+s\left(\frac{\omega}{\sqrt[3]{4}}+\frac{1-\omega}{4}\right)\sqrt[3]{\frac{q_1(t)}{c_2^2}}. \end{cases} \tag{9}$$

It is obvious that if $s=0$, then the second firm in (9) is naive, while at $s=1$ means it updates its production based on market share maximization. Economically, profit maximization only is mainly a short-term goal and is primarily restricted to the accounting analysis of the financial situation. Furthermore, it is primarily concerned as to how the company will survive and grow in the existing competitive business environment [38]. On the other hand, market share can allow firms to improve profitability either by lowering prices, using advertising, or introducing new or different products. It can also grow the size of its market share by appealing to other audiences or demographics. In our paper, we introduce a weighted average decision-making mechanism between those two mechanisms discussed above. This includes the main contribution in this paper that is to compare between the maps (6) and (9) in order to see which model is more stable and gives large region of stability [39].

3. Properties of Map (6)

3.1. Analytical Results. The map (6) can make negative or unbounded trajectories if the initial condition $(q_{0,1},q_{0,2})$ is chosen far from $O=(0,0)$. It is obvious that if $q_{i0}>(1/2c_ik_i), i=1,2$, negative values for $q_i(t+1)$ can be obtained.

Proposition 1. *The map (6) has two fixed points that are* $O_1=(0,0)$ *and* $O_2=((1/8c_1)\sqrt[4]{(c_1/c_2)},(1/8c_1)\sqrt[4]{(c_1/c_2)^3})$.

Proof. Setting $q_1(t+1)=q_1(t)$ and $q_2(t+1)=q_2(t)$ in (6) and solving algebraically, we get the two fixed points. □

Proposition 2. *The fixed point* O_1 *is an unstable point.*

Proof: The Jacobian matrix of map (6) at O_1 becomes

$$\begin{pmatrix} \frac{0}{0} & \frac{0}{0}\\ \\ \frac{0}{0} & \frac{0}{0} \end{pmatrix}, \tag{10}$$

which contains indefinite form and then the point is unstable and the proof is completed.

Proposition 3. *The fixed point* O_2 *is locally asymptotically stable provided that*

$$k_1>\frac{16}{3}\sqrt[4]{\frac{c_2}{c_1}}-\sqrt{\frac{c_2}{c_1}}k_2. \tag{11}$$

Proof. At O_2, the Jacobian matrix becomes

$$\begin{pmatrix} 1-\frac{3k_1}{8}\sqrt[4]{\frac{c_1}{c_2}} & \frac{k_1}{8}\sqrt[4]{\frac{c_2}{c_1}}\\ \\ \frac{k_2}{8}\sqrt[4]{\frac{c_1}{c_2}} & 1-\frac{3k_2}{8}\sqrt[4]{\frac{c_2}{c_1}} \end{pmatrix}, \tag{12}$$

whose trace and determinant are given by

$$\begin{aligned} \tau&=2-\frac{3k_1}{8}\sqrt[4]{\frac{c_1}{c_2}}-\frac{3k_2}{8}\sqrt[4]{\frac{c_2}{c_1}},\\ \delta&=1-\frac{3k_1}{8}\sqrt[4]{\frac{c_1}{c_2}}-\frac{3k_2}{8}\sqrt[4]{\frac{c_2}{c_1}}+\frac{1}{8}k_1k_2. \end{aligned} \tag{13}$$

Substituting (13) in Jury conditions [40] gives

$$\Delta_1 := 1 - \tau + \delta = \frac{k_1 k_2}{8},$$
$$\Delta_2 := 1 + \tau + \delta = 4 - \frac{3k_1}{4}\sqrt[4]{\frac{c_1}{c_2}} - \frac{3k_2}{4}\sqrt[4]{\frac{c_2}{c_1}} + \frac{k_1 k_2}{8}, \quad (14)$$
$$\Delta_3 := 1 - \delta = \frac{3k_1}{8}\sqrt[4]{\frac{c_1}{c_2}} + \frac{3k_2}{8}\sqrt[4]{\frac{c_2}{c_1}} - \frac{k_1 k_2}{8}.$$

Since k_1 and k_2 are positive speeds of adjustment parameters then $\Delta_1 > 0$ is always satisfied. $\Delta_2 > 0$ and $\Delta_3 > 0$ give

$$4 - \frac{3}{4}\sqrt[4]{\frac{c_1}{c_2}}k_1 - \frac{3}{4}\sqrt[4]{\frac{c_2}{c_1}}k_2 + \frac{1}{8}k_1 k_2 > 0,$$
$$\frac{3}{8}\sqrt[4]{\frac{c_1}{c_2}}k_1 + \frac{3}{8}\sqrt[4]{\frac{c_2}{c_1}}k_2 - \frac{1}{8}k_1 k_2 > 0. \quad (15)$$

Combining the above inequalities completes the proof. □

Proposition 4. *The fixed point O_2 can be destabilized due to flip bifurcation only.*

Proof. The Jacobian (12) has the following eigenvalues:

$$\lambda_{\pm} = 1 - \frac{3k_1}{16}\sqrt[4]{\frac{c_1}{c_2}} - \frac{3k_2}{16}\sqrt[4]{\frac{c_2}{c_1}} \pm \frac{\sqrt{9\left(\sqrt{c_1}k_1 - \sqrt{c_2}k_2\right)^2 + 4\sqrt{c_1 c_2}k_1 k_2}}{16\sqrt[4]{c_1 c_2}}. \quad (16)$$

It is clear that $9\left(\sqrt{c_1}k_1 - \sqrt{c_2}k_2\right)^2 + 4\sqrt{c_1 c_2}k_1 k_2$ is always positive, and therefore, we have only two real eigenvalues. So the point becomes unstable because of flip bifurcation. □

3.2. Numerical Results. The following numerical simulation experiments validate the above theoretical results. We start our numerical experiments by assuming the following parameters' set $(c_1 > c_2)$, $c_1 = 0.7, c_2 = 0.5$. At this set, $O_2 = (0.1942423762, 0.2298306788)$ and the Jacobian becomes

$$\begin{pmatrix} -0.22373 & 0.34475 \\ 0.54388 & -0.37898 \end{pmatrix}, \quad (17)$$

where we assume $k_1 = 3$ and $k_2 = 4$. The eigenvalues then become $\lambda_{\pm} = (0.138563, -0.741273)$ with $|\lambda_{\pm}| < 1$ and then O_2 is locally asymptotically stable. Keeping the costing shift parameters c_1 and c_2 as previously, we now study the influence of k_1 or k_2 on the stability of O_2. Figures 1(a) and 1(b) show that O_2 is locally asymptotically stable for all values of k_1 and k_2; until we get the cycle of period 2, the point O_2 becomes unstable. Indeed, the simulation shows some interesting behavior of the dynamic of map (6) around the point O_2. To present that dynamics, we have to study the effects of k_1 or k_2 separately. Assuming the following parameters set, $c_1 = 0.7, c_2 = 0.5$, and $k_1 = 2$. As k_2 increases to 6.54, a period-2 cycle (represented by squares in Figure 1(c)) is born around the fixed point O_2. It is plotted with its basins of attraction represented by the light green colors in Figure 1(c) while the grey color refers to divergent (or nonconvergent) points in the phase plane. This cycle turns into a cycle of period four as k_2 increases to 7.14 with quite complicated basins of attraction as displayed in Figure 1(d). Other basins of attraction for the cycle of period four are formed in Figure 1(e) at $k_2 = 7.24$ where nonconvergent points appeared in white color within the basins. The basins of attraction become more complicated as the period-8 starting to appear at $k_2 = 7.24$ as depicted in Figure 1(f). Increasing k_2 further gives rise to four disconnected pieces and two chaotic attractors and then one chaotic attractor. We give in Figures 1(g) and 1(h) examples of two and one chaotic attractors and their basins at $k_2 = 7.53$ and $k_2 = 7.69$, respectively. The white color in the basins denotes the nonconvergent points in the phase plane. The same discussion can be performed for the other parameter k_1 under the same values of costs. This makes us to display the 2D-bifurcation diagram in the (k_1, k_2) – plane on which interesting readers can detect more about the dynamics of map (6) around O_2. Figure 2(a) presents the 2D-bifurcation in the (k_1, k_2) –plane with examples of attractive basins of period-7 (Figure 2(b)), period-9 (Figure 2(c)), and period-10 (Figure 2(d)). Furthermore, the 2D-bifurcation diagram shows that the dynamics of map (6) do not permit the appearance of period-3 and period-5.

Now, we study the case when $c_1 < c_2$ by assuming the set of parameters' values, $c_1 = 0.5, c_2 = 0.9$. In this case, we do not want to repeat the above discussions and only we give some simulations represented by Figures 3(a) to 3(f) at this set in order to see the difference in dynamics in this case and the previous one. All these results so far show a peculiar shape of the basins of attraction and require from us to investigate other characteristics of map (6). From the above discussion and the numerical experiments, we highlight that the assumptions $c_1 > c_2$ and $c_1 < c_2$ affect the stability region obtained by the second condition of (14) for the interior equilibrium point in the (k_1, k_2) – plane. We have seen that at $c_1 > c_2$ $(c_1 = 0.7, c_2 = 0.5)$, we get $k_1 \in (0, 4.9)$ and $k_2 \in (0, 5.8)$ while in the case $c_1 < c_2$ $(c_1 = 0.5, c_2 = 0.9)$, we have $k_1 \in (0, 6.166)$ and $k_2 \in (0, 4.625)$ for the same condition.

3.3. Critical Curves and Phase Plane Zones. The structure of the basins of attraction of map (6) at any ϱ that may represent O_2 or periodic cycle or any chaotic attractor is constructed by some boundaries. These boundaries are calculated as follows.

Proposition 5. *The origin point $O = (0, 0)$ has four real preimages.*

Proof. Setting $q_1(t+1) = 0$ and $q_2(t+1) = 0$ in (6) and solving the system algebraically, we get

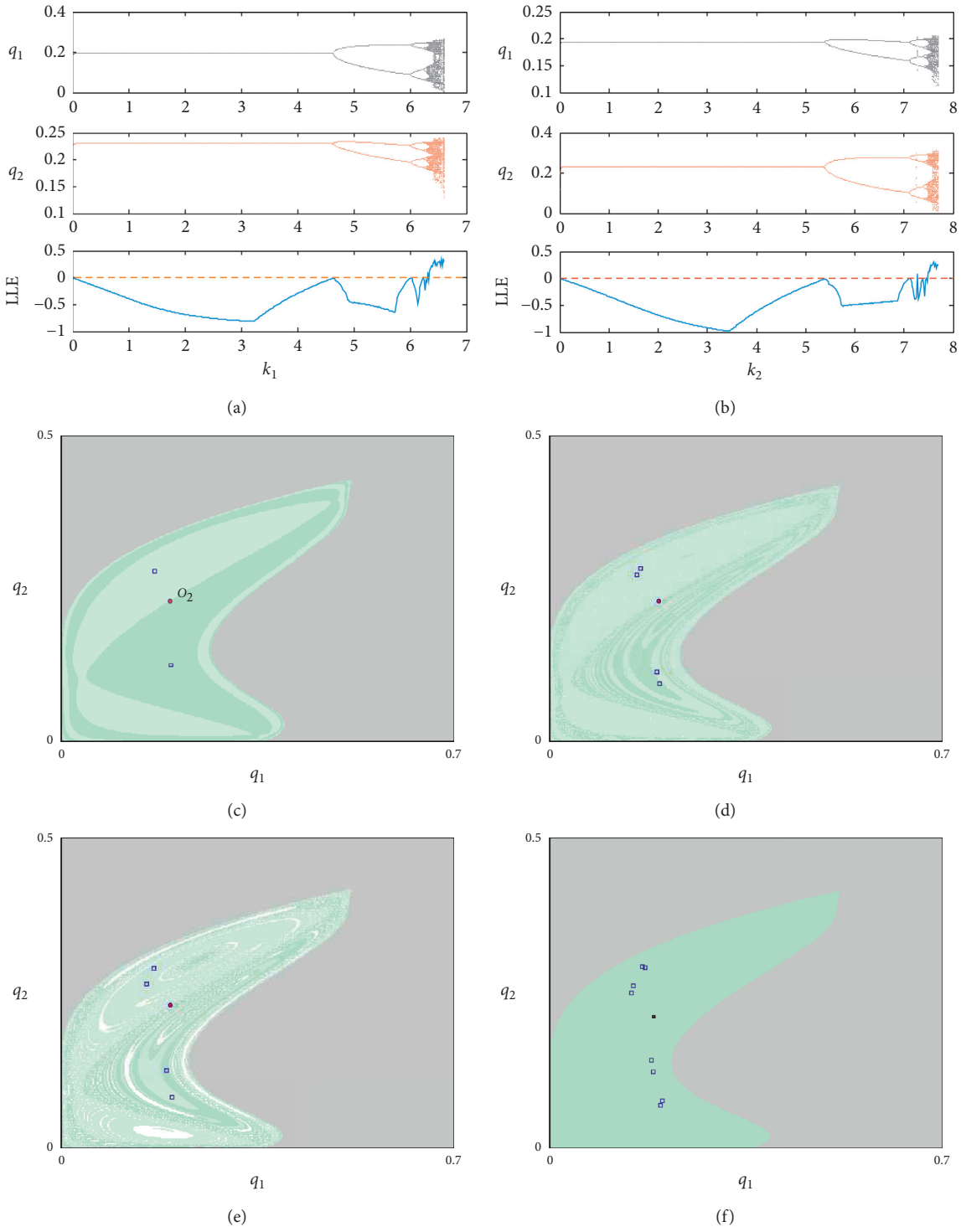

Figure 1: Continued.

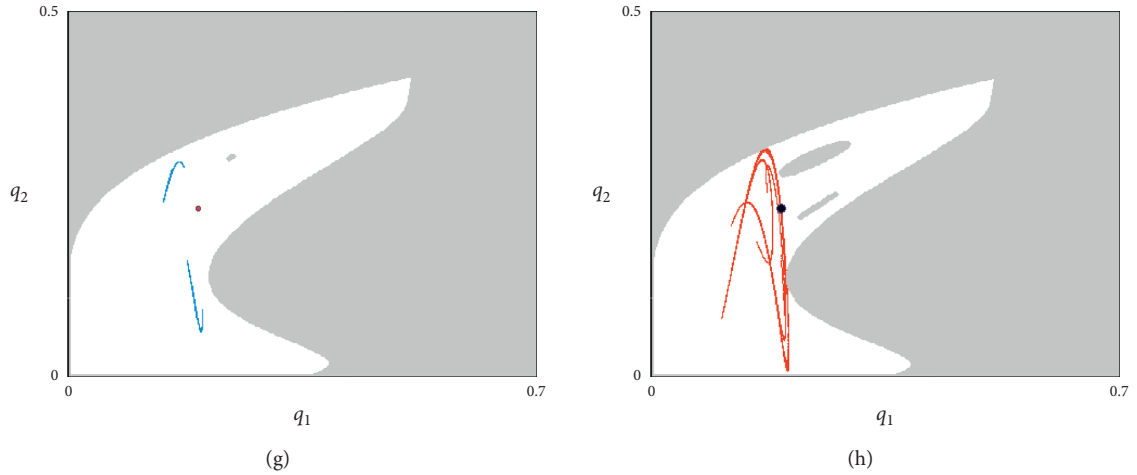

FIGURE 1: (a) Bifurcation diagram and LLE on varying k_1. (b) Bifurcation diagram and LLE on varying k_2. (c) The basins of attraction of period-2 cycle at $k_2 = 6.54$. (d) The basins of attraction of period-4 cycle at $k_2 = 7.14$. (e) The basins of attraction of period-4 cycle at $k_2 = 7.24$. (f) The basins of attraction of period-8 cycle at $k_2 = 7.43$. (g) The basins of attraction of two chaotic attractors at $k_2 = 7.53$. (h) The basins of attraction of a chaotic attractor at $k_2 = 7.69$. Other parameters' values are, $c_1 = 0.7$ and $c_2 = 0.5$.

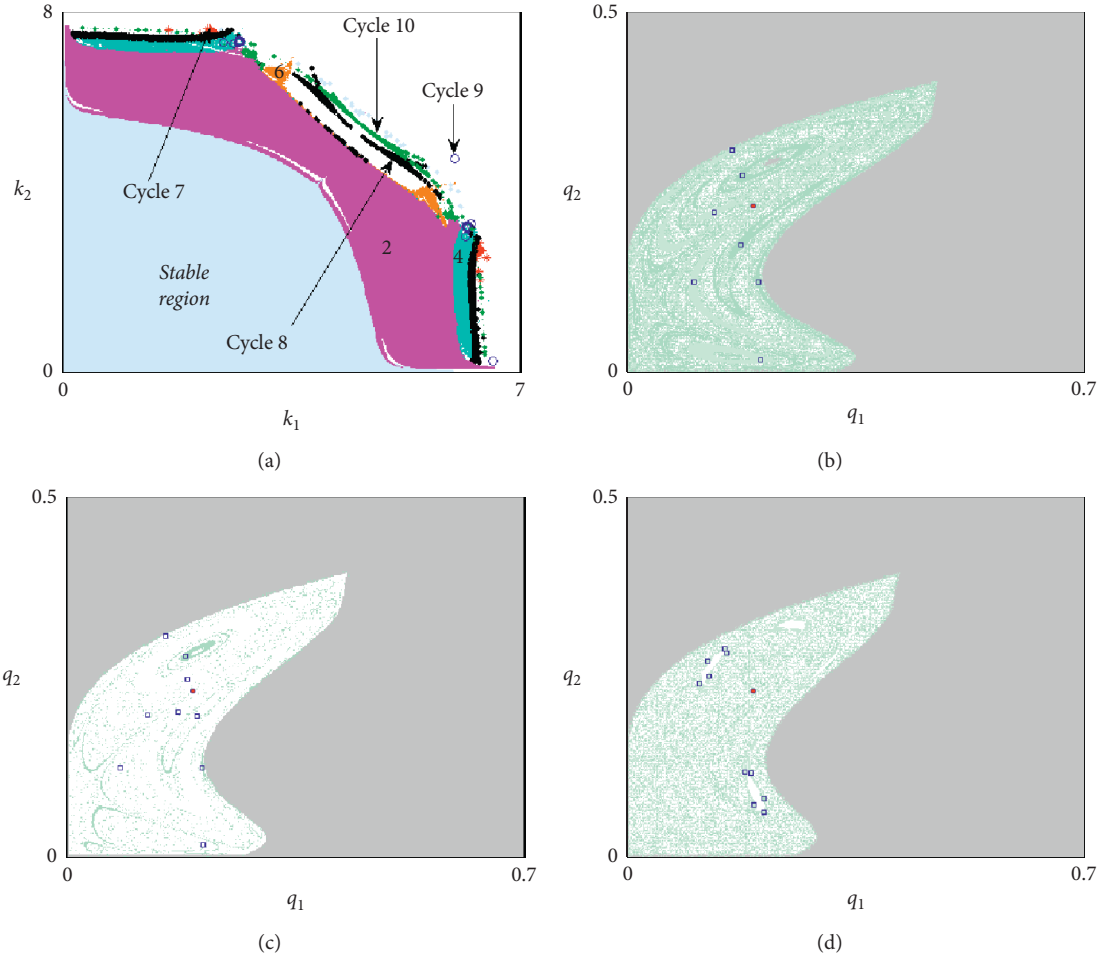

FIGURE 2: (a) The 2D-bifurcation in the (k_1, k_2) – plane. (b) The basins of attraction of period-7 cycle at $k_1 = 2.288$ and $k_2 = 7.5362$. (c) The basins of attraction of period-9 cycle at $k_1 = 2.713$ and $k_2 = 7.3140$. (d) The basins of attraction of period-10 cycle at $k_1 = 2.933$ and $k_2 = 7.263$. Other parameters' values are, $c_1 = 0.7$ and $c_2 = 0.5$.

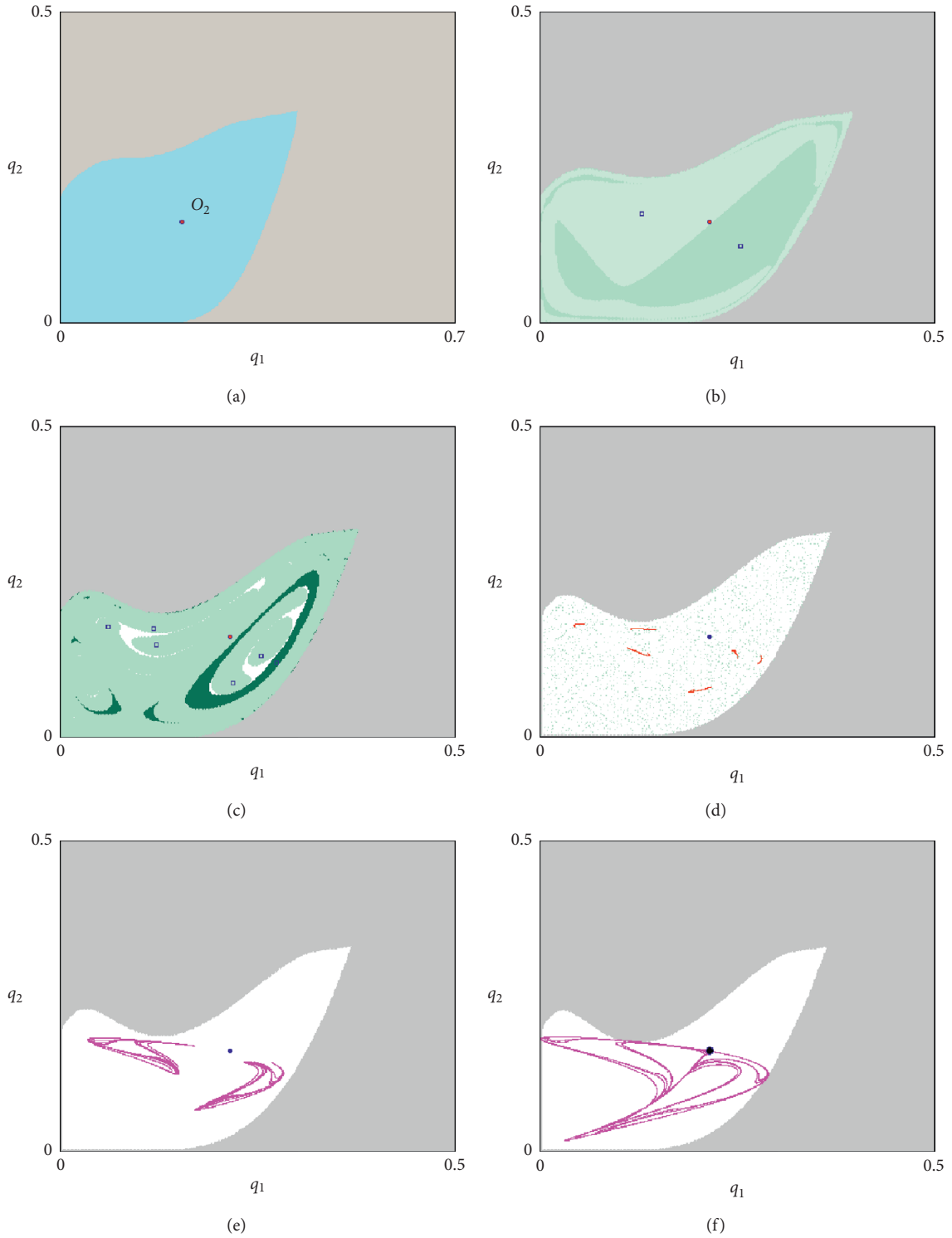

FIGURE 3: (a) The basins of attraction of the fixed point O_2 at $k_1 = 3$ and $k_2 = 3$. (b) The basins of attraction of period-2 cycle at $k_1 = 6.06$ and $k_2 = 3$. (c) The basins of attraction of period-6 cycle at $k_1 = 7.06$ and $k_2 = 3$. (d) The basins of attraction of six chaotic attractors at $k_1 = 7.3$ and $k_2 = 3$. (e) The basins of attraction of two chaotic attractors at $k_1 = 7.33$ and $k_2 = 3$. (f) The basins of attraction of a chaotic attractor at $k_1 = 7.68$ and $k_2 = 3$. Other parameters' values are $c_1 = 0.5$ and $c_2 = 0.9$.

$$
\begin{aligned}
O_{-1}^{(0)} &= (0,0),\\
O_{-1}^{(1)} &= \left(\frac{1}{2c_1k_1},0\right),\\
O_{-1}^{(2)} &= \left(0,\frac{1}{2c_2k_2}\right),\\
O_{-1}^{(3)} &= (\mathring{q}_1\mathring{q}_2),
\end{aligned}
\tag{18}
$$

where $O_{-1}^{(3)}\otimes$ is obtained by solving algebraically the following system:

$$
\begin{aligned}
1+k_1\left(\frac{1}{4}\sqrt{\frac{\mathring{q}_2}{\mathring{q}_1}}-2c_1\mathring{q}_1\right)&=0,\\
1+k_2\left(\frac{1}{4}\sqrt{\frac{\mathring{q}_1}{\mathring{q}_2}}-2c_2\mathring{q}_2\right)&=0.
\end{aligned}
\tag{19}
$$

□

Proposition 6. *Let $\omega_1 = O_{-1}^{(0)}O_{-1}^{(1)}$ and $\omega_2 = O_{-1}^{(0)}O_{-1}^{(2)}$ be the two line segments of the coordinates q_1 and q_2. Also, let ω_1^{-1} and ω_2^{-1} be their preimages. Then, the boundary of the basins of attraction of any ϱ is denoted by $\digamma$ and is given by*

$$
\digamma = \left(\cup_{n=0}^{\infty}T^{-n}(\omega_1)\right)\cup\left(\cup_{n=0}^{\infty}T^{-n}(\omega_2)\right),
\tag{20}
$$

where T^{-n} refers to the set of all preimages of rank-n.

These boundaries are displayed in Figure 4. Furthermore, the figure shows the critical curve LC_{-1} that is calculated by vanishing the determinant of the Jacobian of (6). It is represented by the following curve:

$$
\begin{cases}
32\left(4c_2k_2q_2-1\right)c_1k_1q_1^{(3/2)}q_2^{(1/2)}-4\left(c_1q_1^2+c_2q_2^2\right)k_1k_2+\\
+8\left(1-4c_2k_2q_2\right)q_1^{(1/2)}q_2^{(1/2)}+k_1q_2+k_2q_1=0.
\end{cases}
\tag{21}
$$

It is represented by red color in Figure 4 as it contains two parts, $LC_{-1}^{(a)}\cup LC_{-1}^{(b)}$. It is hard to plot or to get an analytical form for LC in order to identify the zones in the phase plane; however, it is simple to see that O_2 has two real preimages of rank-1 and hence it belongs to Z_2. Furthermore, both ω_1^{-1} and ω_2^{-1} have no preimages and they belong to Z_0. With the preimages of the origin, we detect that the phase plane of map (6) is divided into three zones, Z_4, Z_2, and Z_0. Therefore, map (6) is a non-invertible map.

4. Properties of Map (9)

4.1. Analytical Results

Proposition 7. *The map (9) has only two fixed points that are $o_1 = (0,0)$ and $o_2 = (\overline{q}_1,\overline{q}_2)$ where*

$$
\begin{aligned}
\overline{q}_1 &= \frac{1}{4^{(3/8)}c_1^{(3/4)}c_2^{(1/4)}}\left(\frac{\omega}{\sqrt[3]{4}}+\frac{1-\omega}{4}\right)^{(3/8)},\\
\overline{q}_2 &= \frac{1}{4^{(1/8)}c_1^{(1/4)}c_2^{(3/4)}}\left(\frac{\omega}{\sqrt[3]{4}}+\frac{1-\omega}{4}\right)^{(9/8)}.
\end{aligned}
\tag{22}
$$

Proof. Setting $q_1(t+1) = q_1(t)$ and $q_2(t+1) = q_2(t)$ in (9) and solving the system algebraically completes the proof. □

Proposition 8. *The fixed point $o_1 = (0,0)$ is unstable.*

Proof. The proof is the same as Proposition 2. □

Proposition 9. *The fixed point $o_2 = (\overline{q}_1,\overline{q}_2)$ is locally asymptotically stable provided that $k < (4-2s/(45-22s)\hbar)$ where*

$$
\hbar = \frac{15^{(5/8)}}{24}\sqrt[4]{\frac{c_1}{c_2}}\frac{\left[\sqrt{2}\,(1-\omega)+2\sqrt[6]{32}\omega\right]}{\left[\left(2\sqrt[3]{2}-1\right)\left(1+2\sqrt[3]{2}+4\sqrt[3]{4}+15\omega\right)\right]^{(5/8)}}.
\tag{23}
$$

Proof. The Jacobian at o_2 becomes

$$
\begin{pmatrix}
J_{11} & J_{12}\\
J_{21} & J_{22}
\end{pmatrix},
\tag{24}
$$

where

$$
\begin{aligned}
J_{11} &= 1-45\hbar,\\
J_{12} &= \sqrt[4]{\frac{c_1}{2c_2}}\frac{k}{\left(1-\omega+2\sqrt[3]{2}\omega\right)},\\
J_{21} &= \frac{s}{6}\sqrt{\frac{c_1}{c_2}}\left(1-\omega+2\sqrt[3]{2}\omega\right),\\
J_{22} &= 1-s,
\end{aligned}
\tag{25}
$$

and the trace and determinant take the following form:

$$
\begin{aligned}
\tau &= 1-s+\frac{k\hbar}{2}(44s-45),\\
\delta &= 2-s+\frac{45}{2}k\hbar,
\end{aligned}
\tag{26}
$$

and then,

$$
\begin{aligned}
\Delta_1 &= \frac{11sk}{12}\sqrt[4]{\frac{c_1}{c_2}}\left(\frac{\sqrt{2}\,(1-\omega)+2\sqrt[6]{32}\omega}{\left(1-\omega+2\sqrt[3]{2}\omega\right)^{(5/8)}}\right),\\
\Delta_2 &= 4-2s+k\hbar\,(22s-45),\\
\Delta_3 &= s+\frac{k\hbar}{2}(45-44s).
\end{aligned}
\tag{27}
$$

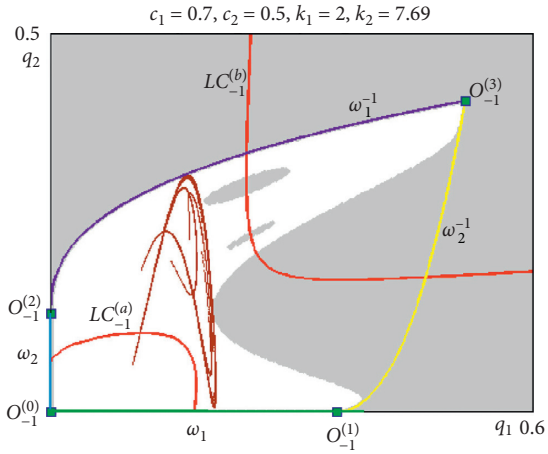

FIGURE 4: The critical curve and preimages of map (6) at the parameters' values, $c_1 = 0.7, c_2 = 0.5, k_1 = 2$, and $k_2 = 7.69$.

It is clear that $\Delta_1 > 0$ and $\Delta_3 > 0$ since $s \in (0,1)$ and $\hbar$ is always positive. While $\Delta_2 > 0$ is attained, if $k < (4 - 2s/(45 - 22s)\hbar)$. The proof is completed.

We should highlight here that if $k > (4 - 2s/(45 - 22s)\hbar)$, then o_2 can be destabilized due to flip bifurcation only. □

4.2. Numerical Results. We assume the following $(c_1 > c_2)$, $c_1 = 0.7, c_2 = 0.5$ with $\omega = 0.2$. At this set, $o_2 = (0.6068957946, 0.4381254240)$ and the Jacobian becomes, at taking $k = 1.2$ and $s = 0.2$,

$$\begin{pmatrix} -0.91172 & 0.17654 \\ 0.048127 & 0.8 \end{pmatrix}, \tag{28}$$

and the eigenvalues are $\lambda_\pm = (-0.916669, 0.804949)$ with $|\lambda_\pm| < 1$ and then o_2 is locally asymptotically stable. Increasing k above the value $(4 - 2s/(45 - 22s)\hbar)$ gives rise to a period-doubling bifurcation, as shown in Figure 5(a). It is clear that the fixed point o_2 is stable for all the values of k until k reaches the value $(4 - 2s/(45 - 22s)\hbar)$ where the first period-2 cycle is born. As discussed in map (6), we give here some complex behaviors of map (9) at different values of the bifurcation parameter k. For instance, at $k = 8.026$, a cycle of period-2 is emerged and is plotted with its basins of attraction in Figure 5(b). At $k = 8.44$, a period-4 cycle is coexisted with its attractive basins in Figure 5(c). It is clear that they are quite complicated basins. The basins become more complicated when the period-8 cycle appears as given in Figure 5(d) at $k = 8.58$. After that higher periodic cycles exist with quite complicated basins and then the map enters the chaos region at $k = 8.83$ and $k = 8.9$ where two chaotic attractors and then one chaotic attractor are emerged and displayed in Figures 5(e) and 5(f), respectively.

The numerical simulation shows that increasing ω which means the second firm gives more interesting to the market share maximization than the profit maximization reduces the stability interval of o_2. The same observation when the firm gives more interesting to the traded-offs between the market share maximization and profit maximization is obtained. It is noticed that low values of the traded-off parameter s keep the stability interval of o_2 larger. Furthermore, when we take values of c_1 and c_2 in the form $c_1 < c_2$, the dynamics of map (9) do not give any new complex dynamics and hence the dynamic is still governed by the change that may be happened on both parameters ω and s.

4.3. Critical Curves and Phase Plane Zones.

$$2c_1 q_1^{(4/3)} - q_1^{(1/3)} - \frac{k}{4}\sqrt{\frac{s}{\sqrt[3]{c_2^2}(s-1)}\left(\frac{\omega}{\sqrt[3]{4}} + \frac{1-\omega}{4}\right)} = 0, \tag{29}$$

which has no real solutions as the expression under the square root is negative. Therefore, o belongs to Z_1 zone.

Proposition 10. *The origin point $o = (0,0)$ has only one real preimage that is $o_{-1}^{(0)} = (0,0)$.*

Proof. Setting $q_1(t+1) = 0$ and $q_2(t+1) = 0$ in (9), we get

$$\begin{aligned} q_1 + kq_1\left(\frac{1}{4}\sqrt{\frac{q_2}{q_1}} - 2c_1 q_1\right) &= 0, \\ (1-s)q_2 + s\left(\frac{\omega}{\sqrt[3]{4}} + \frac{1-\omega}{4}\right)\sqrt[3]{\frac{q_1}{c_2^2}} &= 0. \end{aligned} \tag{30}$$

The first equation in (29) gives $q_1 = 0$ or $1 + k((1/4)\sqrt{(q_2/q_1)} - 2c_1 q_1) = 0$. Substituting $q_1 = 0$ in the second equation of (29) gives $q_2 = 0$, then we get $o_{-1}^{(0)} = (0,0)$. Now, we have the following case:

$$\begin{aligned} 1 + k\left(\frac{1}{4}\sqrt{\frac{q_2}{q_1}} - 2c_1 q_1\right) &= 0, \\ (1-s)q_2 + s\left(\frac{\omega}{\sqrt[3]{4}} + \frac{1-\omega}{4}\right)\sqrt[3]{\frac{q_1}{c_2^2}} &= 0. \end{aligned} \tag{31}$$

Solving (30) gives □

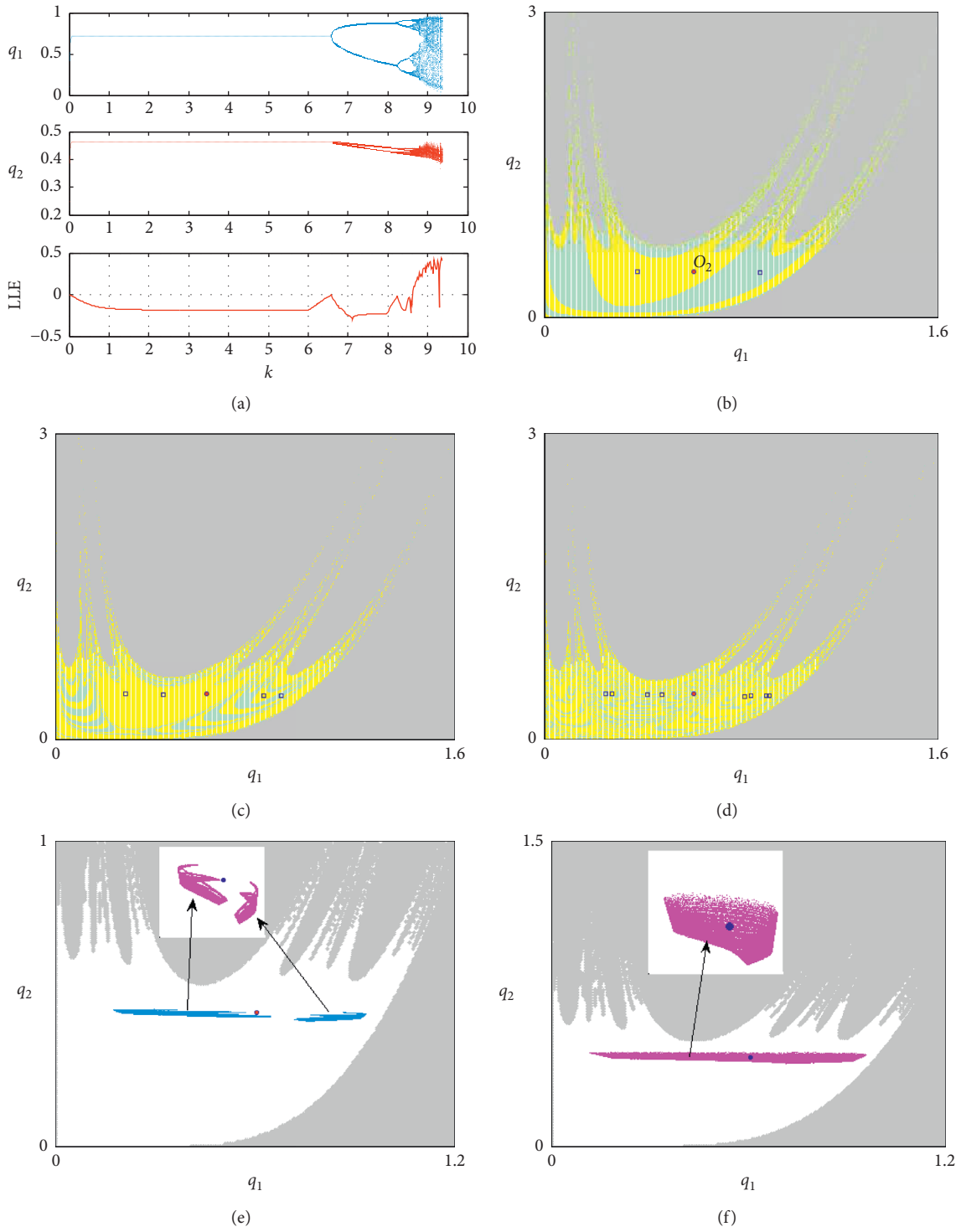

FIGURE 5: (a) Bifurcation diagram and LLE on varying k. (b) The basins of attraction of period-2 cycle at $k = 8.026$. (c) The basins of attraction of period-4 cycle at $k = 8.44$. (d) The basins of attraction of period-8 cycle at $k = 8.58$. (e) The basins of attraction of two chaotic attractors at $k = 8.83$. (f) The basins of attraction of a chaotic attractor at $k = 8.9$. Other parameters' values are $c_1 = 0.7, c_2 = 0.5, \omega = 0.2$, and $s = 0.2$.

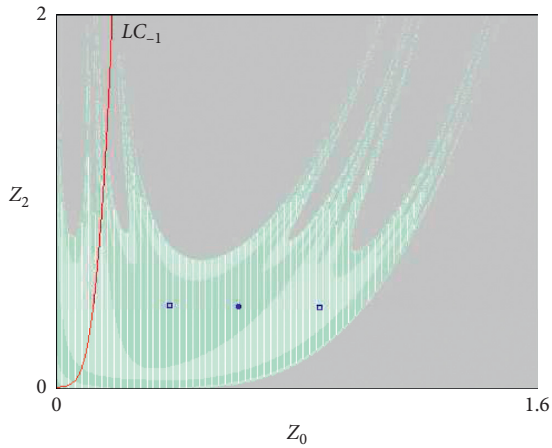

Figure 6: The critical curve and zones of map (9) at the parameters' values, $c_1 = 0.7, c_2 = 0.5, k = 2, \omega = 0.2$, and $s = 0.2$.

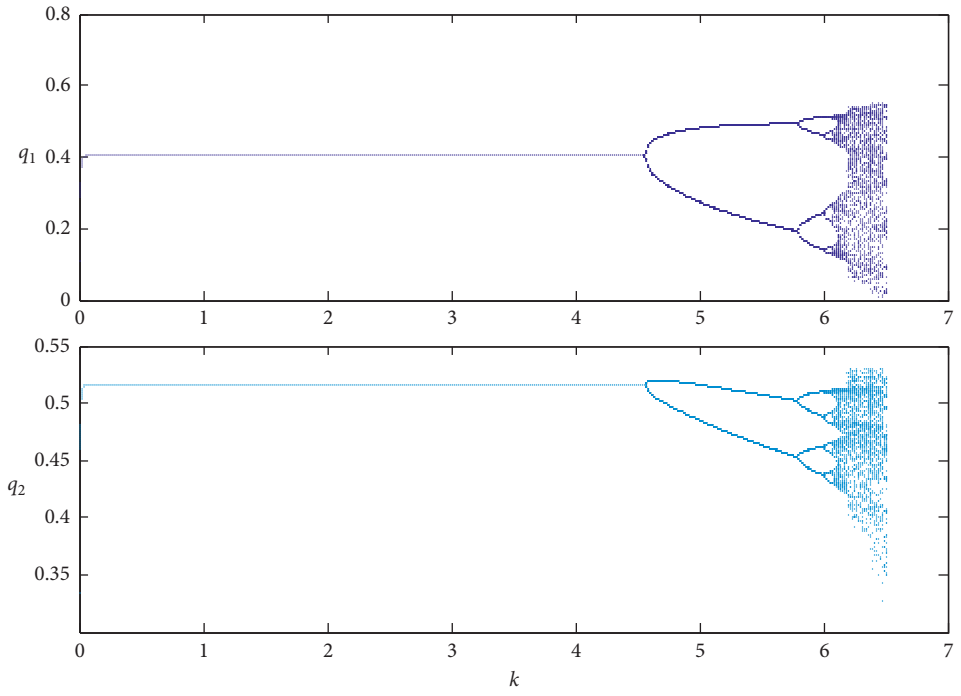

(a)

Figure 7: Continued.

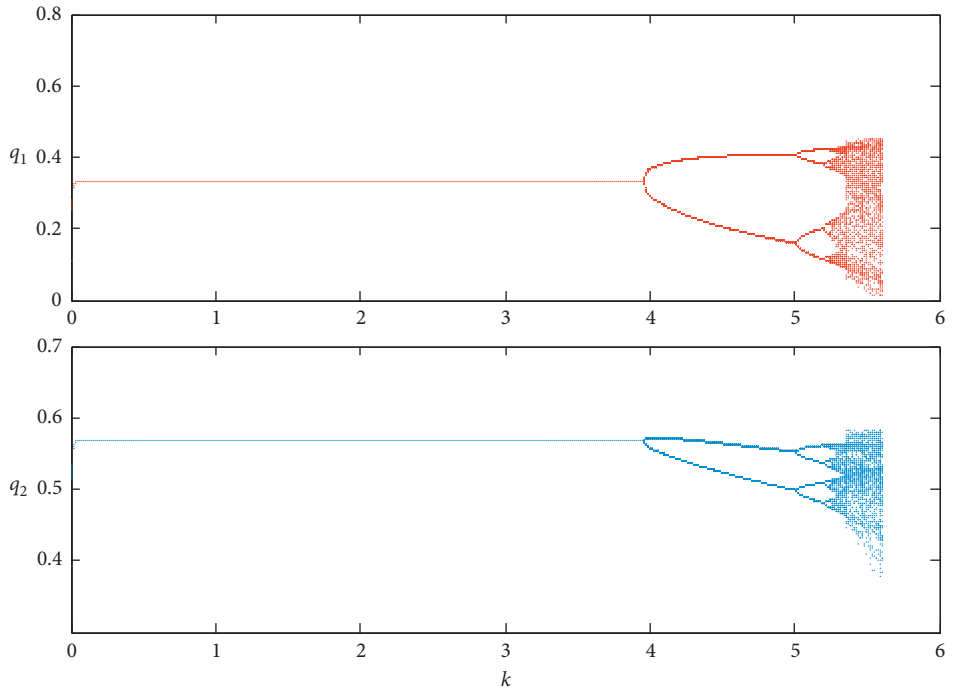

(b)

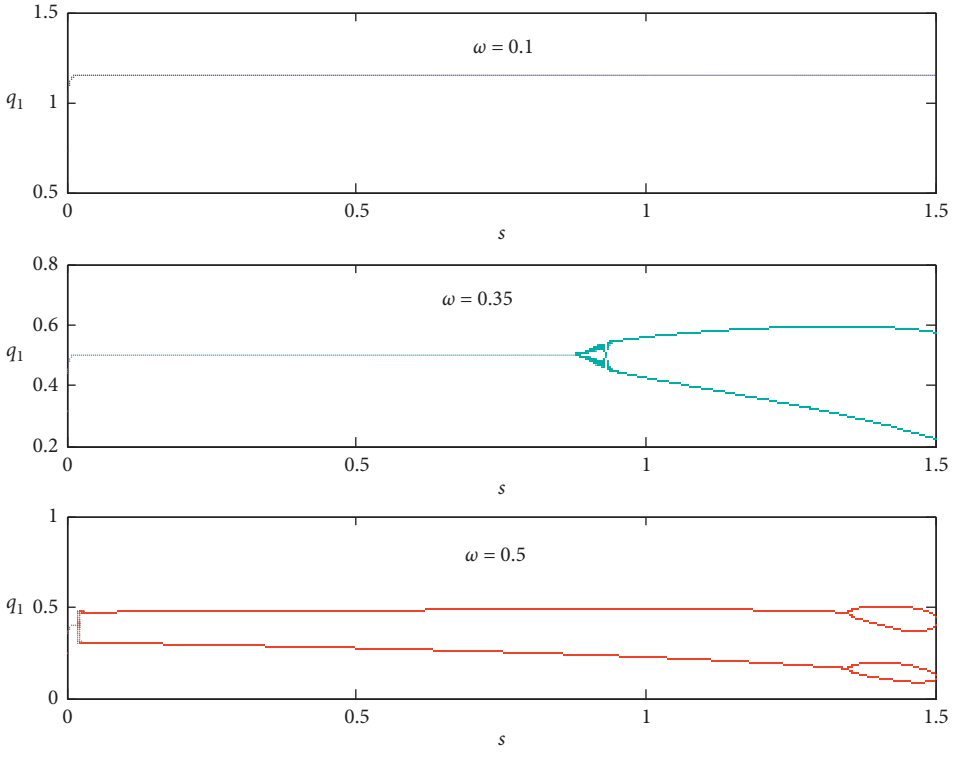

(c)

Figure 7: Continued.

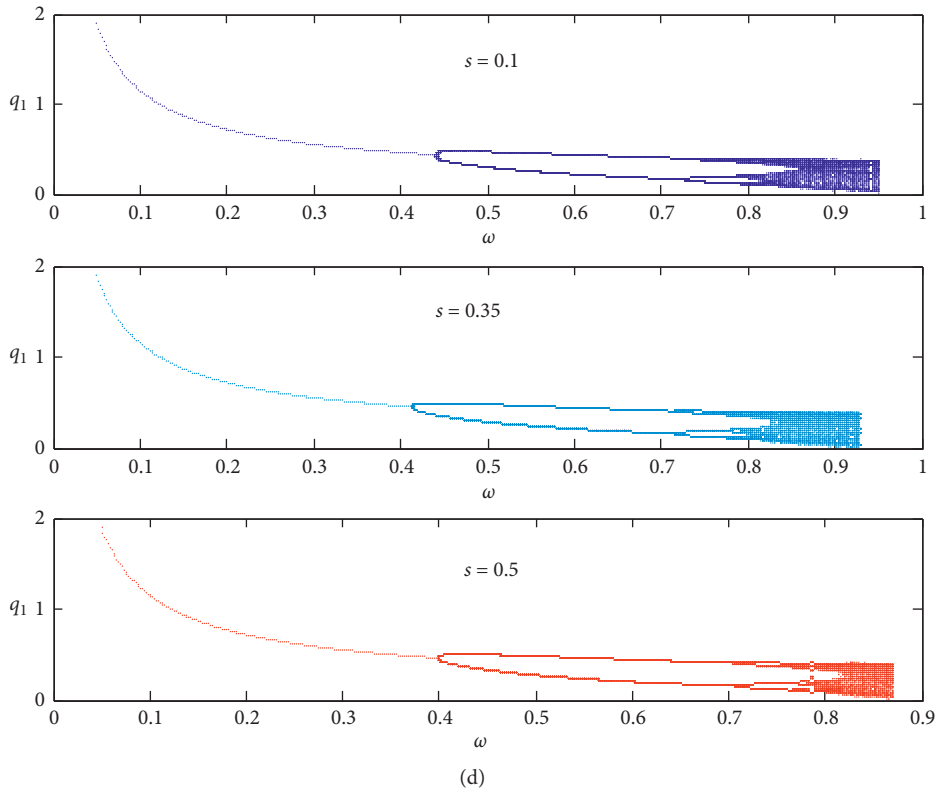

(d)

Figure 7: (a) Bifurcation diagram on varying k at $c_1 = 0.7, c_2 = 0.5, \omega = 0.5$, and $s = 0.5$. (b) Bifurcation diagram on varying k at $c_1 = 0.7, c_2 = 0.5, \omega = 0.7$, and $s = 0.5$. (c) Bifurcation diagram on varying s at $c_1 = 0.7, c_2 = 0.5, k = 5$, and different values for ω. (d) Bifurcation diagram on varying ω at $c_1 = 0.7, c_2 = 0.5, k = 5$, and different values for s.

Proposition 11. *The fixed point o_2 has no real preimages.*

Proposition 12. *Any point in the form $(0, q), q \neq 0$ has two real preimages.*

Proposition 13. *Any point in the form $(q, 0), q \neq 0$ has no real preimages.*

Now, LC_{-1} for map (9) is given by the following curve:

$$\begin{cases} 96sc_1kq_1^{(13/6)}q_2^{(1/2)} - 96c_1kq_1^{(13/6)}q_2^{(1/2)} - 24sq_1^{(7/6)}q_2^{(1/2)} + 24q_1^{7/6}q_2^{(1/2)} - 3skq_2q_1^{(2/3)} + \\ + 3kq_2q_1^{(2/3)} - \dfrac{ks}{\sqrt[3]{c_2^2}}\left(\dfrac{\omega}{\sqrt[3]{4}} + \dfrac{1-\omega}{4}\right)q_1 = 0. \end{cases} \tag{32}$$

It is plotted in Figure 6 with red color at the parameters' values, $c_1 = 0.7, c_2 = 0.5, k = 2, \omega = 0.2$, and $s = 0.2$. Simulation shows that any point belonging to LC_{-1} has two real preimages. However, it is hard to plot LC but we can conclude that the phase plane of (9) may be divided into only two zones that are Z_2 and Z_0. Therefore, map (9) is a noninvertible map.

5. Comparison between the Maps T and T_1

The above analysis and discussion about the two maps show that the model described by map (9) is quite complicated than those of map (6); however, map (9) gives a large stability region for the fixed point under the same set of parameters. This is clear when comparing the 1D bifurcation diagram for the two maps. This means that the firm adopting the trade-offs between the market share maximization and the profit maximization will be more stable in the market competition than those using a gradient-based mechanism such as the bounded rationality. It is also observed from the numerical experiments that when the second firm updates its outputs based on the average of market share and profit maximization, the stability region of the fixed point reduces and becomes almost like those provided by map (6) under the same set of parameters' values. Figure 7(a) shows the bifurcation diagram at $c_1 = 0.7, c_2 = 0.5, \omega = 0.5$, and $s = 0.5$. Increasing ω further to 0.7 and keeping the other parameters' values fixed, the region of stability region of the

fixed point reduces, as shown in Figure 7(b). Furthermore, Figures 7(c) and 7(d) show the influences of the parameters s and ω on the dynamics of map (9). From an economic perspective, one can see that low values of the parameter ω means the second firm pays more attention for the profit maximization (just as the first firm decision-making mechanism) than market share and hence the interior equilibrium point becomes stable for any value of s in the interval $[0, 1]$. As ω increases further, the stability interval of the equilibrium point with respect to s is reduced, as shown in Figure 7(c). Similar discussion is for the influences of the parameter ω given in Figure 7(d).

6. Conclusion

In this manuscript, we have studied two nonlinear duopoly models whose players adopted gradient-based mechanism and trade-off mechanism. We have shown that the fixed points in both models become unstable due to flip bifurcation only. The duopoly in the first model has been compared with the duopoly of the second model whose second firm uses trade-off between market share maximization and profit maximization. Our contributions showed that the second model was more stabilizing than the first model. It has been investigated that the trade-off mechanism can give better stability region for the fixed point. We found that when the second firm in the second model adopts the average between market share and profit maximization, the region of stability was reduced. Furthermore, using higher weights of the trade-off makes the stability region to shrink and hence the second firm should adopt low weights to become more stable in the market. We have also investigated that both maps are noninvertible, and for this reason, the basins of attraction of any dynamic behavior of the maps were quite complicated. In future study, we intend to apply the trade-off mechanism to oligopoly models with more than two firms.

Data Availability

The datasets generated during the current study are available from the corresponding author on reasonable request.

Conflicts of Interest

The author declares no conflicts of interest.

Acknowledgments

This research was supported by King Saud University, Riyadh, Saudi Arabia, Project number (RSP-2020/167).

References

[1] C. W. Cobb and P. H. Douglas, "A theory of production," *American Economic Review*, vol. 18, pp. 139–165, 1928.

[2] A. Dixit and J. Stiglitz, "Monopolistic competition and optimum product diversity," *American Economic Review*, vol. 67, no. 3, pp. 297–308, 1977.

[3] N. Singh and X. Vives, "Price and quantity competition in a differentiated duopoly," *The RAND Journal of Economics*, vol. 15, no. 4, pp. 546–554, 1984.

[4] F. Cavalli, A. Naimzada, and F. Tramontana, "Nonlinear dynamics and global analysis of a heterogeneous Cournot duopoly with a local monopolistic approach versus a gradient rule with endogenous reactivity," *Communications in Nonlinear Science and Numerical Simulation*, vol. 23, no. 1-3, pp. 245–262, 2015.

[5] M. Kopel, "Simple and complex adjustment dynamics in Cournot duopoly models," *Chaos, Solitons & Fractals*, vol. 7, no. 12, pp. 2031–2048, 1996.

[6] E. Ahmed and H. N. Agiza, "Dynamics of a cournot game with n-competitors," *Chaos, Solitons & Fractals*, vol. 9, no. 9, pp. 1513–1517, 1998.

[7] T. Puu, "The chaotic duopolists revisited," *Journal of Economic Behavior & Organization*, vol. 33, no. 3-4, pp. 385–394, 1998.

[8] H. N. Agiza, "Explicit stability zones for Cournot game with 3 and 4 competitors," *Chaos, Solitons & Fractals*, vol. 9, no. 12, pp. 1955–1966, 1998.

[9] G. I. Bischi, C. Mammana, and L. Gardini, "Multistability and cyclic attractors in duopoly games," *Chaos, Solitons & Fractals*, vol. 11, no. 4, pp. 543–564, 2000.

[10] A. Agliari, L. Gardini, and T. Puu, "The dynamics of a triopoly Cournot game," *Chaos, Solitons & Fractals*, vol. 11, no. 15, pp. 2531–2560, 2000.

[11] G. I. Bischi and A. Naimzada, "Global analysis of a dynamic duopoly game with bounded rationality," in *Advances in Dynamic Games and Applications. Annals of the International Society of Dynamic Games*, J. A. Filar, V. Gaitsgory, and K. Mizukami, Eds., Birkhäuser, Boston, MA, USA, 2000.

[12] S. S. Askar and M. F. Elettreby, "The impact of cost uncertainty on Cournot oligopoly games," *Applied Mathematics and Computation*, vol. 312, pp. 169–176, 2017.

[13] S. S. Askar, "The impact of cost uncertainty on Cournot duopoly game with concave demand function," *Journal of Applied Mathematics*, vol. 2013, 2013.

[14] S. S. Askar, "Duopolistic Stackelberg game: investigation of complex dynamics and chaos control," *Operational Research*, vol. 20, pp. 1685–1699, 2018.

[15] S. S. Askar, "The influences of asymmetric market information on the dynamics of duopoly game," *Mathematics*, vol. 8, no. 7, p. 1132, 2020.

[16] H. N. Agiza, A. S. Hegazi, and A. A. Elsadany, "Complex dynamics and synchronization of a duopoly game with bounded rationality," *Mathematics and Computers in Simulation*, vol. 58, no. 2, pp. 133–146, 2002.

[17] H. N. Agiza and A. A. Elsadany, "Nonlinear dynamics in the Cournot duopoly game with heterogeneous players," *Physica A: Statistical Mechanics and Its Applications*, vol. 320, pp. 512–524, 2003.

[18] J. Ma, F. Zhang, and Y. He, "Complexity analysis of a master-slave oligopoly model and chaos control," *Abstract and Applied Analysis*, vol. 2014, 2014.

[19] J. Andaluz, A. A. Elsadany, and G. Jarne, "Nonlinear Cournot and Bertrand-type dynamic triopoly with differentiated products and heterogeneous expectations," *Mathematics and Computers in Simulation*, vol. 132, pp. 86–99, 2017.

[20] G. I. Bischi, M. Gallegati, and A. Naimzada, "Symmetry-breaking bifurcations and representative firm in dynamic duopoly games," *Annals of Operations Research*, vol. 89, pp. 252–271, 1999.

[21] G. I. Bischi, L. Gardini, and M. Kopel, "Analysis of global bifurcations in a market share attraction model," *Journal of*

Economic Dynamics and Control, vol. 24, no. 5-7, pp. 855–879, 2000.

[22] L. Fanti, L. Gori, and M. Sodini, "Nonlinear dynamics in a Cournot duopoly with isoelastic demand," *Mathematics and Computers in Simulation*, vol. 108, pp. 129–143, 2015.

[23] A. K. Naimzada and R. Raimondo, "Chaotic congestion games," *Applied Mathematics and Computation*, vol. 321, pp. 333–348, 2018.

[24] Y. Peng and Q. Lu, "Complex dynamics analysis for a duopoly Stackelberg game model with bounded rationality," *Applied Mathematics and Computation*, vol. 271, pp. 259–268, 2015.

[25] E. Ahmed and M. F. Elettreby, "Controls of the complex dynamics of a multi-market Cournot model," *Economic Modelling*, vol. 37, pp. 251–254, 2014.

[26] J. Peng, Z. Miao, and f. Peng, "Study on a 3-dimensional game model with delayed bounded rationality," *Applied Mathematics and Computation*, vol. 218, no. 5, pp. 1568–1576, 2011.

[27] W. Elberfeld and E. Wolfstetter, "A dynamic model of Bertrand competition with entry," *International Journal of Industrial Organization*, vol. 17, no. 4, pp. 513–525, 1999.

[28] M. Janssen and E. Rasmusen, "Bertrand competition under uncertainty," *The Journal of Industrial Economics*, vol. 50, no. 1, pp. 11–21, 2003.

[29] A. K. Naimzada and L. Sbragia, "Oligopoly games with nonlinear demand and cost functions: two boundedly rational adjustment processes," *Chaos, Solitons & Fractals*, vol. 29, no. 3, pp. 707–722, 2006.

[30] J. Ma and F. Si, "Complex dynamics of a continuous bertrand duopoly game model with two-stage delay," *Entropy*, vol. 18, no. 7, p. 266, 2016.

[31] T. Puu, *Disequilibrium Economics: Oligopoly, Trade, and Macrodynamics*, Springer International Publishing Ag, part of Springer Nature, Berlin, Germany, 2018.

[32] K. Sydsaeter and P. Hammond, *Essential Mathematics for Economic Analysis*, Prentice-Hall, England, UK, 2005.

[33] S. S. Askar, "On dynamical multi-team Cournot game in exploitation of a renewable resource. Chaos," *Solitons & Fractals*, vol. 32, no. 1, pp. 264–268, 2003.

[34] T. Negishi, "Monopolistic competition and general equilibrium," *The New Palgrave Dictionary of Economics*, vol. 6, 1987.

[35] S. S. Askar, "Tripoly Stackelberg game model: one leader versus two followers," *Applied Mathematics and Computation*, vol. 328, pp. 301–311, 2018.

[36] S. S. Askar and M. Abouhawwash, "Quantity and price competition in a differentiated triopoly: static and dynamic investigations," *Nonlinear Dynamics*, vol. 91, no. 3, pp. 1963–1975, 2018.

[37] J. Zhang, Q. Da, and Y. Wang, "The dynamics of Bertrand model with bounded rationality," *Chaos, Solitons & Fractals*, vol. 39, no. 5, pp. 2048–2055, 2009.

[38] B. T. Gale, "Market share and rate of return," *The Review of Economics and Statistics*, vol. 54, no. 4, p. 412, 1972.

[39] GI. Bischi, C. Chiarella, M. Kopel, and F. Szidarovszky, *Nonlinear Oligopolies: Stability and Bifurcations*, Springer-Verlag Berlin Heidelberg, Berlin, Germany, 2010.

[40] T. Puu, "Chaos in duopoly pricing," *Chaos, Solitons & Fractals*, vol. 1, no. 6, pp. 573–581, 1991.

Hindawi
Complexity
Volume 2021, Article ID 8826253, 13 pages
https://doi.org/10.1155/2021/8826253

Research Article

The Dynamic Impacts of the Global Shipping Market under the Background of Oil Price Fluctuations and Emergencies

Zihan Chen,[1] Xiaokong Zhang ,[2] and Jian Chai [2]

[1]*Accounting School, Henan University of Economics and Law, Zhengzhou 450046, China*
[2]*School of Economics and Management, Xidian University, Xi'an 710126, China*

Correspondence should be addressed to Xiaokong Zhang; xkzhang_1996@stu.xidian.edu.cn and Jian Chai; chaijian0376@126.com

Received 9 September 2020; Revised 13 December 2020; Accepted 30 December 2020; Published 11 February 2021

Academic Editor: Xueyong Liu

With growing uncertainty about the evolution of the global landscape, it is of great practical significance to explore the nonlinear dynamic adjustment relationship among the world oil market, the global bulk shipping market, the stock market, and economic growth in China. This paper applied the TVP-SV-VAR model and selected quarterly data from 1998 to 2020 to explore the dynamics. The results indicated that the impact intensity of BDI on China's economy had a "positive" to "negative" change in different lag periods. This was mainly due to the fact that the negative impact of higher freight prices on China's economy outweighed the positive impact of higher trade volumes on China's economy. The impact intensity of BDI on GDP had a distinct medium- to long-term effect. A positive BDI shock had a dampening effect on stock prices in the short and medium term, while a positive BDI shock could promote stock market prosperity in the long-term perspective. The impulse responses of SSE and GDP to BDI showed that the external shipping market shocks to China's stock market and economic growth gradually became smaller over time. For impulse response at three different time points, the impact intensity of the BDI to GDP varied at different time points, with the largest shock during the financial crisis in 2008, followed by the shock during the oil price crash in 2014, and the smallest during the COVID-19 epidemic. This demonstrated that the external shipping market's influence on Chinese economic growth and stock market has gradually weakened over time, illustrating the enhancement of Chinese risk-resilience capacity.

1. Introduction

With the further advance of economic globalization and the rapid development of international trade, the scope and degree of international trade markets increasingly have extended and strengthened. Meanwhile, the surging demand for maritime trade derived from the international trade market has made the global shipping market increasingly prominent. Dry bulk transport, including coal, iron ore, and grain, is the mainstay of the international shipping industry, which is related to the basic survival demands of nations, the basic material guarantee for the survival of the countries, and the essential condition for maintaining the standard of living desired by the nationals. Therefore, in a certain sense, compared with container transport, general cargo transport, and liquid bulk transport, the dry bulk market, which is responsible for the transportation of major raw materials and materials, plays an increasingly crucial role in the international shipping market and international trade. The Baltic Dry Index (BDI) is an international authoritative index for measuring international shipping conditions, the barometer and wind vane of the international shipping market, the leading index reflecting international trade conditions, and the microcosm of the global economy. In 2008, when the BDI reached a record high, a large number of investors were attracted to the maritime industry. The financial crisis broke the gold rush and shipping rates plummeted. The slump and depression in the shipping industry had continued until 2013, when the shipping market was rejuvenated, and the BDI returned to 2000. However, in 2014, the Ebola virus ravaged the whole of Africa. The Danish Poyan Oil Company applied to the court for bankruptcy, the supply of ships and bunker oil was seriously affected, and the BDI began to decline precipitously

in the market downturn. The shipping market then went into a slow recovery, yet its upward trend was dampened by the sudden onset of COVID-19. The main factors influencing the fluctuation of the BDI include global GDP growth rate, global demand for iron ore and coal transportation, global demand for grain transportation, global supply of ship tonnage, average international bunker price, war, and natural disasters. Among them, fuel oil prices, economic, climate, and unexpected events have a more profound impact on BDI. Firstly, fuel costs can account for 40% of a ship's operating costs. Drastic changes in oil prices may cause a certain degree of disturbance to the BDI. Secondly, from the trend of BDI over the years, the bulk freight rate is determined by the relationship between supply and demand, but the concentration of dry bulk transport industry is low, and the change of the supply side (effective capacity) is relatively slow. Therefore, the short-term fluctuation of the BDI is mainly dominated by the demand side (transport demand), which is greatly influenced by the change of economic prosperity. In terms of the major regions connected by BDI routes, key routes from China and the United States are included. In recent years, China, as a major demander of bulk dry bulk cargoes, has seen a growing demand for imports of bulk raw materials, most notably iron ore and coal, which rank among the highest in terms of seaborne imports. Thus, as a bellwether of trade data for trade-active countries, the BDI is closely related to the trade volume and GDP growth of China and the US and, even more so, reflects the degree of economic prosperity in China. In addition, other contingencies at the supply and demand level can also phase in freight rates, such as the financial crisis and COVID-19.

As a result, the shipping market is dependent on the oil market and on international trade. As the world's largest trading country, the interaction between the oil market and shipping market has a profound impact on investor sentiment and trade volume, ultimately exacerbating China's macroeconomic fluctuations. Especially, in recent years, against the backdrop of structural changes in internal supply and demand, sharp fluctuations in oil prices and frequent unexpected events, the BDI fluctuates frequently and its influence on China's economy should not be underestimated. The stock market acts as a macroeconomic barometer, and the macroeconomic functions profoundly affect the stock market volatility. Many scholars have confirmed the existence of a positive correlation between the BDI, the US stock market, and the US dollar index, but there are rare studies on the mechanism of the influence of the BDI and the Chinese stock market. Against the background of increasing economic uncertainty, it is of great practical significance to study the linkages among the world oil market, global shipping market, China's stock market, and economy. There have been numerous excellent reviews in the literature of the two-two relationship among the oil market, shipping market, stock market, and GDP, but studies which include the world oil market, global shipping market, Chinese stock market, and GDP in the same system are little investigated. Furthermore, there are only few studies that consider the nonlinear dynamic linkage between the variables. Thus, this paper attempts to use the TVP-SV-VAR model to analyze the nonlinear dynamic adjustment relationship among the world oil market, global shipping market, Chinese stock market, and economic growth and fully explore the inner influence mechanism between the variables. Only by identifying the potential shock effects of the world oil market and global shipping market, can we clarify the direction and path of policy adjustment based on the driving factors, thus effectively preventing the impact of oil prices and ocean freight rates, while reducing the possibility of unexpected shocks to Chinese economy and stock market. In addition, this paper examines the linkages and shock effects between markets under the major emergencies of the "financial crisis," "international oil price crash," and "COVID-19," in order to provide useful scientific reference for industry insiders.

2. Literature Review

2.1. The Effect of the Oil Market on BDI, Stock Market, and Economic Growth. As a leading indicator of global shipping costs and a unit of measurement of commodity trading volume, the BDI was closely related to fluctuations in the world oil market. On the one hand, crude oil price was transmitted directly to the BDI through global shipping and transportation costs. On the other hand, changes in international market factors such as the global economic cycle, business cycle, and major emergencies would act on both the BDI and the international crude oil market at the same time, thus triggering a synchronized volatility trend in both markets [1]. There was a significant cross-correlation between the BDI and crude oil price, and the short-term multiple fractal characteristics were stronger than the long-term ones [2]. In accordance with this, Arigoni et al. [3] structured different scenarios of the effects of high and low BDI and oil prices and found same conclusions.

Oil price shocks have a significant impact on factor inputs in the production sector as well as on macroeconomic performance. In terms of macroeconomics, theoretical studies have shown that the positive shock of oil prices affects the input of relevant downstream production sectors through the cost channels of upstream raw materials and then affects the output [4–6]. In this process, imported inflation caused by oil prices directly affects the economy, triggering the reverse adjustment of the monetary and fiscal policies, which further indirectly affects the economic growth. As the largest oil importer, the Chinese economy cannot avoid the shock of international oil prices. Existing research studies have attempted to explore the response of Chinese economy to oil price shocks. Cheng et al. [7], based on a GARCH model, showed that uncertainty of oil price had a negative impact on China's real GDP. Zhao et al. [8] established a DSGE model to confirm that the influence of different types of oil price fluctuations had different approaches on economic growth, and rising oil prices driven by demand would produce long-term negative effects on China's GDP. Kim et al. [9] found that Chinese economy had a time-varying response to the oil price shock.

As far as the stock market was concerned, the causal relationship between the international crude oil market and

the stock market largely depended on the development stage, energy structure, global crude oil market, and other factor endowments [10, 11]. The existing research studies showed that crude oil market was the Granger cause of stock market volatility [12, 13]. Phan et al. [14, 15] empirically demonstrated that the introduction of oil prices could significantly improve the accuracy of stock price forecasts. In addition, most studies showed that the two were preceded by a nonlinear time-lagged effect. Wen et al. [16] further suggested that oil price shocks had a negative effect in the short run but would turn positive in the long run. Ding et al. [17] used a SVAR model to prove that international crude oil price fluctuations had a significant Granger effect on investor sentiment in the Chinese stock market, and investor sentiment was contagious by international crude oil price fluctuations with an average lag of about 8 months.

2.2. The Effect of BDI on the Stock Market and Economic Growth. Numerous studies have analyzed the volatility spillovers and linkage mechanisms among the BDI, stock market, and economic growth. Existing research studies showed that the BDI had a long-term cointegration relationship with the US stock market Standard and Poor's Dow Jones Indices. Changes in the BDI could help explain the Dow Jones Indices [18]. Alizadeh and Muradoglu [19] further demonstrated that using the BDI for predicting other stock market fluctuations could significantly improve forecast performance. Besides, Lin et al. [20] confirmed that the BDI had a significant time-varying volatility spillover effects on commodity and stock markets by using the VAR-BEKK-GARCH-X model. Given the volatility spillover relationship among the BDI, commodity, and stock market, the BDI was closely related to global trade volatility; thus, the research related to the Baltic Dry Index (BDI) as a leading economic indicator was a hot issue in academic research [21–23]. A large number of scholars have favored the BDI as a leading indicator for predicting the macroeconomy [24, 25].

In summary, there has been a large amount of literature examining the two-two relationship among international oil markets, shipping markets, stock markets, and economic growth, providing evidence of their correlation and giving a factual and theoretical basis for the in-depth study of this paper. However, on the one hand, there are relatively few studies that include oil markets, stock markets, shipping markets, and GDP in the same system, and furthermore, there are only a few papers that consider the nonlinear dynamic linkages between the variables. On the other hand, the relationships among variables may present different results depending on the country, region, sample range, system changes, and methodological selection. Consequently, this paper employed the TVP-SV-VAR model to explore the nonlinear linkages between different markets and Chinese economic growth, which could theoretically enrich the current relevant studies and provided factual evidence for the nonlinear linkages between different markets and the Chinese economy in practice.

3. Methodology

Vector autoregression is a fundamental tool in econometric analysis and is widely used. However, the coefficient and variance in the traditional VAR model are constant. In many cases, the data generation process for economic variables appears to have randomly fluctuating drift coefficients. In addition, with constant changes such as institutional changes and policy preferences, large structural abrupt changes may occur in the economic system. At this time, the estimated time-varying coefficient of the VAR model may be biased because it ignores the possible changes of volatility in the disturbance. It is a great challenge to characterize and interpret the dynamic adjustment characteristics between observed variables, and thus, VAR is limited in use. In recent years, in order to capture the potential time-varying nature of the economic structure, random fluctuations are gradually incorporated into the TVP-VAR model. The TVP-SV-VAR model sets all parameters as a first-order random walk process, allows temporary and permanent deviations of parameters, and enables us to capture the possible time-varying properties of economic structure in a flexible and robust way, which can well describe the nonlinear and dynamic characteristics between variables. As a result, it is more advantageous at the practical application level.

The TVP-SV-VAR model is a variant of the traditional VAR model. The structural VAR model can be defined as follows:

$$Ay_t = F_1 y_{t-1} + \cdots + F_s y_{t-s} + \mu_t, \quad t = s+1, \ldots, n, \tag{1}$$

where $y_t$is a $k \times 1$ vector of observed variables, $A, F_1, \ldots, F_s$ is a $k \times k$ matrix of coefficients, and $\mu_t \sim N(0, \Sigma\Sigma)$ can be described as a $k \times 1$ structural shock. Assuming that the coefficient matrix A is a lower-triangular, the recursive method can be used to identify the structural relationship. Equation (1) can be transformed into the following form:

$$y_t = X_t \beta_t + A_t^{-1} \Sigma_t \varepsilon_t, \varepsilon_t \sim N(0, I_k), \tag{2}$$

where the parameter β_t, matrix A_t, and $\Sigma_t$are all temporally variable parameters. It is assumed that the parameters to be evaluated follow the random walk process, which implies that temporary and permanent shifts in the coefficients are allowed. The drift coefficients can be used to capture possible nonlinearity, such as gradual or structural changes. The error term can be used to capture temporary shifts:

$$\begin{aligned} &\beta_{t+1} = \beta_t + \mu_{\beta_t}, \alpha_{t+1} = \alpha_t + \mu_{\alpha_t}, \\ &h_{t+1} = h_t + \mu_{h_t}, \\ &\begin{bmatrix} \varepsilon_t \\ \mu_{\beta_t} \\ \mu_{\alpha_t} \\ \mu_{h_t} \end{bmatrix} \sim N\left(0, \begin{bmatrix} I_k & 0 & 0 & 0 \\ 0 & \Sigma_\beta & 0 & 0 \\ 0 & 0 & \Sigma_\alpha & 0 \\ 0 & 0 & 0 & \Sigma_h \end{bmatrix}\right), \end{aligned} \tag{3}$$

where $t = s+1, \ldots, n, \beta_{s+1} \sim N(\mu_{\beta_0}, \Sigma_{\beta_0}), \alpha_{s+1} \sim N(\mu_{\alpha_0}, \Sigma_{\alpha_0})$, and $h_{s+1} \sim N(\mu_{h_0}, \Sigma_{h_0})$. The model is a nonlinear state-space model considering the time variability of the

perturbation term. Therefore, the maximum likelihood estimation requires repeated filtering for each set of parameters until the maximum value is reached, and the calculation is too large. This paper adopts the Bayesian method and MCMC simulation to effectively estimate the TVP-SV-VAR model so as to better depict the time-varying characteristics of coefficients and random volatility.

4. Data and Preliminary Analysis

4.1. Variable and Data. This paper focused on the nonlinear dynamic relationship among the world oil market, the global shipping market, the Chinese stock market, and GDP. The variables were selected as follows: (1) the selection of oil prices: firstly, Brent price and WTI price are important benchmark crude oil prices in the international oil market, and both futures markets have good price discovery functions. Numerous studies have shown that the price discovery function of the WTI crude oil futures market is more representative of the international benchmark crude oil price level [26–28]. With the development of the global economy, the advantages of Brent in terms of the scale of global spot trade and market liquidity are gradually revealed. Most of the findings have revealed that Brent plays an increasingly crucial role in the international crude oil pricing benchmark. Attanasi [29] proved that Brent futures market dominated in the international crude oil price discovery. In addition, Qingsong et al. [2] used multiple fractal trend mutual analysis to prove that the BDI and Brent had strong multiple fractal characteristics than WTI. Therefore, the Brent spot price was chosen as a proxy variable for the crude oil market in this paper; (2) the selection of stock price: the Shanghai Composite Index and the Shenzhen Component Index are two representative stock price indices in China. In terms of the range of constituent stocks, the constituent stocks of the Shanghai Composite Index are all stocks listed on the Shanghai Stock Exchange, reflecting the overall price movements of stocks listed on the Shanghai Stock Exchange. The Shenzhen Component Index is calculated by taking the stocks of 500 listed companies, mainly information technology companies, as the representative of the market. As a result, the Shanghai Composite Index is more representative than the Shenzhen Component Index. In terms of research on Chinese economic cycle and stock market, a large amount of literature has used the Shanghai Composite Index to represent the movement of stock prices [30, 31]. This paper also chose the Shanghai Composite Index to represent the changes in stock prices in China. For the ease of description, the SSE was used instead of the Shanghai Composite Index; (3) the BDI index was adopted to represent changes in global shipping prices, and quarterly GDP was utilized as a proxy variable for Chinese economic growth.

For data processing, on the one hand, there were generally statistical problems such as too high lagged order and more parameters to be estimated when modeling using daily high-frequency data of BDI, Brent, and SSE, resulting in biased estimation results. On the other hand, since the GDP only had quarterly and annual data, in order to facilitate the analysis and ensure sufficient sample capacity, the mixed-frequency data were transformed into quarterly data with the same frequency. The data period was from the first quarter of 1992 to the second quarter of 2020, and the data were from the Wind database. In order to remove the effect of seasonal variation, all variables were seasonally adjusted using the X-12 technique. Next, a standardized treatment that removed the long-term trend and divided it by the standard deviation was applied to all variables in order to portray the short-term volatility of the variables and to remove the effects of the magnitudes.

4.2. Preliminary Analysis

4.2.1. Unit Root Test. The TVP-SV-VAR model requires the observed variables to be stationary, and in order to prevent the occurrence of pseudoregression, the unit root test should be performed on each variable before modeling. In this paper, ADF was used to check the stationarity of the variables. There are three main types, which include only the Intercept term, Intercept and trend term, and None. In general, as long as one type of unit root test passes (i.e., the null hypothesis is rejected), the variable is considered to be stationary. The results are shown in Table 1. The results showed that the BDI, Brent, and SSE rejected the null hypothesis at the 1% significance level, and GDP also passed tests for "Intercept," "Intercept and trend," and "None" at the 5%, 10%, and 1% significance levels, respectively. In conclusion, all variables followed $I(0)$ and could be further analyzed empirically.

4.2.2. Parameter Test. This article used OxMetrics 6 software and the TVP-SV-VAR package written by Jouchi Nakajima, a measurement economist at the Bank for International Settlements, to estimate the model. According to the AIC, BIC, and SC criteria, the optimal lag for the TVP-SV-VAR was identified as 2. Next, to compute the posterior estimates, we draw 10,000 samples using Monte Carlo Markov Chains (MCMC). The estimation results are shown in Table 2 and Figure 1. Table 2 provides the distribution of posteriors, the convergence diagnostics of Geweke, and inefficient factors computed by using MCMC sampling. For the convergence diagnosis, at the 5% significance level, the null hypothesis of convergence to the posterior distribution was rejected, implying that all parameters converge to the posterior distribution of the MCMC simulation, and we achieved the expected effect. Furthermore, the inefficient factors were rather low, within 100. The inefficient factor of $(\Sigma_h)_2$ was the largest, as high as 97.65, which meant that there were only 102 (10000/97.65) irrelevant samples in 10,000 simulations. That was why the number of efficient samples for parameters and state variables were sufficient. Figure 1 successively reveals sample autocorrelations, sample paths, and posterior densities of parameters for each row. The sample autocorrelations at the first row decreased rapidly and kept slightly ranging around the 0 level, illustrating that the majority of the sample was of low autocorrelation. The second row showed that the sample paths were stable without many

Table 1: The results of unit root test.

Variables	Intercept		Intercept and trend		None	
	Statistics	P values	Statistics	P values	Statistics	P values
BDI	−4.5724	0.0003***	−4.5421	0.0024***	−4.6027	<0.0001***
Brent	−4.4513	0.0005***	−4.4115	0.0035***	−4.4810	<0.0001***
SSE	−5.5503	<0.0001***	−5.5171	<0.0001***	−5.5834	<0.0001***
GDP	−3.2930	0.0185***	−3.3143	0.0713*	−3.2511	0.0014***

***,**, and * show the significance at the 1%, 5%, and 10%, respectively.

Table 2: The results of TVP-SV-VAR parameter estimation.

Parameter	Mean	Std. dev.	95% interval	Geweke	Inef.
$(\Sigma_\beta)_1$	0.0229	0.0026	[0.0184, 0.0288]	0.890	5.80
$(\Sigma_\beta)_2$	0.0226	0.0026	[0.0182, 0.0284]	0.692	4.44
$(\Sigma_\alpha)_1$	0.0666	0.0208	[0.0382, 0.1184]	0.822	36.20
$(\Sigma_h)_1$	0.6182	0.1454	[0.3684, 0.9318]	0.071	30.74
$(\Sigma_h)_2$	0.9799	0.2776	[0.5439, 1.5799]	0.053	97.65

Note: Σ_β and Σ_α are the values multiplied by 100.

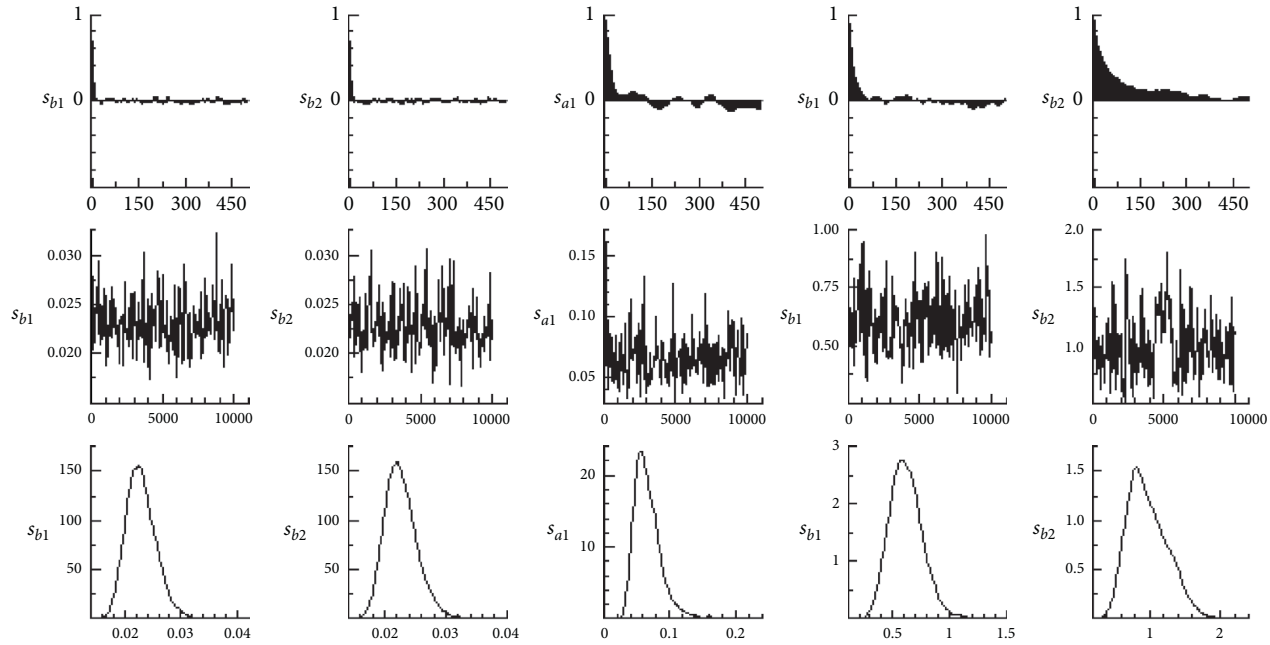

Figure 1: Sample autocorrelations (top), sample paths (middle), and posterior densities (bottom).

extreme values, which meant that the samples produced from MCMC were effective.

5. Empirical Results

This section mainly relied on two types of time-varying impulse response functions from the TVP-SV-VAR model to analyze the nonlinear dynamic interactions among the world oil market, the global shipping market, the Chinese stock market, and economic growth. The impulse response was sorted into the impulse response at different periods ahead and impulse response at different time points. Both impulse responses are influenced by the same factors and depict time-varying characteristics, but the impulse response is represented from a different perspective. Firstly, we chose shocks arising at 3 different periods ahead in terms of the response of variables at every time point: 2-quarter, 4-quarter, and 8-quarter, portraying short-, medium-, and long-term phases, respectively. Next, we chose shocks arising at different time points to describe the time-varying impulse response: 2008Q4, 2014Q2, and 2020Q1, representing the three periods of the global financial crisis, the international oil price crash, and COVID-19, respectively.

5.1. The Effect of BDI on Stock Prices and GDP in China

5.1.1. The Effect of Impulse Responses from Shocks at Three Different Periods Ahead. The impulse response of GDP to the BDI showed time-varying characteristics, as shown in Figure 2(a). The direction of the impulse response function

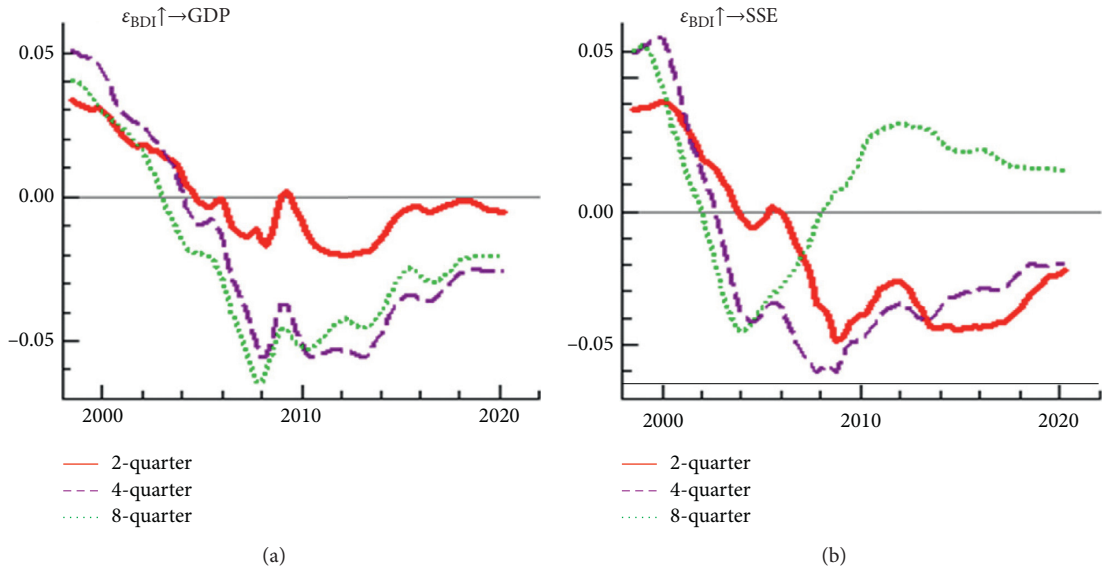

Figure 2: Impulse responses from shocks at three different periods ahead: (a) BDI ⟶ GDP; (b) BDI ⟶ SSE.

under different lag periods was basically the same. Specifically, it can be divided into three stages. The first stage was from 1998 to 2007. In this period, the impulse response of GDP to the BDI varied widely. The second stage was from 2008 to 2014, when the impact of the BDI on GDP was relatively smooth. The third stage was after 2015, when the impulse response of GDP to the BDI began to reverse, and the fluctuations became obvious. For the shock direction and intensity, in the first stage, there was a shift from "positive" to "negative" shocks. This was mainly due to the gradual increase in trade after the Asian financial crisis in 1997, when the economies of all countries began to recover. And, with China's accession to the WTO, China had become the world's number one processing plant with its low cost and promising market. China's economy began to boom. In this context, due to the economic recovery and the huge trade volume, the freight rates in the shipping market remained high, but the negative impact brought by the rise in shipping freight rates did not offset the positive impact brought by China's accession to the WTO on the economic interests of China. In other words, the positive impact of the increase in "trade volume" on China's economy was far greater than the negative impact of the increase in "freight rate" on China's economy. After that, during the period of 2004–2007, under the multiple drivers of the continuous growth of oil demand, frequent emergencies, and speculation, the international oil price began to enter the rising channel. Driven by the recovery of international trade demand and soaring oil prices, the BDI also showed favorable fluctuations and began to rise sharply, with the highest point breaking through 10,000 points, hitting a new historical high. After China's accession to the WTO, the volume of trade was huge, and the soaring BDI undoubtedly formed a constraint on the development of China's outbound-oriented economy. That is to mention, the negative impact of the increase in "freight prices" on China's economy outweighed the positive impact of the increase in "trade volume" on China's economy. In the second stage, the BDI produced negative shocks to GDP, with a smooth impulse response and the strongest shocks. After the 2008 financial crisis, the international oil price and the BDI plummeted. At this stage, GDP had the greatest response to the BDI shocks, indicating that the impact of the BDI on GDP was more pronounced during the period of increasing uncertainty in the international political and economic situations. In the third stage, the impulse response trend of GDP to the BDI began to reverse and to climb upward. It still showed a negative correlation, but the intensity of the shock gradually decreased. The impact of rising freight rates on China's economy stepped into a downward channel, which may be related to China's entry into the new normal of economic development and the transformation of the economic structure. The nonlinear dynamic response trends converged from different lag periods, but the lag 8 periods had the smallest shock strength, while the lag 2 and lag 4 periods' shocks were the strongest. As the lag period continues to increase, the impact intensity of the BDI to GDP gradually decreased.

The impact of the BDI on the SSE Composite Index was time-varying (BDI ⟶ SSE), as shown in Figure 2(b). Similar to the GDP response, the stock price response to the BDI shock also showed a general trend from "positive" to "negative," but the difference was that the lag 8 period turned to positive after a short period of negative range fluctuation. For the perspective of different periods, the BDI mainly produced negative impact on stock price under lag 2 and lag 4 periods. For lag 8 period, there was a shift from "positive" to "negative" to "positive" impact on stock price, but it mainly showed positive impact. The results indicated that positive BDI shocks had a dampening effect on stock prices in the short and medium term, and the positive BDI shocks promoted stock market prosperity in the long-term perspective. Rising ship freight rates may make shipping stocks perform strongly, and there was a structural bull market. However, rising transportation costs for bulk commodity

trade raised the cost of imports, which may have affected corporate performance. Thus, in the short and medium term, rising BDI dampened the stock market boom. From a long-term perspective, the continuous rise of BDI signaled the recovery and prosperity of the global economy, which was conducive to the formation of stable economic growth expectations for investors, further promoting stock market prosperity. Similar to GDP, it can also be divided into three stages: 1998–2007 (the impulse response function changed greatly and was unstable), 2008–2014 (the impulse response function fluctuated smoothly), and after 2015 (the impulse response function started to climb). For the shock direction and intensity, in the first stage, the impulse function under different lag periods were successively from "positive" to "negative." In the second stage, the lag 2 and 4 period impulse curves were less amplitude and basically stable, but the impact intensity was the strongest, while the lag 8 period impulse curve began to reverse, from "negative" to "positive." In the third stage, whether in the short, medium, or long term, the intensity of BDI shocks gradually converged.

5.1.2. The Effect of Impulse Responses from Shocks at Three Different Time Points. Figure 3 reflects the potential impact of BDI on Chinese stock market and economic growth at three different time points. The impulse response of GDP to the BDI (Figure 3(a)) depicted that the direction of shocks at three time points, 2018Q4, 2014Q2, and 2020Q1, were consistent and largely negative. However, the shocks varied in intensity at different time points, with the largest shock under the financial crisis, followed by the oil price crash, and the smallest shock under COVID-19. It indicated that the impact of China's economy on external shipping market shocks gradually decreased over time; that is, higher freight rates had a lower negative impact on the Chinese economy, which may be related to the gradual decrease in the dependence of the Chinese economy on foreign trade. From the impulse response of SSE to the BDI (Figure 3(b)), we found that the impulse response at different time points showed a trend from "positive" to "negative" to "positive." There was a negative impact in the short and medium term, but the long-term promotion effect was obvious, which further verified the previous analysis. For impact intensity, it also showed that the shock weakened over time and the ability to resist risks increased.

5.2. The Effect of Brent on BDI, Chinese Stock Prices, and GDP

5.2.1. The Effect of Impulse Responses from Shocks at Three Different Periods Ahead. According to the impulse response of GDP to Brent at three different periods ahead, the impulse response had significant nonlinear time-varying characteristics, which largely depended on the Chinese stage of economic development such as industrial structure optimization and business cycle fluctuations (Figure 4(a)). The impulse response of GDP to Brent was mainly divided into three stages, which were from 1998 to 2003 as the first stage, from 2004 to 2012 as the second stage, and from 2012 to 2020 as the third stage. In the first stage, the impulse response intensity from the short term, medium term, and long term was small. According to China's national conditions, this paper considered that China was building the basic framework of the socialist market economy system and was in the initial stage. In this stage, the impact of the international crude oil market had limited impact on Chinese economy. In the second stage, the impulse response intensity of GDP to Brent from the short term, medium term, and long term was more severe. There are two main reasons: the first point was that basic conditions for Chinese economic response to the international crude oil market have matured during the initial improvement of the socialist market economic system, such as the exchange rate system; the second point is that the rapid development of Chinese heavy chemical industry in this stage indirectly drove the demand for crude oil. However, due to the limited element endowments of crude oil, China was highly dependent on international crude oil imports, which further intensified the response of GDP to Brent. In the third stage, the impulse response intensity from the short term was still intense; however, the impulse response intensity from the medium-term and long-term shocks gradually weakened. Based on Chinese development characteristics, we found that China had entered a stage of comprehensively deepening reform and development since 2012, in which the optimization of the industrial structure and economic development entered a new normal. Besides, the tertiary industry had the rapid development, and the proportion of energy-intensive industries has declined in this stage. The response of different industries to crude oil prices was heterogeneous in China, among which the metal mining and processing industries that used crude oil and its related products as power resources had the greatest negative effects. Therefore, the impulse response of GDP to Brent was blocked because of industrial optimization and structural transformation to a certain extent.

From the impact direction, the short-term impulse response function of Brent to GDP was positive. In terms of the direction of shocks, the short-term impulse response function of Brent to GDP was positive. It showed that there was a strong positive correlation between oil prices and China's economic growth, and higher oil prices stimulated economic growth in the short run. China was in a medium to high stage of development, with rapid industrial development and a strong demand for oil. When world oil prices rose, there was a time lag in decision-making in the industrial sector. Therefore, in the short term, rising oil prices boosted economic growth. In the medium and long term, oil prices affected economic development by influencing the cost of upstream production of raw materials to affect the downstream related production sector of factor inputs and the consumption side of the product price level and ultimately affected economic development. As a result, over time, the industrial sector became aware of the increased production costs associated with higher oil prices. Companies started taking practical actions and reduced their future production plans. Therefore, the existence of higher oil prices in the medium and long term had a negative impact on the economy. However, the impulse response of

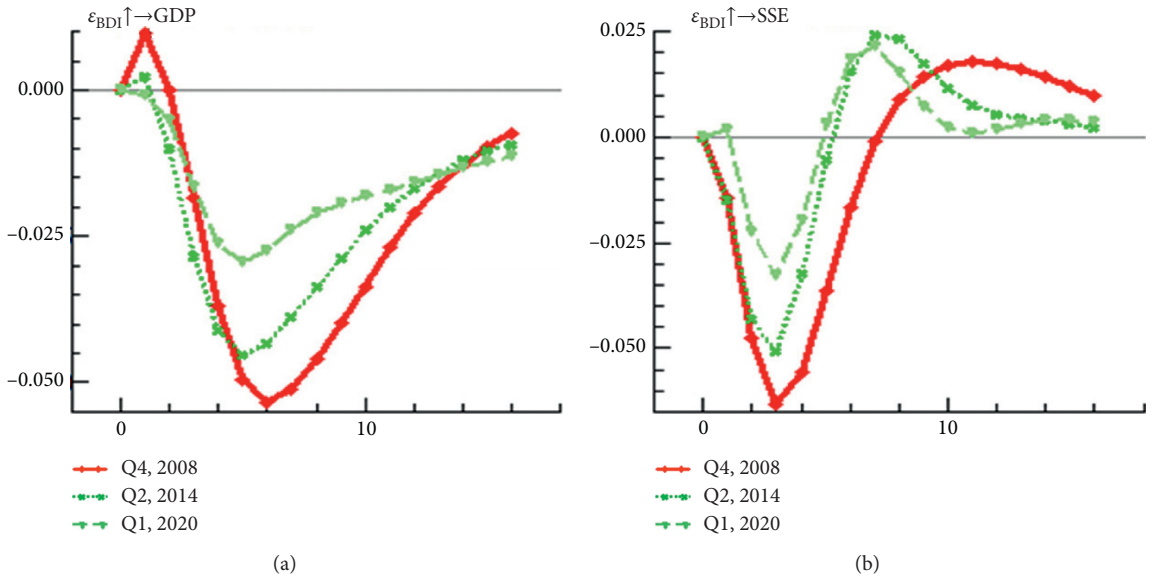

Figure 3: Impulse responses from shocks at three different time points: (a) BDI ⟶ GDP; (b) BDI ⟶ SSE.

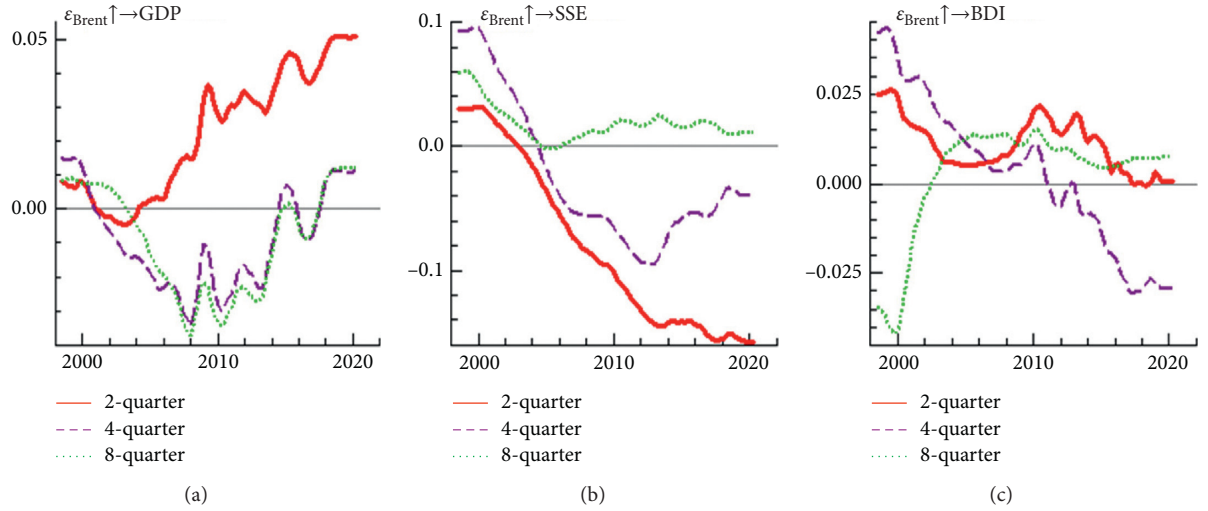

Figure 4: Impulse responses from shocks at three different periods ahead: (a) Brent ⟶ GDP; (b) Brent ⟶ SSE; (c) Brent ⟶ BDI.

GDP to Brent turned from negative to positive. Oil price growth had a positive relationship with economic growth in this stage, which verified the research results of Du et al. [32] and Mo et al. [33].

The impulse response of SSE to Brent had obvious nonlinear characteristics (Figure 4(b)). The oil price affected the stock market in two main aspects. On the one hand, oil prices increased the cost of production, which affected corporate performance and ultimately stock prices. On the other side, it was transmitted through the intermediary variable of sentiment. The stronger the investor panic was, the greater the awareness of short selling was, which negatively affected stock prices. The first phase was from 1998 to 2005. The short-, medium-, and long-term impulse responses were positive, and the impact intensity gradually reduced. The stock market was in a growth period with a strong speculative atmosphere, which combined with the low oil price formed a positive stock market response to the crude oil market shock. The second stage was after 2006, when China achieved full liquidity of the stock market, and the stock market reform was basically completed. At this stage, the impulse response function was negative in the short and medium term but positive in the long term. In this paper, it was argued that the positive oil price shock deeply affected the production costs and investor sentiment of the whole industrial chain and thus played a restraining role on the stock market. So, the impulse response function in the short and medium term was consistent with economic theory. However, in the long run, Chinese economy had maintained a medium-to-high-speed development all year round, and oil prices had risen simultaneously with Chinese economic growth. Therefore, the long-term impulse response function conformed to the actual situation in China.

The impulse response of the BDI to Brent can be divided into two phases (Figure 4(c)). The first phase was from 1998 to 2004. In this phase, the impulse response of BDI to Brent

was positive in the short and medium term, but negative in the long term. In the short term, positive fluctuations in crude oil prices were transmitted through transportation costs to the BDI, causing freight rates to rise, which was consistent with the short- and medium-term impulse response trends at this stage. But in the long run, the shipping market was more depressed at this stage, and rising oil prices played a restraining role on the shipping market. The second stage was after 2005. In this stage, the impulse response of the BDI to Brent was positive in the short term, which was consistent with economic logic. In the medium term, the impulse response of the BDI to Brent had a negative impact. In the long term, the impact was again positive. This may be due to the fact that the characteristics of oil as a commodity gradually emerged, and it rapidly rose due to speculation, unexpected events, and other factors, but the demand for iron ore, grain, and other dry bulk transport was relatively stable. Therefore, in the medium term, oil prices were running counter to the BDI phenomenon.

5.2.2. The Effect of Impulse Responses from Shocks at Three Different Time Points. The impact intensity of Brent on GDP at different time points showed heterogeneity (Figure 5(a)). From the impact direction, the impulse response of GDP to Brent shifted from "positive" to "negative" in period 6 during the 2008 financial crisis and the 2014 oil price crash. However, during the COVID-19 period, the impulse response of GDP to Brent always remained positive. From the impact intensity, the oil price shock to the Chinese economy during the 2008 financial crisis was the strongest and most harmful. Furthermore, the intensity impact of the oil price on China's economy in case of unexpected events gradually diminished over time, and the intensity impact of the oil price on China's economy even turned positive during COVID-19. This may be related to China's structural economic transformation and environmental policies such as "oil to gas."

As economic globalization continued to advance, the connection between markets was becoming closer, and the interaction between the international crude oil market and the Chinese stock market was strengthening, which was reflected in a more intense impulse response of the stock market to oil prices. Specifically, the impulse response trend of SSE to Brent at different time points was similar (Figure 5(b)). The impulse response of the stock market to Brent was predominantly negative. The impact intensity was the highest when the lag was two periods, and then, it gradually changed from negative to positive and finally converged to 0. The results presented that the impact intensities at different time points were heterogeneous. Brent's impact intensity on the SSE was the highest during COVID-19 and the lowest during the financial crisis. The impact intensity of Brent on the stock market was stronger during COVID-19 and the 2014 oil price crash than the impact intensity of Brent on the stock market during the 2008 financial crisis. In addition, as China's stock market continued to open up and develop over time, the stock market had become more susceptible to investor sentiment and economic uncertainty and had become more responsive to major events. So, the impact intensity of oil price on the stock market increased.

The impulse response of the BDI to Brent exhibited distinct time-varying characteristics (Figure 5(c)). The impulse response of the BDI to Brent reached a maximum in the second period and then gradually weakened. The results showed that in the short run, the impact intensity of Brent on the BDI during the oil price crash and financial crisis was less than that of the COVID-19 period, and impact intensity decayed to zero after the 14^{th} period. During the 2008 financial crisis, the impulse response of the BDI to Brent was consistently positive, and the duration of Brent to BDI shocks was longer.

5.3. The Dynamic Nexus between GDP and the Stock Market in China

5.3.1. The Effect of Impulse Responses from Shocks at Three Different Periods Ahead. According to Chinese empirical data, the impulse response of GDP to SSE had a significant promotion effect (Figure 6(b)) at three different periods ahead. From impact intensity, a prosperous stock market boosted a prosperous economy. From the impulse response of SSE to GDP (Figure 6(a)), the Chinese stock market and the economic growth showed a positive correlation at three different periods ahead before 2008. After 2008, it began to reverse and showed a negative effect. This may be related to the successive introduction of countercyclical economic policies after the financial crisis, which led investors to gradually build up an expectation that the authorities would implement austerity policies when the economy overheats. In summary, there was a negative feedback adjustment mechanism between the stock market and the economy in China after 2008.

5.3.2. The Effect of Impulse Responses from Shocks at Three Different Time Points. Figure 7(b) demonstrates that the impulse response of GDP to SSE was positive at three different time points. Figure 7(a) demonstrates that the impulse response of SSE to GDP at three different time points was negative. It was further verified that there was a negative feedback adjustment mechanism between the Chinese economy and the stock market after 2008. And, the absolute value of the impact intensity of GDP on the stock market at different time points was greater than the absolute value of the impact intensity of SSE on GDP. In other words, the impact of the economy on the stock market was greater than the impact of the stock market on the economy.

5.4. Variance Decomposition of SSE and GDP. Table 3 shows the variance contribution of influencing factors to China's stock market. It can be seen from Table 3 that the main reason for the change of China's stock market was Brent, which had a greater impact on the stock market than BDI. Overall, the impact of the stock market on itself gradually decreased over time. First, GDP had little effect on the stock

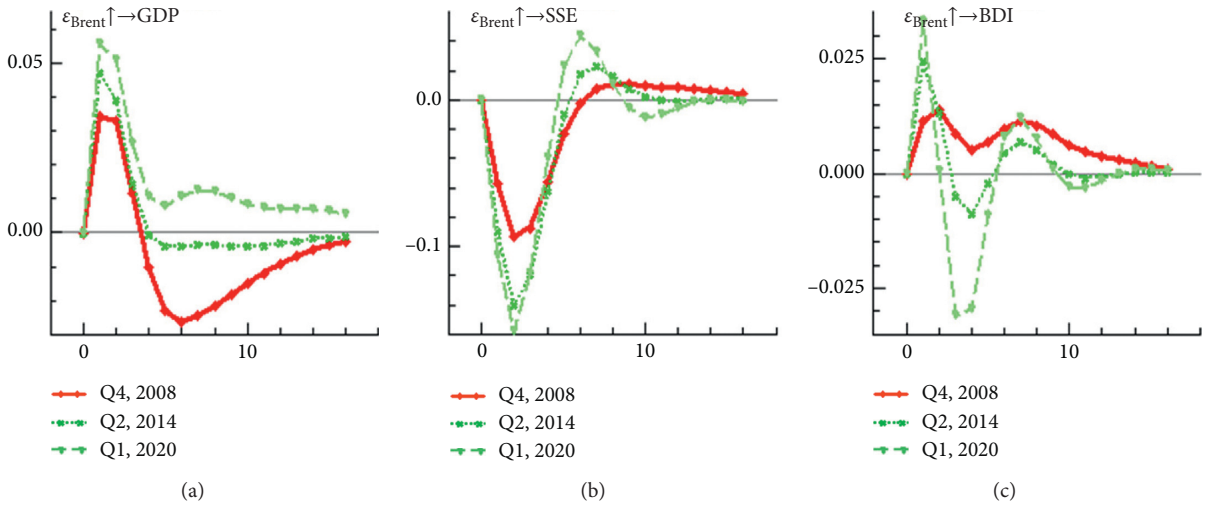

Figure 5: Impulse responses from shocks at three different time points: (a) Brent ⟶ GDP; (b) Brent ⟶ SSE; (c) Brent ⟶ BDI.

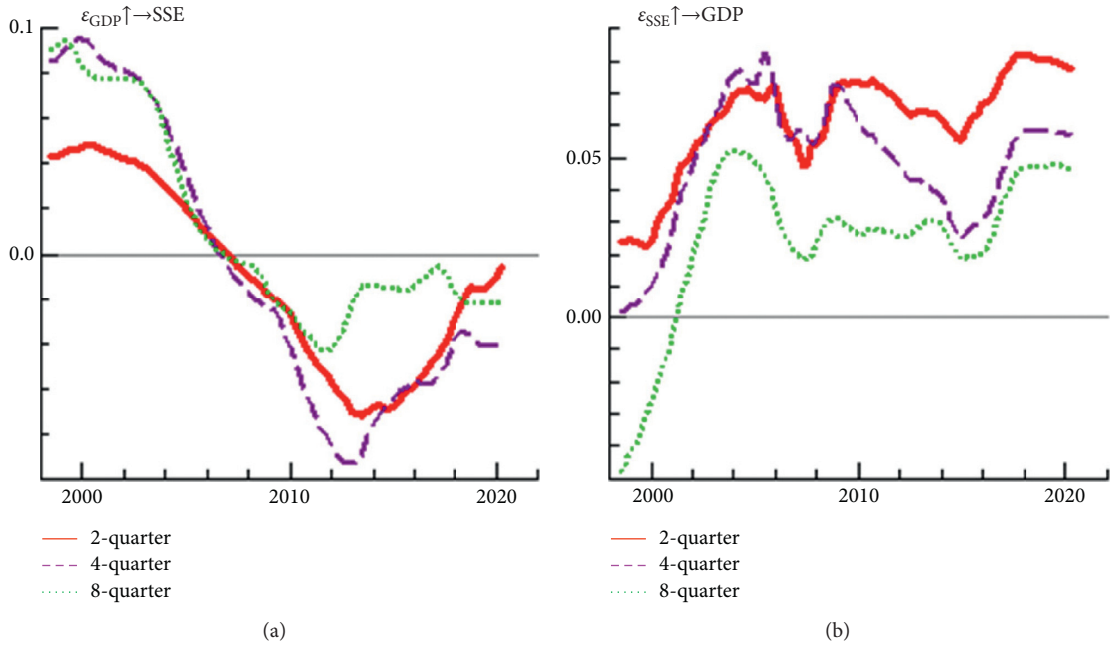

Figure 6: Impulse responses from shocks at three different periods ahead: (a) GDP ⟶ SSE; (b) SSE ⟶ GDP.

market in the current GDP. As the stock market is a barometer of the macro economy, GDP in the current period acted on the stock market by influencing investors' expectations. Therefore, the stock market was more influenced by investors' expectations of GDP. With the continuous extension of GDP lag period, investor expectations were constantly strengthened, and the impact on the stock market was also increasing. Second, Brent's impact on stocks has deepened over time. As oil is known as the blood of modern industry, the industrial sector is highly dependent on oil. As a traditional manufacturing country, China's energy external dependence is high, and the fluctuation of oil price has a profound influence on China's economy. The fluctuation of oil price affects the performance of listed companies and investors' economic expectations, thus causing stock market turbulence. Last, the contribution rate of BDI reached its peak in the third phase. Since the BDI mainly measures dry bulk shipments, they have less impact on the economy than oil. Therefore, the impact of the BDI on the stock market decreased slowly with the extension of the lag period.

Table 4 shows the variance contribution of GDP influencing factors. As can be seen from Table 4, the main influencing factor of GDP change was itself. With the continuous extension of the lag period, the contribution rate gradually decreased from 88.20% to 73.40%. In terms of external factors, Brent's contribution to the Chinese economy was the highest, at around 20%. As the lag period goes on, the contribution of the stock market and BDI to China's

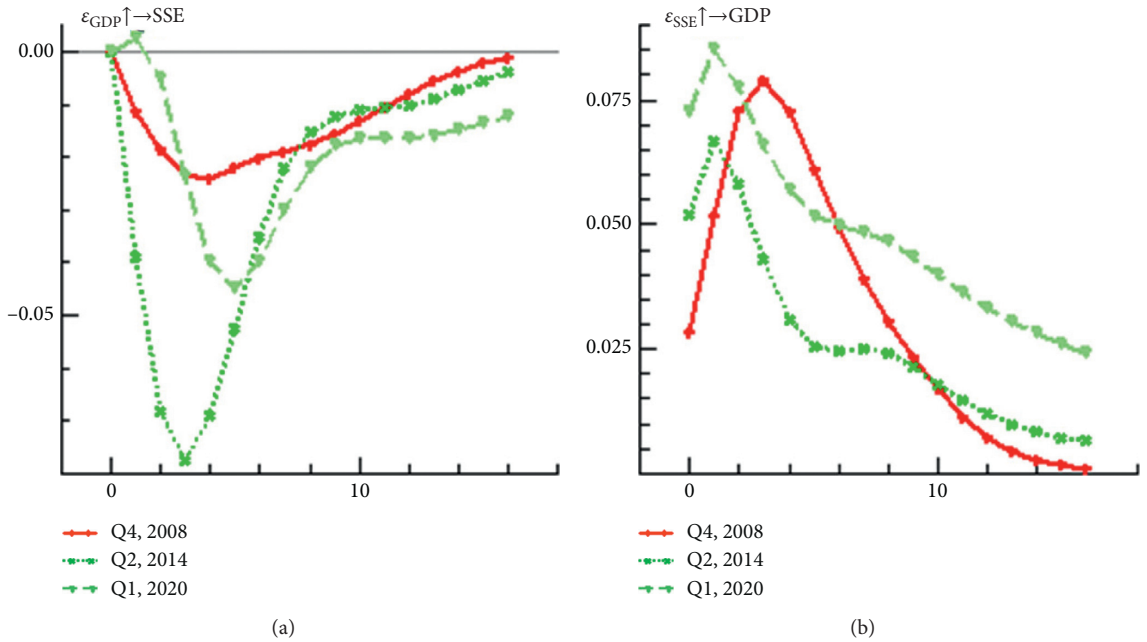

Figure 7: Impulse responses from shocks at three different time points: (a) GDP ⟶ SSE; (b) SSE ⟶ GDP.

Table 3: Variance decomposition of SSE.

Period	SSE	GDP	Brent	BDI
1	92.0898	0.0000	2.8734	5.0368
2	86.3341	0.3192	2.0115	11.3352
3	81.7636	0.7420	6.8049	10.6895
4	77.2484	2.6126	10.6633	9.4758
5	73.8604	5.3409	11.8618	8.9369
6	72.2636	7.2789	11.6972	8.7603
7	71.6974	7.8701	11.8249	8.6076
8	71.2704	7.7403	12.5623	8.4270
9	70.7282	7.6774	13.3012	8.2912
10	70.2546	7.8582	13.6581	8.2291

Table 4: Variance decomposition of GDP.

Period	GDP	SSE	Brent	BDI
1	88.1979	0.2228	11.5774	0.0019
2	80.8341	0.3045	18.4991	0.3623
3	77.3571	0.8465	21.4826	0.3138
4	75.5825	1.4968	22.5697	0.3510
5	74.8401	2.0422	22.5425	0.5752
6	74.4040	2.2692	22.4427	0.8841
7	74.1303	2.2880	22.3733	1.2084
8	73.8841	2.2835	22.3617	1.4707
9	73.6276	2.3354	22.3798	1.6572
10	73.4008	2.4142	22.4091	1.7760

economy gradually increased, but their contributions were generally low, which further demonstrated the importance of oil to manufacturing-oriented China.

6. Conclusions

This paper applied the TVP-SV-VAR model to analyze the nonlinear and time-varying effects of the world oil market and global shipping market on stock market and economic growth in China. The study used quarterly frequency data for the 1998Q1–2020Q2 period. The empirical results provide strong support for the presence of time-varying characteristics between the variables under study as follows:

First, from the impact direction, the impacts of the international shipping market on China's economy in different lag periods show a "positive" to "negative" shift. This is mainly due to the gradual increase in trade after the Asian financial crisis in 1997, when the economies of various countries begin to recover. And, with China's accession to the WTO, China has become the world's number one processing plant with its low cost and promising market. Against this backdrop, the negative impact of rising shipping costs cannot offset the positive impact of WTO accession on China's economic interests; that is, the positive impact of the increase in trade volume on China's economy is far greater than the negative impact of the increase in freight prices on China's economy. Then, as trade growth declines, BDI fluctuations begin to have a negative impact on the Chinese economy; that is, the negative impact of higher freight prices on China's economy outweighs the positive impact of higher trade volumes on China's economy. From the impact intensity, the impact of the BDI on China's economy and stock market is more pronounced during the period of increased uncertainty in the international political and economic

situations. From the lag period, the impact intensity of the BDI on GDP has a distinct medium- to long-term effect as the lag period increases and the intensity of the shock increases. In addition, a positive BDI shock has a dampening effect on stock prices in the short and medium term, while a positive BDI shock can promote stock market prosperity in the long-term perspective. The impulse responses of SSE and GDP to BDI show that the external shipping market shocks to Chinese stock market and economic growth gradually become smaller over time, indicating that the ability to resist risks increases in China.

Second, the impulse response of China's economy and securities market to the fluctuation of international oil prices is affected by China's economic development, energy structure, major international emergencies, and the level of oil prices, which has a nonlinear time-varying characteristic. From the impact direction, the oil price has a strong positive correlation with China's economic growth due to the time lag in decision-making in the industrial sector, and rising oil prices can stimulate economic growth in the short-term. Over time, the industrial sectors gradually realize the problem of higher production costs caused by higher oil prices, and companies start to take practical actions and reduce their future production plans. In the medium to long term, therefore, the existence of higher oil prices has a negative impact on the economy. Furthermore, the intensity impact of the oil price on China's economy in case of unexpected events has gradually diminished over time, and the intensity impact of the oil price on China's economy even turned positive during COVID-19. This may be related to China's structural economic transformation and environmental policies such as the "oil to gas." In addition, as China's stock market continues to open up and develop over time, the stock market has become more susceptible to investor sentiment and economic uncertainty and has become more responsive to major events. So, the impact intensity of oil price on the stock market has increased.

Last, after the 2008 financial crisis, the stock market boom has promoted economic prosperity, and economic prosperity has dampened stock market boom conversely, which proves that there existed a negative feedback adjustment mechanism between the stock market and the economy. Besides, the absolute value of the impact intensity of GDP on the stock market at different time points is greater than the absolute value of the impact intensity of the stock market on GDP; i.e., the economy affects the stock market more than the stock market affects the economy.

Data Availability

All data used have been included in the Wind database and are also available from the corresponding author upon request.

Conflicts of Interest

The authors declare that there are no conflicts of interest regarding the publication of this paper.

Acknowledgments

This work was supported by the National Natural Science Foundation of China (NSFC) (71874133), Annual Basic Scientific Research Project of Xidian University (2019), and Youth Innovation Team of Shanxi Universities.

References

[1] X. Zhang, T. Xue, and H. E. Stanley, "Comparison of econometric models and artificial neural networks algorithms for the prediction of baltic dry index," *IEEE Access*, vol. 1, 2018.

[2] R. Qingsong, W. Yao, and L. Xinsheng, "Cross-correlations between baltic dry index and crude oil prices," *Physica A: Statistical Mechanics and its Applications*, vol. 453, 2016.

[3] A. Arigoni, A. Newman, C. Turner, and C. Kaptur, "Optimizing global thermal coal shipments," *Omega*, pp. 118–127, Elsevier, Amsterdam, Netherlands, 2017.

[4] P.-y. Nie and Y.-C. Yang, "Effects of energy price fluctuations on industries with energy inputs: an application to China," *Applied Energy*, vol. 165, pp. 329–334, 2016.

[5] B. Ou, X. Zhang, and S. Wang, "How does China's macroeconomy response to the world crude oil price shock: a structural dynamic factor model approach," *Computers & Industrial Engineering*, vol. 63, no. 3, pp. 634–640, 2012.

[6] S. A. Basher, A. A. Haug, and P. Sadorsky, "Oil prices, exchange rates and emerging stock markets," *Energy Economics*, vol. 34, no. 1, pp. 227–240, 2012.

[7] D. Cheng, X. Shi, J. Yu, and D. Zhang, "How does the Chinese economy react to uncertainty in international crude oil prices?" *International Review of Economics & Finance*, vol. 64, 2019.

[8] L. Zhao, X. Zhang, S. Wang, and S. Xu, "The effects of oil price shocks on output and inflation in China," *Energy Economics*, vol. 53, pp. 101–110, 2016.

[9] W. J. Kim, S. Hammoudeh, J. S. Hyun, and R. Gupta, "Oil price shocks and China's economy: reactions of the monetary policy to oil price shocks," *Energy Economics*, vol. 62, pp. 61–69, 2017.

[10] H. Bloch, S. Rafiq, and R. Salim, "Economic growth with coal, oil and renewable energy consumption in China: prospects for fuel substitution," *Economic Modelling*, vol. 44, pp. 104–115, 2015.

[11] T. Liang, J. Chai, Y.-J. Zhang, and Z. G. Zhang, "Refined analysis and prediction of natural gas consumption in China," *Journal of Management Science and Engineering*, vol. 4, no. 2, pp. 91–104, 2019.

[12] P. K. Narayan and S. S. Sharma, "New evidence on oil price and firm returns," *Social Science Electronic Publishing*, vol. 35, no. 12, 2011.

[13] P. K. Narayan and S. S. Sharma, "Firm return volatility and economic gains: the role of oil prices," *Economic Modelling*, vol. 38, pp. 142–151, 2014.

[14] D. H. B. Phan, S. S. Sharma, and P. K. Narayan, "Oil price and stock returns of consumers and producers of crude oil," *Journal of International Financial Markets, Institutions and Money*, vol. 34, pp. 245–262, 2015.

[15] D. H. B. Phan, S. S. Sharma, and P. K. Narayan, "Stock return forecasting: some new evidence," *International Review of Financial Analysis*, vol. 40, pp. 38–51, 2015.

[16] X. Wen, Y. Guo, Y. Wei, and D. Huang, "How do the stock prices of new energy and fossil fuel companies correlate?

evidence from China," *Energy Economics*, vol. 41, pp. 63–75, 2014.
[17] Z. Ding, Z. Liu, Y. Zhang, and R. Long, "The contagion effect of international crude oil price fluctuations on Chinese stock market investor sentiment," *Applied Energy*, vol. 187, pp. 27–36, 2017.
[18] O. Erdogan, K. Tata, B. C. Karahasan et al., "Dynamics of the co-movement between stock and maritime markets," *International Review of Economics & Finance*, vol. 25, 2013.
[19] A. H. Alizadeh and G. Muradoglu, "Stock market efficiency and international shipping-market information," *Journal of International Financial Markets, Institutions and Money*, vol. 33, pp. 445–461, 2014.
[20] A. J. Lin, H. Y. Chang, and J. L. Hsiao, "Does the baltic dry index drive volatility spillovers in the commodities, currency, or stock markets?" *Transportation Research Part E: Logistics and Transportation Review*, vol. 127, pp. 265–283, 2019.
[21] E. Melike, "Baltic dry index as a major economic policy indicator: the relationship with economic growth," *Procedia-Social and Behavioral Sciences*, vol. 210, pp. 416–424, 2015.
[22] F. Lin and N. C. S. Sim, "Trade, income and the baltic dry index," *European Economic Review*, vol. 59, pp. 1–18, 2013.
[23] F. Lin and D. Fu, "Trade, institution quality and income inequality," *World Development*, vol. 77, pp. 129–142, 2016.
[24] L. Han, J. Jin, L. Wu, and H. Zeng, "The volatility linkage between energy and agricultural futures markets with external shocks," *International Review of Financial Analysis*, vol. 68, 2020.
[25] L. Han, Li Wan, and Y. Xu, "Can the baltic dry index predict foreign exchange rates?" *Finance Research Letters*, vol. 32, 2020.
[26] Y.-J. Zhang, "Speculative trading and WTI crude oil futures price movement: an empirical analysis," *Applied Energy*, vol. 107, pp. 394–402, 2013.
[27] D. Zhang, Q. Ji, and A. M. Kutan, "Dynamic transmission mechanisms in global crude oil prices: estimation and implications," *Energy*, vol. 175, pp. 1181–1193, 2019.
[28] S. J. Byun, "Speculation in commodity futures markets, inventories and the price of crude oil," *The Energy Journal*, vol. 38, no. 5, pp. 93–113, 2017.
[29] E. D. Attanasi, "Bitumen prices and structural changes in north American crude oil markets," *Natural Resources Research*, vol. 25, no. 4, pp. 1–10, 2016.
[30] L. Tingting, L. Chao, and S. Rui, "The structure and dynamics of granular complex networks deriving from financial time series," *International Journal of Modern Physics C (IJMPC)*, vol. 31, 2020.
[31] H. Ding, H.-G. Kim, and S. Y. Park, "Crude oil and stock markets: causal relationships in tails?" *Energy Economics*, vol. 59, pp. 58–69, 2016.
[32] L. Du, H. Yanan, and C. Wei, "The relationship between oil price shocks and China's macro-economy: an empirical analysis," *Energy Policy*, vol. 38, no. 8, pp. 4142–4151, 2010.
[33] B. Mo, C. Chen, H. Nie, and Y. Jiang, "Visiting effects of crude oil price on economic growth in BRICS countries: fresh evidence from wavelet-based quantile-on-quantile tests," *Energy*, vol. 178, no. 1, pp. 234–251, 2019.

Hindawi
Complexity
Volume 2021, Article ID 6670222, 15 pages
https://doi.org/10.1155/2021/6670222

Research Article

5D Nonlinear Dynamic Evolutionary System in Real Estate Market

Jingyuan Zhang

Business School, Hunan University, Changsha 410082, Hunan, China

Correspondence should be addressed to Jingyuan Zhang; jingyuanzh@hnu.edu.cn

Received 14 October 2020; Revised 3 December 2020; Accepted 28 December 2020; Published 11 January 2021

Academic Editor: Huajiao Li

In this paper, we propose a new predator-prey nonlinear dynamic evolutionary model of real estate enterprises considering the large, medium, and small real estate enterprises for three different prey teams. A 5D predator-prey nonlinear dynamic evolutionary system in the real estate market is established, where the large, medium, and small real estate enterprises correspond to three differential equations, provincial and local officials, and the central government correspond to the other two differential equations. Nonlinear dynamic analysis on a 5D predator-prey evolutionary system in the real estate market, containing the analysis of equilibrium points and stabilities, is made. The corresponding discrete system is simulated, and the simulation results about Lyapunov spectrum, bifurcation diagram, sequence diagram, and phase diagram are given. Compared with the work of Yang et al. in which all real estate enterprises corresponded to one differential equation, in our proposed model, the large, medium, and small real estate enterprises correspond to three differential equations which is more accordant with the specific circumstance of real estate companies.

1. Introduction

Since the reform in 1978, China began to implement the system of market economy which brings the upward trend in real estate investment. According to the statistics of the National Administration of Industry and Commerce in 2018, there are altogether 97,000 real estate developers registered in the National Administration of Industry and Commerce. The total number of permanent residents in China, consisting of more than 500 million urban residents and 300 million migrant workers, is over 8.8 million. There are more than 90,000 real estate enterprises with a permanent urban population of more than 800 million. According to data released by the National Bureau of Statistics, housing prices in major cities are still rising mostly, especially for new commercial residential buildings. So in China, real estate enterprises are very large groups and are also very important.

Nonlinear characteristics exist in systems with various research directions, such as chaotic circuit [1–7], neural network [8–15], and image encryption [16–18]. Competition of enterprises also has nonlinear characteristics. Puu [19] studied the adjustment process of three oligopolists, under Coumot and Stackelberg action. It is demonstrated that, with an isoelastic demand function and constant marginal costs, the system can result in periodic or in chaotic behavior. Based on the analysis, several useful issues are investigated either analytically or numerically. Agiza et al. [20] investigate the dynamics of a nonlinear discrete-time duopoly game, where the players have heterogeneous expectations. Two players with different expectations are considered: one is boundedly rational and the other thinks with adaptive expectations. The stability conditions of the equilibria were discussed. How the dynamics of the game depend on the model parameters was found. They demonstrate that as some parameters of the game are varied, the stability of Nash equilibrium is lost by period-doubling bifurcation. The chaotic features were justified numerically via computing Lyapunov exponents, sensitive dependence on initial conditions, and the fractal dimension. Ma and Pu [21] modeled a dynamic triopoly game characterized by firms with different expectations by three-dimensional nonlinear difference equations, where the market has quadratic inverse demand function and the firm possesses cubic total cost function. The local stability of Nash equilibrium was studied. Numerical simulations were presented to show that the

triopoly game model behaved chaotically with the variation of the parameters. Elsadany [22, 23] used three nonlinear difference equations to study the dynamic Cournot game with the characteristics of three bounded rational actors and analyzed the stability of the system. The global complexity analysis is helpful for behavior taking some effective measures, avoiding the collapse of the output dynamic competition game, and obtaining some practical and theoretical significance in the practice. Ahmed and Agiza [24] derived the dynamical system of n competitors in a Cournot game and studied the stability of its fixed point "Nash equilibrium." The effect of a modification of the price demand relation was pointed out. Zhao and Lv [25] studied a three-species food chain model with a Beddington-De Angelis functional response. The equilibrium states of the system were identified and their stability was analyzed analytically. The simulation results showed chaotic long-term behavior over a broad range of parameters. Elettreby and Hassan [26] proposed two different versions of the multiteam model where a team of two firms compete with another team. The firms in each team help each other. The equilibrium solutions and the conditions of their local asymptotic stability were studied. Elettreby and Mansour [27] studied an incomplete information dynamical system. Then, they suggested a modification of this system which was applied to the standard Cournot game. The equilibrium solutions and the conditions of their locally asymptotic stability for the static and the dynamic in monopoly and duopoly cases were studied. Elettreby [28] proposed a new multiteam prey-predator model, in which the prey teams help each other. Its local stability was studied. In the absence of a predator, there was no help between the prey teams. The global stability and persistence of the model without help were studied. Upadhyay et al. [29] studied the influence of top predator interference on the dynamics of food chain models including intermediate predators and top predators and found that there were different types of attraction sets including chaos. Elettreby and El-Metwally [30] applied the multiteam concept to the predator model and studied the global stability and persistence of the model without help. Liu et al. [31] investigated the appointed-time consensus problem under directed and periodical switching topologies. From a motion-planning perspective, a novel distributed appointed-time algorithm was developed for a multiagent system with double-integrator dynamics. Cotter and Roll [32] studied a comparative anatomy of residential REITs and private real estate markets: returns, risks, and distributional characteristics. REITs have somewhat less market risk than equity. Residential REIT characteristics differ from those of the S&P/Case–Shiller (SCS) private real estate markets. This is partly attributable to methods of index construction. They suggested that investment in residential real estate is far more risky than what might be inferred from the widely followed SCS series. The evolution of the real estate market is very complex and changeable, similar to the biological evolutionary process, falling within the scope of complexity. Motivated by this, the study uses the biological evolutionary process to explain the economic phenomenon in the real estate market. However, little research has quantitatively analyzed this process in the real estate market from the biological view. Yang and Tang [33] established a model on a three-dimension predator-prey evolutionary system in the real estate market. The model involved the relationship among private enterprises, provincial and local officials, and the central government in the real estate market using the population ecology theory of mutual relations. The complex dynamical behaviors of such a predator-prey model are investigated by means of numerical simulation. However, [33] considered all private enterprises as a prey team, and just one equation corresponds to the private enterprises. In fact, according to a 2015 real estate enterprise sales ranking, the private enterprises were divided into three levels [33]: first class: sales ≥ 100 billion; the second class: 20 billion $\leq$ sales < 100 billion; and the third class: sales < 20 billion. The first kind of private enterprises has great strength, can assist the third type of enterprises, or join cooperation evolution and development with the second category of private enterprises. Private enterprises in the second category compete or cooperate with other companies, having their own characteristics. The third-class private enterprises have relatively weak strength, requiring the help of other companies, in order to maintain survival in the real estate market. Thus, in [33], it is relatively unspecific for considering three types of real estate companies as a prey team, which does not fit the specific circumstance of real estate companies. In this paper, we propose a new model considering the large, medium, and small real estate enterprises for three different prey teams. A 5D predator-prey evolutionary system in the real estate market is established, where the large, medium, and small real estate enterprises correspond to three differential equations, provincial and local officials, and the central government correspond to the other two differential equations. Compared with literature [33] in which all real estate enterprises corresponded to a differential equation, in our proposed model, the large, medium, and small real estate enterprises correspond to three differential equations.

2. Model and Nonlinear Dynamic Analysis

2.1. Model. Let x be the density of large real estate companies, y the density of medium real estate companies, z the density of small real estate companies, u the density of provincial and local officials as predators, and v the center government, which can be growth-oriented central leaders who are intelligent designers of institutions that moderate the predator-prey relationship. The ecosystem on the top of the predator-prey interactions is the institutional framework subject to adjustment by the central government and a, b, c, d, e, f, h are parameters. Large enterprises can help medium-sized and small enterprises, and large enterprises, medium-sized enterprises, and small enterprises are affected by each other; and α, β, and γ are their influence coefficients. The nonlinear differential equation can be established as follows:

$$\begin{cases} \dfrac{\mathrm{d}x}{\mathrm{d}t} = ax(1-x) - xu + \alpha xyzu, \\ \dfrac{\mathrm{d}y}{\mathrm{d}t} = by(1-y) - yu + \beta xyzu, \\ \dfrac{\mathrm{d}z}{\mathrm{d}t} = cz(1-z) - zu + \gamma xyzu, \\ \dfrac{\mathrm{d}u}{\mathrm{d}t} = -\mathrm{d}u^2 + exu + fyu + gzu, \\ \dfrac{\mathrm{d}v}{\mathrm{d}t} = hv - \dfrac{v^2}{u}, \end{cases} \tag{1}$$

where in the absence of any predation u, each team of preys grows logistically; this is a $x(1-x)$, b$y(1-y)$, $cz(1-z)$; and the terms $-xu$, $-yu$, and $-zu$ denote the reduction in the prey growth rate because of the effect of the predation. The teams of preys help each other against the predator, that is, a $xyzu$ term exists. In the absence of any prey for sustenance, the predator's death rate results in inverse decay, that is, the term $-\mathrm{d}u^2$. The prey's contribution to the predator growth rate is exu, fyu, and gzu, that is proportional to the available prey as well as the size of the predator population. hv measures the value of self-reproduction of top predator v. In this paper, it is central government $-v^2/u$ denotes the effect of predator u on v.

2.2. Nonlinear Dynamic Analysis for the Model

2.2.1. Solution of Equilibrium Points. In order to find the equilibrium points, the right side of equation (1) is set as zero, and we can obtain equation (2) as follows:

$$\begin{cases} ax(1-x) - xu + \alpha xyzu = 0, \\ by(1-y) - yu + \beta xyzu = 0, \\ cz(1-z) - zu + \gamma xyzu = 0, \\ -\mathrm{d}u^2 + exu + fyu + gzu = 0, \\ hv - \dfrac{v^2}{u} = 0. \end{cases} \tag{2}$$

Solving equation (2), we can get the equilibrium points $E_j = (x, y, z, u, v)$ $(j = 1, 2, \ldots, 12)$ as follows:

$$\begin{aligned} &E1\left(0, 0, \frac{dc}{dc+g}, \frac{gc}{dc+g}, 0\right), \\ &E2\left(0, 0, \frac{dc}{dc+g}, \frac{gc}{dc+g}, \frac{hgc}{dc+g}\right), \\ &E3\left(0, \frac{db}{db+f}, 0, \frac{fb}{db+f}, 0\right), \\ &E4\left(0, \frac{db}{db+f}, 0, \frac{fb}{db+f}, \frac{hfb}{db+f}\right), \\ &E5\left(\frac{da}{da+e}, 0, 0, \frac{ea}{da+e}, 0\right), \\ &E6\left(\frac{da}{da+e}, 0, 0, \frac{ea}{da+e}, \frac{hea}{da+e}\right), \\ &E7\left(0, \frac{bcd-cg+bg}{bcd+cf+bg}, \frac{bcd+cf-bf}{bcd+cf+bg}, \frac{bcf+bcg}{bcd+cf+bg}, 0\right), \\ &E8\left(0, \frac{bcd-cg+bg}{bcd+cf+bg}, \frac{bcd+cf-bf}{bcd+cf+bg}, \frac{bcf+bcg}{bcd+cf+bg}, \frac{hbcf+hbcg}{bcd+cf+bg}\right), \\ &E9\left(\frac{acd-cg+ag}{acd+ce+ag}, 0, \frac{acd+ce-ae}{acd+ce+ag}, \frac{ace+acg}{acd+ce+ag}, 0\right), \\ &E10\left(\frac{acd-cg+ag}{acd+ce+ag}, 0, \frac{acd+ce-ae}{acd+ce+ag}, \frac{ace+acg}{acd+ce+ag}, \frac{hace+hacg}{acd+ce+ag}\right), \\ &E11\left(\frac{abd-bf+af}{abd+be+af}, \frac{abd+be-ae}{abd+be+af}, 0, \frac{abe+abf}{abd+be+af}, 0\right), \\ &E12\left(\frac{abd-bf+af}{abd+be+af}, \frac{abd+be-ae}{abd+be+af}, 0, \frac{abe+abf}{abd+be+af}, \frac{habe+habf}{abd+be+af}\right). \end{aligned} \tag{3}$$

2.2.2. Stability Analysis of Equilibrium Point. Jacobian matrix of the system described by (1) can be calculated easily as shown in

$$J = \begin{bmatrix} a(1-2x)-u(1-\alpha yz) & \alpha xzu & \alpha xyu & -x(1-\alpha yz) & 0 \\ \beta yzu & b(1-2y)-u(1-\beta xz) & \beta xyu & -y(1-\beta xz) & 0 \\ \gamma yzu & \gamma xzu & c(1-2z)-u(1-\gamma xy) & -z(1-\gamma xy) & 0 \\ eu & fu & gu & -2\mathrm{d}u+ex+fy+gz & 0 \\ 0 & 0 & 0 & \dfrac{v^2}{u^2} & \dfrac{hu-2v}{u} \end{bmatrix}. \tag{4}$$

Proposition 1. *When v is equal to 0, the equilibrium points (E1, E3, E5, E7, E9, and E11) are unstable.*

Proof. From the 5th expression of equation (2), we can get $v(t)=0$ or $v(t)=hu\ (t)$. Substituting $v=0$, $v=hu$ into equation (4), we can get

$$J = \pm h\begin{bmatrix} a(1-2x)-u(1-\alpha yz) & \alpha xzu & \alpha xyu & -x(1-\alpha yz) \\ \beta yzu & b(1-2y)-u(1-\beta xz) & \beta xyu & -y(1-\beta xz) \\ \gamma yzu & \gamma xzu & c(1-2z)-u(1-\gamma xy) & -z(1-\gamma xy) \\ eu & fu & gu & -2\mathrm{d}u+ex+fy+gz \end{bmatrix}, \tag{5}$$

where "±" means that "+" corresponds to $v=0$ and "−" corresponds to $v=hu$. It is known that when $v=0$, one of the eigenvalues of the Jacobian matrix is h. Because $h>0$, the equilibrium point is not stable.

That is the end of the proof.

For the equilibrium point $E_2\ (0,0,dc/dc+g,gc/dc+g,hgc/dc+g)$, the eigenvalues of the corresponding Jacobian matrix can be obtained as $\lambda=-h,a-(gc/dc+g),b-(gc/dc+g),-c,-(dg\,c/dc+g)$. Obviously, all eigenvalues are negative and the equilibrium point $E2\ (0,0,dc/dc+g,gc/dc+g,hgc/dc+g)$ is locally asymptotically stable when the following conditions are met:

$$\begin{cases} a<\dfrac{gc}{dc+g}, \\ b<\dfrac{gc}{dc+g}. \end{cases} \tag{6}$$

For the equilibrium point $E4\ (0,db/db+f,0,fb/db+f,hfb/db+f)$, the eigenvalues of the corresponding Jacobian matrix can be obtained as $\lambda=-h,a-(fb/db+f),c-(fb/db+f),-b,-(df\,b/db+f)$. Obviously, all eigenvalues are negative and the equilibrium point $E4\ (0,db/db+f,0,fb/db+f,hfb/db+f)$ is locally asymptotically stable when the following conditions are satisfied:

$$\begin{cases} a<\dfrac{fb}{db+f}, \\ b<\dfrac{fb}{db+f}. \end{cases} \tag{7}$$

For the equilibrium point $E_6\ (da/da+e,0,0,ea/da+e,hea/da+e)$, the eigenvalues of the corresponding Jacobian matrix can be obtained as $\lambda==-h,-a,b-(ea/da+e),c-(ea/da+e),-(de\,a/da+e)$. Obviously, all eigenvalues are negative and the equilibrium point $E_6\ (da/da+e,0,0,ea/da+e,hea/da+e)$ is locally asymptotically stable when the following conditions are satisfied:

$$\begin{cases} b<\dfrac{ea}{da+e}, \\ c<\dfrac{ea}{da+e}. \end{cases} \tag{8}$$

For the equilibrium point $E8\ (0, bcd - cg + bg/\ bcd + cf + bg,\ bcd + cf - bf/bcd + cf + bg, bcf + bcg/bcd + cf + bg, hbcf + hbcg/bcd + cf + bg)$, from the Jacobian matrix (4), the following equation can be obtained:

$$J = -h\begin{bmatrix} a - u(1-\alpha yz) & 0 & 0 & 0 \\ yzu & b(1-2y) - u & 0 & -y \\ yzu & 0 & c(1-2z) - u & -z \\ eu & fu & gu & -2du + fy + gz \end{bmatrix} = -h[a - u(1-\alpha yz)]\begin{bmatrix} b(1-2y) - u & 0 & -y \\ 0 & c(1-2z) - u & -z \\ fu & gu & -du \end{bmatrix}. \tag{9}$$

The Jacobian determinant is as follows:

$$|J - \lambda E| == [-h - \lambda][a - u(1-\alpha yz) - \lambda]\begin{vmatrix} b(1-2y) - u - \lambda & 0 & -y \\ 0 & c(1-2z) - u - \lambda & -z \\ fu & gu & -du - \lambda \end{vmatrix} = -(-h - \lambda)(A - \lambda)\left[\lambda^3 + (du - B - C)\lambda^2 + (CB + guz + fuy - duB - duC)\lambda + duBC - guzB + fuyC\right], \tag{10}$$

where $\begin{cases} A = a - u(1-\alpha yz); \\ B = b(1-2y) - u; \\ C = c(1-2z) - u. \end{cases}$ Using the Routh Hurwitz condition, the following condition is necessary and sufficient when all roots of the characteristic equation of the system (1) at the equilibrium point have a negative real part:

$$\begin{cases} A < 0, \\ du - B - C > 0, \\ CB + guz + fuy - duB - duC > 0, \\ duBC - guzB + fuyC > 0, \\ (du - B - C)(CB + guz + fuy - duB - duC) > duBC - guzB + fuyC. \end{cases} \tag{11}$$

For the equilibrium point $E10\ (acd - cg + ag/\ acd + ce + ag, 0, acd + ce - ae/\ acd + ce + ag, ace + acg/\ acd + ce + ag, hace + hacg/acd + ce + ag)$, from the Jacobian matrix (4), equation (12) can be obtained:

$$J = -h\begin{bmatrix} a(1-2x) - u & xzu & 0 & -x \\ 0 & b - u(1-\beta xz) & 0 & 0 \\ 0 & xzu & c(1-2z) - u & -z \\ eu & fu & gu & -du \end{bmatrix} = -h[b - u(1-\beta xz)]\begin{bmatrix} a(1-2x) - u & 0 & -x \\ 0 & c(1-2z) - u & -z \\ eu & gu & -du \end{bmatrix}. \tag{12}$$

The Jacobian determinant is as follows:

$$|J - \lambda E| = [-h - \lambda][b - u(1-\beta xz) - \lambda]\begin{vmatrix} a(1-2x) - u - \lambda & 0 & -x \\ 0 & c(1-2z) - u - \lambda & -z \\ eu & gu & -du - \lambda \end{vmatrix} = -(-h - \lambda)(B1 - \lambda)\left[\lambda^3 + (du - A1 - C1)\lambda^2 + (A1C1 + zgu + eux - duA1 - duC1)\lambda + duA1C1 - zguA1 + euxC1\right], \tag{13}$$

where $\begin{cases} A1 = a(1-2x) - u; \\ B1 = b - u(1-\beta xz); \\ C1 = c(1-2z) - u. \end{cases}$ Using the Routh Hurwitz condition, the following condition is necessary and sufficient when all roots of the characteristic equation of the system (1) at the equilibrium point have a negative real part:

$$\begin{cases} B1 < 0, \\ \mathrm{d}u - A1 - C1 > 0, \\ A1C1 + zgu + eux - \mathrm{d}uA1 - \mathrm{d}uC1 > 0, \\ \mathrm{d}uA1C1 - zguA1 + euxC1 > 0, \\ (\mathrm{d}u - A1 - C1)(A1C1 + zgu + eux - \mathrm{d}uA1 - \mathrm{d}uC1) \\ > \mathrm{d}uA1C1 - zguA1 + euxC1. \end{cases} \tag{14}$$

For the equilibrium point $E12\,(abd - bf + af/abd + be + af, abd + be - ae/abd + be + af, 0, abe + abf/\quad abd + be + af, habe + habf/abd + be + af)$, from the Jacobian matrix (4), equation (15) can be obtained:

$$J = -h\begin{bmatrix} a(1-2x) - u & 0 & xyu & -x \\ 0 & b(1-2y) - u & xyu & -y \\ 0 & 0 & c - u(1-\gamma xy) & 0 \\ eu & fu & gu & -\mathrm{d}u \end{bmatrix} = -h[c - u(1-\gamma xy)]\begin{bmatrix} a(1-2x) - u & 0 & -x \\ 0 & b(1-2y) - u & -y \\ eu & fu & -\mathrm{d}u \end{bmatrix}. \tag{15}$$

The Jacobian determinant is as follows:

$$\begin{aligned} |J - \lambda E| &= [c - u(1-\gamma xy) - \lambda]\begin{vmatrix} a(1-2x) - u - \lambda & 0 & -x \\ 0 & b(1-2y) - u - \lambda & -y \\ eu & fu & -\mathrm{d}u - \lambda \end{vmatrix} \\ &= -(-h - \lambda)(C2 - \lambda)\left[\lambda^3 + (\mathrm{d}u - A2 - B2)\lambda^2\right. \\ &\quad \left. + (A2B2 + eux + fuy - \mathrm{d}uB2 - \mathrm{d}uA2)\lambda + \mathrm{d}uA2B2 - euxB2 + fuyA2\right] = 0, \end{aligned} \tag{16}$$

where $\begin{cases} A2 = a(1-2x) - u; \\ B2 = b(1-2y) - u; \\ C2 = c - u(1-\gamma xy). \end{cases}$ Using the Routh Hurwitz condition, the following condition is necessary and sufficient when all roots of the characteristic equation of system (1) at the equilibrium point have a negative real part:

$$\begin{cases} C2 < 0, \\ \mathrm{d}u - A2 - B2 > 0, \\ A2B2 + eux + fuy - \mathrm{d}uB2 - \mathrm{d}uA2 > 0, \\ \mathrm{d}uA2B2 - euxB2 + fuyA2 > 0, \\ (\mathrm{d}u - B2 - A2)(A2B2 + eux + fuy - \mathrm{d}uB2 - \mathrm{d}uA2) > \mathrm{d}uA2B2 - euxB2 + fuyA2. \end{cases} \tag{17}$$

We have discussed the stability of all the equilibria of the system. Now, we validate the above conclusions, and the validation method is as follows: at first, we suppose the coefficients are a, b, c, d, e, f, g, h, α, β, γ; then, by the Jacobi matrix, we find its eigenvalues. According to the characteristics of the positive and negative polarity of the eigenvalues, we can judge the stability of equilibrium points and then substitute into the supposed coefficient of a, b, c, d, e, f, g, h, α, β, γ into stability judgment inequalities (6), (8), (11), (14), and (17) and verify the inequality of stability judgment conditions. For example, if the characteristic roots of the Jacobian matrix are all negative corresponding to the preassumed coefficients, then the equilibrium point is stable. Subsequently, the preassumed coefficients are replaced into the inequality system for stability judgment condition, and if the inequality set is true, the theoretical analysis process is proved to be correct. On the contrary, if the characteristic roots of the Jacobian matrix are not all negative corresponding to the preassumed coefficients, then the equilibrium point is unstable. Subsequently, the preassumed coefficients are replaced into the inequality system for stability judgment condition, and if the inequality set is not true, the theoretical analysis process is proved also to be correct. Here, Table 1 shows the equilibrium points (viz, the solution of equation (2)), the corresponding eigenvalue, the stability, and the conditional inequality systems true or no when the preassumed coefficients are $a = 1$, $b = 1.14$, $c = 2.93$, $d = 1.3$, $e = 0.21$, $f = 0.1$, $g = 0.35$, $h = 2$, $\alpha = 0.05$, $\beta = 2$, $\gamma = 0.8$. □

3. System Simulation Results

To facilitate the simulation of the system, we discretize equation (1). The system equation after discretization is shown in

Table 1: The equilibrium points, the corresponding eigenvalue, the stability, and the conditional inequality systems true or no.

Equilibrium points	Eigenvalues	Stability	Is the inequality set true?
(0, 0, 0.9158, 0.2466, 0)	−2.6495; −0.3545; 0.7534; 0.8934; 2	Unstable	No
(0, 0, 0.9158, 0.2466, 0.4931)	−2;−0.3545;−2.6495; 0.7534; 0.8934	Unstable	No
(0, 0.9368, 0, 0.0721, 0)	−0.1007; −1.061; 0.9279; 2.8579; 2	Unstable	No
(0, 0.9368, 0, 0.0721, 0.1441)	−2;−1.061; 0.1007; 0.9279; 2.8579	Unstable	No
(0.8609, 0, 0, 0.1391, 0)	−0.8217;−0.22; 1.0009; 2.7909; 2	Unstable	No
(0.8609, 0, 0, 0.1391, 0.2781)	−2; −0.22; −0.8217; 1.0009; 2.7909	Unstable	No
(0, 0.7381, 0.8981, 0.2986, 0)	−2.589; −0.4959;−0.7761; 0.7113; 2	Unstable	No
(0, 0.7381, 0.8981, 0.2986, 0.5971)	−2;−−0.7761;−0.4959;−2.589; 0.7113	Unstable	No
(0.6563, 0, 0.8827, 0.3437, 0)	−0.5767 + 0.2056i;−0.5767 − 0.2056i;−2.5361; 1.1945; 2	Unstable	No
(0.6563, 0, 0.8827, 0.3437, 0.6873)	−2;−0.5767 + 0.2056*i*;−0.5767 − 0.2056*i*;−2.5361; 1.1945	Unstable	No
(0.806, 0.8298, 0, 0.194, 0)	−0.3516; −0.7237; −0.9289; 2.8398; 2	Unstable	No
(0.806, 0.8298, 0, 0.194, 0.3881)	−2; −0.3516; −0.9289;−0.7237; 2.8398	Unstable	No

$$\begin{cases} x(n+1) = x(n) + ax(n)(1 - x(n)) - x(n)u(n) + \alpha x(n)y(n)z(n)u(n), \\ y(n+1) = y(n) + by(n)(1 - y(n)) - y(n)u(n) + \beta x(n)y(n)z(n)u(n), \\ z(n+1) = z(n) + cz(n)(1 - z(n)) - z(n)u(n) + \gamma x(n)y(n)z(n)u(n), \\ u(n+1) = u(n) - \mathrm{d}u^2(n) + ex(n)u(n) + fy(n)u(n) + gz(n)u(n), \\ v(n+1) = v(n) + hv(n) - \dfrac{v^2(n)}{u(n)}. \end{cases} \tag{18}$$

Using MATLAB simulation, we can obtain a Lyapunov spectrum and bifurcation diagram about parameters α, β, γ and output sequence diagrams as follows:

3.1. α Is Changed and Other Parameters of System (18) Are Fixed. We use $a = 1$, $b = 1.14$, $c = 2.93$, $d = 1.3$, $e = 0.21$, $f = 0.1$, $g = 0.35$, $h = 2$, $\beta = 0.2$, $\gamma = 0.5$ and simulate the Lyapunov spectrum and bifurcation diagram versus parameters α whose results are shown in Figures 1 and 2. From Figure 1, the following conclusions can be obtained: when $\alpha < 0.8$, we can know LE1 > 0, LE2 < 0, and LE3 < 0, and the chaos is generated in the system; when $0.8 < \alpha < 1$, we can know LE1 < 0, LE2 < 0, and LE3 < 0, and the periodic window is generated in the system; when $\alpha > 1$, we can know LE1 > 0, LE2 < 0, and LE3 < 0, and the periodic window turns into chaos in the system. In short, as α increases, the system experiences chaos-period-chaos. Figure 2 is the flip bifurcation diagram versus α. According to Figure 2, when α is used as 0.05, 0.95, and 2, we can obtain sequence diagrams shown in Figure 3–5, respectively, and phase diagrams shown in Figures 6–9, respectively.

3.2. β Is Changed and Other Parameters of System (18) Are Fixed. We use $a = 1$, $b = 1.14$, $c = 2.93$, $d = 1.3$, $e = 0.21$, $f = 0.1$, $g = 0.35$, $h = 2$, $\alpha = 0.05$, $\gamma = 0.5$ and simulate the Lyapunov spectrum and bifurcation diagram versus parameters β whose results are shown in Figures 10 and 11. From Figure 10, the following conclusions can be obtained: when $\beta < 1.12$, we can know LE1 > 0, LE2 < 0, and LE3 < 0, and the chaos is generated in the system; when $1.12 < \beta < 1.24$, we can know LE1 < 0, LE2 < 0, and LE3 < 0, and the periodic window is generated in the system; when $1.24 < \beta < 3.5$, we can know LE1 > 0, LE2 < 0, and LE3 < 0, and the periodic window turns into chaos in the system; when $\beta > 3.5$, we can know LE1 < 0, LE2 < 0, and LE3 < 0, and the chaos turns into a periodic window in the system.

In short, as β increases, the system experiences chaos-period-chaos-period. Figure 11 is flip bifurcation diagram versus β. According to Figure 11, when β is used as 0.7, 1.2, and 3, we can obtain sequence diagrams shown in Figures 12–14, respectively, and phase diagrams shown in Figures 15–18, respectively.

3.3. γ Is Changed and Other Parameters of System (18) Are Fixed. We use $a = 1$, $b = 1.14$, $c = 2.93$, $d = 1.3$, $e = 0.21$, $f = 0.1$, $g = 0.35$, $h = 2$, $\alpha = 0.05$, $\beta = 2$ and simulate the Lyapunov spectrum and bifurcation diagram versus parameters β whose results are shown in Figures 19 and 20. From Figure 19, when $\gamma = 0.096$ and $\gamma = 0.184$, we can know LE1 = 0, LE2 < 0, and LE3 < 0. From Figure 20, it is clear that when $0 < \gamma < 0.096$, the system has a 4-fold periodic; when $0.096 < \gamma < 0.2$, the system has a 8-fold periodic. From Figure 19, when $0.2 < \gamma < 0.376$, we know that LE1 > 0, LE2 < 0, and LE3 < 0, and the system is chaotic; when $\gamma = 0.376$ and $\gamma = 0.392$, we know that LE1 = 0, LE2 < 0, and LE3 < 0. Hence, from Figure 20, we

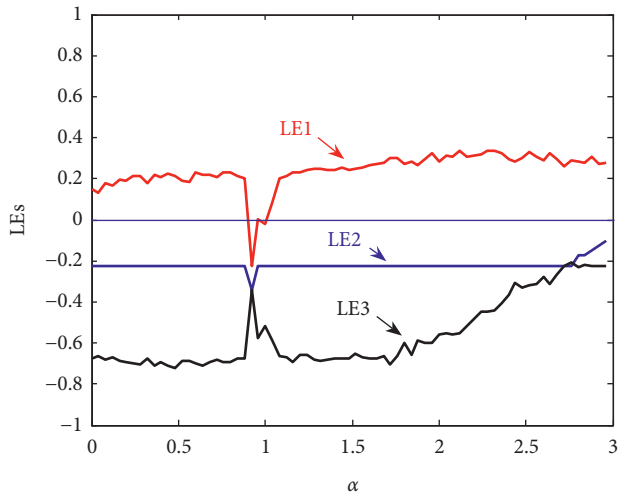

Figure 1: Lyapunov spectrum versus α when $a = 1$, $b = 1.14$, $c = 2.93$, $d = 1.3$, $e = 0.21$, $f = 0.1$, $g = 0.35$, $h = 2$, $\beta = 0.2$, $\gamma = 0.5$.

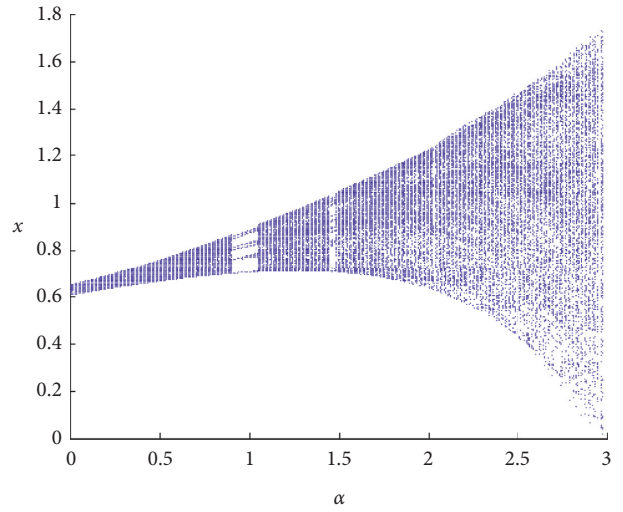

Figure 2: Flip bifurcation diagram versus parameters α when $a = 1$, $b = 1.14$, $c = 2.93$, $d = 1.3$, $e = 0.21$, $f = 0.1$, $g = 0.35$, $h = 2$, $\beta = 0.2$, $\gamma = 0.5$.

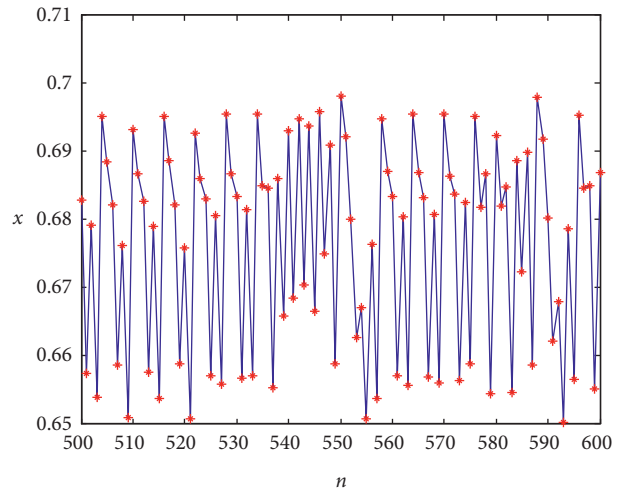

Figure 3: x–n sequence diagram which denotes that the system is chaotic when $\alpha = 0.05$.

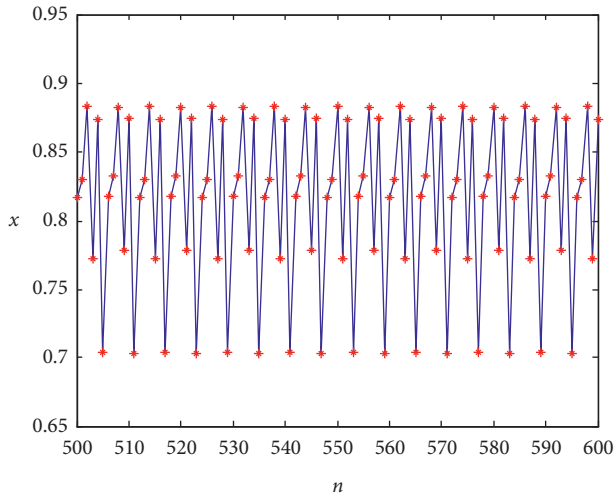

Figure 4: x–n sequence diagram which denotes that the system is periodic when $\alpha = 0.95$.

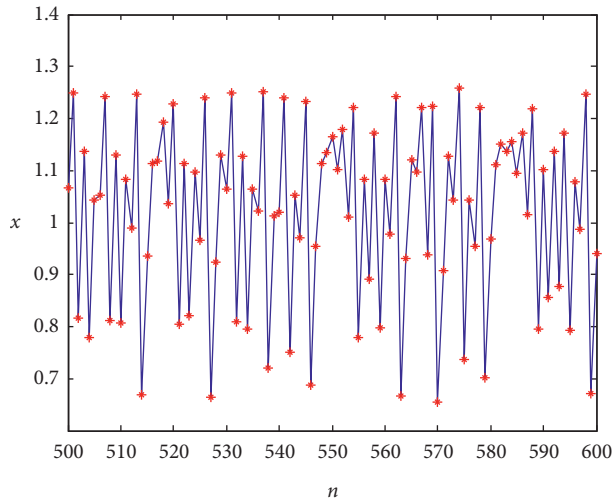

Figure 5: x–n sequence diagram which denotes that the system is chaotic when $\alpha = 2$.

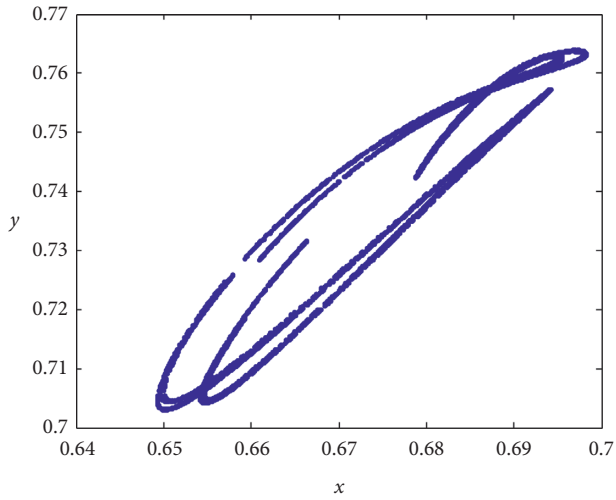

Figure 6: x–y phase diagram which denotes that the system is chaotic when $\alpha = 0.05$.

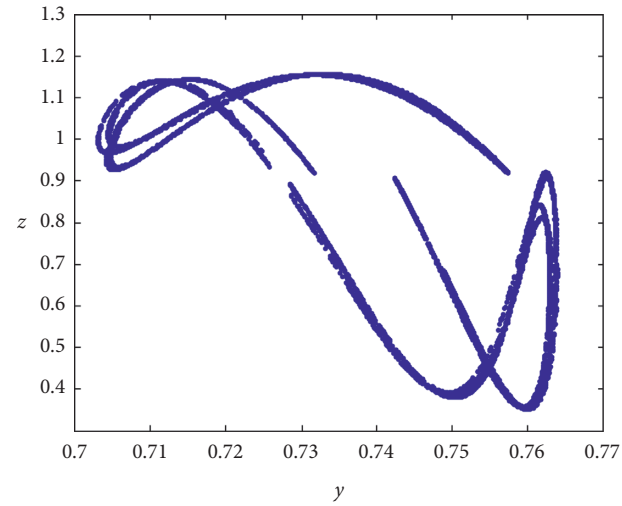

Figure 7: y-z phase diagram which denotes that the system is chaotic when $\alpha = 0.05$.

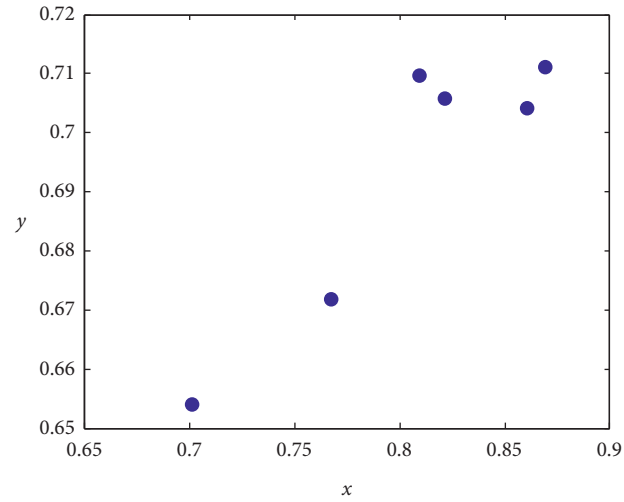

Figure 8: x-y phase diagram which denotes that the system is periodic when $\alpha = 0.95$.

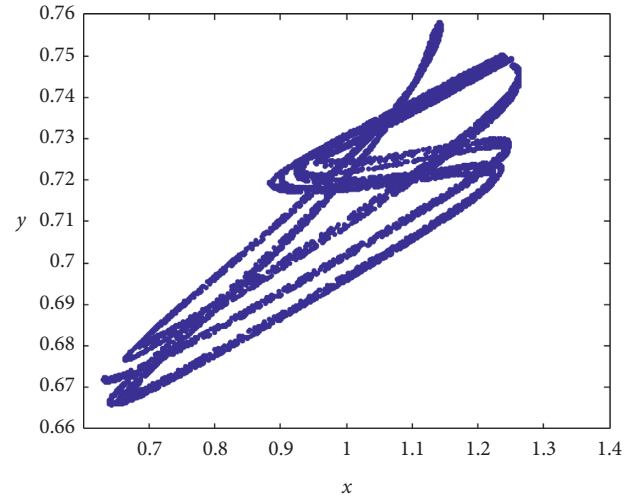

Figure 9: x-y phase diagram which denotes that the system is chaotic when $\alpha = 2$.

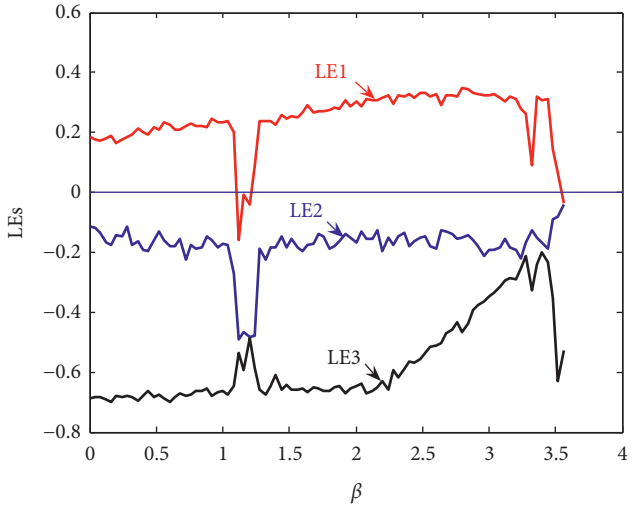

Figure 10: Lyapunov spectrum versus β when $a=1$, $b=1.14$, $c=2.93$, $d=1.3$, $e=0.21$, $f=0.1$, $g=0.35$, $h=2$, $\alpha=0.05$, $\gamma=0.5$.

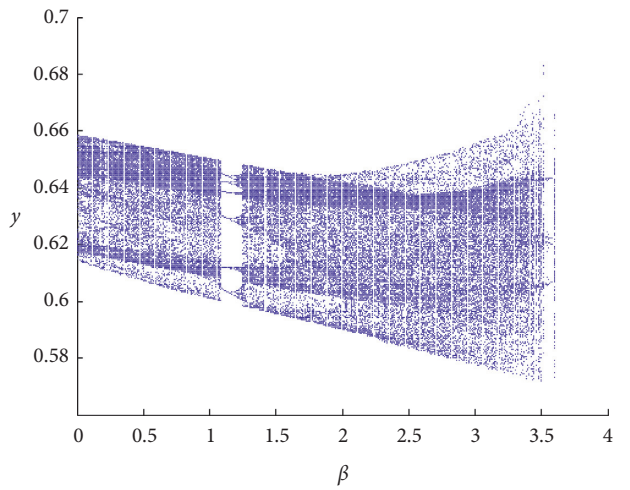

Figure 11: Flip bifurcation diagram versus parameters β when $a=1$, $b=1.14$, $c=2.93$, $d=1.3$, $e=0.21$, $f=0.1$, $g=0.35$, $h=2$, $\alpha=0.05$, $\gamma=0.5$.

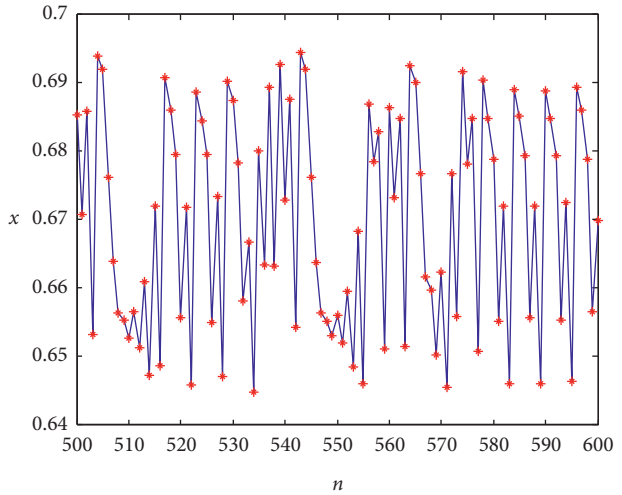

Figure 12: x–n sequence diagram which denotes that the system is chaotic when $\beta=0.7$.

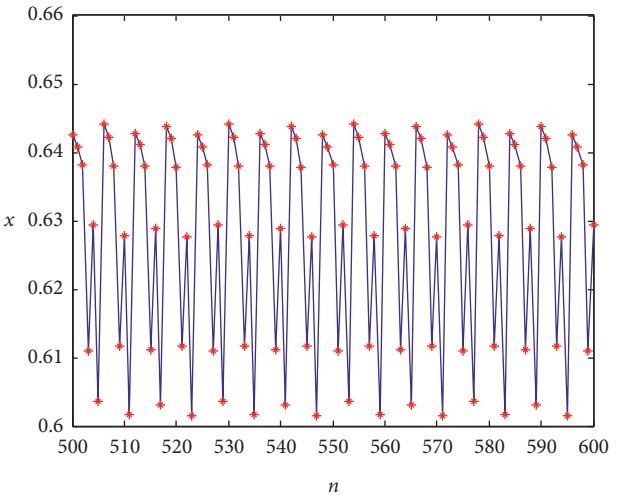

Figure 13: x–n sequence diagram which denotes that the system is periodic when $\beta=1.2$.

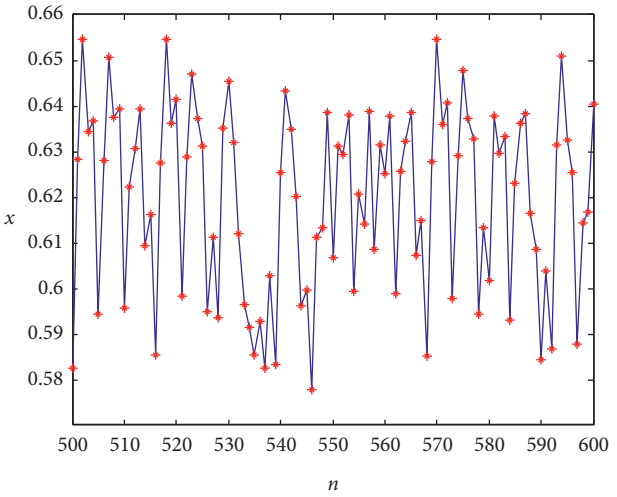

Figure 14: x–n sequence diagram which denotes that the system is chaotic when $\beta=3$.

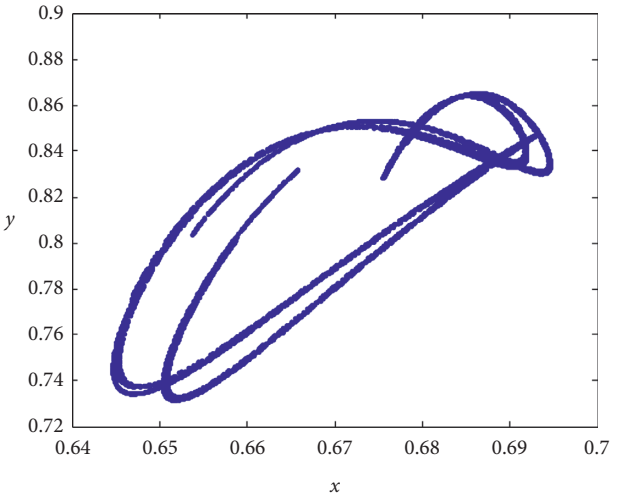

Figure 15: x-y phase diagram which denotes that the system is chaotic when $\beta=0.7$.

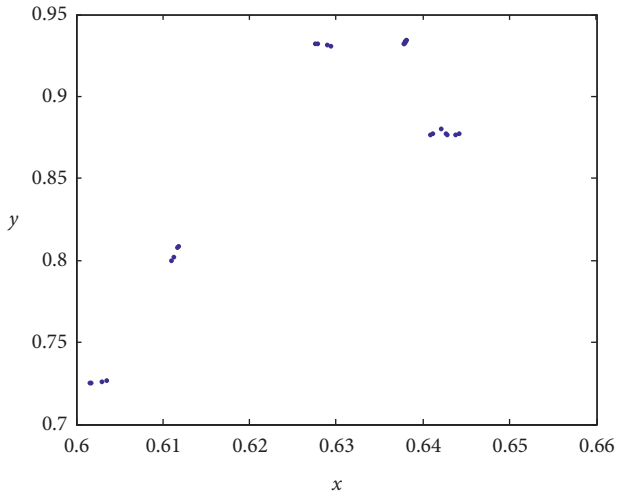

Figure 16: x–y phase diagram which denotes that the system is periodic when $\beta = 1.2$.

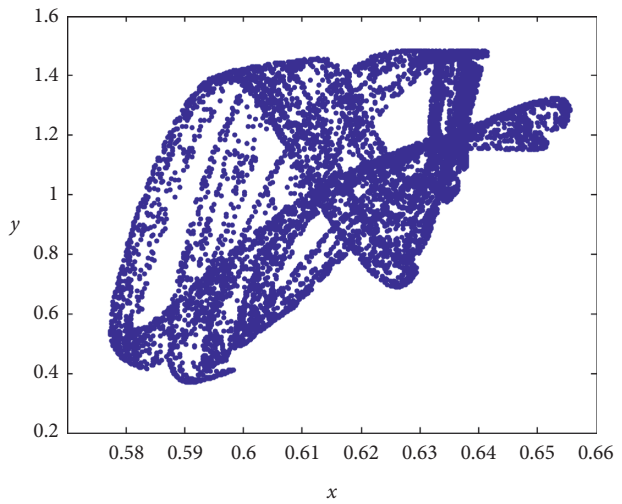

Figure 17: x–y phase diagram which denotes that the system is chaotic when $\beta = 3$.

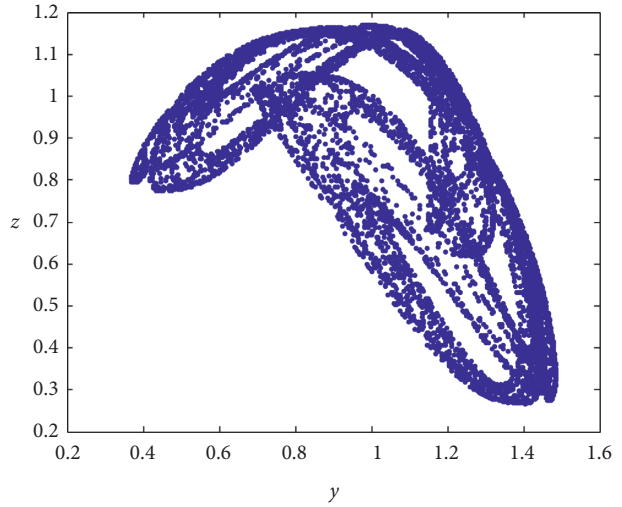

Figure 18: y-z phase diagram which denotes that the system is chaotic when $\beta = 3$.

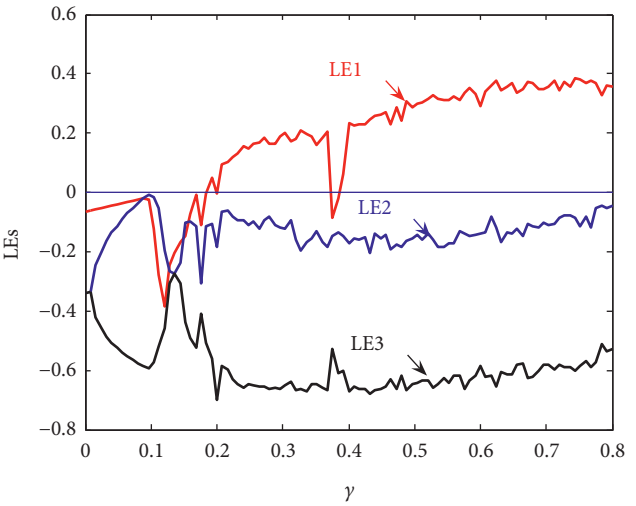

Figure 19: Lyapunov spectrum versus γ when $a = 1$, $b = 1.14$, $c = 2.93$, $d = 1.3$, $e = 0.21$, $f = 0.1$, $g = 0.35$, $h = 2$, $\alpha = 0.05$, and $\beta = 2$.

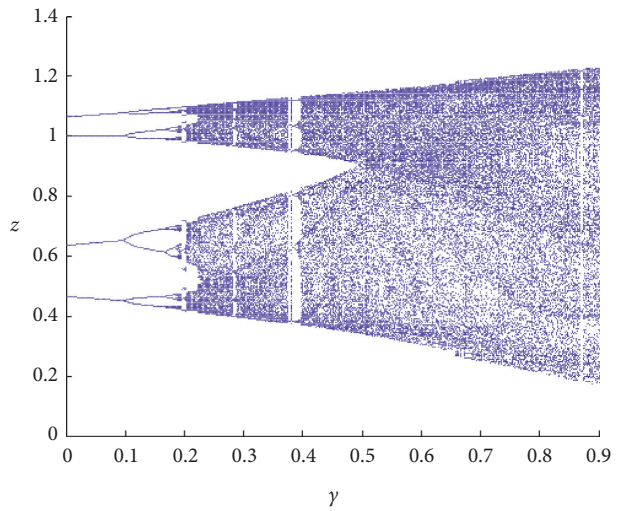

Figure 20: Flip bifurcation diagram versus parameters γ when $a = 1$, $b = 1.14$, $c = 2.93$, $d = 1.3$, $e = 0.21$, $f = 0.1$, $g = 0.35$, $h = 2$, $\alpha = 0.05$, and $\beta = 2$.

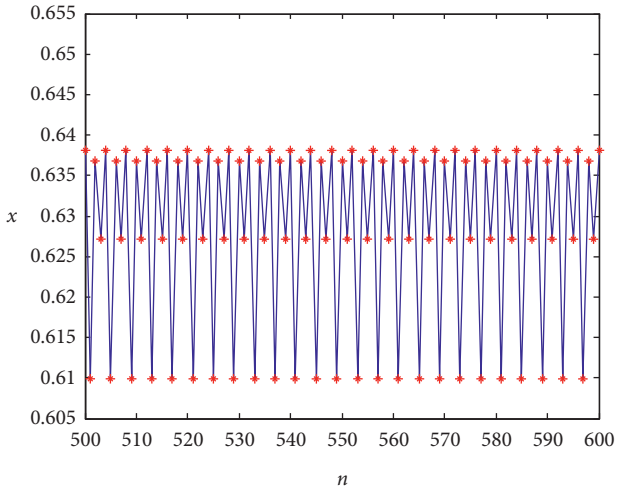

Figure 21: x-n sequence diagram which denotes that the system is 4-fold periodic when $\gamma = 0.08$.

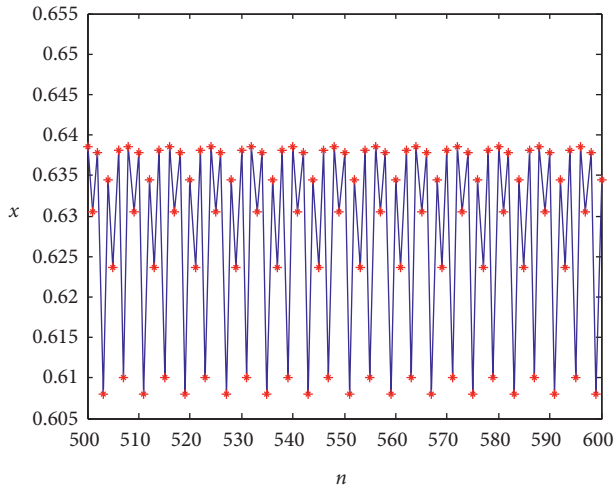

Figure 22: x-n sequence diagram which denotes that the system is 8-fold periodic when $\gamma = 0.15$.

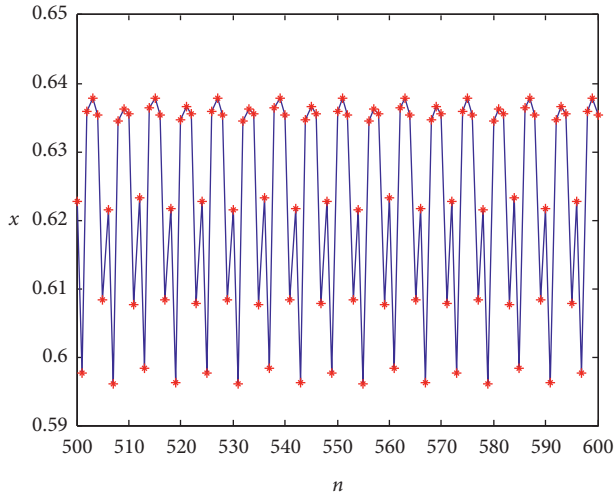

Figure 23: x-n sequence diagram which denotes that the system is periodic when $\gamma = 0.39$.

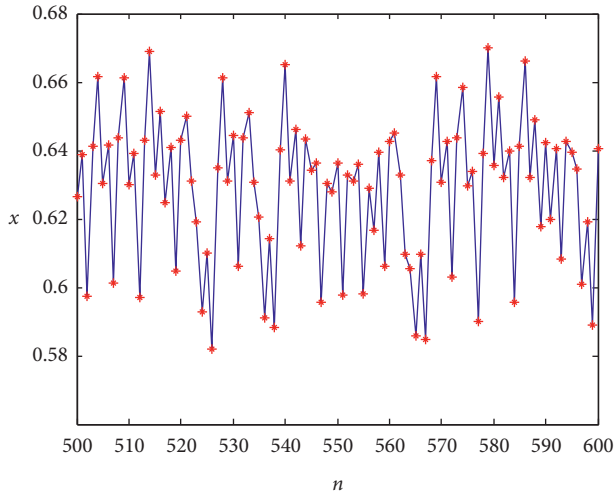

Figure 24: x-n sequence diagram which denotes that the system is chaotic when $\gamma = 0.8$.

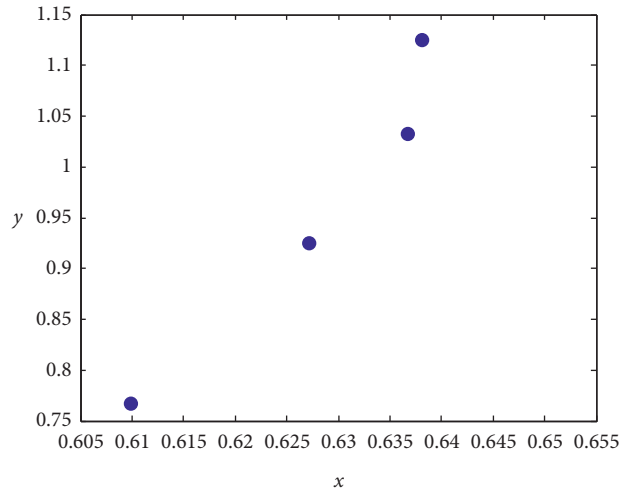

Figure 25: x-y phase diagram which denotes that the system is 4-fold periodic when $\gamma = 0.08$.

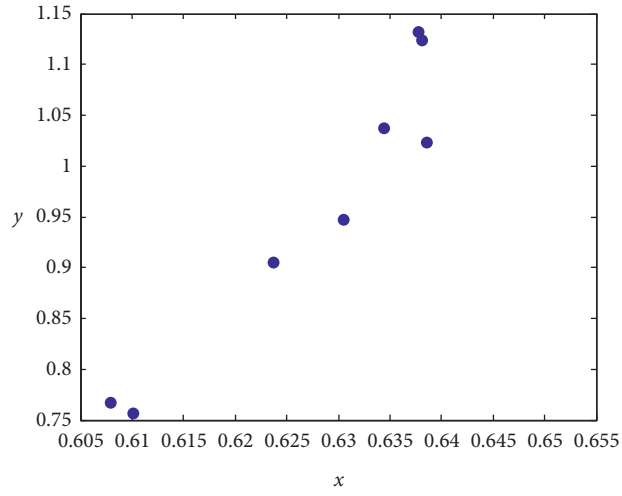

Figure 26: x-y phase diagram which denotes that the system is 8-fold periodic when $\gamma = 0.15$.

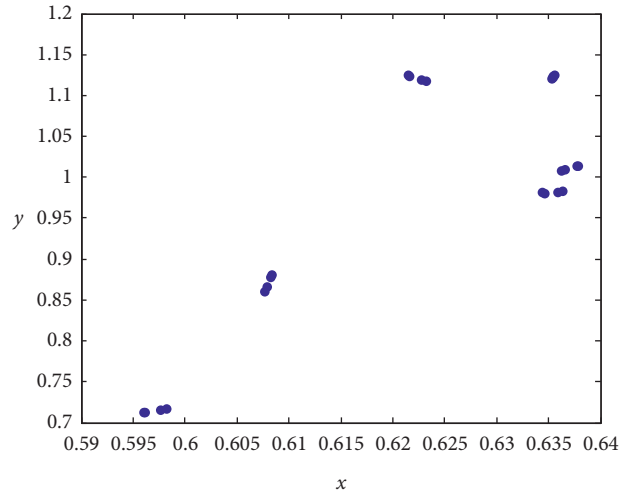

Figure 27: x-y phase diagram which denotes that the system is periodic when $\gamma = 0.39$.

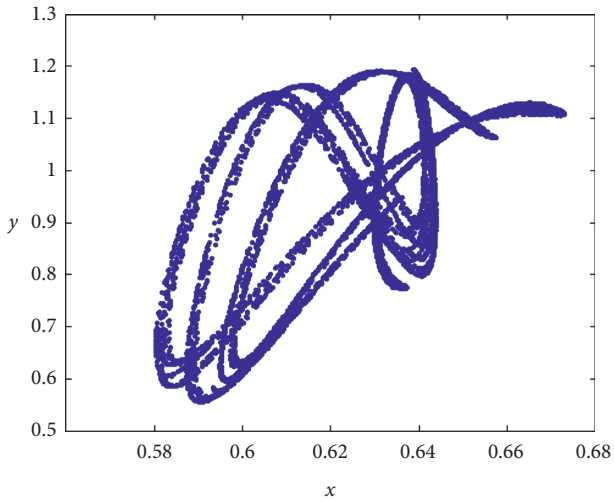

Figure 28: x-y phase diagram which denotes that the system is chaotic when $\gamma = 0.8$.

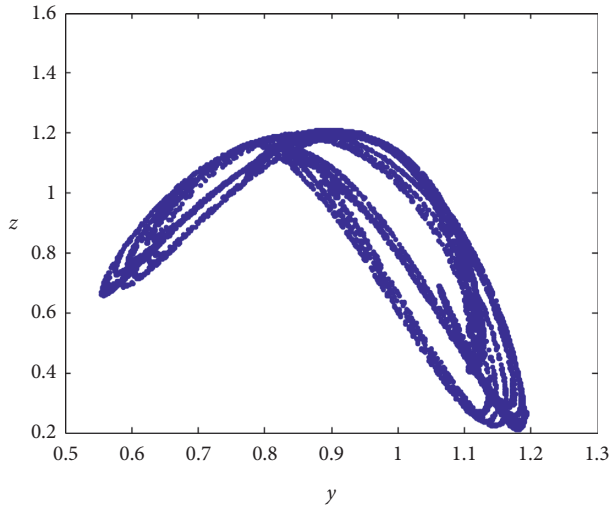

Figure 29: y-z phase diagram which denotes that the system is chaotic when $\gamma = 0.8$.

know that when $0.376 < \gamma < 0.39$, the system is periodic. When $\gamma > 0.392$, we know that LE1 > 0, LE2 < 0, and LE3 < 0, and the system is chaotic. In short, as γ increases, the system experiences a route of 4-fold periodic, 8-fold periodic, and chaos-period-chaos. Figure 20 is the flip bifurcation diagram versus β. According to Figure 20, when γ is used as 0.08, 0.15, 0.39, and 0.8, we can obtain sequence diagrams shown in Figure 21–24, respectively, and phase diagrams shown in Figure 25–29, respectively.

3.4. Multistability of the System. Multistability means that when parameters are fixed and the initial values are different, the system presents different attractors. When using $a = 1$, $b = 1.14$, $c = 2.93$, $d = 1.3$, $e = 0.21$, $f = 0.1$, $g = 0.35$, $h = 2$, $\alpha = 0.05$, $\beta = 2$, and $\gamma = 0.08$, we simulate the multistability of

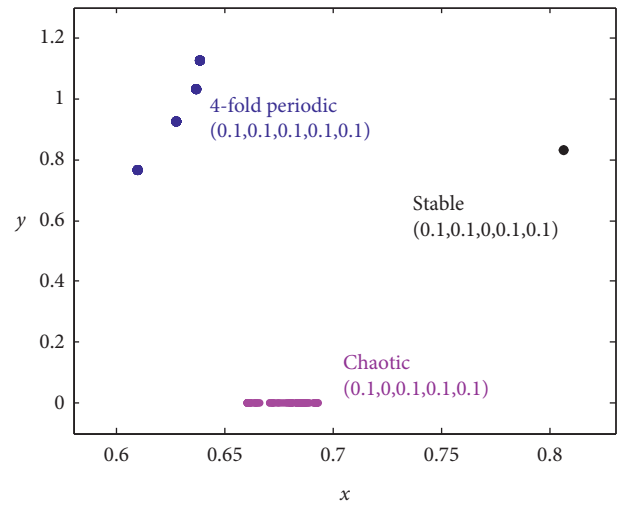

Figure 30: When $a = 1$, $b = 1.14$, $c = 2.93$, $d = 1.3$, $e = 0.21$, $f = 0.1$, $g = 0.35$, $h = 2$, $\alpha = 0.05$, and $\beta = 2$, $\gamma = 0.08$, multistability results of the system where the blue points denote 4-fold periodic states correspond to initial value (0.1, 0.1, 0 .1, 0.1, 0.1), the black point denotes a stable state of equilibrium point corresponding to initial value (0.1, 0.1, 0, 0.1, 0.1), and the rose points denote chaotic state corresponding to initial value (0.1, 0, 0.1, 0.1, 0.1).

the system, and simulation results are shown in Figure 30 where the blue points denote 4-fold periodic states corresponding to initial value (0.1, 0.1, 0 .1, 0.1, 0.1), the black point denotes a stable state of equilibrium point corresponding to initial value (0.1, 0.1, 0, 0.1, 0.1), and the rose points denote chaotic state corresponding to initial value (0.1, 0, 0.1, 0.1, 0.1).

When using $a = 1$, $b = 1.14$, $c = 2.93$, $d = 1.3$, $e = 0.21$, $f = 0.1$, $g = 0.35$, $h = 2$, $\alpha = 0.05$, $\beta = 2$, and $\gamma = 0.15$, we simulate the multistability of the system, and simulation results are shown in Figure 31 where the blue points denote 8-fold periodic states corresponding to initial value (0.1, 0.1, 0.1, 0.1, 0.1), the black point denotes a stable state of equilibrium point corresponding to initial value (0.1, 0.1, 0, 0.1, 0.1), and the rose points denote chaotic state corresponding to initial value (0.1, 0, 0.1, 0.1, 0.1).

From the above results, we can know that, under different initial value conditions, three kinds of attractors coexist, so the system is multistable.

In this paper, to facilitate the simulation of the system, we discretize equation (1) just as what literature [33] did. Compared with the corresponding continuous-time system, the discrete system has the following different points: (i) the system states are discrete and sequence output is discrete and (ii) the curves in the phase diagrams are formed by discrete points.

4. Comparison with Literature [33]

In [33], it is relatively unspecific for considering all real estate companies as a prey team, which does not fit the specific circumstance of real estate companies. Our model considers the large, medium, and small real estate enterprises for three different prey teams. Compared with the 3D

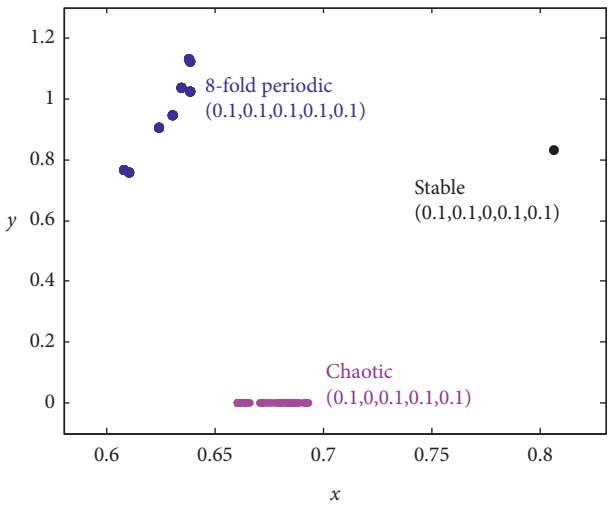

FIGURE 31: When $a = 1$, $b = 1.14$, $c = 2.93$, $d = 1.3$, $e = 0.21$, $f = 0.1$, $g = 0.35$, $h = 2$, $\alpha = 0.05$, $\beta = 2$, and $\gamma = 0.15$, multistability results of the system where the blue points denote 8-fold periodic states corresponding to initial value (0.1, 0.1, 0 .1, 0.1, 0.1), the black point denotes a stable state of equilibrium point corresponding to initial value (0.1, 0.1, 0, 0.1, 0.1), and the rose points denote chaotic state corresponding to initial value (0.1, 0, 0.1, 0.1, 0.1).

model in literature [33], our model is more accordant with the specific circumstance of real estate companies and emerges richer dynamic characteristics. In [33], the range of the positive Lyapunov exponent is narrower, and the corresponding chaos range is also narrower. On the contrary, in our paper, the range of the positive Lyapunov exponent is wider, and the corresponding chaos range is also wider. In addition, in our model, there are "period-chaos-period" or "chaos-period-chaos" bifurcation characteristics.

5. Conclusion

In this paper, a 5D predator-prey evolutionary model of real estate enterprises was proposed. This model considers the large, medium, and small real estate enterprises for three different prey teams. We made a nonlinear dynamic analysis on a 5D predator-prey evolutionary system in the real estate market and simulated the corresponding discrete system. The simulation results about the Lyapunov spectrum, bifurcation diagram, sequence diagram, and phase diagram were given. In this paper, the range of the positive Lyapunov exponent is wide, and the corresponding chaos range is also wide. The system has rich dynamic characteristics showing "period-chaos-period" or "chaos-period-chaos" bifurcation performance.

Data Availability

All the data used to support the findings of this study are available from the corresponding author upon request.

Conflicts of Interest

The authors declare that they have no conflicts of interest.

Acknowledgments

The work was supported by the Social Science Foundation of Hunan Province of China (18YBA089).

References

[1] H. R. Lin, C. Wang, and Y. Tan, "Hidden extreme multistability with hyperchaos and transient chaos in a hopfield neural network affected by electromagnetic radiation," *Nonlinear Dynamics*, vol. 99, pp. 2369–2386, 2020.

[2] C. H. Wang, H. Xia, and L. Zhou, "A memristive hyperchaotic multiscroll jerk system with controllable scroll numbers," *International Journal of Bifurcation and Chaos*, vol. 27, no. 6, Article ID 1750091, 2017.

[3] R. P. Wu and C. Wang, "A new simple chaotic circuit based on memristor," *International Journal of Bifurcation and Chaos*, vol. 26, no. 9, Article ID 1650145, 2016.

[4] M. H. Zhu, C. H. Wang, Q. L. Deng, and Q. H. Hong, "Locally active memristor with three coexisting pinched hysteresis loops and its emulator circuit," *International Journal of Bifurcation and Chaos*, vol. 30, no. 13, Article ID 2050184, 2020.

[5] Q. Deng, C. Wang, and L. Yang, "Four-wing hidden attractors with one stable equilibrium point," *International Journal of Bifurcation and Chaos*, vol. 30, no. 6, Article ID 2050086, 2020.

[6] C. H. Wang, H. Xia, and L. Zhou, "Implementation of a new memristor-based multiscroll hyperchaotic system," *Pramana-Journal of Physics*, vol. 88, no. 2, 2017.

[7] X. Zang and C. Wang, "Multiscroll hyperchaotic system with hidden attractors and its circuit implementation," *International Journal of Bifurcation and Chaos*, vol. 29, no. 9, Article ID 1950117, 2019.

[8] H. Lin, C. Wang, Q. Hong, and Y. Sun, "A multi-stable memristor and its application in a neural network," *IEEE Transactions on Circuits and Systems II: Express Briefs*, vol. 67, no. 12, pp. 3472–3476, 2020.

[9] H. R. Lin, H. Wang, W. Yao, and Y. M. Tan, "Chaotic dynamics in a neural network with different types of external stimuli," *Communications in Nonlinear Science and Numerical Simulation*, vol. 90, Article ID 105390, 2020.

[10] W. Yao, C. Wang, Y. Sun, C. Zhou, and H. Lin, "Exponential multistability of memristive cohen-grossberg neural networks with stochastic parameter perturbations," *Applied Mathematics and Computation*, vol. 386, Article ID 125483, 2020.

[11] W. Yao, C. Wang, Y. Sun, C. Zhou, and H. Lin, "Synchronization of inertial memristive neural networks with time-varying delays via static or dynamic event-triggered control," *Neurocomputing*, vol. 404, pp. 367–380, 2020.

[12] Y. M. Tan and C. H. Wang, "A simple locally active memristor and its application in HR neurons," *Chaos*, vol. 30, no. 5, Article ID 53118, 2020.

[13] C. Zhou, C. H. Wang, Y. C. Sun, and W. Yao, "Weighted sum synchronization of memristive coupled neural networks," *Neurocomputing*, vol. 403, pp. 225–232, 2020.

[14] H. Lin, C. Wang, Y. Sun, and W. Yao, "Firing multistability in a locally active memristive neuron model," *Nonlinear Dynamics*, vol. 100, no. 4, pp. 3667–3683, 2020.

[15] W. Yao, C. H. Wang, and J. D. Cao, "Hybrid multi-synchronization of coupled multistable memristive neural networks with time delays," *Neurocomputing*, vol. 363, pp. 281–294, 2019.

[16] S. Wang, C. Wang, and C. Xu, "An image encryption algorithm based on a hidden attractor chaos system and the

knuth-durstenfeld algorithm," *Optics and Lasers in Engineering*, vol. 128, Article ID 105995, 2020.

[17] C. Xu, J. Sun, and C. Wang, "An image encryption algorithm based on random walk and hyperchaotic systems," *International Journal of Bifurcation and Chaos*, vol. 30, no. 4, Article ID 2050060, 2020.

[18] G. F. Cheng, C. H. Wang, and C. Xu, "A novel hyper-chaotic image encryption scheme based on quantum genetic algorithm and compressive sensing," *Multimedia Tools and Applications*, vol. 79, pp. 39-40, 2020.

[19] T. Puu, "The chaotic duopolists revisited," *Journal of Economic Behavior and Organization*, vol. 33, no. 3, pp. 385–394, 1998.

[20] H. N. Agiza, A. A. Elsadany, and A. A. Elsadany, "Chaotic dynamics in nonlinear duopoly game with heterogeneous players," *Applied Mathematics and Computation*, vol. 149, no. 3, pp. 843–860, 2004.

[21] J. Ma and X. Pu, "Complex dynamics in nonlinear triopoly market with different expectations," *Discrete Dynamics in Nature and Society*, vol. 2011, Article ID 902014, 12 pages, 2011.

[22] A. A. Elsadany, "Competition analysis of a triopoly game with bounded rationality," *Chaos, Solitons & Fractals*, vol. 45, no. 11, pp. 1343–1348, 2012.

[23] A. A. Elsadany, "A dynamic cournot duopoly model with different strategies," *Journal of the Egyptian Mathematical Society*, vol. 23, no. 1, pp. 56–61, 2015.

[24] E. Ahmed and H. N. Agiza, "Dynamics of a cournot game with *n*-competitors," *Chaos, Solitons & Fractals*, vol. 9, no. 9, pp. 1513–1517, 1998.

[25] M. Zhao and S. Lv, "Chaos in a three-species food chain model with a beddington-deangelis functional response☆," *Chaos, Solitons & Fractals*, vol. 40, no. 5, pp. 2305–2316, 2009.

[26] M. F. Elettreby and S. Z. Hassan, "Dynamical multi-team cournot game," *Chaos, Solitons & Fractals*, vol. 27, no. 3, pp. 666–672, 2006.

[27] M. F. Elettreby and M. Mansour, "On cournot dynamic multi-team game using incomplete information dynamical system," *Applied Mathematics and Computation*, vol. 218, no. 21, pp. 10691–10696, 2012.

[28] M. F. Elettreby, "Two-prey one-predator model," *Chaos, Solitons & Fractals*, vol. 39, no. 5, pp. 2018–2027, 2009.

[29] R. K. Upadhyay, R. K. Naji, S. N. Raw, and B. Dubey, "The role of top predator interference on the dynamics of a food chain model," *Communications in Nonlinear Science and Numerical Simulation*, vol. 18, no. 3, pp. 757–768, 2013.

[30] M. F. Elettreby and H. El-Metwally, "Multi-team prey-predator model," *International Journal of Modern Physics C*, vol. 18, no. 10, pp. 1609–1617, 2007.

[31] Y. Liu, Y. Zhao, W. Ren, and G. Chen, "Appointed-time consensus: accurate and practical designs," *Automatica*, vol. 8, pp. 425–429, 2018.

[32] J. Cotter and R. Roll, "A comparative anatomy of residential REITs and private real estate markets: returns, risks and distributional characteristics," *Real Estate Economics*, vol. 43, no. 1, pp. 209–240, 2015.

[33] Y. J Yang and W. Z. Tang, "Research on a 3d predator-prey evolutionary system in real estate market," *Complexity*, vol. 2018, Article ID 6154940, 13 pages, 2018.

Hindawi
Complexity
Volume 2020, Article ID 8872307, 18 pages
https://doi.org/10.1155/2020/8872307

Research Article

Volatility Similarity and Spillover Effects in G20 Stock Market Comovements: An ICA-Based ARMA-APARCH-M Approach

Shanglei Chai,[1] **Zhen Zhang**,[2] **Mo Du**,[3] **and Lei Jiang**[4]

[1]*School of Business, Shandong Normal University, Jinan 250014, China*
[2]*Institute of Systems Engineering, Dalian University of Technology, Dalian 116024, China*
[3]*School of Accounting, Shandong Youth University of Political Science, Jinan 250103, China*
[4]*School of Economics, Zhejiang University of Finance & Economics, Hangzhou 310018, China*

Correspondence should be addressed to Zhen Zhang; zhen.zhang@dlut.edu.cn

Received 30 August 2020; Revised 11 November 2020; Accepted 1 December 2020; Published 11 December 2020

Academic Editor: Xueyong Liu

Financial internationalization leads to similar fluctuations and spillover effects in financial markets around the world, resulting in cross-border financial risks. This study examines comovements across G20 international stock markets while considering the volatility similarity and spillover effects. We provide a new approach using an ICA- (independent component analysis-) based ARMA-APARCH-M model to shed light on whether there are spillover effects among G20 stock markets with similar dynamics. Specifically, we first identify which G20 stock markets have similar volatility features using a fuzzy C-means time series clustering method and then investigate the dominant source of volatility spillovers using the ICA-based ARMA-APARCH-M model. The evidence has shown that the ICA method can more accurately capture market comovements with nonnormal distributions of the financial time series data by transforming the multivariate time series into statistically independent components (ICs). Our findings indicate that the G20 stock markets are clustered into three categories according to volatility similarity. There are spillover effects in stock market comovements of each group and the dominant source can be identified. This study has important implications for investors in international financial markets and for policymakers in G20 countries.

1. Introduction

Given the rising trend of contagion in global financial market, the G20, which was born after the 2008 financial crisis, has become the most important forum of global cooperation to address the crisis [1]. The spillover effects imply that a huge impact on a financial market will increase the returns and relevance of that market and other markets [2]. A further explanation is that the volatility of the stock markets will move together over time (i.e., comovements). So, how do we measure the comovements of the stock markets? Some existing studies [3–5] show that the comovements can be measured by the similarity among multiple markets because volatility similarity enhances information flows across markets and thus lead to comovements among them. That is, we can find that whenever the price of one market drops, its connected markets will also go down, and vice versa. Therefore, the volatility similarity measured by clustering analysis is applied to quantify comovements of stock markets in this study.

Motivated by this factor, we model on multivariate financial time series as it has long been a standard for studying volatility spillover and comovements [6]. However, the extant empirical literature has dealt with spillover effects focusing on shocks to volatility by multivariate GARCH models, which have the following disadvantages.

First, GARCH models are limited to solving two-dimensional or three-dimensional problems [7–12]. However, the fact cannot be ignored that there are far more than two or three interconnected financial markets at risk nowadays, which is lack of relevant research in the existing literature. To fill this gap, we intend to address high-dimensional volatility modeling problem in G20 financial markets; therefore, a new approach is necessary to deal with such situations.

Second, the existing literature does not include studies of volatility similarity and spillover effects in G20 stock market comovements. In today's increasing economic globalization economy and financial liberalization, it is generally believed that financial markets tend to fluctuate in a similar trend with each other. The fluctuations from more than two markets that have some underlying factors in common may simultaneously transmit to one market [13–16]. It is necessary to quantify the common volatility spillovers as a composite index of market comovements around the world.

Third, multicollinearity might occur when multiple financial market volatility factors act as explanatory variables to explain the volatility spillovers to the same market. If there is a certain correlation between explanatory variables, the result does not truly explain the spillover effects. Therefore, some statistically independent components that represent the volatilities of original multivariate time series must be decomposed.

To overcome these disadvantages, the idea of dimensionality reduction is needed to reflect the information of all indicators through a few indicators. Methods such as principal component analysis (PCA) or independent component analysis (ICA) can be used to decompose the information into unrelated parts in the low-dimensional space for more meaningful interpretation. Principal component analysis assumes that principal components obey Gaussian distribution; however, the actual data usually do not obey Gaussian distribution, such as the fat-tailed and nonnormal of financial time series data. ICA can solve such problems well. The use of ICA in financial data analysis is an exploratory effort to uncover some of the underlying driving mechanisms. This is the essential difference between ICA and other data processing methods, such as principal component analysis and factor analysis.

Therefore, we introduce ICA for volatility spillover effects modeling in G20 stock market comovements. Although the basic model of ICA was mainly applied to signal processing in the previous literature, it has recently shown more advantages when used in financial time series modeling [17]. The strongest point is that ICA can deal with more large-scale data than other competitive models with extremely low computational costs, thereby avoiding the curse of dimensionality. It also reproduces some higher moment features with the heavy-tailed and higher kurtosis distribution that really exist in the financial market [18–20]. In addition, it does not require joint estimation because each one of the components is independent. Based on the above analysis, it is appropriate to introduce ICA to study the co-movements of G20 stock markets in this paper.

Our study aims to address these essential problems as follows. (i) How can we identify the comovements of stock market in G20 countries, or which stock markets in G20 have similar volatility patterns? (ii) Among the markets with similar volatility, are there spillover effects in market comovements? (iii) If there are spillovers in two or more markets, which is the dominant source of spillovers? To address question (i), an ARMA-APARCH-M model and fuzzy C-means clustering method are adopted to explore the comovements according to volatility similarity. To address questions (ii) and (iii), we propose an ICA-based ARMA-APARCH-M model for investigating volatility spillovers of G20 stock market comovements.

This study is organized as follows. Section 2 discusses the relevant literature. In Section 3, we introduce the methodology and theoretical considerations. The data and empirical results are presented in Section 4. Conclusions are offered in Section 5.

2. Literature Review

The analysis of volatility spillover effects between cross-national stock markets is of high interest in the empirical financial literature, with increasing attention being paid to this issue [6, 21–26]. The transmission of volatility risk is analyzed by examining the spillover effect of volatility between financial markets. In these literatures, the generalized autoregressive conditional heteroskedasticity (GARCH) model, developed by Bollerslev [27], is widely used. Although this model can capture many characteristics of financial time series, its hypothesis ignores the symbol of new information. The negative shocks from bad news tend to trigger higher volatility than the arrival of good news. This phenomenon suggests that it is unreasonable for a simple GARCH model to set positive and negative shocks as symmetrical and equal impacts.

In view of the asymmetric impact, many extension models have been put forward, e.g., Ding et al.'s [28] APARCH (asymmetric power ARCH) model. Since then, the GARCH model with asymmetric items has been widely used in the following studies of stock markets' volatility [23, 29–31]. Mensi et al. [23] employed the bivariate APARCH model to capture volatility spillover effects between the U.S. and BRICS stock markets. Except for the GARCH models, some other conventional econometric methods are used for volatility spillover effects studies, such as the ARMA model [32], Markov regime-switching model [33, 34], and VAR framework [35–38]. However, a large number of parameters have to be estimated in these models when it comes to more than two or three financial assets. To overcome the curse of dimensionality, some network models have been proposed in recent years [1, 18, 20, 39–44]. Geng et al. [18] construct volatility networks of energy companies using the connectedness network approach and provide a reference for risk management.

No matter which method is used to examine the volatility spillover effects of financial markets, there is a common defect in the existing literature. That is, they have not considered the common volatility spillovers as composite index to measure risk contagion brought by the simultaneous movement. Volatility in a market is transmitted from more than two or three markets, which may have common latent elements and move together. Such a transmission of volatility across markets that are moving together is generally referred to volatility spillover effects of market comovements. This can be captured by a composite index that represents the weighting value of multiple stock return residuals as the comovements of financial variables.

To solve the problems described above, ICA which has been popularized in recent years has been adopted. It aims at extracting the independent components of implicit information from the original data without knowing signal-mixing process. Despite its popularity in signal processing, ICA has been recently applied in financial settings, e.g., stock price forecasting [45], realized volatility analysis [46], conditional covariance forecasting [14], portfolio selection [47], gold price analysis [48], and structural shock identification of VAR models [49]. The ICA method has an advantage that it can extract the underlying information in financial time series and provide more valuable information for financial forecasting [45]. The application of ICA in the study can overcome the curse of dimensionality and capture the volatility spillover effects from multiple financial markets to one market.

As an essential concept, the comovements' recognition across international stock markets has attracted many scholars to research [3, 19, 50–57]. Sheng et al. [57] analyze market comovements across eight major stock markets and verify the existence of volatility spillover. Chen [52] examines the comovements of stock markets using a novel Bayesian factor model. Although these studies recognize the concept of comovements, they do not quantify the comovements of stock markets. Since Aghabozorgi and Teh [3] refer to the fluctuations of stock markets in a homogeneous group as comovements, we employ volatility similarity analysis to quantify the comovements. Volatility similarity is defined as a close distance between volatility influencing factors representing fluctuation features, i.e., market movements are organized into homogeneous groups where the distance of within-group objects is minimized and the distance of cross-group objects is maximized. For distance calculation, the method of grouping time series by clustering analysis has been recently applied to address financial time series issues [58–65]. These scholars agree that clusters generated on account of similarity are very accurate and meaningful. Hence, we use volatility similarity measured by a fuzzy C-means (FCM) clustering analysis to quantify comovements of stock markets.

3. Methodology

To examine the volatility similarity and spillover effects in G20 stock market comovements, an ICA-based ARMA-APARCH-M approach has been proposed. As shown in Figure 1, we adopted three steps to solve the problems mentioned in the introduction. The ARMA-APARCH-M model is employed to acquire the residuals of return series and then use ICA to generate the independent components (ICs). Each calculated independent component is a composite index representing the weighting value of multiple stock return residuals. As potential components that capture volatility are statistically independent, we can fit a univariate ARMA-APARCH-M model to each IC. In this way, the volatility spillover effects from multiple financial markets to one in comovements can be examined.

3.1. Independent Component Analysis (ICA). ICA is a method of statistical and numerical analysis to extract the independent components of unknown signals or random variables. This method was originally developed to deal with blind source separation (BSS), also known as the cocktail party problem. The so-called cocktail party problem is that in a banquet full of various conversations and music, people can still focus on hearing what they want to hear despite the different sounds around them. Without knowing the mixing mechanism, it only looks for statistically independent components that are hidden in the complex phenomenon using a linear or nonlinear decomposition of the observed data.

Suppose that $\mathbf{X} = [\mathbf{x}_1, \mathbf{x}_2, \ldots, \mathbf{x}_m]^T$ denotes a given multivariate matrix of size $m \times n$, and $\mathbf{x}_i$ refers to the observed mixture signal. The basic ICA model [66] is given by

$$\mathbf{X} = \mathbf{AS} = \sum_{i=1}^{m} a_i s_i, \tag{1}$$

where $\mathbf{A}$ is the unknown mixing matrix and $\mathbf{S}$ is the source matrix that cannot be directly observed. The ICA model explains how to generate observations by mixing components s_i. Independent component (IC) is a latent variable that cannot be directly observed. ICA aims to find a specific $m \times m$ demixing matrix $\mathbf{W}$ such that

$$\mathbf{Y} = [\mathbf{y}_i] = \mathbf{WX}, \tag{2}$$

where $\mathbf{y}_i$ is the i^{th} row of the matrix $\mathbf{Y}$, $i = 1, 2, \ldots, m$. It is used to estimate the independent latent source signals (s_i). The independent components (ICs) $\mathbf{y}_i$ must be statistically independent. When demixing matrix $\mathbf{W}$ is the inverse of mixing matrix $\mathbf{A}$, i.e., $\mathbf{W} = \mathbf{A}^{-1}$, ICs ($\mathbf{y}_i$) can be used to estimate the latent source signals s_i. In this study, we adopt the FastICA algorithm proposed by Hyvärinen and Oja [66] to solve the demixing matrix W, as it has been shown to work well with financial data [14]. It is an algorithm on the basis of a fixed-point iteration process to maximize the non-Gaussianity of $\mathbf{w}^T\mathbf{x}$. The derivative of the nonquadratic function G is denoted by g. It is completed by the following four steps:

Step 1: choose an initial weight vector $\mathbf{W}$

Step 2: let $\mathbf{W}^+ = E\{\mathbf{X}g(\mathbf{W}^T\mathbf{X})\} - E\{g'(\mathbf{W}^T\mathbf{X})\}\mathbf{W}$

Step 3: let $\mathbf{W}^+ = \mathbf{W}^+/\|\mathbf{W}^+\|$

Step 4: if not converged, go back to 2

3.2. ARMA-APARCH-M Model. To explain the asymmetric effects of positive and negative shocks in financial markets, Ding et al. [28] propose an asymmetric power ARCH (APARCH) model in consideration of long memory property, which is

$$r_t = \mu + \varepsilon_t, \quad \varepsilon_t|\psi_{t-1} \sim N\left(0, \sigma_t^2\right), \tag{3}$$

$$\sigma_t^\delta = \alpha_0 + \sum_{i=1}^{q} \alpha_i\left(\left|\varepsilon_{t-i}\right| - \gamma_i\varepsilon_{t-i}\right)^\delta + \sum_{j=1}^{p} \beta_j\sigma_{t-j}^\delta, \tag{4}$$

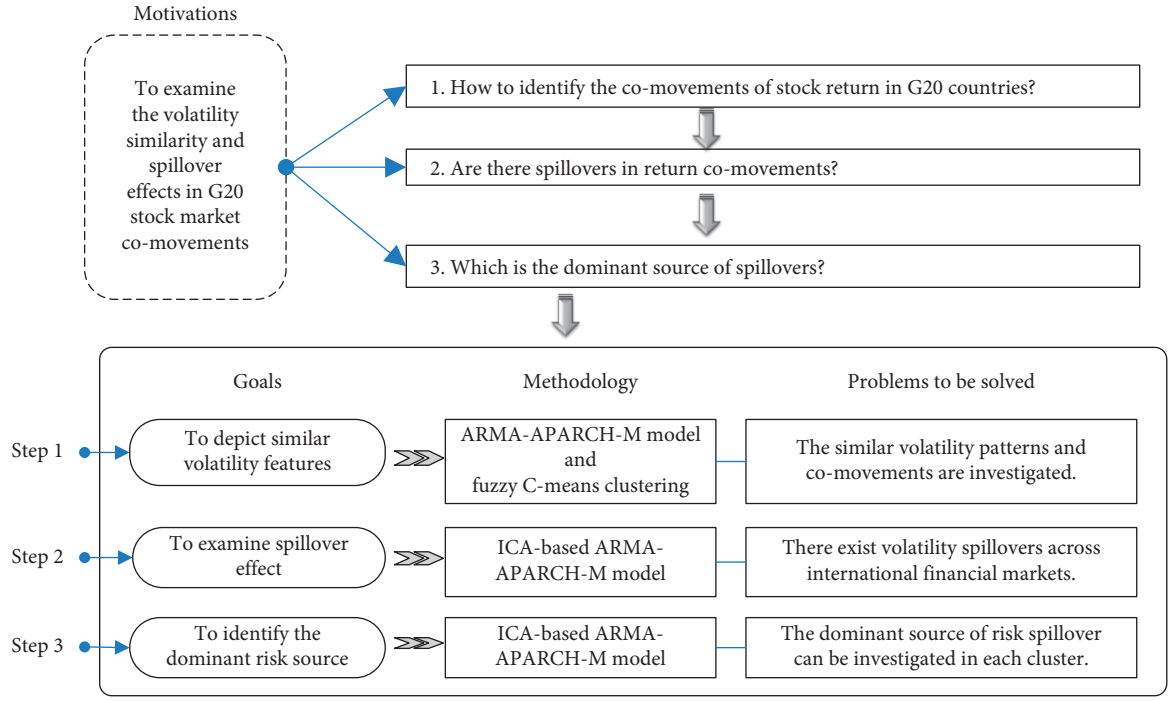

Figure 1: The frame diagram of the methodology.

where r_t is the logarithmic returns of stock markets, defined as the sum of a conditional mean μ and a zero-mean disturbance ε_t. The conditional standard deviation σ_t can be estimated by the relevant lagged information over multi-periods. The coefficient γ_i represents the asymmetric effect. The estimated parameter δ is not preset, but estimated from the sample data.

However, in financial investments, the greater the risk, the greater the expected return, a phenomenon called risk reward when risk increases. Therefore, the APARCH model is extended to an APARCH-M model so that the conditional variance can directly influence the mean of returns. In addition, evidence has shown that the financial time series is sequence autocorrelated because it is influenced by its own inertia and lag effect. We incorporate autoregressive moving average (ARMA) in the APARCH-M model, which is named ARMA-APARCH-M.

$$\begin{aligned} r_t &= \mu + \sum_{i=1}^{m} \varphi_i r_{t-i} + \omega\sigma_t + \varepsilon_t + \sum_{j=1}^{n} \theta_j \varepsilon_{t-j} \\ &= \mu + \mathrm{ARMA}(m,n) + \omega\sigma_t + \varepsilon_t, \end{aligned} \tag{5}$$

$$\sigma_t^{\delta} = \alpha_0 + \sum_{i=1}^{p} \alpha_i \left(|\varepsilon_{t-i}| - \gamma_i \varepsilon_{t-i}\right)^{\delta} + \sum_{j=1}^{q} \beta_j \sigma_{t-j}^{\delta}, \tag{6}$$

where $\{\varphi_1, \varphi_2, \ldots, \varphi_m, \theta_1, \theta_2, \ldots, \theta_n\}$ is the set of AR(m) and MA(n) coefficients and ω is the contribution rates of risk to returns. The definitions of other symbols are same to equations (3) and (4).

3.3. ICA-Based ARMA-APARCH-M Model. Suppose we need to investigate whether there are volatility spillovers from other z financial markets $(z = 2, \ldots, n)$ to one financial market x in the comovements process. First, the mean return equations are established for z markets:

$$\begin{aligned} r_{1t} &= \mu_1 + \sum_{i=1}^{m} \varphi_{1i} r_{1,t-i} + \omega_{1t}\sigma_{1t} + \varepsilon_{1t} + \sum_{j=1}^{n} \theta_{1j} \varepsilon_{1,t-j} r_{2t} \\ &= \mu_2 + \sum_{i=1}^{m} \varphi_{2i} r_{2,t-i} + \omega_{2t}\sigma_{2t} + \varepsilon_{2t} + \sum_{j=1}^{n} \theta_{2j} \varepsilon_{2,t-j} \vdots r_{zt} \\ &= \mu_z + \sum_{i=1}^{m} \varphi_{zi} r_{z,t-i} + \omega_{zt}\sigma_{zt} + \varepsilon_{zt} + \sum_{j=1}^{n} \theta_{zj} \varepsilon_{z,t-j}, \end{aligned} \tag{7}$$

where $r_{1t}, r_{2t}, \ldots, r_{zt}$ are the logarithmic returns of z financial markets, $\sigma_{1t}, \sigma_{2t}, \ldots, \sigma_{zt}$ represent the internal market risks of stock markets, $\varepsilon_{1t}, \varepsilon_{2t}, \ldots, \varepsilon_{zt}$ are the return residual sequences, and $\omega_{1t}, \omega_{2t}, \ldots, \omega_{zt}$ are contribution rates of the internal market risks to returns. Then, ICA is applied to transform the residual sequences into several statistically independent components that represent comprehensive indices of multiple market fluctuations.

$$\begin{aligned} s_{1t} &= w_{11}\varepsilon_{1t} + w_{12}\varepsilon_{2t} + \cdots + w_{1k}\varepsilon_{kt} \\ s_{2t} &= w_{21}\varepsilon_{1t} + w_{22}\varepsilon_{2t} + \cdots + w_{2k}\varepsilon_{kt} \\ &\vdots \\ s_{kt} &= w_{k1}\varepsilon_{1t} + w_{k2}\varepsilon_{2t} + \cdots + w_{kk}\varepsilon_{kt}, \end{aligned} \tag{8}$$

where $s_{1t}, s_{2t}, \ldots, s_{kt}$ are the independent components named as $\mathrm{IC}_1, \mathrm{IC}_2, \ldots, \mathrm{IC}_k$ and $\varepsilon_{1t}, \varepsilon_{2t}, \ldots, \varepsilon_{kt}$ are the return residual sequences.

Third, a univariate ARMA-APARCH-M model is established to examine spillover effects from other z financial

markets $(z = 2, \ldots, n)$ to one financial market x in the comovements process. That is, the independent components $s_{1t}, s_{2t}, \ldots, s_{kt}$ are substituted into the mean equation of financial market x as explanatory variables to obtain an ICA-based ARMA-APARCH-M model as

$$r_{xt} = \mu_x + \sum_{i=1}^{m} \varphi_{xi} r_{x,t-i} + \omega_x \sigma_{xt} + \delta_1 s_{1t} + \delta_2 s_{2t} + \cdots + \delta_k s_{kt} + \varepsilon_{xt} + \sum_{j=1}^{n} \theta_{xj} \varepsilon_{x,t-j}, \tag{9}$$

where $\delta_1, \delta_2, \ldots, \delta_k$ are contribution rates of the independent components $s_{1t}, s_{2t}, \ldots, s_{kt}$ to returns. If $\delta_i (i = 1, \ldots, k)$ is significantly not zero, the new comprehensive index $s_i (i = 1, \ldots, k)$ has volatility spillover effects on market x.

4. Data and Empirical Results

4.1. Data. To empirically investigate volatility similarity and spillover effects of stock market comovements, we use daily closing prices of G20 stock markets from January 02, 2006, to June 18, 2018. Notably, the G20 is a global organization dealing with financial risks, and it includes nineteen countries plus the European Union as a whole. They are S&P 500 (US), Nikkei 225 (Japan), DAX (Germany), CAC 40 (France), FTSE 100 (UK), MIB (Italy), TSX (Canada), RTS (Russia), SSE Composite (China), MERVAL (Argentina), All Ordinaries (Australia), Bovespa (Brazil), BSE Sensex (India), Jakarta Composite (Indonesia), IPC (Mexico), TASI (Saudi Arabia), INVSAF 40 (South Africa), ISE 100 (Turkey), and KOSPI (South Korea). The long-term trends of G20 stock prices time series denoted as p_t are shown in Figure 2.

They are inherently nonstationary which means that the distribution of time series changes over time. This universal feature of financial time series makes volatility modeling a challenging task that attracts a large number of scholars to discuss [35, 36, 67]. To settle this issue, the returns r_t are calculated as $r_t = \ln(p_t/p_{t-1}) = \ln(p_t) - \ln(p_{t-1})$, which is the difference in logarithmic price. Some volatility characteristics of return series for G20 stock markets are shown in Figure 3.

First, the fluctuation trend appears to be clustered together in bunches. This phenomenon indicates that there may be conditional heteroskedasticity, which needs to be tested further. Second, there exists significant asymmetric response to positive and negative shocks, which is also called leverage effect. To further explain, the fact is that stock markets tend to be more violent on bad news and less violent on good news. During the 2008 financial crisis, the price fell like a cliff, while the stock volatility jumped dramatically. Therefore, asymmetric terms cannot be ignored when modeling on volatility of financial time series. Third, the volatility features of some stock return series are similar to others in their comovements. For example, the stock markets of the US and UK have similar volatility trends as they are impacted by common factors, such as economic development, international trade, and investment. It indicates that volatility similarity may exist in G20 stock market comovements, which must be examined further. Therefore, we intend to initially identify the comovements and accurately determine which G20 stock markets have similar volatility features.

Before modeling volatility, we briefly analyze the descriptive statistics of G20 stock markets. The mean, standard deviation (S.D.), skewness, kurtosis, Jarque-Bera statistic, ADF test for unit root, and ARCH effect test for heteroskedasticity are presented in Table 1. The skewness of each return series is nonzero, which indicates that the series distribution is biased relative to the normal distribution. The kurtosis of each return series is greater than 3, that is, the convexity of the distribution is greater than the normal distribution. The Jarque-Bera statistics are relatively large and their associated probability p values are all close to zero.

To sum up, we can reject the null hypothesis and therefore draw a conclusion that the return series do not obey the normal distribution. In this context, some conventional models of normal hypothesis are not applicable. To overcome this drawback, ICA is used for modeling as it can reproduce high kurtosis in return series [17]. The ADF test results of the return series show that it is a stationary series, confirming the necessity of the logarithmic difference transformation on price series. The F-statistic and $T \times R^2$ testing results clearly reject the null hypothesis of no ARCH effect. The evidence shows that GARCH models should also be designed to measure heteroskedasticity. In conclusion, we provide a new approach using an ICA-based ARMA-APARCH-M model to address the cross-markets volatility spillover effects of market comovements.

4.2. Empirical Results

4.2.1. Results of Comovements Identification. One approach of detecting comovements is clustering analysis [3]. The time series clustering methods are summarized into three types: original data, feature extraction, and model parameters [68]. Among these methods, we choose model-based fuzzy C-means clustering. After establishing the ARMA-APARCH-M model to extract volatility features of high-dimensional stock return time series, a fuzzy C-means (FCM) method is used for clustering the model parameters that describe the volatility characteristics. The coefficient results estimated by the ARMA-APARCH-M model are presented in Table 2. All the parameters are significantly nonzero; thus, the actual data satisfy the hypothesis conditions of the model. The asymmetry coefficient γ in the test is statistically significant, which means that this asymmetric behavior does exist, that is, the negative impact on the fluctuation is more severe than the positive impact of the same magnitude.

This result is consistent with the conclusions of Ning et al. [69] and Bekaert et al. [67]. The asymmetry in volatility clusters of stock markets is found to be more obvious than in other financial markets [69]. Compared with a positive impact of the same size, the increase in negative impact and conditional variance is greater [67]. The risk return coefficient ω is nonzero, which denotes that the risk factor has a significant impact on returns. Thus, the risk factor should be considered in the model. The power parameter of conditional heteroskedasticity comes through $\delta > 0$, which is

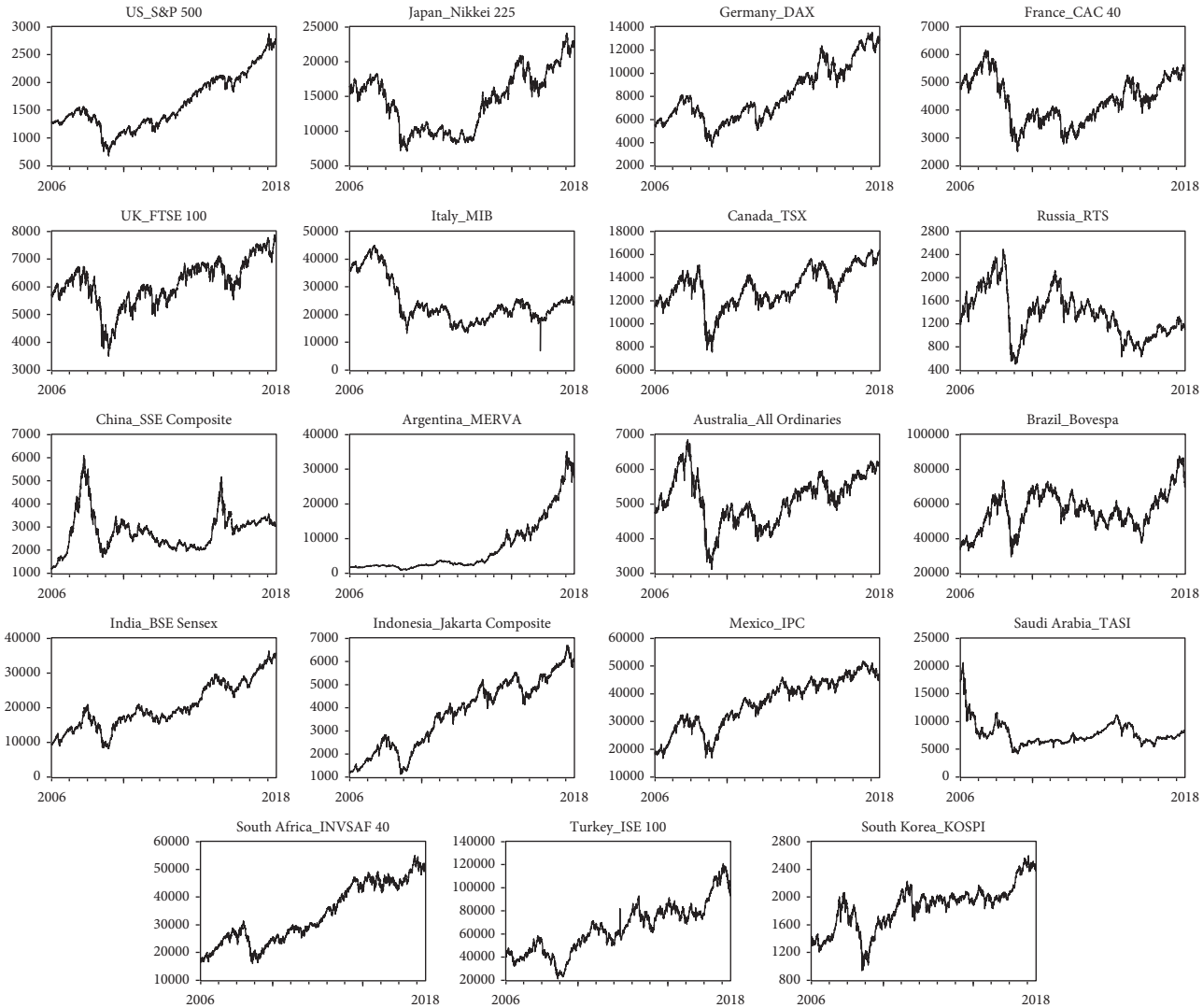

Figure 2: The volatility characteristics of G20 stock prices. (a) US_S&P 500, (b) Japan_Nikkei 225, (c) Germany_DAX, (d) France_CAC 40, (e) UK_FTSE 100, (f) Italy_MIB, (g) Canada_TSX, (h) Russia_RTS, (i) China_SSE Composite, (j) Argentina_MERVAL, (k) Australia_All Ordinaries, (l) Brazil_Bovespa, (m) India_BSE Sensex, (n) Indonesia_Jakarta Composite, (o) Mexico_IPC, (p) Saudi Arabia_TASI, (q) South Africa_INVSAF 40, (r) Turkey_ISE 100, and (s) South Korea_KOSPI.

neither one in the Taylor/Schwert's model setting nor two in the Bollerslev's model setting, which verifies the rationality of the APARCH model. It is not a specific value setting but rather a parameter estimation. Thus, it can more accurately evaluate the impact of conditional variance. After extracting volatility features by the ARMA-APARCH-M model, we use the fuzzy C-means (FCM) method to cluster G20 stock markets into three categories, as shown in Figure 4. The proposed model identifies clusters of return series with similar volatility patterns and handles simultaneous comovements across international stock markets.

The figure indicates that there exists apparent difference between three groups obtained by clustering the G20 stock markets. Different clusters correspond to different dynamic patterns corresponding to volatility coefficients.

Cluster 1: S&P 500 (US), DAX (Germany), CAC 40 (France), FTSE 100 (UK), MIB (Italy), TSX (Canada), and All Ordinaries (Australia).

Cluster 2: Nikkei 225 (Japan), SSE Composite (China), MERVAL (Argentina), BSE Sensex (India), Jakarta Composite (Indonesia), TASI (Saudi Arabia), and ISE 100 (Turkey).

Cluster 3: RTS (Russia), Bovespa (Brazil), IPC (Mexico), INVSAF 40 (South Africa), and KOSPI (South Korea).

In cluster 1, the members are mainly well-developed stock markets in Europe and America. The closer economic ties and trade links between these countries have made the volatility features of financial markets more similar to each other.

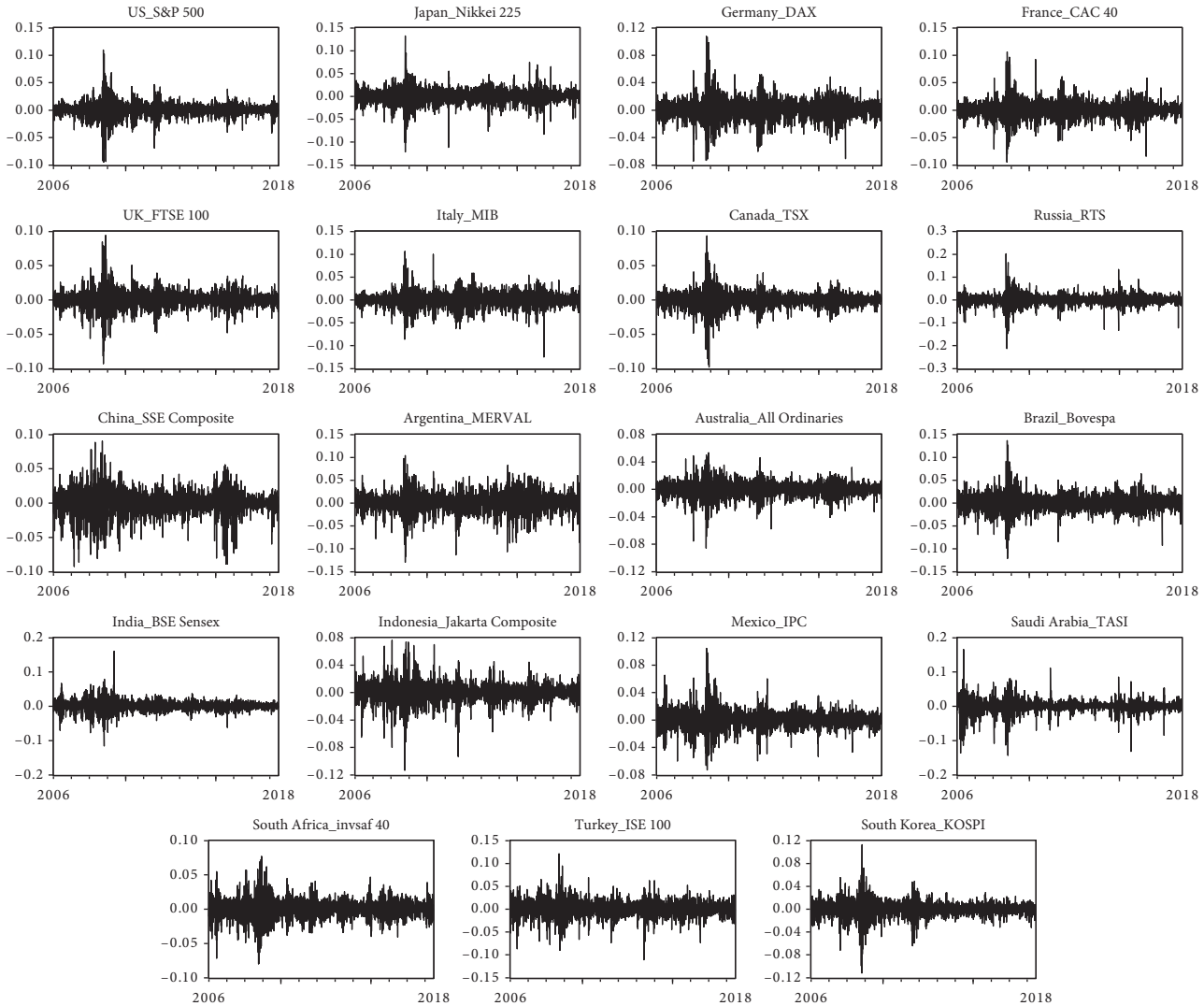

Figure 3: The volatility characteristics of G20 stock returns. (a) US_S&P 500, (b) Japan_Nikkei 225, (c) Germany_DAX, (d) France_CAC 40, (e) UK_FTSE 100, (f) Italy_MIB, (g) Canada_TSX, (h) Russia_RTS, (i) China_SSE Composite, (j) Argentina_MERVAL, (k) Australia_All Ordinaries, (l) Brazil_Bovespa, (m) India_BSE Sensex, (n) Indonesia_Jakarta Composite, (o) Mexico_IPC, (p) Saudi Arabia_TASI, (q) South Africa_INVSAF 40, (r) Turkey_ISE 100, and (s) South Korea_KOSPI.

It is special that almost all cluster 1 markets experienced peak volatility in October 2008 when Lehman Brothers closed down. This may be due to the sharp fluctuations of the US market during the financial turmoil, which was immediately transmitted to other member markets in cluster 1. In addition, the comovements with drastic volatile characteristics across multiple markets in cluster 1 exist significantly in the period of the European sovereign debt crisis from late 2009 to the end of 2012 and the Brexit vote on June 23, 2016. Although the volatility of each market is caused by the crisis to inconsistent extent, some similarities are shown obviously in volatility patterns and therefore volatility spillover effects may exist in cluster 1. To further confirm the existence of this effect, more accurate quantification is necessary in the following subsection. In line with our finding, Morales-Zumaquero and Sosvilla-Rivero [70] show that the US stock market is closely related to the other six stock markets, i.e., those of the UK, EU, Australia, Switzerland, Canada, and Japan.

In cluster 2, the members are mainly less well-developed stock markets in Asia, such as Japan, China, India, Indonesia, and Saudi Arabia. As shown by Zhou et al. [71]; the volatility of the Chinese market is more pronounced by the spillover effect of Japan rather than the United States and the United Kingdom. Moreover, the Indian market also has an impact on the Chinese market. Meanwhile, they also specifically point out that these volatility spillover effects exist in both directions. The large fluctuations in the Chinese market in February 2007 have been transferred to the Asian market. These facts may be attributed to the growing trend of financial integration in Asia. Thus, these Asian stock markets are clustered into one group based on volatility similarity.

In cluster 3, the members are mainly emerging stock markets that are less mature and open to foreign investors than the other markets in cluster 1. Three of these countries are the BRICS members, e.g., Russia, Brazil, and South Africa. Due to the weak openness of their domestic financial

Table 1: Summary descriptive statistics of G20 stock returns.

Stock indices	Mean	S. D.	Skewness	Kurtosis	Jarque-Bera	ADF test:	ARCH LM test:	
							F-statistic	$T \times R^2$
US_S&P 500	0.0002	0.0120	−0.3770	14.9110	19246.8700	−44.9070	128.3470	123.5320
Japan_Nikkei 225	0.0001	0.0152	−0.5150	11.2390	9314.9420	−59.3620	127.2750	122.5390
Germany_DAX	0.0003	0.0137	−0.0420	9.2260	5238.1310	−57.4980	102.3060	99.2350
France_CAC 40	0.0000	0.0141	−0.0050	9.5690	5831.4690	−59.6110	129.2030	124.3240
UK_FTSE 100	0.0001	0.0117	−0.1440	11.1940	9084.7360	−43.2410	206.3210	194.0850
Italy_MIB	−0.0001	0.0152	−0.2310	8.2470	3748.7100	−58.4250	121.9480	117.5950
Canada_TSX	0.0001	0.0110	−0.7060	14.8520	19249.2100	−25.9650	426.8940	377.4150
Russia_RTS	0.0000	0.0215	−0.4130	14.6270	18359.0100	−51.3530	184.1580	174.3580
China_SSE Composite	0.0003	0.0168	−0.6120	7.3980	2815.7120	−57.0240	111.4290	107.7900
Argentina_MERVAL	0.0009	0.0197	−0.4830	7.0170	2306.2880	−54.7720	191.8890	181.2690
Australia_All Ordinaries	0.0000	0.0106	−0.5830	8.6680	4524.2370	−58.5830	340.7710	308.5220
Brazil_Bovespa	0.0000	0.0170	−0.0390	9.1410	5096.1870	−58.9570	103.6580	100.5060
India_BSE Sensex	0.0000	0.0141	0.1040	13.0620	13687.0800	−54.2680	61.4310	60.3250
Indonesia_Jakarta	0.0001	0.0132	−0.6660	11.5470	10109.4500	−52.3560	118.3860	114.2820
Mexico_IPC	0.0000	0.0123	0.1030	10.1870	6984.7720	−34.9620	65.1940	63.9470
Saudi Arabia_TASI	0.0000	0.0171	−0.9680	16.6220	25581.3500	−39.3160	197.4790	186.2460
South Africa_INVSAF 40	0.0000	0.0132	−0.1170	6.9040	2066.9090	−57.3320	157.3460	150.1490
Turkey_ISE 100	0.0000	0.0164	−0.2950	7.1410	2364.6120	−56.5210	40.7560	40.2750
South Korea_KOSPI	0.0000	0.0123	−0.5950	12.9000	13434.3900	−56.9490	167.4950	159.3580

Note: S. D. is the standard deviation of G20 stock return time series. The Jarque-Bera is the normality test statistic. The critical values of the ADF test are −3.432180 at 1% level, −2.862234 at 5% level, and −2.567183 at 10% level.

Table 2: The coefficient results estimated by the ARMA-APARCH-M model.

Stock indices	μ	φ	ω	θ	α_0	α	γ	β	δ
US_S&P 500	0.0008	−0.3444	−0.0655	0.1482	−0.1697	0.9753	−0.0655	0.0008	−0.3444
Japan_Nikkei 225	−0.0008	−0.5427	0.0755	0.1949	−0.1120	0.9543	0.0755	−0.0008	−0.5427
Germany_DAX	0.0002	−0.3315	0.0002	0.1254	−0.1260	0.9735	0.0002	0.0002	−0.3315
France_CAC 40	−0.0003	−0.3307	0.0276	0.1126	−0.1651	0.9726	0.0276	−0.0003	−0.3307
UK_FTSE 100	−0.0009	−0.3532	0.1028	0.1329	−0.1266	0.9732	0.1028	−0.0009	−0.3532
Italy_MIB	−0.0002	−0.3033	0.0101	0.1342	−0.1117	0.9770	0.0101	−0.0002	−0.3033
Canada_TSX	0.0001	−0.2143	−0.0022	0.1196	−0.0976	0.9872	−0.0022	0.0001	−0.2143
Russia_RTS	0.0003	−0.2347	−0.0236	0.1237	−0.0754	0.9823	−0.0236	0.0003	−0.2347
China_SSE Composite	−0.0001	−0.1577	0.0414	0.1407	−0.0013	0.9936	0.0414	−0.0001	−0.1577
Argentina_MERVAL	−0.0003	−0.5958	0.0879	0.2202	−0.0503	0.9460	0.0879	−0.0003	−0.5958
Australia_All Ordinaries	−0.0003	−0.3938	0.0536	0.1503	−0.1124	0.9706	0.0536	−0.0003	−0.3938
Brazil_Bovespa	−0.0012	−0.2782	0.0861	0.1144	−0.0681	0.9771	0.0861	−0.0012	−0.2782
India_BSE Sensex	0.0002	−0.2702	0.0267	0.1745	−0.0703	0.9844	0.0267	0.0002	−0.2702
Indonesia_Jakarta Composite	−0.0005	−0.3691	0.1101	0.2050	−0.0638	0.9759	0.1101	−0.0005	−0.3691
Mexico_IPC	−0.0007	−0.2580	0.0836	0.1386	−0.0903	0.9833	0.0836	−0.0007	−0.2580
Saudi Arabia_TASI	0.0012	−0.3862	−0.0848	0.2432	−0.0741	0.9744	−0.0848	0.0012	−0.3862
South Africa_INVSAF40	−0.0006	−0.3108	0.0870	0.1349	−0.1104	0.9772	0.0870	−0.0006	−0.3108
Turkey_ISE 100	0.0011	−0.4093	−0.0432	0.1610	−0.0746	0.9658	−0.0432	0.0011	−0.4093
South Korea_KOSPI	−0.0006	−0.2821	0.0795	0.1408	−0.0774	0.9808	0.0795	−0.0006	−0.2821

Note: μ, φ, ω *and*, θ denote the coefficients of the mean equation, while $\alpha_0, \alpha, \gamma, \beta$, *and* δ denote the coefficients of the conditional variance equation. φ *and* θ are the coefficients of ARMA process indicating autoregressive and moving average. ω is the risk return which exhibits the impact from the conditional variance to return. γ is the asymmetry coefficient. δ is the power parameter of conditional heteroskedasticity.

markets, they were less impacted by the global financial crisis.

The most important implication of comovements identification is risk management in the stock markets. We can uncover volatility similarities by the method that reveals comovements of stock markets across the world. The motivation of this process is to inspire the investors' interest for higher returns in stock markets by using relevant information of the comoving markets in the same cluster as prior knowledge. Our results demonstrate the benefits of our study, wherein the empirical discussion allows better understanding of the comovements across multiple markets. Therefore, the risk measured by volatility can be detected in one stock market that is similar to other comoving markets.

4.2.2. Volatility Spillover Effects in Cluster 1. Using an ICA-based ARMA-APARCH-M model, we seek to answer

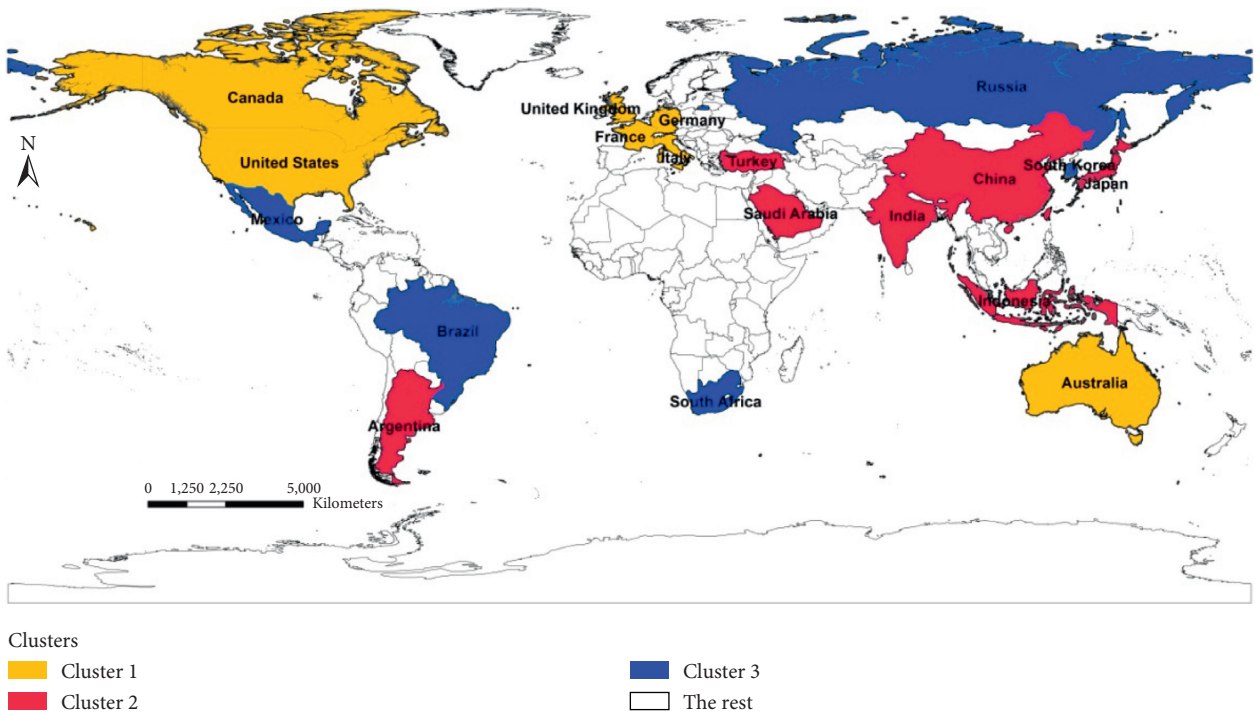

Figure 4: The clustering results of G20 stock markets.

questions (ii) and (iii) mentioned in the introduction. That is, among markets with similar volatility, are there spillover effects in market comovements? If there are spillover effects in two or more markets, which is the dominant source of spillovers? To address these questions, we use the FastICA algorithm [66] in each cluster to examine the spillover effects from multiple markets to one market. Take cluster 1 for example. We choose the S&P 500 (US) as the objective or the explained variable to investigate whether the other six stock markets (DAX, CAC 40, FTSE 100, MIB, TSX, and All Ordinaries) with similar volatility patterns in cluster 1 have volatility spillover effects to the S&P 500 and which is the dominant source. The residual series of six stock returns drawn by the ARMA-APARCH-M model are shown in Figure 5.

First, we employ ICA to the residual series $\varepsilon_{1t}, \varepsilon_{2t}, \varepsilon_{3t}, \varepsilon_{4t}, \varepsilon_{5t}$, and ε_{6t} of DAX (Germany), CAC 40 (France), FTSE 100 (UK), MIB (Italy), TSX (Canada), and All Ordinaries (Australia). The demixing matrix $\mathbf{W}_1$ is given by equation (10). The numbers in matrix $\mathbf{W}_1$ are the weights of each independent component (IC), which is a composite index obtained by the linear combination of residual series. The weight of each stock market in each independent component is clear.

$$\mathbf{W}_1 = \begin{pmatrix} 23.6145 & 109.2491 & -4.9218 & -143.9797 & -2.5157 & -2.1065 \\ 64.4442 & 76.0391 & -187.6554 & 3.0148 & -3.1082 & 7.5524 \\ -58.7561 & -34.8238 & 8.2896 & 26.5095 & -20.7591 & 16.6815 \\ 17.2218 & 11.9073 & 45.4227 & -0.2849 & -106.0729 & 27.1261 \\ 0.7523 & -0.5108 & -1.5688 & -5.5844 & 29.5780 & 88.8336 \\ -165.2102 & 205.4445 & -39.5022 & -8.1738 & 0.0620 & -1.1539 \end{pmatrix}. \quad (10)$$

Then, we further discover something valuable from the weights of each independent component, IC_1, IC_2, IC_3, IC_4, IC_5, or IC_6. In IC_1, ε_{4t} has the maximum absolute value of the weight (−143.9797) in the first row of the matrix $\mathbf{W}_1$, which is significantly higher than that of other sequences $\varepsilon_{1t}, \varepsilon_{2t}, \varepsilon_{3t}, \varepsilon_{5t}$, and ε_{6t}. Therefore, it is believed that IC_1 mainly represents the residual series ε_{4t}, i.e., MIB (Italy). Respectively, IC_2 mainly represents the residual series ε_{3t}, i.e., FTSE 100 (UK); IC_3 mainly represents the residual series ε_{1t}, i.e., DAX (Germany); IC_4 mainly represents the residual series ε_{5t}, i.e., TSX (Canada); IC_5 mainly represents the residual series ε_{6t}, i.e., All Ordinaries (Australia); and IC_6 mainly represents the residual series ε_{2t}, i.e., CAC 40 (France). The ICs shown in Figure 6 are statistically

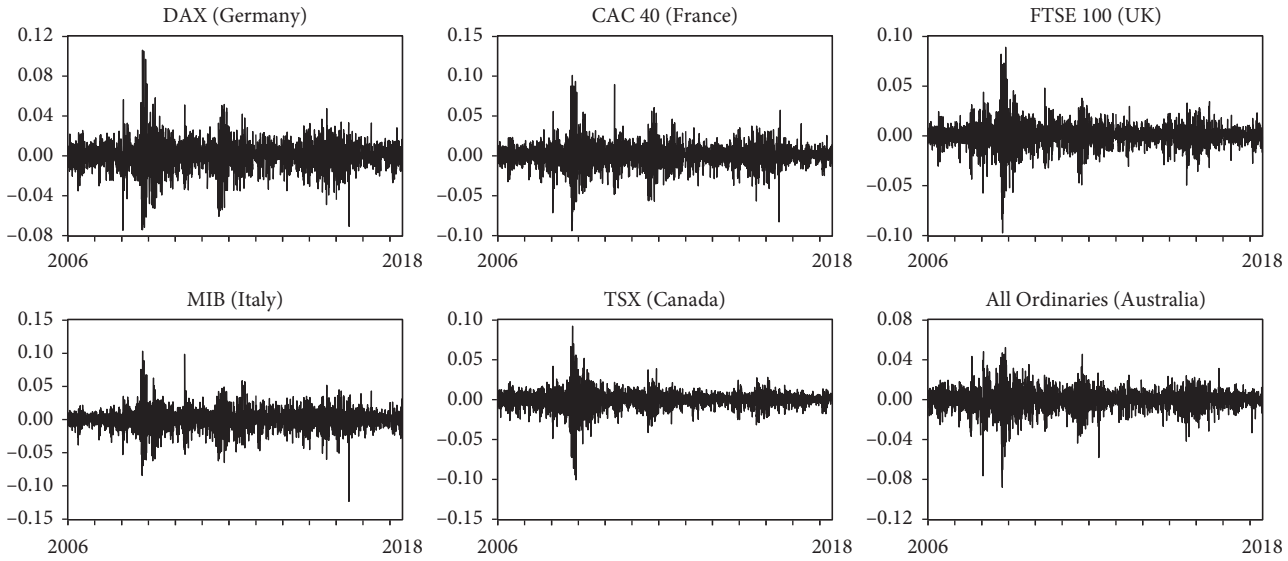

Figure 5: The residual series given by the ARMA-APARCH-M model. (a) DAX (Germany), (b) CAC 40 (France), (c) FTSE 100 (UK), (d) MIB (Italy), (e) TSX (Canada), and (f) All Ordinaries (Australia).

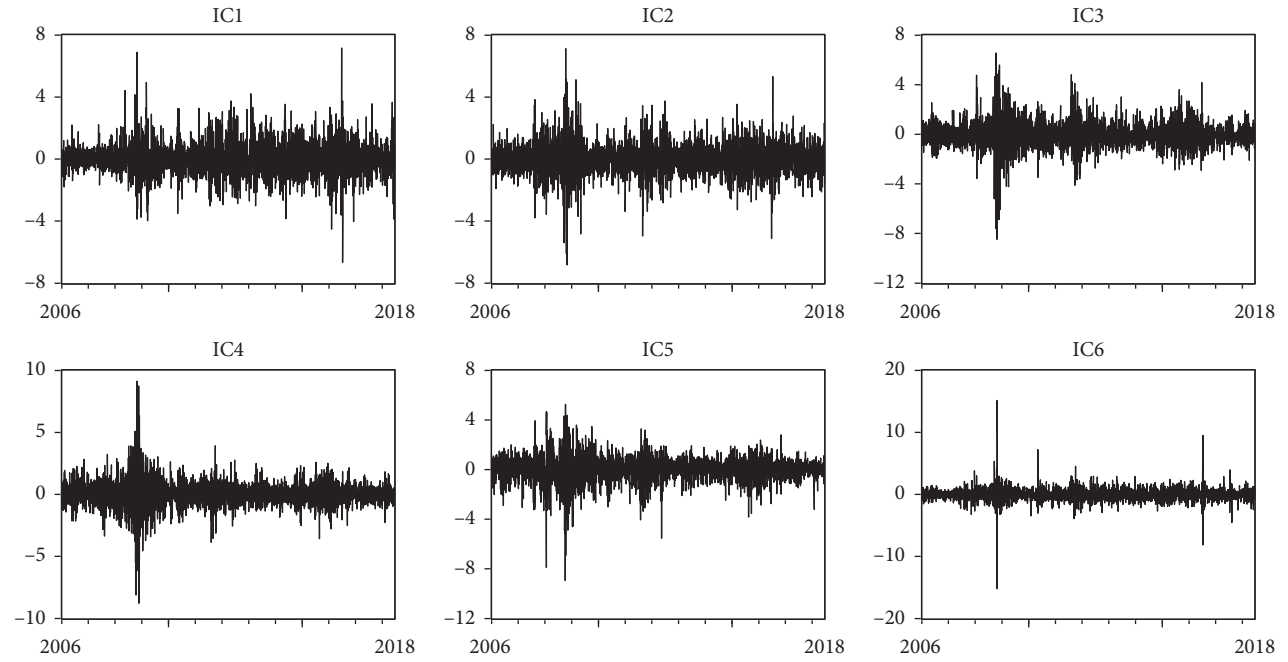

Figure 6: The time series of $IC_1, IC_2, IC_3, IC_4, IC_5$, and IC_6 for cluster 1. (a) IC_1, (b) IC_2, (c) IC_3, (d) IC_4, (e) IC_5, and (f) IC_6.

independent; thus, multicollinearity is avoided in the following model.

After estimating the ICs, we fit a univariate ARMA-APARCH-M model to each of them. That is, IC_1, IC_2, IC_3, IC_4, IC_5, and IC_6 are incorporated as explanatory variables to equation (9). The coefficient results estimated by the ICA-based ARMA-APARCH-M model for cluster 1 are listed in Table 3. The mean equation and the conditional variance equation are given by equations (11) and (12), respectively. The contribution of each IC is listed, which denotes the volatility spillover effects from each IC to S&P 500 (US) in equation (11). The results show that there are volatility spillovers from independent components (ICs) to S&P 500 (US). According to the coefficients in Table 3, the ICs can be ordered as follows: $IC_3, IC_4, IC_5, IC_1, IC_2$, and IC_6. Therefore, the dominant source of volatility spillovers is IC_3 representing DAX (Germany), followed by IC_4 representing TSX (Canada), IC_5 representing All Ordinaries (Australia), IC_1 representing MIB (Italy), IC_2 representing FTSE 100 (UK), and IC_6 representing CAC 40 (France), as shown in Figure 7.

Table 3: The results estimated by the ICA-based ARMA-APARCH-M model for cluster 1.

Variable	Coefficient	Std. error	z-statistic	Prob.
IC_1	−0.0016	0.0001	−17.5293	$p \le 0.001$
IC_2	−0.0015	0.0001	−17.1906	$p \le 0.001$
IC_3	−0.0073	0.0001	−84.0053	$p \le 0.001$
IC_4	−0.0026	0.0001	−24.7667	$p \le 0.001$
IC_5	0.0021	0.0001	23.7606	$p \le 0.001$
IC_6	0.0007	0.0001	7.2746	$p \le 0.001$

Note: The coefficient denotes the contribution of each IC which indicates the impact from each IC to S&P 500 (US) in mean equation of return.

$$\begin{aligned} r_{xt} &= 0.0001 + 0.1174^{*} r_{x,t-1} + 0.0434^{*} \sigma_{xt} + \varepsilon_{xt} \\ &\quad - 0.3212^{*} \varepsilon_{x,t-1} - 0.0016^{*} \mathrm{IC}_1 - 0.0015^{*} \mathrm{IC}_2 \\ &\quad - 0.0073^{*} \mathrm{IC}_3 - 0.0026^{*} \mathrm{IC}_4 + 0.0021^{*} \mathrm{IC}_5 \\ &\quad + 0.0007^{*} \mathrm{IC}_6, \end{aligned} \tag{11}$$

$$\begin{aligned} \sigma_{xt}^{1.4777} &= 0.1261^{*} \left(\left| \varepsilon_{x,t-1} \right| - 0.2791^{*} \varepsilon_{x,t-1} \right)^{1.4777} \\ &\quad + 0.8591^{*} \sigma_{x,t-1}^{1.4777}. \end{aligned} \tag{12}$$

This may make sense for the fact that the return series of the G20 stock markets tend to move together over the same periods. It is widely believed that there exist volatility spillover effects across international financial markets, and the comovements among them become more apparent during the global financial crisis [72]. Consistent with that, Shahzad et al. [73] indicated that the US stock market is a major recipient of spillover effects from European markets. Similarly, BenSaïda et al. [35] revealed that the German market largely contributes to the risk of other markets (US, UK, France, Netherlands, Switzerland, Hong Kong, and Japan), with 94.8% of risk spillovers, followed by UK with 85.3%.

4.2.3. Volatility Spillover Effects in Cluster 2. Repeat the abovementioned procedures for cluster 2. We choose Nikkei 225 (Japan) as the objective or the explained variable to investigate whether the other six stock markets (SSE Composite, MERVAL, BSE Sensex, Jakarta Composite, TASI, and ISE 100) with similar volatility patterns in cluster 2 have volatility spillovers to Nikkei 225 and which is dominant. The demixing matrix $\mathbf{W}_2$ is given by the following equation:

$$\mathbf{W}_2 = \begin{pmatrix} -2.3828 & -7.1177 & -15.0659 & -15.6862 & -1.1394 & 68.2009 \\ 5.1260 & 4.1618 & -80.8038 & 22.3446 & 2.8544 & 3.7693 \\ 61.0537 & -0.9735 & -3.2500 & -11.3021 & -0.1312 & 1.7050 \\ 2.8788 & 0.8582 & -0.9470 & 5.1762 & -59.2972 & 2.5249 \\ 2.6402 & 1.0968 & 11.9850 & -82.7679 & 5.5286 & 0.4012 \\ -3.2147 & 53.6616 & -5.3618 & -6.9119 & -1.8459 & -6.4739 \end{pmatrix}. \tag{13}$$

From the weights of each independent component, $IC_1, IC_2, IC_3, IC_4, IC_5$, or IC_6, we can see that IC_1 mainly represents ISE 100 (Turkey), IC_2 represents BSE Sensex (India), IC_3 represents SSE Composite (China), IC_4 represents TASI (Saudi Arabia), IC_5 represents Jakarta Composite (Indonesia), and IC_6 represents MERVAL (Argentina), as shown in Figure 8.

The ICs are statistically independent; therefore, multicollinearity is avoided in the following model. The coefficient results estimated by the ICA-based ARMA-APARCH-M model for cluster 2 are shown in Table 4. The mean equation of return and the conditional variance equation are given by equations (14) and (15), respectively. The contribution of each IC is listed, which denotes the impact from each IC to Nikkei 225 (Japan) in equation (14).

$$\begin{aligned} r_t &= -0.0003 - 0.0451^{*} r_{t-1} + 0.0469^{*} \sigma_t + \varepsilon_t \\ &\quad - 0.0599 \varepsilon_{t-1} + 0.0010^{*} \mathrm{IC}_1 - 0.0029^{*} \mathrm{IC}_2 \\ &\quad + 0.0021^{*} \mathrm{IC}_3 - 0.0015^{*} \mathrm{IC}_4 - 0.0044^{*} \mathrm{IC}_5 \\ &\quad + 0.0006^{*} \mathrm{IC}_6, \end{aligned} \tag{14}$$

$$\begin{aligned} \sigma_t^{1.1540} &= 0.0002 + 0.1183^{*} \left(\left| \varepsilon_{t-1} \right| - 0.3823^{*} \varepsilon_{t-1} \right)^{1.1540} \\ &\quad + 0.8720^{*} \sigma_{t-1}^{1.1540}. \end{aligned} \tag{15}$$

The results show that there exist volatility spillover effects from independent components to Nikkei 225 (Japan). According to the coefficients in Table 4, the six ICs can be ordered as follows: $IC_5, IC_2, IC_3, IC_4, IC_1$, and

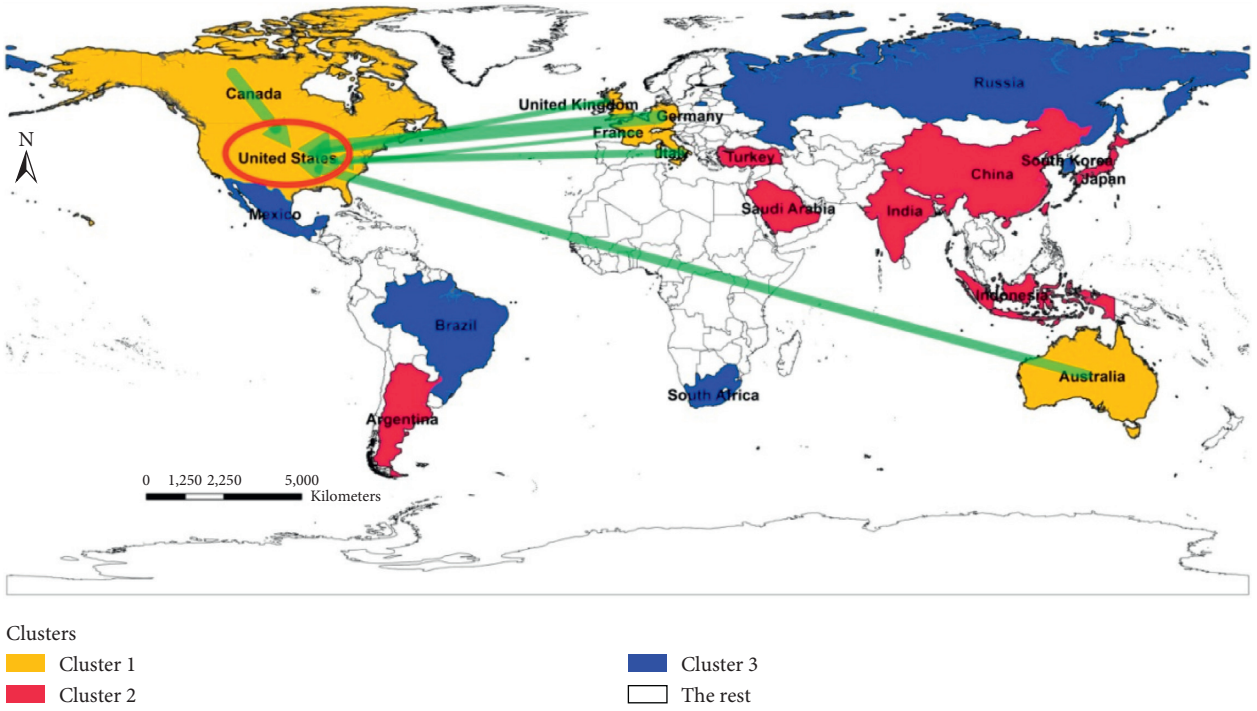

Figure 7: The volatility spillovers from DAX (Germany), CAC 40 (France), FTSE 100 (UK), MIB (Italy), TSX (Canada), and All Ordinaries (Australia) to S&P 500 (US).

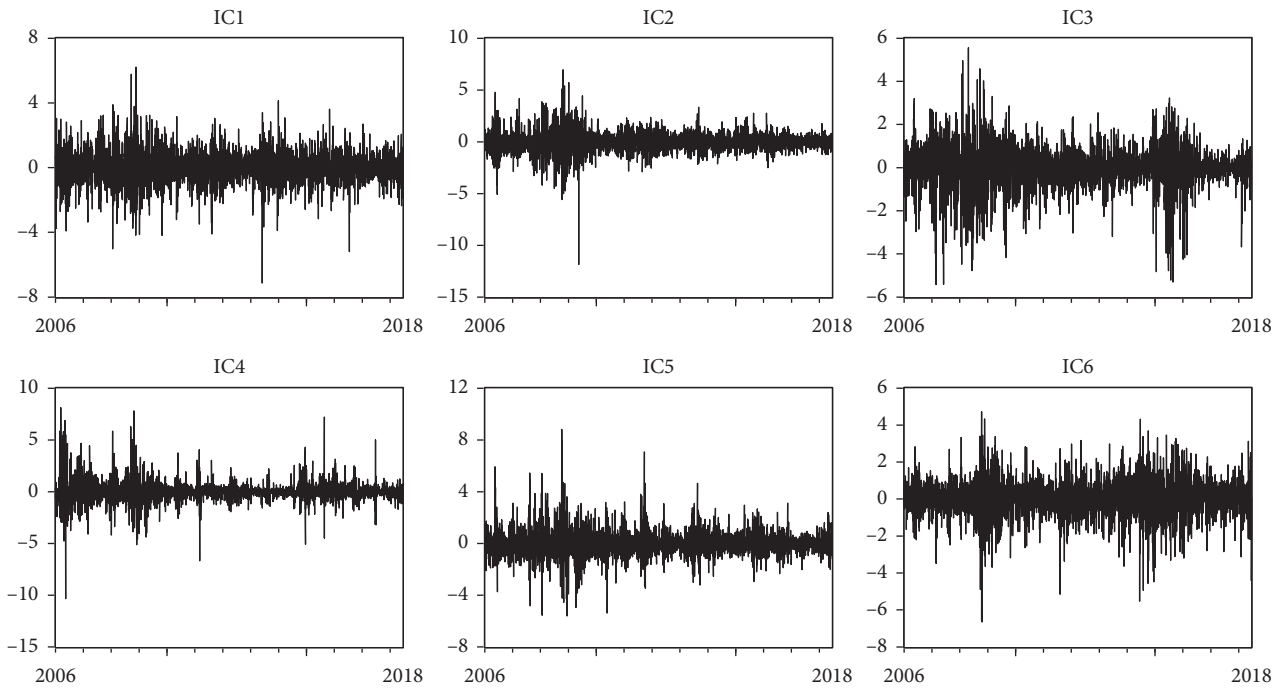

Figure 8: The time series of $IC_1, IC_2, IC_3, IC_4, IC_5$, and IC_6 for cluster 2. (a) IC_1, (b) IC_2, (c) IC_3, (d) IC_4, (e) IC_5, and (f) IC_6.

IC_6. The dominant source of volatility spillovers is Jakarta Composite (Indonesia), followed by BSE Sensex (India), SSE Composite (China), TASI (Saudi Arabia), ISE 100 (Turkey), and MERVAL (Argentina), as shown in Figure 9. Different from this result, Zhou et al. [71] concluded that the Japanese stock market is more impacted by the US market, which is in accordance with the finding of Lien et al. [74]. However, there is another finding in Zhou et al.'s [71] study that volatility spillover effects of equity markets from China to Japan gradually increased from late 2006 and became more pronounced between February and July in 2007. This may be supportive to explain our

Table 4: The results estimated by the ICA-based ARMA-APARCH-M model for cluster 2.

Variable	Coefficient	Std. error	z-statistic	Prob.
IC_1	0.0010	0.0002	5.5578	$p \leq 0.001$
IC_2	−0.0029	0.0002	−16.9653	$p \leq 0.001$
IC_3	0.0021	0.0002	11.3034	$p \leq 0.001$
IC_4	−0.0015	0.0002	−9.1943	$p \leq 0.001$
IC_5	−0.0044	0.0002	−25.2339	$p \leq 0.001$
IC_6	0.0006	0.0002	3.2686	$p \leq 0.001$

Note: the coefficient denotes the contribution of each IC which indicates the impact from each IC to Nikkei 225 (Japan) in mean equation of return.

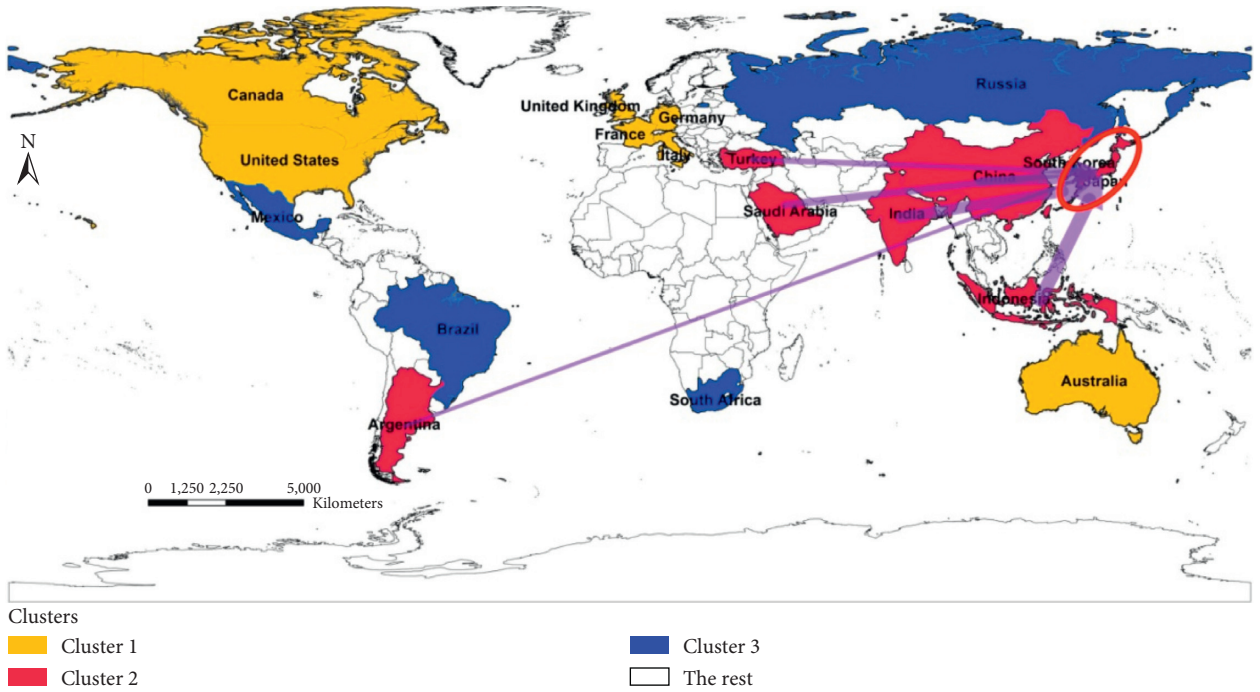

Figure 9: The volatility spillovers from SSE Composite (China), MERVAL (Argentina), BSE Sensex (India), Jakarta Composite (Indonesia), TASI (Saudi Arabia), and ISE 100 (Turkey) to Nikkei 225 (Japan).

result that there exist relatively significant volatility spillover effects between stock markets in China and Japan, since the relationship between these two markets had been experiencing the climax period from the end of 2006 to July 2007.

4.2.4. Volatility Spillover Effects in Cluster 3. Repeat the abovementioned procedures for cluster 3. We choose RTS (Russia) as the objective or the explained variable to investigate whether the four stock markets (Bovespa, IPC, INVSAF 40, and KOSPI) with similar volatility patterns in cluster 3 have volatility spillovers to RTS and which is dominant. The demixing matrix $\mathbf{W}_3$ is given by the following equation:

$$\mathbf{W}_3 = \begin{pmatrix} -6.1012 & -12.3333 & 89.1063 & -36.2422 \\ 5.9370 & 82.6484 & -16.2380 & -1.3493 \\ 79.5860 & -71.0763 & -10.1331 & -4.9205 \\ 2.6659 & 14.2862 & -6.2117 & -81.6311 \end{pmatrix}. \quad (16)$$

From the weights of each independent component, IC_1, IC_2, IC_3, or IC_4, we can see that IC_1 mainly represents INVSAF 40 (South Africa), IC_2 represents IPC (Mexico), IC_3 represents Bovespa (Brazil), and IC_4 represents KOSPI (South Korea), as shown in Figure 10.

The ICs are statistically independent; thus, multicollinearity is avoided in the following model. The coefficient results estimated by the ICA-based ARMA-APARCH-M model for cluster 3 are shown in Table 5. The mean equation

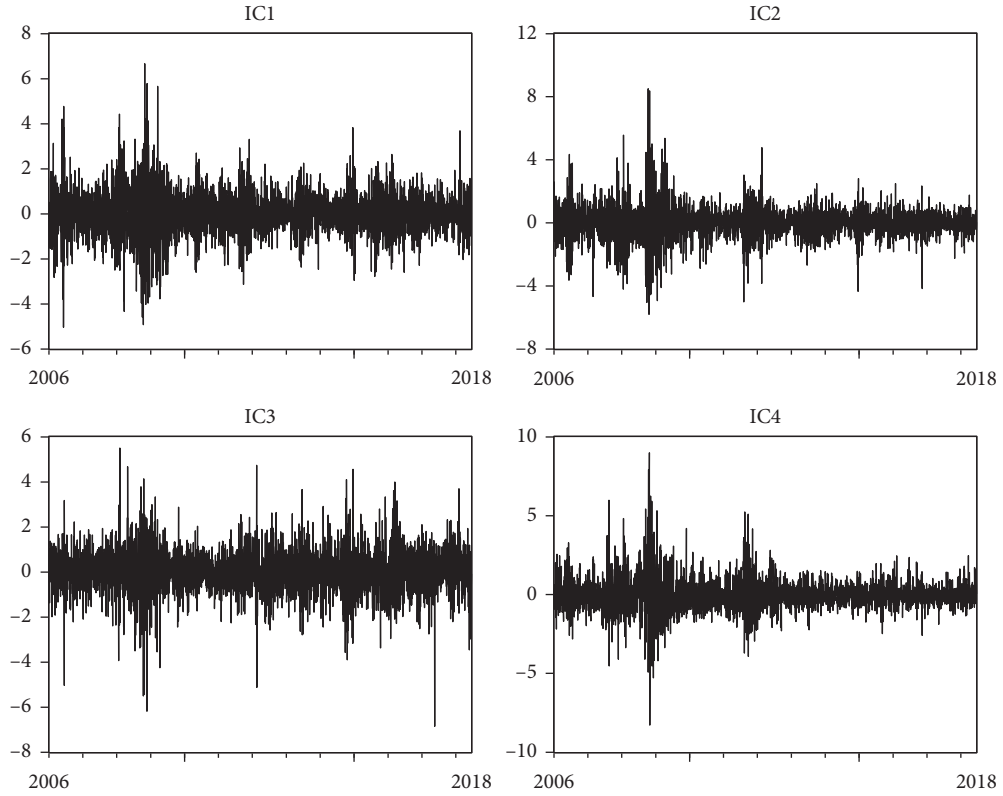

Figure 10: The time series of IC_1, IC_2, IC_3, and IC_4 for cluster 3. (a) IC_1, (b) IC_2, (c) IC_3, and (d) IC_4.

Table 5: The results estimated by the ICA-based ARMA-APARCH-M model for cluster 3.

Variable	Coefficient	Std. error	z-statistic	Prob.
IC_1	0.0071	0.0002	29.3460	$p \le 0.001$
IC_2	0.0057	0.0002	25.0421	$p \le 0.001$
IC_3	0.0025	0.0002	10.6856	$p \le 0.001$
IC_4	−0.0062	0.0002	−26.0124	$p \le 0.001$

Note: the coefficient denotes the contribution of each IC which indicates the impact from each IC to RTS (Russia) in mean equation of return.

of return and the conditional variance equation are given by equations (17) and (18), respectively. The contribution of each IC is listed, which denotes the impact from each IC to RTS (Russia) in equation (17).

$$\begin{aligned} r_t = {} & -0.0001 - 0.9998 * r_{t-1} + 0.0083 * \sigma_t + \varepsilon_t \\ & + 1.0021 * \varepsilon_{t-1} + 0.0071 * \mathrm{IC}_1 + 0.0057 * \mathrm{IC}_2 \\ & + 0.0025 * \mathrm{IC}_3 - 0.0062 * \mathrm{IC}_4, \end{aligned} \tag{17}$$

$$\begin{aligned} \sigma_t^{1.1540} = {} & 0.0002 + 0.1183 * \left(\left|\varepsilon_{t-1}\right| - 0.3823 * \varepsilon_{t-1}\right)^{1.1540} \\ & + 0.8720 * \sigma_{t-1}^{1.1540}. \end{aligned} \tag{18}$$

There are clear volatility spillovers from independent components (ICs) to RTS (Russia). According to the coefficients in Table 5, the four ICs can be ordered as follows: IC_1, IC_4, IC_2, and IC_3. The dominant source of volatility spillovers is INVSAF 40 (South Africa), followed by KOSPI (South Korea), IPC (Mexico), and Bovespa (Brazil), as shown in Figure 11.

One possible reason for the spillover transmission of South African and Brazilian markets towards the Russian market may be the increasing cooperation and win-win outcomes among BRICS countries in recent years. BRICS countries have been less impacted by the global financial crisis in light of the weak openness of their domestic financial markets; therefore, the volatility features of these

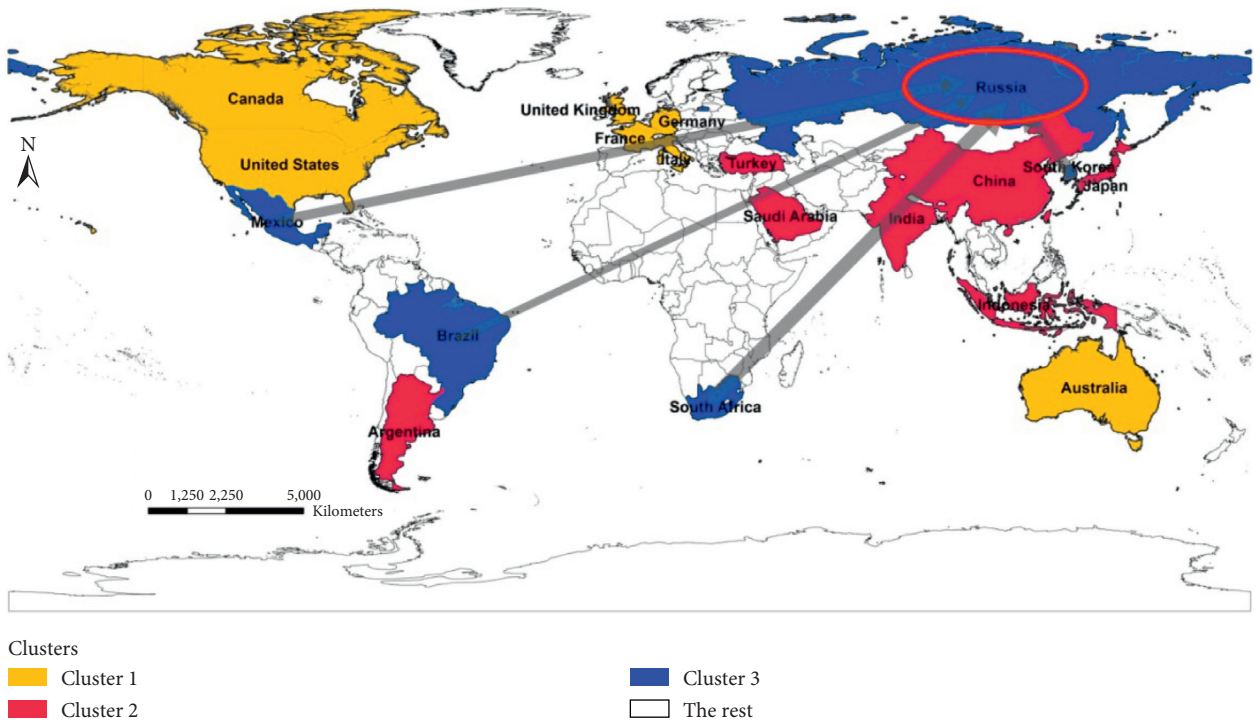

Figure 11: The volatility spillovers from Bovespa (Brazil), IPC (Mexico), INVSAF 40 (South Africa), and KOSPI (South Korea) to RTS (Russia).

markets are significantly different from those of the European and American markets in cluster 1.

5. Conclusion

In this study, the volatility similarity and spillover effects of G20 stock market comovements are examined using the ICA, ARMA-APARCH-M model, and fuzzy C-means clustering methods. This is a high-dimensional volatility problem of financial time series, involving nineteen financial markets. We cluster the G20 stock markets into three categories according to the volatility similarity and examine volatility spillover effects of the stock market comovements in each cluster.

The contribution of this study to the extant literature lies in three folds. First, an innovative method is adopted to examine the volatility spillover effects in G20 stock market comovements. This is due to the fact that financial volatility arises from some underlying factors representing the financial variables' comovements. Second, we can capture the common volatility spillovers from multiple markets to one as the comovements of financial variables. Third, this study has some implications for investors and policymakers in G20 stock markets. They are clustered into three categories, and there are spillover effects in stock market comovements of each cluster. Furthermore, the dominant source of volatility spillovers can be identified from multiple markets.

Some valuable findings can be drawn from the volatility similarity and spillover effects analysis on G20 stock market comovements, summarized as follows. First, we do confirm a striking feature of volatility similarity existing in the comovements of G20 stock markets. Second, there exist spillover effects in stock market comovements group. Third, the dominant source can be identified from the spillover process. Furthermore, given that the changing interactions between stock markets are important reference for investment decision and policy making, our conclusion based on the proposed method provides practical implications to the participants of G20 financial markets.

The investors should be warned that it is becoming increasingly difficult to build portfolios to reduce systemic risk through real-time monitoring and tracking of major financial markets as the dynamic interactions among these heterogeneous agents increase. Investors seeking potential investment opportunities in complex financial systems should pay close attention to the interdependent dynamics among these comoving markets and adjust their investment strategies and asset allocation accordingly. They can identify cross-market volatility spillovers in advance and further seek the arbitrage opportunities to achieve the goal of improving their investment efficiency. For policy makers, risk regulation in the early stages of a financial crisis requires close attention to these heterogeneous, dynamic, and interactive financial markets. They can better formulate and implement strong relevant policy measures to stabilize the financial system by closely monitoring which are the dominant volatility transmitters.

For future study, we suggest conducting detailed explorations on the price risk caused by volatility spillovers of high-frequency trading data in stock markets. Quantifying the risk based on volatility is very important to investors and policy makers. Future work will help to effectively measure and monitor the risk of stock markets in real time.

Data Availability

The datasets used and analyzed during the current study are available from the corresponding author on reasonable request.

Conflicts of Interest

The authors declare that they have no conflicts of interest.

Acknowledgments

This work was supported by the National Natural Science Foundation of China (nos. 71704098, 71971039, and 72003110) and the Natural Science Foundation of Shandong Province (no. ZR2016GQ03).

References

[1] W. Zhang, X. Zhuang, Y. Lu, and J. Wang, "Spatial linkage of volatility spillovers and its explanation across G20 stock markets: a network framework," *International Review of Financial Analysis*, vol. 71, Article ID 101454, 2020.

[2] R. P. Mclver and S. H. Kang, "Financial crises and the dynamics of the spillovers between the US. and BRICS stock markets," *Research in International Business and Finance*, vol. 54, Article ID 101276, 2020.

[3] S. Aghabozorgi and Y. W. Teh, "Stock market co-movement assessment using a three-phase clustering method," *Expert Systems with Applications*, vol. 41, no. 4, pp. 1301–1314, 2014.

[4] A. Y. Lin and Y. N. Lin, "Market similarity and cross-border investment performance," *Finance Research Letters*, Article ID 101751, 2020.

[5] M. Raddant and D. Y. Kenett, "Interconnectedness in the global financial market," *Journal of International Money and Finance*, vol. 110, Article ID 102280, 2021.

[6] X. V. Vo and T. T. A. Tran, "Modelling volatility spillovers from the US equity market to ASEAN stock markets," *Pacific-Basin Finance Journal*, vol. 59, p. 101246, 2020.

[7] W. Ahmad, P. Sadorsky, and A. Sharma, "Optimal hedge ratios for clean energy equities," *Economic Modelling*, vol. 72, pp. 278–295, 2018.

[8] S. A. Basher and P. Sadorsky, "Hedging emerging market stock prices with oil, gold, VIX, and bonds: a comparison between DCC, ADCC and GO-GARCH," *Energy Economics*, vol. 54, pp. 235–247, 2016.

[9] L. Bauwens, S. Laurent, and J. V. K. Rombouts, "Multivariate GARCH models: a survey," *Journal of Applied Econometrics*, vol. 21, no. 1, pp. 79–109, 2006.

[10] M. Caporin and M. McAleer, "Do we really need both BEKK and DCC? a tale of two multivariate GARCH models," *Journal of Economic Surveys*, vol. 26, no. 4, pp. 736–751, 2012.

[11] S. Chrétien and J.-P. Ortega, "Multivariate GARCH estimation via a Bregman-proximal trust-region method," *Computational Statistics & Data Analysis*, vol. 76, pp. 210–236, 2014.

[12] R. Engle, "Dynamic conditional correlation," *Journal of Business & Economic Statistics*, vol. 20, no. 3, pp. 339–350, 2002.

[13] T. K. Chue, F. A. Gul, and G. M. Mian, "Aggregate investor sentiment and stock return synchronicity," *Journal of Banking & Finance*, vol. 108, Article ID 105628, 2019.

[14] A. García-Ferrer, E. González-Prieto, and D. Peña, "A conditionally heteroskedastic independent factor model with an application to financial stock returns," *International Journal of Forecasting*, vol. 28, no. 1, pp. 70–93, 2012.

[15] D. Gjika and R. Horváth, "Stock market comovements in central Europe: evidence from the asymmetric DCC model," *Economic Modelling*, vol. 33, pp. 55–64, 2013.

[16] T. Strohsal and E. Weber, "Time-varying international stock market interaction and the identification of volatility signals," *Journal of Banking & Finance*, vol. 56, pp. 28–36, 2015.

[17] P. Poncela, "Further research on independent component analysis," *International Journal of Forecasting*, vol. 28, no. 1, pp. 94–96, 2012.

[18] J.-B. Geng, Y.-J. Du, Q. Ji, and D. Zhang, "Modeling return and volatility spillover networks of global new energy companies," *Renewable and Sustainable Energy Reviews*, vol. 135, Article ID 110214, 2021.

[19] Y. Hu, X. Li, and D. Shen, "Attention allocation and international stock return comovement: evidence from the Bitcoin market," *Research in International Business and Finance*, vol. 54, Article ID 101286, 2020.

[20] F. Wu, W.-L. Zhao, Q. Ji, and D. Zhang, "Dependency, centrality and dynamic networks for international commodity futures prices," *International Review of Economics & Finance*, vol. 67, pp. 118–132, 2020.

[21] J. Beirne, G. M. Caporale, M. Schulze-Ghattas, and N. Spagnolo, "Global and regional spillovers in emerging stock markets: a multivariate GARCH-in-mean analysis," *Emerging Markets Review*, vol. 11, no. 3, pp. 250–260, 2010.

[22] J. L. M. Marcelo, J. L. M. Quirós, and M. D. M. M. Quirós, "Asymmetric variance and spillover effects: regime shifts in the Spanish stock market," *Journal of International Financial Markets, Institutions and Money*, vol. 18, no. 1, pp. 1–15, 2008.

[23] W. Mensi, S. Hammoudeh, D. K. Nguyen, and S. H. Kang, "Global financial crisis and spillover effects among the US. and BRICS stock markets," *International Review of Economics & Finance*, vol. 42, pp. 257–276, 2016.

[24] G. Milunovich and S. Thorp, "Valuing volatility spillovers," *Global Finance Journal*, vol. 17, no. 1, pp. 1–22, 2006.

[25] T. Miyakoshi, "Spillovers of stock return volatility to Asian equity markets from Japan and the US," *Journal of International Financial Markets, Institutions and Money*, vol. 13, no. 4, pp. 383–399, 2003.

[26] A. Ng, "Volatility spillover effects from Japan and the US to the Pacific-Basin," *Journal of International Money and Finance*, vol. 19, no. 2, pp. 207–233, 2000.

[27] T. Bollerslev, "Generalized autoregressive conditional heteroskedasticity," *Journal of Econometrics*, vol. 31, no. 2, pp. 307–327, 1986.

[28] Z. Ding, C. W. J. Granger, and R. F. Engle, "A long memory property of stock market returns and a new model," *Journal of Empirical Finance*, vol. 1, no. 1, pp. 83–106, 1993.

[29] A. BenSaïda, "Good and bad volatility spillovers: an asymmetric connectedness," *Journal of Financial Markets*, vol. 43, pp. 78–95, 2019.

[30] L. Charfeddine and H. Al Refai, "Political tensions, stock market dependence and volatility spillover: evidence from the recent intra-GCC crises," *The North American Journal of Economics and Finance*, vol. 50, Article ID 101032, 2019.

[31] M. K. Newaz and J. S. Park, "The impact of trade intensity and market characteristics on asymmetric volatility, spillovers and asymmetric spillovers: evidence from the response of international stock markets to US shocks," *The Quarterly Review of Economics and Finance*, vol. 71, pp. 79–94, 2019.

[32] G. Gannon, "Simultaneous volatility transmissions and spillover effects: US. and Hong Kong stock and futures markets," *International Review of Financial Analysis*, vol. 14, no. 3, pp. 326–336, 2005.

[33] G. M. Gallo and E. Otranto, "Volatility spillovers, interdependence and co-movements: a Markov switching approach," *Computational Statistics & Data Analysis*, vol. 52, no. 6, pp. 3011–3026, 2008.

[34] Q. Ji, W. Bahloul, J.-B. Geng, and R. Gupta, "Trading behaviour connectedness across commodity markets: evidence from the hedgers' sentiment perspective," *Research in International Business and Finance*, vol. 52, Article ID 101114, 2020.

[35] A. BenSaïda, H. Litimi, and O. Abdallah, "Volatility spillover shifts in global financial markets," *Economic Modelling*, vol. 73, pp. 343–353, 2018.

[36] F. X. Diebold and K. Yilmaz, "Better to give than to receive: predictive directional measurement of volatility spillovers," *International Journal of Forecasting*, vol. 28, no. 1, pp. 57–66, 2012.

[37] D. Philippas and C. Dragomirescu-Gaina, "Exposing volatility spillovers: a comparative analysis based on vector autoregressive models," *Finance Research Letters*, vol. 18, pp. 302–305, 2016.

[38] X. Su, "Dynamic behaviors and contributing factors of volatility spillovers across G7 stock markets," *The North American Journal of Economics and Finance*, vol. 53, Article ID 101218, 2020.

[39] E. Baumöhl, E. Kočenda, Š. Lyócsa, and T. Výrost, "Networks of volatility spillovers among stock markets," *Physica A: Statistical Mechanics and its Applications*, vol. 490, pp. 1555–1574, 2018.

[40] M. Hu, D. Zhang, Q. Ji, and L. Wei, "Macro factors and the realized volatility of commodities: a dynamic network analysis," *Resources Policy*, vol. 68, Article ID 101813, 2020.

[41] Q. Ji, B.-Y. Liu, J. Cunado, and R. Gupta, "Risk spillover between the US and the remaining G7 stock markets using time-varying copulas with Markov switching: evidence from over a century of data," *The North American Journal of Economics and Finance*, vol. 51, Article ID 100846, 2020.

[42] X. Liu, H. An, H. Li, Z. Chen, S. Feng, and S. Wen, "Features of spillover networks in international financial markets: evidence from the G20 countries," *Physica A: Statistical Mechanics and its Applications*, vol. 479, pp. 265–278, 2017.

[43] Š. Lyócsa, T. Výrost, and E. Baumöhl, "Return spillovers around the globe: a network approach," *Economic Modelling*, vol. 77, pp. 133–146, 2019.

[44] W. Mensi, F. Z. Boubaker, K. H. Al-Yahyaee, and S. H. Kang, "Dynamic volatility spillovers and connectedness between global, regional, and GIPSI stock markets," *Finance Research Letters*, vol. 25, pp. 230–238, 2018.

[45] L.-J. Kao, C.-C. Chiu, C.-J. Lu, and J.-L. Yang, "Integration of nonlinear independent component analysis and support vector regression for stock price forecasting," *Neurocomputing*, vol. 99, pp. 534–542, 2013.

[46] A. Kumiega, T. Neururer, and B. Van Vliet, "Independent component analysis for realized volatility: analysis of the stock market crash of 2008," *The Quarterly Review of Economics and Finance*, vol. 51, no. 3, pp. 292–302, 2011.

[47] A. Hitaj, L. Mercuri, and E. Rroji, "Portfolio selection with independent component analysis," *Finance Research Letters*, vol. 15, pp. 146–159, 2015.

[48] L. Xian, K. He, and K. K. Lai, "Gold price analysis based on ensemble empirical model decomposition and independent component analysis," *Physica A: Statistical Mechanics and its Applications*, vol. 454, pp. 11–23, 2016.

[49] C. Gouriéroux, A. Monfort, and J.-P. Renne, "Statistical inference for independent component analysis: application to structural VAR models," *Journal of Econometrics*, vol. 196, no. 1, pp. 111–126, 2017.

[50] T. Box, "Qualitative similarity and stock price co-movement," *Journal of Banking & Finance*, vol. 91, pp. 49–69, 2018.

[51] H. Bu, W. Tang, and J. Wu, "Time-varying co-movement and changes of comovement structure in the Chinese stock market: a causal network method," *Economic Modelling*, vol. 81, pp. 181–204, 2019.

[52] P. Chen, "Understanding international stock market co-movements: a comparison of developed and emerging markets," *International Review of Economics & Finance*, vol. 56, pp. 451–464, 2018.

[53] K.-I. Inaba, "Information-driven stock return comovements across countries," *Research in International Business and Finance*, vol. 51, p. 101093, 2020.

[54] R. MacDonald, V. Sogiakas, and A. Tsopanakis, "Volatility co-movements and spillover effects within the Eurozone economies: a multivariate GARCH approach using the financial stress index financial stress index," *Journal of International Financial Markets, Institutions and Money*, vol. 52, pp. 17–36, 2018.

[55] C. P. Nguyen, T. V. H. Nguyen, and C. Schinckus, "Institutions, economic openness and stock return co-movements: an empirical investigation in emerging markets," *Finance Research Letters*, vol. 28, pp. 137–147, 2019.

[56] M. Niţoi and M. M. Pochea, "What drives European union stock market co-movements?" *Journal of International Money and Finance*, vol. 97, pp. 57–69, 2019.

[57] X. Sheng, J. Brzeszczyński, and B. M. Ibrahim, "International stock return co-movements and trading activity," *Finance Research Letters*, vol. 23, pp. 12–18, 2017.

[58] A. Arratia and A. Cabaña, "A graphical tool for describing the temporal evolution of clusters in financial stock marketsfinancial stock markets," *Computational Economics*, vol. 41, no. 2, pp. 213–231, 2013.

[59] J. G. Dias, J. K. Vermunt, and S. Ramos, "Clustering financial time series: new insights from an extended hidden Markov model," *European Journal of Operational Research*, vol. 243, no. 3, pp. 852–864, 2015.

[60] F. Durante and E. Foscolo, "An analysis of the dependence among financial markets by spatial contagionfinancial markets by spatial contagion," *International Journal of Intelligent Systems*, vol. 28, no. 4, pp. 319–331, 2013.

[61] P. D'Urso, L. De Giovanni, R. Massari, R. L. D'Ecclesia, and E. A. Maharaj, "Cepstral-based clustering of financial time series," *Expert Systems with Applications*, vol. 161, Article ID 113705, 2020.

[62] P. D'Urso, C. Cappelli, D. D. Lallo, and R. Massari, "Clustering of financial time series," *Physica A: Statistical Mechanics and its Applications*, vol. 392, no. 9, pp. 2114–2129, 2013.

[63] P. D'Urso, L. De Giovanni, and R. Massari, "GARCH-based robust clustering of time series," *Fuzzy Sets and Systems*, vol. 305, pp. 1–28, 2016.

[64] H. Esmalifalak, A. I. Ajirlou, S. P. Behrouz, and M. Esmalifalak, "(Dis) integration levels across global stock markets: a multidimensional scaling and cluster analysis," *Expert Systems with Applications*, vol. 42, no. 22, pp. 8393–8402, 2015.

[65] S.-H. Liao and S.-Y. Chou, "Data mining investigation of co-movements on the Taiwan and China stock markets for future investment portfolio," *Expert Systems with Applications*, vol. 40, no. 5, pp. 1542–1554, 2013.
[66] A. Hyvärinen and E. Oja, "Independent component analysis: algorithms and applications," *Neural Networks*, vol. 13, no. 4-5, pp. 411–430, 2000.
[67] G. Bekaert, E. Engstrom, and A. Ermolov, "Bad environments, good environments: a non-Gaussian asymmetric volatility model," *Journal of Econometrics*, vol. 186, no. 1, pp. 258–275, 2015.
[68] T. W. Liao, "Clustering of time series data-a survey," *Pattern Recognition*, vol. 38, pp. 1857–1874, 2005.
[69] C. Ning, D. Xu, and T. S. Wirjanto, "Is volatility clustering of asset returns asymmetric?" *Journal of Banking & Finance*, vol. 52, pp. 62–76, 2015.
[70] A. Morales-Zumaquero and S. Sosvilla-Rivero, "Volatility spillovers between foreign exchange and stock markets in industrialized countries," *The Quarterly Review of Economics and Finance*, vol. 70, pp. 121–136, 2018.
[71] X. Zhou, W. Zhang, and J. Zhang, "Volatility spillovers between the Chinese and world equity markets," *Pacific-Basin Finance Journal*, vol. 20, no. 2, pp. 247–270, 2012.
[72] K. H. Liow, "Volatility spillover dynamics and relationship across G7 financial markets," *The North American Journal of Economics and Finance*, vol. 33, pp. 328–365, 2015.
[73] S. J. H. Shahzad, J. A. Hernandez, M. U. Rehman, K. H. Al-Yahyaee, and M. Zakaria, "A global network topology of stock markets: transmitters and receivers of spillover effects," *Physica A: Statistical Mechanics and its Applications*, vol. 492, pp. 2136–2153, 2018.
[74] D. Lien, G. Lee, L. Yang, and Y. Zhang, "Volatility spillovers among the US. and Asian stock markets: a comparison between the periods of Asian currency crisis and subprime credit crisis," *The North American Journal of Economics and Finance*, vol. 46, pp. 187–201, 2018.

Hindawi
Complexity
Volume 2020, Article ID 8859706, 14 pages
https://doi.org/10.1155/2020/8859706

Research Article

Analyzing the Characteristics and Causes of Location Spatial Agglomeration of Listed Companies: An Empirical Study of China's Yangtze River Economic Belt

Deyu Meng,[1] Guoen Wei,[2] and Pingjun Sun[3]

[1]*College of Management, Qingdao Agricultural University, Qingdao 266109, China*
[2]*College of Geography and Ocean Sciences, Nanjing University, Nanjing 210023, China*
[3]*College of Geographical Sciences, Southwest University, Chongqing 400700, China*

Correspondence should be addressed to Pingjun Sun; sunpj031@nenu.edu.cn

Received 12 September 2020; Revised 14 November 2020; Accepted 28 November 2020; Published 10 December 2020

Academic Editor: Huajiao Li

Enhancing urban development vitality and optimizing the allocation of regional industrial factors require a comprehensive analysis of listed companies, such as the overall distribution network, agglomeration evolution trend, industrialization layout, and driving mechanism. Using 1,624 A-share listed companies in China's Yangtze River Economic Belt as research area, this study integrated trend surface analysis (TSA), exploratory spatial data analysis (ESDA), standard deviation ellipse (SDE), and spatial regression model methods. The main results are as follows: (1) The overall quantity scale of the listed companies in the Yangtze River Economic Belt has achieved significant growth, but the spatial difference of location selection persists. The spatial configuration formed a hierarchical urban distribution pattern with the Yangtze River Delta region as the agglomeration core and the provincial capitals as the fulcrum. (2) Listed companies accelerate the expansion of the Yangtze River Delta region. Chengdu, Wuhan, Changsha, and other central-western provincial capitals gradually increased the region's attractiveness. High-high and low-low agglomerations remain the main forms of agglomeration. (3) There are significant differences in the location selection of listed companies with varying specialization levels, forming a relatively different alienated high-value distribution structure among various industry types. (4) The levels of knowledge spillover, city scale, and policy support level are major factors affecting the location selection process of listed companies in the Yangtze River Economic Belt. For low-level city network with few listed companies, city scale and knowledge spillover levels are significant determinants for the development of headquarters' economy. For high-level city network, along with the level of knowledge spillovers and policy support, globalization level has an important contribution to the shaping of the location advantages of attracting the layout of listed companies.

1. Introduction

With the rise of cross-border trade and emerging technological revolutions, the dominant production factor inputs have been gradually shifting from capital and labor into innovation, technology, and information. Listed companies have increasingly provided crucial support to regional organizations to participate in the global market competition under the new normal of economic development. These enterprises have become a new type of "carriage," promoting sustainable development in the modern national economy and playing a leading role in guiding technology development. They have also been essential in integrating scientific and technological inventions, promoting industrial upgrading, and meeting social development needs in the regional product development chain [1]. A listed company is a market-oriented modern enterprise formed by the agglomeration of various production factors. It reflects the level of capital securitization and direct financing capacity of a particular region and, to a certain extent, represents the dominant position of a country or region in the global division of labor system and the international innovation pattern [2, 3].

Affected by regional policy adjustments and changes in corporate business strategies, the location selection and

distribution law of listed companies in emerging developing countries represented by China has been changed consistently in recent years. This has resulted in changes to the industrial innovation strength and production agglomeration pattern and has created an incentive effect on the allocation optimization of regional production factors and reward mechanisms for industries. Researching location spatial agglomeration of listed companies is particularly important for emerging economies in the growth period of capital markets [4]. The evolution and development of density, scale, and operating performance are mainstream research areas in analyzing the spatial agglomeration of listed companies, using various methods, such as nuclear density [5], spatial autocorrelation [6], Gini coefficient [7], and location quotient [8]. Majority of the studies have focused on country, state, and provincial levels [2, 9] and have paid little attention to the change of attractiveness of new urban forms (e.g., urban agglomerations, metropolitan areas, and economic belts) in the location selection of listed companies. Moreover, adapting to the rapid development of urbanization and urban hierarchical systems in emerging countries is complex and difficult. Thus, establishing a comprehensive analytical framework with multiple methods is essential for the study of the location of spatial agglomeration of listed companies in the new urban agglomeration.

Along with the opportunities and challenges brought about by the transformation of the industrial structure in emerging economies, the basic roles of listed companies in urban development and upgrading of industrial parks have been continuously improved; recent studies have focused on enhancing regional location attractiveness to listed companies and analyzing the driving mechanism of the location selection of listed companies [10, 11]. Urban geographical location, financial prosperity, knowledge spillover effect, and export-oriented economic scale are considered as critical elements for the spatial layout of headquarters. The internal and external structural elements of sociology and management (e.g., entrepreneur's investment motives, policy support, innovation reward of enterprises, and demonstration driving effect of scale agglomeration) are also being considered as important components [6, 12]. In terms of driving mechanism research, the influence of geospatial elements on the location of spatial agglomeration of listed companies can be difficult to analyze using traditional approaches, such as least squares regression and panel Tobit regression. Therefore, exploring the driving influence of spatial dependence on the location selection of listed companies is necessary for optimizing the layout structure of listed companies and formulating investment promotion strategies of industrial parks and regions that enhance location's attractiveness.

The study area is the Yangtze River Economic Belt (YEB), one of the highest economic density areas in China, which covers 11 provincial administrative regions, namely, Shanghai, Jiangsu, Zhejiang, Anhui, Jiangxi, Hubei, Hunan, Sichuan, Chongqing, Yunnan, and Guizhou (Figure 1). The region has a high total economic value and sizeable industrial sector [13, 14]. Its vibrant atmosphere for innovation and creativity has formed a spatial economic cluster of listed companies based on national central cities (e.g., Shanghai, Wuhan, Chongqing, Chengdu) and urban agglomerations (e.g., the Yangtze River Delta, urban agglomerations in the middle reaches of the Yangtze River, and Chengdu-Chongqing urban agglomeration) [15]. The regional differences in the location selection of listed companies and the "path-dependent effect" of regional headquarters economy development are becoming more and more obvious, bringing challenges to the allocation of urban factor resources and the sustainable development of industries in the YEB region [7]. Therefore, to measure the spatial agglomeration evolution of the listed companies and to explore the driving mechanism of location selection become an important basis promoting the rational layout of industrial factors and realizing the overall sustainable economic development of the YEB region.

Based on the concepts of regional coordinated development and enterprise management to build the analysis framework of "pattern evolution-typical alienation-driving mechanism," trend surface analysis (TSA), exploratory spatial data analysis (ESDA), standard deviation ellipse (SDE), and location quotient model (LQM) were employed to analyze the location characteristics of spatial agglomerations of the listed companies. GIS technology and spatial regression model are used to analyze the driving mechanism that affects the spatial agglomeration of listed companies from the perspective of the overall and "typical regions" (stratification of the regional city network system based on the quantity of listed companies). This study intends to focus on solving two research problems: (1) to reveal the evolution characteristics of spatial agglomeration of the location selection of listed companies in the YEB region; (2) to clearly explore the key factors of the city network with different scales of listed companies in the YEB region to attract and cultivate listed companies. By solving these problems, this study aims to provide a basis for fully understanding the spatial preference and temporal changes of the location selection of listed companies in the YEB region and provide targeted suggestions for improving the networked layout of listed companies in the YEB region, as well as different levels of city networks along the line to enhance the location attractiveness of listed companies and shape the location advantages of industrial agglomeration.

2. Materials and Methods

2.1. Research Methods. This study adopts the "pattern evolution-typical alienation-driving mechanism" framework (Figure 2) and is composed of two main components: (1) pattern evolution and (2) typical alienation and driving mechanism. In pattern evolution analysis, the spatial agglomeration characteristics of listed companies are explored in terms of overall distribution network, agglomeration evolution trend, industrialization layout using GIS spatial interpolation, trend surface analysis, exploratory spatial data analysis method, standard deviation ellipse, and location quotient. For typical alienation and driving mechanism analysis, based on the clustering of the distribution of listed

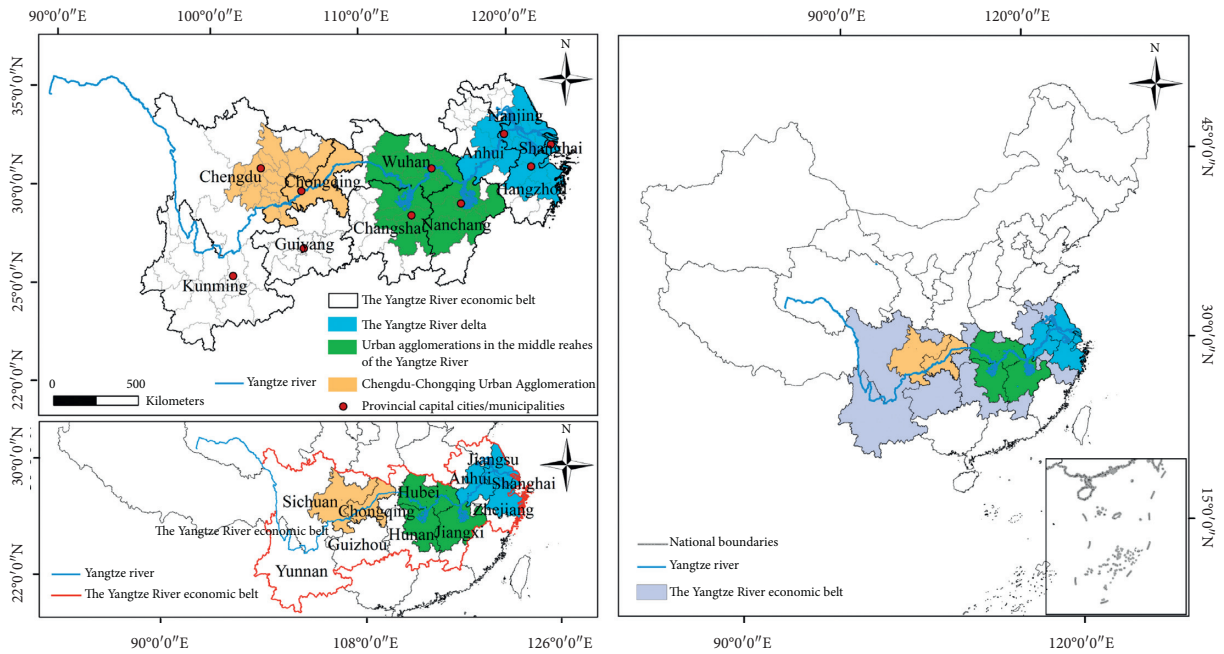

Figure 1: Geographical location map of the YEB region.

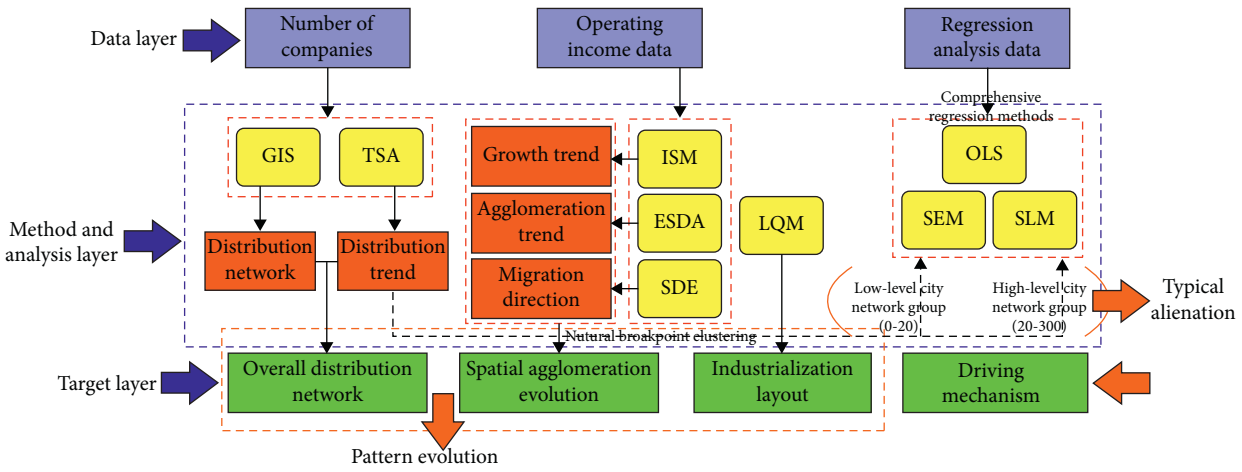

Figure 2: Research ideas framework.

companies, the "typical regions" are divided into two types, low-level city network with few listed companies and high-level city network with a large number of listed companies, which is taken as the basis for the cities which have different scales of listed companies to adopt targeted strategies to develop headquarters economy. The OLS model, spatial lag model, and the spatial error model are employed to analyze the driving mechanism of the spatial agglomeration of listed companies for the entire area and for "typical regions." The research ideas and the functions of each method are shown in Figure 2.

2.1.1. Trend Surface Analysis. The trend surface is an approximate processing result. This method fits the observation points to a trend line in the form of trend gradient on the orthogonal plane formed by the X axis and the Y axis, which can simulate the difference in spatial distribution trends of listed companies in the north-south and east-west directions. The formula is as follows:

$$z_i(x_i, y_i) = T_i(x_i, y_i) + \varepsilon_i, \quad (1)$$

where (x_i, y_i) are the planar spatial coordinates; x and y represent the east-west and north-south directions in

geographic space, respectively. z_i (x_i, y_i) is the number of listed companies. T_i (x_i, y_i) represents the trend value of the number of listed companies in the range. The Trend Surface tool in ArcGIS software was used to describe the trend of the observed values [16].

2.1.2. Exploratory Spatial Data Analysis

(1) Global Spatial Autocorrelation. The global spatial autocorrelation method is used to analyze the spatial agglomeration of listed companies. Global Moran's I index can reflect the spatial autocorrelation of geographical elements distribution, which is given by the following expression:

$$\text{Moran's}I = \frac{\sum_{i=1}^{n}\sum_{i=1}^{n} W_{ij}\left(x_i - \overline{x}\right)\left(x_j - \overline{x}\right)}{\sum_{i=1}^{n}\left|x_j - \overline{x}\right|^2 \sum_{i=1}^{n}\sum_{j=1}^{n} W_{ij}}, \quad (2)$$

where i and j are the numbers of listed companies in the region and W_{ij} is a spatial weight matrix. Moran's I values fall within the range [-1, 1]. When the value is positive, the observation is positively correlated in spatial distribution, and when the value is negative, the correlation is negative. When the value is 0, the distribution of the observed value is random.

(2) Local Spatial Autocorrelation. The local spatial autocorrelation can be used to comprehensively reflect the regional variability of the spatial agglomeration. In this study, we used local Moran's I to test the regional variability of the spatial agglomeration of listed companies, which are given by the expressions

$$\text{local Moran's } I = \frac{\left(x_i - \overline{x}\right)}{S^2}\sum_{j=1}^{n} W_{ij}\left(x_j - \overline{x}\right),$$
$$S^2 = \frac{1}{n}\sum_{i=1}^{n}\left(x_i - \overline{x}\right)^2. \quad (3)$$

A positive index value indicates that the region-adjacent units are close to an agglomeration with similar value. When the index is negative, the adjacent units are heterogeneous.

2.1.3. Standard Deviation Ellipse. This method mainly includes three elements: angle θ, long axis standard deviation, and short-axis standard deviation, which are used to reflect the degree of geographic concentration, the dominant distribution direction, and the migration direction of center-of-gravity of listed companies in the YEB region. The formula for the center-of-gravity coordinates is

$$\overline{X}_w = \frac{\sum_{i=1}^{n} w_i x_i}{\sum_{i=1}^{n} w_i},$$
$$\overline{Y}_w = \frac{\sum_{i=1}^{n} w_i y_i}{\sum_{i=1}^{n} w_i}, \quad (4)$$

such that (x_i, y_i) is the spatial location of provincial units and w_i is the spatial weight of provincial units.

2.1.4. Location Quotient of Specialization Level. The location quotient method is used to measure the location selection preference of listed companies with different specialization levels under the industry classification of the YEB region [8]. We used the total operating income data of listed companies as the measurement indicators and divided the whole industry into labor-intensive industries, capital-intensive industries and technology-intensive industries based on the Dongcai industry classification. The specific classification rules are as follows: Listed companies in household appliances, food and beverage, apparel and textiles, trade and retail, and light industry manufacturing were classified as labor-intensive industries. Listed companies in real estate, steel, utilities, basic chemicals, building materials, nonferrous metals, and transportation were classified as capital-intensive industries. Listed companies in defense military industry, mechanical equipment, computers, automobiles, medical biology, and computer networks were classified as technology-intensive industries.

2.1.5. Regression Analysis Model. A comprehensive regression model was employed to analyze the factors affecting the spatial agglomeration characteristics of listed companies in the YEB region and "typical regions." The methodology includes the use of the OLS model, the spatial error model (SEM), and the spatial lag model (SLM) and selects the optimal model based on the goodness of fit, Schwarz criterion, and Akaike information criterion. The OLS model is a traditional regression model based on the least square method. The SEM focuses on unobservable spatial dependence between variables and can detect the spatial interaction effect between error terms. The SLM emphasizes the neighborhood effect and focuses on the overlooked spatial interdependence between dependent variables and can detect the influence of spatial distance on behavior [17]. The formula of the OLS model is not introduced. For the SLM, the formula is as follows:

$$y = \sigma w_{ij} y_i + x_i\beta + \varepsilon_i,$$
$$\varepsilon_i \sim N\left(0, \sigma^2 I\right), \quad (5)$$

where y is the number of listed companies in the city; x is the influencing factor affecting the layout of listed companies; β is the coefficients of the regression model, which is related to the explanatory power of the influencing factors on the spatial agglomeration of listed companies; and ε is a random error.

The SEM is given by the expression

$$y = x_i\beta + \lambda w_{ij}\varepsilon_j + \mu_i, \quad (6)$$

where λ is the parameter for the spatial correlation strength between residuals and μ_i is a random disturbance term.

2.2. Data Sources. In this study, all the A-share listed companies (704 companies in 2008, 1624 companies in 2017) in 126 cities in total along the YEB region were used in the analysis, with the research period from 2008 to 2017. The

research starting point (2008) coincides with the beginning of the global financial crisis, analyzing the spatial agglomeration characteristics and causes of listed companies in the YEB region in the post-financial crisis era. Prefecture-level cities were used as the basic geographical unit in the study. Attribute information, securities code, industry category, and city of listed companies were derived mainly from the Choice, Wind, and CSMAR databases in China and were appended with the corresponding company's spatial information. Additional data on the factors affecting spatial distribution were derived from City Statistical Yearbook and City Statistical Bulletin.

3. Results

3.1. The Spatiotemporal Evolution of the Location of Spatial Agglomeration of Listed Companies

3.1.1. Overall Distribution Network Analysis. Figures 3 and 4 present the spatial agglomeration of listed companies along the YEB region in various provinces and regions. The listed companies are mainly concentrated in the Yangtze River Delta region, forming a hierarchical regional layout network that has the Yangtze River Delta region as the agglomeration core, the Yangtze River as the primary link, and the provincial capitals as fulcrums. For the given study period, the number of listed companies in the YEB region increased rapidly, from 704 in 2008 and 1097 in 2013 to 1624 in 2017. In the Yangtze River Delta area, listed companies accounted for 63.2% (2008), 67.9% (2013), and 71.6% (2017) of the total study area. Shanghai, Jiangsu, and Zhejiang have led the sustained development of the headquarters economy in the YEB region. In contrast, Guizhou, Chongqing, Yunnan, Jiangxi, and other central and western provinces with relatively slow economic development have fewer listed companies. This suggests that the location selection of listed companies in the YEB region has significant regional differences and the economic development of headquarters in each province is not balanced. The headquarters economy in the Yangtze River Delta region has been actively expanding, probably due to factors such as the economic strength advantage and economic externalities. The scale of listed companies around the provincial capital cities has grown significantly. In 2008, Shanghai and Hangzhou were at the forefront in terms of the number of listed companies. By 2017, the listed companies in Chongqing, Chengdu, Changsha, Wuhan, Nanjing, and other provincial capital cities have increased in magnitude from the third echelon to the second echelon. This suggests that as the provincial capital cities continue to siphon resource elements (e.g., technology, labor services, and capital), the location's attractiveness is increasing for listed companies.

Figure 5 shows the trends in the distribution of listed companies. The listed companies in the YEB region exhibit the following spatial distribution trend: "the quantity of companies is high in the northeast and low in the southwest." The east-west direction presents a U-shaped structure which is raised at both ends and dipping in the middle. The results also show that over time the upward momentum of the eastern region has decelerated. The overall quantity scale of listed companies in the central and western regions is weaker than in the eastern regions, but this gap is significantly shrinking. In the north-south direction, the slope line rises from south to north, and the value of the slope has gradually decreased over time. This indicates that the overall quantity scale of listed companies in the northern region is larger than in the southern region and that this difference has shrunk over time. This contraction in scale disparity between the northern and southern regions may be related to the rapid development of headquarters economy in Zhejiang and Hunan provinces.

3.1.2. Spatial Agglomeration Evolution Analysis

(1) Growth Trend Evolution Analysis of Listed Companies. Figure 6 shows the evolution trend of quantity growth transfer of listed companies based on the comprehensive division of incremental subtraction and natural breakpoint classification method. The cities in the YEB region are divided into four categories: unchanged regions (0), slow growth (1–15), rapid growth (15–45), and extreme growth (45–90). In terms of growth structure, we found that the quantity growth structure of listed companies in the YEB region has been relatively stable, with the majority classified as unchanged or having slow growth. The proportion of the area of unchanged regions was 51.9% for the periods of 2008–2013 and 2013–2017, while the proportions of those with slow growth were 44.3% and 38.9%, respectively. In terms of spatial characteristics, the scale transfer classification shows significant regional heterogeneity. Rapid growth and extreme growth are concentrated in the Yangtze River Delta region, with Shanghai and Hangzhou being core to form the core peripheral structure of the incremental gradient attenuation. This reflects the city grade gradient difference and the core edge diffusion effect of the location's attractiveness. Slow growth cities in the central and western regions are spatially fragmented. Over time, the quantity scale of listed companies has increased in a number of cities, including Chengdu, Wuhan, and Changsha, and the trend evolution pattern of listed companies in the central and western regions has gradually formed around the agglomeration of provincial capital cities.

(2). Analysis of the Trend of Spatial Agglomeration and Concentration Scope of Listed Companies. Table 1 summarizes the change in the global autocorrelation index, and Figure 7 presents the evolution of local autocorrelation trend and spatial center-of-gravity. In terms of the evolution of spatial agglomeration distribution, the results show a significant spatial agglomeration trend, with high-high and low-low agglomerations distributed in the east and west regions, respectively. In the global autocorrelation analysis, global Moran's I index values for 2008, 2013, and 2017 are 0.128, 0.228, and 0.283, respectively. The z-test values have become more significant, reflecting the continued increase in the spatial concentration of listed companies in the YEB region. In the local autocorrelation analysis, we employed

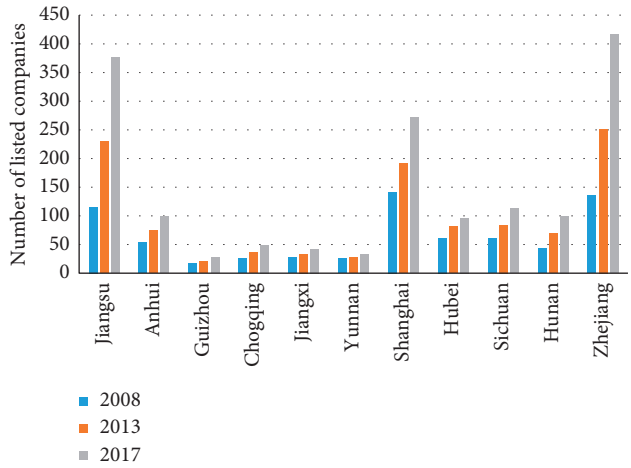

Figure 3: The distribution of listed companies in the provinces of the YEB region in 2008, 2013, and 2017.

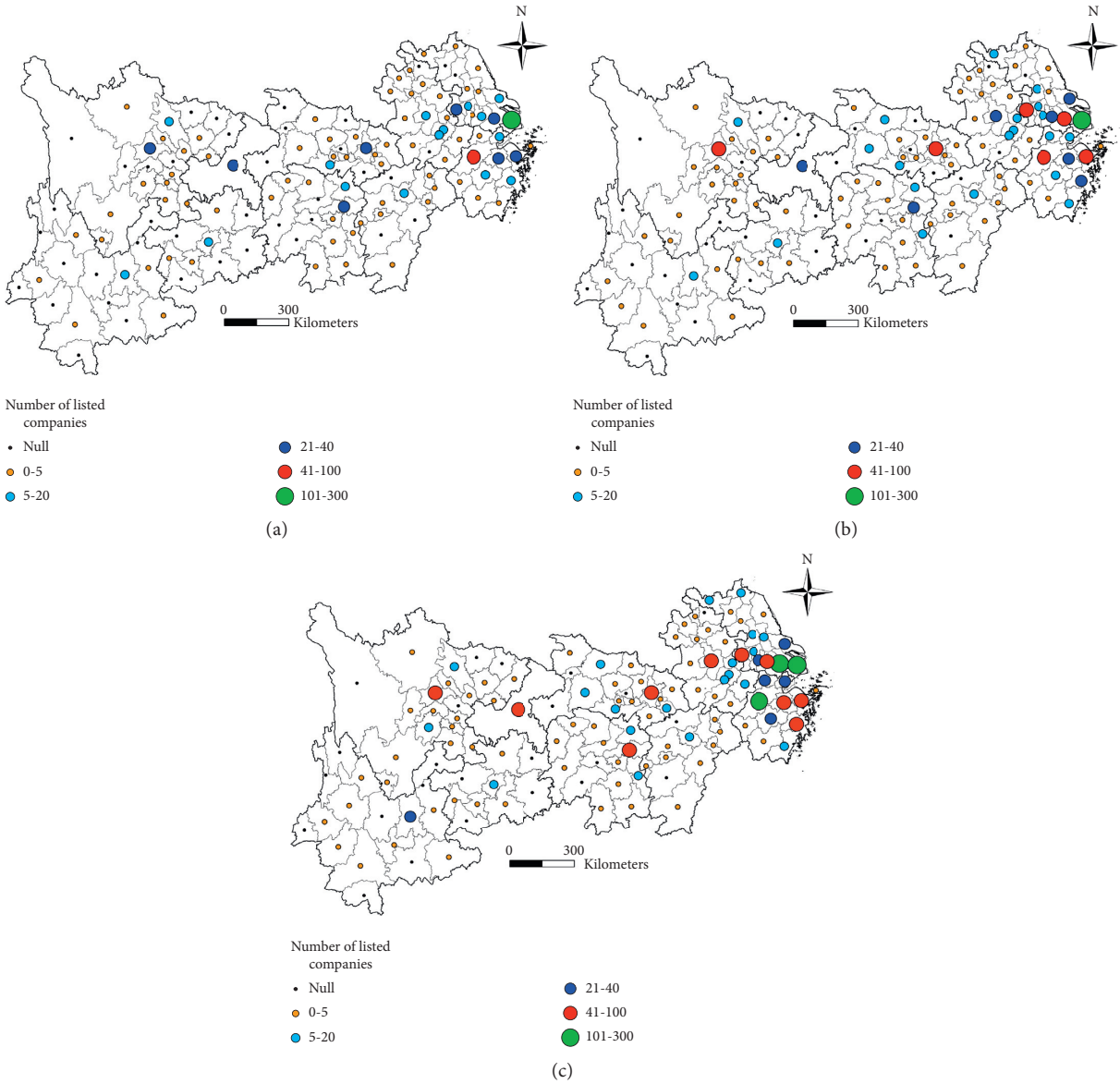

Figure 4: The distribution network of listed companies in cities of the YEB region in (a) 2008, (b) 2013, and (c) 2017.

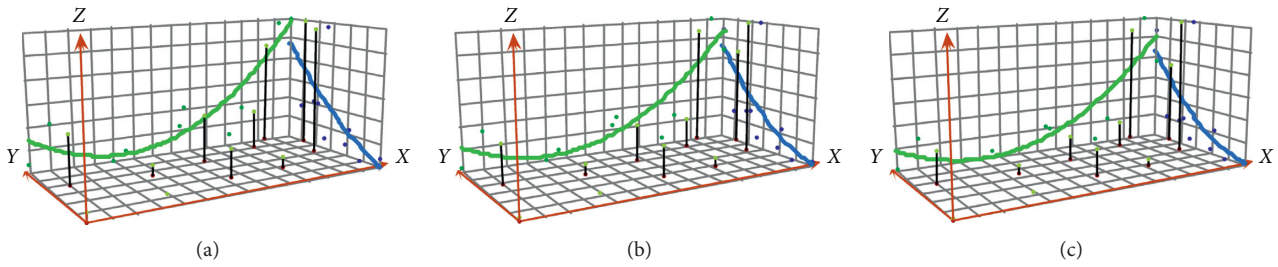

Figure 5: The trend distribution of listed companies in (a) 2008, (b) 2013, and (c) 2017.

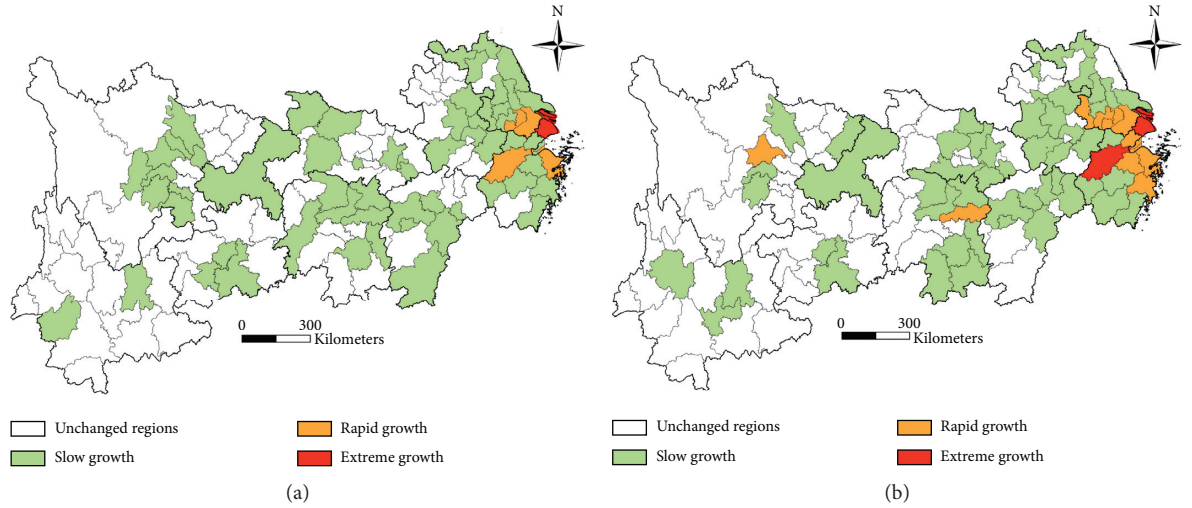

Figure 6: The classification of quantity growth trend of listed companies in the YEB region for (a) 2008 and (b) 2017.

Table 1: Global Moran's I index of spatial agglomeration of listed companies in the YEB region.

	2008	2013	2017
Moran's I	0.129	0.228	0.283
Σ (I)	0.00059	0.00073	0.0008
Z (I)	5.616	8.699	10.323

Note. σ (I) is variance.

the natural breakpoint method to group the cities into four types according to local Moran's I index: high-high (HH) agglomeration, low-low (LL) agglomeration, high-low (HL) agglomeration, low-high (LH) agglomeration. HH and LL agglomerations are the dominant agglomeration types in the YEB region that are distributed in the east and west regions, respectively. Having vibrant education and financial, technological, and information sectors, the Yangtze River Delta region has strong geographical attractiveness, forming HH agglomeration zones in Shanghai, Hangzhou, and Nanjing that are gradually spreading to the south. Due to the weak location conditions of the economic base and industrial business environment in western Yunnan and southern Sichuan, the overall development of the headquarters economy in the region has been restricted, and relatively stable LL agglomeration groups have been formed. In addition, Zhenjiang, Taizhou, Yangzhou, Ma'anshan, Xuancheng, and other cities have formed an LH cluster because of the relative disparity in business and financial environments with high-value areas. Affected by possible factors such as administrative division, topographic isolation, and weak industrial cooperation in the central and western regions, Wuhan, Changsha, Chengdu, Guiyang, Kunming, and other provincial capitals have insufficient linkages with other cities. The spatial diffusion effect of the headquarters economy remains weak and forms an HL agglomeration with fragmented distribution.

In terms of the evolution of the spatial center-of-gravity, the development center of listed companies shifted from the west towards the eastern coast, and the rate of migration slowed gradually. The spatial center-of-gravity changed between 30.46°–30.52°N and 116.25°–117.19°E and moved along the direction of "western-central-eastern" in Anqing city, Anhui. The migration speed of center-of-gravity decreased from 10.45 km/yr (2008–2013) to 9.28 km/yr (2013–2017). The standard deviation ellipse shifted

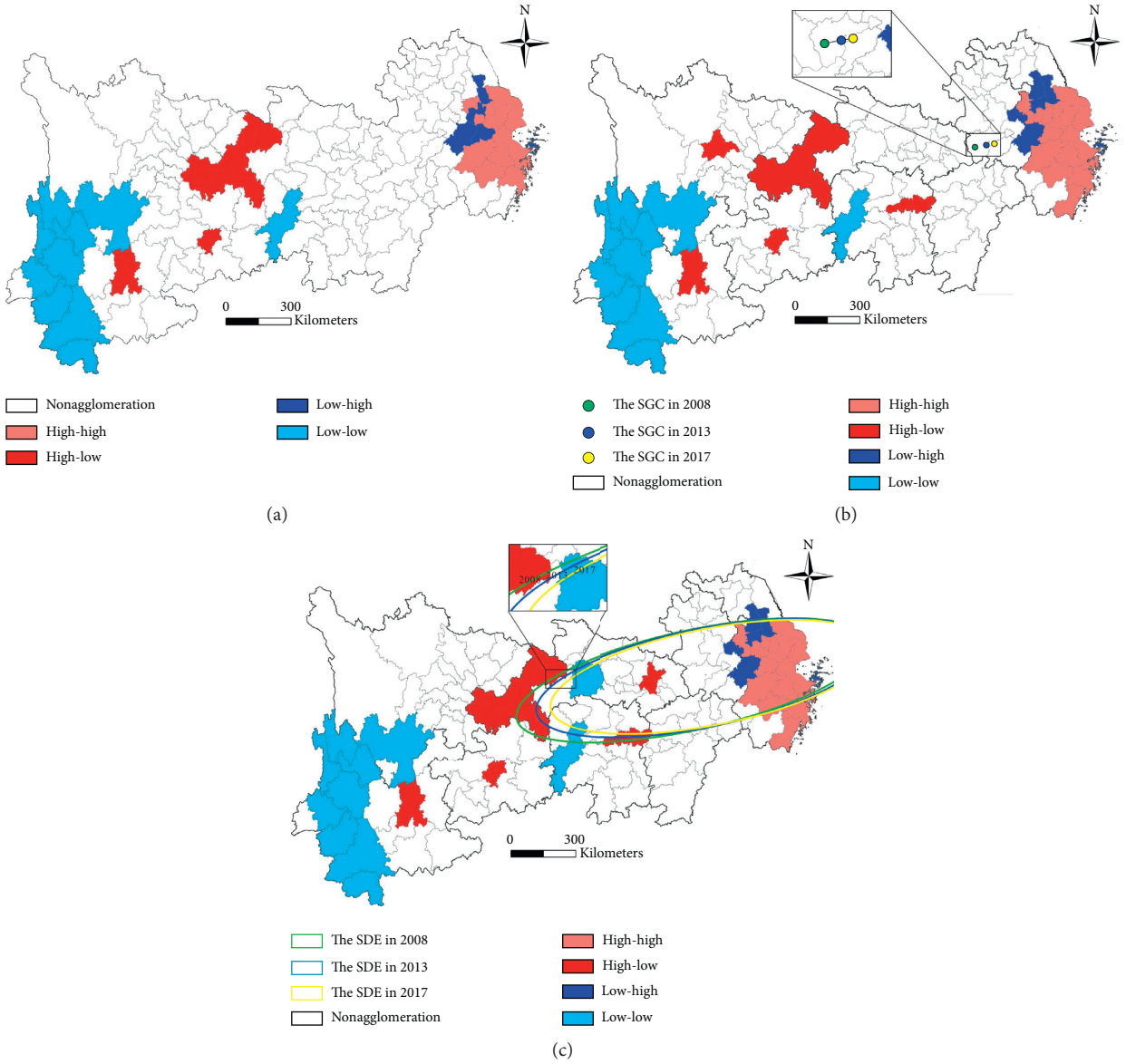

Figure 7: The spatial agglomeration classification, spatial gravity center (SGC), and standard deviation ellipse (SDE) of listed companies in the YEB region for (a) 2008, (b) 2013, and (c) 2017.

eastwards along with the migration of the spatial center-of-gravity, and the area was reduced from 606,750 km^2 to 538,234 km^2. The spatial center-of-gravity is the center of the ellipse formed by the high concentration of listed companies in the region, and its movement can reflect the extension direction of the high-value group with a large number of listed companies. The spatial center-of-gravity moves steadily eastward and the elliptical range continues to spread eastward, comprehensively showing that the attractive advantage created by the high economic strength, financial service level, and technological innovation environment in the eastern coastal area is still in the strengthening stage for listed companies. Meanwhile, the migration speed of the spatial center-of-gravity of listed companies to the east has slowed down, which is in line with the conclusion that the upward trend of the eastern region in the spatial distribution trend analysis has slowed down, indicating that, on the basis of the improvement of policy structure and regional development environment, the central and western regions will still have the opportunity to show a gradually optimized competitive advantage in the competition of spatial agglomeration of listed companies in the future.

3.1.3. Spatial Evolution of the Industrialization Location Layout of Listed Companies. Figure 8 reflects the spatial agglomeration characteristics among listed companies with different specialization levels from different industry types using the method of location quotient and Inverse Distance Weighted (IDW), and the index in the legend reflects the specialization levels of listed companies in each region. The results show that labor-intensive listed companies with high-

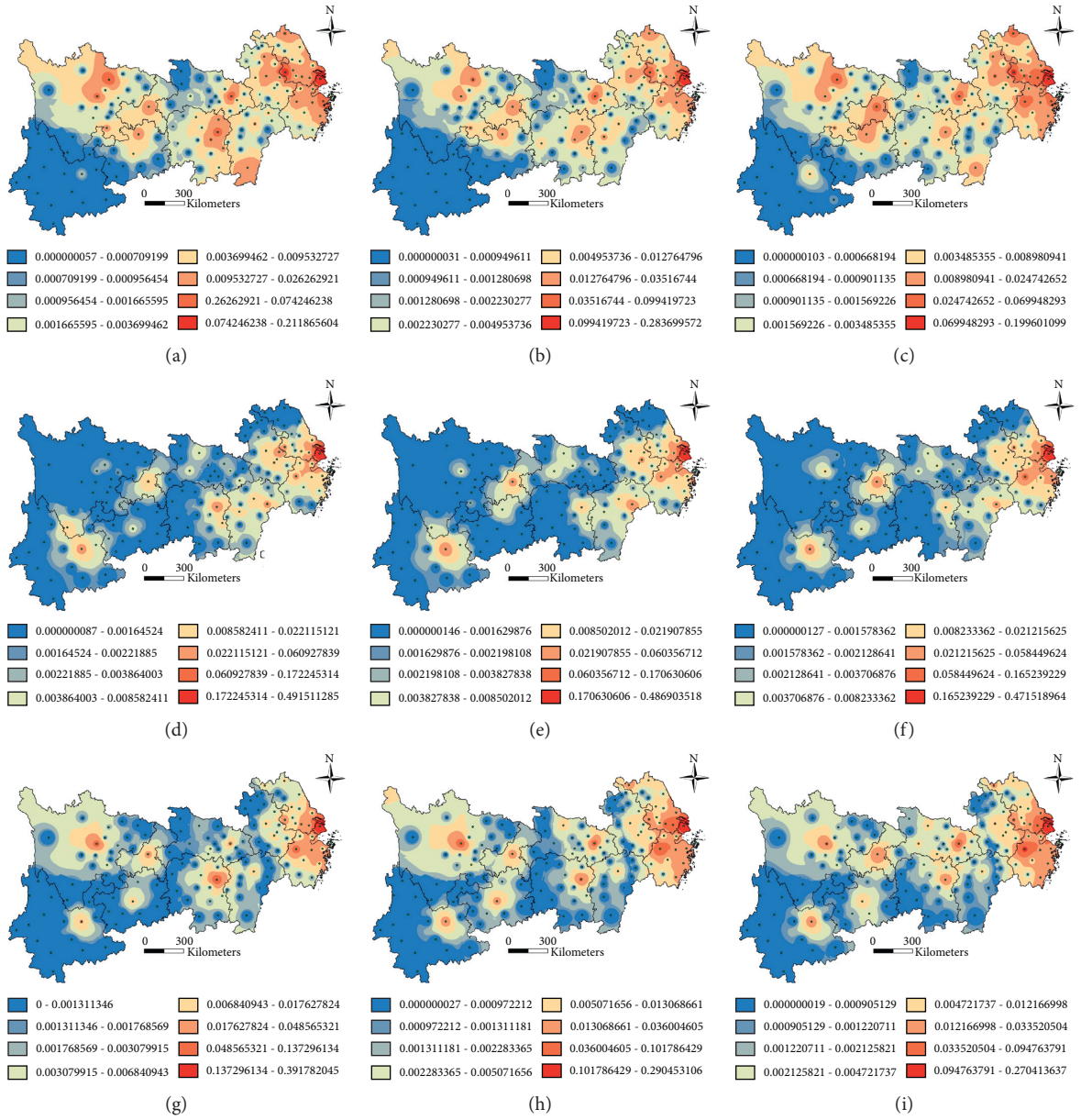

FIGURE 8: The spatial agglomeration of the specialization levels of listed companies in three major industrial types in (a, d, g) 2008; (b, e, h) 2013; and (c, f, i) 2017.

specialization levels gradually spread from a bead-chain distribution into flaky pattern distribution. In 2008, there were three major bead chains, namely, the Chengdu-Mianyang, Changsha-Zhuzhou-Xiangtan-Yueyang, and the Yangtze River Delta region with Nanjing, Shanghai, and Ningbo as centers. In 2017, the flaky high-value agglomeration area in the Yangtze River Delta was gradually formed, with Shanghai, Hangzhou, and Nanjing as core and Ningbo, Suzhou, and other places as the flanks. The trend of outward expansion and integration in the Chengdu-Mianyang and Chongqing-Guiyang chains continued increasing, in line with China's high-quality workforce migration trend (i.e., transfer to eastern coastal and provincial capitals) and the transition of labor-intensive enterprises towards high specialization in the Yangtze River Delta.

High capital-intensive listed companies with high-specialization levels tend to congregate in the Yangtze River Delta region, forming a layout structure more concentrated in the east than in the west. For 2008–2017, affected by the Yangtze River Delta integration strategy and regional capital factor allocation management experience, capital-intensive listed companies increasingly gathered in the Yangtze River Delta region and gradually formed a cluster distribution pattern with Shanghai as the core and Hangzhou, Ningbo, Jiaxing, and Suzhou as the series support. In the central-western regions, only Chengdu, Yingtan, Chongqing,

Changsha, and other places have relatively high-levels of specialization, exhibiting pronounced polarized distribution characteristics.

Technology-intensive listed companies with high-specialization levels huddled in provincial capital cities and accelerated the diffusion around the urban agglomeration and metropolitan areas. In 2008, the high-specialization listed companies exhibited a fragmented pattern and were only located in central cities, such as Chengdu, Changsha, Hangzhou, Nanjing, and Shanghai. In 2013, a distribution area of high-specialization levels of technology-intensive listed companies was formed with Wuhan City Circle as the boundary in Hubei province. In 2017, the fragmented structure changed, and the high-value areas in the east region expanded southwards and westwards, covering much of the Yangtze River Delta's urban agglomeration. Due to trans-boundary cooperation among technology-intensive enterprises, a high-specialization cluster of technology-intensive listed companies was created in the Chengdu-Chongqing urban agglomeration. The urban agglomerations and metropolitan areas have become the first choice for technology-intensive listed companies with high-specialization levels.

3.2. Driving Mechanism Affecting Location Spatial Agglomeration of Listed Companies. The production and operation of listed companies require a large reserve of scientific and technological talents [18], the scale of urban industrial economy largely determines the degree of perfection of the regional industrial chain [19], and the degree of economic openness and geographic location affect the convenience for enterprises' foreign trade cooperation and transnational operations [7]. Besides, the strength of the local financial support and the policy environment determines the degree of infrastructure modernization and policy incentives, affecting the operating costs of listed companies [5]. Based on this, we select the factors that influence the location spatial agglomeration of listed companies, such as city scale, globalization level, technological input, knowledge spillover, and level of policy support. The following parameters were used: regional GDP, actual utilization of foreign capital, total expenditure on science and technology, number of institutions for higher learning, and total general government expenditure. The dummy variables, based on the urban administrative level ("1" for prefecture-level city, "2" for provincial capital city, and "3" for municipality directly under the central government), were used to reflect the geographic location parameter. The summary of indicator details is presented in Table 2. The data for these indicators were obtained mainly from the 2017 China Statistical Yearbook and the China City Statistical Yearbook, supplemented by provincial, city, and municipal statistical yearbooks. To analyze the driving mechanism by parts, we divided "typical regions" into low-level city network (0–20) and high-level city network (20–300) based on the number of city listed companies (see Figure 4). A comprehensive analysis of the driving factors of spatial agglomeration can then be implemented for the YEB region and "typical regions," in order to clarify the key elements of the city networks with different quantity of listed companies to achieve the headquarter economy development.

Table 3 summarizes the calculation results of SLM and SEM regression analysis. The OLS regression model has a poor fit (R-squared is small; AIC and SC are both larger than SLM and SEM), primarily because it fails to consider the influence of the spatial dimensions of listed companies. The SLM and SEM incorporate lag and error terms into the framework that can explain the correlation between the spatial distribution of listed companies and the various driving factors. The results indicate that in both the overall region and the "typical regions", the SLM and SEM are both significant at the 0.1% level. The SEM has a larger log-likelihood value and smaller AIC and SC values than the SLM; the SEM's R^2 is also comparatively better. These findings suggest that the influence of uncertain factors on the spatial layout of listed companies cannot be ignored, and the SEM is more suitable in explaining the influencing factors for the spatial distribution of listed companies and is therefore used in the subsequent analyses.

In terms of the overall area, the top three factors are knowledge spillover level ($B = 29.737$), city scale ($B = 20.756$), and level of policy support ($B = 17.225$). This suggests that the intellectual resources of colleges and universities deliver high-quality, innovative talents for enterprises, which are essential in the location selection of listed companies. The city scale positively affects regional economic strength, infrastructure construction level, consumer market capacity, and modern service level, which can ensure reliability in business operations. The high level of policy support can help in the effective implementation of government programs and market operations. It can also make contributions in terms of providing enterprises with financial support, promoting fair market competition, and encouraging transnational cooperation strategies. The results also show that the regression coefficients for technology development level and geographic locations are −20.327 and −17.931, respectively. This suggests that while the technological input and the geographic location of Changsha, Wuhan, Chengdu, Ningbo, Suzhou, Taizhou, and other outside cities in the Yangtze River Delta have not been optimal, the enormous growth in the number of listed companies has weakened the overall influence of these two factors.

For low-level city network with few listed companies, the two main factors are city scale ($B = 7.654$) and knowledge spillover level ($B = 5.055$). This suggests a strong dependence of low-level city network on the scale of cities. Cities, particularly in the central and western regions, should prioritize in enhancing the capacity of industry support and economic development strength towards the development of headquarters economy. The impact of knowledge spillover is related to the demand for intellectual resources and skill competency in listed companies. In most cities in the central and western regions, limited resources in universities and the relative scarcity of high-quality talents can significantly inhibit the appeal of cities in attracting agglomeration of listed companies.

For high-level city network with a large number of listed companies, the top three determinants are knowledge spillover level ($B = 37.815$), policy support level ($B = 15.471$),

Table 2: Details of the driving factors used in the model.

Driving factors	Definition	Indicator
City	To some extent, affects the environment for the survival and development of listed companies	GDP
Globalization	Affects the convenience of enterprises to carry out cross-border cooperation in technology, capital, production, operation, and labor services	Actual utilization of foreign capital
Technology	To a certain extent, determines the ease of industrial transformation and product power of listed companies	Total expenditure on science and technology
Knowledge	Affects the enterprise's production-university-research cooperation and innovative atmosphere	The number of ordinary institutions of higher learning
Policy	Affects the smooth implementation of the company's layout and business strategy	The general public budget expenditure of the government
Location	The administrative level of a city is directly related to the concentration of resource elements and regional social and economic activities	Administrative level

Note. "City" is city scale; "globalization" is the globalization level; "technology" refers to the technological input; "knowledge" refers to the level of knowledge spillover; "policy" is the level of policy support; and "location" refers to the geographical location.

Table 3: Results of SLM and SEM regression analysis of each dimension.

Level of quantity	SLM			SEM		
	a	b	c	a	b	c
City	19.385 ***	7.334***	12.247 **	20.756 ***	7.654 ***	8.344 *
Globalization	1.862 *	−0.982 *	7.399 *	2.527 *	−0.966 *	14.32 **
Technology	−17.336 ***	−3.901 **	−24.783 ***	−20.327 ***	−3.66 **	−27.073 ***
Knowledge	27.995 ***	5.541 ***	35.974 ***	29.737 ***	5.055 ***	37.815 ***
Policy	15.732 ***	2.575 **	21.291 **	17.225 ***	2.999 **	15.471 **
Location	−15.657 ***	2.332 **	−26.892 **	−17.931 ***	1.953 **	−21.025 **
R-squared	0.928	0.732	0.951	0.935	0.735	0.956
Log-likelihood	−387.062	−186.632	−75.277	−383.633	−186.396	−74.6621
AIC	790.125	389.265	166.554	781.267	386.793	163.324
SC	811.508	408.992	174.11	799.977	404.054	169.935
N	107	88	19	107	88	19

Note. a indicates the YEB region; *b* indicates low-level city network; *c* indicates high-level city network. $^{***}p < 0.01$; $^{**}p < 0.1$; $^{*}p < 0.05$. AIC means Akaike information criterion; SC is the Schwarz criterion.

and globalization level ($B = 14.32$). With the acceleration of industrial structure transformation and upgrading in the high-level city network, the demand for industry-university-research cooperation, technological innovation talents, and educational resources has increasingly become crucial in the modern high-end industrial system. Likewise, the strong influence of policy support suggests that policies relating to urban agglomeration planning and city construction have a considerable effect on shaping the location advantages in high-level city network. High-quality government service and work efficiency have provided significant contributions to the improvement of the business environment of listed companies. The impact of the level of globalization is prominent because high-level city network has a higher level of specialization, having stronger demands for international labor and transnational technology cooperation. The higher the level of globalization, the stronger the participation in the global industrial division of labor system, which may help companies to improve competitiveness in overseas markets and market visibility.

4. Discussion

4.1. Overall Distribution Structure Analysis. GIS spatial interpolation and TSA methods were employed to study the location selection characteristics of listed companies in the YEB region, showing the spatial distribution network of listed companies with the Yangtze River Delta region as the core and the following distribution trend: "the quantity of companies is high in the northeast and low in the southwest," similar to the findings of previous studies [6, 8, 12]. This verifies the disparity in headquarters economic development between the east and west regions of the YEB region and reaffirms the significant advantages of the Yangtze River Delta in attracting listed companies [20]. The scale of listed companies in the provincial capital cities of Chongqing, Chengdu, Changsha, Wuhan, Nanjing, and other cities increased rapidly at the end of the study period. This suggests that the regional development strategies and financial support policies, which are based on the provincial capital cities used as the core, have

yielded significant results for enhancing the location attractiveness for listed companies. In order to boost the headquarters economy in the YEB region, the government has to recognize the spatial differences in the location selection process of listed companies and help improve the economic radiation capacity of the Yangtze River Delta region and provincial capital cities to the surrounding cities.

4.2. Spatial Agglomeration Evolution Analysis. The findings show that the listed companies in the YEB region have an apparent "Matthew effect." Listed companies had the Yangtze River Delta region as the first choice for their headquarter location, followed by provincial capitals. The location attraction of other cities in the central and western regions had been insufficient, leading to the formation of a strict urban hierarchy growth order [21]. The spatial autocorrelation analysis shows that the spatial agglomeration of listed companies in the YEB region has been increasing gradually, indicating that cities with high-scale listed companies have the ability to radiate economic activities and can form coordinated growth structures with surrounding cities. The spatial center-of-gravity shifted from the west to the east coast, but the rate of migration slowed. These findings highlight the strength of the eastern region in cultivating and attracting headquarters of listed companies. The results also suggest that the shifting government policies, construction strategies, and resource reallocation towards the central and western regions in recent years have enhanced competitiveness and attractiveness of these regions in the development of the headquarters economy. The distribution of industries by specialization levels shows that listed companies with high specialization tend to flock in eastern cities, provincial capitals, and urban agglomerations. Since modern urban systems are often better equipped to deal with interregional resource allocation and business interaction, they are more likely to strengthen the joint force of professional development.

4.3. Driving Factors Analysis. In comparison to the findings from previous studies that found regional economic scale as the principal determinant, our findings suggest that the level of knowledge spillover has become the primary factor affecting the location selection of listed companies in the YEB region [4]. This means that in the era of the knowledge economy, intellectual resources are becoming crucial elements for listed companies to create wealth and improve market competitiveness [22]. The important impact of city scale and knowledge spillover level for low-level city network indicates that strengthening their industrial construction capacity and investment in science and education resources is key to attracting the spatial agglomeration of listed companies. This supports China's current preferential policies towards the development of the central and western regions. Globalization was found to have a significant impact on high-level city network, which reflects a crucial requirement of listed companies in the east region for transnational operations and cooperation. In order to further develop the headquarters economy for this particular city type, vertical integration and extension of the industrial chain have to be strengthened, and transnational development strategies have to be implemented to improve the status of the international division of labor.

4.4. Policy Implications. In the postepidemic era, the global economic and financial landscape is facing in-depth adjustments; the listed companies in YEB region also have many problems, such as imbalanced spatial agglomeration layout and significant gap between east and west, which makes it urgent to rely on listed companies to accelerate resource integration and industrial innovation, and achieve the coordinated development of regional economy and industrial strength. (1) The knowledge spillover level, the city scale, and the level of policy support play important role for overall region. Cities in the YEB region should speed up the construction of school-enterprise alliances and the integration of production-education-research, strengthen financial investment in education, and cultivate corporate management talents and technological research teams. Meanwhile, the government should focus on the change of the global financial market and accelerate the reform and innovation of the domestic financial system, to provide a great policy environment for the development of listed companies. (2) The knowledge spillover level, policy support level, and globalization have made outstanding contributions to the layout of listed companies in high-level city network. The eastern cities, represented by Shanghai, Hangzhou, and Nanjing, should progress in cultivating high-end international talents, creating a highly conducive business environment, and pushing for industrial internationalization. At the same time, it is necessary to integrate into the construction of the national strategies, such as the Yangtze River Economic Belt and the Belt and Road Initiative, relying on the cross-regional alliance of industrial parks to strengthen the cooperation with cities in the central and western regions for enhancing the radiating and leading effect of the headquarters economy. Emerging cities in the central-western regions, represented by Chongqing, Wuhan, and Chengdu, should focus on the construction of more industrial parks and urban agglomerations and strengthen the cooperation in enterprise listing, cross-regional operation, and industrial chain construction with the marginal cities to consolidate their location attractiveness. (3) The city scale and knowledge spillover level are the most critical factors in cultivating and attracting the layout of listed companies in low-level city network represented by small- and medium-sized cities in the central and western regions. These cities should focus on improving their own industrial capacity, vigorously connect with the construction strategy of urban agglomeration and metropolitan area, transform industrial comparative advantages into city economic advantages, actively cultivate their talent teams, improve basic conditions for regional development, and attract the industrial transfer and spatial layout of listed companies.

5. Conclusion

This study took all A-share listed companies in the YEB as the research object, established the framework "pattern evolution-typical alienation-driving mechanism," and explored the evolution of the spatial agglomeration and the driving mechanisms of listed companies from 2008 to 2017. An integrated method system was developed; it combines trend surface analysis, exploratory spatial data analysis, standard deviation ellipse, SEM regression, and SLM regression in the analysis. The main conclusions of the study are as follows.

The location selection of listed companies has gradually formed a spatial distribution network where the Yangtze River is the link, the provincial capital cities act as the fulcrum, and the Yangtze River Delta region serves as the agglomeration core. The spatial difference of the layout of listed companies persists, showing the following spatial distribution trend: "the quantity of companies is high in the northeast and low in the southwest."

The YEB region has formed a strict urban hierarchy growth order. The number of listed companies in most cities is unchanged or has slow growth. In the central and western regions, the pattern of scale transfer has gradually formed around the development of provincial capital cities. Spatial autocorrelation analysis shows that the spatial agglomeration of listed companies has become more pronounced. HH and LL agglomerations are the main agglomeration types and are found mainly in the east and west regions of the YEB region. The spatial center-of-gravity and the ellipse range have shifted from the west to the eastern coast, and the location selection of high-specialization levels of listed companies showed significant variations among the three major industry types (i.e., labor-intensive, capital-intensive, and technology-intensive).

Knowledge spillover level, city scale, and policy support level are the main driving factors for attracting listed companies in the YEB region. Low-level city network with few listed companies has heavy dependency on city scale and knowledge spillover levels. In high-level city network, aside from the level of knowledge spillovers and policy support, the level of globalization was found to be a crucial driving mechanism.

Based on the unbalanced tendency shown by the spatial agglomeration of listed companies in the YEB region and the dominant factors affecting the distribution of listed companies in different city networks, targeted development suggestions are put forward, such as accelerating the construction of school-enterprise alliances and the integration of production-education-research, relying on the construction of industrial parks and urban agglomerations, accelerating cross-regional collaboration, and improving industrial development capabilities.

This study still has several limitations, which can be improved in future studies. First, our analysis of the location spatial agglomeration characteristics of listed companies did not consider distribution elements, such as asset intelligence, profit levels, and debt structure. Second, due to difficulties in data acquisition, several driving factors were overlooked, such as geographical terrain, entrepreneur choice preference, and regional market conditions. Despite these research constraints, this study was able to establish the framework of "pattern evolution-typical alienation-driving mechanism" and explored the key factors for attracting listed companies in the YEB region at different levels. The results can provide a useful reference for local governments to optimize the conditions for attracting investment and urban infrastructure and promote the overall coordinated and sustainable development of the headquarters economy in the YEB region.

Data Availability

The research data used to support the findings of this study are available from the corresponding author upon request.

Conflicts of Interest

The authors declare that there are no conflicts of interest regarding the publication of this paper.

Acknowledgments

Special thanks are due to the professional language editing service from EditX. This research was funded by the Program of National Natural Science Foundation of China, under grant no. 41501173, and Talent Introduction Program Project of Southwest University, under grant no. SWU019020.

References

[1] D. Maditinos, Z. Sevic, and C. Tsairidis, "Intellectual capital and business performance: an empirical study for the Greek listed companies," *European Research Studies Journal*, vol. 3, pp. 145–168, 2017.

[2] M. D. Rice and D. I. Lyons, "Geographies of corporate decision-making and control: development, applications, and future directions in headquarters location research," *Geography Compass*, vol. 4, no. 4, pp. 320–334, 2010.

[3] J. Garcia-Algarra, G. G. Bengoechea, and M. L. Mouronte-Lopez, "Reducing trade inequality: a network-based assessment," *Complexity*, vol. 2020, Article ID 1593215, 9 pages, 2020.

[4] L. Li, C. M. Li, Z. X. Dai et al., "Research on spatial-temporal change and mechanism of listed companies in China," *Surveying and Mapping Science*, vol. 44, pp. 324–329, 2019.

[5] J. P. Zhao and M. H. Lu, "Characteristics and influencing factors of spatial distribution of headquarters of listed firms in Beijing," *Economic Geography*, vol. 40, pp. 12–20, 2020.

[6] L. Zhang, H. Zhang, and H. Yang, "Spatial distribution pattern of the headquarters of listed firms in China," *Sustainability*, vol. 10, no. 7, 2564 pages, 2018.

[7] H. F. Wang, X. Zhang, X. Xiong et al., "Spatial agglomeration and changing trend of China's bio-industry: based on empirical data analysis of listed companies," *Economic Geography*, vol. 38, pp. 101–107, 2018.

[8] Y. X. Zhong, Y. Fu, W. D. Guo et al., "Spatial pattern evolution and driving factors of China's listed companies," *Scientia Geographica Sinica*, vol. 38, pp. 485–494, 2018.

[9] S. Mariann, "Spatial distribution of the top 500 companies on regional and county levels in Hungary-a repeated analysis," *Regional Statistics*, vol. 7, pp. 148–170, 2017.

[10] C. Gu, L. Hu, and I. G. Cook, "China's urbanization in 1949-2015: processes and driving forces," *Chinese Geographical Science*, vol. 27, no. 6, pp. 847–859, 2017.
[11] M. Manniste, A. Hazak, and E. Listra, "European listed companies' share price reactions to global credit crunch: typology of winners and losers," *International Journal Of Trade Economics and Finance*, vol. 2, pp. 478–483, 2014.
[12] J. Y. Lin, "The study on the characteristics of regional distribution evolution and the path dependence of listed companies in China," *Shanghai Economic Research*, pp. 37–43, 2018.
[13] X. Xu, G. Yang, Y. Tan, J. Liu, and H. Hu, "Ecosystem services trade-offs and determinants in China's Yangtze River economic belt from 2000 to 2015," *Science of The Total Environment*, vol. 634, pp. 1601–1614, 2018.
[14] Y. Li, H. Shao, N. Jiang et al., "The evolution of the urban spatial pattern in the Yangtze River economic belt: based on multi-source remote sensing data," *Sustainability*, vol. 10, 2018.
[15] Y. Zhong, A. Lin, L. He, Z. Zhou, and M. Yuan, "Spatio-temporal dynamics and driving forces of urban land-use expansion: a case study of the Yangtze River economic belt, China," *Remote Sensing*, vol. 12, no. 2, p. 287, 2020.
[16] H. Wang and R. Zuo, "A comparative study of trend surface analysis and spectrum-area multifractal model to identify geochemical anomalies," *Journal of Geochemical Exploration*, vol. 155, pp. 84–90, 2015.
[17] F. Li, X. Wang, H. Liu et al., "Does economic development improve urban greening? Evidence from 289 cities in China using spatial regression models," *Environmental Monitoring and Assessment*, vol. 190, pp. 1–19, 2018.
[18] Z. Sun and L. P. Xiao, "Industrial Characteristics,Corporate governance and firm's R and D investment——evidence from A shares of listing corporation of strategic emerging industries in China," *Journal of Economic Management*, vol. 8, pp. 23–34, 2015.
[19] Y. M. Sun and X. W. Meng, "Research on macroeconomic environment, industry characteristics and zero debt behavior of listed companies," *Macroeconomics*, vol. 2, pp. 33–45, 2019.
[20] J. Li, X. Huang, M.-P. Kwan, H. Yang, and X. Chuai, "The effect of urbanization on carbon dioxide emissions efficiency in the Yangtze River Delta, China," *Journal of Cleaner Production*, vol. 188, pp. 38–48, 2018.
[21] E. Aksel, "Exploring economic development through headquarters: the spatial distribution of Turkey's large industrial enterprises and its implications for urban systems," *Professional Geographer*, vol. 68, pp. 138–148, 2015.
[22] G. Venanzoni, M. Carlucci, and L. Salvati, "Latent sprawl patterns and the spatial distribution of businesses in a southern European city," *Cities*, vol. 62, pp. 50–61, 2017.

Hindawi
Complexity
Volume 2020, Article ID 8876017, 17 pages
https://doi.org/10.1155/2020/8876017

WILEY | Hindawi

Review Article

A Scientometric Review of Digital Currency and Electronic Payment Research: A Network Perspective

Qing Shi and Xiaoqi Sun

The Institute for China's Overseas Interests, Shenzhen University, Shenzhen, Guangdong 518060, China

Correspondence should be addressed to Xiaoqi Sun; sunxiaoqi@szu.edu.cn

Received 1 September 2020; Revised 1 October 2020; Accepted 18 October 2020; Published 9 November 2020

Academic Editor: Xueyong Liu

The potential implications of digital currencies and electronic payment (DC/EP) have become a hot global research area. To present the knowledge bases and research fronts of this field, we apply a scientometric approach to analyze 454 publications obtained from the Web of Science core collection. Results show that, first, the knowledge bases can be classified into three main topics: (1) the usage and diversification effect of private digital currencies from the point of investment and asset allocation; (2) the price dynamics and market efficiency of private digital currencies; and (3) other economic roles of digital currencies and corresponding change brought into the monetary system. Second, several research trends can be inferred using sliding window analysis and burst detection, namely, how the introduction of digital currencies changes consumers' choice in payment instrument and their money demand; how social media and investor sentiment affect the market of digital currencies; and the impact of digital currencies on the central bank, monetary policy, and central bank digital currency. Third, core scholars and countries involved in the research of DC/EP are identified, and it is found that collaboration has been rising especially among European scholars and countries. With these systematic analyses, we offer recommendations for scholars and practitioners in future research of DC/EP.

1. Introduction

The global spread and use of the Internet and mobile phones contribute to the development of new forms of money and financial payments [1, 2]. Specifically, digital currencies and electronic payments (DC/EP) are introduced to conduct convenient and effective financial transactions. Digital currencies, or digital money, are referred to as any types of currencies using FinTech, which include cryptocurrencies issued by private entities, central bank digital currencies, and other forms of digital money, while electronic payments are referred to as the payments using digital instruments such as mobile wallets. These financial innovations, which bring a range of impacts on various aspects of financial markets and the wider economy, have drawn increasing attention from academia, enterprises, and governments and become a hot global research topic [3, 4].

The employment of DC/EP has been facilitated by the innovation of blockchain based on the decentralized ledger technology (DLT), which promises to offer secured peer-to-peer transactions and auditable and transparent transfer of assets, thus reducing the trust gap [5, 6]. The applications of DC/EP are multitude. It benefits consumers and merchants through more efficient and less expensive services for e-commerce and cross-border payments [7–9]. Also, some types of digital currencies can be potentially used as alternative investment instruments [10, 11]. Moreover, besides private end-users, DC/EP may provide central banks and the banking industry with additional monetary policy tools [12–14]. And the regulation society may also rely on the data generated by DC/EP for filtering and signal extraction, such as intelligent auditing, tracing functionality, and promoting cooperation among regulatory agencies [15]. Nonetheless, potential risks and disruptions may arise with regard to

business models, financial systems, and regulation regimes [16–18].

Given the rising importance of DC/EP initiatives, a review study is demanded. There exist some survey works on the related literature. For example, Bohme et al. [19] reviewed the economics, technology, and governance of Bitcoin. Tschorsch and Scheuermann [20] carried out a review on the protocol and building blocks under decentralized digital currencies and explored the design space as well as fundamental structures at the core of the protocol. Holub and Johnson [21] and Corbet et al. [22] reviewed the literature on cryptocurrencies. Dashkevich et al. [23] performed a survey on the applications of blockchain technology to functions by the central bank. The existing literature reviews adopted a descriptive statistical approach to analyze the frequency and distributions of knowledge units and investigate the context of critical articles, however, ignoring the structure features embodied in the network of knowledge units and its potential change. Through scientometric methods, we aim to reveal the structure features of DC/EP knowledge networks, including cocitation network, cooccurrence network, and collaboration network, thereby providing a roadmap for prospective scholars in this field.

A CiteSpace study typically consists of several components, notably a body of scientific literature which is obtained through the objective criteria of selection and exclusion, a set of scientometric metrics and visual analytic tools that can highlight significant patterns and trends, and theories that guide the interpretation of visualized intellectual structures and dynamic patterns [24]. Scientometric methods include author cocitation analysis (ACA) [25], document cocitation analysis (DCA) [26], coword analysis [27], and many other variations. Compared to traditional reviews, a scientometric review has the advantages of dealing with big data, providing a more rigorous research output, finding pivotal points in an intellectual structure, detecting the emerging trends in a specific field, and employing various network-based visualization technologies to make a more intuitive impression [23, 28, 29]. Therefore, this approach has become increasingly applied in different areas of academic research, such as identifying the research trends on green construction [30], showing the intellectual landscape of propoor tourism research [31], finding the opportunities and challenges in destination branding [32], mapping the evolution and research framework of carbon footprint [33], and arising number of scientometric studies in the fields of finance and economics [34, 35]. These papers demonstrate the advantage and fitness of scientometric methods for exploring academic knowledge bases and corresponding cutting-edge issues. Despite the popularity of scientometric methods, to our knowledge, a few publications have applied it to analyze the rapidly rising literature in the area of DC/EP, neither to visualize the knowledge base nor to detect the research frontiers. Our work is thus to fill this gap.

To sum up, this paper makes two contributions to the literature by using the scientometric approach and CiteSpace. First, we use a new review method to investigate the DC/EP related studies, which systematically explore and visualize the knowledge bases, intellectual structure, and emerging hot topics and research fronts in the area of DC/EP. Second, we extend the application of CiteSpace to a new literature field, that is, DC/EP research.

The remainder of this paper is organized as follows. Section 2 illustrates the scientometric research method, including network construction, network-related metrics, parameter setting in the CiteSpace, and data sources. Section 3 uses CiteSpace network analysis to explore the intellectual structure of DC/EP through clustering analysis of citations and timeline mapping of its evolutionary path. Section 4 conducts sliding window analysis and citation bursts detection to demonstrate structural changes of cocitation networks and find probable bursts of research interest followed by a clustering analysis of terms and keywords to further analyze the emerging hot topics and research fronts. Section 5 investigates core scholars and countries through clustering analysis and maps the collaboration network to highlight the major strength in the field of DC/EP. The last section is the concluding part.

2. Methodology and Data

2.1. Network Construction. Network analysis is one of the foundations of the CiteSpace studies. The network consists of nodes and edges linking these nodes. In matrix language, one network can be expressed as the following equation:

$$G^{v} = \begin{bmatrix} e_{11}^{v} & e_{12}^{v} & \cdots & e_{1n}^{v} \\ e_{21}^{v} & e_{22}^{v} & \cdots & e_{2n}^{v} \\ \vdots & \vdots & \ddots & \vdots \\ e_{n1}^{v} & e_{n2}^{v} & \cdots & e_{\mathrm{nn}}^{v} \end{bmatrix}, \tag{1}$$

where e_{ij}^{v} denotes the connection between node i and node j of network type v, which is defined by the node type. For citing references, if two nodes show simultaneously in the same reference, then these two nodes are connected, that is, $e_{ij} > 0$; otherwise $e_{ij} = 0$. The value of e_{ij} is called the weight of the edge. The more two nodes show together, the larger e_{ij} is. For cited references, two nodes are connected if both are cited simultaneously by one reference, that is, $e_{ij} > 0$. In other words, the network is weighted but undirected network. Figure 1 is an example illustration for the network construction.

For citing references, we construct four networks in which authors, countries, terms, and keywords are set as nodes, respectively. The author network is used to analyze collaboration between authors and to identify key authors in the network using centrality indicators; the country network is constructed to investigate the collaboration between countries; and the keyword network can identify the current hot topics and previous hot topics.

For cited references, we construct a cocitation network in which cited references are set as nodes. Through cocitation network, we reveal the intellectual structure of DC/EP by analyzing clusters and key nodes and learn the evolution of research fronts and knowledge bases and the critical articles in the evolution process.

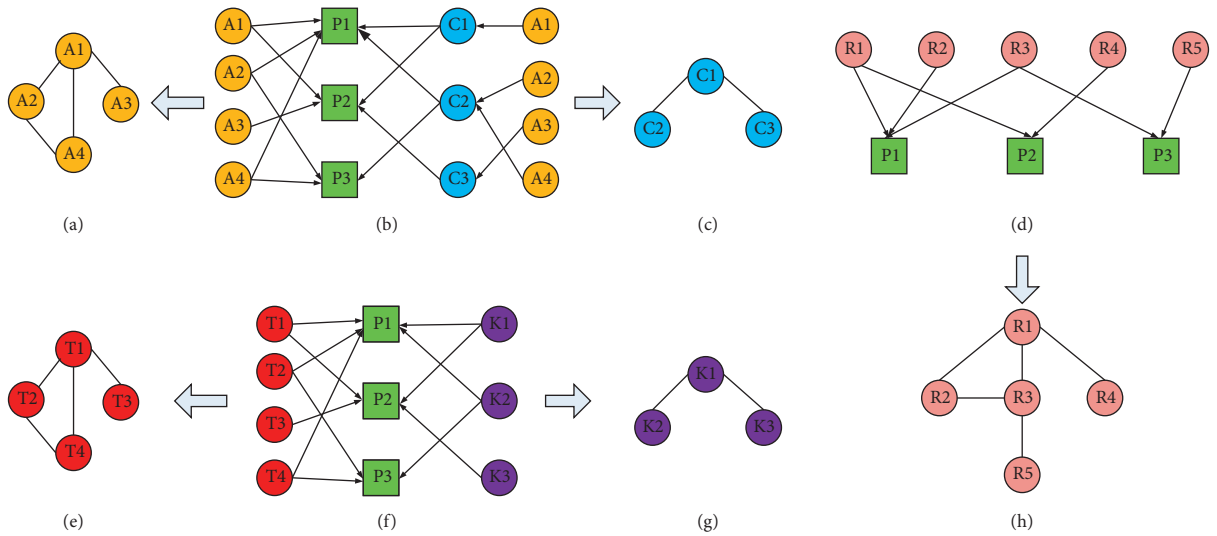

Figure 1: Pictorial view of network construction. Note: A is the abbreviation of author, C is country, P is paper, R is reference, T is term, and K is keyword. The thickness of a line denotes the weight of the edge. The color of a circle represents the node type. (a) Author-collaboration network. (b) Author-article-country relationship. (c) Country-collaboration network. (d) Reference-article relationship. (e) Terms co-occurrence network. (f) Terms-article-keywords relationship. (g) K.eywords cooccurrence network. (h) Cocitation network.

Sliding window analysis identifies the evolution of cocitation network and demonstrates structural changes in the research trend over time. Field knowledge is updated year by year and consequently the associated network evolves over time. To investigate the emerging trends, we divide the article series from 2000 to 2020 into fragments with a length of 5 years (the size of the sliding windows could neither be too small nor too large. If too small, there will be a limited number of references and in turn the chosen nodes, in the constructed network, which makes the clustering meaningless. For example, if the size of sliding windows is 2 (year), there are only 8 nodes in the 2000-2001 network. On the other hand, if the size is too large, the constructed networks become difficult to capture the detailed information of structural changes. After balancing information loss and statistical significance, the size is chosen to be 5 (year) and the starting year is 2000 so that every constructed network consists of at least 30 nodes) through sliding windows with a sliding step of 1 year (see Figure 2), and each fragment is used to construct a network. The reason to adopt the sliding windows approach is to fully use the feature of memory and transitivity contained in fragments [36]. After the sliding window process, we obtain a series of 17 networks from which we can learn the change of modularity and thus analyze the evolution features.

2.2. Network Indicators and Scientometric Metrics. Betweenness centrality, clustering-related indicators, modularity, silhouette, and burst-related indicators are the main metrics for visualizing and analyzing.

The betweenness centrality of node i, $\mathrm{bc}(i)$, is defined as the following equation:

$$\mathrm{bc}(i) = \sum_{s \neq i \neq t} \frac{p_{\mathrm{st}}^{i}}{p_{\mathrm{st}}}, \tag{2}$$

where p_{st} is the number of the shortest paths between nodes s and t and p_{st}^{i} is the number of these shortest paths that pass through node i. High betweenness centrality emphasizes the importance of nodes in connecting different clusters and identifies potentially revolutionary scientific publications.

Clustering: cocitation similarities (σ) between articles i and j are calculated through cosine coefficients. Let A be the set of articles that cites i and B the set of papers that cites j; then the similarity can be defined as the following equation:

$$\sigma_{\mathrm{ij}} = \frac{|A \cap B|}{\sqrt{|A| \cup |B|}}, \tag{3}$$

where $|A \cap B|$ is the cocitation counts, $|A|$ is the citation counts of i, and $|B|$ is the citation counts of j. Define a cluster of a network G as one subgraph G_k such that $G = \cup_{k=1} G_k$ and $G_m \cap G_n = \varnothing$ for all $m \neq n$, and a cut function f as the following equation (see more in Shi and Malik [37]):

$$f(G_m, G_n) = \sum_{i \in G_m, j \in G_n} \sigma_{ij}. \tag{4}$$

The goal of clustering is to maximize $\sum_{k=1} f(G_k, G_k)$ and minimize $\sum_{k=1} f(G_k, G - G_k)$, and spectral clustering is an efficient approach to that end [38]. In CiteSpace, clusters are automatically generated based on the abovementioned ideas.

To better visualize the clusters, CiteSpace labels generated clusters by ranking algorithms such as TF*IDF, log-likelihood ratio (LLR) tests, or mutual information. LLR algorithm is adopted here to select the labels for corresponding clusters. The rationale behind this choice is that the terms selected by LLR highlight the unique aspect of a cluster, and LLR is good at generating high intraclass similarity and low interclass similarity [38]. The other clustering-related visualization tool is timeline mapping, which is a global visualization of the network. Cluster labels are shown vertically at the right-hand side, and the publication years of the articles are shown in an upper horizontal timeline. Timeline mapping is a helpful tool in obtaining the

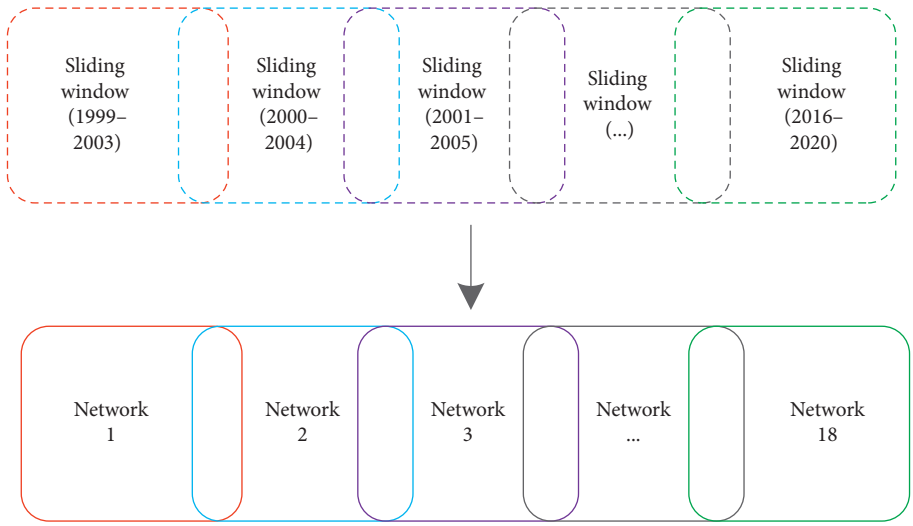

Figure 2: Sliding window process.

timespan, evolution process of one cluster, and the influential articles along the evolution process.

Modularity Q and silhouette are two metrics used for assessing the cluster-related features in a network. Assume a network can be divided into c communities, then Q can be calculated from a symmetric $c \times c$ matrix whose elements, along the main diagonal, q_{mm} denote the fraction of edges connecting nodes in the same community m while the other elements $q_{mn}\,(m \neq n)$ represent the fraction of edges linking nodes in the different communities m and n, according to [39], and Q is defined by the following equation:

$$Q = \sum_{m} \left[q_{mm} - \left(\sum_{n} q_{mn} \right)^2 \right]. \tag{5}$$

The modularity measures the extent to which a network can be divided into independent clusters and is a global measure of the overall structure of the network, and its score ranges from 0 to 1. The larger Q is, the more well-structured a network is. Since modularity is defined for any network, one may use modularity values to compare different networks [38]. $Q > 0.3$, a usual empirical threshold of significance, means that the detected community structure is significant. As argued by Chen et al. [40], the intellectual structure of a scientific field can be analyzed by the modularity of the associated cocitation network, which evolves over time, and newly published articles may introduce a profound structural variation on the network.

Silhouette is proposed by Rousseeuw [41], measuring the quality of a clustering configuration, and suggests the uncertainty that one needs to consider when interpreting the nature of the cluster. Let D be the cluster in which node i is present and C is any cluster which is different from D, $a(i)$ is the average length of all edges within D, and $b(i)$ is the minimum of the average length of all edges going from i to C; then define S as the following equation:

$$S(i) = \frac{b(i) - a(i)}{\max\{a(i), b(i)\}}. \tag{6}$$

The value of S ranges between −1 and 1, with 1 representing a perfect separation from other clusters. Empirically, the result is persuasive if the silhouette value is 0.7–0.9 and it is reasonable if the score is above 0.5.

Citation burstiness analysis detects potential articles that drive emerging research interests. The burstiness of the frequency of an article over time indicates a specific duration in which an abrupt change of the frequency takes place [29] and is developed to find a set of fast-rising terms used by scholars in their latest publications. Kleinberg [42] developed an algorithm to calculate and detect abrupt changes and its idea later was introduced into the software CiteSpace by [43]; see equations (7)–(9). Assume the citation growth model is expressed as the following equation:

$$F(t) = \mathrm{ae}^{\mathrm{bt}}, \tag{7}$$

where a is the initial citation times (i.e., $F(0)$), b is the annual growth rate of citation, and t is time. Therefore, the 2-time citation growth (one parameter setting in CiteSpace) can be expressed as the following equation:

$$\frac{F(t_2)}{F(t_1)} = e^{b(t_2 - t_1)} = 2. \tag{8}$$

Take log transformation on both sides of the right-hand of equation (8); we obtain

$$d = t_2 - t_1 = \frac{\ln 2}{b}. \tag{9}$$

There are two attributes for a citation burstiness, that is, the intensity of burst (b) and burst duration (the number of years that citation grows at b) [40]. Different term/article has different burstiness.

2.3. Data Collection and Parameters Setting in CiteSpace. There are several primary databases that can be adopted in the process of scientometric analysis, like Web of Science

(WoS), Scopus, and Google Scholar. With a comparative assessment of these databases, Olawumi and Chan [44] have pointed out that WoS covers various core journals' publishing houses and most relevant journals in its records. In this sense, we select the core collections of the WoS as the data source to include only high-quality SCI/SSCI publications. 114 records published from 1995 to 2020 are collected initially. However, the 114 records do not include relevant publications if the terms "digital currency," "electronic payment," and "digital money" do not explicitly appear in the titles, abstracts, or index terms. Therefore, in the second step, we expand the dataset with a citation indexing method following Chen et al. [40]. The assumption of the approach is intuitive; that is, citing at least one of the 114 records makes the citing article relevant to the topic. According to Chen et al. [40], the citation index-based expansion has the advantage of obtaining a self-contained dataset. Finally, a total of 454 records were obtained after data merging and deduplication.

In this review, CiteSpace (version 5.6.R5) is used as a knowledge management tool to get an in-depth understanding of the intellectual structure and emerging frontiers of the concerned research area. The software gradually develops along the path of scientometric, citation analysis, cocitation analysis, and cocitation visualization; is outstanding in clustering literature, visualizing the intellectual structure; and is specifically designed to facilitate the detection of emerging trends and abrupt changes in scientific literature [24, 45].

The basic parameters include a time interval from 1995 to 2020, time slice = 1 year, term source = title/abstract/author, key words/key words plus. Time slicing is a dividing strategy, and time slicing by one year means dividing the whole period of 1995–2020 into 26 subperiods, resulting in 26 networks. Setting a small number for time slicing can reveal the evolution trend and its features. Top N per slice is a parameter setting to select nodes to be shown in the corresponding networks. In this study, we set $N = 100$ to choose the most relevant and critical data, which means that only the top-cited 100 records are shown in each network. Besides, we choose the pruning algorithm of "pathfinder within the merged network" to simplify the resulting 26 cocitation networks and emphasize the key structure. Figure 3 illustrates the basic framework of the running CiteSpace.

3. The Intellectual Network of DC/EP

After running CiteSpace, we conduct a cluster analysis of the cocitation network to show the knowledge bases and intellectual structure of DC/EP from a perspective of spatial distribution as well as a chronological evolutionary path.

3.1. Summary Description. CiteSpace divides the cocitation network into several clusters of cocited references such that references are tightly connected within the same clusters, but loosely connected between different clusters. The overview clusters mapping of cited references in our dataset are shown in Figure 4, where cluster labels are in red, and node labels are in black with font size proportional to citation counts. The modularity (Q) of the network is 0.82, which is higher than the threshold level of 0.3, indicating that the clustering is significant.

Table 1 lists the largest eight clusters of cited references, marked out by different colors in Figure 4, which are ranked by their sizes. Cluster #1 is the biggest one with 60 articles. All clusters in Table 1 are highly homogeneous, since their silhouette values are all larger than 0.9, implying that the reference cluster of this study is effective and meaningful. The average year of publication of a cluster indicates its recentness. Cluster #2 is the most recently formed cluster with an average year of 2018.

Figure 5 shows a timeline visualization of the cocitation clusters to illustrate the chronological dynamics of each cluster. For example, the evolutionary path of the largest cluster, Cluster #1, is exhibited in the first line. It could be seen that the forming year of this cluster is 2010, with a rising number of in-cluster references around 2013. The most cited reference in this cluster was published in 2016 by Dyhrberg [46], marked as the biggest yellow node along the timeline, and the article with the high betweenness centrality in this cluster appeared in 2015 [47], surrounded with a thick purple ring in the timeline.

3.2. Knowledge Bases. Knowledge base analysis provides a foundation for future DC/EP research. Two types of key references in the cocitation network can be seen as forming the knowledge bases of the research field: (1) landmark nodes with high citation frequency, suggesting their intracluster importance, and (2) boundary spanner nodes with high betweenness centrality, indicating their intercluster importance.

Table 2 lists the top eleven cited articles. Both Cluster #1 and Cluster #9 have 4 articles in the top landmarks. The remaining three are all from Cluster #5. The most cited article in our dataset is Dyhrberg [46] with 116 citations, followed by Cheah and Fry [48] and Dwyer [49], both with 101 citations. These three top-cited articles are all from Cluster #1, which will be discussed in more detail in the following Subsection 3.3.

Urquhart [50] from Cluster #9, which ranks the fourth, pioneered in studying the market efficiency of Bitcoin. The work is followed by another two highly cited articles from the same cluster, Nadarajah and Chu [51] and Bariviera [52]. All of them concluded that the market of Bitcoin is inefficient or only efficient in specific periods. Besides, Bariviera [52] further showed that price volatility, measured as the logarithmic difference between intraday high and low prices, exhibits long memory during all the period, which reflects a different underlying dynamic process generating the prices and volatility. This is echoed by Katsiampa [53], also with a high citation in Cluster #9, which explored the optimal conditional heteroskedasticity model with regard to goodness-of-fit to Bitcoin price data and found that the AR-CGARCH

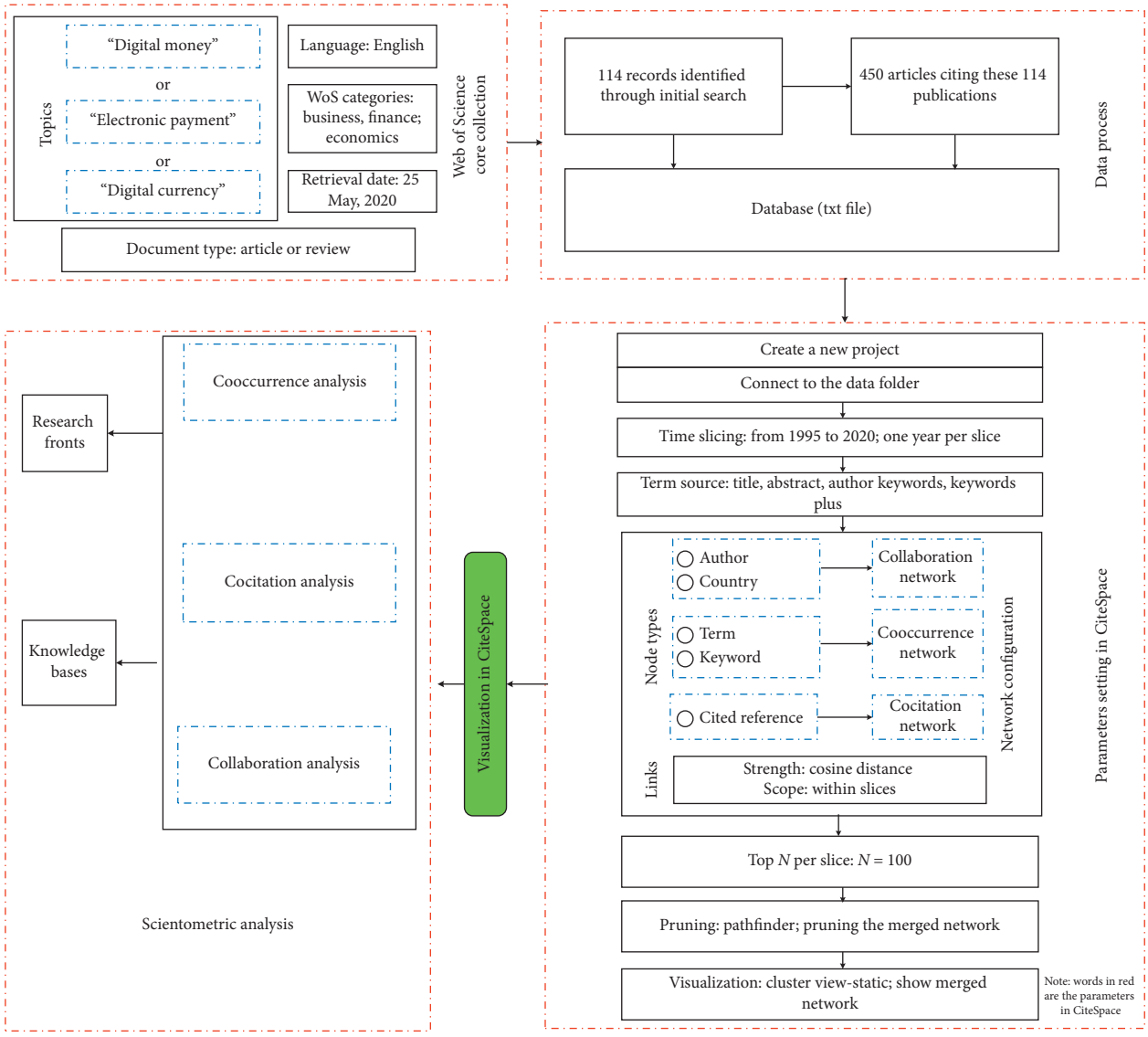

Figure 3: Framework of this study.

model, including both a short-run and a long-run component of the conditional variance, is the best.

The fifth and sixth ranking papers are both from Cluster #5, broadly focusing on the usage of private digital currencies. Specifically, Baur et al. [54] analyzed the statistical properties of Bitcoin to study the prevailing usage of private digital currencies and found that they are mainly used as a speculative investment rather than an alternative currency and medium of exchange, whereas Bouri et al. [11] used a dynamic conditional correlation model to examine whether Bitcoin can act as a hedge and safe haven for major world stock indices, bonds, oil, gold, the general commodity index, and the US dollar index. Interestingly, their work indicates that Bitcoin is a poor hedge and is suitable as a safe haven against weekly extreme down movements in Asian stocks only.

Table 3 shows seven structurally essential references, with the highest betweenness centrality values, in the synthesized network. These references are important in terms of not only how they connect individual nodes in the network but also how they connect aggregated groups of nodes. Two of these nodes are in Cluster #2 and two in Cluster #1. These works can be seen as bridge works in promoting paradigm shift or theme-switching of DC/EP research.

Platanakis and Urquhart [55] from Cluster #2 are with the highest betweenness value and analyze the potential out-of-sample portfolio benefits resulting from including Bitcoin in a stock-bond portfolio for a range of eight popular asset allocation strategies. Selgin [47] from Cluster #1 ranks the second, which casts fundamental insights into the monetary system. It argues that a properly designed synthetic commodity money may supply the foundation for a monetary regime, and this regime does not require oversight by any monetary authority, yet it is able to generate a stable macroeconomy.

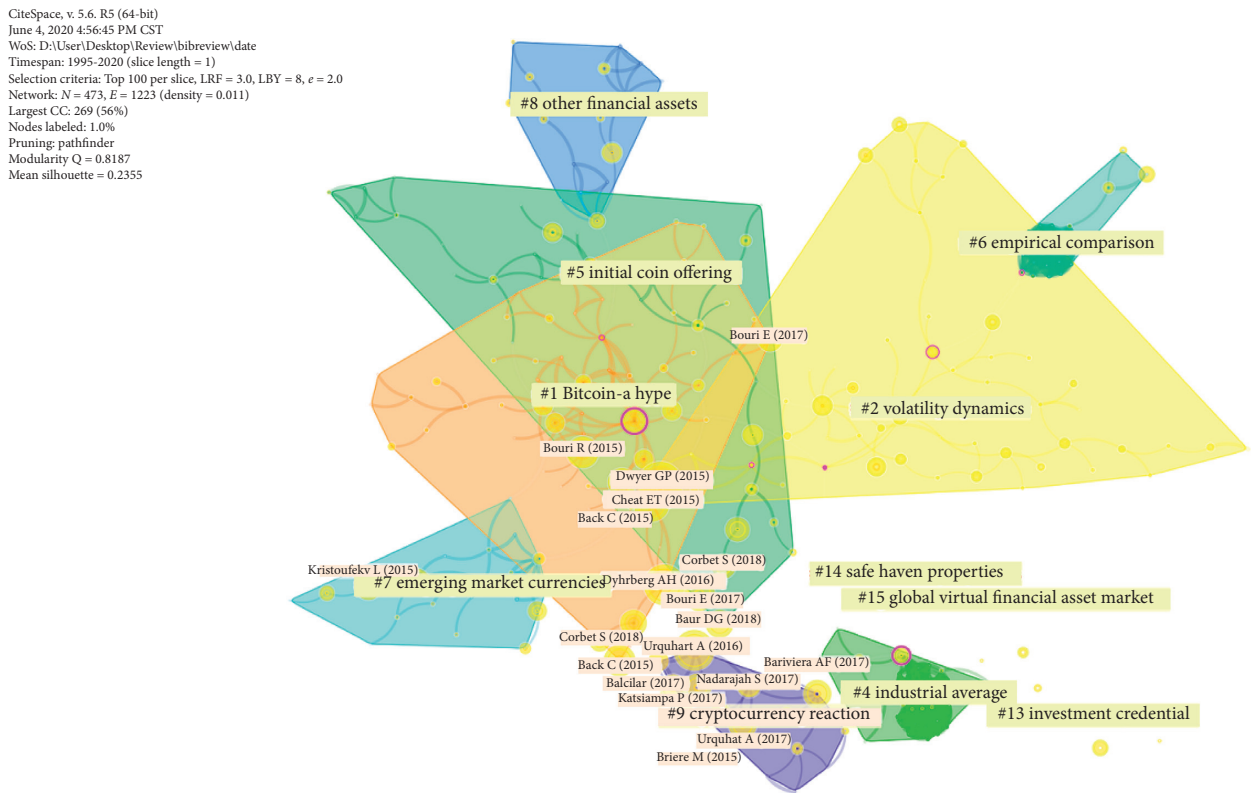

Figure 4: Clusters of cited references on DC/EP (1995–2020). Clusters are in different colors, and their labels are in red text. Landmark articles are labeled in black with font size proportional to citation counts.

Table 1: Major clusters of cited references on DC/EP (1995–2020).

Cluster #	Size	Silhouette	Label (LLR)	Year ave.
1	60	0.945	Bitcoin-a hype	2015
2	54	0.918	Volatility dynamics	2018
4	36	0.971	Industrial average	2014
5	31	0.959	Initial coin offering	2017
6	25	0.998	Empirical comparison	2016
7	20	0.981	Emerging market currencies	2013
8	16	0.997	Other financial assets	2015
9	14	0.964	Cryptocurrency reaction	2017

Alvarez-Ramirez et al. [56] from Cluster #4 rank the third and study long-range correlations and informational efficiency of the Bitcoin market.

3.3. Review of Major Clusters. Tables 4 and 5 list five critical citing papers and five key cited publications in the major Clusters #1 and #2, respectively.

The core members of Cluster #1 represent major milestones in DC/EP, notably Dyhrberg [46] with the highest citations. Using an asymmetric GARCH model, Dyhrberg [46] explored the hedging capability of Bitcoin and found that Bitcoin can be used as a hedge against both stocks in the Financial Times Stock Exchange Index and American dollar in the short term. The second most cited references are Cheah and Fry [48], which discovered speculative bubbles in the Bitcoin market through econometric modeling of Bitcoin prices, and Dwyer [49] theoretically explained how applied financial technologies and limitation of the quantity produced can create an equilibrium in which a digital currency has a positive value. Ciaian et al. [57] incorporated specific factors of digital currencies in studying the price formation process and thus obtained a high citation.

More recent works with significance in DC/EP are contained in Cluster #2. Phillip et al. [58] top the other in citations in Cluster #2. They integrated stylized attributes in a single model to measure the varied nature and price dynamics of 224 different cryptocurrencies and demonstrated that most of them have leverage effects and Student's t error distributions. The other most cited reference is Kim [59], which examined transaction costs of Bitcoin in international transactions using Bitcoin quotes data in 16 different currencies and found that the transaction cost of Bitcoin is lower than that of the retail foreign exchange rate.

Among the five major citing articles related to Clusters #1 and #2, four articles are similar, namely, Bedi and Nashier [60], Ahmed [61], Charfeddine et al. [62], and Klarin [63], which are all published in 2020. Their high coverage of references in both clusters suggests significant relevance to the field of DC/EP. Bedi and Nashier [60] have the highest citation coverage in both Clusters #1 and #2. Adopting a similar method to that of Dyhrberg [46] that used modified conditional VAR as a measurement of risk, Bedi and Nashier [60] examined the diversification capability of Bitcoin. Different from Dyhrberg [46], they only focused on various fiat currency assets and

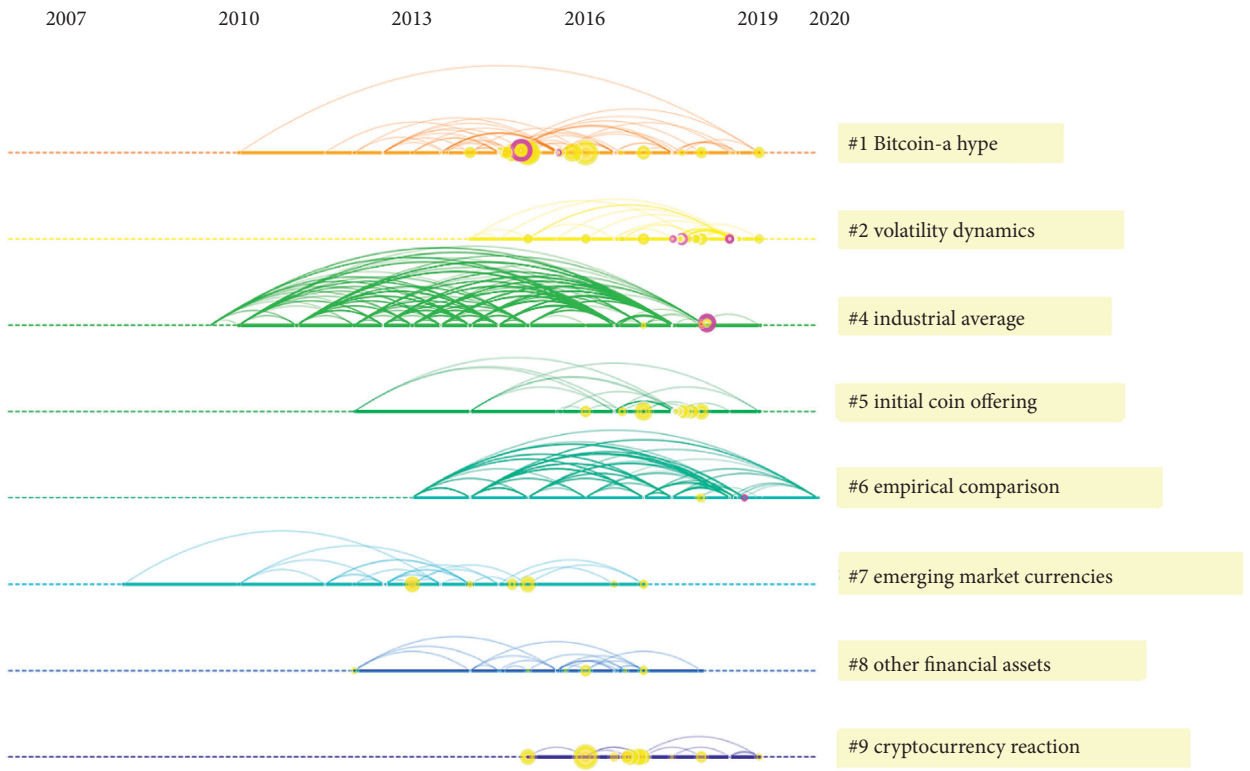

Figure 5: Timelines of cocitation clusters. Major clusters are labeled on the right with different colors. Yellow circles on the horizontal lines represent high citation articles and purple circles denote high betweenness nodes.

performed comprehensive risk-adjusted portfolio evaluations across three asset allocation strategies, providing insights into the sharp disparity in Bitcoin trading volumes across national currencies from a portfolio theory perspective. The other citing articles also focus on the price dynamics and economic role of Bitcoin in asset allocation, with modifications to either asset classes, data frequency, or risk measurement methods.

4. Emerging Trends of DC/EP

In this section, we detect emerging trends of DC/EP research with CiteSpace from two perspectives: (1) cocitation analysis in terms of references and (2) cooccurrence analysis in terms of keywords and terms.

4.1. Detecting Emerging Trends from Cocitation Network. Emerging trends in the DC/EP research from cocitation network are detected by combining sliding window analysis and burst detection. The collective intellectual structure of the cocitation network in a specific area evolves over time. Newly published articles may introduce profound structural variation, which temporally reduce the modularity of the cocitation network [40, 64] and lead to emerging trends in the research field. To detect these emerging trends, the dynamics of modularity is investigated by sliding window analysis. Figure 6 shows the dynamics of the modularity of the 17 constructed cocitation networks. It could be seen that the local minimum of modularity appeared in 2003, 2010, and 2013, which suggests that structural variations occurred, or some new research trends emerged, around these years.

To detect what these trends are and which publications play important roles in forming them, we analyze the citation burst of publications in the whole dataset. If a publication has a citation burst starting from 2003, 2010, or 2013, it is likely to introduce a structural change to the cocitation network and lead to a new research trend. Figure 7 lists the publications whose beginning citation burst years are 2003, 2010, or 2013.

The publications with citation burst year beginning in 2003 mainly studied the factors that affect buyers' trust in sellers and their intention to purchase goods on the electronic markets. For example, Doney and Cannon [65] examined, both theoretically and empirically, the cognitive processes through which buyers develop trust of a seller. Gefen [66] tested the hypothesis that familiarity and trust influence buyers' intention to purchase online goods using survey data from 217 potential e-commerce users and found that people's disposition to trust is the primary factor that affects their trust in the vendor. Based on economic theories and data from online experiments, Ba and Pavlou [67] examined the extent to which trust can be induced by a proper feedback mechanism in the electronic markets and how risk factors affect trust formation. They demonstrated that appropriate feedback mechanisms can induce calculus-based credibility trust without repeated interactions between two transacting parties. Trust can mitigate information asymmetry by reducing transaction-specific risks, thus generating price premiums for reputable sellers. It could be inferred from these cited references that rising interest in buyer's choice behavior of an electronic transaction in the

Table 2: Most cited references.

Citation counts	References	Cluster #
116	Dyhrberg, 2016, FINANC RES LETT, V16, P85	1
101	Cheah and Fry, 2015, ECON LETT, V130, P32	1
101	Dwyer, 2015, J FINANC STABIL, V17, P81	1
94	Urquhart, 2016, ECON LETT, V148, P80	9
86	Baur et al., 2018, FINAN RES LETT, V0, P0	5
79	Bouri et al., 2017, FINANC RES LETT, V20, P192	5
65	Nadarajah and Chu, 2017, ECON LETT, V150, P6	9
62	Katsiampa, 2017, ECON LETT, V158, P3,	9
61	Ciaian et al., 2016, APPL ECON, V48, P1799	1
58	Bariviera, 2017, ECON LETT, V161, P1	9
58	Corbet et al., 2018, ECON LETT, V165, P28	5

Table 3: Cited references with the highest betweenness centrality.

Rank	Centrality	References	Cluster #
1	0.39	Platanakis and Urquhart, 2019, BRIT ACCOUNT REV, V0, P0	2
2	0.33	Selgin, 2015, J FINANC STABIL, V17, P92	1
3	0.23	Alvarez-Ramirez et al., 2018, PHYSICA A, V492, P948	4
4	0.17	Dyhrberg, 2018, ECON LETT, V171, P140	2
5	0.10	Hendrickson, 2016, ECON INQ, V54, P925	1
6	0.10	Urquhart, 2019, INT REV FINANC ANAL, V63, P49	6
7	0.10	Feng, 2018, FINANC RES LETT, V26, P63	5

Table 4: Citing articles and cited references of Cluster #1.

Cluster #1 Bitcoin-a hype			
Citing articles		Cited references	
Coverage %	Author (year): title	Cites	Author (year), journal, volume, page
49	Bedi and Nashier (2020): On the Investment Credentials of Bitcoin: A Cross-Currency Perspective	116	Dyhrberg (2016), FINANC RES LETT, V16, P139
32	Ahmed (2020): Is There a Risk-Return Trade-Off in Cryptocurrency Markets? The Case of Bitcoin	101	Cheah and Fry (2015), ECON LETT, V130, P32
25	Charfeddine et al. (2020): Investigating the Dynamic Relationship between Cryptocurrencies and Conventional Assets: Implications for Financial Investors	101	Dwyer (2015), J FINANC STABIL, V17, P81
24	Saiedi (2020): Global Drivers of Cryptocurrency Infrastructure Adoption	61	Ciaian et al. (2016), APPL ECON, V48, P1799
22	Klarin (2020): The Decade-Long Cryptocurrencies and the Blockchain Rollercoaster: Mapping the Intellectual Structure and Charting Future Directions	53	Bohme et al. (2015), J ECON PERSPECT, V29, P213

research of DC/EP might start from 2003. This trend may be related to the gradual development of e-commerce after the Internet technology booming.

As to the publications with citation burst year beginning in 2010, Schuh and Stavins [68] studied the determinants of the use of different payment instruments. They demonstrated that the changes in relative convenience and cost as well as the changes in relative characteristics of substitute payment instruments contribute to the corresponding choice. Bolt et al. [12] empirically analyzed the impact of surcharging on the demand for debit card based on consumer and retailer survey data in the Netherlands and found that surcharging steers consumers away from using debit cards towards cash services. Zinman [69] tested the neoclassical consumer choice model, concerning debit card use versus credit card use, in the presence of behavioral considerations, such as self-control issues, complex intertemporal trade-offs, and low pecuniary stakes, and concluded that the neoclassical model adequately explains consumer choice even on a margin where behavioral alternatives have strong intuitive appeal. In summary, these references suggest a rising trend in DC/EP research that focuses on the determinants of consumer's choice of different payment instruments.

Further, for the publications with citation burst year beginning in 2013, Ching and Hayashi [70] and Carbo-Valverde and Linares-Zegarra [71] studied the effectiveness of rewards card programs on consumer payment choice with respect to debit/credit cards and cash and suggested that rewards may significantly modify preferences for payment

Table 5: Citing articles and cited references of Cluster #2.

Cluster #2 volatility dynamics			
Citing articles		Cited references	
Coverage %	Author (year): title	Cites	Author (year), journal, volume, page
36	Bedi and Nashier (2020): On the Investment Credentials of Bitcoin: A Cross-Currency Perspective	31	Phillip et al. (2018), ECON LETT, V163, P6
25	Ahmed (2020): Is There a Risk-Return Trade-Off in Cryptocurrency Markets? The Case of Bitcoin	31	Kim (2017), FINANC RES LETT, V23, P300
20	Dong and Hao (2020): The Asymmetric Effect of Volatility Spillover in Global Virtual Financial Asset Markets: The Case of Bitcoin	27	Raskin and Yermack (2015), HDB DIGITAL CURRENCY, V0, P31
20	Charfeddine et al. (2020): Investigating the Dynamic Relationship between Cryptocurrencies and Conventional Assets: Implications for Financial Investors	26	Gandal (2018), J MONETARY ECON, V95, P86
17	Klarin (2020): The Decade-Long Cryptocurrencies and the Blockchain Rollercoaster: Mapping the Intellectual Structure and Charting Future Directions	25	Vidal-Tomas (2018), FINANC RES LETT, V27, P259

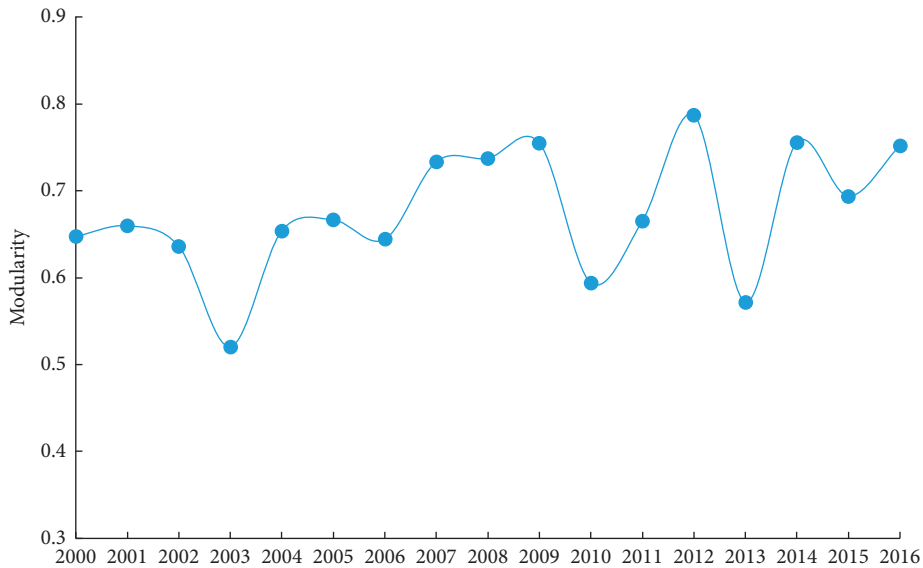

Figure 6: The dynamics of modularity from 2000 to 2020, that is, 17 cocitation networks constructed from sliding windows with a size of 5 (year) and step length of 1 (year).

instruments and their economic impacts vary significantly across types of rewards and merchant activities. Klee [72] studied the relationship between money demand and consumer payment behavior based on empirical evidence from grocery store transaction data and showed that there are statistically significant effects of transaction costs, opportunity costs, and product characteristics on the choice of payment instrument, which, in turn, affect money demand. He et al. [73] emphasized the ignorance of the payment system and bank's role in the provision of convenient, efficient, and safe instruments by mainstream banking theory and introduced a risk of theft, including fraud, embezzlement, counterfeiting, and many other kinds of opportunistic behavior, and a safe-keeping role for banks into modern monetary theory. The general equilibrium model can generate the concurrent circulation of cash and bank liabilities as media of exchange, or inside and outside money, as well as yield novel policy implications, such that negative nominal interest rates are feasible and for some parameters optimal. These articles probably indicate an emerging trend that reflects on how consumer's choice of payment instruments affects money demand and in turn influences the bank's role and their policy implications.

4.2. Detecting Emerging Trends from Keywords Network. The above subsection analyzes the emerging trends of research in DC/EP from the perspective of cocitation network. In this subsection, we use CiteSpace to conduct a network analysis concerning the terms and keywords occurring in the dataset. Twelve clusters are formed with modularity of 0.77. Table 6 lists the top four clusters in terms of their recentness, whereas Table 7 shows five keywords in each of these clusters with the highest frequency. The keywords followed by "*" are with citation bursts, notably "digital currency" and "money" (see Figure 8).

References	Strength	Begin	End	1995–2020
Lee MKO., 2001, INT J ELECTRON COMM, V6, P75	5.6219	2003	2008	
Hoffman DL., 1999, COMMUN ACM, V42, P80	8.3864	2003	2007	
Jarvenpaa S L., 2000, ITM, V1, P45	7.7384	2003	2007	
Ba SL., 2002, MIS QUART, V26, P243	4.9954	2003	2008	
Doney PM., 1997, J MARKETING, V61, P35	3.9959	2003	2005	
Gefen D., 2000, OMEGA–INT J MANAGE S, V28, P725	4.5058	2003	2007	
McKnight DH., 2001, INT J ELECTRON COMM, V6, P35	10.6506	2003	2008	
Borzekowski R., 2008, J MONEY CREDIT BANK, V40, P149	11.7265	2010	2016	
Jonker N., 2007, ECONOMIST–NETHERLAND, V155, P271	9.2111	2010	2015	
Schuh S., 2010, J BANK FINANC, V34, P1745	9.6846	2010	2017	
Zinman J., 2009, J BANK FINANC, V33, P358	5.2929	2010	2013	
Bolt W., 2010, J BANK FINANC, V34, P1738	6.1718	2010	2017	
Ching AT., 2010, J BANK FINANC, V34, P1773	7.6843	2013	2017	
Klee E., 2008, J MONETARY ECON, V55, P526	5.7397	2013	2016	
Carbo-Valverde S., 2011, J BANK FINANC, V35, P3275	4.8293	2013	2017	
He P., 2008, J MONETARY ECON, V55, P1013	3.8222	2013	2016	
Borzekowski R., 2008, INT J IND ORGAN, V26, P889	3.8222	2013	2016	

Figure 7: The publications with citation burst year beginning in 2003, 2010, or 2013.

Table 6: Most recently formed clusters of keywords.

Cluster #	Size	Silhouette	Ave. year	Label (LLR)
10	13	0.913	2019	Confirmatory bias
11	12	0.958	2019	Price discovery
1	23	0.902	2018	Yellow metal
5	16	0.947	2018	Central bank

Cluster #10 is mainly related to behavioral finance and focuses on how social media and investor sentiment affects cryptocurrency markets [74, 75]. Cluster #11 focuses on the price discovery determinants and volatility dynamics of digital currencies [76, 77]. Cluster #1 is a larger one on the topic of hedge, diversification effect of digital currencies, and their comparison with gold [78, 79].

The topic of Cluster #5 is the most distinct one that concentrates on the impact of digital currency on the central bank, monetary policy, and central bank digital currency (CBDC). For example, following an analysis of private digital currencies, Dow [80] considered proposals for the state issue of digital currency and concluded that regulation updating should be a main focus. Bindseil [81] made a further discussion on the pros and cons of CBDC. To cope with the potential drawbacks, they proposed a two-tier remuneration of CBDC as a solution and a tested and simple tool to control the quantity of CBDC in both normal and crisis times. Also, Hampl and Havranek [82] examined the use of central bank equity as an unconventional monetary policy tool and argued that it may weaken the financial strength of the central bank and endangers long-term price stability.

Table 7: Top five keywords in each recent cluster.

	Freq.	Keyword
Cluster #10	29	Price
	18	Portfolio diversification
	9	Sentiment
	5	Social media
	5	Performance
Cluster #11	27	Digital currency*
	23	Exchange
	18	Stock
	10	Price discovery
	9	Bubble
Cluster #1	51	Gold
	23	Dollar
	18	Currency
	10	Time series
	9	Long memory
Cluster #5	18	Money*
	10	Garch
	7	Monetary policy
	5	Volatilityspillover
	4	Connectedness

Note: the keywords followed by "*" are with citation bursts.

5. Collaboration Network of DC/EP

In this section, we analyze the international academic collaboration network and demonstrate the main distribution of DC/EP research in the networks of authors and countries.

5.1. Core Scholars and Collaboration Network. The authors with high citations can be viewed as core scholars. Table 8 summarizes the top ten cited authors and reflects their

Table 8: Most cited authors.

Author	Citing counts	Cluster #	Label (LLR)
Dyhrberg	120	3	Hedging effectiveness
Baur et al.	118	7	Energy commodities
Bouri et al.	117	10	Investor reaction
Urquhart	115	3	Hedging effectiveness
Cheah and Fry	108	9	Global driver
Corbet et al.	105	3	Hedging effectiveness
Nakamoto	101	5	Price fluctuation
Dwyer	101	9	Global driver
Kristoufek et al.	88	10	Investor reaction
Ciaian et al.	85	3	Hedging effectiveness

relative influences in the field of DC/EP. Dyhrberg ranks the first with 120 papers citing his work, followed by Baur et al. and Bouri et al. Four of them are from Cluster #3. Both Cluster #9 and Cluster #10 have the two top-cited authors. The analysis indicates that the topic of "hedging effectiveness," "global driver," and "investor reaction" have drawn more research interest than others.

Further knowledge of the existing collaboration among authors can enhance productivity in DC/EP; therefore, we conduct a network analysis regarding authors and the resulted clusters are shown in Figure 9. Links show the existing collaboration among authors, and productive authors in the collaboration network are labeled. Our network of authors indicates that although the research in this emerging field by international scholars has not been highly collaborative, several partnership networks have been rising. For example, a four-node collaboration network exists among Zhang, Li, Shen, and Wang. Besides, Roubaud, Bouri, and Urquhart are also located in a highly collaborative network.

5.2. Core Countries and Collaboration Network. Papers published in the field of DC/EP can be clustered by country (region). Figure 10 shows the collaboration network of countries. It is clearly shown that the USA; several European countries such as France, England, and Germany; and Asian countries like China and South Korea have important positions in the network. Collaboration especially among the European countries is intense. Many nodes are surrounded by a purple ring, indicating a high betweenness centrality.

Table 9 summarizes the top ten countries in terms of the number of publications in the dataset. Among all the countries, the USA conducts the highest contribution in terms of the number of both published articles (88) and average citations (78). England ranks the second by the count of publications (49), while it is replaced by Canada regarding the average citations (34). China is also a productive country in DC/EP with a total publication of 41. However, as to the average citations, it is the lowest of the ten countries at a level of 8, which demonstrates that the studies from Chinese scholars have not attracted comparative attention. Nonetheless, some Chinese scholars only publish their papers in Chinese, which are omitted in the English database. Thus, interpretations based on English publications about China's role in global DC/EP research should be cautious. As to the centrality of these countries, France, Germany, and Canada rank the top three, while China and India are the lowest with a score of zero, indicating that the collaboration among the European countries is comparatively high, while China and India do DC/EP research independently and are not so involved into a global research network of DC/EP.

6. Discussion on Limitations of This Study

While this study summarizes and extends the knowledge bases on DC/EP, there are some limitations. First, selection bias is a common problem facing scientometric analysis [83]. For example, the references for this research were collected only from WoS, which limits the coverage of some recent relevant articles as well as working papers. Future research should use a wider range of databases to provide additional information on the trend analysis in recent years. To limit the scope of search among working papers, especially to identify those with relatively good quality, future scholars may consider focusing on the top economics and finance conferences as well as working papers of top financial research institutions.

Designing a good searching is indeed a big challenge for scientometric studies. Which terms or phrases should be used? How many terms should be searched? Using too many terms may cause a lot of irrelevant papers to be included and thus increase the computing burden for CiteSpace, while too little terms are likely to decrease the representativeness of scientometric studies. Keeping the balance between efficiency and representativeness is a trade-off for scientometric studies using CiteSpace at the current stage. Therefore, designing a robust metric or developing an approach for a good balance could be meaningful research in the future. Currently, we heavily rely on multiple rounds of experiments to find a good database for this study. In this study, we use topic searching that contains the information of title, abstract, keywords, and keywords plus and index-expansion strategy, which can retrieve the relevant articles as possible

No.	Keywords	Strength	Begin	End	1995–2020
1	Electronic payment	9.1486	2000	2017	
2	Information technology	6.0394	2001	2017	
3	Model	10.3311	2002	2013	
4	Trust	15.0737	2003	2013	
5	Internet	3.8902	2003	2017	
6	Behavior	3.3634	2003	2018	
7	Determinant	3.3548	2003	2016	
8	E commerce	7.4437	2004	2011	
9	E-commerce	4.7484	2004	2017	
10	Electronic commerce	7.7192	2005	2008	
11	Consumer	5.514	2006	2017	
12	Impact	4.691	2006	2015	
13	Adoption	5.9756	2008	2017	
14	Retail payment	3.5035	2010	2016	
15	Cash	6.1457	2013	2017	
16	Money	4.1666	2015	2017	
17	Pay	3.5385	2016	2017	
18	Digital currency	5.5286	2017	2018	

Figure 8: Keywords with the strongest citation bursts, ranked by the beginning year of burst.

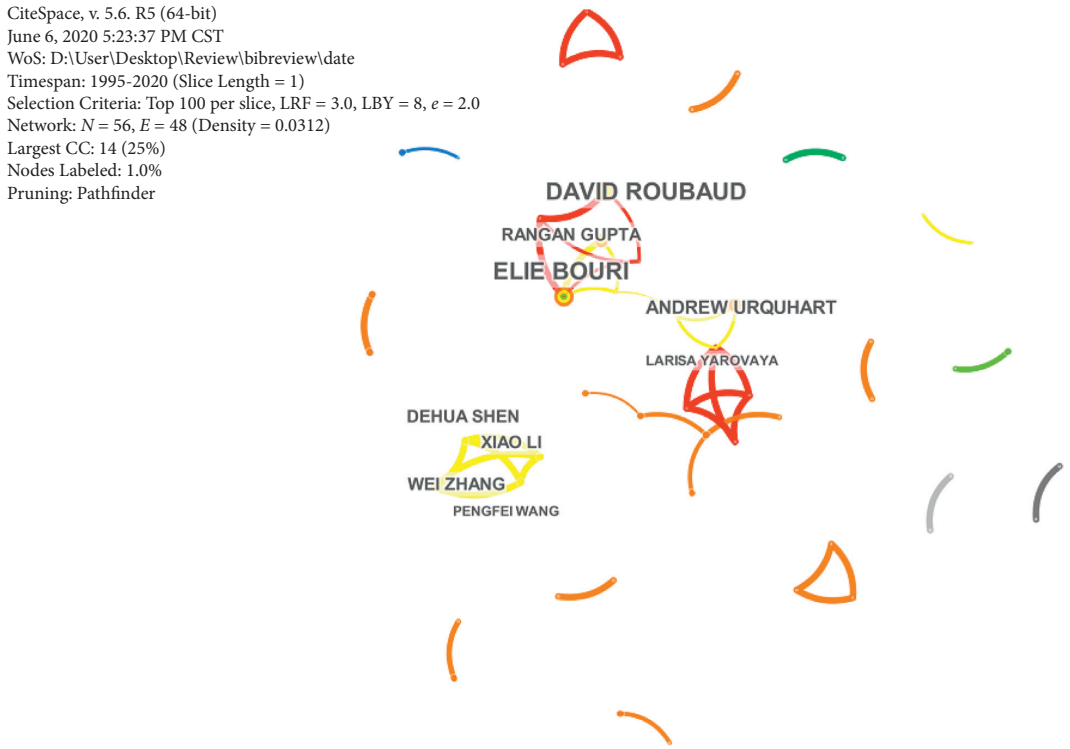

Figure 9: Collaboration of the authors in the field of DC/EP.

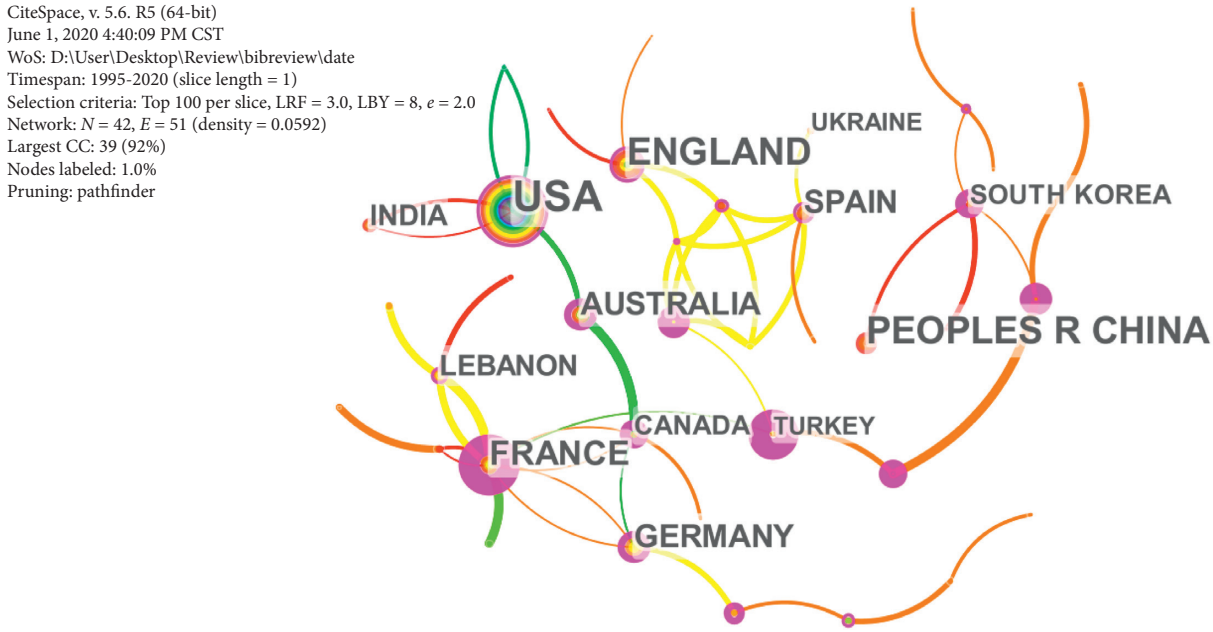

Figure 10: Network of countries in the field of DC/EP.

Table 9: Contributions of countries on DC/EP.

Country	Centrality	Counts	Total citations	Ave. citations
USA	0.18	88	6843	78
England	0.18	49	989	20
PRC	0.00	41	325	8
France	1.06	30	620	21
Australia	0.26	25	228	9
Spain	0.18	24	334	14
Germany	0.33	23	222	10
India	0.00	17	109	6
Lebanon	0.18	17	506	30
Canada	0.41	16	472	34

as it could. Nonetheless, it is still impossible to collect all related papers. This kind of information loss is the necessary cost to bear for searching in scientometric studies.

Second, the algorithm used to perform the network analysis is predefined by the software according to the default rules of cocitation analysis, therefore less tailored discretion. Besides, CiteSpace requires the same ratio for the articles published at different time points. Thus, the most recent papers will not be included in the study sample, resulting in calculation inaccuracy, whose drawback is partly reduced in this study by analyzing the high coverage rate papers in major clusters.

7. Conclusion and Future Research Remarks

This study performs a scientometric study with the utilization of CiteSpace to obtain the knowledge bases and research frontiers in the field of DC/EP from the perspective of network analysis. Our main conclusions are as follows.

First, through network analysis of cited references, we construct a knowledge map of DC/EP including mainly eight clusters and visualize the development path. From the knowledge map and timeline visualization, two major clusters are selected, labeled as "Bitcoin-a hype" and "Volatility dynamics," respectively, with the log-likelihood algorithm. In terms of citation frequency and betweenness centrality, knowledge bases in this field are recognized, which could be classified into three main topics: (1) the usage and diversification effect of private digital currencies from the point of investment and asset allocation [11, 46, 54, 55]; (2) the price dynamics and market efficiency of private digital currencies [48, 51–53, 56–58]; (3) other economic roles of digital currencies and corresponding change brought into the monetary system [47, 59].

Second, we study the evolution of the cocitation network based on a 5-year sliding window analysis. The modularity of these constructed networks exhibits sharp drops in the years 2003, 2010, and 2013, indicating structural changes may appear in the research trend. Combining with citation burst detection, we infer several research trends: (1) buyer's choice behavior of electronic transaction [65–67]; (2) the determinants of consumer's choice of different payment instruments [12, 68, 69]; and (3) how consumer's choice of payment instruments affects money demand and in turn affects bank's role [14, 70–72].

Third, the network of terms and keywords is analyzed. Ranked by recentness, four major clusters are derived. Combining with burst detection, we demonstrate two probable research fronts: (1) how social media and investor sentiment affect the market of digital currencies [74, 75]; (2) the impact of digital currencies on central bank, monetary policy, and central bank digital currency [80–82].

Finally, we identify core scholars and countries involved in the research of DC/EP and their collaboration networks. Dyhrberg ranks the first in terms of citing counts. At the

country's level, the USA and France achieve the highest total local citation score and centrality, respectively. Academic collaboration in DC/EP has been rising, especially among the European scholars and countries.

With the results of our study, future research on DC/EP could make progress from several perspectives. First, while the roles of digital currencies in financial markets have been empirically studied, theoretical analysis of the underlying economic model is comparatively rare. More efforts should be devoted to expanding the scope of digital economic theory. Second, compared to digital currencies issued by private entities, central bank digital currency deserves further attention, especially the impact on modern monetary theory, international trade and payment, and cross-border collaboration.

Data Availability

The bibliographic records are retrieved from the Web of Science, and the processed data used to support the findings of this study are available at supplementary materials.

Conflicts of Interest

The authors declare that they have no conflicts of interest regarding this paper.

Acknowledgments

The authors appreciate the financial support from the Humanities and Social Sciences Foundation of the Ministry of Education of China (Grant no. 20YJC790110), the Basic and Applied Research Co-Foundation of Guangdong (Grant no. 2019A1515110693), and the National Natural Science Foundation of China (Grant no. 41901246).

Supplementary Materials

Data used for this study. (*Supplementary Materials*)

References

[1] C. Lagarde, *Winds of Change: The Case for New Digital Currency*, C. Department, Ed., p. 12, International Monetary Fund, Washington, DC, USA, 2019.

[2] L.-Y. Leong, T.-S. Hew, K.-B. Ooi, and A. Y.-L. Chong, "Predicting the antecedents of trust in social commerce—A hybrid structural equation modeling with neural network approach," *Journal of Business Research*, vol. 110, pp. 24–40, 2020.

[3] D. He, R. B. Leckow, V. Haksar et al., "Fintech and financial services: initial considerations," in *Staff Discussion Notes,* p. 49, International Monetary Fund, Washington, DC, USA, 2017.

[4] M. Raskin and D. Yermack, "Digital currencies, decentralized ledgers and the future of central banking," in *Research Handbook on Central Banking*, P. Conti-Brown, Ed., Edward Elgar Publishing, Cheltenham, UK, 2018.

[5] M. Swan, *Blockchain: Blueprint for a New Economy*, O'Reilly Media, Inc, Sebastopol, CA, USA, 2015.

[6] T. Mancini-Griffoli, M. M. Peria, I. Agur et al., "Casting light on central bank digital currencies," in *Staff Discussion Notes*p. 39, International Monetary Fund, Washington, DC, USA, 2018.

[7] J. Chapman, R. Garratt, S. Hendry, A. McCormack, and W. McMahon, *Project Jasper: Are Distributed Wholesale Payment Systems Feasible Yet?*, Bank of Canada, Ottawa, Canada, 2017.

[8] S. Morris and H. S. Shin, *Distributed Ledger Technology and Large Value Payments: A Global Game Approach*, Princeton University, Princeton, NJ, USA, 2018.

[9] D. Duffie, "Digital currencies and fast payment systems," in *Mimeo,* Stanford University, Stanford, CA, USA, 2019.

[10] J. Carrick, "Bitcoin as a complement to emerging market currencies," *Emerging Markets Finance and Trade*, vol. 52, no. 10, pp. 2321–2334, 2016.

[11] E. Bouri, P. Molnár, G. Azzi, D. Roubaud, and L. I. Hagfors, "On the hedge and safe haven properties of bitcoin: is it really more than a diversifier?" *Finance Research Letters*, vol. 20, pp. 192–198, 2017.

[12] W. Bolt, N. Jonker, and C. van Renselaar, "Incentives at the counter: an empirical analysis of surcharging card payments and payment behaviour in the Netherlands," *Journal of Banking & Finance*, vol. 34, no. 8, pp. 1738–1744, 2010.

[13] K. S. Rogoff, *The Curse of Cash: How Large-Denomination Bills Aid Crime and Tax Evasion and Constrain Monetary Policy*, Princeton University Press, Princeton, NJ, USA, 2017.

[14] D. He, "Monetary policy in the digital age," *Finance and Development*, vol. 55, no. 2, 2018.

[15] H. Hassani, X. Huang, and E. Silva, "Banking with blockchain-ed big data," *Journal of Management Analytics*, vol. 5, no. 4, pp. 256–275, 2018.

[16] N. A. Plassaras, "Regulating digital currencies: bringing bitcoin within the reach of the IMF," *Chicago Journal of International Law*, vol. 14, no. 1, p. 26, 2013.

[17] B. Nelson, "Financial stability and monetary policy issues associated with digital currencies," *Journal of Economics and Business*, vol. 100, pp. 76–78, 2018.

[18] K. Hong, K. Park, and J. Yu, "Crowding out in a dual currency regime? Digital versus fiat currency," *Emerging Markets Finance and Trade*, vol. 54, no. 11, pp. 2495–2515, 2018.

[19] R. Böhme, N. Christin, B. Edelman, and T. Moore, "Bitcoin: economics, technology, and governance," *Journal of Economic Perspectives*, vol. 29, no. 2, pp. 213–238, 2015.

[20] F. Tschorsch and B. Scheuermann, "Bitcoin and beyond: a technical survey on decentralized digital currencies," *IEEE Communications Surveys & Tutorials*, vol. 18, no. 3, pp. 2084–2123, 2016.

[21] M. Holub and J. Johnson, "Bitcoin research across disciplines," *The Information Society*, vol. 34, no. 2, pp. 114–126, 2018.

[22] S. Corbet, B. Lucey, A. Urquhart, and L. Yarovaya, "Cryptocurrencies as a financial asset: a systematic analysis," *International Review of Financial Analysis*, vol. 62, pp. 182–199, 2019.

[23] N. Dashkevich, S. Counsell, and G. Destefanis, "Blockchain application for central banks: a systematic mapping study," *IEEE Access*, vol. 8, pp. 139918–139952, 2020.

[24] C. Chen, "Science mapping: a systematic review of the literature," *Journal of Data and Information Science*, vol. 2, no. 2, pp. 1–40, 2017.

[25] H. D. White and K. W. McCain, "Visualizing a discipline: an author co-citation analysis of information science, 1972-1995," *Journal of the American Society for Information Science*, vol. 49, no. 4, pp. 327–355, 1998.

[26] H. Small, "Co-citation in the scientific literature: a new measure of the relationship between two documents," *Journal of the American Society for Information Science*, vol. 24, no. 4, pp. 265–269, 1973.

[27] M. Callon, J.-P. Courtial, W. A. Turner, and S. Bauin, "From translations to problematic networks: an introduction to co-word analysis," *Social Science Information*, vol. 22, no. 2, pp. 191–235, 1983.

[28] M. J. Grant and A. Booth, "A typology of reviews: an analysis of 14 review types and associated methodologies," *Health Information & Libraries Journal*, vol. 26, no. 2, pp. 91–108, 2009.

[29] C. M. Chen, *CiteSpace: A Practical Guide for Mapping Scientific Literature*, Nova Science Publishers, Hauppauge, NY, USA, 2016.

[30] I. Y. Wuni, G. Q. P. Shen, and R. Osei-Kyei, "Scientometric review of global research trends on green buildings in construction journals from 1992 to 2018," *Energy and Buildings*, vol. 190, pp. 69–85, 2019.

[31] L. Yu, G. Wang, and D. W. Marcouiller, "A scientometric review of pro-poor tourism research: visualization and analysis," *Tourism Management Perspectives*, vol. 30, pp. 75–88, 2019.

[32] J. L. Ruiz-Real, J. Uribe-Toril, and J. C. Gazquez-Abad, "Destination branding: opportunities and new challenges," *Journal of Destination Marketing & Management*, vol. 17, p. 13, 2020.

[33] Y. Yang and G. F. Meng, "The evolution and research framework of carbon footprint: based on the perspective of knowledge mapping," *Ecological Indicators*, vol. 112, p. 16, 2020.

[34] A. Andrikopoulos and G. Trichas, "Publication patterns and coauthorship in the journal of corporate finance," *Journal of Corporate Finance*, vol. 51, pp. 98–108, 2018.

[35] B. Burton, S. Kumar, and N. Pandey, "Twenty-five years of the European Journal of Finance (EJF): a retrospective analysis," *The European Journal of Finance*, p. 25, 2020.

[36] X. Gao, H. An, W. Fang, H. Li, and X. Sun, "The transmission of fluctuant patterns of the forex burden based on international crude oil prices," *Energy*, vol. 73, pp. 380–386, 2014.

[37] J. Shi and J. Malik, "Normalized cuts and image segmentation," *IEEE Transactions on Pattern Analysis and Machine Intelligence*, vol. 22, no. 8, pp. 888–905, 2000.

[38] C. Chen, F. Ibekwe-SanJuan, and J. Hou, "The structure and dynamics of cocitation clusters: a multiple-perspective cocitation analysis," *Journal of the American Society for Information Science and Technology*, vol. 61, no. 7, pp. 1386–1409, 2010.

[39] M. E. J. Newman and M. Girvan, "Finding and evaluating community structure in networks," *Physical Review E*, vol. 69, no. 2, p. 15, 2004.

[40] C. Chen, Z. Hu, S. Liu, and H. Tseng, "Emerging trends in regenerative medicine: a scientometric analysis in CiteSpace," *Expert Opinion on Biological Therapy*, vol. 12, no. 5, pp. 593–608, 2012.

[41] P. J. Rousseeuw, "Silhouettes: a graphical aid to the interpretation and validation of cluster analysis," *Journal of Computational and Applied Mathematics*, vol. 20, pp. 53–65, 1987.

[42] J. Kleinberg, "Bursty and hierarchical structure in streams," *Data Mining and Knowledge Discovery*, vol. 7, no. 4, pp. 373–397, 2003.

[43] C. M. Chen, "Detecting and mapping thematic changes in transient networks," in *Proceedings of the Eighth International Conference on Information Visualisation, 2004. IV 2004*, E. Banissi, Ed., IEEE Computer Society, London, UK, pp. 1023–1032, July 2004.

[44] T. O. Olawumi and D. W. M. Chan, "A scientometric review of global research on sustainability and sustainable development," *Journal of Cleaner Production*, vol. 183, pp. 231–250, 2018.

[45] B. Lin and T. Su, "Mapping the oil price-stock market nexus researches: a scientometric review," *International Review of Economics & Finance*, vol. 67, pp. 133–147, 2020.

[46] A. H. Dyhrberg, "Hedging capabilities of bitcoin. is it the virtual gold?" *Finance Research Letters*, vol. 16, pp. 139–144, 2016.

[47] G. Selgin, "Synthetic commodity money," *Journal of Financial Stability*, vol. 17, pp. 92–99, 2015.

[48] E.-T. Cheah and J. Fry, "Speculative bubbles in bitcoin markets? an empirical investigation into the fundamental value of Bitcoin," *Economics Letters*, vol. 130, pp. 32–36, 2015.

[49] G. P. Dwyer, "The economics of bitcoin and similar private digital currencies," *Journal of Financial Stability*, vol. 17, pp. 81–91, 2015.

[50] A. Urquhart, "The inefficiency of bitcoin," *Economics Letters*, vol. 148, pp. 80–82, 2016.

[51] S. Nadarajah and J. Chu, "On the inefficiency of bitcoin," *Economics Letters*, vol. 150, pp. 6–9, 2017.

[52] A. F. Bariviera, "The inefficiency of Bitcoin revisited: a dynamic approach," *Economics Letters*, vol. 161, pp. 1–4, 2017.

[53] P. Katsiampa, "Volatility estimation for Bitcoin: a comparison of GARCH models," *Economics Letters*, vol. 158, pp. 3–6, 2017.

[54] D. G. Baur, K. Hong, and A. D. Lee, "Bitcoin: medium of exchange or speculative assets?" *Journal of International Financial Markets, Institutions and Money*, vol. 54, pp. 177–189, 2018.

[55] E. Platanakis and A. Urquhart, "Should investors include bitcoin in their portfolios? a portfolio theory approach," *The British Accounting Review*, vol. 52, no. 4, p. 19, 2019.

[56] J. Alvarez-Ramirez, E. Rodriguez, and C. Ibarra-Valdez, "Long-range correlations and asymmetry in the bitcoin market," *Physica A: Statistical Mechanics and Its Applications*, vol. 492, pp. 948–955, 2018.

[57] P. Ciaian, M. Rajcaniova, and D. A. Kancs, "The economics of bitcoin price formation," *Applied Economics*, vol. 48, no. 19, pp. 1799–1815, 2016.

[58] A. Phillip, J. S. K. Chan, and S. Peiris, "A new look at cryptocurrencies," *Economics Letters*, vol. 163, pp. 6–9, 2018.

[59] T. Kim, "On the transaction cost of bitcoin," *Finance Research Letters*, vol. 23, pp. 300–305, 2017.

[60] P. Bedi and T. Nashier, "On the investment credentials of bitcoin: a cross-currency perspective," *Research in International Business and Finance*, vol. 51, p. 21, 2020.

[61] W. M. A. Ahmed, "Is there a risk-return trade-off in cryptocurrency markets? the case of bitcoin," *Journal of Economics and Business*, vol. 108, p. 21, 2019.

[62] L. Charfeddine, N. Benlagha, and Y. Maouchi, "Investigating the dynamic relationship between cryptocurrencies and conventional assets: implications for financial investors," *Economic Modelling*, vol. 85, pp. 198–217, 2020.

[63] A. Klarin, "The decade-long cryptocurrencies and the blockchain rollercoaster: mapping the intellectual structure and charting future directions," *Research in International Business and Finance*, vol. 51, p. 16, 2020.

[64] C. Chen, "Predictive effects of structural variation on citation counts," *Journal of the American Society for Information Science and Technology*, vol. 63, no. 3, pp. 431–449, 2012.

[65] P. M. Doney and J. P. Cannon, "An examination of the nature of trust in buyer-seller relationships," *Journal of Marketing*, vol. 61, no. 2, pp. 35–51, 1997.
[66] D. Gefen, "E-commerce: the role of familiarity and trust," *Omega*, vol. 28, no. 6, pp. 725–737, 2000.
[67] S. Ba and P. A. Pavlou, "Evidence of the effect of trust building technology in electronic markets: price premiums and buyer behavior," *MIS Quarterly*, vol. 26, no. 3, pp. 243–268, 2002.
[68] S. Schuh and J. Stavins, "Why are (some) consumers (finally) writing fewer checks? the role of payment characteristics," *Journal of Banking & Finance*, vol. 34, no. 8, pp. 1745–1758, 2010.
[69] J. Zinman, "Debit or credit?" *Journal of Banking & Finance*, vol. 33, no. 2, pp. 358–366, 2009.
[70] A. T. Ching and F. Hayashi, "Payment card rewards programs and consumer payment choice," *Journal of Banking & Finance*, vol. 34, no. 8, pp. 1773–1787, 2010.
[71] S. Carbó-Valverde and J. M. Liñares-Zegarra, "How effective are rewards programs in promoting payment card usage? empirical evidence," *Journal of Banking & Finance*, vol. 35, no. 12, pp. 3275–3291, 2011.
[72] E. Klee, "How people pay: evidence from grocery store data," *Journal of Monetary Economics*, vol. 55, no. 3, pp. 526–541, 2008.
[73] P. He, L. Huang, and R. Wright, "Money, banking, and monetary policy," *Journal of Monetary Economics*, vol. 55, no. 6, pp. 1013–1024, 2008.
[74] S. Zhang, X. Zhou, H. Pan, and J. Jia, "Cryptocurrency, confirmatory bias and news readability—Evidence from the largest Chinese cryptocurrency exchange," *Accounting & Finance*, vol. 58, no. 5, pp. 1445–1468, 2019.
[75] P. Xie, J. Wu, and H. Du, "The relative importance of competition to contagion: evidence from the digital currency market," *Financial Innovation*, vol. 5, no. 1, p. 19, 2019.
[76] L. Rognone, S. Hyde, and S. S. Zhang, "News sentiment in the cryptocurrency market: an empirical comparison with forex," *International Review of Financial Analysis*, vol. 69, p. 17, 2020.
[77] O. Entrop, B. Frijns, and M. Seruset, "The determinants of price discovery on bitcoin markets," *Journal of Futures Markets*, vol. 40, no. 5, pp. 816–837, 2020.
[78] T. Takaishi, "Rough volatility of bitcoin," *Finance Research Letters*, vol. 32, p. 8, 2020.
[79] S. J. H. Shahzad, E. Bouri, D. Roubaud, and L. Kristoufek, "Safe haven, hedge and diversification for G7 stock markets: gold versus bitcoin," *Economic Modelling*, vol. 87, pp. 212–224, 2020.
[80] S. Dow, "Monetary reform, central banks, and digital currencies," *International Journal of Political Economy*, vol. 48, no. 2, pp. 153–173, 2019.
[81] U. Bindseil, "Central bank digital currency: financial system implications and control," *International Journal of Political Economy*, vol. 48, no. 4, pp. 303–335, 2019.
[82] M. Hampl and T. Havranek, "Central bank equity as an instrument of monetary policy," *Comparative Economic Studies*, vol. 62, no. 1, pp. 49–68, 2020.
[83] Y. A. Su, Y. N. Yu, and N. Zhang, "Carbon emissions and environmental management based on big data and streaming data: a bibliometric analysis," *Science of the Total Environment*, vol. 733, p. 11, 2020.